

976/77

DATE DUE

Digitized by Google



64

F

Mineralogy and Geology of the Wagnerite Occurrence on Santa Fe Mountain, Front Range, Colorado

GEOLOGICAL SURVEY PROFESSIONAL PAPER 955





Mineralogy and Geology of the Wagnerite Occurance on Santa Fe Mountain, Front Range, Colorado

By DOUGLAS M. SHERIDAN, SHERMAN P. MARSH,
MARY E. MROSE, and RICHARD B. TAYLOR

GEOLOGICAL SURVEY PROFESSIONAL PAPER 955

A detailed mineralogic study of wagnerite, a rare phosphate mineral occurring in the report area in Precambrian gneiss; this is the first recorded occurrence of wagnerite in the United States



UNITED STATES DEPARTMENT OF THE INTERIOR

THOMAS S. KLEPPE, *Secretary*

GEOLOGICAL SURVEY

V. E. McKelvey, *Director*

Library of Congress Cataloging in Publication Data

Main entry under title:

Mineralogy and geology of the wagnerite occurrence on Santa Fe Mountain, Front Range, Colorado.
(Geological Survey Professional Paper 955)

Includes bibliographical references.

1. Wagnerite—Colorado—Santa Fe Mountain. 2. Geology—Colorado—Santa Fe Mountain.

I. Sheridan, Douglas M., 1921- II. Series: United States Geological Survey Professional Paper 955.

QE391.W3M56 549'.72 76-10335

For sale by the Superintendent of Documents, U.S. Government Printing Office

Washington, D.C. 20402

Stock Number 024-001-02844-1

CONTENTS

	Page		Page
Metric-English equivalents	IV	Descriptive mineralogy—Continued	
Abstract	1	Wagnerite	5
Introduction	1	Other minerals	8
Acknowledgments	2	Mineral assemblages and textural relations	11
Geologic setting	2	Chemistry	14
Occurrence	3	X-ray crystallography	15
Descriptive mineralogy	5	Origin	19
Methods used for optical determinations	5	References cited	22

ILLUSTRATIONS

	Page
FIGURE 1. Map of east-central Front Range showing Santa Fe Mountain wagnerite locality and location of figure 2	2
2. Map showing distribution of rutile-bearing light-colored gneisses in the Santa Fe Mountain-Beaver Brook-Soda Creek area	3
3. Geologic map of wagnerite locality, Santa Fe Mountain	4
Photomicrographs:	
4. Large ameboid-shaped grain of wagnerite	6
5. Large blocky grain of wagnerite poikiloblastically enclosing rows of rutile grains	7
6. Complex intergrowth of closely spaced grains of wagnerite and plagioclase	7
7. Part of a large wagnerite grain that is crowded with tiny inclusions	8
8, 9. Rims of apatite on wagnerite	8, 9
10. Prismatic to blocky inclusions of apatite in wagnerite	9
11, 12. Wagnerite strongly oriented parallel to foliation defined by fibrolitic sillimanite	11, 12
13, 14. Prismatic sillimanite cutting wagnerite and other minerals	12, 13
15. Corundum containing numerous needles of sillimanite	13
16. Corundum and rutile along grain boundaries of wagnerite	13
17. X-ray powder photographs of wagnerite, ferroan wagnerite, magniotriplite, and triplite	20

TABLES

	Page
TABLE 1. Modes of light-colored gneisses, Santa Fe Mountain wagnerite locality, Colorado	5
2. Optical data for wagnerite from Santa Fe Mountain, Colorado	5
3. Comparison of optical data for wagnerite	6
4. Optical data for other minerals from wagnerite locality, Santa Fe Mountain, Colorado	10
5. Chemical analyses of wagnerite	14
6. Microprobe analysis of wagnerite from Santa Fe Mountain, Colorado	15
7. Crystallographic, compositional, and density data compared for wagnerite, ferroan wagnerite, magniotriplite, and triplite	16
8. X-ray powder diffraction data for wagnerite, $Mg_2(PO_4)F$	17

METRIC-ENGLISH EQUIVALENTS

Metric unit		English equivalent
Length		
millimetre (mm)	=	0.03937 inch (in)
metre (m)	=	3.28 feet (ft)
kilometre (km)	=	.62 mile (mi)
Area		
square metre (m ²)	=	10.76 square feet (ft ²)
square kilometre (km ²)	=	.386 square mile (mi ²)
hectare (ha)	=	2.47 acres
Volume		
cubic centimetre (cm ³)	=	0.061 cubic inch (in ³)
litre (l)	=	1.105 cubic inches
cubic metre (m ³)	=	35.31 cubic feet (ft ³)
cubic metre	=	.00081 acre-foot (acre-ft)
cubic hectometre (hm ³)	=	210.7 acre-feet
litre	=	2.113 pints (pt)
litre	=	1.06 quarts (qt)
litre	=	.26 gallon (gal)
cubic metre	=	.00026 million gallons (Mgal or mil gal)
cubic metre	=	6.290 barrels (bbl) (1 bbl=42 gal)
Weight		
gram (g)	=	0.035 ounce, avoirdupois (oz avdp)
gram	=	.0022 pound, avoirdupois (lb avdp)
ounce (oz)	=	1.7 tons, short (2,000 lb)
ounce	=	.98 ton, long (2,240 lb)
Specific combinations		
kilogram per square centimetre (kg/cm ²)	=	0.96 atmosphere (atm)
kilogram per square centimetre	=	.98 bar (0.9869 atm)
cubic metre per second (m ³ /s)	=	35.3 cubic feet per second (ft ³ /s)

Metric unit	English equivalent	
Specific combinations—Continued		
litre per second (l/s)	=	.0353 cubic foot per second
cubic metre per second per square kilometre [(m ³ /s)/km ²]	=	91.47 cubic feet per second per square mile [(ft ³ /s)/mi ²]
metre per day (m/d)	=	3.28 feet per day (hydraulic conductivity) (ft/d)
metre per kilometre (m/km)	=	3.28 feet per mile (ft/mi)
kilometre per hour (km/h)	=	911.3 foot per second (ft/s)
metre per second (m/s)	=	3.28 feet per second
metre squared per day (m ² /d)	=	10.764 feet squared per day (ft ² /d) (transmissivity)
cubic metre per second (m ³ /s)	=	22.826 million gallons per day (Mgal/d)
cubic metre per minute (m ³ /min)	=	264.9 gallons per minute (gal/min)
litre per second (l/s)	=	15.85 gallons per minute
litre per second per metre [(l/s)/m]	=	4.83 gallons per minute per foot [(gal/min)/ft]
kilometre per hour (km/h)	=	.62 mile per hour (mi/h)
metre per second (m/s)	=	2.237 miles per hour
gram per cubic centimetre (g/cm ³)	=	62.43 pounds per cubic foot (lb/ft ³)
gram per square centimetre (g/cm ²)	=	2.048 pounds per square foot (lb/ft ²)
gram per square centimetre	=	.0142 pound per square inch (lb/in ²)
Temperature		
degree Celsius (°C)	=	1.8 degrees Fahrenheit (°F)
degrees Celsius (temperature)	=	[(1.8 × °C) + 32] degrees Fahrenheit

MINERALOGY AND GEOLOGY OF THE WAGNERITE OCCURRENCE ON SANTA FE MOUNTAIN, FRONT RANGE, COLORADO

By DOUGLAS M. SHERIDAN, SHERMAN P. MARSH,
MARY E. MOSE, and RICHARD B. TAYLOR

ABSTRACT

The first known occurrence in the United States of wagnerite, a rare magnesium fluophosphate, is on Santa Fe Mountain near Idaho Springs in the Colorado Front Range. Wagnerite occurs as a minor constituent of thin lenses of sillimanite-plagioclase gneiss of Precambrian age. Other minerals in the gneiss are corundum, rutile, pale-brown biotite, apatite, monazite, zircon, and tourmaline. The sillimanite-plagioclase gneiss is a local lithologic variant of a persistent layer of rutile-bearing sillimanite-quartz gneiss and related rocks that has been traced 15 km along a Z-shaped fold southeastward from the northern flank of Santa Fe Mountain.

The wagnerite from Santa Fe Mountain is anhedral, mostly fine grained, and pale yellow to yellowish tan. Luster is vitreous to slightly resinous. Cleavage (100) is very poor. In transmitted light, grains are colorless and nonpleochroic. The indices of refraction and the optic angle show a range in values: $\alpha=1.565-1.571$, $\beta=1.567-1.572$, $\gamma=1.578-1.585$ (all ± 0.002); $(+2V)=28^{\circ}-33^{\circ}$ ($\pm 1^{\circ}$). Dispersion is $r > v$, weak.

Textural relations indicate that a single stable mineral assemblage characterizes the sillimanite-plagioclase gneiss: wagnerite+plagioclase (albite)+fibrolitic sillimanite+magnesian biotite. To this assemblage may be added small amounts of rutile, monazite, zircon, and apatite, minerals inferred to represent phases belonging to a relatively early stage of crystallization during high-grade regional metamorphism. Corundum, prismatic sillimanite, and some apatite crystallized later but probably during the same regional metamorphism.

Chemical analysis of the wagnerite from Santa Fe Mountain led to the formula $(\text{Mg}, \text{Fe}, \text{Mn})_{2.08} \text{PO}_4(\text{F}, \text{Cl})_{0.96}$, with $\text{Mg}:\text{Fe}:\text{Mn}=0.97:0.02:0.01$; this formula is close to the empirical formula $\text{Mg}_2(\text{PO}_4)\text{F}$.

Single crystal X-ray-diffraction studies showed that the wagnerite from Santa Fe Mountain is monoclinic, space group $P2_1/a$, with $a=11.9263 \pm 0.0007$ Å, $b=12.6707 \pm 0.0008$ Å, $c=9.6411 \pm 0.0005$ Å, $\beta=108.285^{\circ} \pm 0.005^{\circ}$, volume $=1,383.57$ Å³. Specific gravity calculated from refined cell data is 3.16 g/cc; specific gravity measured by the pycnometer method is 3.15 g/cc. A strong monoclinic subcell is present with the b -axis halved (6.335 Å); the subcell is in space group $P2_1/a$ with $Z=8$, and its cell parameters are comparable with those reported in the literature for triplite-group minerals. The X-ray powder-diffraction pattern taken in Fe/Mn radiation has the following strong lines (hkl , d , I): 141, 2.970 Å (100); 402, 2.839 Å (85); 202, 3.114 Å (60); 122, 3.287 Å (60); 023, 2.748 Å (30); 421, 2.697 Å (21).

A comparison of crystallographic data for wagnerite, ferroan wagnerite, magniotriplite, and triplite indicates that, despite their high magnesium content, ferroan wagnerite and magniotriplite are members of the triplite group and have a true cell that is different from that of wagnerite. So-called "ferroan wagnerite," from Hålsjöberget, Sweden, and from the Albères massif, eastern Pyrenees, France, is actually

magniotriplite; this material should not be referred to as ferroan wagnerite. Although X-ray powder-diffraction patterns of ferroan wagnerite and magniotriplite resemble the diffraction pattern of wagnerite, the pattern for wagnerite has a line at 5.66 Å which distinguishes it from triplite-group minerals.

Rutile-bearing gneisses in the east-central Front Range are believed to have formed by metamorphism of bentonitic clays that were generated during intense weathering of intermediate to basic tuffs and flows in Precambrian time. The clays were partly reworked by surface waters; fluorine of probable volcanic source was adsorbed locally. After a thick succession of interlayered volcanic and sedimentary rocks accumulated, high-grade regional metamorphism took place. The thin layers and lenses of reworked weathered materials recrystallized to form rutile-bearing sillimanite-quartz gneiss and related feldspathic rocks. Wagnerite formed locally, instead of apatite, where the amount of calcium was insufficient to accommodate the available phosphate.

INTRODUCTION

Wagnerite, a rare magnesium fluophosphate mineral, occurs as a minor constituent of thin layers of rutile-bearing gneiss in regionally metamorphosed rocks of Precambrian age on the northern flank of Santa Fe Mountain, 3.5 km southeast of Idaho Springs in the east-central Front Range, Clear Creek County, Colorado (fig. 1). This is the first recorded occurrence of wagnerite in the United States (Sheridan and others, 1971).

Sheridan and Marsh examined the Santa Fe Mountain area in 1968 during field investigation of rutile-bearing gneisses in this region. Petrographic studies of rock samples from this area subsequently disclosed the presence of an unknown biaxial positive mineral that has a small optic angle. Optical, X-ray, and chemical investigations proved this mineral to be wagnerite. Additional samples were obtained by Sheridan and Marsh in 1969 and a geologic map of the wagnerite locality was prepared (fig. 3).

This report describes the occurrence and properties of wagnerite from Santa Fe Mountain, Colo. Also included are descriptions of other minerals and the mineral assemblages, a comparison of the optical, chemical, and X-ray data for Colorado wagnerite with data for wagnerite from other localities in the world, and a discussion of

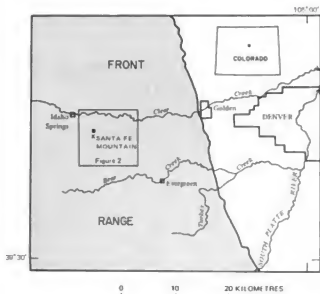


FIGURE 1.—Map of east-central Front Range showing Santa Fe Mountain wagnerite locality (black square) and location of figure 2.

origin of the Colorado wagnerite. Responsibilities and credits are: Sheridan and Marsh provided the geologic field data and, together with Taylor, determined the descriptive mineralogy, petrography, and mineral assemblages; Mrose provided detailed X-ray data, discussions of the chemistry and X-ray crystallography, and comparison of wagnerite with ferroan wagnerite, magniotriplite, and triplite.

ACKNOWLEDGMENTS

We wish to thank Cabins, Inc. of Wheatridge, Colo., for its cooperation in permitting us to sample and study this wagnerite occurrence on their property. It is pertinent to mention that although wagnerite is a rare mineral, neither the wagnerite nor the corundum, which also occurs at this locality, can be regarded as having special museum or specimen value. These minerals are minor constituents of a metamorphic rock and, as such, are important to the geologist as unusual mineral phases in an uncommon metamorphic assemblage rather than to a mineral collector.

We are grateful to numerous U.S. Geological Survey colleagues for their help during this study. John W. Adams, George A. Desborough, Fred A. Hildebrand, and James M. Nishi made microchemical and other tests during the early part of the investigation. Laura E. Reichen provided the quantitative chemical analysis, Johnnie Gardner provided a fluorine determination, and Robert B. Finkelman made a microprobe analysis. Ray E. Wilcox, Irving J. Witkind, and Glenn A. Izett gave helpful advice during petrographic determinations of optical

data. Judith Konnert calculated the powder pattern for wagnerite from near Werfen, Austria, and also carried out least-squares analysis of the Colorado wagnerite.

All specimens used in these investigations, except those from the Colorado locality, were kindly supplied by several individuals: ferroan wagnerite from eastern Pyrenees by François Fontan of the Laboratoire de Minéralogie-Cristallographie (Toulouse, France); type magniotriplite, by Dr. Prof. G. Barsanov of the Fersman Mineralogical Museum (Leningrad, U.S.S.R.); and all other study materials, by Paul Desautels of the U.S. National Museum (Washington, D. C.).

GEOLOGIC SETTING

The wagnerite locality lies in the east-central part of the block of uplifted Precambrian rocks that form the core of the Colorado Front Range. Bedrock in the general vicinity of the occurrence is composed of a thick folded succession of gneisses of high metamorphic grade. These interlayered metasedimentary and metavolcanic rocks contain mineral assemblages in general correlative with the sillimanite zone and the upper part of the amphibolite facies. The regional metamorphism accompanied a long Precambrian period of deformation that involved two stages of plastic folding. Tight to open west-northwest-trending folds were formed first and, in some areas, were modified subsequently by more northerly trending crossfolds. Although granitic plutons were emplaced in this general region during three major periods of igneous activity in the Precambrian Era, the closest major igneous bodies are more than 5 km from the wagnerite locality. The geologic setting, therefore, is regional metamorphic rather than contact metamorphic.

Feldspar-rich gneiss (chiefly plagioclase, quartz, microcline, and biotite) and biotite gneiss (chiefly biotite, plagioclase, and quartz) are the principal metamorphic rocks in the east-central Front Range. Much of the biotite gneiss is sillimanitic, and some contains garnet-bearing and cordierite-bearing layers. Interlayered with the feldspar-rich gneiss and the biotite gneiss are variable amounts of hornblende gneiss, amphibolite, and calcisilicate gneiss.

Thin layers and lenses of rutile-bearing light-colored gneisses occur at several stratigraphic levels within this thick succession of gneisses. These range in thickness from 15 cm to 50 m and contain from trace amounts to about 5 percent of rutile. A remarkably persistent layer has been traced along a z-shaped fold for about 13 km south-eastward from the northern flank of Santa Fe Mountain (fig. 2). The distribution of the rutile-bearing gneisses and other Precambrian rocks in the east-central Front Range is shown in a generalized map by Marsh and Sheridan (1976, fig. 2).

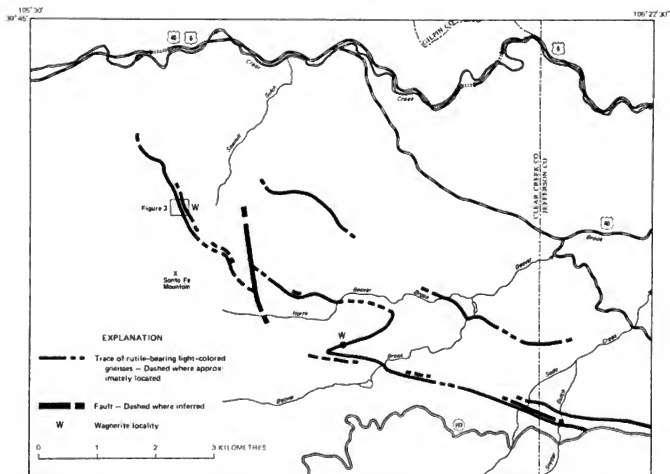


FIGURE 2.—Map showing distribution of rutile-bearing light-colored gneisses in the Santa Fe Mountain-Beaver Brook-Soda Creek area.

The rutile-bearing light-colored gneisses are composed of several lithologic varieties that are interlayered and gradational along strike. The most common varieties are sillimanite-quartz gneiss, biotite-quartz-plagioclase gneiss, and rocks gradational between these two types. Less common regionally, but locally predominant, is a sillimanitic topaz-quartz gneiss (Sheridan and others, 1968), which is present in several localities between Santa Fe Mountain and the eastern margin of the Front Range. At Santa Fe Mountain a local variant of the rutile-bearing light-colored gneisses is a sillimanite-plagioclase gneiss containing wagnerite and corundum.

OCCURRENCE

At the Santa Fe Mountain wagnerite locality, rutile-bearing light-colored biotite-quartz-plagioclase gneiss forms two northwest-trending layers that are separated by hornblende gneiss (fig. 3). Wagnerite occurs in a corundum-bearing sillimanite-plagioclase gneiss that forms a lens within the biotite-quartz-plagioclase gneiss

in the eastern layer and that interfingers with biotite-quartz-plagioclase gneiss in the western layer. Small bodies of simple quartz-feldspar pegmatite intrude the succession of metamorphic rocks here as they do ubiquitously throughout the Precambrian terrane of the east-central Front Range.

Although rutile-bearing gneisses at this stratigraphic level persist continuously for 1.5 km to the northwest and for 11.5 km to the southeast (fig. 2), the principal occurrence of wagnerite is within the area shown in figure 3. Wagnerite has also been identified as a trace constituent of rutile-bearing biotite-quartz-plagioclase gneiss in the area between Beaver Brook and North Beaver Brook (fig. 2).

The wagnerite-bearing sillimanite-plagioclase gneiss is white or light gray, fine to coarse grained, poorly foliated, and texturally complex. Aggregates of prismatic sillimanite, as much as 12 cm long and 1 cm thick, and grains of corundum, as long as 2.3 cm, are diversely oriented in a fine- to medium-grained matrix rich in plagioclase and

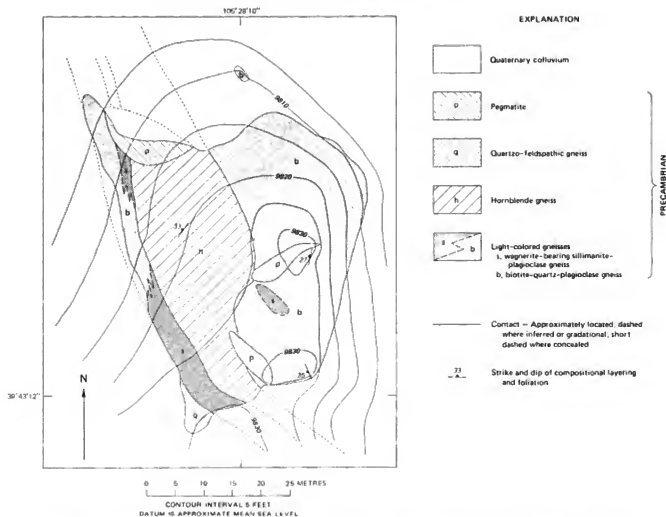


FIGURE 3.—Geologic map of wagnerite locality, Santa Fe Mountain. Geology and topography by D. M. Sheridan and S. P. Marsh.

fibrolitic sillimanite. Wagnerite is recognizable in hand specimens and outcrops as aggregates of small yellow to yellowish-tan grains that commonly are complexly intergrown with other minerals of the rock. Such aggregates are generally small, mostly 2 to 5 mm across. Smaller individual grains of wagnerite are also common but are recognized readily only in thin section. Other constituents of the gneiss are biotite, rutile, apatite, monazite, zircon, tourmaline, muscovite, and, locally, chlorite. Foliation in the sillimanite-plagioclase gneiss is in general obscure in the outcrops, owing to the diversely oriented large grains of corundum and aggregates of prismatic sillimanite. In some thin sections, however, foliation is well shown and is defined by aggregates of fibrolitic sillimanite, elongate grains of plagioclase, and oriented flakes of biotite.

Modes of the light-colored gneisses of the wagnerite locality were determined by the point-count method (1,000 points each) and are reported in table 1. Modes 1-7

represent wagnerite-rich rocks in which plagioclase and sillimanite are the principal constituents. Modes 8 and 9 represent wagnerite-bearing rock with more biotite than sillimanite. Because rock specimens for these thin sections were selected preferentially to study the wagnerite, the modes do not represent normal mineralogical percentages. We estimate that wagnerite and corundum each form about 1 percent of the average rock and that rutile makes up 1-2 percent. In the sillimanite-plagioclase gneiss, quartz is present only in trace amounts as tiny rounded inclusions in other minerals.

The biotite-quartz-plagioclase gneiss, the associated hornblende gneiss, and the quartzo-feldspathic gneiss (fig. 3) are fine to medium grained moderately well foliated rocks. Some parts of the hornblende gneiss and the light-colored biotite-quartz-plagioclase gneiss show well-developed compositional layering on a scale of a few centimetres, but other parts contain massive layers 1 m thick.

TABLE 1.—Modes (volume percent) of light-colored gneisses, Santa Fe Mountain wagnerite locality, Colorado

Modes	Wagnerite-bearing sillimanite-plagioclase gneiss									Biotite-quartz-plagioclase gneiss		
	1	2	3	4	5	6	7	8	9	10	11	12
Field No. SF—	11-4X2	11-4X	21A	21AX	11-4X2	58X	23A1	11-2X	11-3X	7A	9A	9D
Quartz.....	Trace								Trace	29.3	38.8	36.0
Plagioclase.....	74.4	47.3	71.6	61.7	45.7	52.4	55.0		68.8	56.3	50.5	46.7
Microcline.....										2		
Sillimanite.....	12.8	45.0	19.8	25.7	38.9	35.5	28.5	2.2	3.3			2.0
Biotite.....	1.5		.1		.3		.3	14.0	10.2	12.5	4.6	10.8
Muscovite (and Sericite).....	4.8	1.8	2.0	.8	3.7	1.0	4.5	3.3	10.1	1.0	4.4	3.3
Wagnerite.....	.7	.9	4.6	6.8	6.9	7.6	10.9	1.4	.3			
Apatite.....	.3	.3	.3	.6	2.1	2.4	1.2	.5	.2			
Rutile.....	4.8	4.7	.9	1.2	.1	.8	1.0	3.1	3.1	.1	.5	.2
Corundum.....			.7		2.2	.3		.5	1.5			
Monazite and (or) zircon.....	.2	Trace	Trace	Trace	.1	Trace	.3	.4	.2	Trace	Trace	Trace
Tourmaline.....											.1	
Chlorite.....	.5		Trace	.2	Trace	Trace	.3		2.3	.6	1.1	1.0
Total.....	100.0	100.0	100.0	100.0	100.0	100.0	100.0	100.0	100.0	100.0	100.0	100.0

Modes 10-12 of biotite-quartz-plagioclase gneiss (table 1) indicate that the principal constituents, in order of increasing abundance, are biotite, quartz, and plagioclase. Rutile (no more than 0.5 percent) is less abundant than in the wagnerite-bearing rock. Wagnerite was not observed in samples of the biotite-quartz-plagioclase gneiss from the Santa Fe Mountain locality.

DESCRIPTIVE MINERALOGY

METHODS USED FOR OPTICAL DETERMINATIONS

Except for optic angles, all optical data for wagnerite and other minerals from Santa Fe Mountain (tables 2, 4) were obtained on single grains that were selected from mineral separates and that were studied petrographically by the spindle-stage procedures described by Wilcox (1959). Most of the determinations of refractive indices were made by use of the focal masking techniques described in detail by Cherkasov (1955a, b; 1957). A few determinations of refractive indices were made by the Becke line method; an interference filter was used that passes a wavelength near the D-line of the spectrum. All except one of the optic angles reported in table 2 were determined from thin sections mounted in a universal stage. The exception was determined on the spindle stage using Mallard's method for a centered acute bisectrix figure.

The refractive indices of 3 grains of wagnerite from Bamle, Norway (U.S. Natl. Mus. spec. C4151), reported in table 3, were determined by spindle stage procedures and focal masking techniques. Our measurement of the optic angle of each of these grains was facilitated by I. J. Witkind, who carefully mounted each grain so that its

optic plane was normal to the spindle axis. The measurement of the optic angle was then made directly by simple rotation of the spindle from one melatope to the other.

WAGNERITE

The wagnerite from Colorado is anhedral, mostly fine grained but ranging to medium grained, and pale yellow to yellowish tan. The luster is vitreous to slightly resinous. Cleavage (100) is very poor and other cleavage was not observed. The specific gravity, determined by Fahey's method (Fahey, 1961) on the material ground for chemical analysis, is 3.13. In transmitted light the wagnerite in thin section is colorless; large grains in immersion mounts are faintly yellowish and nonpleochroic. The mineral is biaxial positive. The indices of refraction and $2V$ (table 2) show a range in values: $\alpha=1.565-1.571$, $\beta=1.567-1.572$, $\gamma=1.578-1.585$ (all ± 0.002); $(+2V)=28-35^\circ$ ($\pm 1^\circ$). Slight

TABLE 2.—Optical data for wagnerite from Santa Fe Mountain, Colorado

Sample No. SF—	Indices of refraction (± 0.002) ^a			Sample No. SF—	Optic angle (measured) ($\pm 1^\circ$) ^b
	α	β	γ		
11-7.....	1.565	1.567-1.568	1.578-1.579	24AX.....	$28^\circ \pm 0.5^\circ$
21.....	1.566	1.567	1.580	23A1.....	$28.5^\circ \pm 1.0^\circ$
24, No. 1.....	1.566	1.568	1.581	11-2.....	$29^\circ \pm 1.0^\circ$
23-A1.....	1.568	1.570	1.582	11-7.....	$29^\circ-31^\circ \pm 1.0^\circ$
21A.....	1.569	1.571	1.583	11-4.....	$31^\circ \pm 1.0^\circ$
24, No. 3.....	1.569	1.570	1.583	21B.....	$31^\circ \pm 0.5^\circ$
24, No. 2.....	1.571	1.572	1.585	21A.....	$31.5^\circ \pm 1.0^\circ$
				24B.....	$32.5^\circ \pm 1.0^\circ$
				23B2X.....	$33^\circ \pm 0.5^\circ$

^aDetermined by spindle stage techniques.

^bDetermined from thin sections on universal stage.

^cDetermined on spindle stage from centered acute bisectrix figure by Mallard's method.

^dUnred.

variation of optical properties occurs within many individual grains, a variation limited to 1° or less in $2V$ and to correspondingly small changes in indices. The birefringence ($\gamma - \alpha$), calculated from refractive index determinations, ranges from 0.013 to 0.015. Dispersion is $r > v$, weak. The extinction angle ($Z\Delta c$) was measured at approximately 23° by universal stage techniques in one thin section, but the (100) cleavage is so poorly developed that a representative value for $Z\Delta c$ cannot be reported. The optical data for wagnerite from Santa Fe Mountain are compared with optical data for wagnerite from several other localities in table 3.

As viewed in thin section, individual grains of wagnerite range in size from 0.02 to 6.1 mm. Most individual grains are in the size range 0.2–0.6 mm. Aggregates of wagnerite grains, complexly intergrown with plagioclase and other minerals of the rock, are also common, ranging in size from 1 mm to 12 mm but most commonly in the size range 2–5 mm. One elongate aggregate observed in hand specimen is 20 mm long but is so complexly intergrown with other minerals that no more than 50 percent of the aggregate is wagnerite.

TABLE 3.—Comparison of optical data for wagnerite

Locality	Source of data	Indices of refraction			$(+)$ $2V$
		α	β	γ	
Santa Fe Mountain, Colo.	(a)	1.565–1.571 ± 0.002	1.567–1.572 ± 0.002	1.578–1.585 ± 0.002	28° – 33° $\pm 1^\circ$
Bamle, Norway ...	(b)	1.569–1.571 ± 0.002	1.570–1.572 ± 0.002	1.582–1.584 ± 0.002	37° – 38° $\pm 1^\circ$
Do.	(c)	1.569	1.570	1.582	36° – 50°
Werfen, Austria	(d)	1.5678	1.5719	1.5824	28° – 24°
Kyakhia, U.S.S.R. ...	(e)	1.577 ± 0.001	1.582 ± 0.001	1.595 ± 0.001	32° $\pm 1^\circ$
Dolní Bory, western Moravia, Czechoslovakia ...	(f)	1.568	1.571	1.582	Small.

* Calculated from published $2V$ as given in sources of data (c) and (d).

Sources of data:

- This report (table 2).
- This report. The indices reported here are the range in values obtained by spindle-stage techniques on 3 grains of wagnerite, U.S. Natl. Mus. spec. 64151 from Bamle, Norway. Measurement of $2V$ was done by orienting the optic plane of each grain normal to the spindle axis; in this manner, measurement of the optic angle was made directly by rotation of the spindle from one melatope to the other.
- Indices of refraction from Michel-Lévy and Lacroix (1888, p. 290). The $2V$ was calculated from $2E=59^\circ 30'$, reported by Doelter (1918, p. 319).
- Indices of refraction from Hegemann and Steinmetz (1927, p. 55). The $2V$ was calculated from $2E=45^\circ 22'$, reported by Hegemann and Steinmetz (1927, p. 55).
- Finko (1962, p. 1425).
- Stančík (1965, p. 67).

The wagnerite appears to be entirely anhedral; no crystal faces were observed despite the study of numerous thin sections. Most commonly the individual grains are elliptical to very irregular or amoeboid (fig. 4) in shape. The larger grains tend to be blocky to rounded and have very irregular boundaries (fig. 5). Some of these grains contain myriads of small inclusions of rutile; others poikiloblastically enclose small grains of plagioclase, sillimanite, monazite, and other minerals.

Some groups of closely spaced wagnerite grains seem to be composed of distinct individuals that are separated by plagioclase and other minerals of the rock. When viewed through crossed polars, however, most of the wagnerite grains in such groups have identical interference color and come to extinction at the same position. Very likely such wagnerite grains are connected in the third dimension and represent a type of branching skeletal growth, which, in the plane of the thin section, shows up mainly as a complex intergrowth approaching that of a poikiloblastic texture (fig. 6).

In addition to poikiloblastic inclusions of grains of other minerals of a size large enough to be readily identi-

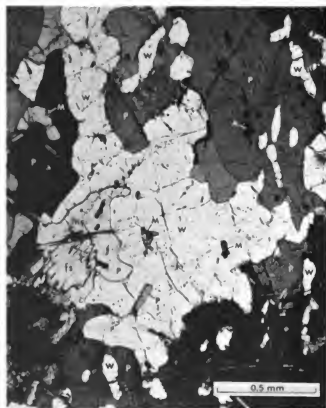


FIGURE 4.—Large grain of wagnerite (W) occupying central part of photomicrograph is amoeboid in shape; smaller grains of wagnerite are elliptical to irregular. Other minerals are plagioclase (P), monazite (M), apatite (A), fibrolitic sillimanite (fs), and muscovite (ms). Crossed polars.

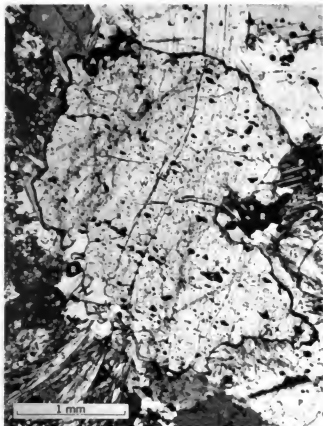


FIGURE 5.—Large blocky grain of wagnerite (W) poikiloblastically encloses rows of grains of rutile (R). Apatite (A) forms a thin rim along the boundary of the wagnerite grain. Other minerals are plagioclase (P), biotite (B), fibrolitic sillimanite (fs), and prismatic sillimanite (S). Crossed polars.

fiably in thin section, many of the medium to large grains of wagnerite show cloudy areas crowded with abundant very tiny inclusions. At low to moderate magnification in plane-polarized light, these cloudy areas are bluish. Commonly, the cloudy areas are located at or near the center of the wagnerite grains, and the surrounding borders of wagnerite are relatively clear of inclusions; in other wagnerite grains, the cloudy areas are located asymmetrically near the edge of the grains (fig. 9). A photomicrograph (fig. 7), taken at high magnification with upper and lower polars removed, shows part of a wagnerite grain clouded with tiny inclusions. Toward the center of the clouded area, the inclusions are principally equidimensional with rounded form, and they commonly range in size from 0.0005 to 0.01 mm. Toward the edge of the clouded area, elongate prismatic inclusions, as long as 0.1 mm, are more abundant and are aligned in a rectilinear pattern. Identification of these tiny inclusions proved impossible by ordinary petrographic methods in thin section, but an attempt was made to learn their mineralogic nature by other methods. During the



FIGURE 6.—Complex intergrowth of closely spaced grains of wagnerite (W) and plagioclase (P). However, as most of the wagnerite grains shown here have the same interference color and come to extinction at the same position, they are probably interconnected in the third dimension and comprise a complex branching skeletal or poikiloblastic growth. Other minerals are rutile (R), monazite (M), apatite (A), and muscovite (ms). Crossed polars.

chemical analysis of wagnerite, the analytical procedure involved digestion of part of the sample in nitric acid. The insoluble residue from this digestion was studied carefully by Mrose through X-ray techniques. This residue, which represents at least part of the inclusions, was found to be sillimanite, rutile, and quartz, plus minor mica and xenotime. If apatite or any other mineral soluble in nitric acid were present as part of the suite of tiny inclusions in the wagnerite, it probably was dissolved during the analytical procedure.

Although many of the wagnerite grains are in direct contact with the other minerals of the rock, many others show a partial to complete enveloping film of apatite (fig. 8). Each rim is formed of a single optically continuous apatite crystal. The thickness of the rim ranges from less than 0.01 mm to 0.2 mm but most commonly is about 0.02 mm. Although the rims of apatite are perhaps most commonly present between wagnerite and plagioclase or fibrolitic sillimanite, they have also been observed between wagnerite and other minerals of the rock, such as biotite, monazite, rutile, muscovite, and chlorite. Where

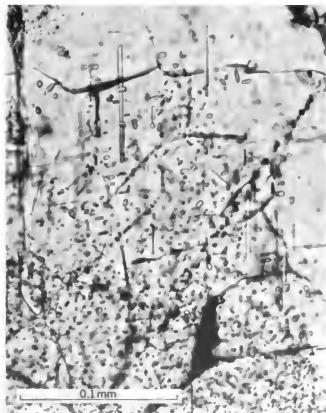


FIGURE 7.—Part of a large wagnerite grain that is crowded with tiny inclusions. Bottom of photomicrograph is toward the interior of wagnerite grain and shows abundant equidimensional to rounded inclusions. Top of photomicrograph is near edge of wagnerite grain and is relatively free of inclusions. Between the clear edge and the densely clouded interior, elongate prismatic inclusions are aligned in rectilinear fashion. Inclusions are chiefly sillimanite, rutile, and quartz. Photomicrograph taken with upper and lower polars removed.

two or more wagnerite grains are closely spaced in the rock, the apatite rims commonly coalesce over part of their extent, forming the thicker observed portions of such rims. Some of the larger wagnerite grains not only have an external rim of apatite but also have internal rims of apatite bordering poikiloblastic inclusions of small grains of plagioclase and other minerals of the rock. Although commonly composed of clear apatite, in one instance the apatite rim has formed around a wagnerite grain containing an asymmetrically located area clouded with tiny inclusions (fig. 9); where the cloudy area extends to the edge of the wagnerite grain, the apatite rim is also crowded with abundant tiny inclusions.

In some thin sections the wagnerite has been partly altered to an unidentified fine-grained material which appears brownish in plane-polarized light and which has no conspicuous identifiable characteristics when viewed with crossed polars or when examined by conoscopic study.



FIGURE 8.—Apatite (A) forms rims on wagnerite (W). Wagnerite grain at top center has only a partial rim of apatite, but all other wagnerite grains shown here are completely rimmed by apatite. Rims on several grains at top center and upper right coalesce and surround a small grain of plagioclase (P). Other minerals are fibrolitic sillimanite (fs) and prismatic sillimanite (S). Crossed polars.

OTHER MINERALS

The optical characteristics of the associated minerals from the Santa Fe Mountain wagnerite-bearing rocks were also studied. These properties together with those of some of the minerals of the associated rocks are reported in table 4.

Plagioclase.—The plagioclase of the wagnerite-bearing sillimanite-plagioclase gneiss is albite (An_0 - An_1), as determined in two samples (SF-21 and SF-24A, table 4). Commonly showing well-developed albite twinning (figs. 6, 12), the plagioclase grains are elongate parallel to the foliation; they range in length from 0.04 to 7 mm but most commonly are about 1.2 mm. The plagioclase in biotite-quartz-plagioclase gneiss (SF-7A, table 4) is also albite (An_0) and occurs as grains averaging about 0.6 mm in length. The plagioclase of these light-colored gneisses is more sodic than the plagioclase of the darker colored metamorphic rocks in this area. Plagioclase in the hornblende gneiss (SF-20B, table 4) is andesine (An_{17}); and plagioclase in the quartz-feldspathic gneiss is oligoclase (An_{27}).

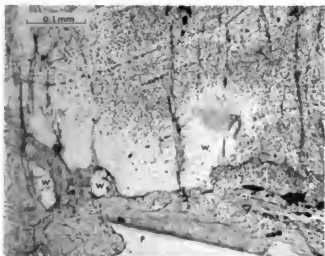


FIGURE 9.—Large grain of wagnerite (W) occupies upper two-thirds of photomicrograph and is rimmed by apatite (A), which completely encloses two smaller grains of wagnerite at left. Where the edge of large wagnerite grain is clear and relatively free from tiny inclusions, as at left center, the adjoining apatite rim is also clear. Where edge of large wagnerite grain is clouded with tiny inclusions, as at right, the adjoining apatite rim is also clouded with inclusions. Other minerals are plagioclase (P), rutile (R), and chlorite (ch). Polars partly crossed.

Biotite.—Most of the biotite in the sillimanite-plagioclase gneiss and the biotite-quartz-plagioclase gneiss is very pale brown, as viewed under the hand lens and in thin section. It resembles the biotite found in the cordierite-bearing biotite gneisses of the east-central Front Range (Gable and Sims, 1969, p. 39) rather than the dark-brown to black biotite of the more common gneisses. Optical data for pale-brown biotite from two samples of sillimanite-plagioclase gneiss (SF-21; SF-11-3) and from one sample of biotite-quartz-plagioclase gneiss (SF-7A) are reported in table 4. All three samples of biotite are biaxial negative ($2V$ estimated no more than 10°). Comparison of the β index (ranging from 1.584 to 1.595) with Winchells' graph (Winchell and Winchell, 1951, p. 374) suggests that this is a low-iron, high-magnesium variety; thus the biotite is probably close to the phlogopite-eastonite part of the compositional field. Biotite flakes range in size from 0.02 to 2.6 mm but average about 0.5 mm in both of the light-colored gneisses.

Sillimanite.—Sillimanite in the sillimanite-plagioclase gneiss occurs in two varieties. Fibrolitic sillimanite occurs in elongate to elliptical aggregates of tiny needles oriented parallel to the foliation (figs. 11, 12) and other mineral lineations; most aggregates are 0.5–10 mm long, although locally some are as long as 19 mm. Coarse prismatic sillimanite crystals are diversely oriented in the rock, commonly cutting other minerals (figs. 13, 14). Single

prismatic sillimanite crystals generally are 0.1–0.2 mm thick and 1.5–2 mm long; aggregates of these crystals are locally as much as 12 cm long and 1 cm in diameter. Refractive indices of prismatic sillimanite from two samples (SF-21 and SF-24A, table 4) are at the lower end of the range of values reported by Deer, Howie, and Zussman (1962, p. 121).

Monazite.—Monazite occurs as small, clear, pale-yellowish grains. These grains range in size from 0.01 to 0.2 mm and are commonly associated with rutile and wagnerite. Refractive indices α and β , determined for sample SF-11-3 (table 4), are in the lower range of values commonly reported.

Apatite.—Two forms of apatite occur in the sillimanite-plagioclase gneiss: (1) individual grains that are rounded to blocky and locally prismatic, clear and colorless to dusky, and about the same average size and distribution as those of wagnerite; (2) partial to complete rims on wagnerite (noted in the description of wagnerite and shown in figs. 5, 8, 9). The apatite that occurs as individual grains ranges in size from 0.02 to 1 mm; aggregates are as much as 6.4 mm across. Locally, prismatic grains of apatite occur as inclusions in wagnerite (fig. 10). The refractive indices determined for individual grains of apatite from two samples (SF-11 and SF-21, table 4) suggest that it is fluorapatite.

Corundum.—Corundum, ranging in color from pink to grayish, occurs in the sillimanite-plagioclase gneiss in grains ranging in size from 0.04 mm to 2.3 cm. Many of the larger grains are subhedral to euhedral and show well-

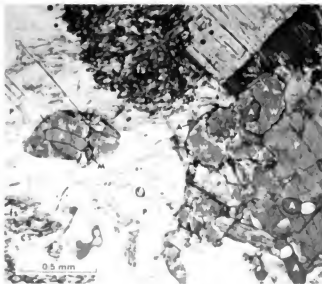


FIGURE 10.—Apatite (A) occurs as prismatic to blocky grains included in wagnerite (W). Other apatite grains are included in plagioclase (P). The wagnerite grain at upper right also has a thin partial rim of apatite. Other minerals are monazite (M), fibrolitic sillimanite (fs), and prismatic sillimanite (S). Crossed polars.

TABLE 4.—Optical data for other minerals from wagnerite locality, Santa Fe Mountain, Colorado

Biaxial minerals							
Mineral	Rock type	Sample No. SF-	Indices of refraction ¹			Optic sign	Remarks
			α	β	γ		
Plagioclase.....	Sillimanite-plagioclase gneiss containing wagnerite, rutile, and corundum.	21	1.532	1.536	1.541	(+)	Composition: ² albite (An ₈).
Do.....	do.....	24A	1.533	1.537	1.542	(+)	Composition: ² albite (An ₈).
Do.....	Rutile-bearing biotite-quartz-plagioclase gneiss.	7A	1.532	1.536	1.541	(+)	Composition: ² albite (An ₈).
Do.....	Hornblende gneiss.	20B	1.544	1.548	1.552	(-)	Composition: ² andesine (An ₁₁).
Biotite.....	Sillimanite-plagioclase gneiss containing wagnerite, rutile, and corundum.	21	1.557	1.595	1.595	(-)	Pleochroism: α =colorless to very pale yellowish tan; β = γ =pale brown.
Do.....	do.....	11-3	1.548	1.584	1.584	(-)	Do.
Do.....	Rutile-bearing biotite-quartz-plagioclase gneiss.	7A	1.549	1.585	1.585	(-)	Do.
Sillimanite.....	Sillimanite-plagioclase gneiss containing wagnerite, rutile, and corundum.	21	1.656	1.658	1.676	(+)	Prismatic variety.
Do.....	do.....	24A	1.654	1.657	1.674	(+)	Do.
Andalusite.....	Feldspathic layer in rutile-bearing biotite-quartz-plagioclase gneiss.	4F	1.628	1.634	1.639	(-)	Pleochroism: α =pink; β = γ =colorless.
Mouzarite.....	Sillimanite-plagioclase gneiss containing wagnerite, rutile, and corundum.	11-3	1.787	1.788	⁽²⁾	(+)	Absorption: $\beta > \alpha = \gamma$.
			$\pm 0.003 \pm 0.003$				
Uniaxial minerals							
Mineral	Rock type	Sample No. SF-	Indices of refraction ¹		Optic sign	Remarks	
			ϵ	ω			
Apatite.....	Sillimanite-plagioclase gneiss containing wagnerite, rutile, and corundum.	11	1.629	1.632	(-)		
Do.....	do.....	21	1.631	1.635	(-)		
Corundum.....	do.....	15	1.759	1.767	(-)	Pink in hand specimen.	
			± 0.003	± 0.003			
Tourmaline.....	do.....	11-3	1.615	1.638	(-)	Dichroism: ϵ =colorless to very pale tan; ω =yellowish brown.	
Do.....	Feldspathic layer in rutile-bearing biotite-quartz-plagioclase gneiss.	4F-1	1.613	1.635	(-)	Dichroism: ϵ =colorless to very pale blue; ω =greenish blue.	
Do.....	do.....	4F-2	1.612	1.635	(-)	Dichroism: ϵ =very pale blue; ω =variegated greenish blue to brownish yellow.	

¹Precision of refractive index determinations is ± 0.002 except where indicated. Determined by spindle stage procedures.²Plagioclase composition determined from curves for low-temperature plagioclase by Smith (1960, pl. 12).³Not determined.

developed pseudo-hexagonal parting; thin sections of such grains commonly show twinning. Many of the smaller grains of corundum are anhedral to angular kernels, many of which resemble graphic shapes. Such small kernels of corundum, 0.06-1 mm across, occur as closely spaced individuals that comprise aggregates 3 mm across in fibrolitic sillimanite clots. Individual grains of corundum within an aggregate commonly have the same interference color and come to extinction at the same position upon rotation of the microscope stage, suggesting that they are connected elements of a single skeletal crystal. Refractive indices for corundum from one sample (SF-15) are reported in table 4.

Andalusite.—Andalusite has been recognized only in a single thin feldspathic layer within the biotite-quartz-plagioclase gneiss. It occurs as blocky pinkish-white grains ranging in size from 0.2 to 1 mm, and it is associated with plagioclase, quartz, muscovite, and chlorite. Optical data for andalusite from one sample (SF-4F) are reported in table 4.

Tourmaline.—Tourmaline occurs sparsely in both the sillimanite-plagioclase gneiss and the biotite-quartz-plagioclase gneiss. It is fairly common as small yellowish-brown to pale-greenish-blue grains in heavy mineral separates prepared from rock samples; although a few grains were observed in thin sections, none was seen in

contact with wagnerite. In a sillimanitic biotite-quartz-plagioclase gneiss that occurs along the trace of the light-colored gneiss unit about 100 m northwest of the wagnerite locality, sparse small aggregates of tourmaline, as much as 2 cm across, are poikiloblastically intergrown with other minerals of the rock; individual brownish crystals are 2–6 mm long and 0.5 mm in diameter. Optical data for tourmaline from rocks of the mapped area (fig. 3) are reported in table 4. The refractive indices suggest that the tourmaline is dravite.

Other minerals from the wagnerite locality.—Quartz occurs only in trace amounts in the sillimanite-plagioclase gneiss, where it is present as small rounded inclusions in other minerals of the rock. In the biotite-quartz-plagioclase gneiss, however, quartz is a major constituent occurring as grains ranging from 0.04 to 3.8 mm in size and averaging about 0.5 mm. Rutile is a characteristic minor constituent of both the light-colored gneisses of the Santa Fe Mountain locality. Commonly splendent red in color, it ranges from yellow to nearly black. Heavy mineral separates indicate that the average rutile content of the sillimanite-plagioclase gneiss is between 1 and 2 percent. The average rutile content of the biotite-quartz-plagioclase gneiss is no more than 0.5 percent. Rutile grains range in size from 0.01 to 0.6 mm, but most are in the range of 0.06–0.1 mm. Although most of the rutile grains are anhedral, some are subhedral to euhedral. Zircon, although identified optically in grains picked from heavy mineral separates, does not appear to be as abundant in the sillimanite-plagioclase gneiss as monazite. Xenotime was identified only in the insoluble residue from the chemical analysis of wagnerite. White mica occurs in both the sillimanite-plagioclase gneiss and the biotite-quartz-plagioclase gneiss. All samples of white mica studied by X-ray proved to be muscovite. Many grains of the muscovite are about the same size as biotite (about 0.5 mm). Sericite (finely crystalline muscovite) is found in plagioclase and along the boundaries of some of the sillimanite aggregates. Chlorite is fairly common as a minor constituent of both of the light-colored gneisses where it apparently formed as an alteration or pseudomorph of biotite. The chlorite seems to have a birefringence of about 0.010 and is colorless in thin section. Universal-stage study of the chlorite in one thin section (SF-11-3X) of wagnerite-bearing rock indicates that (+) 2 θ of the mineral is about 13°.

MINERAL ASSEMBLAGES AND TEXTURAL RELATIONS

During petrographic studies of wagnerite-bearing gneiss, special attention was focused on mineral assemblages and on textures, structures, and intergranular relations. Although one or more of the minerals listed in the following assemblage may be missing from a

particular specimen, textural relations indicate that a single stable-state assemblage characterizes this rock: wagnerite + plagioclase (albite) + fibrolitic sillimanite + magnesian biotite. To this assemblage may be added small amounts of rutile, monazite, zircon, and apatite, minerals inferred to represent phases belonging to an early stage of crystallization during the high-grade regional metamorphism. Rock textures indicate that corundum, prismatic sillimanite, and some of the apatite (the form that occurs as rims on wagnerite) crystallized later, but very likely during the same regional metamorphism.

Fibrolitic sillimanite, plagioclase, biotite, and wagnerite define the foliation of the sillimanite-plagioclase gneiss. Commonly elongate aggregates of fibrolitic sillimanite aligned in foliation surfaces also form a linear structure. Elongate grains of plagioclase and wagnerite, flattened in the foliation plane, are intergrown to varying degrees. Small grains and grain clusters of wagnerite concentrated at boundaries between other minerals (fig. 11) are strongly oriented in the plane of foliation. Similarly, wagnerite grains enclosed within

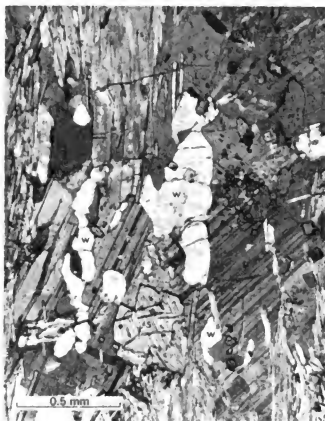


FIGURE 11.—Foliation in sillimanite-plagioclase gneiss is defined by fibrolitic sillimanite (fs). Grains of wagnerite (W) that are concentrated along grain boundaries of other minerals are also strongly oriented in the plane of the foliation. Other minerals are plagioclase (P), prismatic sillimanite (S), and monazite (M). Crossed polars.



FIGURE 12.—Foliation in sillimanite-plagioclase gneiss is defined by fibrolitic sillimanite (fs). Grains of wagnerite (W) that are enclosed within grains of plagioclase (P) are also strongly oriented in the plane of the foliation. A single optical orientation is shared by numerous grains of wagnerite. Other minerals are monazite (M) and prismatic sillimanite (S). Crossed polars.

single grains of plagioclase commonly are also strongly oriented (fig. 12). In part, such groups of wagnerite grains are complexly intergrown skeletal growths; a single optical orientation is commonly shared by dozens of separate but closely spaced grains. (See figs. 6, 12.) Such common orientation may be confined within a single plagioclase grain or may cross host-crystal boundaries, or a single plagioclase grain may enclose several differently oriented skeletal wagnerite growths. Some of the larger wagnerite grains enclose rows of rutile grains (fig. 5) or may surround other minerals that define the foliate fabric.

In contrast, prismatic sillimanite and corundum in coarse grains disrupt the foliate fabric of the wagnerite-bearing gneiss. Prismatic sillimanite typically cuts plagioclase, wagnerite, and fibrolitic sillimanite (figs. 13, 14). It cuts across the foliation and fails to parallel the lineation of the fibrolitic sillimanite. Corundum grains similarly interrupt the foliation. Small anhedral corundum grains, groups of small grains in optical continuity, skeletal crystals enclosing other minerals, and large subhedral to euhedral crystals of corundum seem to represent varying stages of crystallization. Characteristically, these

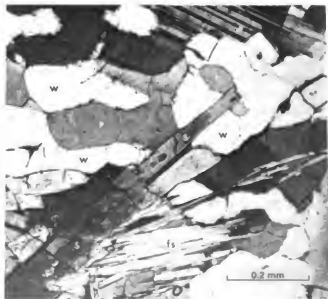


FIGURE 13.—Prismatic sillimanite (S) cuts wagnerite (W) and plagioclase (P). Other grains are fibrolitic sillimanite (fs). Crossed polars.

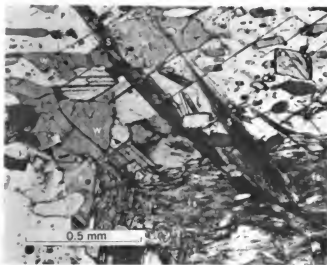


FIGURE 14.—Prismatic sillimanite (S) cuts wagnerite (W), plagioclase (P), and fibrolitic sillimanite (fs). Crossed polars.



FIGURE 15.—Corundum (C) contains numerous tiny needles of sillimanite that are oriented parallel to the alignment of fibrolitic sillimanite (fs) in sillimanite-plagioclase gneiss. A small grain of plagioclase (P) is partly enclosed by corundum. Plane-polarized light.

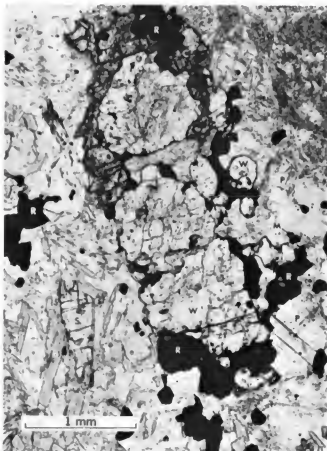


FIGURE 16.—Grain of wagnerite (W) at top center is partly surrounded by a border of corundum (C). Numerous grains of rutile (R) occur along the grain boundaries of wagnerite in this specimen. Other minerals are plagioclase (P), biotite (B), monazite (M), and prismatic sillimanite (S). Plane-polarized light.

corundum grains are developed in aggregates of fibrolitic sillimanite and contain remnants of sillimanite needles that still retain the linear orientation of the fibrolitic aggregates (fig. 15). Rarely, wagnerite is surrounded in part by a corundum border (fig. 16).

Apatite and wagnerite have several textural relationships. Locally, prisms of apatite are surrounded by wagnerite (fig. 10); some aggregates of apatite grains are surrounded by a border of elongate wagnerite grains; a considerable proportion of the wagnerite grains are partially or completely rimmed by apatite. (See figs. 5, 8, 9.) Rims of apatite occur not only on exterior surfaces of wagnerite but also between the wagnerite and its poikiloblastic inclusions. Apatite rims have been observed between wagnerite and the following minerals: plagioclase, fibrolitic sillimanite, biotite, monazite, rutile, muscovite, and chlorite. The rims, therefore, do not appear to be a simple reaction rim of the type that occurs only between a specific pair of minerals.

TABLE 5.—Chemical analyses of wagnerite
[Landsr. (...) indicate not determined]

	This report (Analyst, Laura Reichen)				Hegemann and Sauerbrey (1927)		Finko (1962)					
Locality	Santa Fe Mountain, Colo.				Werfen, Austria		Khabba, Buryat, U.S.S.R.					
Color	Pale yellow				Pale yellow		Pale yellow			Orange		
Composition	Theoretical (percent)	Determined (percent)	Recalculated ¹	Ratios	Determined ² (percent)	Ratios	Determined (percent)	Ratios	Determined (percent)	Recalculated ³	Ratios	
MgO	49.59	45.97	48.31	2.03	48.35	2.00	40.42	1.99	42.63	42.84	2.01	
FeO	1.64	1.72	1.72		0.95		9.90		4.88	8.67		
MnO	0.47	0.49	0.49		0.70		2.00		0.45	0.45		
Fe ₂ O ₃									4.17			
CaO		1.36		1.00		1.00		1.00			1.00	
P ₂ O ₅	43.65	41.84	42.89		43.45		41.60		41.56	41.56		
F	11.68	10.3	10.72		11.49		11.08		10.00	10.05		
Cl		0.46	0.48	0.96		0.99		0.99			0.96	
H ₂ O ⁺		0.00					tr.		0.65	0.65		
H ₂ O ⁻		0.00										
Al ₂ O ₃		1.05										
TiO ₂		0.44		O=4.06		O=4.00		O=4.00			O=4.08	
SiO ₂		1.84										
Subtotal	104.92	105.37	104.61		104.94		105.00		104.14	104.22		
Less F = O	4.92	4.35	4.51		4.84		4.65		4.19	4.22		
Less Cl = O		0.10	0.10									
Total	100.00	100.94	100.00		100.10		100.35		99.95	100.00		
Formula	Mg ₂ PO ₄ F				(Mg,Fe,Mn) _{2.03} PO ₄ Cl _{0.96}		(Mg,Fe,Mn) _{2.00} PO ₄ F _{0.99}		(Mg,Fe,Mn) _{2.01} PO ₄ (OH) _{0.96}			
					Mg:Fe:Mn=97:0:02:0:01		Mg:Fe:Mn=98:0:01:0:01		Mg:Fe:Mn=99:0:01:0:01			

¹Recalculated to 100 after deducting CaO as fluorapatite, Al₂O₃, TiO₂, and SiO₂.²Calculated to oxide values by the authors of this report from the original analysis.³Recalculated to 100 by the authors of this report after first converting Fe₂O₃ to FeO.⁴Determined by specific ion electrode method by Johnnie Gardner, U.S. Geological Survey.⁵And soluble SiO₂.

From the textural and mineralogical relations we make the following interpretations. The foliate fabric defined by wagnerite, plagioclase, fibrolitic sillimanite, and biotite apparently formed early during high-grade regional metamorphism. Except for prismatic sillimanite, corundum, some apatite, and minor chlorite and muscovite, the minerals of the sillimanite-plagioclase gneiss apparently crystallized at about the same time. Development of corundum and the large diversely oriented aggregates of prismatic sillimanite occurred later but probably during the same high-grade regional metamorphism. The larger grains of wagnerite may also belong to this later stage of crystallization. Chlorite and sericite probably formed still later under lower grade metamorphic conditions.

CHEMISTRY

Sample preparation for chemical analysis.—Because wagnerite occurs at the Santa Fe Mountain locality as a minor constituent of rutile-bearing gneiss, 1,000–1,500 g of the gneiss that showed the greatest visible concentra-

tions of wagnerite was used to prepare a sample large enough for chemical analysis. The sample of gneiss was broken into ¼-in. (6 mm) pieces, then it was ground to approximately 65 mesh (0.208 mm); the ground material was repeatedly washed with water and the fines decanted. After air drying, this material was sieved and the portion between 0.208 mm and 0.104 mm was retained; this fraction was then separated into light and heavy fractions, by use of bromoform (sp. gr., 2.86). The heavy fraction (> 2.86), which contained wagnerite, rutile, corundum, mica, sillimanite, and fluorapatite, was put through a Frantz isodynamic magnetic separator; splits were taken at 0.3 amps, 0.5 amps, and 1.3 amps. Wagnerite was concentrated in the 0.5 amp fraction. Compound grains (wagnerite-rutile, wagnerite-sillimanite, wagnerite-fluorapatite, and sillimanite-rutile) were removed by hand-picking under the binocular microscope. Four and one-half grams of visibly pure wagnerite were obtained for chemical analysis.

Methods of analysis.—The complete chemical analysis of wagnerite from Santa Fe Mountain, Colo., is given in table 5. The analytical methods used are as follows:

1. P_2O_5 . A portion of the sample was dissolved with nitric acid, and after a preliminary separation as ammonium phosphomolybdate, weighed as $Mg_3P_2O_7$.
2. F, Cl. Both fluorine and chlorine were determined on the combined filtrates from two successive sodium-carbonate fusions and water leaches of another fraction of the sample. Fluorine was weighed as CaF_2 (Groves, 1951) and chlorine as $AgCl$. Because of the apparent low fluorine value (9.03 percent) obtained by this method, another fluorine determination by the specific-ion-electrode method was made; this value (10.3 percent) is the one reported in table 5.
3. FeO. The wagnerite sample was not noticeably affected by boiling for 15 minutes with 1:8 sulfuric acid, the usual method of attack for the determination of FeO. However, the mineral was completely dissolved by heating for 24 hours at 65°C in 1:15 hydrochloric acid, to which a measured excess of standard potassium dichromate had been added to react with released ferrous iron.
4. H_2O . Total water was determined by the Penfield method.
5. MgO, CaO, Al_2O_3 , Fe_2O_3 , TiO_2 , MnO, and insoluble. Nitric acid was used to dissolve the sample for these determinations. Repeated evaporations to dryness with the acid were necessary to completely dissolve the wagnerite. After a small insoluble fraction had been removed, the filtrate was evaporated to dryness so that the interfering phosphorus could be separated by a double extraction with sodium-carbonate fusion and water leach. Conventional methods then were used for the determination of the cations (Peck, 1964).

Chemical analysis and formula.—The analysis, after correction for impurities (fluorapatite, sillimanite, rutile, and quartz), led to the formula $(Mg, Fe, Mn)_{2.08}PO_4$ (F, Cl)_{0.96}, with Mg:Fe:Mn=0.97:0.02:0.01, close to the empirical formula $Mg_2(PO_4)F$. The presence of sillimanite, rutile, and quartz as impurities in the analyzed sample was confirmed by X-ray powder patterns taken of the insoluble residue obtained from digestion of part of the sample in nitric acid. Fluorapatite as a contaminant in the analyzed sample was suspected, but its presence could not readily be verified inasmuch as it probably was dissolved during analytical procedures. However, energy-dispersive microprobe analyses of five polished grains of carefully selected, pale-yellow, transparent fragments of wagnerite were made by Robert B. Finkelman of the U.S. Geological Survey. The results given in table 6, showing an absence of Ca in the pure mineral, provide semiquantitative data that support the corrections made for impurities—including the subtraction of a fluorapatite phase—in recalculating the chemical analysis. (See table 5.)

TABLE 6.—Microprobe analysis of wagnerite from Santa Fe Mountain, Colorado (semiquantitative data) (Analysis, Robert B. Finkelman)

Constituents ¹	Weight percent (average of 5 grains)
MgO.....	≈50
FeO.....	2
MnO.....	≈1
P_2O_5	40

¹Si, Al, Ca, and Ti were below the limits of detection (≈0.5 percent). Fluorine could not be observed in this system.

The analysis of the Santa Fe Mountain wagnerite is compared in table 5 with other wagnerite analyses reported in the literature.

X-RAY CRYSTALLOGRAPHY

Single-crystal X-ray data.—Single-crystal X-ray study, made by the precession method, was carried out on a transparent, equant, pale-yellow fragment of wagnerite from Santa Fe Mountain, Colo. The precession photographs confirmed the monoclinic symmetry and space group $P2_1/a$ (for $c < a$) and yielded the following preliminary crystallographic data: $a = 11.94 \pm 0.01$ Å, $b = 12.68 \pm 0.01$ Å, $c = 9.65 \pm 0.01$ Å, $\beta = 108^\circ 10' \pm 20'$. The refined cell values, obtained by a least-squares refinement of the powder data (Appleman and Evans, 1973), are in excellent agreement with those reported by Coda, Guiseppe, and Tadini (1967) for wagnerite from Werfen, Austria (table 7). The specific gravity calculated for wagnerite from the refined cell data is 3.16, in good agreement with the measured value (3.13) obtained on a 500-mg sample by the pycnometer method.

Precession photographs of the Colorado wagnerite showed the presence of a strong monoclinic subcell with the b -axis halved (6.335 Å); this subcell is in space group $I2/a$, with $Z=8$, which data confirm the observations of Coda, Guiseppe, and Tadini (1967). The cell parameters of the subcell of the Colorado wagnerite are comparable with those reported in the literature for the triplite-group minerals—triplite, $(Mn, Fe, Mg, Ca)_2(PO_4)(F, OH)$ (Waldrop, 1969), and zwieselite, $(Fe, Mn, Mg, Ca)_2(PO_4)(F, OH)$ (C. T. Tennyson, in Strunz, 1970, p. 316).

X-ray powder data.—An X-ray powder diffraction pattern of the wagnerite from Santa Fe Mountain, Colo., was taken in a Debye-Scherrer powder camera fitted with a Wilson adapter (114.59 mm dia.) in Fe/Mn radiation ($\lambda FeK\alpha = 1.9373$ Å). Film measurements were corrected for expansion; the intensities of the observed lines were estimated visually by comparison with a calibrated intensity strip. Indexed X-ray powder-diffraction data for the Colorado wagnerite are cited in table 8 where they are compared with data for the calculated powder pattern of

wagnerite from Werfen, Austria (based on the structural data of Coda and others, 1967); also, with data for wagnerite from Bamle, Norway (Henriques, 1957); from Kyakhta, U.S.S.R. (Finko, 1962); and from Dolni Bory, western Moravia, Czechoslovakia (Staněk, 1965).

Identity of ferroan wagnerite with magniotriplite, triplite, and zwieselite are fluophosphates with the chemical formula $X_2(PO_4)_F$, where $X = Mg, Fe^{+2}, Mn^{+2}$, and (or) Ca . In wagnerite, ferroan wagnerite, and magniotriplite, Mg is the dominant cation, generally with lesser amounts of Fe^{+2} , Mn^{+2} , and Ca substituting in part for Mg ; the dominant cation in triplite is Mn^{+2} ; in zwieselite the dominant cation is Fe^{+2} . In these minerals, $(OH)^{-1}$ may substitute in part for F^{-1} . Strunz (1970) includes triplite, zwieselite, and wagnerite in the triplite series, a subgroup of the triplite-triploidite group. On the basis of recent crystallographic data (table 7), the minerals in the triplite series can be divided into two subgroups: (1), one containing magniotriplite, triplite, and zwieselite, with the b axis ≈ 6.5 Å and symmetry $I2/a$; (2), the other containing wagnerite, with the b axis ≈ 12.5 Å and symmetry $P2_1/a$. Comparison of the structures of wagnerite (Coda and others, 1967) and triplite (Waldrop, 1969) indicates that the minerals are not isotopic; Waldrop (1969) noted that triplite and zwieselite show identical reflection intensities and, on this basis, suggested that they are isotopic.

Ferroan wagnerite from Hällsjöberget (Hörsjöberget), Sweden (Henriques, 1957)—formerly talktriplite of Igelström (1882)—and from pegmatites of the Albères massif, eastern Pyrenees, France (Fontan and others, 1970), and magniotriplite from Turkestan ridge, U.S.S.R. (Ginzburg and others, 1951), were identified as such solely on the basis of X-ray powder photography and chemical analysis. As far as is known, magniotriplite and so-called "ferroan wagnerite" have never been characterized crystallographically. Because of their high magnesium content, ferroan wagnerite from both of the localities and magniotriplite (type material) were examined by X-ray powder diffraction and single-crystal techniques in order to establish their structural relation to wagnerite and (or) triplite.

X-ray powder diffraction patterns of wagnerite, ferroan wagnerite, magniotriplite, and triplite are compared in figure 17. It is interesting to note that the patterns of the two ferroan wagnerites and the magniotriplite are identical and show a closer resemblance in spacings to the pattern of wagnerite than to that of triplite. The powder pattern of wagnerite, however, is visually distinguishable from the powder patterns of ferroan wagnerite and magniotriplite by the presence of a line at 5.66 Å (table 8). This line also clearly showed up on films taken of wagnerite from Bamle, Norway (USNM C4151), Salzburg, Austria (USNM C4150), and Werfen, Austria (USNM

TABLE 7.—Crystallographic, compositional, and density data compared for wagnerite, ferroan wagnerite (= magniotriplite), magniotriplite, and triplite

	Wagnerite		Ferroan wagnerite (= magniotriplite)		Magniotriplite		Triplite	
	Present study ^a	Coda and others (1967)	This report ^b	This report ^c	This report ^d	This report ^e	Waldrop (1969)	
Unit cell data								
a (Å)	11.928 (7)	11.952 (8)	11.921	12.045	12.015	12.015	12.065 (1)	
b (Å)	12.620 (9)	12.679 (9)	6.381	6.422	6.415	6.415	6.534 (1)	
c (Å)	9.641 (5)	9.644 (7)	9.711	9.769	9.767	9.767	10.789 (1)	
d (Å)	0.943 (1.9-200)	0.931 (1.7-200)	1.876 (1.1-225)	1.876 (1.1-225)	1.876 (1.1-225)	1.876 (1.1-225)	1.809 (1.1-259)	
Cell volume (Å ³)	1,383.37	1,388.12	704.70	717.14	716.74	716.74	796.56	
Space group	$P2_1/a$ (PO ₄ F Cl) ₄₀	$P2_1/a$ (PO ₄ F Cl) ₄₀	$P2_1/a$ (OH) ₄₀	$P2_1/a$ (OH) ₄₀	$P2_1/a$ (OH) ₄₀	$P2_1/a$ (OH) ₄₀	$P2_1/a$ (OH) ₄₀	
Composition	$Mg, Fe, Mn, Ca, P, O, F, Cl$	$Mg, Fe, Mn, Ca, P, O, F, Cl$	$Mg, Fe, Mn, Ca, P, O, F, Cl$	$Mg, Fe, Mn, Ca, P, O, F, Cl$	$Mg, Fe, Mn, Ca, P, O, F, Cl$	$Mg, Fe, Mn, Ca, P, O, F, Cl$	$Mg, Fe, Mn, Ca, P, O, F, Cl$	
Z	16	16	8	8	8	8	8	
Density, d_m (g/cm ³)	3.16	3.15	3.47	3.55	3.57	3.57	3.62	
Density, d_c (g/cm ³)	3.16	3.15	3.47	3.55	3.57	3.57	3.62	
Chemical analysis	This report	Hegenmatt and Schumacher (1927)	Henriques (1957)	Fontan and others (1970)	Ginzburg and others (1951)	Wolfe and Henrich (1967), Henrich (1951)	Wolfe and Henrich (1967), Henrich (1951)	
Localities of mineral	Santa Fe Mountain, Colo.	Werfen, Austria	Hällsjöberget (Hörsjöberget), Sweden	Eastern Pyrenees, France	Turkestan ridge, U.S.S.R.	Mica hole, Ferroan County, Colo.	Mica hole, Ferroan County, Colo.	

^aWhen in parentheses are one standard deviation; data for 11.928 (7), real

11.928 (7) Å. Actual ratios and cell volumes calculated by authors of this report.

^bCell parameters obtained by refinement of powder data (table 6).

^cCell parameters obtained by measurement of precession films.

^dCalculated by authors of this report.

TABLE 8.—X-ray powder diffraction data for wagnerite, $Mg_3(PO_4)_2$

This report				Henniques (1957)				Finko (1962)				Šaňák (1965)			
Höllgraben, near Werfen, Austria				Santo Fe Mountain, Colorado				Bævre, Norway				Kyakhta, U.S.S.R.			
Calculated Pattern ¹				Calculated ²				Observed ³				Observed ⁴			
d_{hkl} (Å)	I	d_{hkl} (Å)	I	d_{hkl} (Å)	I	d_{hkl} (Å)	I	d_{hkl} (Å)	I	d_{hkl} (Å)	I	d_{hkl} (Å)	I	d_{hkl} (Å)	I
200	5.676	6	5.662	5.662	7	5.635	20	5.635	20	5.635	20	5.635	20	5.635	20
120	5.535	2	5.529	5.529	7	5.170	10	5.170	10	5.170	10	5.170	10	5.170	10
021	5.212	5	5.209	5.211	7	5.170	10	5.170	10	5.170	10	5.170	10	5.170	10
002	4.578	2	4.577	4.577	7	4.208	10	4.208	10	4.208	10	4.208	10	4.208	10
202	4.280	1	4.275	4.275	7	4.015	10	4.015	10	4.015	10	4.015	10	4.015	10
221	4.235	7	4.228	4.226	11	3.279	80	3.279	80	3.279	80	3.279	80	3.279	80
122	3.827	3	3.825	3.827	5	3.236	20	3.236	20	3.236	20	3.236	20	3.236	20
310	3.626	1	3.618	3.618	5	3.107	90	3.107	90	3.107	90	3.107	90	3.107	90
221	3.537	5	3.532	3.533	5	2.765	30	2.765	30	2.765	30	2.765	30	2.765	30
230	3.390	1	3.385	3.385	5	2.744	50	2.744	50	2.744	50	2.744	50	2.744	50
122	3.289	54	3.287	3.287	60	2.695	60	2.695	60	2.695	60	2.695	60	2.695	60
320	3.249	9	3.243	3.244	5	2.544	20	2.544	20	2.544	20	2.544	20	2.544	20
202	3.117	67	3.114	3.114	60	2.472	50	2.472	50	2.472	50	2.472	50	2.472	50
032	3.105	1	3.104	3.104	5	2.422	15	2.422	15	2.422	15	2.422	15	2.422	15
213	3.308	1	3.306	3.306	5	2.378	10	2.378	10	2.378	10	2.378	10	2.378	10
141	2.973	100	2.970	2.970	100	2.258	20	2.258	20	2.258	20	2.258	20	2.258	20
132	2.845	1	2.843	2.843	85	2.197	50	2.197	50	2.197	50	2.197	50	2.197	50
402	4.845	80	4.839	4.839	85	2.152	10	2.152	10	2.152	10	2.152	10	2.152	10
400	2.838	4	2.831	2.831	85	2.107	10	2.107	10	2.107	10	2.107	10	2.107	10
141	2.825	4	2.823	2.823	85	2.072	10	2.072	10	2.072	10	2.072	10	2.072	10
330	2.819	1	2.815	2.815	85	2.037	10	2.037	10	2.037	10	2.037	10	2.037	10
223	2.806	18	2.804	2.804	11	1.992	10	1.992	10	1.992	10	1.992	10	1.992	10
410	2.770	1	2.763	2.763	85	1.957	10	1.957	10	1.957	10	1.957	10	1.957	10
240	2.767	3	2.765	2.766	3	1.922	10	1.922	10	1.922	10	1.922	10	1.922	10
023	2.750	21	2.749	2.748	30	1.887	10	1.887	10	1.887	10	1.887	10	1.887	10
421	2.704	17	2.698	2.697	21	1.852	10	1.852	10	1.852	10	1.852	10	1.852	10
133	2.557	2	2.556	2.555	5	1.817	10	1.817	10	1.817	10	1.817	10	1.817	10
242	2.547	1	2.545	2.545	5	1.782	10	1.782	10	1.782	10	1.782	10	1.782	10
213	2.515	2	2.513	2.513	5	1.747	10	1.747	10	1.747	10	1.747	10	1.747	10
232	2.509	2	2.506	2.506	5	1.712	10	1.712	10	1.712	10	1.712	10	1.712	10
341	2.476	3	2.472	2.468	15	1.677	10	1.677	10	1.677	10	1.677	10	1.677	10
033	2.474	1	2.473	2.473	15	1.642	10	1.642	10	1.642	10	1.642	10	1.642	10
051	2.444	1	2.442	2.442	15	1.607	10	1.607	10	1.607	10	1.607	10	1.607	10
204	2.400	1	2.399	2.399	15	1.572	10	1.572	10	1.572	10	1.572	10	1.572	10
522	2.366	5	2.363	2.363	7	1.537	10	1.537	10	1.537	10	1.537	10	1.537	10
333	2.365	2	2.363	2.363	7	1.502	10	1.502	10	1.502	10	1.502	10	1.502	10
214	2.359	3	2.357	2.357	7	1.467	10	1.467	10	1.467	10	1.467	10	1.467	10
430	2.356	1	2.352	2.352	7	1.432	10	1.432	10	1.432	10	1.432	10	1.432	10
114	2.353	1	2.352	2.352	7	1.397	10	1.397	10	1.397	10	1.397	10	1.397	10
423	2.352	3	2.328	2.328	7	1.362	10	1.362	10	1.362	10	1.362	10	1.362	10
421	2.324	9	2.320	2.320	9	1.327	10	1.327	10	1.327	10	1.327	10	1.327	10
251	2.316	1	2.314	2.314	9	1.292	10	1.292	10	1.292	10	1.292	10	1.292	10
512	2.309	1	2.304	2.304	9	1.257	10	1.257	10	1.257	10	1.257	10	1.257	10
004	2.289	17	2.289	2.289	5	1.222	10	1.222	10	1.222	10	1.222	10	1.222	10
314	2.268	4	2.266	2.266	5	1.187	10	1.187	10	1.187	10	1.187	10	1.187	10
143	2.256	19	2.255	2.251	6	1.152	10	1.152	10	1.152	10	1.152	10	1.152	10
014	2.253	2	2.252	2.252	6	1.117	10	1.117	10	1.117	10	1.117	10	1.117	10
132	2.242	1	2.241	2.241	6	1.082	10	1.082	10	1.082	10	1.082	10	1.082	10
124	2.240	8	2.239	2.239	6	1.047	10	1.047	10	1.047	10	1.047	10	1.047	10
341	2.239	5	2.236	2.236	6	1.012	10	1.012	10	1.012	10	1.012	10	1.012	10
223	2.239	3	2.237	2.237	6	0.977	10	0.977	10	0.977	10	0.977	10	0.977	10
510	2.235	1	2.230	2.230	6	0.942	10	0.942	10	0.942	10	0.942	10	0.942	10
242	2.225	21	2.221	2.220	6	0.907	10	0.907	10	0.907	10	0.907	10	0.907	10
052	2.218	1	2.217	2.217	6	0.872	10	0.872	10	0.872	10	0.872	10	0.872	10
522	2.202	44	2.198	2.197	11	0.837	10	0.837	10	0.837	10	0.837	10	0.837	10
332	2.183	1	2.181	2.181	6	0.802	10	0.802	10	0.802	10	0.802	10	0.802	10
252	2.182	2	2.180	2.180	6	0.767	10	0.767	10	0.767	10	0.767	10	0.767	10
431	2.151	1	2.147	2.147	6	0.732	10	0.732	10	0.732	10	0.732	10	0.732	10
513	2.147	1	2.145	2.145	6	0.697	10	0.697	10	0.697	10	0.697	10	0.697	10
404	2.140	13	2.138	2.137	4	0.662	10	0.662	10	0.662	10	0.662	10	0.662	10

See footnotes at end of table, p. 19

TABLE 8.—X-ray powder diffraction data for wagnerite, $Mg_2(PO_4)F$ —Continued

This report			Henriques (1957)			Finko (1962)			Sando (1965)		
Hillgraben, near Werfen, Austria			Santa Fe Mountain, Colorado			Bamide, Norway			Kysakha, U.S.S.R.		
Calculated pattern ^a			Calculated ^b			Observed ^c			Observed ^d		
d _{hkl} (Å)	I		d _{hkl} (Å)	I		d _{hkl} (Å)	I		d _{hkl} (Å)	I	
520	2.137	1	2.133
545	2.121	6	2.119
742	2.117	15	2.114	2.114	7	2.111	20	2.113	30	2.12	20
114	2.090	2	2.089
134	2.083	1	2.083
124	2.009	1	2.009
602	1.9820	11	1.9771
261	1.9810	15	1.9793	1.9782	15	1.979	30	1.977	50
162	1.9341	4
160	2.077	14	2.076	2.076	13	2.071	30	2.09	70	2.08	40
143	2.073	11	2.076
061	2.059	26	2.058	2.058	7	2.057	30	1.995	70	2.06	40
352	2.055	1	2.053
334	2.024	1	2.022
204	1.9237	24	1.9226	1.9229	11	1.922	10	1.929	60
244	1.9136	9	1.915	10	1.905	60
214	1.9020	4
261	1.8932	5	1.894	10
621	1.8902	20	1.8856	1.8856	18	1.887	30	1.859	30	1.888	80
044	1.8558	6	1.8551	1.8552	4
360	1.8450	6	1.8430	1.8428	3	1.834	10
623	1.8172	7	1.8154	1.8128	5
362	1.8100	4
543	1.7954	11	1.7925	1.7918	11	1.794	20	1.805	20	1.795	30
344	1.7737	5	1.7719	1.7720	4	1.771	10
025	1.7593	9	1.7589	1.7585	11
263	1.7512	4
425	1.7504	6
522	1.7488	9
630	1.7374	19	1.7365	1.7368	5	1.739	10	1.757	40	1.747	20
541	1.7261	5
461	1.7255	21	1.7233	11	1.725	30	1.733	50	1.724	30
324	1.6712	25	1.6698	1.6701	11	1.670	30	1.684	50	1.670	50
244	1.6446	4	1.6436	1.6440	5
345	1.6288	7	1.6278	1.6275	11	1.632	20
461	1.6134	4
206	1.6055	5
080	1.5849	5
164	1.5844	4
263	1.5840	25	1.5829	1.585	20	1.594	60	1.585	60
602	1.5820	21	1.5790	1.5831	11	1.580	30	1.587	70
720	1.5712	11	1.5675	1.5673	4
406	1.5645	6	1.558
364	1.5577	28	1.5566	1.5565	18	1.558	20	1.567	70	1.558	60
225	1.5532	16	1.5524	1.5526	18	1.554	20	1.555	30
625	1.5409	20	1.5387	1.5388	7	1.541	10	1.538	50	1.541	20
280	1.5265	12	1.5253	1.5253	6	1.528	20	1.528	10
345	1.5064	8	1.5048	1.5054	2	1.507	10
802	1.4946	5
741	1.4917	4
282	1.4863	8	1.4852	1.4862	7	1.489	20	1.494	30	1.488	40
743	1.4741	7	1.4711	1.4717	7	1.474	20	1.474	80
526	1.4633	13	1.4620	1.4619	5	1.464	1.465	30
823	1.4376	11	1.4343	1.4341	4	1.448	<10
606	1.4268	8	1.4251	1.4253	5	1.426	10	1.425	20
265	1.4246	7
804	1.4226	4
800	1.4190	6
381	1.4171	14	1.4158	1.4157	7	1.417	20	1.421	40

See footnotes at end of table, p. 19.

TABLE 8.—X-ray powder diffraction data for wagnerite, $Mg_2(PO_4)F$ —Continued

This report				Henriques (1957)				Finko (1962)				Smith (1966)			
Höllgraben, near Werfen, Austria				Santa Fe Mountain, Colorado				Ramli, Norway				Krykha, western Moravia, Czechoslovakia			
Calculated Pattern ¹				Calculated ²				Observed ³				Observed ⁴			
d_{hkl}	d_{hkl} (Å)	I		d_{hkl} (Å)	d_{hkl} (Å)	I		d_{hkl} (Å)	I			d_{hkl} (Å)	I		
563	1.4116	4	
446	1.4029	9	
444	1.3987	12		1.3973	1.3982	5D	
482	1.3846	5	
065	1.3839	15		1.3854	1.3832	7		1.385	30	1.384	80	1.384	40		
465	1.3795	8	
463	1.3763	14		1.3749	1.3747	9		1.376	10	1.348	50	1.365	20		
722	1.3641	9		1.3615	1.3616	3	
842	1.3519	9		1.3489	1.3489	3	
661	1.3466	8		1.3445	1.3438	3	
345	1.3385	7		1.3376	1.3382	3	
762	1.3277	6		1.3253	1.3256	2	
425	1.3268	5		1.3256
426	1.3122	10		1.3104	1.3104	5		1.322	30
583	1.2816	8		1.2802	1.2801	4		1.284	80
265	1.2766	14		1.2759	1.2758	4	
665	1.2698	8	
147	1.2409	9	
7 10 1	1.2376	5	
7 10 2	1.2259	7		1.2251
366	1.2253	9		1.2243	1.2251	4		1.232	60
284	1.2232	5	
385	1.2167	4	
680	1.2150	13		1.2132	1.2144	6		1.220	70
941	1.2077	13		1.2049	1.2054	5		1.210	60
3 10 0	1.2022	6	

¹Calculated from the crystal structure data of Coda, Guiseppe, Tadino (1967) in space group $P2_1/a$, $a = 11.957$ Å, $b = 12.679$ Å, $c = 9.641$ Å, $\beta = 100^\circ 18'$. All possible calculated d_{hkl} values listed for $d \geq 2.000$ Å, for calculated intensities with $I \geq 1$; calculated d_{hkl} values for $d < 1.9999$ Å given only for those with $I \geq 1$. Calculated integrated intensity data normalized to a maximum of 100.

²Calculated from these unit-cell parameters obtained from least-squares refinements of the observed X-ray powder data with listed indexing by use of the computer program of Appleman and Evans (1973): $a = 11.926$ Å, $b = 12.671$ Å, $c = 9.641$ Å, $\beta = 100^\circ$.

³All possible calculated d_{hkl} values listed for $d \geq 2.000$ Å, calculated d_{hkl} values for $d < 1.9999$ Å listed only for those observed.

⁴Camera diameter, 114.59 mm. Mn-filtered Fe radiation ($\lambda FeK\alpha = 1.9373$ Å). Wilson-type pattern. Film shrinkage negligible. Intensities estimated visually by direct comparison with a calibrated standard film strip. D = diffuse.

⁵Guenier camera. $CoK\alpha$ radiation.

⁶Sample 112, pale yellow. Camera diameter, 57.3 mm. Unfiltered Fe radiation.

⁷Camera diameter, 114.6 mm. Mn-filtered Fe radiation ($\lambda FeK\alpha = 1.9373$ Å).

R5306), when taken in iron radiation, but it was not present in any of the patterns taken of triplite from 18 different localities. The line at 5.66 Å should be looked for in distinguishing patterns of wagnerite from those of the triplite series.

Preliminary crystallographic data for ferroan wagnerite and magniotriplite, based on precession photography, are given in table 7 where they are compared with data for wagnerite and triplite. Comparison of these data indicates that despite their high Mg content both the ferroan wagnerite from Hällsjöberget, Sweden, and the Albères massif, eastern Pyrenees, France, and the magniotriplite from the Turkestan ridge, U.S.S.R., are isostructural with triplite. Refined cell parameters and indexed powder data for both ferroan wagnerites and magniotriplite (Mrose, unpublished data) lead to the conclusion that the so-called "ferroan wagnerite" is actually magniotriplite, the Mg-dominant member of the triplite series, and that, therefore,

this material should not be referred to as ferroan wagnerite.

ORIGIN

The origin of the wagnerite at Santa Fe Mountain is linked inseparably with the origin of light-colored rutile-bearing Precambrian gneisses in the east-central Front Range. Although the genetic history of these rutile-bearing gneisses is admittedly debatable, we think that their field relations and their chemical and petrographic characteristics suggest very strongly that they were originally products of subaerial weathering (Marsh and Sheridan, 1976). According to this hypothesis, intense weathering of tuffs and flows of intermediate to basic composition occurred at several different times during the accumulation of a thick succession of volcanic and sedimentary rocks in Precambrian time. The resulting weathered products were bentonitic clays enriched in

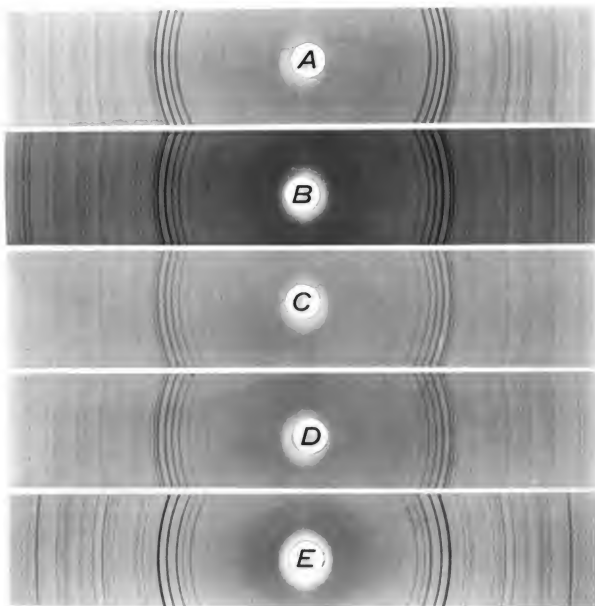


FIGURE 17.—X-ray powder photographs with Fe/Mn radiation (camera diameter: 114.59 mm): *A*) wagnerite, Santa Fe Mountain, Colo.; *B*) ferroan wagnerite (formerly talkriplite of Igelsurom, 1882), Hållsjöberget (Hörsjöberget), Sweden; *C*) ferroan wagnerite, Albères massif, eastern Pyrenees, France; *D*) magniotriplite, Turkestan ridge, U.S.S.R. (Fersman Mineralogical Museum, Moscow; type material); *E*) triplite, Chatham, Conn. (USNM 93792; analyzed material).

titania (leucoxene), alumina (clay), and silica (clay and quartz) as compared to the unweathered volcanic rocks. Surface waters partly reworked these clays, distributing them as thin layers and lenses of somewhat variable composition. Various amounts of sedimentary materials were added to the clays and interlayered with them. Fluorine of probable volcanic source was adsorbed by the weathered products in varying amounts in different localities. After accumulation of additional layers of

volcanic and sedimentary rocks, high-grade regional metamorphism took place throughout a long and complex period of Precambrian tectonism. Early in this period, the weathered products and their admixtures recrystallized to several varieties of rutile-bearing gneiss, some rich in sillimanite and quartz, some characterized by pale biotite and soda-rich plagioclase, and others gradational between these types. Wagnerite crystallized contemporaneously with fibrolitic sillimanite, biotite, and

plagioclase in a local variant of the rutile-bearing gneiss. Foliation and lineation were formed in all the metamorphosed rocks during this early stage of crystallization. Somewhat later, this same long period of regional metamorphism culminated in conditions that promoted the growth of coarse crystals of some of the minerals. A certain amount of redistribution of fluorine, a type of fluorine metasomatism, occurred within the rutile-bearing layers. Coarse crystallization was enhanced by these volatiles. In some areas, such as the area described initially by Sheridan, Taylor, and Marsh (1968), topaz crystallized during concurrent growth of prismatic sillimanite. At the Santa Fe Mountain locality, large crystals of corundum, aggregates of prismatic sillimanite, and the larger grains of wagnerite were formed. During this same stage of crystallization, rims of apatite developed on wagnerite. Sericite and chlorite formed in a lower grade metamorphic environment, either during a retrograde stage of waning metamorphic intensity or perhaps during an even later event.

The origin of the principal types of Precambrian metamorphic rock in the east-central Front Range is, of course, fundamental to the genetic history of the wagnerite locality. Biotite gneiss, commonly sillimanitic, is one of the principal rocks in this region and was considered by Ball (in Spurr and Garrey, 1908, p. 44) to represent metamorphosed shaly sediments. Subsequent investigators have agreed with this conclusion and have considered the sillimanitic varieties as representing alumina-rich shales and the nonsillimanitic varieties as representing sandy shales or graywackes. The origin of feldspar-rich gneiss, the other principal metamorphic rock in this region, has been more problematical. Given various names, such as quartz monzonite gneiss and microcline gneiss, the feldspar-rich gneiss has been considered as an old intrusive igneous rock (Lovering and Goddard, 1950, p. 23) and as a metasedimentary rock (Moench and others, 1962, p. 38; Sheridan and others, 1967, p. 23). Hedge (1969, p. 12, 120-123) considered the feldspar-rich gneiss to be metamorphosed felsic volcanic rock because the gneiss is similar in chemical composition to acid volcanic rocks found in island arc association with basalts. Hornblende gneiss and amphibolite, also abundant in parts of this region, very likely were originally intermediate to basic tuffs and flows, and calc-silicate gneiss and impure marble were sedimentary rocks ranging in character from calcareous shale to argillaceous limestone. The early Precambrian history in this region, therefore, probably involved an accumulation of a thick, layered succession composed predominantly of volcanic and sedimentary rocks.

Thin layers and lenses of light-colored rutile-bearing gneiss occur at several stratigraphic levels in the Precambrian terrane of the east-central Front Range. The

distribution, characteristics, and probable origin of these rutile-bearing gneisses have been discussed by Marsh and Sheridan (1976). Sillimanite-quartz gneiss, one of the principal varieties of rutile-bearing rock, has a simple but unusual mineral and chemical composition, containing very little else except quartz, sillimanite, and accessory rutile; it is chemically similar to many bentonitic clays. Rankama and Sahama (1950, p. 209, 563) have noted that clays produced by weathering are commonly low in calcium and high in aluminum and titanium. Serdyuchenko (1968) believed that metamorphic rocks containing kyanite, sillimanite, or corundum in many places in the world are metamorphosed kaolinite-bauxite-weathering crusts. Kyanite-quartz rock in India was considered by Dunn (1929, p. 248) to have been originally a surface decomposition of basalt to bauxitic clay. Espenshade and Potter (1960, p. 24-25) concluded that sediments containing clay or bauxite were the precursors of kyanite quartzite and sillimanite quartzite in some districts of the southeastern United States. Topaz is present in notable amounts in some of the rutile-bearing rocks in the east-central Front Range, emphasizing the local importance of fluorine. It is likely that volcanic emanations provided this fluorine to the original weathered materials. In support of this hypothesis is the observation of Rankama and Sahama (1950, p. 764) that fluorine is added to the "exogenic cycle by volcanic processes" and that fluorine is strongly adsorbed in soils, bentonite, and bottom muds.

Although the details of the very early history of the rutile-bearing gneisses in the Front Range are matters involving considerable speculation, the present characteristics of these gneisses are the result of high-grade regional metamorphism. The rutile-bearing gneisses occur as persistent stratum-like layers and lenses in a thick succession of gneisses whose mineralogy, textures, and structural features all give evidence of folding and metamorphic recrystallization under high temperature and pressure. The regional character of the metamorphism, rather than a "contact" phenomena, is indicated by the absence of adjacent bodies of igneous rock. The high grade of metamorphism is indicated by the abundance of sillimanite in the light-colored gneisses and by the common presence of the pair sillimanite-microcline in pelitic gneiss layers of this region.

The texture and mineralogy of the wagnerite-bearing sillimanite-plagioclase gneiss indicate that all the minerals, except sericite and chlorite, are products of the regional high-grade metamorphism. The appearance of the rock, with its coarse prismatic sillimanite and the large grains of corundum diversely oriented in a foliated matrix of finer minerals, is similar in many respects to the porphyroblastic textures observed in other gneisses of this region. For example, calc-silicate gneiss and impure

marble locally contain large porphyroblasts of garnet, epidote, and other minerals. Similarly, large randomly oriented porphyroblasts of andalusite occur in the mica schist unit of the nearby Ralston Buttes district (Sheridan and others, 1967, p. 8) 17 km northeast of the Santa Fe Mountain locality. We believe that such porphyroblasts developed in local sites where local pressure-temperature conditions and volatile concentrations favored the growth of coarse crystals late in the regional metamorphism.

Although bodies of pegmatite are present at the Santa Fe Mountain locality, they are not genetically related to the wagnerite. The pegmatites are of simple quartz-feldspar composition and contain no wagnerite.

The occurrence of wagnerite as a regional metamorphic mineral at Santa Fe Mountain is believed to be the direct result of the rather abnormal composition of the light-colored gneiss in which it is found. Apatite, not wagnerite, is the ubiquitous phosphate-bearing mineral in all the other gneisses. A calcium deficiency in the wagnerite-bearing gneiss is inferred from the high Na:Ca ratio of the plagioclase and the paucity of other calcium-bearing minerals. Although some apatite is present in the gneiss, calcium in the rock was apparently insufficient to accommodate all the available phosphate. The wagnerite further reflects the high Mg:Fe ratio, consistent with the pale biotite that is rich in Mg and deficient in Fe as compared with the biotite in most other gneisses of this region.

REFERENCES CITED

- Appleman, D. E., and Evans, H. T., Jr., 1975, Indexing and least-squares refinement of powder diffraction data: U.S. Dept. Commerce, Natl. Tech. Inf. Service PB2-1618, 67 p.
- Cherkasov, Yu. A., 1955a, Dispersiynnyy metod izmereniya pokazatelya prelomleniya [Dispersion method for measuring the index of refraction]: Sbornik Nauch.-Tekh. Inform., Min. Geol. Otkhrany Nedr., No. 1, p. 140-142 (in Russian).
- , 1955b, Novyy variant immersionnogo metoda [A new variant of the immersion method]: Issledovaniya mineral'noy syr'ya. Vses. Nauch.-issled.-ouatel'skiy Inst. Mineral'noy Syr'ya, p. 52-57 (in Russian).
- , 1957, O primeneniye "fokalnogo ekranirovaniya" pri izmereniyakh pokazatelya prelomleniya immersionnyim metodom [Application of "focal screening" to measurement of indices of refraction by the immersion method], in E. V. Rozhkova, ed., Sovremennyye metody mineralogicheskogo issledovaniya gornykh porod, rud i mineralov [Modern methods of mineralogical investigations of rocks, ores, and minerals]: Moscow, Gosudar. Nauchno-Tekh. Izd., Litera, Geol.-Okrane Nedr., p. 184-207 (English translation in Internat. Geology Rev., v. 2, 1960, p. 218-235).
- Coda, A., Guiseppe, G., and Tadini, C., 1967, The crystal structure of wagnerite: Acad. Naz. Lincei Atti, Cl. Sci. Fis., Mat. e Nat. Mem., v. 45, p. 212-224.
- Derr, W. A., Howie, R. A., and Zussman, J., 1962, Ortho- and ring silicates, v. 1 of Rock-forming minerals: New York, John Wiley and Sons, Inc., 333 p.
- Doelter, C., 1918, Wagnerit, Magnesium-Fluoro-orthophosphat, in Doelter, C., Handbuch der Mineralchemie: Dresden und Leipzig, Verlag von Theodor Steinkopff, v. 3, no. 1, p. 318-320.
- Dunn, J. A., 1929, The aluminous refractory minerals—kyanite, sillimanite, and corundum in northern India: Geol. Survey India Mem. 52, pt. 2, p. 145-274, and indexes.
- Espenshade, G. H., and Potter, D. B., 1960, Kyanite, sillimanite, and andalusite deposits of the southeastern States: U.S. Geol. Survey Prof. Paper 336, 121 p.
- Fahey, J. J., 1961, A method for determining the specific gravity of sand and ground rock or minerals: U.S. Geol. Survey Prof. Paper 424-C, p. C372-C373.
- Finko, V. I., 1962, Pervaya nakhodka wagnerita v SSSR [The first specimen of wagnerite from the U.S.S.R.]: Akad. Nauk SSSR Doklady, v. 145, no. 6, p. 1424-1427 (in Russian).
- Fontan, F., Berzati, P.-V., Lacomme, A., and Subra, A., 1970, Sur quelques phosphates des pegmatites du massif des Albères, Pyrénées-Orientales: Soc. Française Minéralogie et Cristallographie Bull., v. 95, p. 583-584.
- Gable, D. J., and Sims, P. K., 1969, Geology and regional metamorphism of some high-grade cordierite gneisses, Front Range, Colorado: Geol. Soc. America Spec. Paper 128, 87 p.
- Ginzburg, A. I., Kruglova, N. A., and Moleva, V. A., 1951, Magnio-triplit—novyy mineral iz gruppy triplita [Magniotriplite—a new mineral of the triplite group]: Akad. Nauk SSSR Doklady, v. 76, no. 1, p. 97-100 (in Russian).
- Groves, A. W., 1951, Silicate analysis [2d ed.]: London, Allen and Unwin, 336 p.
- Hedge, C. E., 1969, A petrogenetic and geochronologic study of migmatites and pegmatites in the central Front Range: Colorado School Mines unpub. Ph. D. thesis, 158 p.
- Hegemann, F., and Steinmetz, H., 1927, Die Mineralgänge von Werfen im Salzkammergut: Zentralblatt Mineralogie, Geologie und Paläontologie, Pt. A, p. 45-56.
- Heinrich, E. W., 1951, Mineralogy of triplite: Am. Mineralogist, v. 36, nos. 3-4, p. 256-271.
- Henriques, Åke, 1957, An iron-rich wagnerite, formerly named talk-triplite, Hållsjöberget (Horsjöberget), Sweden: Arkiv Mineralogi och Geologi, v. 2, no. 6, p. 149-153.
- Igelström, L. J., 1882, Nya mineral från Wermland, 2:o Talktriplit, ett nytt mineral från Horsjöberget i Wermland: Svenska Vetenskapsakademien, Stockholm, Handl. Öfv., v. 39, p. 86-91.
- Lovering, T. S., and Goddard, E. N., 1950, Geology and ore deposits of the Front Range, Colorado: U.S. Geol. Survey Prof. Paper 225, 319 p.
- Marsh, S. P., and Sheridan, D. M., 1976, Rutile in Precambrian sillimanite-quartz gneiss and related rocks, east-central Front Range, Colorado: U.S. Geol. Survey Prof. Paper 959-G.
- Michel-Lévy, A., and Lacroix, Alf., 1888, Les Minéraux des Roches: Paris, Libr. Polytech., 334 p.
- Moench, R. H., Harrison, J. E., and Sims, P. K., 1962, Precambrian folding in the Idaho Springs-Central City area, Front Range, Colorado: Geol. Soc. America Bull., v. 73, no. 1, p. 35-58.
- Peck, L. C., 1964, Systematic analysis of silicates: U.S. Geol. Survey Bull. 1170, 89 p.
- Rankama, K. K., and Sahama, T. G., 1950, Geochemistry: Chicago Univ. Press, 912 p.
- Serdychenko, D. P., 1968, Metamorphosed weathering crusts of the Precambrian, their metallogenic and petrographic features in Proceedings of section 4, Geology of Pre-Cambrian, Internat. Geol. Cong., Rept. 23d Sess., Czechoslovakia, 1968, v. 4, p. 37-42.
- Sheridan, D. M., Marsh, S. P., Mroos, M. F., and Taylor, R. B., 1971, Wagnerite from Santa Fe Mountain, Colorado: a new occurrence [abs.]: Canadian Mineralogist, v. 10, part 5, p. 919.
- Sheridan, D. M., Maxwell, C. H., and Albee, A. L., 1967, Geology and uranium deposits of the Ralston Buttes district, Jefferson County, Colorado, with sections on Paleozoic and younger sedimentary rocks by Richard Van Horn: U.S. Geol. Survey Prof. Paper 520, 121 p.

- Sheridan, D. M., Taylor, R. B., and Marsh, S. P., 1968, Rutile and isopar in Precambrian gneiss, Jefferson and Clear Creek Counties, Colorado: U.S. Geol. Survey Circ. 567, 7 p.
- Smith, J. R., 1960, Optical properties of low-temperature plagioclase, appendix 3, in Hess, H. H., Stillwater igneous complex, Montana: Geol. Soc. America Mem. 80, p. 191-219, incl. diagrams and tables, pl. 12.
- Spurr, J. E., and Garrey, G. H., 1908, Economic geology of the Georgetown quadrangle (together with the Empire district), Colorado, with general geology, by S. H. Ball: U.S. Geol. Survey Prof. Paper 63, 422 p.
- Staněk, Josef, 1965, První výskyt wagneritu v Československu [The first occurrence of wagnerite from Czechoslovakia]: Brno, Moravské Muzeum, Čas. Moravského Muzea v Brně, v. 50, p. 67-70 (in Slovak).
- Strunz, H., 1970, Mineralogische Tabellen: Akad. Verlagsgesellschaft Geos & Portig K.-G., Leipzig, 621 p.
- Waldrop, L., 1969, The crystal structure of triplite, $(\text{Mn,Fe})_2\text{FPO}_4$: Zeitschr. Kristallographie, v. 130, p. 1-14.
- Wilcox, R. E., 1959, Use of the spindle stage for determination of principal indices of refraction of crystal fragments: Am. Mineralogist, v. 44, nos. 11-12, p. 1272-1293.
- Winchell, A. N., and Winchell, Horace, 1951, Description of minerals, Pt. 2 of Elements of optical mineralogy—an introduction to microscopic petrography [4th ed.]: New York, John Wiley & Sons, 551 p.
- Wolfe, C. W., and Heinrich, E. W., 1947, Triplite crystals from Colorado: Am. Mineralogist, v. 32, nos. 9-10, p. 518-526.

QE
75
P910
+

1

Geology of the Minturn 15-Minute Quadrangle, Eagle and Summit Counties, Colorado

GEOLOGICAL SURVEY PROFESSIONAL PAPER 956

*Prepared in cooperation with the
Colorado Mining Industrial Development Board*



Geology of the Minturn 15-Minute Quadrangle, Eagle and Summit Counties, Colorado

By OGDEN TWETO and THOMAS S. LOVERING

GEOLOGICAL SURVEY PROFESSIONAL PAPER 956

*Prepared in cooperation with the
Colorado Mining Industrial Development Board*

*Geology of the region surrounding a
major zinc mining district and the
Vail recreational area, with emphasis on
the Minturn Formation of Pennsylvanian age*



UNITED STATES DEPARTMENT OF THE INTERIOR

CECIL D. ANDRUS, *Secretary*

GEOLOGICAL SURVEY

V. E. McKelvey, *Director*

Library of Congress catalog-card No. 77-600036

For sale by the Superintendent of Documents, U.S. Government Printing Office
Washington, D.C. 20402
Stock Number 024-001-02995-2

CONTENTS

	Page		Page
Abstract	1	Rock formations — Continued	
Introduction	3	Pennsylvanian and Permian Systems — Continued	
Geography	3	Minturn Formation — Continued	
History of investigation	3	Jacque Mountain Limestone Member	46
English and metric units	5	Changes in thickness and facies	47
Rock formations	6	Fossils, age, and correlations	48
Precambrian rocks	7	Origin	52
Biotite gneiss	8	Maroon Formation	53
Cross Creek Granite and related migmatite and		Stratigraphic relations	53
diorite	8	Thickness	54
Cross Creek Granite	8	Character	54
Migmatite	12	Fossils and age	55
Diorite	13	Origin	55
Inferred history	14	Triassic System	56
Age and correlation	14	Chinle Formation	56
Cambrian System	15	Jurassic System	57
Sawatch Quartzite	15	Entrada Sandstone	57
Peerless Formation	19	Morrison Formation	57
Ordovician System	21	Cretaceous System	58
Harding Sandstone	22	Dakota Sandstone	58
Devonian and Mississippian Systems	23	Upper Cretaceous and Tertiary igneous rocks	58
Chaffee Group	24	Pando Porphyry sill	58
Parting Formation	24	Dike rocks	61
Dyer Dolomite	27	Volcanic rocks	62
Gilman Sandstone	28	Physiography and upper Tertiary and Quaternary	
Leadville Limestone (or Dolomite)	30	unconsolidated deposits	63
Pre-Belden unconformity and Moles Formation	32	Tertiary and Pleistocene(?) colluvium	66
Pennsylvanian and Permian Systems	33	Pre-Bull Lake glaciations	65
Belden Formation	34	Bull Lake Glaciation	66
Minturn Formation	38	Eagle River and tributaries from Sawatch Range	66
Subdivision	39	Gore Creek drainage	67
Lithology	41	Piney River	67
Sedimentary features	43	Pinedale Glaciation	68
Type section	43	Landslide	68
Clastic unit A	43	Alluvium	69
Clastic unit B and the dolomite bed of Dows	43	Structure	69
Clastic unit C and the reef dolomite of Lionshead	43	Gore fault	71
Clastic unit D	44	Gore Range	74
Clastic unit E and Wearyman and Hornsilver	44	Sawatch Range	75
Dolomite Members	44	Central sedimentary belt	75
Robinson Limestone Member	44	Bedding faults in Gilman area	77
Clastic unit F	45	Economic geology	77
Elk Ridge Limestone Member	45	Type section	79
Clastic unit G	45	References cited	89
White Quail Limestone Member	45	Index	93
Clastic unit H	46		

ILLUSTRATIONS

	Page
PLATE 1. Geologic map and sections of the Minturn quadrangle	In pocket
FIGURE 1. Index map of west-central Colorado showing geographic setting of the Minturn quadrangle	4
2. English-metric conversion scales	5
3-7. Photographs:	
3. Canyon of the Eagle River at Belden and Gilman	7
4. Cross Creek Granite	10
5. Migmatite from the Gore Range	12
6. Gneissic diorite	13
7. Sawatch Quartzite in contact with Precambrian rocks	15
8. Index map of Gilman area and canyon of the Eagle River	18
9-12. Photographs:	
9. Thin-bedded dolomite of Dyer Dolomite	27
10. Belden Formation in roadcut on U.S. Highway 24	35
11. Channeled contact between Belden and Minturn Formations	35
12. Cliff exposures of lower part of the Minturn formation	39
13. Diagram showing subdivisions and general character of the Minturn Formation	40
14. Photographs of crossbedded gritty dolomite and conglomeratic dolomite in Minturn Formation in the Pando area	42
15. Photograph of dolomite reef in Minturn Formation at Lionhead	44
16. Photograph of Jacque Mountain Limestone Member of the Minturn Formation	46
17. Photomicrograph of biotitic oolitic limestone in Jacque Mountain Member of the Minturn Formation	47
18. Photograph of columnar structure in sill of Pando Porphyry	59
19. Photomicrograph of Pando Porphyry showing sericitic alteration	60
20. Photomicrograph of Pando Porphyry showing chloritic alteration	60
21. Photograph of glacial topography in Gore Range	63
22. Photograph of dip slopes on flank of Sawatch Range	63
23. Photograph showing typical topography in area of Minturn Formation	64
24. Map showing relation of Minturn quadrangle to major structural features and Colorado mineral belt	70
25. Geologic sketch map and section of Gore fault on south slope of Bald Mountain	72
26. Photograph of deformed strata in Gore fault zone at head of Spraddle Creek	73

TABLES

TABLE	Page
1. General stratigraphic section in the Minturn quadrangle	6
2. Chemical analyses, norms, and modes of Cross Creek Granite as compared with Boulder Creek Granite	11
3. Approximate modes of Cross Creek Granite as measured on stained polished slabs 6-10 square inches in size	12
4. Fossils in the Belden Formation	38
5. Fossil collection localities, Minturn Formation	49
6. Megafossils of the Robinson Limestone Member of the Minturn Formation	51
7. Fusulinds in the Robinson Limestone Member of the Minturn Formation	52
8. Fauna of the White Quail Member of the Minturn Formation	53

MEASURED SECTIONS

	Page
Section of the Sawatch Quartzite	16
Section of the Peerless Formation	20
Section of the Harding Sandstone	23
Section of the Parting Formation	25
Section of the Dyer Dolomite	27
Section of the Gilman Sandstone	29
Section of the Leadville Dolomite	31
Emended type section of the Belden Formation and section of the Molas Formation	35
Type section of the Minturn Formation	79

GEOLOGY OF THE MINTURN 15-MINUTE QUADRANGLE, EAGLE AND SUMMIT COUNTIES, COLORADO

By OGDEN TWETO and THOMAS S. LOVERING

ABSTRACT

The Minturn quadrangle is an area of about 230 square miles (600 square kilometres) in the mountains of central Colorado, 75 miles (120 kilometres) west of Denver. In its northeastern part it includes a segment of the high and extremely rugged Gore Range, and in its southwestern part it includes the northeastern flank of the Sawatch Range. These two ranges consist mainly of Precambrian rocks. A lower but mountainous area between them, which occupies a large part of the quadrangle, consists of sedimentary rocks, mainly of Pennsylvanian and Permian age.

Mining operations at Gilman, in the southern part of the quadrangle, were long the chief industry in the quadrangle. The Gilman district is credited with a production through 1972 of about \$328 million in zinc, silver, copper, lead, and gold. The ore deposits of this district are discussed in a separate report.¹ Since the early 1960's a skiing and recreational industry has burgeoned at Vail, in the middle part of the quadrangle, and has surpassed mining as an economic activity in the area.

The rocks exposed in the Minturn quadrangle are of six major categories: (1) Precambrian crystalline rocks, (2) a thin but economically significant sequence of pre-Pennsylvanian Paleozoic sedimentary rocks, (3) a thick sequence of Pennsylvanian and Permian sedimentary rocks, (4) a thin sequence of Mesozoic sedimentary rocks preserved in an area of only about a square mile (2.6 square kilometres) in the northwest corner of the quadrangle, (5) scattered Upper Cretaceous and Tertiary intrusive igneous and volcanic rocks, and (6) unconsolidated Quaternary surficial deposits, mainly of glacial origin.

The Precambrian X rocks exposed in the Gore and Sawatch Ranges consist mainly of migmatite and granitic rocks, but they also include biotite gneiss, diorite, and dike rocks, such as pegmatite and aplite. Biotite gneiss, the oldest rock, was widely converted to migmatite during early phases of granitic intrusion. Biotite-quartz diorite and minor hornblende diorite form many small bodies that were emplaced during and following migmatization and in advance of the main bodies of granitic rocks. The granitic rocks are formally defined here as the Cross Creek Granite. Extensive bodies of this granite in the Sawatch and Gore Ranges are inferred to be parts of a single large batholith. The Cross Creek Granite varies in composition from granodiorite to granite, but most of it is quartz monzonite that is near granodiorite in composition. The granite bodies are typically concordant with the enclosing gneisses and have gradational contacts with the gneisses. The Cross Creek is dated isotopically as about 1,700 million years in age.

The sequence of pre-Pennsylvanian Paleozoic rocks consists, from the base upward, of the Sawatch Quartzite, Peerless Formation,

Harding Sandstone, Chaffee Group, and Leadville Limestone (or Dolomite). These rocks are exposed only in small areas, principally along the canyon of the Eagle River and on the lower slopes of the Sawatch Range; some are exposed also in small fault slices along the Gore fault, a major fault along the southwestern side of the Gore Range. The Gore fault marks the western border of an ancient highland that was elevated repeatedly during Paleozoic time, especially late Paleozoic. Consequently, all the Paleozoic formations thin or pinch out toward the Gore Range.

The Sawatch Quartzite, of Late Cambrian age, rests with profound unconformity upon a planar surface cut over Precambrian rocks. The Sawatch consists almost entirely of medium-bedded medium-grained white or lightly tinted quartzite, but it contains local lenses of fine conglomerate at the base and scattered small lenses of brown-weathering dolomitic sandstones in its middle part. It is about 200 ft (60 m (metres)) thick near the Eagle River and about 100 ft (30 m) thick where preserved along the Gore fault.

The Peerless Formation, of Late Cambrian age, conformably overlies the Sawatch Quartzite and locally is in gradational contact with the Sawatch. The Peerless consists of dolomitic sandstone, sandy dolomite, dolomite, shaly dolomite, and dolomitic edgewise conglomerates. The rocks are locally glauconitic and ferruginous, and they are variously colored brown, maroon, green, and buff. The Peerless is 65–70 ft (20 m) thick near the Eagle River, and a maximum of 20 ft (6 m) of it is preserved near the Gore fault.

The Harding Sandstone, of Middle Ordovician age, lies with erosional unconformity upon the Peerless Formation. The unit consists of white quartzite, green sandstone and conglomerate, and gray and green shale. As exposed along the Eagle River, it ranges in thickness from 14 to 50 ft (4–15 m) and it may be as much as 80 ft (24 m) thick in some of the mine workings at Gilman. It is absent near the Gore fault.

As defined in this report, the Chaffee Group, of Late Devonian and Early Mississippian² age, consists from the base upward of the Parting Formation, Dyer Dolomite, and Gilman Sandstone. Near Gilman, the Parting Formation lies with erosional and slight angular unconformity upon the Harding Sandstone; in other areas it overlaps older sedimentary formations, and in places along the Gore fault it lies upon Precambrian rocks. The Parting consists mainly of coarse-grained tan to white quartzite and conglomerate; locally, green shale is also a prominent component. The Parting is typically about 45 ft (14 m) thick near the Eagle River, though it locally reaches 65 ft (20 m). A maximum of about 20 ft (6 m) is preserved near the Gore fault. The Dyer Dolomite lies conformably and with locally gradational contact upon the Parting Formation. The Dyer consists of thin-bedded gray and buff dolomite. It is 75–80 ft (23–24 m) thick near the Eagle River and is absent near the Gore fault. The Gilman

¹ The report on the ore deposits of the Gilman district, Eagle County, has been designated as Geological Survey Professional Paper 1017.

Sandstone, formerly classed as a member of the Leadville Limestone, lies with erosional unconformity upon the Dyer Dolomite and is overlain with erosional unconformity by the Leadville as here redefined. The Gilman consists of sandstone, dolomite, chert, and breccia in various proportions. It is typically about 20 ft (6 m) thick but ranges from 10 to 50 ft (3–15 m) in thickness. In the mineralized area near Gilman, the Gilman Sandstone has been considerably modified in composition and structure by solution and collapse.

The Leadville Limestone (or Dolomite) as here redefined consists of carbonate rocks of Mississippian age overlying the Gilman Sandstone and underlying either the regolithic Lower Pennsylvanian Molas Formation or the Middle Pennsylvanian Belden Formation. In most of Colorado, the Leadville is a limestone, but across the width of the Colorado mineral belt — a distance of as much as 40 mi (65 km) — it is entirely a dolomite. In the Minturn quadrangle, the boundary between the limestone and the dolomite facies is in the valley of Cross Creek, midway between Gilman and Minturn. Northwest of Cross Creek, the Leadville consists of light-gray-weathering foraminiferal limestone, and it is referred to as the Leadville Limestone. Southwest of Cross Creek, the Leadville consists of fine-grained dark-gray dolomite and various recrystallized dolomite facies, referred to as Leadville Dolomite. The fine-grained dark dolomite is concluded to have replaced original limestone during an early stage of Laramide orogeny in Late Cretaceous time, and various recrystallizations of this material occurred later. The top of the Leadville is a karst erosion surface marked by local pockets of regolithic silt referred to the Molas Formation. Because of the uneven karst surface, the thickness of the Leadville varies widely over the region. Along the Eagle River in the Minturn quadrangle, the Leadville is 110–140 ft (33–42 m) thick; it is absent at the Gore fault. The Leadville is the principal host rock of ore deposits in the Gilman district.

Regolithic silt of the Molas Formation is present only locally at the top of the Leadville and is generally only a few inches to a few feet thick. Where present, it is mapped with the Belden Formation. As seen in mine workings, material of the Molas fills solution channels and caves in the Leadville beneath the karst surface, though no layer of Molas may be evident at this surface.

The Leadville, or locally the Molas, is overlain by as much as 10,500 ft (3,220 m) of predominantly clastic rocks of Pennsylvanian and Permian age. These rocks are divided into three formations, the Belden Formation, about 200 ft (60 m) in maximum thickness, the overlying Minturn Formation, as much as 6,300 ft (1,920 m) thick, and the Maroon Formation, as much as 4,200 ft (1,280 m) thick.

The Belden Formation consists of interbedded black shale, limestone, and fine-grained sandstone. Fossils from the type section, near Gilman, indicate an early Middle Pennsylvanian (Atokan) age. An emended type section is presented. The Belden is about 200 ft (60 m) thick near the Eagle River, and it pinches out northeastward toward the Gore fault, probably by nondeposition.

The Minturn Formation, a type section of which is presented in this report, consists predominantly of grit, conglomerate, and sandstone in lenticular beds. These rocks are highly arkosic, micaceous, coarse grained, and poorly sorted. They are mainly gray or of various light pastel colors, but a zone 400–700 ft (120–210 m) above the base is dull red, and a zone several hundred feet thick at the top is bright red. The clastic rocks are inferred to be marine-margin piedmont deposits derived from a highland east of the Gore fault. Several beds of marine limestone are intercalated in the coarse clastic rocks, particularly in the upper half of the formation. The lower half contains a few thinner beds of dolomite and, at several horizons, scattered dolomite reefs. Seven of the most distinctive and persistent limestones or dolomites were designated as members of the Minturn in the Pando area, immediately south of the quadrangle (Tweto, 1949): the Wearyman, Hornsilver, Resolution, Robinson, Elk Ridge, White Quail, and Jacque Mountain Members. All are present

in the Minturn quadrangle, but only the last four are widespread. Fossils from the limestones indicate that the Minturn is Middle Pennsylvanian (Atokan and Des Moinesian) in age. The Minturn overlaps the eroded edges of all older formations and extends onto Precambrian rocks near the Gore fault. It is about 6,300 ft (1,920 m) thick near the Eagle River, but it thins abruptly by onlap against the old highland near the Gore fault; there, the Robinson Limestone Member, 4,200 ft (1,280 m) above the Belden in the area farther west, is almost in contact with the granite. Westward, the Minturn rocks become finer grained, and they intertongue with gypsum of the Eagle Valley Evaporite near the western boundary of the quadrangle. The Jacque Mountain Limestone Member marks the top of the Minturn Formation.

The Maroon Formation resembles the Minturn in lithology, but it is entirely red, and, in general, it is less coarse grained. It is about 4,200 ft (1,280 m) thick in the northwestern part of the quadrangle and thins eastward toward the Gore fault. The Maroon is unfossiliferous in the Minturn quadrangle, but, from stratigraphic relations and scant fossils found elsewhere, it is concluded to be Middle and Late Pennsylvanian and Early Permian in age.

In a small area on Red and White Mountain, in the northwestern part of the quadrangle, the Maroon is overlain by Mesozoic rocks comprising the Chinle Formation, Entrada Sandstone, Morrison Formation, and Dakota Sandstone. These units have a total thickness of about 535 ft (160 m).

The Upper Cretaceous and Tertiary igneous rocks of the quadrangle are (1) Pando Porphyry, of Late Cretaceous age, in a sill that intrudes the Belden Formation in the Gilman-Red Cliff area; (2) patches of basalt and tuff of Miocene age in the Piney River area, and (3) scattered dacitic dikes of probable middle Tertiary age in the Gore Range. The unconsolidated deposits consist of (1) a thick colluvium of Pliocene and Pleistocene(?) age in the Red and White Mountain-Piney River area, (2) glacial tills of pre-Bull Lake, Bull Lake, and Pinedale ages, (3) landslide deposits, and (4) stream alluvium and gravels of Pleistocene and Holocene age.

The Minturn quadrangle is divided structurally into three main units, corresponding to the parts in the Gore Range, the Sawatch Range, and the intervening area. The Gore Range is a large fault block of Precambrian rocks, only a part of which is included in the quadrangle. The Gore fault, the bounding fault on the southwestern side of this block, is a complex fault that has several strands. It originated in Precambrian time and underwent movements at many times from then to the late Tertiary. It is, in general, a vertical or steep normal fault. The Sawatch Range, only a small part of which lies within the quadrangle, is a huge anticline. The range consists largely of Precambrian rocks in the core of the anticline; a thin cover of Paleozoic sedimentary rocks, broken by a few small faults, forms dip slopes on the northeastern flank of the anticline, southwest of the Eagle River.

The area between the Gore and Sawatch Ranges is broadly synclinal and only moderately deformed. The principal folds are three north-northwest-trending synclines arranged echelon in a north-west-trending line. The southeastern — or Black Gore — syncline has a broad, gently dipping southwestern limb that is a part of the flank of the Sawatch anticline and a narrow northeastern limb that turns up steeply against the Gore fault. The middle — or Vail — syncline is a bowed, doubly plunging syncline that is prominently exposed on the sides of the valley of Gore Creek at Vail. The northwestern — or Red and White — syncline occupies most of the area between the mouth of Gore Creek and the Piney River. The southeastern nose of the syncline is blunt and forms an abrupt north-west-dipping monocline along the north side of Gore Creek from the Eagle River to Red Sandstone Creek. This monocline separates a southern area that is structurally a part of the flank of the Sawatch Range anticline from a northern area that is a part of a large struc-

tural basin that lies northwest of the quadrangle. All three of the synclines are accentuated in the subsurface because of the thinning of the Paleozoic formations toward the Gore Range.

The sedimentary rocks are broken by steep faults in places, but most of the faults have displacements of less than 100 ft (30 m). In the mine workings and canyon walls at Gilman, bedding faults are numerous, and steep faults are rare. The bedding faults, though inconspicuous, played an important role in ground preparation prior to mineralization at Gilman. Faults in the Precambrian rocks in this area are reactivated fractures associated with the Homestake shear zone, a broad northeast-trending Precambrian shear zone that lies mainly to the south of the quadrangle. Most of the faults terminate upward at the base of the Sawatch Quartzite.

INTRODUCTION

GEOGRAPHY

The Minturn quadrangle is an area of about 230 mi² (600 km²) in the mountains of central Colorado, 75 mi (120 km) west of Denver (fig. 1). In its northeastern part it includes a segment of the high and extremely rugged Gore Range, and in its southwestern part it includes the northeastern flank of the Sawatch Range. The Eagle River, which drains all but the northernmost part of the quadrangle, flows along the base of the Sawatch Range. A broad northwest-trending belt between the Eagle River and the high crestral ridge of the Gore Range is mountainous but generally lower than the high crests to the northeast and southwest.

Easy access to the area is provided by U.S. Highway 6 and I-70 which follow Gore Creek westward across the middle of the quadrangle. Access from the south is provided by U.S. Highway 24 and the Denver and Rio Grande Western Railroad, which follow the Eagle River northwestward. Until recent years, population of the quadrangle was centered in the three small towns of Red Cliff, Gilman, and Minturn, along the Eagle River. In the early 1960's, a fourth settlement, Vail, was established as a ski resort on Gore Creek near the mouth of Mill Creek (pl. 1).

Mining conducted in the Red Cliff-Gilman area was long the principal industry within the quadrangle. Red Cliff, the oldest settlement in the quadrangle, was established as a mining town in 1879. The center of mining operations later shifted to Gilman, which since 1918 has been a "company town" of the New Jersey Zinc Co. The mines at Gilman are a principal source of employment for the residents of Minturn also, but Minturn is, in addition, a railroad town that was established as a base for the extra locomotive equipment necessary to move trains over the Continental Divide at Tennessee Pass, 12 mi (19 km) south of Red Cliff.

About 85 percent of the quadrangle is in the White River and Arapahoe National Forests. The forest land supports a summertime sheep-grazing industry and a

small lumbering industry. It also supports a skiing and recreational industry which, though only recently established, has surpassed mining as a principal economic activity in the quadrangle. Superb mountain scenery, the virtual absence of habitations outside the valleys of the Eagle River and Gore Creek, and snow and slope conditions ideal for skiing make the area attractive for such activities.

The Gore Range, the predominating topographic feature, rises 5,000 ft (1,525 m) above the valley of Gore Creek at Vail to a crest-line more than 13,000 ft (4,000 m) in elevation. Below the steep and craggy rock slopes of this intensely glaciated range is a broad area of forested, rounded ridges that extends southwestward to the foot of the Sawatch Range. Many grassy slopes and ridges dot the forested area, which is characterized by dense growths of spruce and alpine fir on the north-facing slopes and by lodgepole pine, aspen, and scattered Douglas-fir on the south-facing slopes.

HISTORY OF INVESTIGATION

The earliest geologic investigations in the Minturn quadrangle were made by Peale (1874, 1876), who described the general stratigraphic sequence and structure along the Eagle River and mapped the area in rapid reconnaissance for the Colorado Atlas (Hayden, 1877). Peale's work provided the geologic framework for various reports on the mines of the Red Cliff-Gilman area (for example, Olcott, 1887; Guiterman, 1890; Means, 1915), although it was gradually supplemented by extrapolation of geologic information from the Leadville district, 20 mi (32 km) to the south, with which the Red Cliff-Gilman area has many parallels (Emmons, 1886; Emmons and others, 1927).

The first detailed geologic map of any part of the quadrangle was prepared by Crawford and Gibson (1925), who mapped the area along the canyon of the Eagle River from 1 mi north of Gilman to about 5 mi (8 km) south of Red Cliff and described the ore deposits. Results of private studies of the ore deposits and vicinity, begun as early as 1912 by the New Jersey Zinc Co., are summarized in reports by Borchardt (1931) and by Radabaugh, Merchant, and Brown (1968).

Geologic mapping of the Minturn quadrangle and study of the Gilman ore deposits in light of the regional geology was begun by us in 1940 for the U.S. Geological Survey in cooperation with the Colorado Metal Mining Fund, a predecessor of the present (1975) Colorado Mining Industrial Development Board. Study of the mineralized area occupied most of the first short field season, and mapping of the quadrangle on a close reconnaissance basis at a scale of 1:48,000 was largely accomplished in the field season of 1941, except for the

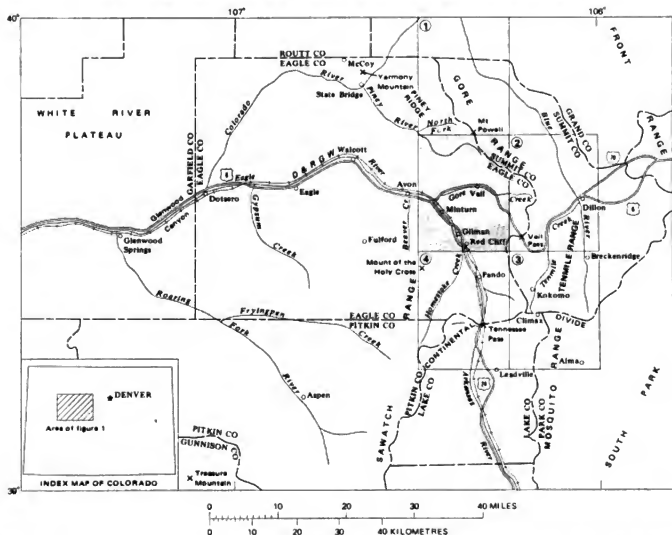


FIGURE 1.—Index map of west-central Colorado showing geographic setting of the Minturn quadrangle (patterned). Adjoining quadrangles are (1) Mount Powell, (2) Dillon, (3) Mount Lincoln, and (4) Holy Cross.

area of Precambrian rocks in the Gore Range. Most of the area in the Gore Range area was mapped during 3 weeks in 1942, and the project was then recessed, owing to wartime pressures for other work. A summary of results to that date (Lovering and Tweto, 1944) was accompanied by the geologic map of the quadrangle, which at that time contained many imperfections and was still blank in the extreme northeast corner. Following work in a few critical areas and in several mines by Tweto in 1946, a summary of the ore deposits was published in 1947 (Tweto and Lovering, 1947). Owing to other demands, the project remained dormant for several years after that date. The last essential stratigraphic and structural fieldwork was completed by Lovering during brief field seasons in 1960–63, and the glacial geology was studied intermittently through

the early 1960's by Tweto. Last improvements in the map of the area in the Gore Range were made in 1969 (Tweto and others, 1970).

With apologies for this long history of delay, we here report on the general geology of the Minturn quadrangle. A separate report (Lovering and others, 1977), deals with the ore deposits of the Gilman district and with the alteration history of the Leadville Limestone. In the many years since the work on the Minturn quadrangle started, studies of various aspects of the geology and of the ore deposits were made by others, and the science of geology made marked advances in concepts, capabilities, and techniques. In the sections that follow we present the results of our interrupted studies as integrated with the later studies of others, without attempting either to achieve balance in the scope of treat-

ment of the various topics or to pursue many topics to the extent that the state of the science nowadays permits. We acknowledge with thanks petrographic data supplied by Tom G. Lovering on our scattered samples of sedimentary and dike rocks from outside the mineralized area.

The geologic map accompanying this report will be found to be geometrically inaccurate in many places, owing to inaccuracies in the topographic base used in the original geologic mapping. Some of the more glaring inaccuracies in the base were latter corrected photogrammetrically, but much of the map remains as plotted on the original base, which was a preliminary version, at a scale of 1 : 48,000, of the 1934 edition of the Minturn 15-minute quadrangle topographic map.

ENGLISH AND METRIC UNITS

Thickness listed in the stratigraphic sections in this report are in feet, as are the contours on the topographic base and the elevations, derived from the contours, in the geologic cross sections. Scales for converting thickness measurements and elevations to metric units are shown in figure 2. Both English and metric values are indicated for other measurements except petrographic dimensions which, in accord with convention, are entirely metric. Conversion units are as follows:

English to metric

Inches (in.) multiplied by 2.54 = centimetres (cm);
Feet (ft) multiplied by 0.3048 = metres (m);
Miles (mi) multiplied by 1.609 = kilometres (km);
Square miles (mi²) multiplied by 2.6 = square kilometres (km²).

Metres to English

Millimetres (mm) multiplied by 0.039 = inches;
Centimetres (cm) multiplied by 0.394 = inches;
Metres (m) multiplied by 3.281 = feet;
Kilometres (km) multiplied by 0.621 = miles.

ROCK FORMATIONS

The rocks of the Minturn quadrangle are divided into many formations or map units (table 1), but on the basis of their occurrence and geologic connotations they fall into six main groups: (1) Precambrian crystalline rocks, (2) a thin sequence of pre-Pennsylvanian Paleozoic sedimentary rocks, (3) a thick sequence of Pennsylvanian and Permian sedimentary rocks, (4) a thin sequence of Mesozoic sedimentary rocks in a small area on Red and White Mountain, (5) scattered Upper Cretaceous and Tertiary intrusive and volcanic rocks, and (6) unconsolidated surficial deposits.

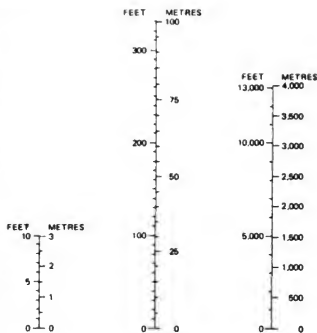


FIGURE 2.—English-metric conversion scales.

The Precambrian rocks, which are principally granite and migmatite, form the high part of the Gore Range in the northeastern part of the quadrangle, and except for a thin cover of sedimentary rocks, they also form the bulk of the flank of the Sawatch Range in the southwestern part of the quadrangle. They are completely covered by sedimentary rocks in the area between the two ranges.

The pre-Pennsylvanian Paleozoic rocks, mainly quartzites and dolomites, are exposed principally in the canyon of the Eagle River (fig. 3) and adjoining lower slopes of the Sawatch Range, although some of them are exposed also in thin fault slices along the Gore fault in the Gore Range. On the flank of the Sawatch Range these rocks form extensive smooth gentle slopes (fig. 22). These slopes are approximate dip slopes, but because they are slightly gentler than the dip, the various formations are in shingled arrangement, with younger units appearing successively downslope and northward. Although thin, aggregating only about 550 ft (168 m), the pre-Pennsylvanian rocks are of special interest as the principal host rocks of the ore deposits of the quadrangle.

The Pennsylvanian and Permian rocks, in contrast, are more than 10,000 ft (3,050 m) thick and are essentially devoid of known mineral deposits in this quadrangle. They occupy the entire area between the Eagle River and the Precambrian rocks of the Gore Range. In this area they form a northwest-trending en echelon

TABLE 1. — General stratigraphic section in the Minturn quadrangle

Age	Name	Thickness, feet (meters)	Character	
Holocene and late Pleistocene	Alluvium and landslide deposits	0-200? (0-90?)	Alluvium, terrace gravels, pond sediments, and landslide debris.	
Pleistocene	Glacial deposits	0-300? (0-90?)	Tills of Pinedale, Bull Lake, and pre-Bull Lake ages.	
Pleistocene(?) and Pliocene	Colluvium	0-75 (0-23)	Sandstone blocks and supergene chert in dirt matrix.	
Miocene	Volcanic rocks	0-200 (0-61)	Tuff and basalt.	
Miocene, Oligocene(?), and Late Cretaceous	Intrusive igneous rocks		Quartz latite, dacite, and quartz basalt porphyries, in sills and dikes.	
Early Cretaceous	Dakota Sandstone	150-160 (46-49)	Medium-bedded to massive light-gray sandstone; is dark gray, thin bedded, and shaly at top; locally conglomeratic at base.	
Late Jurassic	Morrison Formation	250 (76)	Interbedded light-gray sandstone, green, gray, and purple shale, and gray limestone.	
	Entrada Sandstone	60 (18)	Massive, cross-bedded buff to orange sandstone.	
Late Triassic	Chinle Formation	70 (21)	Red and purple siltstone, mudstone, and fine-grained sandstone; Gartsa Member, at base, is 10-26 ft (3-7.5 m) of coarse white sandstone and conglomerate.	
Early Permian, Late and Middle Pennsylvanian	Maroon Formation	1,700-4,200 (518-1,281)	Red sandstone, siltstone, grit, and conglomerate.	
Middle Pennsylvanian	Minturn Formation	2,100-6,300 (640-1,921)	Grit, conglomerate, sandstone, and shale in lenticular bodies, and some intercalated limestone and dolomite in persistent beds; predominantly gray but red in upper part and in an irregular zone near base. Some of the limestones are named members; see figure 13 for subdivisions.	
	Belden Formation	0-200 (0-61)	Dark gray to black shale, limestone, and minor sandstone, in thin beds.	
Early Pennsylvanian	Molas Formation	0-10 (0-3)	Gray, yellow, and brown regolithic silt and clay containing abundant chert fragments.	
Early Mississippian	Leadville Limestone (or Dolomite)	0-140 (0-43)	Dark-gray limestone or dolomite; massive in upper part; medium bedded and cherty in lower part. Dolomite is extensively recrystallized.	
Early Mississippian(?) and Late Devonian	Chaffee Group	Gilman Sandstone	0-50 (0-15)	Interbedded yellow-gray sandstone, sandy and cherty dolomite, and breccia.
Late Devonian		Dyer Dolomite	0-80 (0-24)	Thin-bedded gray dolomite.
		Parting Formation	0-65 (0-20)	Coarse-grained white to tan quartzite and conglomerate; subordinate interbedded green shale.
Middle Ordovician	Harding Sandstone	0-80? (0-24?)	White, gray, and green sandstone and quartzite, and green shale.	
Late Cambrian	Peerless Formation	0-70 (0-21)	Brown, red, green, and buff sandy dolomite, dolomitic sandstone, dolomite, and dolomitic shale; irregularly glauconitic and ferruginous.	
	Sawatch Quartzite	0-220 (0-67)	Medium- to thick-bedded, medium-grained white quartzite.	
Precambrian X	Cross Creek Granite		Coarse-grained, generally porphyritic gneissic to massive quartz monzonite or granodiorite.	
	Diorite		Mainly biotite-quartz diorite, gneissic to massive.	
	Gneisses		Mainly migmatite; some biotite gneiss.	



FIGURE 3.—Canyon of the Eagle River at Belden (in canyon bottom) and Gilman (at top of cliffs). Cliffs of stratified rock in middle part of canyon wall are Sawatch Quartzite, which lies on Precambrian rocks. Discontinuous cliffs higher on canyon wall are Chaffee Group and Leadville Dolomite. Vertical distance between Belden and Gilman is about 600 ft (200 m).

line of synclines. The sedimentary rocks terminate abruptly to the northeast at the Gore fault. This fault flanks the Gore Range and separates the sedimentary and crystalline rocks in the northeastern part of the quadrangle.

The Mesozoic sedimentary rocks are preserved only as a cap about 535 ft (163 m) thick on Red and White Mountain, near the northwest corner of the quadrangle.

The Upper Cretaceous and Tertiary igneous rocks occur only in scattered small bodies, the largest of which is a quartz latite porphyry sill intercalated in the basal Pennsylvanian rocks along the canyon of the Eagle River. The sill is of Late Cretaceous age. Tuff and basalt in small areas in the northwestern corner of the quadrangle are of Miocene age, and small dikes in the Gore Range are of probable middle Tertiary age.

The unconsolidated materials are principally glacial drift, which is widespread throughout most of the quadrangle. The high part of the Gore Range, however, was swept clean by the glaciers, and glacial drift is rare there.

PRECAMBRIAN ROCKS

The Precambrian rocks were mapped only in reconnaissance and were not studied in great detail. Hence, they are divided into only four units on the map (pl. 1), although many other units might be distinguished in more detailed studies. The oldest and least abundant of these units is biotite-quartz-plagioclase gneiss, referred to as biotite gneiss. This gneiss is similar to, and correlated with, the old gneiss of the Front Range and other areas of Precambrian rocks in Colorado, where it has been assigned names such as Idaho Springs Formation (Ball, 1906) or Black Canyon Schist (Hunter, 1925). Presumably, this old gneiss was once far more abundant in the Gore and Sawatch Ranges than it is now, but most of it was converted to migmatite or destroyed during the plutonic-metamorphic episode in which a granite here called the Cross Creek Granite was emplaced. Hence, far more migmatite than biotite gneiss is depicted on the map (pl. 1).

The migmatite and granite are accompanied in many places by a gneissic biotite diorite that seems to grade

into both rocks. The diorite is abundant in most areas where both granite and migmatite are present, but much of it is in small bodies that were not distinguished in mapping. Only the larger bodies of dioritic rocks are shown on the map, and in most of them the diorite is mixed with granite, migmatite, and pegmatite.

BIOTITE GNEISS

The predominating rock of the unit here called biotite gneiss is a dark- to medium-gray strongly foliated gneiss consisting of alternating layers that are rich, respectively, in biotite or in quartz and plagioclase. The grain size is variable, and in the facies in which the biotite is coarse and abundant, the rock is a schist. Some of the gneiss contains sillimanite either as scattered needles or as waxy white clots, and some contains small dull-red almandine garnets. In places the gneiss contains lenses or layers of calc-silicate rock or of quartzite a few inches to a few feet thick, and locally it contains a little hornblende gneiss or amphibolite. In general these other rock varieties are much less abundant in the biotite gneiss of the Minturn quadrangle than they are elsewhere in the Precambrian of Colorado.

The biotite gneiss consists of 20-40 percent quartz, 30-60 percent plagioclase (oligoclase/andesine, An_{30-35}), and 15-30 percent biotite. Sillimanite, garnet, cordierite, microcline, or hornblende may constitute as much as 10 percent of some varieties, and magnetite, apatite, and zircon are ubiquitous minor components. Microcline generally constitutes no more than a few percent of the rock, if present at all, except in varieties grading into migmatite, in which it may be a major component. In composition and general character the biotite gneiss is closely similar to that of the Front Range, described in detail by Sims and Gable (1964, p. C14-C19) and by Moench (1964, p. A11-A16).

Although only scattered bodies of biotite gneiss are shown on the geologic map (pl. 1), the gneiss is more abundant than indicated, as it occurs also in many small bodies within the migmatite and the granite. It is, however, much less abundant than in many other areas of comparable size in the Precambrian terranes of Colorado. Viewed regionally, this sparsity is a fairly local feature associated with the Cross Creek Granite and accompanying migmatite. The gneiss is much more abundant a few miles south of the quadrangle in the Sawatch Range, a few miles north of the quadrangle in the Gore Range, and a few miles east of the quadrangle in the Tenmile Range.

The biotite gneiss is the oldest rock recognized in the Minturn quadrangle, just as similar gneiss (together with associated gneisses not present in the quadrangle)

are the oldest rocks recognized in the Front Range and elsewhere in Colorado. Isotopic dating by the whole-rock rubidium-strontium method indicates that similar and presumably correlative gneisses of the Front Range and the Black Canyon of the Gunnison were formed by metamorphism 1.7 to 1.8 b.y. (billion years) ago (Hedge and others, 1967; Peterman and others, 1968; Hansen and Peterman, 1968). Age of the sedimentary rocks that were parent to the gneiss remains undetermined but, as suggested by isotopic data, probably does not exceed 2 b.y. (Z. E. Peterman, oral commun., 1970).

CROSS CREEK GRANITE AND RELATED MIGMATITE AND DIORITE

The Precambrian rocks of the Gore and Sawatch Ranges in the Minturn quadrangle are predominantly Cross Creek Granite, which is accompanied in most places by closely related diorite and migmatite. These three kinds of rocks are intimately mixed, grade into one another, and seem to be joint products of a major episode of granitic intrusion and attendant plutonic metamorphism. Because of the intermixing and intergrading, mapping of these rocks is a highly subjective process, and maps made by different workers, or even by the same worker at different times, are likely to differ appreciably.

CROSS CREEK GRANITE

The rock unit here designated the Cross Creek Granite¹ is an inhomogeneous batholithic unit ranging in composition from granodiorite to granite. The unit forms the northern end of the Sawatch Range, where it occupies an area of about 50 mi² (130 km²), and it takes its name from Cross Creek in its type area, where it is well exposed in clean and fresh glaciated outcrops. The unit also forms the bulk of the Gore Range, not only within the Minturn quadrangle but also in adjoining parts of the range in the Dillon quadrangle to the east and in the Mount Powell quadrangle to the north (Tweto and others, 1970). The granite bodies in the two ranges are so similar that they are inferred to be parts of a single large batholith. This inference is supported by magnetic data (Tweto and others, 1970, p. C33, pl. 1) which suggest that the granite is continuous in the subsurface between the Gore and Sawatch Ranges near the latitude of Gore Creek.

So far as is known, the Cross Creek Granite is restricted to the northwest side of a major Precambrian fracture zone called the Homestake shear zone (Tweto and Sims, 1963). This broad northeast-trending zone is

¹The term Cross Creek Granite was used in the 1964 preliminary report (Tweto and Tweto, 1964) but has not been formally introduced and published. In the interim "granite of Cross Creek" has been used (Pearson and others, 1966; Bergendahl, 1969; Tweto, 1970).

centered only a few miles south of the Minturn quadrangle in the Sawatch Range (Tweto, 1974) and some of its border fractures extend into the southwestern part of the Minturn quadrangle (fig. 24). In the Gore Range the shear zone is exposed only to the east of the Minturn quadrangle, south of the latitude of Gore and Black Gore Creeks. As the Homestake shear zone had a left-lateral horizontal displacement of at least several miles (Tweto and Sims, 1963, p. 1003-1004), the Cross Creek batholith is possibly displaced with respect to some unknown continuation to the south or southeast. More likely, however, the shear zone coincides with the edge of the batholith because border facies characterize the batholith along the shear zone. Thus, there may be no offset extension of the batholith southeast of the shear zone.

FIELD RELATIONS

The Cross Creek batholith is characterized by very abundant inclusions of partly granitized gneiss, or migmatite, and by complex relations with bordering wallrocks. The inclusions of gneiss range in size from small fragments only inches across to many square miles. In some areas, as on the west slope of the Gore Range just south of the northern boundary of the Minturn quadrangle, the rock of the batholith is essentially a breccia of gneiss fragments a few inches to several feet in diameter in a matrix of granite. More typically, however, the inclusions are remnants of layers of biotite gneiss or migmatite that have been distended or engulfed and have been partly assimilated by the granite. The gneiss bodies are generally but not everywhere elongate parallel to the foliation in the gneiss, and the primary foliation in the granite, though younger, is parallel to this same direction. Reaction between granite and gneiss was extensive, and hence the contacts between the two rocks are commonly vague or completely gradational. In border areas of the batholith, long tongues of gneiss showing these features project into the granite, and, conversely, irregular but basically concordant bodies of the granite project into the gneiss.

Along or near many contacts between granite and gneiss are lenticular bodies of diorite ranging from a few feet to a few thousand feet in length. The diorite grades both into granite and into biotite gneiss or migmatite, but some of it is at least slightly older than the granite, as it is cut by the granite. Moreover, gneissic diorite occurs as inclusions in the granite, and in some of these the foliation is discordant with that in the granite, although dimensionally the inclusions parallel the foliation in the granite. In many places, granite, diorite, and migmatite are so closely intermixed and are so gradational that only the predominating type could be mapped at the scale used.

Most areas of contact between Cross Creek Granite

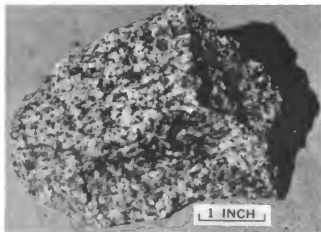
and migmatite or diorite are characterized by abundant pegmatite and aplite. The pegmatite is of several different ages, as some predates the diorite, some post-dates the diorite but predates the granite, some is a facies of the granite, some seems to have replaced granite, and some is in sharply defined dikes cutting the granite. In contrast, most aplite is in dikes that cut the granite, although some is in irregular bodies that grade into the granite and seems to be a textural facies of the same age as the granite.

CHARACTER

In its most typical facies, the Cross Creek Granite is a medium- to coarse-grained irregularly porphyritic gray to pinkish gray slightly to markedly foliated quartz monzonite. Departures from this norm are common, however. Appearance of the rock, and also the composition, varies with amount, color, and size of potassium feldspar (microcline) crystals, which are erratically distributed. In some of the rock the potassium feldspar is bright rose or salmon pink, and, if abundant, it gives the rock a pink cast, but in other parts of the rock the potassium feldspar is light gray to white and inconspicuous. Some parts of the rock contain only very little potassium feldspar, in inconspicuous small grains (fig. 4A), whereas other parts are characterized by abundant coarse grains or crystals of the feldspar (fig. 4B). In some places these crystals attain lengths of 2 in. (5 cm) and constitute as much as 50 percent of the rock. In places, the large potassium feldspar crystals are oriented so as to give a pronounced fluxion structure or grain to the rock, but in other places they have random orientation. If oriented, the feldspar crystals may or may not correspond in orientation to foliation and lineation defined by other minerals in the rock.

Degree of foliation and lineation likewise ranges widely. Most of the rock is gneissic in some degree, but some is essentially structureless. A complete sequence exists from structureless to strongly foliated, banded varieties that resemble, or grade into, coarse-grained biotite gneiss. Coarse banding or streakiness generally characterizes the foliated varieties. The banding may be compositional or textural or both. In some places it reflects only slight differences in biotite or feldspar content between layers or streaks, but in others it is due to streaks of diorite, or to lenses or layers of partly assimilated, or granitized, migmatite or biotite gneiss. In general, the granite is most strongly foliated in the vicinity of gneiss bodies and is only weakly foliated where uncontaminated by gneiss.

In lithology and mode of occurrence, the Cross Creek Granite closely resembles the Boulder Creek Granite of the Front Range (Lovering and Tweto, 1953, p. 8-16; Sims and Gable, 1967, p. E29-E35).



A



B

FIGURE 4.—Cross Creek Granite. A. Nonporphyritic granodiorite facies; B. porphyritic granodiorite facies.

PETROGRAPHY AND COMPOSITION

The predominant quartz monzonite facies of the Cross Creek Granite is composed of 35–50 percent oligoclase, 15–30 percent potassium feldspar, 20–30 percent quartz, 8–15 percent biotite, and minor amounts of accessory minerals. The oligoclase, quartz, and biotite are in fairly constant ratio to each other in the various facies of the rock, but the proportion of potassium feldspar to these other minerals ranges widely. With decrease in the potassium feldspar, the

rock grades toward granodiorite, and with increase it grades toward true granite.

Detailed study of the many different facies of the Cross Creek Granite has not been attempted. In table 2, results of chemical and modal analyses of a sample judged to be representative of the most common variety of the quartz monzonite are presented along with similar data for quartz monzonite typical of the Boulder Creek Granite (or Granodiorite). Approximate modes as determined from polished slabs stained to identify the potassium feldspar are given in table 3, illustrating the variability of the rock even in single samples.

The Cross Creek Granite typically has a hypautomorphic-granular and seriate porphyritic texture. In general, the potassium feldspar crystals are the largest in the rock, although locally aggregates of quartz are larger. Exclusive of the potassium feldspar crystals, the grains have a maximum diameter of about 8 mm, and an average of about 2 mm. Most thin sections exhibit a rude gneissic structure due to weak preferred orientation of biotite and to some segregation of biotite in bands. In the more gneissic varieties, quartz and plagioclase grains are also elongated and crudely oriented.

The potassium feldspar grains generally are in the form of prisms partly or wholly bounded by crystal faces. The crystals vary widely in size, and as brought out by staining, they may range in a given slab of rock from 2 mm to 5 cm in maximum dimension. Almost all the potassium feldspar shows the grid twinning of microcline, and many of the larger crystals can be seen in hand specimen to be Carlsbad twins. The microcline is slightly to markedly perthitic, having a content of albite lamellae that ranges from only a percent or two to as much as 25 percent.

In many localities the potassium feldspar crystals show clear evidence of being younger than the other constituents of the rock. In outcrop, this is shown by the gradation of granite with abundant pink feldspar crystals into small pegmatite dikes and, in places by the orientation of the feldspar crystals athwart the gneissic structure in the rock. In thin section, the microcline shows evidence of having replaced other minerals, particularly plagioclase and biotite, and it commonly contains inclusions of these and other minerals, including quartz, apatite, sphene, magnetite-ilmenite, and minor untwinned potassium feldspar. In some samples the plagioclase and biotite inclusions are altered, although the microcline is fresh. In some samples also, the inclusions show cataclastic effects, such as bent and fractured twinning lamellae in plagioclase or crumpled biotite leaves, even though the enclosing microcline is not deformed. Thus, the microcline crystals are more in

TABLE 2. — Chemical analyses, norms, and modes of Cross Creek Granite as compared with Boulder Creek Granite

¹Chemical analyses of Cross Creek Granite by M. Seesveld, U.S. Geological Survey. Data for Boulder Creek Granite from Sims and Gable (1967, p. E34). Leaders (...) indicate not detected.

	Cross Creek Granite ¹	Boulder Creek Granite ²
Chemical analyses (in weight percent)		
SiO ₂	69.46	64.37
Al ₂ O ₃	15.14	15.86
Fe ₂ O ₃	1.22	1.78
FeO	1.62	3.04
MgO88	1.69
CaO	2.02	2.37
Na ₂ O	3.24	3.09
K ₂ O	4.60	5.00
MnO04	.05
H ₂ O ⁺55	.52
H ₂ O ⁻04	.06
TiO ₂39	.72
P ₂ O ₅25	.32
CO ₂03	.23
Cl02	.03
F07	.12
S00	.14
BaO15	.23
SrO08	...
Subtotal	99.80	99.64
Loss O03	.13
Total	99.77	99.51
Bulk density	2.65	2.66
Powder density	2.69	2.73
Norms		
Quartz	29.10	19.44
Orthoclase	24.46	29.47
Albite	27.25	26.20
Anorthite	9.73	10.29
Hypersthene	2.92	6.34
Magnetite	1.86	2.55
Ilmenite76	1.37
Corundum	1.12	1.63
Apatite34	.66
Pyrite48
Fluorite07	.16
Calcite50
Modes (in volume percent)		
Quartz	27.1	18.3
Potassium feldspar	25.6	34.4
Plagioclase	36.6	32.9
Biotite	9.3	11.9
Muscovite	Trace	1.0
Magnetite- ilmenite	4	.6
Apatite2	.4
Zircon1	.2
Calcite3
Composition of plagioclase ... An ₂₈		
	An ₂₈	An ₂₇

¹ Perphyritic quartz monzonite, top of cliffs at knob outlined by 10,000-ft contour on north shoulder of Mount of the Holy Cross, Holy Cross (15-minute quadrangle 1) and (1.6 km) south of Mustang quadrangle line (See Tweto, 1974).

² Quartz monzonite, Mount Pugh, Central City quadrangle in Front Range, from Sims and Gable (1967, p. E34).

the nature of porphyroblasts than of phenocrysts, as they seem to have grown in the rock after the other constituents had crystallized, and after the stress environment that produced foliation among the other constituents had changed or had disappeared. It is not known at this time, however, whether all the microcline in all the Cross Creek Granite is paragenetically late like this or whether this is a feature only of the batholithic border areas, which happen to be the ones most studied.

The normal plagioclase of the Cross Creek Granite is oligoclase, which ranges in composition from An₂₂ to An₂₈ in different specimens. In some samples that contain late microcline, the oligoclase grains have narrow, sharply defined outer rims that are more sodic and generally less altered than the main grains. The plagioclase of the rims is mostly oligoclase with a composition of An₁₁ to An₁₈, but locally it is albite with a composition of An₈ to An₁₀. Locally, grain contacts between microcline and oligoclase are marked by patches of antiperthitic intergrowths of microcline in oligoclase.

Most quartz in the granite exhibits strong strain shadows and is somewhat fractured. Some quartz was evidently introduced with the microcline, however, as some grains of the strained and fractured quartz are surrounded by aggregates of finer grained, less deformed quartz. The fine-grained quartz also occurs in microscopic veinlets cutting early quartz and other minerals, including the late microcline.

Biotite of the granite is green brown where fresh, but in most localities it is altered and is green, or faded. It is accompanied by exsolved iron and titanium oxides.

Accessory minerals of the granite are magnetite, ilmenite, pyrite, apatite, sphene, and zircon. The pyrite is present only locally, and the apatite and sphene are irregularly distributed, being relatively abundant in some thin sections and absent in others. Muscovite is present in small amounts in most thin sections, occurring both as an alteration product of biotite and in association with late quartz veinlets.

All samples of the Cross Creek Granite studied show cataclastic effects in some degree, and some samples show at least two generations of cataclasis, one that preceded introduction of the large microcline crystals and one or more that followed. Evidence of the early cataclasis is shown by deformed inclusions of plagioclase, biotite, and apatite in undeformed microcline and by replacement relations of microcline against granulated aggregates of other minerals. Younger cataclasis is shown by mortar structure along the edges of the microcline crystals and, where deformation was severe, by jagged fracture zones zigzagging back and forth along cleavages in the microcline. Most of the alteration observed in inclusions in microcline

seems to be associated with such fractures; hence it is interpreted to be younger than the microcline rather than older.

MIGMATITE

The migmatite map unit includes several varieties of rocks intermediate between granite or diorite and biotite gneiss. One common variety is of the classical type, consisting of alternating thin layers of dark biotite-rich gneiss and light-colored granitic or pegmatitic material (fig. 5). The layers in this rock are generally less than 1 in. (2.5 cm.) thick, but the granite or pegmatitic layers swell in places into knots or lenses several inches to a few feet thick. The gneiss layers are similar compositionally to biotite gneiss, consisting essentially of biotite, quartz, and plagioclase but locally containing microcline, sillimanite, or garnet. In some places, as in the outcrops near the mouth of Homestake Creek at the south edge of the quadrangle, milky blue cordierite is a prominent constituent of the gneissic layers. The granitic layers consist essentially of quartz, microcline, and plagioclase but generally contain prominent muscovite, also. They are typically richer in quartz and iron oxides than most granite. Banded migmatite occurs principally in the area west of the Eagle River between the mouth of Homestake Creek and Fall Creek and in the higher parts of the Gore Range.

Another variety of migmatite consists of biotite gneiss which has been partly granitized by introduction of feldspars in grains or crystals 0.2–0.8 in. (0.5–2 cm.) long, forming a prominently speckled rock that superficially resembles a coarse granite but which consists in large part of biotite gneiss. The introduced, or newly crystallized, feldspars in such rock are generally complex perthitic and myrmekitic intergrowths of different feldspars and quartz. Migmatite of this type occurs in many small bodies in both the Sawatch and Gore Ranges, either bordering granitic rock or isolated from it.

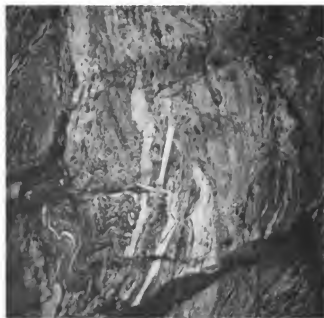


FIGURE 5.—Migmatite in the Gore Range, showing typical mixture of biotite gneiss (dark) and granitic materials (light), and streaking and crenulation resulting from rock flowage.

Another variety of migmatite is intimately associated with, and grades into diorite. It consists of layers, laminae, and wisps of biotite gneiss separated by thin layers of diorite or embedded in larger bodies of diorite. Relations observed at the outcrop in many places suggest that the diorite in such occurrences formed in part by reaction with biotite gneiss (fig. 6) and that the migmatite of this occurrence is a mixture of modified gneiss with the diorite. Migmatite of this kind and associated diorite characterize the border of the Cross Creek batholith along Cross Creek at the quadrangle boundary and immediately southward, and it is also widespread along the border zones of banded migmatite bodies in the Gore Range.

TABLE 3.— Approximate modes of Cross Creek Granite as measured on stained polished slabs 6–10 square inches in size

[Determined by R. C. Pearson, U.S. Geological Survey]

Sample	1			2				3		
	A	B	C	A	B	C	D	A	B	C
Quartz	30.2	26.3	29.4	29.7	25.6	25.8	30.0	29.6	23.9	26.1
Potassium feldspar	19.4	26.8	24.4	14.3	24.6	15.5	15.9	27.9	25.9	27.8
Plagioclase	39.1	37.7	36.4	41.0	37.3	42.6	40.6	34.0	38.2	36.6
Biotite	9.8	8.8	8.8	14.3	11.8	15.1	12.5	7.4	11.3	9.2
Accessory minerals	1.5	.4	1.0	.7	.7	1.0	1.0	1.1	.7	.3
Totals	100.0	100.0	100.0	100.0	100.0	100.0	100.0	100.0	100.0	100.0

SAMPLE DESCRIPTIONS AND LOCALITIES

1. Porphyritic quartz monzonite, cliffs on east side of canyon of the Eagle River at Gilman.
2. Porphyritic quartz monzonite, between 8,450- and 8,500-ft. contours in bottom of valley of Cross Creek, on southeast side of creek.
2. Porphyritic quartz monzonite, railroad cut on east side of canyon of the Eagle River, 2,100 ft. (700 m.) north of mouth of Rock Creek.

Still another variety of material mapped as migmatite is coarsely interlayered igneous rock, such as granite, quartz monzonite, granodiorite, or diorite, and biotite gneiss or banded migmatite. In such material, comparatively pure and presumably intrusive igneous rock in generally concordant layers a few inches to many feet thick alternates with biotite gneiss or banded migmatite in layers of similar thickness. Material of this kind is widespread in the Gore Range. Where the gneiss fraction predominates, it was mapped as migmatite, and where the igneous fraction predominates, it was mapped as granite or diorite. Thus, much of the rock mapped as Cross Creek Granite in this range differs only in degree from the migmatite unit.

Finally, breccias of gneiss fragments in a granite matrix in the Gore Range were mapped as migmatite where the fragments predominate, and as granite where the matrix predominates.

DIORITE

Several varieties of diorite occur in close association with the Cross Creek Granite, but they have not been studied in detail. Most of the varieties are older than the Cross Creek, as they are cut by the granite or by pegmatites related to it, or occur as inclusions in the granite, or have been partly granitized by the granite. Some varieties seem to have crystallized at the same time as the granite, however, and at least one variety is younger than the granite. As a group, the diorites are thought to be closely related to the Cross Creek batholith in age and origin. The diorites occur in countless small bodies as well as in the scattered larger ones indicated on the map (pl. 1). Most of these bodies are concordant, paralleling the foliation in bordering gneiss or granite, but crosscutting bodies of diorite are also found. Many diorite bodies are laced by dikes of diorite pegmatite consisting of andesine, quartz, and biotite.

The most abundant variety of diorite is dark gray, medium-grained, slightly gneissic, biotite-quartz diorite. Locally, this rock contains minor hornblende. Biotite-quartz diorite is closely associated with migmatite, especially near granite contacts, and as noted above, part of it formed by recrystallization of biotite gneiss (fig. 6). The bulk of the diorite, however, is believed to be magmatic and intrusive in origin. The diorite typically consists of 30–45 percent plagioclase, which is andesine, An_{32-44} , 20–33 percent biotite, 15–30 percent quartz, and 2–5 percent magnetite-ilmenite and other accessory minerals. Where partly granitized, the diorite contains a few percent of potassium feldspar, and more quartz, less biotite, and a slightly more sodic plagioclase than the normal rock. Where the adjoining rocks include amphibolite, the diorite generally contains hornblende, and where they include



FIGURE 6.—Gneissic diorite showing structure inherited from original migmatite. It occurs in upper Piney River area, Gore Range.

calc-silicate rock, it contains as much as several percent of epidote. Where cut by granite pegmatites, the diorite is commonly recrystallized to a form rich in coarse biotite.

Various gneissic diorites and diorite gneisses are similar in composition and occurrence to the diorite just described. They are believed to be fundamentally the same rock but were subjected to a magmatic or tectonic movement environment that induced a gneissic structure.

Hornblende and hornblende-biotite diorites occur principally in dikes or small pluglike bodies, although some are of the same occurrence as the biotite-quartz diorites just described. Most of the hornblende diorites thus appear to be younger than the biotite-quartz diorites, but only rarely are they seen to cut Cross Creek Granite. Most of the hornblende diorites lack foliation, though a few are markedly gneissic. The

plagioclase of the hornblende diorites is as calcic as labradorite (An_{55}), and quartz is only a minor constituent or is absent.

On the whole, the suite of diorites accompanying the Cross Creek Granite is similar to—although more abundant than—the suite accompanying the Boulder Creek Granite of the Front Range (Lovering and Tweto, 1953; Harrison and Wells, 1959; Sims and Gable, 1967).

INFERRED HISTORY

From field relations and petrography, development of the Cross Creek Granite batholith is inferred to have begun with the intrusion of small bodies of diorite and the migmatization of preexisting biotite gneiss in advance of the rising batholith of granitic rocks. The early diorite reacted extensively with the biotite gneiss, transforming some of the gneiss into diorite and diorite migmatite. Concurrently, other biotite gneiss was migmatized and was riddled by early pegmatites in advance of the main batholith. The batholith was emplaced as magma of a composition ranging from granodiorite to calcic quartz monzonite. Emplacement occurred under conditions that promoted extensive reaction between magma and wallrocks, causing extensive assimilation and granitization of gneiss as well as the formation of granite-gneiss mixtures, here classed as migmatite, along with the earlier or banded migmatite. The biotite gneiss and migmatite wallrocks were plastic in this environment, and they were deformed by and along with the granite of the invading and moving batholith, resulting in parallel foliations and generally concordant contacts. Minor diorite and abundant pegmatite developed within the batholith and its border zones, both during and following batholith emplacement.

Movement of the batholith, or parts of it, continued as crystallization proceeded, resulting in local deformation of early minerals. Finally, potassium essential to the formation of microcline, and accompanying sodium and silicon were introduced into the essentially consolidated rocks from deeper levels in the batholith. Microcline crystals of porphyroblastic habit, sodic rims of oligoclase, and late quartz veinlets and rims formed as a result, transforming much of the primary granodiorite and calcic quartz monzonite to a more alkalic quartz monzonite or, locally, to true granite.

Petrographic relations would allow an interpretation that the microcline is a product of some geologic event later than the emplacement and crystallization of the Cross Creek batholith and that the rocks of the batholith were deformed and even altered in the interim. Field relations and isotopic dating indicate, however, that the microcline is related to the crystallization history of the batholith and that the present microcline-bearing rock is a product of a single

continuous process rather than of two processes separated by a geologically appreciable time interval. The microcline is restricted to the granitic rocks of the batholith or to metasedimentary rocks immediately bordering granite, and hence it is most likely related to the batholith in origin. If it were related to some other geologic event, such as the intrusion of a younger granite at depth, then it would not be likely to be so exactly coincident in occurrence with the batholith but would extend either less or more widely. Similarly, if the microcline were significantly younger than the rest of the rock, then microcline-bearing facies should yield younger isotopic ages than other facies, but as discussed in the following section, the greatest ages obtained thus far are on the porphyritic, microcline-bearing facies.

AGE AND CORRELATION

As indicated previously, the Cross Creek Granite resembles the Boulder Creek Granite (or Granodiorite) of the Front Range both in composition and occurrence. Both granite units range in composition from granodiorite to true granite, are characteristically gneissic, are generally concordant and syntectonic, have gradational contacts resulting from reaction with their gneissic wallrocks, and are accompanied by diorites that range in age from pregranite to postgranite. These characteristics are those of the oldest (Precambrian X) of three general age groups of granites recognized in Colorado (Tweto, 1964; Hutchinson and Hedge, 1967). The Cross Creek Granite is accordingly classed on geologic grounds as a member of the old group and as an approximate—if not exact—correlative of the Boulder Creek Granite.

Isotopic dating corroborates the geologic correlation. Age of the Boulder Creek Granite is established as 1.70 b.y. (Petersman and others, 1968) or 1.71 b.y. (Hutchinson and Hedge, 1967). Age of the Cross Creek Granite, on the basis of a recently determined six-point rubidium-strontium isochron, is firmly established as 1.71 b.y. (C. E. Hedge, written commun., 1974). The samples used to establish this isochron came from the Cross Creek and Grouse Creek drainages just west of the Minturn quadrangle. Some samples from Cross Creek valley within the Minturn quadrangle and from the Gore Range in the Dillon quadrangle, analyzed earlier by Hedge (written commun., 1968) also yielded ages of about 1.7 b.y. Other samples, however, gave younger ages, as did samples dated by the potassium-argon method (Pearson and others, 1966, p. 1115). The younger ages probably reflect heating and consequent migration of elements in local areas during the second episode of granitic intrusion in Colorado, 1.35–1.45 b.y. ago. Granites of this age, which include the Silver

Plume Granite of the Front Range, the St. Kevin Granite of the Sawatch Range, and many others, have not been observed in the Minturn quadrangle but occur as podiform dikes in Cross Creek Granite just east of the quadrangle, south of Gore Creek.

CAMBRIAN SYSTEM

Rocks of Cambrian age in the Minturn quadrangle and surrounding region are assigned to two formations, the Sawatch Quartzite and the Peerless Formation, both of Late Cambrian age. The Sawatch Quartzite rests with profound unconformity upon a virtually planar surface cut over Precambrian rocks of various kinds. The contact between the quartzite and the predominantly dolomitic rocks of the Peerless Formation is gradational in most places but locally is sharply defined. Both units were included in the Sawatch Quartzite as originally defined by Eldridge (1894) in the Crested Butte area, on the western side of the Sawatch Range. In the Leadville area, where these strata were earlier known as "Lower Quartzite" or "Cambrian quartzite," the part nowadays comprising the Peerless was commonly distinguished as "transition shale" or "Red-cast beds" (Emmons, 1886, p. 58-60). These informal terms were supplanted in 1932 when Behre (1932) assigned the reddish dolomitic strata to the Peerless Shale Member of the Sawatch Quartzite. Because the term "shale" is a misnomer as applied to the Peerless in most places and because the unit is readily mappable over a wide area, it has been classed as the Peerless Formation since 1947 (Singewald, 1947).

SAWATCH QUARTZITE

The Sawatch Quartzite consists of about 200 ft (60 m) of nearly uniform medium- to thick-bedded light-colored quartzite. The quartzite is perhaps the most resistant rock in the quadrangle, and it generally forms cliffs or ledges wherever exposed. On the dip slopes, however, it breaks down to sharply angular fragments or blocks and is poorly exposed. The quartzite is well displayed in the walls of Eagle Canyon where it forms nearly vertical cliffs rising abruptly above somewhat gentler cliffy slopes of Precambrian rocks (fig. 3). It is exposed also in the walls of canyons southwest of the Eagle River, though it is partly buried by talus along most of these canyons. It is not seen northeast of the canyon of the Eagle River, except in a few narrow fault slices along the Gore fault, the largest of which is on the southern spur of Bald Mountain, west of Booth Creek (fig. 25).

The surface of Precambrian rocks on which the quartzite rests seems to be planar wherever exposed in the Minturn quadrangle (fig. 7), but only a mile or two

south of the quadrangle, in the area of the Homestake shear zone, the surface has a relief of as much as 50 ft (15 m) (Tweto, 1949, p. 160; Tweto and Sims, 1963, p. 1008). In most places the Precambrian rocks beneath the quartzite are weathered and are soft and crumbly to depths of a few inches to a few feet, but in some places they are fresh. Where bedding-plane movement has occurred at the base of the quartzite, the soft, altered Precambrian rock is deformed into ridges or mounds as much as 5 ft (1.5 m) high, giving a deceptive appearance of relief in the depositional surface.

Basal beds of the Sawatch Quartzite are generally somewhat coarser grained than the remainder of the quartzite, and locally they contain lenses of quartz granule conglomerate a few inches thick. The granules in such conglomerate are typically $1/8$ – $1/4$ in. (3–6 mm) in diameter and are well rounded; they consist of quartz of various colors, white predominating. In most places the basal 10–30 ft (3–9 m) of the quartzite is gray, pink, or light tan, but in some places this part is white like the remainder of the formation.

The main body of the Sawatch is predominantly vitreous white quartzite made up of well-sorted rounded and subrounded medium-sand quartz grains. Along the canyon of the Eagle River, the zone between 75 and 160 feet (23 and 48 m) above the base of the quartzite contains scattered lenses of brown-weathering dolomitic sandstone or sandy dolomite. This feature was not noted elsewhere in the quadrangle or adjoining areas,



FIGURE 7.—Sawatch Quartzite (bedded rock) resting upon nearly planar surface cut over Precambrian rocks (at base of photograph). Roadcut on U.S. Highway 24, 600 ft (180 m) northwest of high bridge near Red Cliff.

though it exists also in Glenwood Canyon, 40 mi (65 km) to the west (Bass and Northrop, 1963, p. J4-J7). A few green shaly partings occur on bedding planes in the quartzite sequence, and, near Gilman, a shaly sandstone bed 4-6 ft (1.2-2.0 m) thick about 70 ft (21 m) above the base of the quartzite serves as a useful stratigraphic marker. The upper 30-40 ft (9-12 m) of the quartzite is very vitreous and brittle and has a crackled appearance in outcrop. This quartzite is white in the Eagle Canyon area, but more commonly in the region it is pink, particularly in the uppermost part. In the Gilman area, the upper vitreous quartzite contains brecciated and mineralized beds that are known locally as the Rocky Point zone. One or more of these beds, each 1-4 ft (0.3-1.2 m) thick may be present in any part of the upper vitreous quartzite, but in most places they are in the upper middle part, 10-20 ft (3-6 m) below the top of the Sawatch Quartzite. The quartzite of the Rocky Point zone is stained yellow by the oxidation products of pyrite and forms a conspicuous color band near the top of the quartzite cliffs.

As seen in thin sections, quartzite of the Sawatch is somewhat variable; the sand grains in most beds are well sorted and rounded, but in some beds they are poorly sorted and are subrounded to subangular. The grains range from 0.2 to 1.3 mm in diameter, though in most of the rock they are 0.25-0.5 mm. In some samples, the sand grains are in a matrix of very small (0.05 mm) angular quartz fragments that resemble a microbreccia. Many of the larger quartz grains contain inclusions of tourmaline, sillimanite, or rutile, and they commonly show strain shadows and lines of fluid inclusions. Accessory detrital minerals are not abundant but include muscovite, biotite, chert, potassium feldspar, sphene, green tourmaline, and zircon. The tourmaline is especially consistent and is seen in all sections of the quartzites. Feldspar is present only in the uppermost quartzite beds, and it is abundant in sandstone of the overlying Peerless Formation. The feldspar grains generally are fresh and most of them are microcline, though some untwinned potassium feldspar is present also.

The Sawatch Quartzite is 190-220 ft (58-67 m) thick in the canyon area of the Eagle River, and it has a similar thickness of about 200 ft (60 m) at the northern end of the Sawatch Range to the west, at the 12,000-ft contour west of the head of West Grouse Creek. The quartzite thins to the northeast and to the south of the canyon area. In the fault slice on Bald Mountain, it consists of about 100 ft (30 m) of white quartzite and relatively coarse quartzite conglomerate lying on Precambrian rocks and overlain by red hematitic mudstone of the Peerless Formation. Near Pando, 5 mi (8 km) south of Red Cliff, the quartzite thins to about

120 ft (37 m) upon crossing the Homestake shear zone and then thins gradually southward to about 100 ft (30 m) in the Leadville area (Tweto and Sims, 1963, p. 1008).

The character of the Sawatch Quartzite is shown in the following stratigraphic section which was measured as a standard of reference for studies in the mine workings.

Section of the Sawatch Quartzite

(Measured along railroad at north end of canyon of the Eagle River, beginning 2,550 ft (778 m) south of highway overpass. See fig. 8.)

	Thickness (feet)	Distance above base (feet)
Sawatch Quartzite:		
Top of formation		220.3
33 Quartzite, white, vitreous, medium-bedded	11.7	208.6
32 Sandy quartzite, white to gray, medium- to thin-bedded, fine-grained, locally slightly glauconitic; weathers conspicuous ocherous brown. Rocky Point zone of Gilman mines	3.0	205.6
31 Quartzite, white, fine-grained, vitreous, medium-bedded	10.5	195.1
30 Dolomite, tan, medium-grained to coarsely crystalline, rough weathering	1.0	194.1
29 Quartzite, white with some pink bands, medium- to fine-grained, vitreous, locally slightly dolomitic, becomes dolomitic and red toward base. Wavy contact with unit below	12.0	182.1
28 Dolomitic shale, orange-red with purple blotches, finely sandy and micaceous, thin- to medium-bedded. Wavy contact with unit below	1.0	181.1
27 Quartzite, light-gray, medium-grained, massive, is dolomitic and pink near base and grades on strike into dolomite	4.7	176.4
26 Quartzite, medium-bedded	2.0	174.4
25 Dolomite, tan pink	9	173.5
24 Quartzite, white, vitreous, medium- to thick-bedded	4.0	169.5
23 Dolomitic sandstone and quartzite in thin beds, crossbedding weathers in relief. Dolomitic sandstone is buff to pink; quartzite is white	4.0	165.5
22 Shale and dolomite in alternating thin beds, purplish-pink, forms shelf along cliff	2.5	163.0
21 Quartzite and dolomitic sandstone, gray and pink, thin-bedded	2.0	161.0
20 Quartzite sandstone, white, medium-grained, sugary, massive	7.8	153.2
19 Quartzite sandstone, white, medium-grained, sugary, and interbedded brown, medium-grained, soft sandy dolomite	12.0	141.2
18 Quartzite sandstone, white, medium-grained, sugary, massive	6.0	135.2

Section of the Sawatch Quartzite—Continued

Sawatch Quartzite—Continued

	Thickness (feet)	Distance above base (feet)
17. Quartzite, white, vitreous, fine- to medium-grained, massive; contains interbedded brown, coarse, soft, sandy dolomite in short lenses 2 in. to 3 ft thick which become less abundant downward. Quartzite beds are 1–5 ft thick; quartzite is argillaceous near base of unit, and at 18 ft above base, contains 7 in. shaly bed	62.1	73.1
16. Limy and shaly sandstone, thin- and irregular-bedded; weathers dark chocolate brown; contains thin micaceous laminae with numerous dark-brown fossil fragments in some laminae. Micaceous at base. White alum efflorescence on outcrop. Unit is bounded above and below by bedding-plane slips	6.0	67.1
15. Sandstone, light-gray, medium-grained; mottled with dark shell fragments of inarticulate brachiopods; is thin bedded and irregular bedded	1.6	65.5
14. Quartzite, light-tan, vitreous, medium-bedded. Weathered surface is marked by thin horizontal pits $\frac{1}{8}$ – $\frac{1}{4}$ in. long	1.5	64.0
13. Quartzitic sandstone, light-tan gray, knobby weathered. Contains abundant small brachiopods (<i>Dicellomus</i> sp.) and shell fragments on weathered surface	1.8	62.2
12. Quartzite, light gray to light-tan, vitreous, medium- to fine-grained, thin- to medium-bedded. Beds separated by thin micaceous partings with knobby or lenticular structure. At base of unit is 6-in. bed of coarse-grained, light-gray, quartzitic sandstone with abundant fossil fragments, chiefly brachiopods	6.0	56.2
11. Sandy quartzite, light gray, fine-grained, massive	3.3	52.9
10. Shaly sandstone, light bluish gray, very thin bedded, finely micaceous; slightly pink on weathered surfaces	.6	52.3
9. Quartzite, white, medium- to fine-grained, gritty	1.0	51.3
8. Covered	1.0	50.3
7. Quartzite, white, medium- to coarse-grained, massive- to medium-bedded; clay speckled (arkose?); weathers mottled tan. Thin lenses of fine conglomerate with thin shaly layer above it at 7 in. from top	15.5	34.8
6. Sandstone, gray-white, finely conglomeratic, quartzitic	2.3	32.5
5. Quartzite, white, massive, lower 3 in. strongly sheared; bedding-plane slips above and below unit	2.0	30.5

Section of the Sawatch Quartzite—Continued

Sawatch Quartzite—Continued

	Thickness (feet)	Distance above base (feet)
4. Quartzite, white, vitreous, massive, medium-grained. 4-in. shaly zone at base of interval; strong shear slip 5 ft above base	6.0	24.5
3. Quartzite, white, gritty, coarse-grained; has thin sandy partings	7.5	17.0
2. Sandy quartzite, white to pink, medium- to coarse-grained, massive; weathers with vertical tubular holes from $\frac{1}{2}$ to $2\frac{1}{2}$ in. long	1.0	16.0
1. Conglomeratic and quartzitic sandstone, light-gray, coarse-grained, medium- to thin-bedded. Wavy basal contact	16.0	0
Total measured thickness of Sawatch Quartzite	220.3	

Precambrian granite:

Top 6 in. to 3 ft is soft, altered, and sheared.

As indicated in the preceding stratigraphic section, fossil fragments are abundant in certain beds in the lower half of the Sawatch Quartzite, but fossils that are complete enough to identify are rare. The only fossils identified from the Sawatch Quartzite in the Minturn quadrangle are tiny inarticulate brachiopods assigned to the upper Cambrian genus *Dicellomus* by Dr. W. C. Bell of the University of Texas (oral commun., 1941). These fossils are from unit 13 of the preceding stratigraphic section. Better preserved and more abundant brachiopods from about the same level in the Sawatch in the Pando area, a few miles south of Red Cliff, also were identified by Bell as *Dicellomus* sp. (Tweto, 1949, p. 159). Later, as quoted by Berg and Ross (1959, p. 107), Bell reported brachiopods in the Sawatch (presumably in the collections discussed here) to be "*Dicellomus* of the *pectenoides* and *nanus* types, both 'lower' Dresbachian." These determinations by Bell represent almost the only reliable information on fossils from the Sawatch. Trilobites are mentioned in the early literature, but they seem to have come mainly from the strata now assigned to the Peerless Formation (Johnson, 1934, p. 20). Trilobite fragments can be distinguished among the fossil fragments in the quartzite of the Gilman and Pando areas, but most of the fragments are of brachiopods.

The quartz sand that later became the Sawatch Quartzite has been widely recognized to have been formed as the Late Cambrian sea gradually transgressed over a surface of very low relief cut in the Precambrian rocks. The rocks at this surface were weathered, and the quartz residue from them was an abundant source of quartz sand. This sand probably was in part derived by direct wave action on the

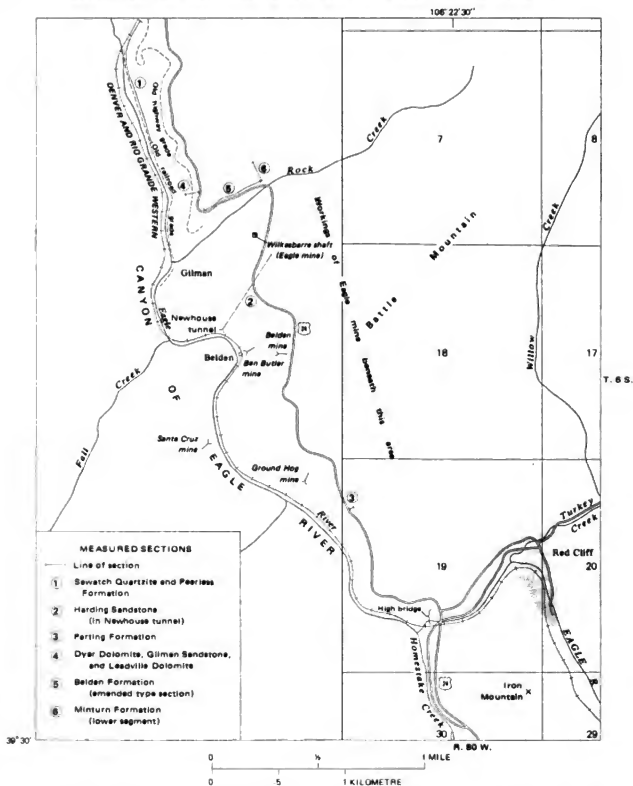


FIGURE 8.—Gilman area and canyon of the Eagle River showing locations of mines referred to and measured sections.

weathered rocks and was in part brought to the sea by streams from land that lay to the east, as regional relations indicate that the transgression was generally eastward (Lochman-Balk, 1956, p. 565-574), and paleocurrent data indicate westward transport of the sand on the sea bottom (Seeland, 1968). The occurrence of fresh detrital microcline and biotite in the uppermost beds of the Sawatch indicates that by that time streams somewhere had removed the weathered mantle and were eroding fresh Precambrian rock. Whether this fresh rock was later covered by Sawatch sediments or remained an island is not known, because the Sawatch has been removed by erosion from so much area since its deposition. However, the rapid thinning of the Sawatch between the Eagle River and Bald Mountain and the relatively coarse conglomerate in the Sawatch at Bald Mountain suggest that land, or an island, may have lain somewhere in the vicinity of the present Gore Range.

PEERLESS FORMATION

The Peerless Formation consists of 65-70 ft (20-21 m) of highly varied but predominantly dolomitic rocks. In most places the lower 20-30 ft (6-9 m) of the Peerless is a sandy dolomite or dolomitic sandstone which commonly is glauconitic and locally is ferruginous or chloritic. This dolomite or sandstone has a slabby appearance in outcrop even though individual beds are as much as 3 ft (1 m) thick, and it weathers dark brown to dark maroon; thus, it contrasts markedly with the underlying white quartzite of the Sawatch. Thin beds of white or pink quartzite in the lower 5-10 ft (1.5-3 m) of the dolomite or sandstone make the contact with the Sawatch a gradational one in many places.

Abundant iron-bearing material characterizes the lower part of the Peerless. The sandstones locally contain red earthy hematite, either in thin beds or as a matrix of the clastic grains. Some of the hematite appears oolitic, but generally the "oolites" are quartz grains heavily coated with hematite. In places the sandstones contain lenses that are as much as 50 percent glauconite, and in other places they contain abundant bright-green iron-rich chlorite, which petrographically appears to be authigenic rather than detrital. Dolomite beds of all the Peerless, but especially of the lower part, commonly contain thin limonitic laminae generally accompanied by sand grains or argillaceous matter, that weather in relief, giving the rock a wavy laminated appearance. Locally, minute limonitic veinlets form a reticulate network in the dolomite. Bright-red hematitic mudstone is also common in the Peerless; near the Gore fault on Bald Moun-

tain, the Peerless is 20 ft (6 m) thick and consists entirely of the red mudstone.

The middle part of the Peerless consists of tan, buff, maroon, and pale-green thin-bedded sandy dolomite, dolomitic shale, dolomite, mudstone, and minor micaceous shale. This unit is soft and nonresistant, and it generally weathers to covered slopes. The upper part of the formation is somewhat thicker bedded than the middle part, and it is also more purely dolomitic, though it, like all the Peerless, differs in lithology from place to place. On the dip slopes west of Gilman and along Cross Creek, the upper 40 ft (12 m) of the Peerless is pure dolomite which is thin bedded, buff, and coarsely crystalline.

The dolomitic rocks of the Peerless are characterized by color mottling and by great variety in sedimentary structures. Bedding planes are wavy, and many are coated with mud or mica or are spotted with mud lumps. Fucoidal markings and worm trails are common on the bedding planes. Ripple marks are conspicuous, and many thin beds have mud cracks filled with material that contrasts in color or composition with the rest of the rock. Many thin beds of the dolomite are flat-pebbled or edgewise conglomerate that consists of slightly abraded pebbles of maroon or purple dolomite in a buff crystalline dolomite matrix. Chips of maroon clay, mudstone, or micaceous shale are also scattered through some of the conglomerates. Other beds are mottled buff and purple, but pebbles cannot be distinguished in them. Some such beds also have various unidentified small curly color markings, as well as concentric structures that may be either concretionary or algal, or both. Many of the markings of various kinds are maroon, as are some beds of the dolomite, and hence the term "Red-cast beds" was once applied to these rocks. As a unit, however, the part of the Peerless above the dark lower beds is mainly buff, though it is spotted or is streaked maroon and pale green in places.

As seen in thin section, the sandy dolomites and dolomitic sandstones of the Peerless consist largely of dolomite, quartz, and feldspars in various proportions, though glauconite and chlorite are also abundant constituents of some samples. The feldspar grains include both microcline and sodic plagioclase, which generally are fresh or only slightly altered. Chlorite, in small irregular flakes and sparse larger, rounded flakes, is most abundant in the arkosic varieties of the rocks. Glauconite is in rounded grains that are among the coarsest in the rocks. Common accessory minerals are muscovite, zircon, and tourmaline; hematite or limonite coats many of the clastic grains. The quartz and feldspar grains are subrounded to subangular and well-

sorted. They range in maximum size from 0.2 mm in some beds to 0.5 mm in others. In some of the dolomitic sandstones the dolomite is concentrated in discrete microlenses or pockets in an otherwise quartzitic rock, whereas in other sandstones the dolomite is a matrix or cement for the clastic grains. In the sandy dolomite, the clastic grains are less well sorted than in the sandstones, and they are scattered unevenly through the dolomite.

Character of the Peerless in the vicinity of Gilman is shown by the following stratigraphic section. As may be seen by comparison with sections measured 1.6 and 2.0 mi (2.6 and 3.2 km) south of Red Cliff (Tweto, 1949, p. 164-165), the Peerless differs markedly from place to place.

Section of the Peerless Formation

[Measured southward along railroad at north end of canyon of the Eagle River, beginning 1,800 ft. (550 m) south of highway overpass. See fig. 8.]

	Thickness (feet)	Distance above base (feet)
Harding Sandstone:		
Sandy quartzite and arkosic sandstone, white, medium- to fine-grained, massive, slightly crossbedded.		
Peerless Formation:		
Top of formation	66.5	
15. Flat-pebble dolomite conglomerate, purplish-pink to buff, medium- and thin-bedded; weathers light chocolate brown; contains partings of purple conglomeratic shale	2.0	64.5
14. Flat-pebble dolomite conglomerate, mottled purplish-pink and light-green, thin-bedded; contains partings of fissile greenish-gray to greenish-buff micaceous dolomitic shale	6.0	58.5
13. Shaly dolomite, mottled green and gray-buff, thin-bedded; weathers with fine siliceous ridges on weathered surface	1.5	57.0
12. Dolomitic shale, greenish-gray to buff-gray, thin-bedded	1.0	56.0
11. Flat-pebble dolomite conglomerate, light-buff, thin-bedded; grades downward into green and purple-pink fissile, sandy shale	1.2	54.8
10. Covered	5.0	49.8
9. Flat-pebble dolomite conglomerate, mottled purple and tan, medium-bedded, buff weathering	1.5	48.3
8. Shale, fissile, greenish-gray, fine-grained	1.5	46.8
7. Dolomite, mottled light-tan and green, medium- to thin-bedded, green-buff weathering	1.5	45.3
6. Dolomitic shale, light-tan, thin-bedded	1.0	44.3
5. Flat-pebble dolomite conglomerate, light-tan with local purple mottling; contains shale fragments and some laminae of green shale	1.0	43.3

Section of the Peerless Formation—Continued

	Thickness (feet)	Distance above base (feet)
Peerless Formation—Continued		
4. Dolomite, greenish- to light-tan, fine-grained, massive, somewhat argillaceous, weathered surfaces are brown and threaded with thin limonitic argillaceous ridges; 4-in. glauconitic shale bed in middle and 2-in. bed at base	3.3	40.0
3. Sandy dolomite, light-gray, coarsely crystalline, medium-bedded; has coarse green glauconitic grains and coarse quartz sand. Weathers tan, with quartz grains and argillaceous ridges in relief, giving rough surface. Contains purple and green shaly fragments in a few thin seams, and near top, a seam of purple, micaceous shale	31.0	9.0
2. Sandy dolomite, pink, massive, brown-weathering, medium-crystalline; has thin coarsely crystalline bands. Weathers rough, with coarse crystals and sand in relief. Grades downward into pink dolomitic crossbedded sandstone	5.0	4.0
1. Sandstone, white, fine-grained, chalky-looking; has thin beds of pink sandy dolomite at top; medium bedded and crossbedded, weathers brown. Conformable contact with underlying quartzite	4.0	0
Total measured thickness of the Peerless Formation	66.5	

Sewatch Quartzite:

Vitreous white quartzite.

Fossils found sparingly in the Peerless Formation at various localities in central Colorado establish the formation as middle Late Cambrian (Franconian Stage) in age. We found no fossils within the quadrangle, but Crawford and Gibson (1925, p. 35) reported the Upper Cambrian trilobite *Saukia pepinensis* and Resser (1942, p. 66) reported the trilobites *Ellipsocephaloides butleri* and *Briscoia* in material from "near Gilman" acquired by C. D. Walcott prior to the mid-1920's. The trilobites reported by Resser are indicative of the Franconian Stage, as are others (*Ptychaspis*, *Idahoia*) reported by Berg and Ross (1959) from the Manitou Park area near Colorado Springs. A trilobite from a bed 44 ft (13 m) above the base of the Peerless in the Holy Cross quadrangle, 1.6 mi (2.6 km) south of Red Cliff was identified by Josiah Bridge of the U.S. Geological Survey (written commun., 1950) as *Pteroccephalia* cf. *P. sanctisabae* Roemer? and as "characteristic of the *Elvinia-Camaraspis* zone of the Franconian Stage." Brachiopods from the same locality were identified by W. C. Bell (reported in the Bridge communication) as *Obolus*

maeschae Lochman, "characteristic of the *Cedaria* and *Crepicephalus* zones of the early Late Cambrian (Dresbachian stage)." Later, however, brachiopods from this same collection were reported by Berg and Ross (1959, p. 107) to have been tentatively identified by Bell as "*Dicellomus?* cf. *mosaica* of the *Conaspis* zone or an unnamed species from the *Cedaria* zone." (The *Conaspis* zone is in the Franconian Stage, above the *Elvinia-Camaraspis* zone and below the *Briscoia* zone).

These data on the age of the Peerless are significant in the evaluation of the unconformity at the top of the Peerless. In the Gilman area, the Peerless is overlain unconformably by the Middle Ordovician Harding Sandstone, and on Bald Mountain and locally in the Pando area (Tweto, 1949, p. 163) it is overlain by the Upper Devonian Parting Formation. In most of the Sawatch Range region, however, it is overlain by the Lower Ordovician Manitou Dolomite (Johnson, 1944). At Glenwood Canyon, 40 mi (64 km) west of Minturn, additional Cambrian strata intervene between the Peerless and the Manitou. Bass and Northrop (1953; 1963) divided the strata of Cambrian age at Glenwood Canyon into two formations, the Sawatch Quartzite, 517 ft (158 m) thick, and the predominantly dolomitic Dotsero Formation, about 100 ft (30 m) thick. Although a well-defined unit with lithology characteristic of the Peerless is present in the area (observation by Tweto), Bass and Northrop did not distinguish it as Peerless because it is overlain by about 150 ft (45 m) of quartzites typical of the Sawatch. They, therefore, placed these quartzites and the 69 ft (21 m) of underlying Peerless equivalent (unit 10 of Sawatch Quartzite stratigraphic section; Bass and Northrop, 1963, p. 6) in the Sawatch Quartzite, which accounts for the relatively great thickness of 517 ft (158 m) reported for this unit, as contrasted with the 220 ft (67 m) at Gilman. The carbonate rocks containing Upper Cambrian fossils above the quartzite were assigned by Bass and Northrop (1953) to the Dotsero Formation as redefined from the original usage of Bassett (1939).

Since the redefinition of the Dotsero, it has been a common practice to correlate the Dotsero and Peerless (for example, Berg, 1960; Stevens, 1961), but this is in error as indicated not only by the presence of a unit with typical Peerless lithology and thickness within the Sawatch as applied by Bass and Northrop, but also paleontologically. The Dotsero is characterized by fossils of late Late Cambrian age (Trempealeuan Stage) as determined by A. R. Palmer (Bass and Northrop, 1953, p. 896), whereas the Peerless is older, of the Franconian—and possibly even Dresbachian—Stage, as discussed above. This difference in age and the presence of 250 ft (75 m) of Cambrian strata between the

Peerless equivalent and the Manitou in Glenwood Canyon strongly suggest that in areas where the Manitou lies on the Peerless some Cambrian strata were removed by erosion before deposition of the Manitou. Such an erosional break between the Upper Cambrian and Lower Ordovician was noted by Berg and Ross (1959) in the Colorado Springs area and as a general feature in Colorado by Tweto (1968a, p. 561).

It is thus likely that in the Minturn quadrangle some part of the Peerless as well as formerly overlying Cambrian strata were removed by erosion prior to Early Ordovician time and that an additional part of the Peerless may have been removed by erosion in pre-Middle Ordovician time, when the Manitou Dolomite was eroded from the area, as discussed below. Some of the eroded Cambrian rocks presumably were carbonate rocks similar to those of the Dotsero Formation.

The central Colorado Upper Cambrian sequence of the Sawatch Quartzite, Peerless Formation, and Dotsero Formation or equivalent is remarkably similar to the Middle Cambrian sequence of the Grand Canyon, described in detail by McKee (1945). Like the Bright Angel Shale of the Grand Canyon, the Peerless displays a very extensive combination of lithic types that indicate shallow-water deposition, rapidly changing environments of deposition, disturbed and noncontinuous deposition, and repeated regressive-transgressive shifts within the broadly transgressive sequence. The abundant flat-pebble conglomerates of the Peerless indicate repeatedly agitated waters and breaks in sedimentation, especially as they include fragile chips of clay or coarse mica shale that can only have been torn by wind or waves from other Peerless sediments nearby. These chips, and also mudcracks, suggest repeated exposure to the air, as on mudflats. In combination, features, such as the shale chips, glauconite, ripple marks, fucoid markings, the conglomerates, and irregular bedding planes, suggest deposition in shallow water. The abundance of iron, as expressed by hematite, limonite, glauconite, and authigenic chlorite, suggests slow deposition under conditions of restricted circulation and high salinity, and the variety of iron minerals suggests changing conditions within this framework (James, 1966). Color mottling in the nonconglomeratic dolomites also suggests these conditions (McKee, 1945, p. 75-77).

ORDOVICIAN SYSTEM

In central Colorado the Ordovician System comprises three formations—the Manitou Dolomite, Harding Sandstone, and Fremont Limestone. These formations, of Early, Middle, and Late Ordovician ages, respectively, are separated one from the other and from post-Ordovician rocks by unconformities that represent

widespread erosion after deposition of each unit (Lovering and Johnson, 1933; Johnson 1944; Sweet, 1954). As a result, the three formations are preserved only in remnants of their original extent. Of these remnants, the Manitou is by far the most extensive and the Harding and Fremont are areally much more restricted. The distribution of these remnants is of economic concern because the Manitou and Fremont are mineralized in many mining districts in central Colorado. The Manitou was referred to as the "White limestone" or "Yule limestone" in older literature in many of the mining districts (Emmons, 1886; Emmons and others, 1927).

In much of the region surrounding the Minturn quadrangle, such as the Leadville area and adjoining Mosquito Range, the western side of the northern Sawatch Range north of Aspen, Glenwood Canyon, and the White River Plateau, the Manitou is the only Ordovician formation present. In the Minturn quadrangle, however, the Manitou is absent and the Ordovician is represented only by the Harding Sandstone. This occurrence of the Harding constitutes an outlier 25 mi (40 km) north of the general area of Harding occurrence, as shown on a map by Sweet (1954, fig. 1). The closest known approach of the Manitou to the Minturn quadrangle is in the Pando area about 8 mi (13 km) south-southeast of Red Cliff, where the Manitou tapers to an eroded edge unconformably beneath the Harding (Tweto, 1956). The Manitou is also present about 9 mi (14 km) southeast of the Minturn quadrangle at Mayflower Gulch in the Kokomo district (Tweto, 1949, p. 156), where it is 20 ft (6 m) thick, lies on Precambrian rocks, and is overlain by the Parting Formation.

The Fremont Limestone is even less widespread than the Harding; its nearest exposures are more than 30 mi (48 km) south of the Minturn quadrangle.

HARDING SANDSTONE

Strata assigned to the Harding Sandstone of Middle Ordovician age consist of white and green quartzite, sandstone, and shale a few feet to perhaps 80 ft (24 m) thick that lie unconformably on the Peerless Formation and are unconformably overlain by the Parting Formation. No fossils have been found in these rocks, but as the rocks are lithologically similar to the Harding exposed in many places along the sides of the Sawatch Range farther south, and as they clearly overlie the Manitou Dolomite south of the Minturn quadrangle in the area between Pando and Tennessee Pass (Tweto, 1956), they are assigned with confidence to the Harding.

The Harding is continuous, although of variable character and thickness, from the north end of the canyon of the Eagle River southward to the quadrangle boundary. Farther south, it is in discontinuous lenses

(Tweto, 1949), and it finally pinches out completely about a mile north of Tennessee Pass (Tweto, 1956). It is continuous westward from the canyon area at least to Beaver Creek, about 2 mi (3 km) west of the quadrangle boundary, but it must pinch out farther west. At Fulford, 7 mi (11 km) west of Beaver Creek, only the Manitou is reported between the Peerless and Parting (Gabelman, 1950). The Harding must also pinch out eastward from the canyon area as it is absent at Bald Mountain and at Mayflower Gulch in the Kokomo district.

The Harding is varied in composition but commonly consists of massive white quartzite in discontinuous lenses at the base; thin-bedded green and maroon sandstone, quartzite, and conglomerate in the middle part; and green shale and sandstone in the upper part. At the north end of Eagle Canyon, the Harding consists of 6 ft (2 m) of massive white quartzite overlain by about 10 ft (3 m) of purple-mottled green clay shale. One-half mile farther south it is represented by a single massive 25-ft (7.5-m) bed of white quartzite. In the Newhouse tunnel of the Eagle mine it is 39 ft (12 m) thick and consists of 22 ft (7 m) of basal white quartzite overlain by 17 ft (5 m) of green-gray quartzites, arkosic quartzites, and sandy green shales. In roadcuts 1.5 mi (2.4 km) south of Gilman, the Harding is only 14 ft (4 m) thick and consists of 2-3 ft (0.6-1 m) of basal white quartzite overlain by 11-12 ft (3.4-3.7 m) of interbedded pink, gray, and green quartzite, conglomerate, sandy shale, and clay shale. On the slopes of the Sawatch Range the Harding consists of at least 35 ft (10.7 m), and possibly as much as 50 ft (15 m), of massive white quartzite. In the lower levels of the Eagle mine the Harding has an apparent thickness of as much as 80 ft (24 m) and consists of 30 ft (9 m) of white and green quartzites overlain by about 50 ft (15 m) of soft variegated clay shale. The shale has been deformed by low-angle faults wherever seen, however, and it may have been thickened by repetition of beds.

Although the Harding normally appears to be merely disconformable with the formations below and above it, small angular discordances exist. In the Pando area, a discordance of as much as 6° between the Peerless and the Harding was measured in cliff exposures, and some of the basal white quartzite occupies steep-sided channels cut in the Peerless (Tweto, 1949, p. 166-169). In the Newhouse tunnel at Gilman (fig. 8), a discordance of 2° was measured between the Harding and the overlying Parting Formation.

Throughout the canyon area and southward into the Pando area, the Harding locally grades at the top into a bed of tough massive green clay from 1 to 2.5 ft (0.3 to 0.75 m) thick that is characteristically marked by dark purple spots and streaks. This clay layer shows no bed-

ding but in places displays a slightly kneaded structure. In places where the Harding is discontinuous, such as south of Red Cliff, this massive clay bevels the Harding and lies directly on the Peerless Formation. The clay bed is interpreted as a residual soil developed on the older rocks prior to the deposition of the overlying Upper Devonian beds. It is a product of unconformity and technically is not a part of either the Harding or the Parting, but its thinness dictates that it be mapped with one or the other. In the Minturn quadrangle it was generally included in the Harding because of its gradational relation with the Harding, but in the Pando area it was included by Tweto (1949, p. 170-173) with the Parting because it lies above the surface of angular discordance between the Harding and Parting.

The Harding Sandstone commonly weathers to a partly or completely covered slope, and the best exposures are found in mine openings. The following section was measured in the Newhouse tunnel, which crosscuts the stratigraphic section from Precambrian rocks at the portal to the Chaffee Group.

Section of the Harding Sandstone

(Measured in Newhouse crosscut tunnel, Gilman. See fig. 8.)

	Thickness (feet)	Distance above base (feet)
Parting Formation:		
White quartzite, uneven-grained, finely conglomeratic.		
Unconformity, 2' discordance		39.2
Harding Sandstone:		
16. Quartzite, green, uneven-grained, sandy and shaly; contains subangular quartz pebbles as much as 1/2 in.	2.3	36.9
15. Shale, green, nodular, sandy. Nodules are pink quartzite, irregular in shape and 1/2-1 in. long	1.2	35.7
14. Shale, green, sandy	.2	35.5
13. Quartzite, white, massive, glassy, fine-grained	2.6	32.9
12. Quartzite, medium-grained; lower part is arkosic and feldspars are kaolinized	.5	32.4
11. Sandstone, green, shaly	.2	32.2
10. Quartzite, greenish gray, medium-grained; stained pinkish brown in scattered 1/4-in. angular spots	3.0	29.2
9. Shale, green, sandy	1	29.1
8. Quartzite, light-green-gray, medium-grained, massive; bottom 3-in. layer is arkosic and contains many white kaolinized grains in slightly chloritic matrix	1.8	27.3
7. Shale, green, sandy	1	27.2
6. Quartzite, light gray to greenish gray, medium-grained, with a few 1/2 to 1-in. pinkish-brown layers	4.8	22.4
5. Quartzite, greenish-gray, fine-grained	.2	22.2
4. Shaly sand parting	.3	21.9
3. Quartzite, white, medium-grained	3.5	18.4

Section of the Harding Sandstone — Continued

	Thickness (feet)	Distance above base (feet)
Harding Sandstone — Continued		
2. Quartzite, white and gray banded; alternating coarse- and fine-grained layers	16.7	1.7
1. Quartzite, white, fine-grained; contains a few very small black grains	1.7	0
Total measured thickness of the Harding Sandstone	39.2	

Peerless Formation:

Dolomite, brown, micaceous, medium-grained sandy.

Petrographic examination of two samples of sandstone from the Harding, one fine-grained and the other coarse-grained, shows that the sandstone consists of quartz, abundant interstitial sericite, minor calcite in scattered small lenses less than 1 mm in length, and accessory tourmaline, green biotite, chlorite, ilmenite/leucokene, sphene, and zircon. Unlike the sandstones of the Peerless, feldspars are absent except as inclusions in some of the quartz grains. The feldspar of this occurrence is an untwinned variety of low refractive index. In the fine-grained sandstone the quartz is in well-sorted grains 0.1-0.2 mm in diameter which have recrystallized to produce irregular interlocking grain boundaries; sericite is in elongated shreds and flakes that have a strong preferred orientation parallel to the bedding but are unevenly distributed. In the coarse-grained sandstone the quartz grains are poorly sorted and range from 0.1 to 2 mm in diameter. Some of the larger grains are well rounded but most are irregular, with interlocking boundaries. Hydromica or sericite fills in around quartz grains and also fills fractures cutting them. A sample of green siltstone from the Harding contains flakes of muscovite as much as 0.2 mm long in a matrix of sericite, clay minerals, and amorphous limonite.

DEVONIAN AND MISSISSIPPIAN SYSTEMS

The Devonian and Mississippian rocks of the Minturn quadrangle and surrounding region consist of a basal quartzite, typically about 40 ft (12 m) thick, and overlying carbonate rocks, typically about 250 ft (75 m) thick. Originally, these strata were divided into two units, the Parting Quartzite and the Leadville Limestone or "Blue Limestone" (Emmons, 1882, 1886). Kirk (1931) later restricted the Leadville to "limestones of Mississippian age," and assigned the carbonate rocks in the lower part of the Leadville of previous usage, along with the Parting strata, to the Upper Devonian Chaffee Formation. Kirk designated the basal quartzite the Parting Quartzite Member of the Chaffee Forma-

tion, and Behre (1932, p. 60) later designated the carbonate strata the Dyer Dolomite Member.

In restricting the Leadville and defining the Chaffee, Kirk selected as the lower boundary of the Leadville an unconformity at the base of a thin sandstone and breccia unit then known to occur in the Leadville area (Emmons and others, 1927, p. 34), in the Mosquito Range (Behre, 1929, p. 38), and in the Gilman area (Crawford and Gibson, 1925, p. 36). This sandstone and breccia unit was later found to be far more widespread and was designated the Gilman Sandstone Member of the Leadville Limestone (Tweto and Lovering, 1947; Tweto, 1949).

Thus, in the usage of the U.S. Geological Survey since 1931, the Devonian and Mississippian rocks of central Colorado have been divided into two formational units: (1) the Chaffee Formation, consisting of the Parting Quartzite Member and the Dyer Dolomite Member, and classified as Upper Devonian; and (2) the Leadville Limestone (or Dolomite), consisting of the Gilman Sandstone Member and an unnamed carbonate rock member, and classified as Lower Mississippian.

Geologic mapping and stratigraphic studies by many workers since 1931 have established that the Parting, Dyer, and Gilman are each a widespread mappable unit in central and northwestern Colorado. Further, the presence of an unconformity between the Gilman and the overlying carbonate rocks of the Leadville was established (Tweto, 1949, p. 179; Banks, 1967, p. 41), and a close relationship in lithology and origin between the Gilman and the Dyer was recognized. In the White River Plateau area, where the Dyer consists of a lower limestone unit and an upper dolomite unit (Bass and Northrop, 1963, p. 21), Campbell (1970) distinguished these units as members and raised the Dyer and Parting in rank to formation and the Chaffee in rank to group.

The classification of Campbell is here adopted with modification. The Parting is designated "Formation" rather than "Quartzite" because it has a mixed lithology or is largely shale in many places. The Dyer is designated the Dyer Dolomite. The Gilman is removed from the Leadville and is designated the Gilman Sandstone, thereby restricting the Leadville to carbonate rocks above the Gilman and below the Pennsylvanian strata. The Chaffee Formation of former usage, plus the Gilman, is designated the Chaffee Group. The Gilman is placed in the Chaffee Group because of its close relation to the Dyer in character, origin, and probably in age. Thus, the Chaffee Group consists, from the base upward, of the Parting Formation, Dyer Dolomite, and Gilman Sandstone.

As discussed in the following sections, the Parting Formation and the lower half or more of the Dyer

Dolomite are established to be Upper Devonian. The upper part of the Dyer Dolomite and the Gilman Sandstone might be either Late Devonian or Early Mississippian in age. Accordingly, the Dyer Dolomite and Chaffee Group are referred to the Upper Devonian and Lower Mississippian(?). The Gilman Sandstone is referred to the Upper Devonian or Lower Mississippian.

CHAFFEE GROUP

The Chaffee Group is exposed in the Minturn quadrangle only in the area near the Eagle River and—in part—in small fault slices along the Gore fault in the Gore Range. Near the Eagle River the group is 140–165 ft (43–50 m) thick—a normal thickness for the region. However, the Chaffee Group thins northeastward toward the Gore Range. In this direction, it overlaps the eroded edges of older formations, and its eroded edge is in turn overlapped by the Pennsylvanian Minturn Formation. In fault slices near the Gore fault, the Parting Formation is the only part of the group preserved beneath the Pennsylvanian rocks. These relations, among others, led Lovering and Johnson (1933) to the concept of a persistent highland in the area of the Gore and Front Ranges in early as well as late Paleozoic time.

Rocks of the Chaffee Group are resistant, and they commonly crop out in cliffs. In the canyon of the Eagle River, they form the lower part of the upper cliffs (fig. 3), which rise above a slope that represents the Harding Sandstone and Peerless Formation.

Though thin, the rocks of the Chaffee Group are of special economic interest because they—along with the overlying Leadville Dolomite—are the host rocks of the principal ore deposits at Gilman, Leadville, and several other mining districts. In such areas, and at Leadville especially, the thin sandy units comprising the Parting and the Gilman provide the principal stratigraphic control in a sequence of mineralized and altered dolomites. In areas where the Dyer and Leadville Dolomites have been replaced by jasperoid, the sandstone in the Gilman—though extensively replaced also—is particularly significant as a stratigraphic marker. Areas of jasperoid northwest of Gilman and west of Minturn are indicated on plate 1 and are discussed in the report on the ore deposits by T. S. Lovering, Tweto, and T. G. Lovering (1977).

PARTING FORMATION

In the southwestern part of the Minturn quadrangle, the Parting Formation consists of 40–65 ft (12–20 m) of predominantly quartzitic rocks. It lies unconformably on the Harding Sandstone in this area, though a few miles to the south it locally lies on the Peerless Formation (Tweto, 1949). As exposed in fault blocks along the Gore fault in the Gore Range, the Parting is 10–30

ft (3-9 m) thick and rests, in different places, on Precambrian rocks, on Sawatch Quartzite, or on a thin remnant of the Peerless Formation (fig. 25).

In the Minturn quadrangle and nearby areas, the Parting Formation consists chiefly of quartzite and quartzite conglomerate, but locally it contains abundant turquoise-green shale which in places is streaked and is mottled maroon. The quartzite is typically light tan to white, poorly sorted, coarse grained, thick bedded to massive, prominently crossbedded, and vitreous. Quartzite conglomerate, characterized by well-rounded to angular white and pink quartz pebbles $\frac{1}{4}$ -2 in. (0.6-5 cm) in diameter, generally is present at the base and occurs also in scattered lenses throughout the unit. Quartzite of the Parting can generally be distinguished from that of the Sawatch—or from the white quartzite present locally in the Harding—in isolated exposures by the coarse and uneven grain, the presence of clear quartz as contrasted to cloudy white quartz of the Sawatch and Harding, and, commonly, by tan color of the rock.

The quartzite of the Parting is composed almost entirely of quartz grains but contains sparse interstitial sericite and a few detrital grains of zircon and leucosene. Some of the quartz grains contain small inclusions of muscovite, green tourmaline, and slender needles of sillimanite, together with lines of minute fluid inclusions. Many of the grains show marked strain shadows. The quartz grains in the nonconglomeratic beds range in size from 0.1 to more than 1 mm; most of them were originally rounded but recrystallization and secondary quartz overgrowths have produced an irregular interlocking texture.

The green shale in the Parting occurs in local thin beds between the heavy quartzite beds and also in thick lenses that locally constitute as much as half the thickness of the formation, as at the north end of the canyon of the Eagle River, south of Cross Creek. Much of the shale is sandy, and some of it contains thin beds of vitreous white quartzite. Thin sections show that the green shale is composed of alternate layers of fine arkosic sand and green chloritic material. The arkosic layers are composed chiefly of quartz, microcline, and a pale-green micaceous mineral tentatively identified as a chlorite. Small flakes of detrital muscovite are common in the arkosic material, and the accessory detrital minerals are tourmaline, sphene, and zircon.

Character of the Parting Formation is illustrated by the following section, measured in the canyon between Red Cliff and Gilman. As measured in sections a few miles farther south (Tweto, 1949, p. 171-173), the uppermost sandstone and quartzite beds of the Parting are dolomitic, and the contact with the overlying Dyer Dolomite is gradational.

Section of the Parting Formation

(Measured on cut along U.S. Highway 24, 0.6 mi (1 km) northwest of high bridge over the Eagle River one-half mile (0.8 km) west of Red Cliff. See fig. 8.)

	Thickness (feet)	Distance above base (feet)
Dyer Dolomite: Covered, 10 ft.		
Parting Formation:		
Approximate top		47.0
15 Quartzite, white, vitreous, coarse-grained, unevenly grained	1.0	46.0
14 Sandy quartzite, light-yellowish gray, thick bedded, contains white vitreous quartzite fragments and bands of intraformational conglomerate of these fragments in sandy quartzite	4.0	42.0
13 Quartzite, white, massive, vitreous, coarse, unevenly grained, slightly conglomeratic, contains buff-gray specks of altered feldspar	4.0	38.0
12 Quartzite, light gray, vitreous, even-grained, medium- to fine grained; abundant buff flecks. Weathers with hackly surface	5.0	33.0
11 Quartzite, white, coarse-grained, slightly sandy, many clear quartz grains as much as $\frac{1}{4}$ in. in diameter	7.0	26.0
10 Sandy quartzite, banded white and greenish gray, coarse-grained; contains clear quartz granules	2.5	23.5
9 Quartzite, white, vitreous, fine grained; contains very few buff specks	7.0	16.5
8 Quartzite, light tan, very coarse and poorly sorted, locally conglomeratic; glassy quartz pebbles	1.5	15.0
7 Sandstone, shaly, greenish gray, brown, weathering, fine grained. Grades down into green-gray shaly and arkosic friable sandstone	1.5	13.5
6 Sandstone, quartzitic, conglomeratic, contains some hematite, grades down into shaly sandstone5	13.0
5 Quartzite, conglomeratic, white, micaceous, vitreous. Contains pebbles of clear and pink quartz and $\frac{1}{4}$ -in. angular fragments of gray shaly sandstone that may be from Harding Sandstone	1.5	11.5
4 Sandy shale and shaly sandstone, light-greenish gray, fine grained, nonmicaceous	4.0	7.5
3 Quartzite, light-pink, medium grained, vitreous, finely banded. Grades downward into white, vitreous, poorly sorted quartzite; is finely conglomeratic at base. Fragments of clear quartz	5.0	2.5
2 Quartzite, banded pink and gray, coarse-grained, conglomeratic, has abundant fragments of pink quartz as much as $\frac{1}{4}$ in. in diameter. Many grains of kaolinitized feldspars as much as $\frac{1}{4}$ in. in diameter	1.5	1.0

Section of the Parting Formation — Continued		
Parting Formation — Continued		
1. Clay-shale, tough, green with purple bands and spots, is micaceous, has kneaded appearance. Probably a regolith	Thickness (feet)	Distance above base (feet)
Total measured thickness of the Parting Formation	1.0	0
	47.0	

Harding Sandstone:

Quartzite, white, vitreous, fine- and even-grained.

In many places the quartzite beds of the Parting contain rusty cavities that can be seen to be molds of brachiopods, pelecypods, or crinoid stems, but generally these are too vaguely imprinted in the coarse quartzite matrix to be more closely identified. On the dip slope traversed by the Tigiwon Road 1.2 mi (1.9 km) northwest of Gilman, somewhat better preserved casts and molds were found in abundance in the Parting. These fossils were identified by Edwin Kirk of the U.S. Geological Survey (written commun., Feb. 5, 1953) as:

Schizophoria striatolata var. *australis* Kindle

Spurifer (*Cyrtospirifer*) *whitneyi* (Hall)

Productella sp.

Paurorhynca endlichi (Meek)

Aviculopecten ? sp. (fragmentary)

Kirk stated "Although poorly preserved, the above listed fossils can be recognized. It is a typical Ouray (Upper Devonian) fauna." A generally similar group of fossils has been reported from the Parting in the southern Sawatch Range (Dings and Robinson, 1957, p. 15). More recently, C. A. Sandberg of the U.S. Geological Survey (written commun., 1971) has reported a conodont fauna containing *?Clydgnathus ormistoni* from the Parting in Glenwood Canyon.

Except for these three invertebrate collections, the chief fossils found in the Parting in central Colorado are fish remains (Bryant and Johnson, 1936; Denison, 1951; Bass and Northrop, 1963, p. J20-J21). On the basis of the fish fossils, particularly the genus *Bothriolepis*, the Parting has been classed as early Late Devonian in age (Denison, 1951; Poole and others, 1967). On the other hand, the brachiopod *Paurorhynca endlichi* and the conodont *?Clydgnathus ormistoni* reported above indicate a late Late Devonian age. This difference in age probably is an expression of different levels of fossil occurrence in the Parting, though it does establish that some of the Parting is younger than was previously known. The Parting is a transgressive unit that progressively thins and becomes younger north-eastward. Most of the fish localities are on the south-west side of the Sawatch Range, 60 mi (97 km) south-west of the Minturn quadrangle, in thin-bedded limy, shaly, and sandy strata nearly 100 ft (30 m) below the

Dyer. The brachiopod locality in the Minturn quadrangle, in contrast, is in quartzite no more than 20 ft (6 m) below the Dyer, and the conodont locality is only 21 ft (6.4 m) below the Dyer. One fish locality is in the Mosquito Range north of Salida, in a red shale unit that underlies the typical quartzite of the Parting. This shale unit extends discontinuously northward to the Leadville area, but it is absent in the Minturn quadrangle. Beds thought by Behre and Johnson (1933) to represent this shale at Gilman are of different character and are herein assigned to the Harding Formation.

From regional studies of the Upper Devonian rocks, and from the fact that most of fish remains in the Parting and correlative units are of fresh or brackish water forms, Denison (1951) concluded that the Parting represents nearshore, shallow-water marine deposits, possibly including freshwater stream-channel and flood-plain deposits. Character of the Parting in the Minturn quadrangle supports such a conclusion. The widely occurring molds of brachiopods and crinoids indicate marine deposition, but the lenticular conglomerates suggest channel deposition, particularly as they show crossbedding of the stream gravel-bar type. General increase in coarseness of the Parting north-eastward suggests a source area and depositional margin not far northeast of the Minturn quadrangle, if not at the site of the Gore Range. From studies of crossbedding and grain size in the Parting from Minturn westward to Rifle, Campbell (1967) concluded that the lower part of the Parting was derived from sources to the east and the upper part was derived from sources to the north. Local areas of nondeposition of the Parting were recognized by Singewald (1931) in the Alma district, 16 mi (25 km) southeast of the Minturn quadrangle.

Throughout the region, the Parting Formation is separated from underlying rocks by a major unconformity. The youngest formation known beneath this unconformity is the Fremont Limestone of Late Ordovician age, and regionally the Parting bevels formations of all ages from Fremont down to Precambrian. Though the unconformity was long thought to represent erosion in Silurian time, the discovery of Silurian and Upper Ordovician limestones in diatremes in the Front Range (Chronic and others, 1969) along with other, indirect evidence suggests that both the Fremont and a Silurian limestone may once have been widespread over the state. If so, these rocks were eroded in Early and Middle Devonian time, when most of the Rocky Mountain region was a land area (Poole and others, 1967; Sandberg and Mapel, 1967). The paleontological data just discussed indicate that in the area of the Minturn quadrangle erosion probably continued through the early part of the Late Devonian also.

DYER DOLOMITE

The Dyer Dolomite lies conformably, locally with gradational contact, upon the Parting Formation and is unconformably overlain by the Gilman Sandstone. The Dyer is uniformly 75–80 ft (23–24 m) thick in most of the area near Gilman and southward to Leadville. In a few places, however, the overlying Gilman Sandstone fills broad channels cut to depths of as much as 25 ft (7.5 m) into the Dyer, reducing the thickness of the Dyer to as little as 50 ft (15 m).

The Dyer consists almost entirely of dolomite, which characteristically is fine grained and thin bedded and breaks into small, sharp, hackly fragments (fig. 9). The dolomite is gray to black; much of it is finely laminated in shades of gray. The laminations are wavy, and Campbell (1970) has interpreted them as stromatolitic in origin. In outcrop, the lower half to two-thirds of the member weathers light buff or yellowish gray, and the upper part weathers dark brown to bluish gray. Argillaceous matter coats many of the bedding planes and occurs also in scattered beds of shaly breccia in the lower, yellow-weathering unit. Such beds are bounded by wavy bedding surfaces that are evident minor discontinuities or diastems; they commonly have a bleached-looking, light-gray or yellow color and lie upon dolomite that is similarly bleached to depths of a few inches. Such argillaceous breccia zones are interpreted as weathered zones formed during periods of interrupted deposition and temporary exposure. Other beds in both the lower and upper parts of the member have a fine

breccia structure but are without argillaceous matter or bleaching. These are interpreted as wave breccias.

Within the canyon of the Eagle River and in adjoining mines, the Dyer contains several distinctive and persistent beds that are useful as stratigraphic markers. A 7-ft (2.1-m) bed that contains abundant black chert in small nodules and lenticular stringers is present 15 ft (4.5 m) above the base. Thin but persistent shale partings occur at 22 and 32 ft (6.7 and 9.8 m) above the base. At 45 ft (14 m) above the base is a bed of dense black dolomite 3–8 ft (1–2.4 m) thick that shows in cliff exposures as a black band at or near the boundary between the yellow- and the blue-gray-weathering parts of the member. At the base of this black bed is a thin sandy stratum known locally as the "sand grain marker."

The "sand grain marker" is typically 1–2 in. (2.5–5 cm) thick, but locally it is as thin as 1/4 in. (6 mm) or as thick as 5 in. (13 cm). It consists of dark dolomite sprinkled with rounded, frosted quartz sand grains generally 0.5–1 mm in diameter. In some places the sand grains are so abundant as to constitute a sandstone. In others, they are so sparse as to require very close scrutiny for identification; nevertheless, this thin stratum has proved to be remarkably persistent and widespread (Lovering and Tweto, 1944, p. 23; Tweto, 1949, p. 175; Banks, 1967). Other sandy zones of similar character occur locally in the upper part of the Dyer, and Campbell (1970) has noted the presence of disseminated quartz sand grains and local thin stringers of sandy dolomite throughout the uppermost part of the Dyer in the White River Plateau area. The frosted, well-rounded grains of the "sand grain marker" and other, local, sandy layers are interpreted to be of eolian origin, blown from coastal dunes into the shallow waters and tidal flats in which the carbonate muds of the Dyer accumulated.

Character of the Dyer is illustrated by the following stratigraphic section, measured in the canyon of the Eagle River.

Section of the Dyer Dolomite

(Measured along first gully north of Rock Creek, beginning at abandoned highway grade below U.S. Highway 24 (See fig. 8))

	Thickness (feet)	Distance above base (feet)
Gilman Sandstone:		
Quartzite and dolomite breccia.		
Unconformity.		77.8
Dyer Dolomite:		
16. Dolomite, gray, brown- to gray- weathering, finely crystalline, brittle, thin-bedded	9.0	68.8
15. Dolomite, dark-bluish gray, finely crystalline, brittle, hackly, thin- bedded, and finely banded	3.5	65.3
14. Dolomite, tan-gray, finely crystalline, brittle, thick bedded	2.0	63.3



FIGURE 9.—Thin-bedded dolomite characteristic of Dyer Dolomite in roadcut of abandoned highway 0.3 mi (0.5 km) northwest of Gilman. Hammer (arrow) shows scale.

Section of the Dyer Dolomite — Continued

Dyer Dolomite — Continued	Thickness (feet)	Distance above base (feet)
13. Dolomite, grayish-black, finely crystalline, thin-bedded, contains $1/8$ - $1/4$ in. mud lumps at top	4.0	59.3
12. Dolomite, black, dark brown-gray weathering, medium-crystalline to finely crystalline, medium-thin-bedded	5.0	54.3
11. Dolomite, shaly, gray, thin-bedded	8	53.5
10. Dolomite, blue-black, finely crystalline, massive. Weathers dark blue-gray to black. "Black marker bed." 2- to 5-in. bed of sandy dolomite at base is "sand grain marker"	8.0	45.5
9. Dolomite, dark gray; weathers light buff to greenish gray; is thinly bedded; forms massive bed	10.0	35.5
8. Dolomitic shale, dark gray, thin-bedded; grades upward into overlying bed. "Shale marker"	3.0	32.5
7. Dolomite, argillaceous, dark bluish-gray grading to gray downward, green buff weathering, fine-grained, irregularly bedded	9.0	23.5
6. Shale, dolomitic, green, thin bedded ..	1.0	22.5
5. Dolomite, cherty, light-gray, buff weathering, fine-grained, thin-bedded. Chert is black, in scattered lenses as much as 18 in. long and 3 in. thick. "Cherty marker"	7.5	15.0
4. Shale, calcareous, gray-green, fissile ..	0.5	14.5
3. Dolomite, light-gray, gray weathering, very fine grained, thin-bedded	4.0	10.5
2. Shaly dolomite, light gray, thin bedded ..	0.5	10.0
1. Dolomite, light gray, finely crystalline, medium-bedded; weathers buff and to smoothly rounded ledge. Contains a few shale partings. Basal 3 ft is very thinly bedded, irregularly bedded, and knobby weathering. Conformable contact with quartzite below	10.0	0
Total measured thickness of Dyer Dolomite	77.8	

Parting Formation:

Sandy quartzite, white and pinkish-white, rust-spotted, coarse- and uneven-grained, is slightly dolomitic in irregular areas.

Under the microscope, typical Dyer Dolomite is seen to consist of dolomite grains averaging about 0.05 mm in diameter, most of which contain minor amounts of opaque dark carbonaceous matter as "dust." This dusty organic matter probably accounts for the dark color of the rock. A few tiny irregular masses, of quartz and of a clay interpreted as halloysite, are also present; no other minerals were observed.

Fossils are rare in the Dyer Dolomite in the northern Sawatch and Mosquito Ranges, but they have been found in several localities farther west and south. We

found none in the Minturn quadrangle, though the Upper Devonian brachiopod *Spirifer whitneyi* var. *animasensis* Girty was reported by Crawford and Gibson (1925, p. 37-38). At Glenwood Canyon, 40 mi (64 km) west of Minturn, the Dyer contains a basal unit of limestone that has yielded an abundant fauna of Upper Devonian brachiopods (Bass and Northrop, 1963, p. J21-26). Similar fossil assemblages have been reported from several localities in the lower part of the Dyer on the western side of the Sawatch Range (Johnson, 1944, p. 329-330) and from the southern end of the range (Dings and Robinson, 1957, p. 15). The fossils from the lower part of the Dyer are the basis for the assignment of the Dyer to the Upper Devonian, though close affinities with Lower Mississippian faunas have been recognized (for example, P. E. Cloud, in Bass and Northrop, 1963, p. J26).

Though the upper part of the Dyer has been classed as Devonian by many authors, it is poorly fossiliferous and its age is not well established. Helen Duncan of the U.S. Geological Survey (in Morris and Lovering, 1961, p. 87) reported that a sparse coral fauna "suggests * * * Early Mississippian age." Both Hallgarth (1959) and Rothrock (1960) concluded from subsurface studies in western Colorado that the upper part of the Dyer passes westward into limestones classed as Lower Mississippian on the basis of lithology and sparse fossils. In southwestern Colorado and adjoining Utah, Baars (1966, p. 2089) reported Early Mississippian endothyrid foraminifera in the upper part of the Ouray Limestone, with which the Dyer is generally correlative. Therefore, we class the Dyer as Late Devonian and Early Mississippian (?) in age.

GILMAN SANDSTONE

The Gilman Sandstone is a thin but widely persistent unit of sandstone, breccia, and dolomite that lies with erosional unconformity upon the Dyer Dolomite and is overlain with erosional unconformity by the Leadville Limestone (or Dolomite). The unit is typically about 20 ft (6 m) thick in the Minturn quadrangle and surrounding region, but it thins locally to about 10 ft (3 m), and in a few places it thickens to as much as 50 ft (15 m). Where thick, the sandstone fills broad channels cut into the underlying Dyer Dolomite. One such channel was observed in the Eagle mine, and others occur south of the quadrangle.

The Gilman is varied in lithology, but in most places a major part is sandstone or sandy dolomite. A basal bed of sandstone 1-2 ft (0.3-0.6 m) thick is commonly present. This bed is generally overlain by a few feet of interbedded sandstone and dolomite in beds that pinch and swell, and this is overlain by lenticular bodies of breccia, dolomite, and sandstone or sandy dolomite. Chert is abundant in some of the breccia and dolomite.

The top of the Gilman is marked in many places by a bed of structureless brown-gray lithographic dolomite called the "waxy bed" by the mine geologists at Gilman and also referred to by that name by Engel, Clayton, and Epstein (1958) and by Banks (1967, p. 41). This bed is irregular in thickness, ranging from a few inches to several feet, and is generally separated from underlying strata by a wavy contact. A more pronounced wavy contact separates it from overlying bedded carbonate rock of the Leadville. Though cut out by unconformity in places, the "waxy bed" has been traced throughout the region from the White River Plateau to the Sangre de Cristo Range (Engel and others, 1958, p. 376; Banks, 1967, p. 36-42).

In cliff exposures of the Chaffee Group and Leadville Limestone (or Dolomite), the Gilman generally shows up as a yellowish-gray massive unit separating thin-bedded gray dolomite of the Dyer below from thick-bedded gray carbonate rocks of the Leadville above. In such exposures, the "waxy bed" commonly forms a shallow indentation in the cliff.

In mineralized areas, the Gilman displays compositional and structural features that are interpreted as products of solution processes. These features are discussed in the report on the ore deposits (Loving and others, 1977). In most unmineralized areas solution features are absent and the sandstone and sedimentary breccia of the Gilman are essentially unmodified. Previous descriptions of the Gilman by us (Loving and Tweto, 1944; Tweto, 1949) were based on studies in the Gilman and Leadville mineralized areas, and they consequently emphasized solution features that are now known to be of restricted occurrence in the Gilman.

Where not modified by solvent action, the unconformity at the base of the Gilman is a smooth but wavy surface that commonly shows relief of several inches in only a few feet along strike, and a relief of several feet over longer distances. Where modified by solvent action, this surface is irregular and is marked by abrupt pits and pinnacles that have relief of as much as several feet. Strata above the modified surface show local sag structures and internal faults and are cut by dikelets of black clay, breccia, quartz sand, or dolomite sand.

Sandstone of the Gilman is yellow to light gray and consists of well-sorted, rounded quartz grains about 0.5 mm in diameter cemented by dolomite, calcite, or silica. Some of the sandstone is speckled with minute particles of white clay. As judged from several thin sections, the sandstone is devoid of detrital heavy minerals. The sandstone closely resembles that of the "sand grain marker" and other thin sand lenses in the Dyer Dolomite, and, like them, it is probably of eolian origin, though obviously reworked in water.

Except in the "waxy bed", the dolomite in the Gilman

is in part identical to the gray, fine-grained, finely laminated dolomite in the underlying Dyer and in part a breccia or edgewise conglomerate of dolomite fragments cemented by dolomite. Both varieties locally contain sparse to abundant quartz grains similar to those of the sandstone, and both varieties occur in cherty or chert-free forms. The "waxy bed," in contrast, is devoid of quartz grains and chert and shows no lamination or bedding.

The chert in the Gilman is predominantly black, but a light-gray to white variety is also present. The chert occurs principally in sharp to somewhat abraded fragments. The fragments are most abundant in the dolomite breccias, but they are scattered through the laminated dolomite also. The chert has been studied in detail by Banks (1970) who distinguished an early variety that was deposited from hypersaline waters penecontemporaneously with the enclosing dolomite, though the chert was broken and redistributed by wave action as dolomite deposition proceeded, and a late chert that transects primary sedimentary structures in the dolomite. Banks attributed the late chert to ground-water action during karst erosion after deposition of the Leadville Limestone.

A section of the Gilman Sandstone in the Gilman area follows. In this locality, the Gilman shows effects of solution and collapse, and also of hydrothermal alteration in some of the dolomite. Sections in other areas show less breccia and little or no hydrothermal alteration (Tweto, 1949, p. 179-180).

Section of the Gilman Sandstone

(Measured in gully in cliffs 0.4 mile northwest of Gilman, at abandoned highway grade below U.S. Highway 24. See fig. 8.)

	Thickness (feet)	Distance above base (feet)
Leadville Dolomite		
Light gray finely crystalline dolomite		
Unconformity, wavy surface.		30.0
Gilman Sandstone		
8 Dolomite "waxy bed"; is dark gray, brown-gray weathering, dense, uniform, hackly fracture, 3-in. layer of black chert at base	9.0	21.0
7 Dolomite, hydrothermally altered; is brownish-gray, porous, vuggy; has zebra-rock structure in patches	1.6	19.4
6 Dolomite, gray, fine-grained; contains sparse black chert	4.6	14.8
5 Sandy dolomite and sandstone, gray, thin-bedded	1.0	13.8
4 Dolomite chert breccia Dolomite fragments are irregular in size and shape; chert fragments are small. Contains scattered chunks of dolomitic sandstone, and a few subangular fragments of limestone as much as 1 ft in diameter. Contact with underlying sandstone very irregular	5.1	8.7

Section of the Gilman Sandstone — Continued

	Thickness (feet)	Distance above base (feet)
Gilman Sandstone — Continued		
3. Sandstone, dolomitic, buff-gray, medium-grained	1.2	7.5
2. Dolomite-chert breccia; has some chunks of sandstone	5.5	2.0
1. Sandstone, dolomitic, tan to gray, medium-grained; single thick bed ...	2.0	0
Total measured thickness of the Gilman Sandstone	30.0	
Unconformity, Dyer Dolomite:		
Dolomite, gray, thin-bedded, and brittle.		

Except for differences in proportions of sandstone and dolomite, the Gilman closely resembles the underlying Dyer in lithology, and like the Dyer, it shows abundant evidence of shallow-water deposition. After detailed study of the upper Dyer and Gilman throughout the region, Banks (1967, 1970) concluded that the dolomite in these units was deposited from shallow hypersaline waters in a mudflat environment subject to agitation by waves and frequent subaerial exposure and that the sand was introduced by wind. Similarly, Campbell (1970) concluded a tidal flat origin for his Coffee Pot Member of the Dyer (equivalent of all the Dyer in the Minturn quadrangle).

The Gilman Sandstone is unfossiliferous, and, like the upper part of the Dyer, it might be either late Devonian or Early Mississippian in age. Kirk (1931) assigned it to the Mississippian Leadville Limestone rather than to his underlying Upper Devonian Chaffee Formation because of the unconformity he recognized at its base. However, the unconformity at its top, not recognized by Kirk, seems to mark a far more significant break in sedimentation. The strata of the Gilman and Dyer below this unconformity are reworked eolian sands and primary dolomites deposited in shallow hypersaline waters. The strata above, in the Leadville, are normal marine limestone, some of which was later hydrothermally dolomitized (Lovering and others, 1977). As seen in local outcrops, the unconformity at the top of the Gilman is a wavy surface with relief of as much as 18 in. (45 cm), but over longer distances the relief is several feet, as indicated by erosional truncation of upper units of the Gilman Sandstone. Some depressions in the surface of unconformity are filled with pebbles of quartzite and chert (Tweto, 1949, p. 179). The quartzite indicates that in some nearby area erosion extended to a stratigraphic level below the Gilman, probably in the Sawatch Quartzite. Banks (1967, p. 41) interpreted the unconformity as a karst erosion surface.

LEADVILLE LIMESTONE (OR DOLOMITE)

In most parts of central Colorado, the carbonate rocks of the Leadville Limestone are predominantly or entirely limestone. Through most of the Minturn quadrangle, however, and southeastward through the Leadville district and the Mosquito Range to the vicinity of Buffalo Peaks, a distance of 42 mi (68 km), the carbonate rocks of the Leadville are dolomite. Through this area the Leadville is accordingly called the Leadville Dolomite. The boundary between the limestone and dolomite facies lies approximately along Cross Creek in the Minturn quadrangle; hence, the Leadville is referred to either as limestone or as dolomite in this report, depending on the area involved.

The Leadville is of prime economic interest because it is the principal host rock of ore deposits at Gilman, Leadville, and Aspen as well as in several lesser mining districts in the Sawatch and Mosquito Ranges. The ore deposits are predominantly in the dolomite facies. East of the Sawatch Range, the belt of dolomite coincides with the width of the Colorado mineral belt (fig. 24).

The Leadville lies unconformably on the Gilman Sandstone and is overlain unconformably either by very thin patches of the Molas Formation or by the Belden Formation of Pennsylvanian age. The unconformity at the top of the Leadville is a karst erosion surface that irregularly truncates the carbonate rocks. In the canyon area between Minturn and Red Cliff and in the Eagle mine, the Leadville ranges from 110 to 140 ft (34 to 43 m) in thickness, except as affected locally by cavities and channels in the karst surface. The Leadville thins to zero at some place beneath the Pennsylvanian rocks east and northeast of the canyon area, for it is absent beneath Pennsylvanian rocks in fault slices along the Gore fault. It also thins southeastward. Two miles (3 km) south of Red Cliff it is 67 ft (20 m) thick, and in the Kokomo district, it is 25 ft (7.6 m) thick (Tweto, 1949, p. 185–186). At Leadville the thickness averages about 80 ft (24 m), although it ranges from 0 to 190 ft (0 to 58 m) (Tweto, 1968b).

The dolomite of the Leadville, from Cross Creek southeastward through Red Cliff to Leadville and beyond, consists of several varieties or facies. Most abundant and oldest is a finely crystalline dark-gray dense dolomite in which bedding is well preserved. Superposed on this are various coarser grained and lighter colored facies resulting from recrystallization under hydrothermal conditions. Bedding is partly obliterated in the recrystallized rocks, making them appear more massive than the medium- to thick-bedded dark dense dolomite. The origin of the dark dense dolomite—whether syngenetic or hydrothermal—has

been considerably debated. (See Radabaugh and others, 1968; Tweto, 1968a.) It was concluded to be hydrothermal by Engel, Clayton, and Epstein (1958), and it is interpreted by us to be hydrothermal.

The character and origin of the various dolomite facies in the Leadville are discussed in the report on ore deposits (Lovering and others, 1977), but as the dolomite facies have a stratigraphic expression in the Gilman area, they are described briefly here. The lower 80–100 ft (24–30 m) of the Leadville in the Gilman area consists of predominant dark-gray to black finely crystalline dolomite and subordinate interbedded medium-gray and medium-crystalline dolomite. The lower 50–65 ft (15–20 m) of the dolomite contains conspicuous black chert. An especially cherty bed about 10 ft (3 m) thick lies about 50 ft (15 m) above the Gilman Sandstone. A persistent streak of fragmental chert—the “chert breccia marker” of the Gilman mines—is at the base of this bed, and above it is dolomite that contains abundant chert in long lenses or thin beds. Banks (1970, p. 3033) concluded that the chert was “precipitated from ground waters as amorphous silica after initial lithification [of the limestone] but prior to or during karst erosion of the formation in Late Mississippian(?) and Early Pennsylvanian time.”

The lower unit of dolomite just described is separated from an upper unit by a brecciated and slightly sandy and shaly dolomite zone 1–4 ft (30–120 cm) thick that is known as the pink breccia. This zone has been markedly affected by bedding fault movement and hydrothermal alteration. It may mark an unconformity within the Leadville, but it has not been identified outside of the mine area.

Above the pink breccia in the Gilman area is an upper unit of the Leadville that consists largely of recrystallized dolomite and is known at Gilman as the “discontinuous banded.” This unit is characterized by abundant patches of zebra rock consisting of alternating bands of black or dark-gray fine-grained dolomite and white coarse-grained vuggy dolomite. The bands are $1/16$ – $1/2$ in. (1.5–13 mm) thick and generally are approximately parallel to the bedding, although markedly discordant locally. The zebra rock in turn has recrystallized irregularly into a coarse-grained, vuggy, light-brown-gray dolomite known locally for its luster as pearly or brown pearly dolomite. Neither zebra rock nor pearly dolomite are confined to the upper unit of dolomite. At Gilman they occur sporadically in the lower unit, and in places elsewhere in the region, as at Leadville, they locally constitute the full thickness of the Leadville. Conversely, dark-gray dense dolomite is abundant at the level of the “discontinuous banded” in many places outside the Gilman area.

Characteristic lithology of the Leadville Dolomite in the Gilman area is shown in the following section:

Section of the Leadville Dolomite

(Measured in gully in cliffs, 0.4 mile northwest of Gilman, starting just below level of U.S. Highway 24. See fig. 8.)

	Thickness (feet)	Distance above base (feet)
Belden Formation:		
Black shale, ocherous at base.		
Unconformity, with karst topography.		126.6
Leadville Dolomite:		
12 Dolomite, light-gray with pinkish-gray streaks, medium- to coarsely crystalline, massive; weathers with light brown, granular, pitted surface; has vuggy zebra-rock structure	13.0	113.6
11 Dolomite, dark-gray, gray-weathering, fine- to medium-crystalline, massive	1.5	112.1
10 Shale, gray, thin-bedded	1.0	111.1
9 Dolomite, light-gray to tan- and blue-gray, medium-coarse-grained, vuggy, massive, slightly calcareous. Weathers brownish and rough	30.5	80.6
8 Dolomite, nearly black, gray-weathering, finely crystalline, dense, massive. Has blocky fracture distinct from that of unit 9. Upper contact is marked by 2-ft shaly breccia zone	7.5	73.1
7 Dolomite, same as in unit 8 but with sharp, hackly, weathered surface, and denser and slightly calcareous. Black shale parting at base	11.0	62.1
6 Dolomite, medium blue-gray, finely crystalline, massive. Weathers blue- to brown-gray and to rounded surfaces. Forms bench at shale parting at top	11.0	51.1
5 Cherty dolomite, bluish gray, blue-gray-weathering, medium-grained, massive. Black chert in lenses $1/2$ –2 in. thick and 3–12 in. long, and in bedding layers 1 in. thick and several feet long; layers 3–6 in. apart. Some zebra-rock structure	5.0	46.1
4 Cherty dolomite, blue-black, dense, finely crystalline, hackly, thin-bedded, contains argillaceous laminae that weather in relief; contains black chert in beds $1/2$ –2 in. thick; interval weathers streaky gray and brown. Base of interval is irregular and wavy, marked by chert	11.3	34.8
3 Dolomite, light gray, medium-fine-grained, massive, dark-brownish-gray weathering, with some vuggy zebra banding. Cherty in upper 3 ft, but chert less abundant and lighter than in interval above. Chert in bedding layers. Some sandy banding with chert	15.3	19.5

Section of the Leadville Dolomite — Continued

	Thickness (feet)	Distance above base (feet)
Leadville Dolomite — Continued		
2. Cherty dolomite, gray-black, dense, fine grained, thin-bedded, hackly. Black chert in 1-in. layers, weathers light gray and brown speckled	10.5	9.0
1. Dolomite, light-gray, buff, and knobby-weathering, finely crystalline; contains thin lenses of chert and chert breccia, and several 1-in. bands of brown-weathering siliceous dolomite	9.0	0
Total measured thickness of Leadville Dolomite	126.6	

Gilman Sandstone:

Dolomite of waxy bed, dark-gray, brown-gray-weathering, dense, somewhat hackly.

The boundary between the dolomite and limestone facies of the Leadville is buried beneath the moraines at the mouth of Cross Creek. The northernmost exposure of the dark dense dolomite facies is on the north side of the bedrock knob west of Bolts Lake (pl. 1). In exposures a mile farther north, near the Minturn Ranger Station, the Leadville above the Gilman is entirely limestone except for irregular patches of coarse-grained vuggy hydrothermal dolomite. This limestone is dark gray, finely crystalline to lithographic, thick bedded to massive, and cherty, and it weathers light bluish gray. Thin sections show abundant recrystallized foraminifera in the limestone.

The limestone facies is poorly exposed in the Minturn area. To the northwest, where it is well exposed, Engel, Clayton, and Epstein (1958) reported that the limestone is divisible into two main units. The lower one, resting on the syngenetic dolomite of the "waxy bed" at the top of the Gilman, consists of medium- to very fine grained, dark- to medium-gray cherty limestone and is commonly about 40 ft (12 m) thick, although it ranges from 30 to 70 ft (9–21 m). The chert is not abundant and is concentrated near the top and bottom of the unit. Exclusive of the chert, the limestone contains from 1.3 to 3.15 percent silica and less than 0.5 percent Al, Fe, Mg, and other minor constituents. The upper unit is a remarkably pure limestone containing 99 percent or more calcite. It is 60–150 ft (18–46 m) thick and is gray, fine grained, and thick bedded. It consists in large part of foraminiferal material but also contains abundant small fragments of other fossils and is locally oolitic.

Despite its composition and the abundance of foraminiferal and other fossil remains in parts of it, the Leadville Limestone of central Colorado is rather poor

in diagnostic fossils. We found no fossils other than recrystallized fragments in it, though the Lower Mississippian brachiopod *Spirifer centronatus* Winchell was reported by Crawford and Gibson (1925, p. 37) from a location a few feet above the Gilman.

The Leadville is classed as Early Mississippian, or late Kinderhookian and Osagean, in age (Weller and others, 1948). A Meramecian or Late Mississippian age for some of the upper strata was reported by Hallgarth and Skipp (1962). However, Skipp later amended her earlier identification of *Endothyra* aff. *E. scitula* Toomey on which the Meramecian age assignment was based (oral commun., Feb. 1969) and, as reported by Conley (1965), she found no foraminifera younger than late Osagean in extensive collections of well preserved microfossils made by Conley in the White River Plateau.

The Leadville is generally recognized as an approximate, if not exact, equivalent of the Madison Limestone of extreme northwestern Colorado and west-central Wyoming. Sando (1967) established that a thin basal dolomitic unit of the Madison in west-central Wyoming is Kinderhookian, that limestone making up the main body of the formation is Osagean, and that a thin upper member is Meramecian.

So far as the Leadville of the Minturn quadrangle is concerned, it is most likely only Lower Mississippian (Kinderhookian and Osagean), because it was here eroded more deeply before deposition of the Pennsylvanian rocks than in areas to the west and northwest.

PRE-BELDEN UNCONFORMITY AND MOLAS FORMATION

As indicated in the preceding section, the Leadville Limestone was unevenly eroded before deposition of overlying marine Pennsylvanian sediments began. Chemical weathering of the limestone during at least the latter part of this erosion period produced a karst erosion surface characterized by caves, sinkholes, and irregular channels, and it also produced a residuum of clay, silt, and chert, derived from the insoluble materials in the limestone. This residuum or regolith, containing varying amounts of admixed materials from other sources, constitutes the Molas Formation.

The Molas Formation was first recognized in southwestern Colorado (Cross and Howe, 1905), where it forms a thin unit associated with the karst erosion surface at the top of the Mississippian limestone and beneath marine Pennsylvanian rocks. Subsequently, it has been recognized at the base of the Pennsylvanian sequence in scattered localities throughout central Colorado, and Henbest (1958) has described generally equivalent units in Wyoming and New Mexico.

In the Minturn quadrangle the Molas occurs principally as a filling in caves and channelways in the Leadville Limestone (or Dolomite), but locally a few inches to a few feet of it lies between the Leadville and the Belden Formation. A few miles south of the quadrangle the Molas reaches a thickness of as much as 70 ft (21 m) in local areas, and at Leadville it is as much as 40 ft (12 m) thick (Tweto, 1968b, p. 688, 701). Where present in such thicknesses, the Molas consists of reworked regolithic materials and silts and sands from other sources. Thus, thickness of the Molas is not a measure of amount or duration of weathering of the Leadville. Because it is so thin and discontinuous in the Minturn quadrangle, the Molas was not mapped as a separate formation but was included with the Belden Formation.

In most exposures in the Minturn quadrangle the Molas has been altered and bleached by hydrothermal action, and the bright yellow and red colors characteristic of the formation elsewhere are uncommon. The principal occurrence is as a filling in caves, which are exposed widely in the mine workings. The Molas of this occurrence consists of sericitic silt, clayey material, very fine grained sandstone, and variable amounts of fragmental chert. Except for some of the chert, these materials are bleached white and are soft and pasty. They normally have a highly contorted, kneaded structure and evidently have flowed plastically independent of their competent wallrocks under the influence of bedding-fault movements and of gravitative adjustments in the massive bodies of sulfide ores. This material is called "shaly lime" by the mine geologists at Gilman, though it is not calcareous.

Lenses of Molas lying at the top of the Leadville (stratigraphic section of the Belden Formation) are principally very fine grained sandstone, some of which is conglomeratic and contains pebbles of quartzite, limestone, and chert. In places a carbonaceous fossil soil zone is preserved at the top of the Molas, immediately beneath the basal shale of the Belden.

The weathering and erosion that produced the regolithic Molas Formation destroyed some part of the stratigraphic record of the Mississippian; therefore, the date at which the Molas began to accumulate cannot be certainly fixed. Erosion probably began in Mississippian time, as rocks representing most of the Upper Mississippian are absent over a wide region in Colorado and bordering areas. The regolith of the Molas, however, probably represents only the latter part of the long time span involved. In the Minturn quadrangle, the Pennsylvanian marine transgression occurred in early Middle Pennsylvanian time. The Molas probably is not much older.

PENNSYLVANIAN AND PERMIAN SYSTEMS

The Mississippian and older rocks of the Minturn quadrangle and neighboring areas are overlain by as much as 10,500 ft (3,220 m) of clastic rocks that are principally Pennsylvanian in age but Permian in the upper part. No physical boundary between the rocks of these two ages has been recognized, and as the time boundary is indistinguishable within unfossiliferous red beds that constitute the upper half of the clastic sequence, the two systems are discussed together.

The Pennsylvanian and Permian rocks were deposited in a long and rather narrow trough that extended from northwestern Colorado southeastward into New Mexico. In central Colorado, this trough lay between two highlands that were the source of the sediments—the Front Range highland on the northeast and the Uncompahgre—San Luis highland on the southwest. Both of these highlands were elements of the so-called Ancestral Rockies, elevated in Pennsylvanian time. Within the trough, coarse clastic sediments were deposited near the bordering highlands, and evaporites were deposited in basins strung along the center of the trough. The regional distribution of these sediments and the general paleotectonic setting have been described by Lovering (1929), Lovering and Johnson (1933), Brill (1952), Curtis (1958), Mallory (1958), and Hallgarth (1967).

The Minturn quadrangle straddles the boundary between the depositional trough and the flank of the Paleozoic Front Range highland to the east. Thus, coarse-grained Pennsylvanian and Permian clastic rocks that cover much of the quadrangle wedge out rapidly against the flank of the Gore Range, which was part of the early highland. The quadrangle also straddles the boundary between the clastic and the evaporite facies of the Pennsylvanian and Permian rocks, and thus the clastic rocks pass westward into gypsiferous fine-grained sediments in the area where the Eagle River leaves the quadrangle.

Many different nomenclatures have been applied to the Pennsylvanian and Permian rocks as a consequence of their relatively great thickness, their lenticularity, their facies changes, and the paucity of diagnostic fossils in their upper half. History of the nomenclature has been reviewed by Brill (1944; 1952) and Tweto (1949) and will be considered only briefly here. Shaly and limy strata at the base of the sequence were originally called Weber shale by Emmons (1882), and coarse clastic rocks of gray aspect above them were called Weber grit. Eldridge (1894) applied the name Maroon formation to all the strata between the Weber shale (or limestone) and what is now recognized as the Jurassic Entrada Sandstone in the Crested Butte area.

In the Tenmile (Kokomo) area immediately southeast of the Minturn quadrangle, Emmons (1898) restricted the Maroon to the lower part of the red-bed sequence above the gray Weber grit and applied the name "Wyoming formation" to the upper part of the red-bed sequence. The term Wyoming was later abandoned, and the term Maroon was applied to all the red beds above the Weber grit (or "Wever? formation") in west-central Colorado (Johnson, 1934). Brill (1942) proposed the name "Battle Mountain formation" for all of the former Weber shale and Weber grit plus all but the uppermost part of the former Maroon. In doing so, he distinguished the former Weber shale as the Belden Shale Member of the Battle Mountain, and he applied the name State Bridge Formation—obtained from a report by Donner (1936, 1949)—to the uppermost and fine-grained part of the red-bed sequence. In the preliminary Minturn report, Lovering and Tweto (1944) applied the term Maroon Formation to all the strata between the Leadville and the Triassic rocks, distinguishing the Belden as a member. In the same year, Brill (1944) abandoned the term Battle Mountain, replacing it with Maroon Formation, and elevated the Belden to formation rank.

On the basis of work in the adjoining Holy Cross quadrangle as well as the work in the Minturn quadrangle, Tweto (1949) defined the Minturn Formation as including the strata, about 6,000 ft (1,830 m) thick, between the Belden and the top of a well-known limestone unit defined as the Jacque Mountain Limestone Member of the Minturn. Pennsylvanian (?) and Permian red beds above the Jacque Mountain were assigned to a restricted Maroon Formation. In this usage, gypsiferous strata were regarded only as facies of the three recognized formations, Belden, Minturn, and Maroon. In the Glenwood Springs area, however, Bass (1958) and Bass and Northrop (1963) applied the southwestern Colorado name Paradox Formation to the main gypsum unit, and referred all Pennsylvanian rocks beneath it (except the Molas) to the Belden, and the pre-Triassic red beds above it to the Maroon Formation. Subsequently, Lovering and Mallory (1962) assigned the gypsiferous rocks to a new formation, the Eagle Valley Evaporite, noting that with disappearance of the Jacque Mountain Limestone Member in the "gypsum basin" immediately west of the Minturn quadrangle, no lithologic basis exists there for distinguishing the Minturn and Maroon Formations. The Eagle Valley was later further described by Mallory (1971).

In summary, the sequence of Pennsylvanian and Permian rocks in the Minturn quadrangle is divided into three units: (1) a thin basal unit, the Belden Formation, 0–200 ft (0–61 m) thick, (2) the Minturn Formation, as much as 6,300 ft (1,920 m) thick, and (3) the Maroon Formation, as much as 4,200 ft (1,280 m) thick. A fourth unit, the Eagle Valley Evaporite, laterally

equivalent to part or all the Minturn and part of the Maroon, is recognizable at the western boundary of the quadrangle but is not distinguished on the map (pl. 1).

BELDEN FORMATION

Interbedded dark-gray to black shale, limestone, and sandstone at the base of the Pennsylvanian sequence in west-central Colorado was first designated the Belden Shale Member by Brill (1942, p. 1385), then the Belden Shale (Brill, 1944, p. 624), and finally the Belden Formation (Brill, 1952, p. 812). The type section as designated by Brill (1942) is in cuts along U.S. Highway 24 on the north side of Rock Creek, opposite Gilman. The name was taken from the station of Belden on the railroad in the canyon bottom below Gilman (fig. 8), and the station name was derived in turn from the Belden mine, in the canyon wall at Gilman.

In the Minturn quadrangle the Belden Formation is exposed only along the canyon of the Eagle River or near the mouths of tributary canyons, as of Turkey Creek and of Rock Creek. In this area the formation is about 200 ft (61 m) thick but it probably wedges out rapidly to the northeast beneath the Minturn Formation, for it is absent along the Gore fault, as is also the lower half of the Minturn Formation. From the Minturn quadrangle the Belden thins southward to as little as 25 ft (7.5 m) (Tweto, 1949; 1953; 1956) and then thickens abruptly to as much as 400 ft (122 m) at Leadville (Tweto, 1968b). Westward from the quadrangle, the Belden thickens to more than 600 ft (183 m) (Brill, 1944, p. 644, 653) and locally to as much as 900 ft (274 m) (Murray, 1958, p. 50). As applied by Bass (1958) and Bass and Northrop (1963), who extended it up to the gypsiferous unit they called the Paradox Formation, it is 600–1,000 ft (183–305 m) thick in the Glenwood Springs quadrangle.

The Belden (fig. 10) consists principally of dark-gray to black shale and interbedded thin-bedded black limestone, but it also contains thin beds of dark-gray fine-grained sandstone and sandy mudstone, and lenses of brown-weathering black dolomite. Locally, it also contains lenses of impure coal a few inches thick and thin beds or lenses of dirty brown anhydrite or gypsum. Proportions of the various constituents range widely, though shale generally predominates. At the type section the Belden contains little sandstone, but elsewhere, particularly to the south, it contains abundant fine-grained sandstone and quartzite.

The base of the Belden is sharply defined and generally is marked by black shale lying unconformably on Leadville Limestone (or Dolomite) or on the regolithic material comprising the Molas Formation. The black shale is the "caprock" of the mineralized area near Gilman; there, the contact with the Leadville

is quite irregular, owing not only to the karst topography at the top of the Leadville but also to low-angle faults along the contact and to slump collapse over a second generation of channels and caves formed by hydrothermal action during mineralization. A porphyry sill of Late Cretaceous age lies within the Belden in the Gilman-Red Cliff area (fig. 18). The sill is 5-30 ft (1.7-9 m) above the base of the Belden and is 30-80 ft (9-24 m) thick.

The top of the Belden is marked in the Gilman area by a channeled surface above which are thick-bedded coarse-grained gray and green micaceous sandstones of the Minturn Formation (fig. 11). In many places, however, the contact with the Minturn is gradational. In such places the contact is placed at the level where sandstone and green-gray micaceous shale begin to predominate over black shale and limestone.

In defining the Belden, Brill (1942, p. 1385-1386) presented a type section that does not clearly indicate the location of the top of the formation, or its thickness.



FIGURE 11.—Channeled contact (at man's hand) between thin-bedded rocks of the type section of the Belden Formation (north of Gilman) and overlying thick-bedded sandstone of the Minturn Formation.

The following emended type section corrects these shortcomings and illustrates in greater detail the character of the Belden.

Emended type section of the Belden Formation and section of the Molas Formation

(Section measured along U.S. Highway 24 on the north side of Rock Creek, 0.25 mi (400 m) north of Gilman. Section begins at U-shaped bend in highway at Rock Creek and extends west southwest along highway to top of Leadville Dolomite at curve where highway turns north. See fig. 6.)

	Thickness (feet)	Distance above base (feet)
Minturn Formation:		
Arkosic sandstone and conglomeratic grit with sparse quartz pebbles.		
Scour-and-fill contact		198.0
Belden Formation:		
27. Clay shale, dolomitic shale, and dolomite, interbedded. Shale is dark gray to grayish black, except some layers at top are dusky red to dark olive gray; is noncalcareous and slightly micaceous, except highly micaceous at top. Some of shale beds cut across underlying beds in troughs as much as 3 ft deep, making pinch- and-swell structure. Dolomite is dark to light gray and in beds 3-12 in. thick	9.5	188.5
26. Shale, bluish gray to dark gray, thin- and irregular-bedded, noncalcareous	6.0	182.5
25. Shale, dolomite, and mudstone, interbedded. Shale is dark gray to black and fissile. Dolomite is mottled		



FIGURE 10.—Belden Formation in roadcut on U.S. Highway 24, 1.2 mi (1.9 km) north of Gilman. Lower part of Minturn Formation is exposed in cliff at upper left.

Extended type section of the Belden Formation and section of the Molas Formation — Continued

	Thickness (feet)	Distance above base (feet)
Belden Formation — Continued		
25. Shale, dolomite, and mudstone — Continued light pinkish gray and light gray; weathers yellowish brown to light orange brown; is thin bedded, vuggy, and medium grained; occurs in beds 3–10 in. thick. Lower 2½ ft of unit is olive-gray dolomitic shale and mudstone. Productid brachiopod impressions in shale 4 ft above base of unit	8.0	174.5
24. Shale and limestone, interbedded; are medium gray; weather light yellowish brown and yellowish gray. Shale is calcareous, micaceous, and laminated. Some is crystalline, in beds 3–6 in. thick	7.0	167.5
23. Dolomite, recrystallized, calcitic, light- gray to white, contains many small vugs lined with coarse crystals of dolomite	0.5	167.0
22. Limestone, shale, and mudstone, dark- gray	4.0	163.0
21. Shale and limestone, interbedded. Shale is dark olive gray to grayish black, fissile, and finely micaceous. Limestone is argillaceous, dense to very fine grained, and medium gray; weathers light olive gray; is medium bedded but breaks into 1-in. rhombic blocks	5.0	155.0
20. Sandy limestone, medium gray; weathers tan; is thin bedded. Quartz sand is fine to very fine grained and most abundant at top	1.0	154.0
19. Shale, somewhat calcareous, and minor interbedded platy dolomitic limestone. Shale is olive gray; weathers light olive gray; is thin and irregular bedded; is fissile and micaceous near top	7.0	147.0
18. Limestone, yellowish-brown to dusky- red, thin-bedded; lower part is micaceous; contains fragments of shale ¼–½ in. in diameter, and small amount of fine sand	1.0	146.0
17. Limestone and shale interbedded. Limestone is dark gray, dense to fine grained, thin to medium bedded; upper 4 in. is banded brown dolomite. Shale is olive gray to dark gray	2.0	144.0
16. Covered zone, mostly dark shale and minor limestone	30.0	114.0
15. Shale and limestone. Shale is medium gray; weathers light gray; is fissile. Limestone is dark to very dark gray, in beds 1–6 in. thick; makes up about 10 percent of unit	4.0	110.0
14. Limestone and shale. Limestone is medium gray; weathers light orange brown; is dense to very fine grained and thin to medium bedded. Shale is		

Extended type section of the Belden Formation and section of the Molas Formation — Continued

	Thickness (feet)	Distance above base (feet)
Belden Formation — Continued		
14. Limestone and shale — Continued medium gray; weathers medium orange brown; is most abundant in lower part of unit	7.0	103.0
13. Limestone, dense, medium-gray to medium-olive-gray, weathers olive gray to yellow brown and blocky, except top 1 ft weathers rounded; 6-in. bed of dark gray shale in middle of unit	4.0	99.0
12. Limestone and shale. Limestone is dark to medium gray, dense to very fine grained, and thin to medium bedded; composes 70 percent of unit. Shale is very dark gray to black, and very thin bedded to fissile	17.0	82.0
11. Shale and limestone, dark gray; weather light orange brown; limestone is platy, in 1- to 2-in. beds	5.0	77.0
10. Mudstone and limestone, clayey, dark- bluish gray, weather olive brown; are thin bedded	7.0	70.0
9. Shale and limestone, interbedded, are dark to very dark gray. Shale is noncalcareous and fissile. Limestone is dense to fine grained, thin to medium bedded, and has flangy to platy fracture, 2 ft bed of limestone at top weathers yellowish brown	20.0	50.0
8. Limestone, dark bluish-gray; weathers yellowish brown to dark brown, somewhat speckled with black; is dense to very fine grained, and medium bedded; has irregular upper and lower surface	3.0	47.0
7. Shale, dark gray to dark greenish- brown; weathers gray to brown; is laminated to very thin bedded	1.5	45.5
6. Mudstone, calcareous, greenish-brown; weathers light buff brown to light brownish gray; has thin, irregular bedding	4.0	41.5
5. Shale, limestone, and shale-chip conglomerate. Shale is black to brownish black; weathers black to gray; is fissile; in top 1.5 ft of unit, is greenish gray, limy, and contains shale fragments as much as 1½ in. across and ¼ in. thick. Limestone is black; weathers light yellow brown to light orange brown; is thin to medium bedded with irregular bedding surfaces; is somewhat vuggy. Unit lies on porphyry sill	10.5	31.0
Porphyry sill, light gray to orange-gray or pinkish gray; weathers buff to yellowish- gray. Approximate thickness of about 60 ft (18 m) is not included in the stratigraphic distances		
4. Shale, black, contorted; lies beneath porphyry sill	2.0	29.0

Emended type section of the Belden Formation and section of the Molas Formation — Continued

Belden Formation — Continued

	Thickness (feet)	Distance above base (feet)
3. Limestone and shale. Limestones is medium to very thin bedded or laminated; is in layers 6–18 in. thick separated by shale partings; contains echinoid spines 3 ft above base.	7.0	22.0
2. Shale and sandstone, interbedded. Shale is grayish black; weathers dark gray; is fissile to very thin and irregular bedded. Sandstone is dark gray, in thin lenticular beds.	18.0	4.0
1. Shale and limestone, dark-gray to black, thin- to medium-bedded. Shale is platy and irregular bedded. Limestone is ahalys and slabby.	4.0	0
Total measured thickness of the Belden Formation	198.0	

Erosional unconformity.

Molas Formation:

Regolithic mudstone and chert; uppermost layer is fissile carbonaceous shale that suggests old soil.	2.0
Sandstone, conglomeratic, white. Matrix is very fine grained, well-sorted quartz and pebbles are white quartz, black limestone and dolomite, and subordinate chert, 1/2–3 in. in diameter	8.0

Total measured thickness of the Molas Formation

10.0

Erosional unconformity marked by pinnacles of Leadville Dolomite rising 10–15 ft (3–4.5 m) above general level of formation; Molas in the depressions between pinnacles.

Leadville Dolomite.

The Belden Formation is moderately to highly fossiliferous. On the basis of its fossils, it has been assigned ages ranging from late Early Pennsylvanian to middle Middle Pennsylvanian, or from Morrowan through Atokan to Des Moinesian. Brill (1944, p. 626) assigned it a Des Moinesian (Cherokee) age based on collections from unspecified localities in west-central and northwestern Colorado. Henbest (in Thomas and others, 1945; also in Henbest, 1946) and Thompson (1945) assigned at least the lower part of the Belden in the Glenwood Springs area to the Morrowan. Bass and Northrop (1963, p. J35) considered the lower 600 ft (183 m) of the Belden in the Glenwood Springs area to be Morrowan in age and the remainder to be Atokan.

The Belden of the type section near Gilman and of nearby localities in the Minturn and Holy Cross quadrangles is classed as Atokan (early Middle Pennsylvanian) in age by Mackenzie Gordon, Jr., and E. L. Yochelson of the U.S. Geological Survey (written commun., Feb. 16, 1966), based on studies of eight collec-

tions of megafossils. The fossils reported by Gordon and Yochelson are listed in table 4. Their statement follows:

The Belden Shale at its type section is relatively fossiliferous throughout, but the fossils are not sufficiently short-ranged to determine a precise age. Nevertheless, it is possible to arrive at an approximate age for this formation. First, the absence of typical Des Moinesian brachiopod species, such as *Desmoinesia muricatus* (Dunbar and Condra) and *Megalobolus mesolobus* (Norwood and Pratt) in the Belden, as well as the presence of *Fusulinella* of late Atokan age in the overlying Minturn Formation eliminates the possibility of Des Moinesian age for the Belden in the Minturn quadrangle. Brill (1944, p. 626) assigned a Des Moinesian (Cherokee) age to the Belden, but his faunal list from unspecified localities includes species that we have not found in the type Belden Shale. It would seem likely, therefore, that Brill's fossils came from areas where Belden-like lithology includes rocks of Des Moinesian age. In a later paper, Brill (1952, p. 814–815) assigned a late Morrowan age to the lower part of the Belden as far south as Glenwood Springs. He assigned an early Des Moinesian (Cherokee) age to the uppermost part at Whiskey Creek Pass, Sangre de Cristo Mountains, and stated that the Belden seems to be a facies that crosses time lines.

The fauna of the Belden Shale in the Minturn region does not contain elements typical of either the fauna of the type Morrow Series of Arkansas or of its Lower Pennsylvanian equivalents in the Great Basin in western Utah and Nevada. The nearest affinities are to be found in the fauna of the upper Pottsville Formation of Ohio and of the Kanawha Member in the upper part of the Pottsville Formation of West Virginia. Of 15 taxa listed in table 4 that have been either definitely or questionably identified to described species, 10 occur in the upper Pottsville of Ohio. A common Belden species has been compared with *Aciculapora eaglenis* (Price) of the Kanawha Formation.

The available evidence points to an Atokan age for the type Belden, though it is not conclusive. Similarities between this fauna and that of the upper Pottsville may be controlled in part by facies. The possibility that the lower part of the Belden might be of late Morrowan age cannot be eliminated entirely.

Extensive search for fusulinids in the Belden of the type section and neighboring areas by L. G. Henbest, Ogden Tweto, and others was generally fruitless, although Henbest found very sparse *Millerella* sp. together with *Endothyra* sp. and *Osgia* or *Girvanella* sp. about 55 ft (17 m) above the Leadville Dolomite and 4 ft (1.3 m) below an ostracode-bearing limestone in the type section of the Belden (L. G. Henbest, written commun., Oct. 2, 1958). As noted by Thompson (1945, p. 42) and Henbest (in Bass and Northrop, 1963, p. J40), the mere presence of *Millerella* does not prove a Morrowan age. Henbest (written commun., Oct. 2, 1958) concluded as follows:

No significant foraminiferal evidence on the age of the Belden shale in the vicinity of the type section has been found. Foraminifera indicating Early(?) Pennsylvanian age have been reported, by me, from Glenwood Springs and Wellsville on the Arkansas River below Salida. The evidence from larger fossils for a Middle Pennsylvanian age of the Belden at the type section is not positive, but I think that it has greater weight than an age determination based solely on correlations with the Wellsville and Glenwood Springs areas. In other words, the Belden shale may, and probably does, differ locally in age. At the type section, a Middle Pennsylvanian age seems most likely.



FIGURE 12.—Lower part of the Minturn Formation, in cliffs on the east side of the Eagle River near Two Elk Creek. Vertical distance from upper switchback in highway to skyline is 1,200–1,400 ft (365–427 m).

The clastic rocks that make up the bulk of the formation are varied but in general are highly arkosic, coarse grained, and poorly sorted. They are extremely lenticular and many of the beds or lenses change rapidly in lithology in short distances. The rocks are also poorly exposed over wide areas. Consequently, the clastic rocks present great difficulties in the tracing of stratigraphic levels and the determination of detailed geologic structure. In contrast, the limestone and dolomite beds interbedded with the clastic rocks are relatively persistent and are moderately well exposed. They constitute the only reliable stratigraphic markers in this thick formation. Though only a few of the carbonate beds have proved to be widely persistent, many others serve as local markers useful in stratigraphic bridging from area to area. In mapping, nearly all the principal carbonate beds were "walked out" as a means of establishing stratigraphic control and determining the presence or absence of faults.

SUBDIVISION

In defining the Minturn Formation, Tweto (1949) designated seven of the principal carbonate beds or zones as members in the Pando area (fig. 13). The lower

three of these—the Wearyman, Hornsilver, and Resolution Dolomite Members—at about 2,600, 2,900, and 3,700 ft (793, 884, and 1,128 m), respectively, above the base of the formation, were newly named at that time. The upper four—the Robinson, Elk Ridge, White Quail, and Jacque Mountain Limestone Members—were named earlier in the adjoining Kokomo district, where they are the host rocks of ore deposits (Emmons, 1898; Koschmann and Wells, 1946). The Jacque Mountain, the highest persistent limestone in the Pennsylvanian-Permian sequence, is the uppermost unit of the Minturn Formation and defines the top of the formation (Tweto, 1949).

Not all of the seven carbonate members are persistent throughout the Minturn quadrangle. Further, the members were defined in the Pando area after most of the mapping in the Minturn quadrangle was completed, and no attempt was subsequently made to trace each one through the Minturn quadrangle. Consequently, only the Robinson, Jacque Mountain, and—to a lesser degree—the White Quail are distinguished widely on the geologic map (pl. 1). The other members are distinguished locally. In the Robinson, which consists of several limestone beds separated by clastic rocks, only

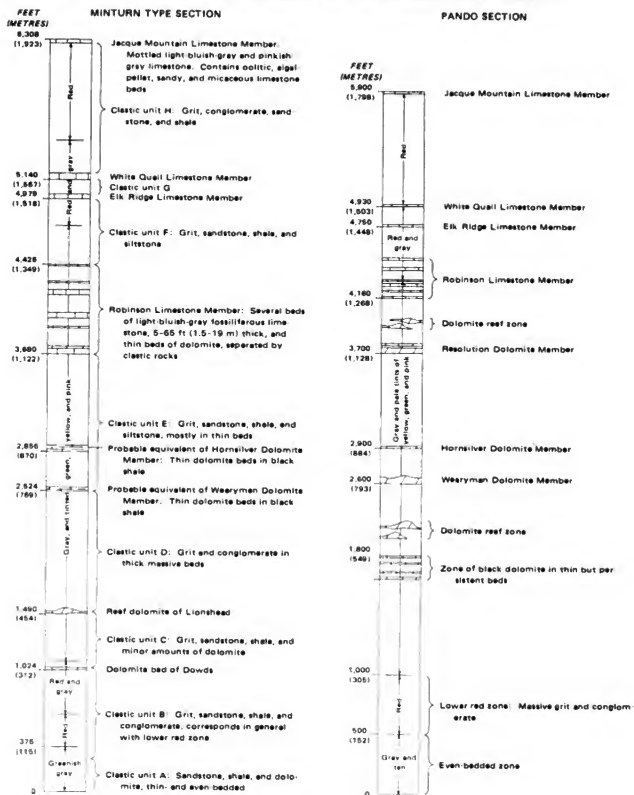


FIGURE 13.—Subdivisions and general character of the Minturn Formation in Minturn quadrangle, and comparison with stratigraphic section in Pando area, Holy Cross quadrangle.

the thickest and most prominent beds are distinguished. These beds are not necessarily the bounding carbonate beds of the member.

Clastic rocks between the various carbonate beds or members are all generally similar except that some of them differ in color, and some units have either more massive or thinner bedding than other parts of the formation. For purposes of reference, the clastic rocks are divided into lettered units A—H, bounded by the carbonate members or by certain carbonate beds of more local occurrence, as indicated in figure 13.

Attempts have been made in the past to subdivide the thick sequence of Pennsylvanian and Permian rocks in the region on the basis of color, as some of the rocks are gray and some are red, but the color boundaries migrate stratigraphically by as much as hundreds of feet in short distances and can be only indefinitely located in thick zones of interbedded red and gray rocks. Thus, except in a very general way, color is unreliable as an indicator of stratigraphic position. The Minturn Formation is predominantly gray, or pale tints of green, yellow, and pink, but it contains a dull red zone in its lower part and a zone of brighter red at its top. In the middle part of the Minturn quadrangle, the lower red zone extends from about 375 ft (114 m) above the base of the Minturn Formation to about 1,075 ft (328 m) above the base; the lower half of this zone is almost entirely red, and the upper half is alternating red and gray. In the Pando area a few miles to the south, in contrast, the lower red zone occupies the interval between 500 and 1,000 ft (152 and 305 m) above the base of the formation (Tweto, 1949, p. 194, 220–222). Similarly, in the Minturn quadrangle, the upper red zone lies about 4,750 ft (1,450 m) above the base of the formation and consists of 700 ft (215 m) of alternating red and gray rocks overlain by 800 ft (245 m) of almost entirely red rocks. In the Pando area (Tweto, 1949), the upper red zone lies 4,300 ft (1,310 m) above the base and consists of about 600 ft (185 m) of alternating red and gray rocks overlain by about 950 ft (290 m) of entirely red rocks.

LITHOLOGY

Exclusive of the volumetrically minor carbonate beds, the Minturn Formation consists of interbedded—or interlensed—grit, sandstone, conglomerate, shale, and siltstone, with grit the predominating and characterizing rock type. As applied here, grit is coarse grained, poorly sorted in size and shape of grains, markedly feldspathic, generally micaceous, and friable to firmly cemented. In most of it, a conspicuous fraction of the grains is very coarse sand (1–2 mm in diameter), and much of it contains abundant particles of granule size (2–4 mm), as well as scattered pebbles, or even cobbles several inches in diameter. Quartz is the most

abundant constituent, but a large fraction of the grains is pink feldspar (microcline) derived from Precambrian pegmatites; plagioclase also is an abundant but less conspicuous component. Many of the feldspar grains are sharp-edged cleavage fragments. Coarse, ragged flakes of detrital muscovite are common in the grit; flakes of dark mica are somewhat less common. In a zone roughly 500–2,500 ft (150–760 m) above the base of the Minturn, the grit also contains rather abundant particles of dark-green chlorite phyllite. Pebbles in the grit are mainly quartz of the bull-quartz type, derived from Precambrian pegmatites and quartz veins, but some are feldspar fragments or rocks of various types, such as pegmatite, granite, and gneisses. The pebbles are well rounded to sharply angular. Pebbles of sedimentary rocks are rare and are found principally in the lower part of the formation.

Most of the sandstone in the Minturn Formation is also feldspathic, micaceous, and poorly sorted; it differs from the grit only in being finer grained and, commonly, in having a smaller proportion of angular grains. Though some relatively pure quartz sandstone is present in the Minturn, particularly in the lowermost part, most of the sandstone and grit is arkose by the definition of Pettijohn (1957, p. 291). Some beds of sandstone and grit contain abundant dark rock and mineral grains and might be called graywackes in the old sense of the term, but they lack the fine-grained matrix that is nowadays implicit in the term (Pettijohn, 1957, p. 301). Petrographic study by Boggs (1966, p. 1414) of 68 samples of sandstone showed very wide ranges in mineral compositions and a mean composition among the detrital grains of 50.5 percent quartz, 34.3 percent feldspar, 6.4 percent micas, 6.3 percent rock fragments, minor amounts of mud coatings and heavy minerals, and a trace of clay minerals. Boggs found that the cement is dominantly calcite but is silica in some samples. His samples apparently came from along Gore Creek and westward along the Eagle River, where rocks of the Minturn are generally finer grained and less feldspathic than those to the south.

Most shales and siltstones of the Minturn Formation are micaceous and sandy, though some gray to black clay shale is also present. Some of the micaceous shale contains as much as 50 percent of detrital mica in flakes 1–3 mm in diameter. Sand and silt in the shale and siltstone are generally arkosic. Boggs (1966, p. 1416) made X-ray diffraction studies of 26 samples of these rocks and found illite present in all samples, chlorite in about half the samples, and mixed-layer clays in several. No discrete kaolinite or montmorillonite were found. In a broader study of the clay mineralogy of the Pennsylvanian rocks in central Colorado, Raup (1966) found that the clay minerals in the finer grained rocks of the Minturn Formation are



A



B

FIGURE 14.—Dolomite in the Minturn Formation in the Pando area. A. Crossbedded gritty dolomite 200 ft (60 m) below base of Robinson Limestone Member, 0.5 mi (0.8 km) south of Minturn quadrangle boundary. B. Conglomeratic dolomite, a local facies of the Hornsilver Dolomite Member, 1.5 mi (2.4 km) south of Minturn quadrangle boundary.

dominantly illite, mixed-layer illite-montmorillonite, mixed-layer chlorite-vermiculite, and, in the lower part of the formation, some kaolinite. The clay and mica fractions in the samples tested ranged from a trace to 100 percent and averaged less than 50 percent. A suite of 12 samples from near Gilman came mainly from the lower red zone in the Minturn.

Carbonate rocks of the Minturn Formation exhibit many unusual lithologic features resulting from the coarse-clastic environment of deposition. Almost all the carbonate beds are locally sandy or gritty, or even contain pebbles. Many grade laterally into grit, conglomerate, or sandstone, passing through such odd facies as conglomerate made up of quartz and pegmatite pebbles in a matrix of dolomite, or dolomite containing 50 percent by volume of coarse arkosic grit (fig. 14). The carbonate rocks are also prominently micaceous in places. Extreme examples are biotitic limestone that contains as much as 10 percent detrital biotite in a matrix of otherwise pure limestone and "schistose" muscovitic limestone that contains so much muscovite in coarse flakes oriented parallel to the bedding that the rock resembles a coarse mica schist.

The limestones of the Minturn are in part very fine grained or sublithographic and in part calcarenitic, consisting of limestone grains and fossil fragments. Most limestone beds or units contain both of these varieties. Boggs (1966), using the classification of Folk (1959), classified most of the limestone as micrite (lithified carbonate mud), biomicrite (carbonate mud with small fossils or fossil fragments), and oomicrite (oolitic carbonate mud). In a detailed study of the Robinson Limestone Member, Tillman (1971) identified four

main facies of limestone: (1) oolite, (2) tubular Foraminifera micrite, (3) phylloid algae facies of biomicrite, and (4) stromatolite facies of laminated micrite. Bedding planes in the limestones are typically rough and scaly, and many near the tops of the limestone units are coated with films of yellowish- or greenish-gray argillaceous matter. In places, such bedding surfaces are studded with small fossils, such as fusulinids. Some limestone units locally contain chert. Most of the limestones are bluish or brownish gray on fresh fracture, but they weather a distinctive light bluish gray. In this respect particularly, the limestones closely resemble those in other Pennsylvanian formations of the region, as in the Hermosa Formation of southwestern Colorado and in the Madera Formation of northern New Mexico.

Dolomite in the Minturn is of three main varieties: (1) Evenly and generally thin-bedded, finely crystalline, dark-gray to black dolomite, most of which weathers brownish gray; (2) massive, vuggy, light-gray to black, brown-weathering, crystalline reef (biohermal) dolomite; and (3) coarsely crystalline, light-gray, buff-to tan-weathering, vuggy hydrothermal dolomite formed either by replacement of limestone or by recrystallization of earlier dolomite. The thin-bedded dark dolomite is generally in layers only 1–5 ft (0.3–1.5 m) thick. This dolomite commonly is interbedded with black shale, and many of the dolomite beds grade on strike into black shale. Some of the dolomite contains abundant black chert, either as long lenticles or as very irregular, scraggly bodies. Also, some of the dolomite is appreciably phosphatic, for it reacts strongly to the qualitative ammonium molybdate test for phosphorus.

The dolomite reefs occur either as isolated bodies surrounded by clastic rocks or as abrupt bulges on thin layers of bedded dolomite or limestone. Most of the reefs have steep and ragged sides; a few have smooth and nearly vertical sides abutted by coarse grits. The reefs are typically a few hundred feet in diameter and 25–100 ft (7.5–30 m) high. However, some are as small as 25 ft (7.5 m) across and 5–10 ft (1.5–3 m) high; others are as large as 1 mi (1.6 km) in diameter. The largest reef in the quadrangle, partly exposed in the bottom of the valley of Two Elk Creek 3 mi (4.8 km) above its mouth, has a visible thickness of almost 500 ft (152.4 m) and a maximum horizontal dimension, including a projecting layer, of about a mile. This and many other reefs contain abundant fossil fragments, particularly in their outer part; some contain areas with concentrically laminated algal structures. The reefs evidently were deposited as algal and bioclastic limestone, and were subsequently dolomitized, perhaps diagenetically.

SEDIMENTARY FEATURES

Many of the lenses of clastic rocks in the Minturn Formation are crossbedded, some of them spectacularly so. Most of the crossbedding is high-angle, medium-scale planar in the classification of McKee and Weir (1953), but simple and trough crossbedding also occur. Scour structures, in addition to those recorded by planar crossbedding, are common also. The scours are of two general magnitudes: (1) small filled channels cut as much as several feet into underlying strata, and (2) channels hundreds of feet wide—seen in cliff exposures—filled by entire beds or lenticular bodies of grit or conglomerate.

Other sedimentary features present in some of the rocks are ripple marks of various kinds and sizes, mud cracks, mud-chip conglomerates, small clastic dikes, raindrop impressions, and, rarely, salt casts.

TYPE SECTION

In defining the Minturn Formation, Tweto (1949) designated the cliffs and area east of Minturn as the type locality but did not present a type section measured at that locality. Instead, he presented a representative section measured in the Pando area, about 10 mi (16 km) to the south. In 1963, T. S. Lovering measured a detailed section of the Minturn at the type locality, presented at the end of this report. That section is here designated the type section of the Minturn Formation, and the section in the Pando area (Tweto, 1949, p. 207–227) is designated a reference section. The main features of the two sections are compared in figure 13.

Because the type section was necessarily measured

over a horizontal distance of several miles in rocks that are shingled against an old highland, the thicknesses measured in the type section are not necessarily a measure of the thickness of the Minturn at any given locality. As shown by cross sections (pl. 1), the distance between the Robinson Limestone Member and the base of the Minturn Formation decreases northeastward toward the Gore Range. This is due to progressive pinchout eastward of clastic beds in the lower part of the formation. The western boundary of the area affected by this pinching is not known but is almost certainly west of the outcrops of the major limestones. Therefore, the vertical distance from any given horizon to the base of the formation probably is less in most localities than that indicated by measurement of stratigraphic thickness along a horizontal course.

CLASTIC UNIT A

The basal unit of the Minturn Formation, here referred to as clastic unit A, is characterized by relatively fine-grained and evenly bedded clastic rocks. The rocks of the unit constitute a transition zone between the underlying shaly and limy Belden Formation and the overlying coarse-grained, lenticular, arkosic grits of the main body of the Minturn Formation. Unit A is 375 ft (115 m) thick in the Minturn type section and about 500 ft (150 m) thick in the Pando section. It consists largely of green-gray and tan sandstone and shale but includes many thin beds of dolomite and a little conglomerate. Grit is essentially absent, thereby distinguishing this unit from the remainder of the formation, and the sandstones and conglomerates are less feldspathic than those in overlying rocks. Raup (1966) found appreciable kaolinite in the shales of this unit, just as in those of the Belden Formation below.

CLASTIC UNIT B AND THE DOLomite BED OF DOWDS

Clastic unit B, about 650 ft (200 m) thick, consists of grit, sandstone, shale, and conglomerate lying between unit A and the top of a distinctive dolomite bed here referred to as the dolomite bed of Dowds. (Named for Dowds siding near the junction of Gore Creek and the Eagle River.) Unit B corresponds in general to the lower red zone in the area near Minturn and is characterized by alternating thin and thick strata. The dolomite bed of Dowds is about 6 ft (2 m) thick; it is mottled greenish gray and black and is cherty. This bed of dolomite is the lowest carbonate bed in the Minturn that is persistent and distinctive enough to serve as a stratigraphic marker.

CLASTIC UNIT C AND THE BLUE DOLomite OF LONSHAD

Clastic unit C, about 450 ft (135 m) thick, consists of strata between the dolomite bed of Dowds and the top of



FIGURE 15.—Dolomite reef in Minturn Formation at Lionshead, on steep slope above Minturn. Note abrupt termination to right (arrow).

a reefy dolomite zone referred to as the reef dolomite of Lionshead. Unit C is similar in lithology to clastic unit B except that it is gray rather than red and contains a few thin beds of dolomite. The reef dolomite of Lionshead consists of discrete reefs strung at intervals along a thin and otherwise inconspicuous bed of dark dolomite. A typical reef in this unit forms the landmark of Lionshead on the slope above Minturn (fig. 15). This reef is 48 ft (14 m) thick but abruptly pinches laterally to two thin dolomite beds separated by several feet of grit.

CLASTIC UNIT D

Clastic unit D, about 1,000 ft (305 m) thick, consists of massive grits and conglomerates between the reef dolomite of Lionshead and the top of a massive grit bed about 200 ft (60 m) thick that is persistent through the cliffs on the east side of the Eagle Valley from Two Elk Creek to Gore Creek (grit marker bed of pl. 1). Clastic unit D constitutes the most massive part of the Minturn Formation. Many of the thickest beds are markedly lenticular; one bed that forms a cliff 200 ft (60 m) high on the shoulder north of Two Elk Creek pinches in a quarter of a mile (0.4 km) along strike to 5 ft (1.5 m). In the Pando area, thin beds of dolomite and also many dolomite reefs occur in this stratigraphic interval, but they are absent at Minturn.

CLASTIC UNIT E AND WEARYMAN AND HORNSILVER DOLOMITE MEMBERS

Clastic unit E, about 1,100 ft (335 m) thick, consists of varied clastic rocks in beds thinner than those in unit D. The base of the unit is marked by the Wearyman Dolomite Member or probable equivalent. The Hornsilver Dolomite Member—or equivalent—is about

330 ft (100 m) above the base. The Wearyman and Hornsilver both change in character northward in the Minturn quadrangle. The Wearyman is a light-colored reef (stromatolitic) dolomite 15–75 ft (4.5–22 m) thick in the Pando area (Tweto, 1949, p. 198) and in the Wearyman Creek and Turkey Creek areas in the southern part of the Minturn quadrangle. On Battle Mountain the Wearyman thins, grades into bedded dolomite, and becomes discontinuous. Farther north, at the Minturn type section at Game Creek, its probable equivalent is a 27-ft (8-m) unit of dark-gray shale that contains thin beds of dolomite (unit 86, Minturn type section). Similarly, the Hornsilver, an 18–28 ft (5.5–8.5 m) of distinctive light-weathering dolomite in the Pando area and in southern part of the Minturn quadrangle, also thins and changes in character on Battle Mountain. In the part of the Minturn type section at Game Creek, the Hornsilver equivalent probably is a dolomitic sandstone and thin beds of dolomite in a predominantly clastic unit 54 ft (16.5 m) thick (unit 94, Minturn type section).

ROBINSON LIMESTONE MEMBER

The name Robinson was first applied by Emmons (1882, p. 220; 1898, p. 2) to a group of three limestone beds separated one from the other by 80–100 ft (24–30 m) of clastic rocks at the Robinson mine in the Kokomo district. Tweto (1949, p. 201) defined the Robinson as a member of the Minturn Formation in the Pando area and adjacent Kokomo district. There, the Robinson consists of 3–5 beds of limestone separated by clastic rocks in a zone 300–400 ft (90–120 m) thick and about 4,200 ft (1,280 m) above the base of the Minturn Formation. In the early mapping of the Minturn quadrangle, Lovering and Tweto (1944) called the limestones of this zone the “Lime Cliffs,” but subsequent mapping in the area between the Minturn quadrangle and the Kokomo district (Tweto, 1953) established that these limestone beds are the same as the Robinson, and the term “Lime Cliffs” was dropped (Tweto, 1949, p. 201).

In the area of the Minturn type section in the Minturn quadrangle, the Robinson member is 746 ft (228 m) thick; it consists of six carbonate beds, each 5–65 ft (1.5–20 m) thick, separated by much thicker intervals of clastic rocks. The increased number of limestone beds and thickness of the member in this area as contrasted with the Pando area result from facies changes in the Resolution Dolomite Member of the Pando area. Northward from the Pando area, thin-bedded dolomite of the Resolution Member grades into thick-bedded to massive light-bluish-gray fossiliferous limestone characteristic of the Robinson, as does also an overlying zone of dolomite reefs and dolomitic grit (fig. 13). These lower limestone beds are accordingly included in the

Robinson, and the Resolution Dolomite Member is not recognized except in the southernmost part of the quadrangle.

The greatest amount of limestone known in the Robinson is along Gore Creek east of the mouths of Mill and Spraddle Creeks. In this area the member includes as many as four major limestone beds 25–75 ft (7.6–22.9 m) thick, as well as several minor beds. From this vicinity, the limestone beds decrease in number and thickness westward toward the evaporite basin, and the limestone also changes in character to a non-resistant and inconspicuous shaly, flaggy non-fossiliferous brownish-gray limestone. On the spur north of Dowds, the Robinson contains no more than two well-defined limestone beds and is a vaguely defined unit of interbedded shaly limestone, shale, and sandstone. Northwestward from this spur, gypsum appears in this limy-shaly zone and gradually supplants the limestone. Cross sections diagramming the changes in the Robinson from Booth Creek westward have been presented by Boggs (1966, fig. 5), and a facies classification of the Robinson over a wider region has been made by Tillman (1971).

Individual limestone beds within the Robinson extend for distances of a few thousand feet to several miles. Generally, as one bed pinches out, it is overlapped by another at a somewhat different stratigraphic level. Thus, the limestone beds have the form of broad lenses, and the member as a whole consists of overlapping lenses of limestone in a matrix of clastic rocks. In places, thin beds of dolomite are also present in the Robinson, and a few limestone beds have dolomite caps. Such dolomite is apparently of early, perhaps diagenetic, origin and is distinct from late hydrothermal dolomite, which irregularly replaces the gray limestone in many places in the southern part of the quadrangle.

In places, limestone beds of the Robinson swell abruptly into massive, vuggy bioherms or reefs consisting of algal bodies, shell fragments, and calcarenite. Most of these bioherms are dolomite, but some are limestone. Good examples, among many, are on the south wall of Gore Creek valley just east of Mill Creek, and on the west wall of the canyon of the Piney River near Moniger Creek.

The Robinson contains a large assemblage of fossils, as discussed under a following heading, but it is characterized particularly by brachiopods, pelecypods, and fusulinids.

CLASTIC UNIT F

Unit F (fig. 13) consists of about 450 ft (138 m) of grit, sandstone, shale, and siltstone, much as in clastic unit E. In the Minturn quadrangle, the lowermost light-red beds of the upper red zone in the Minturn Formation oc-

cur in the upper part of this unit, though most of the unit is gray. In the Pando area, in contrast, the lowest red beds of the upper red zone are in the middle part of the Robinson Limestone Member (fig. 13).

ELK RIDGE LIMESTONE MEMBER

The name Elk Ridge Limestone was first applied by Koschmann and Wells (1946, p. 67) to two beds of limestone separated by 175–225 ft (52–68 m) of red clastic rocks in the Kokomo district. The Elk Ridge was designated a member of the Minturn Formation by Tweto (1949, p. 202) who noted that in the Pando area it is a single limestone bed 7.5–21 ft (2.3–6.4 m) thick. In the Minturn quadrangle the member is also a single bed and, as elsewhere, is discontinuous, passing abruptly into black shale in places. In the area of the Minturn type section it is 30 ft (9 m) thick, but in most places it is no more than half this thickness. It has not been identified with certainty north of Gore Creek. The limestone in the Elk Ridge is in part dark, fine grained, and thin bedded, and in part bluish gray like the Robinson. This lighter variety is mottled pale pink in many places and is generally sandy and locally oolitic.

CLASTIC UNIT G

About 130 ft (40 m) of grit, sandstone, and shale between the Elk Ridge and White Quail Limestone Members constitutes clastic unit G. In the Minturn type section these rocks are gray or pink, but to the southeast in the Pando area and the Kokomo district they are predominantly red.

WHITE QUAIL LIMESTONE MEMBER

The name White Quail was first applied by Emmons (1898) to limestone beds that are the major host rocks of ore deposits in the Kokomo district. Koschmann and Wells (1946, p. 67) further described this unit in the Kokomo district as two, and locally three, beds of dark fossiliferous limestone 5–30 ft (1.5–9 m) thick, separated by clastic rocks, in a zone about 200 ft (60 m) thick. Limestones of this zone were designated the White Quail Limestone Member of the Minturn Formation by Tweto (1949, p. 203). In the Pando area, the zone is reduced to a single 10-ft (3-m) bed of dark-colored oolitic limestone or locally to about 10 ft (3 m) of dolomite and black shale. It thickens northward in the Minturn quadrangle, however, reaching 35–50 ft (10–15 m) in the general area of Mill, Booth, and Middle Creeks. From this area it thins westward toward the evaporite basin and also changes to silty limestone or calcareous siltstone, just as does the Robinson. It has not been identified farther west than the mountain spur north of Dowds.

Throughout the area, the White Quail contains lenses

of black shale, and parts of it grade abruptly along the bedding into clastic rocks, causing marked differences in thickness from place to place. In general, the upper beds grade into grit, and the lower beds into shale or siltstone.

In the southern part of the quadrangle and in the Pando area, the White Quail is a dark-bluish- or greenish-gray, dark-weathering, irregularly oolitic limestone that in many places contains scattered gastropods, cephalopods, and pelecypods. It maintains these general characteristics northward to Gore Creek, except that the weathered surfaces gradually change to light grayish yellow. At Mill Creek the White Quail consists of a lower limestone unit about 15 ft (4.5 m) thick and an upper one about 20 ft (6 m) thick, separated by 10–12 ft (3–3.6 m) of dark shale. The limestones are in alternate thick and thin beds, and the thin beds are calcarenites consisting almost entirely of shell fragments.

North of Gore Creek the limestone changes from dark gray to light gray and assumes many of the characteristics of the Jacque Mountain Limestone Member higher in the section. For this reason, it was misidentified as Jacque Mountain in the original mapping (Lovering and Tweto, 1944) in the Spraddle Creek area, near the Gore fault. In this area much of the limestone is foraminiferal, accentuating the oolitic appearance, and on weathered surfaces it is characterized by very abundant pinhole cavities. It contains thin beds that consist largely of fossil fragments, and contains scattered coiled cephalopods in the thicker beds. It was classified in this general area by Boggs (1966, p. 1408–1410) as biomicrite, oomicrite, and algal oomicrite.

CLASTIC UNIT H

Grit, conglomerate, sandstone, and shale 1,000–1,200 ft (305–365 m) thick lying between the White Quail Limestone Member below and the Jacque Mountain Limestone Member above are referred to as clastic unit H. This unit is almost entirely red, though locally it contains some gray beds in its lower part. Through most of the area the red color is bright, ranging from orange red to maroon, but as the evaporite basin is approached, the color becomes dull red, or grayish red. The clastic rocks of the unit include much conglomerate and are in general coarser than in most of the other clastic units except in unit D.

JACQUE MOUNTAIN LIMESTONE MEMBER

The Jacque Mountain Limestone Member, which defines the top of the Minturn Formation (Tweto, 1949), is the most persistent and consistent limestone bed in the Pennsylvanian and Permian sequence. The

limestone was named by Emmons (1898) for Jacque Mountain (later called Jacque Peak) in the Kokomo district. It has been traced from the Kokomo district northwestward beyond the northern boundary of the Minturn quadrangle, and it has been identified with reasonable certainty in a separate area of Pennsylvanian and Permian rocks 15 mi (24 km) farther northwest along the Colorado River near McCoy (Murray, 1958, p. 54). It also has been identified along the Continental Divide east of the Mosquito-Tenmile Range (observation by Tweto; also Singewald, 1951, p. 11; Brill, 1952, p. 819). Like all the limestones, the Jacque Mountain fades out in the evaporite basin just west of the Minturn quadrangle. Lovering and Mallory (1962) traced it from the Gore Creek area westward to a terminus on the north side of the Eagle River at a point almost exactly on the quadrangle boundary. Boggs (1966) reported that it extends discontinuously about 5 mi (8.1 km) farther west along the north side of the Eagle River, but W. W. Mallory (written commun., 1968) has stated that this extension cannot be confirmed.

The Jacque Mountain (fig. 16) is typically 20–25 ft (6–7.6 m) thick and consists of gray to light-bluish-gray fine-grained limestone with a distinctive combination of features. It is generally oolitic in some part, particularly in the upper beds. Some part or all of the limestone commonly contain clastic materials, such as grit, sand, or micas (fig. 17), and in many places the



FIGURE 16.—Jacque Mountain Limestone Member of the Minturn Formation, on ridge between the heads of Mill and Two Elk Creeks.

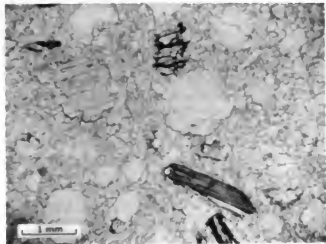


FIGURE 17.—Photomicrograph of biotitic oolitic limestone in Jacques Mountain Limestone Member of Minturn Formation, showing fresh and altered biotite flakes (dark), and oolites recrystallized to large single crystals. Crossed polars.

limestone contains lenses of grit, conglomerate, or siltstone. Locally, the oolites and clastic grains define a crossbedded structure in an otherwise sublitographic limestone (micrite). Beds of intraformational limestone conglomerate are common. Some beds are welded aggregates of irregular pellets a few millimeters in diameter, at least some of which seem to be algal. In places the limestone contains concentric algal structures a few inches to 2 ft (7 cm to 0.6 m) in diameter. In many exposures, some bedding planes are marked by cusps and hollows an inch or two across that look like disorganized cross-ripples. Pink mottling of the gray or bluish-gray limestone is common, particularly in the intraformational conglomerates, and locally some beds are pink throughout. Styolites in the limestone are typically micaceous and are stained red by hematite. Throughout, but perhaps most commonly in the upper oolitic beds, the limestone contains widely scattered coiled cephalopods 2–4 in. (5–10 cm) in diameter, and locally it also contains straight cephalopods, high-spired gastropods, and fragments of pelecypods. These fossils are generally recrystallized to sparry calcite. In at least one occurrence, at the head of Mill Creek, oolites in the top bed of the Jacques Mountain are very soft but coarsely crystalline and were tentatively identified as gypsum. Boggs (1966, p. 1410) classified the limestone in the Jacques Mountain as biomicrite, oomicrite, and algal oomicrite in the east-central part of the quadrangle, and as micrite and intraclast and stromatolitic limestone near the evaporite basin. A series of sections of the limestone along Gore Creek and the Eagle River has been diagrammed by Lovering and Mallory (1962).

CHANGES IN THICKNESS AND FACIES

The Minturn Formation thins rapidly toward the Gore Range by onlap, or the shingling out of the lower units (pl. 1, secs. A–A', B–B', E–E'). On the mountain southeast of the junction of Gore and Black Gore Creeks, typical blue-gray fossiliferous limestone of the Robinson Member is separated from Precambrian rocks by only 50–100 ft (15–30 m) of grit. Similar relations are known on Copper Mountain, in the northern part of the Kokomo district (Tweto, 1949, p. 195; Bergendahl and Koachmann, 1971, pl. 1) where limestone of the Robinson member also lies within 50 ft (15 m) of Precambrian rocks. The same relations also are known or reasonably inferred at several places along the Gore fault north of Gore Creek, as at Bighorn and Pitkin Creeks and near the head of Middle Creek.

As the base of the Robinson Limestone Member lies 3,700–4,200 ft (1,130–1,280 m) above the Belden as measured from the valley of the Eagle River (fig. 13), the relations just described indicate that a minimum of about 4,000 ft (1,220 m) of clastic rocks beneath the Robinson pinches out between the Eagle River and the flank of the Gore Range. Much of the thinning evidently is localized near the Gore fault, for more than a thousand feet (305 m) of grit is exposed beneath the Robinson at Booth Creek, only a mile or two (1.6 or 3.2 km) from the fault. As discussed in the section on structure, the Gore fault is an ancient fault that in Pennsylvanian time formed an abrupt border between the highland area to the east and the basin of sedimentation to the west. In the area along the fault clastic rocks of the Minturn Formation are very coarse. Conglomerates exposed in fault slices on the south slope of Bald Mountain contain abundant 2-ft (0.6-m) boulders and some as large as 4 ft (1.2 m) in diameter.

Westward from the vicinity of the Gore fault, the clastic rocks become finer grained toward the evaporite basin. A partial section measured on the western side of the mountain spur north of Dowds showed predominant sandstone and siltstone and only 5 percent of grit in clastic unit E. Clastic units F and G contain no grit, 15 percent sandstone, 78 percent shale and siltstone, and 7 percent carbonate rocks. These proportions contrast with predominant grit and abundant conglomerate farther east, as described in the Minturn type section. The section near Dowds also illustrates the thinning between carbonate members of the Minturn. The White Quail and Robinson are separated by about 500 ft (150 m) of clastic rocks, in units F and G, in contrast to 700 ft (213 m) in the Minturn type section. Clastic unit E is reduced even more severely, from 1,100 ft (335 m) in the type section to only 350 ft (105 m). Clastic units C and D have the same thickness at Dowds as in the type section, but it should be noted that this part of the type

section is the same distance from the depositional shoreline as in the locality near Dowds.

Westward from Dowds, the Minturn intertongues with, and grades into, gypsum of the Eagle Valley Evaporite (Mallory, 1971, pl. 2). On the north side of the Eagle River, thick units of gypsiferous shale and siltstone alternate with thin units of gypsum, most of which is silty. South of the river, near Stone Creek, gypsum is much more abundant, but its stratigraphic relations are obscured by slumps and landslides. This gypsum probably is the same as that in two beds that are exposed near Avon, 2 mi (3.2 km) to the west. Burchard (1911, p. 362) described these as a lower bed 130 ft (40 m) thick and an upper bed 50–75 ft (15–23 m) thick, separated by 40–50 ft (12–15 m) of clay, calcareous shale, and shaly limestone. Because of the small area of exposure and the obscurity due to slumping, Eagle Valley Evaporite is not distinguished on the quadrangle map (pl. 1).

FOSSILS, AGE, AND CORRELATIONS

The Minturn Formation and equivalents have been classed as mostly or entirely Middle Pennsylvanian in age by many workers (Roth and Skinner, 1930; Brill, 1944, 1952; Henbest, 1946; Tweto, 1949; Stevens, 1962; Bass and Northrop, 1963; Murray and Chronic, 1965). Extensive fossil collections from the Minturn quadrangle, Pando area, and Kokomo district establish that the lower five-sixths of the formation, up through the White Quail Limestone Member, is Atokan and Des Moinesian in age. The age of the uppermost part, comprising clastic unit H and the Jacque Mountain Limestone Member, is not so definitely established but is also classed as Pennsylvanian and very likely Des Moinesian, as indicated below.

Diagnostic fossils—both megafossils and fusulinids—are most abundant in the limestones of the Robinson Limestone Member. Megafossils are also found at various levels from the base of the formation up to the Robinson, but fusulinids have not been found lower than the Hornsilver Dolomite Member. Above the Robinson, the Elk Ridge has yielded a few megafossils and fusulinids. The White Quail has yielded diagnostic megafossils but the few fusulinids found in it are too poorly preserved for identification. Though searched extensively for identifiable fossils, the Jacque Mountain has yielded only a sparse molluscan fauna.

Data on fossils are summarized below from reports by Mackenzie Gordon, Jr., and E. L. Yochelson of the U.S. Geological Survey (written commun., Feb. 16, 1966) on 31 collections of megafossils, and by L. G. Henbest (written commun., May 5, 1958 and Oct. 2, 1958) on 44 collections of fusulinids. The localities of the fossil col-

lections to which we refer in the present report are listed in table 5.

Gordon and Yochelson noted that colonies of the coral *Chaetetes* are the principal fossils in the lower part of the Minturn Formation, and that this form "ranges through about 3,000 feet of beds in this area, the lowest recorded occurrence being approximately 1,420 feet above the base of the Minturn."

From a shale bed about 40 ft (12 m) above the base of the Minturn (loc. 14582-PC) they reported:

Linoproductus cf. *L. prattenianus* (Norwood and Pratten)
Juresania nebrascensis (Owen)
Aviculopecten sp.

From a dolomite reef at a stratigraphic level below the Wearyman Dolomite Member and above the reef dolomite of Lionshead (locs. 9875-PC and 9879-PC) Gordon and Yochelson reported:

Chaetetes sp.
Desmoinesia nana (Meek and Worthen)?
Linoproductus sp. indet.
Anthracospirifer rockymontanus (Marcou)
optimus (Hall)
Condathyrus perplexa (McCheesney)
Sirelochoondria cf. *S. tenuilincata* (Meek and Worthen)
Lima? sp. indet.
Edmondia sp.
Weidyceras sp.

From the Hornsilver Dolomite Member (loc. 14579-PC) Gordon and Yochelson reported:

Caninoid coral undet.
Chaetetes sp.
Multithecopora? sp.
Derbyia crassa (Meek and Hayden)?
Kozłowska? sp. A
Anthracospirifer rockymontanus (Marcou)
Condathyrus perplexa (McCheesney)
Crurithyrus planiconvexa (Shumard)
Cleothyrudina orbicularis (McCheesney)
Composita ovata Mather
Beecheria boudens (Morton)
Glabrocingulum sp. indet.

From limestone about at the stratigraphic level of the Resolution Dolomite Member, or possibly of the Hornsilver Member (loc. 9874-PC) they reported:

Chaetetes sp.
Cidarid spines
Meekella striatocostata (Meek)
Antiquatonia coloradensis (Girty)
Linoproductus prattenianus (Norwood and Pratten)?
Anthracospirifer rockymontanus (Marcou)
Condathyrus perplexa (McCheesney)?
Composita subtilita (Hall)?

and stated:

Occurrence of these fossils with a small timid species of *Fusulinella* indicates a late Atokan age for the collection, according to Henbest (oral commun., 1966). The megafossils are all rather long-ranging Pennsylvanian species not restricted to beds of Atokan age.

TABLE 5.— *Fossil collection localities, Minturn Formation, Minturn quadrangle and vicinity, Colorado*

(Abbreviations for 15-minute quadrangle are: M, Minturn; HC, Holy Cross; ML, Mount Lincoln)

Collection No.	Quadrangle	Locality	Description and remarks
9864-PC	M	Turkey Creek, about 5.5 mi (9 km) northeast of Red Cliff, near mouth of tributary gulch from north that enters Turkey Creek at 10,050-ft contour.	Lower of two prominent beds of limestone of Robinson Member exposed at this locality.
9865-PC	M	Roadcut on U.S. Highway 6 southeast of junction of Gore and Black Gore Creeks, 0.25 mi (400 m) south of highway bridge over Gore Creek.	Limestone of Robinson Member.
9867-PC	M	Meadow at head of Spraddle Creek between 10,600- and 10,800-ft contours, and outcrops on slope on northwest side of creek, about 0.75 mi (1.2 km) southwest of top of Bald Mountain.	Limestone of White Quail Member.
9868-PC	M	Knob marked by closed 10,450-ft contour on ridge on southeast side of Spraddle Creek, about 1.7 mi (2.7 km) south-southwest of top of Bald Mountain.	Limestone of White Quail Member.
9874-PC	M	Crest of ridge between Spraddle and Booth Creeks, at 11,300-ft contour.	Limestone bed probably at about stratigraphic level of Resolution or Hornaiver Member.
9875-PC	M	Two Elk Creek, about 1.7 mi (2.7 km) from its mouth, near 8,750-ft contour at trail and creek.	Dolomite reef stratigraphically below Wearyman Dolomite Member.
9876-PC	M	Ledges in hay meadow on north side of Gore Creek and U.S. Highway 6, 0.5 mi (0.8 km) west of Red Sandstone Creek. (Locality was later covered by Highway 1-70.)	Limestone of Robinson Member.
9879-PC	M	Same as 9865-PC.	
12062-PC	HC	Summit of Ptarmigan Hill (12,154-ft survey point) 0.35 mi (0.56 km) south of boundary of Minturn quadrangle. See Pando map (Tweto, 1953).	Dolomite and black shale of White Quail Member. Unit 101 of Pando stratigraphic section (Tweto, 1949, p. 208).
12063-PC	HC	Southwest shoulder of Ptarmigan Hill. See Pando map (Tweto, 1953).	Calcareous shale equivalent to fourth highest of five limestone beds in Robinson Member. Unit 55 of Pando stratigraphic section (Tweto, 1949, p. 212).
12093-PC	HC	Same as 12063-PC.	
12094-PC	HC	Same as 12062-PC.	
13049-PC	M	Two Elk Creek, at mouth of tributary gulch from north, at 9,100-ft contour.	Limestone boulders from ledges in Robinson Member higher in gulch.
13057-PC	HC	Same as 12063-PC.	
13058-PC	ML	Ridge crest outlined by 11,750-ft contours, 3,400 ft (1,020 m) east of common corner of Minturn, Holy Cross, Mount Lincoln, and Dillon quadrangles, and 500 ft (150 m) south of Dillon quadrangle boundary. See Pando map (Tweto, 1953).	Limestone of Jacque Mountain Member.
13059-PC	M	Same as 9864-PC.	
13060-PC	M	Same as 9867-PC.	
13061-PC	M	Same as 9867-PC.	
13062-PC	M	Same as 9865-PC.	
13064-PC	M	Ridge between Turkey and Wearyman Creeks, 200 ft (60 m) below crest of mountain with triangulation station Shrine on it at elevation 11,876 ft.	Limestone of Jacque Mountain Member.

TABLE 5. — Fossil collection localities, Minturn Formation, Minturn quadrangle and vicinity, Colorado — Continued

Collection No.	Quadrangle	Locality	Description and remarks
14578-PC	ML	100 ft (30 m) east of crest of ridge followed by Eagle County-Summit County boundary, at 12,250-ft contour; 1.4 mi (2.25 km) south of Dillon quadrangle boundary. See Pando map (Tweto, 1953).	Limestone of White Quail Member.
14579-PC	HC	Tributary gulch of Resolution Creek, NW 1/4 sec. 36, T. 6 S., R. 80 W., at 10,700-ft contour. See Pando map (Tweto, 1953).	Dolomite and limestone of Hornsiver Member.
14582-PC	M	Roadcut on U.S. Highway 24 on north side of Rock Creek, 0.25 mi (400 m) north of Gilman.	Green-gray shale with limestone nodules, 40 ft (12 m) above base of Minturn Formation.
14583-PC	M	Same as 9867-PC.	
14584-PC	M	Same as 9867-PC.	
f5757-5760	HC	Southwestern shoulder of Ptarmigan Hill. See Pando map (Tweto, 1953).	Collections from limestone beds of Robinson Member in Pando measured section (Tweto, 1949, p. 211-212): f5757—unit 42; f5758—unit 39; f5759—unit 65; f5760—unit 60.
f5761-5766	ML	Type locality of Robinson Member, in Kokomo district, quarry at site of former town of Robinson. (Locality was later buried beneath tailings ponds).	From the three limestone beds present in the Robinson Member at this locality: f5761b—lower bed; f5761, f5762, f5762b—middle bed at base, middle, and top, respectively; f5765, f5766—upper bed at base and 5 ft (1.5 m) above base, respectively.
f5790	ML	Nearly same as 14578-PC, but on crest of ridge, between 12,300- and 12,350-ft contours.	Limestone of White Quail Member.
f7036-7039	M	Lime Creek, about 3 mi (5 km) above mouth, NW 1/4 sec. 3, T. 6 S., R. 80 W., in clearing on slope above Lime Creek trail.	From three lowest limestone beds of Robinson Member: f7036—base of upper bed, 90 ft (27 m) above second bed; f7037—upper part of second bed; f7038—nodular limestone within second bed; f7039—lowest bed.

Megafossils from the Robinson Member are listed in table 6, which includes one collection, 13049-PC, from float judged to be from the Robinson but not included in the table as prepared by Gordon and Yochelson, who also stated:

Brachiopods characteristic of the Robinson Member and apparently restricted to it in this region are: *Mesolobus mesolobus* (Norwood and Pratt), *Chonetina jeffordsi* Stevens, *Desmonesia muricata* (Dunbar and Condra), *Antiquatonia* aff. *A. hermosana* (Girty), and *Neospirifer coloradoensis* Stevens. These fossils suggest a correlation between the Robinson Member and units 7 to 9 of Stevens (1962) in the McCoy area, about 30 miles northwest of Minturn.

Fusulinids from systematic collections from the Robinson Member in three localities in or near the Minturn quadrangle are listed in table 7, as collected and identified by L. G. Henbest. Of a collection made earlier by Tweto at the same locality as megafossil collections 9864-PC and 13059-PC (table 5), Henbest said (written commun., April 29, 1941):

Two early species of *Fusulina* are present. One is new, and the other is either *Fusulina taosensis* Needham 1937, or a very closely related form. Though the stratigraphic record of these two species is but poorly known, the evolutionary status of these forms indicates

early Des Moines age or perhaps a position in the upper part of the Lampasas Series of Cheney (1940). *Fusulina taosensis* was originally found in the lower part of the Magdalena Group east of Taos, N. Mex. I think that the evidence for an age at least as early as the early Des Moines is good.

Other Foraminifera noted by Henbest from the collections reported in table 7 are:

Bradyina sp.
Calcitonella sp.
Calcivertella sp.
Climacaminna sp.
Cribrodium sp.
Earlandia perparva Plummer
Earlandia sp.
Endothyra sp.
Globobuccina sp.
Monotaxis sp.
Orthoceras sp.
Polystaxis sp.
Quawanella sp.
Serpulopsis sp.
Spiroplectammina sp.
Tetrataxis mulsapensis Cushman and Waters
Tetrataxis sp.
Trepelopsis gnanidis Cushman and Waters
Trepelopsis sp.

TABLE 6. — *Megafauna of the Robinson Limestone Member of the Minturn Formation*
(X, present; ?, questionable occurrence)

Name	Collection No.					
	1004-1009-PC	1005-PC	1006-PC	1007-PC	1008-PC	1009-PC
Coral						
<i>Crinoid</i> sp.		X				
<i>Lophophyllid coral</i>	X					
<i>Chaetetes</i> cf. <i>C. malleoporeus</i>						
Mine Edwards and Hains	X	X				
Bryozoa						
<i>Fenestellid</i>		X				
Echinoderm						
<i>Crinoid stems</i>	X	X	X	X		
<i>Echinoid spines</i>			X			
Brachiopods						
<i>Dorthis crassa</i> (Meek and Hayden)		X		X		
<i>Dorthis</i> sp. indet.	X					
<i>Mesolobus striatostriatus</i> (Owl)		X	X			
<i>Mesolobus mesolobus</i>						
(Norwood and Pratt)		X				
<i>Chonetes affinis</i> Stevens						
<i>Eratasma macropora</i> Barwell						
<i>Eratasma</i> sp.						
<i>Desmanella muricata</i> (Dunbar and Gaudry)				X		
cf. <i>D. insignis</i> (Girty)		X				
<i>Antiquitella</i> aff. <i>A. hermiana</i> (Girty)	X					
sp.				X		
<i>Leptodictya protuberans</i>						
(Norwood and Pratt)	?	X	X			
sp. indet.						
<i>Punctostrophia lenticularis</i> (Shumard)		X				
<i>Antrochoceras rochmansi</i> (Marshall)		X				
<i>Neoschisma coloradensis</i> Stevens		X				
<i>Crurithyris planicosta</i> (Shumard)?		X				
<i>Candylodonta purpurina</i> (McChesney)		X				
<i>Compsochasma</i> (Hall)		X				
sp.				X		
<i>Brachyura</i> cf. <i>B. hendersoni</i> (Morton)	X					
<i>Echinodonta</i> sp. A.						
Pelecypoda						
<i>Perspecta</i> cf. <i>P. akensis</i> Newell						
sp.		X				
<i>Concordium</i> sp.		X				
<i>Schizodus</i> sp.				X		
<i>Spindus</i> sp.		X				
<i>Asterella</i> sp.		X				
Gastropoda						
<i>Belosiphon</i> indet.	X		X			
<i>Knights</i> (<i>Cymatospira</i>) <i>monifera</i> (Norwood and Pratt)		?				
<i>Worthenia subulata</i> (Conrad)		X				
<i>Planorbis</i> (<i>Drepanophorus</i>) <i>parvus</i> (Swallow)		X				
High-spired gastropod						
<i>Gastropoda</i> indet.		X				
Cephalopods						
<i>Pseudoschisma</i> <i>lucense</i> (McChesney)		X		X		

NOTE: In reports prepared later than this table, E. L. Yochelson (written commun., Nov. 14, 1966) and Mackenzie Gordon, Jr. and W. J. Swade (written commun., Nov. 21, 1966) reported the brachiopods *Antiquitella coloradensis* (Girty) and *Crurithyris* sp., the gastropod *Candylodonta* sp., and indeterminate corals in collections from red-mottled cherty limestone of the Robinson Member 1 mi (1.6 km) west of Bald Mountain.

In summarizing the results of studies of the Foraminifera, Henbest said:

All of the fusulinid bearing units, except those with the problematic fauna of F7036, have foraminiferal faunas that indicate a Middle Pennsylvanian age. Of these, none younger than the middle part of the Middle Pennsylvanian was recognized. The fauna represented by F7036 suggests an early Late Pennsylvanian age, but the foraminiferal evidence is opposed by field evidence. Two to observed

that the zone of F7036 is overlain at another locality by beds containing *Mesolobus* sp. A definite solution of this problem remains to be determined.

In addition to the fusulinid species from the Robinson reported by Henbest, other species were reported by Tillman (1971, p. 599) as identified by G. J. Verville: *Fusulina curta*, *F. distenta*, *F. truncatula*, *F. platensis*, and *Wedekindella coloradensis*.

Fauna of the White Quail Member is shown in table 8 as reported by Gordon and Yochelson (written commun., 1966), who noted that:

"*Maximites cherokeeensis* was described originally from the Mulky coal of the Cherokee Shale in Henry County, Missouri, and except for the White Quail specimens this genus and species is not known elsewhere." Regarding *Mesolobus euampygus*, they also noted that: this is the only bed in the Minturn section in which this species has been found. This occurrence suggests a correlation between the White Quail Member and unit 15 of the section recorded by Stevens (1962, p. 618-624) in the McCoy area, the only bed in which he encountered *M. euampygus*.

Most collections of microfossils from the White Quail proved to be devoid of identifiable fusulinids, but in one collection (F5790) Henbest identified "*Profusulinella* sp. or immature specimens of a higher fusulinid."

Fossils in the Jacque Mountain Limestone Member as reported by Gordon and Yochelson (written commun., 1966) include (locs. 13058-PC, 13064-PC):

Schizodus sp.

Perrinites sp.

Dolorothoceras sp.

Donatoceras sp. indet.

Gordon and Yochelson stated:

The *Donatoceras* *** is distinct from the species in the White Quail Member. It is too poorly preserved to name formally but probably is the same species that was collected by Kochmann and Williams near the head of Searles Gulch in the Kokomo district [Kochmann and Wells, 1946, p. 69]. This earlier specimen was described and figured as *Donatoceras* sp. (of Colorado) by Miller and Youngquist (1949, p. 46, pl. 15, figs. 1-7) in their volume on American Permian Nautiloids. Despite this implication of Permian age, Gordon regards the Jacque Mountain species as rather closely related to Cherokee age forms such as *Donatoceras umbilicatum* Hyatt and *D. williamsi* Miller and Owen and rather unlike most known Permian species.

The genera so far recorded from the Jacque Mountain Member range widely through Pennsylvanian and Permian rocks. There is no demanding reason, especially when one considers the rapidity of sedimentary accumulation in the Minturn section, to regard the Jacque Mountain Member as any age but merely slightly younger than the White Quail Member.

In summarizing the age of the Minturn Formation, Gordon and Yochelson stated:

The Minturn Formation is regarded as Middle Pennsylvanian in age, and includes beds of Atokan and Des Moines age. The Robinson and White Quail Members are dated as Des Moines age in age by the

TABLE 7. — *Fusulinids in the Robinson Limestone Member of the Minturn Formation*

Palmgum Hill (Holy Cross quadrangle)			Lime Creek (Minturn quadrangle)		Robinson Member (type locality) (Mount Lincoln quadrangle)	
Limestone No.	Locality No.	Name	Locality No.	Name	Locality No.	Name
4	f5760	<i>Fusulina pristina</i> Thompson				
3	f5759	<i>Fusulina</i> sp.	f7036	? <i>Iowacella</i> sp. aff. <i>I. waternensis</i> (Thompson, Verville, and Lokke)	f5766	<i>Wedekindellina euthysepta</i> (Henbest) <i>Fusulina rockymontana</i> Roth and Skinner
					f5765	<i>Fusulina rockymontana</i> Roth and Skinner
2	f5757	<i>Fusulina</i> sp. (early form) <i>Fusulinella</i> or <i>Fusulina</i> sp. <i>Millerella</i> sp.	f7038	<i>Fusulina illinoensis</i> Dunbar and Henbest	f5762b	<i>Wedekindellina euthysepta</i> (Henbest) <i>Fusulina</i> sp.
			f7037	<i>Wedekindellina euthysepta</i> (Henbest) or <i>W. excentrica</i> (Roth and Skinner) <i>Fusulina</i> sp.	f5761	<i>Fusulina rockymontana</i> Roth and Skinner
					f5762	<i>Wedekindellina</i> sp.
1	f5758	<i>Fusulina</i> sp. cf. <i>F. rockymontana</i> Roth and Skinner ? <i>Fusulinella devexa</i> Thompson <i>Wedekindellina euthysepta</i> (Henbest)	f7039	<i>Fusulina novamexicana</i> Needham <i>Wedekindellina euthysepta</i> (Henbest) <i>Millerella</i> -like foraminifer	f5761-b	<i>Wedekindellina excentrica</i> Roth and Skinner

megafossil content. The Hornsriver and Robinson Members are dated as early Des Moinesian in age by fusulinids. The presence of *Fusulinella* in a collection of unknown horizon dates at least some of the lower part of the Minturn Formation as late Atokan in age.

As indicated by the preceding statements of Gordon and Yochelson, and by Stevens (1962), some of the limestones of the Minturn correlate with limestones in the McCoy area, 12 mi (19 km) northwest of the Minturn quadrangle, where the term "McCoy formation" was formerly applied to the Pennsylvanian rocks (Donner, 1949). On the basis of fossils and, in some cases, physical stratigraphy, the Minturn also is approximately or in some part is equivalent to the Paradox Formation as used by Bass and Northrop (1963) in the Glenwood Springs area, to the Gothic Formation of Langenheim (1952) on the western side of the Sawatch Range, to the Morgan Formation of northwestern Colorado and northeastern Utah (Thomas and others, 1945) to the Hermosa Formation of southwestern Colorado (Bass, 1944; Henbest, 1946), to the lower part of the Fountain Formation of the eastern side of the Front Range (Mallory, 1958), and to the upper part of the Sandia and the lower part of the Madera Formations of the Magdalena Group of northern New Mexico (Henbest, 1946; Brill, 1952; Myers, 1968).

ORIGIN

The Minturn Formation records two alternating environments of deposition: (1) a marine facies, comprising carbonate rocks, black shales, intertonguing evaporites, and probably some even-bedded siltstones

and sandstones, and (2) a nonmarine, largely fluviatile, facies comprising the bulk of the grits and conglomerates and at least some of the associated sandy and micaceous shales. A nonmarine origin of many of the coarse clastic rocks is not directly proved but is inferred from their extreme lenticularity, very poor sorting, general coarseness of grain, extensive crossbedding, channel structures, and the presence in some of them of land plants. The plant remains are not abundant but include fossil tree roots (stigmara), *Lepidodendron*, *Sigillaria*, *Walchia*, fern impressions, and rare petrified wood. In addition, rush, reed, and twiglike impressions are fairly common. Although some of these are marine as indicated by their occurrence in fossiliferous dolomites, most are probably terrestrial, as also are thin coaly or carbonaceous seams in well-defined cyclothemic sequences (Tweto, 1949, p. 211–214; Brill, 1952, p. 820).

Distribution of the two general classes of rocks suggests that normal shallow-water marine sedimentation was interrupted repeatedly by floods of coarse clastic debris derived from the highland area immediately to the east. This debris probably was deposited in the form of shallow-water deltas, bar and back-bar deposits, river flood-plain deposits, and alluvial fans in a recurrent piedmont. When marine conditions prevailed, they extended laterally onto the highland, as shown by the limestones on Precambrian rocks near the Gore fault, and when fluviatile conditions prevailed, they extended to the margins of the evaporite basin.

TABLE 8. — Fauna of the White Quail Member of the Minturn Formation

(X, present; ? , questionable occurrence)

Name	Collection locality and Nos.		
	Snyder Creek	Platteau Hill	Radius Ridge
	9667-PC	13092-PC	14578-PC
	9668-PC	13094-PC	
	13060-PC		
	13061-PC		
	14583-PC		
	14584-PC		
Plants:			
Reedlike plant	X
<i>Lepidodendron</i> sp.	X
Echinoderms:			
Echinoid spines	X
Brachiopods:			
<i>Derbyia crassa</i> (Meek and Hayden)?	X
<i>Mesolobus euamptus</i> (Girty)	X	...
<i>Linoproductus prattenianus</i> (Norwood and Pratten)?	X
<i>Anthracospirifer</i> aff. <i>A. rockymontanus</i> (Marcou)	X
<i>Condathyrus perplexa</i> (McCheaney)	X	...
<i>Composita</i> sp.	X
Pelecypods:			
<i>Nuculoides</i> ? sp. indet	X
<i>Polidoceras</i> sp.	X	...
<i>Myalina</i> sp.	X
<i>Asculopecten</i> sp.	X
<i>Schizodus</i> sp. A.	X
sp. B	X
<i>Pleurophorus</i> sp.	X
Gastropods:			
<i>Bellerophon</i> sp. indet	X
<i>Knightsites</i> (<i>Retapira</i>)? sp.	X
<i>Euphemites</i> sp.	X	?
<i>Bellerophonitid</i> sp. indet	X
<i>Glabrocingulum</i> ? sp.	X	...
Cephalopods:			
<i>Brachycycloceras</i> sp.	X
<i>Kionoceras</i> ? sp.	X
<i>Mooroceras normale</i> Miller, Dunbar, and Condit	X	...	X
<i>Metaceras</i> sp. A.	X	X	X
<i>Domatoceras</i> sp. A.	X	...	X
<i>Liroceras</i> sp.	X	...	X
<i>Ephippioceras ferratum</i> (Cox)	X	...	X
<i>Maximites</i> cf. <i>M. cherokeensis</i> (Miller and Owen)	X

Boggs (1966) and Mallory (1971) have interpreted the sediments of the evaporite basin as products of shallow hypersaline waters in the center of the trough that extended through west-central Colorado, and with this we concur. The open sea with normal marine conditions lay to the northwest, in the area of the Morgan Formation, which closely resembles the marine facies of the Minturn. Evidently, the waters of the Morgan sea repeatedly swept southeastward along the border of the Front Range highland, depositing the marine beds of the Minturn Formation, and just as repeatedly, they are forced back by deposition of the coarse clastic sediments. To what extent subsidence in the basin or trough, pulses of uplift in the highland, or climatic factors control the interplay between spreading of

the sea and the building of clastic dams in it is unappraised, but most likely, all three were involved.

From the absence of kaolinite in all but the basal part of the combined Belden and Minturn, and from the abundance of fresh feldspars, both Raup (1966) and Boggs (1966) concluded that the clastic sediments of the Minturn were derived from a source area—the highland to the east—that was undergoing rapid erosion under conditions of a semiarid to arid climate. Parallels in composition and sedimentary structure between the Minturn rocks and modern sediments in parts of the semiarid West suggest that this was so. Hubert (1960), however, concluded that because of the generally red color of the Fountain Formation—an analog of the Minturn—lateritic weathering under humid conditions prevailed. This interpretation of red sediments in the Minturn and Fountain has been refuted by Walker (1967).

MAROON FORMATION STRATIGRAPHIC RELATIONS

The Maroon Formation as redefined by Tweto (1949) consists of the Pennsylvanian and Permian red beds lying above the Minturn Formation. As applied in the Minturn quadrangle, the Maroon includes all the strata—as much as 4,200 ft (1,280 m) in thickness—between the Jacque Mountain Member of the Minturn and the Upper Triassic Chinle Formation. The base of the Chinle, which in most places is marked by a distinctive sandstone—the Garita Member—was also recognized as the top of the Maroon Formation by Bass and Northrop (1963) in the Glenwood Springs quadrangle and, farther west, by Donnell (1954; 1958).

Throughout the area west and northwest of the Minturn quadrangle, however, other units have been recognized by various authors in the few hundred feet of strata immediately beneath the Chinle. Stratigraphically lowest of these, lying 100–750 ft (30–230 m) below the Chinle, is a distinctive white to orange sandstone called a tongue of the Weber Sandstone in the Maroon Formation by Donnell (1954) and Bass and Northrop (1963), called Weber Sandstone by Brill (1944) and Murray (1958), and called Schoolhouse Sand by Thompson (1949) or Schoolhouse Tongue by Brill (1952). About 50–150 ft (15–45 m) above the tongue of the Weber and 50–100 ft (15–30 m) below the Chinle, in the area west of Glenwood Springs is a cherty dolomite bed a few feet thick designated the South Canyon Creek Dolomite Member of the Maroon Formation by Bass and Northrop (1950), who recognized it as a probable tongue of the Phosphoria Formation.

All the strata between the tongue of the Weber and the Chinle, including the South Canyon, were assigned

to the State Bridge Formation by Brill (1944; 1952), although in one measured section (1944, p. 643) he assigned these strata to the Dinwoody or Moenkopi Formations. At its type locality at State Bridge, 10 mi (16 km) northwest of the Minturn quadrangle, the State Bridge is distinguished from the underlying Maroon Formation by a change from the predominating coarse red sandstones of the Maroon to red siltstone and shale (Donner, 1949). A few miles northwest of State Bridge, Murray (1958) found that the tongue of the Weber ends abruptly; he inferred an erosional unconformity between the Maroon and State Bridge, and such an unconformity has subsequently been confirmed elsewhere in the region (Freeman, 1971).

The part of the State Bridge above the South Canyon Member (Stewart and others, 1972), or above an arbitrary datum 100 ft (30.4 m) higher (MacLachlan, 1959; Oriol and Craig, 1960), has been correlated on lithologic grounds with the Lower Triassic Moenkopi Formation.

It is not yet established whether equivalents of the Weber, South Canyon, and State Bridge or Moenkopi are included within the Maroon Formation as applied in the Minturn quadrangle. More likely, these units are younger than any of the Maroon in the quadrangle. The tongue of the Weber pinches out about 12 mi (20 km) west of the quadrangle, in the area between Walcott and Eagle. The South Canyon or a probable equivalent—the Yarmony Limestone Member of Sheridan (1950)—has not been identified closer to the quadrangle than Walcott or the State Bridge area. The Maroon within the quadrangle contains much siltstone in its upper part, and thus it might include strata equivalent to the lower part, at least, of the State Bridge. However, siltstone is abundant throughout the Maroon, even in the coarse-grained facies of the Pando and Kokomo areas. Therefore, the mere presence of siltstone in the red-bed sequence does not establish presence of the State Bridge.

THICKNESS

In the Minturn quadrangle the Maroon is largely restricted to the area north of Gore Creek, although a few small patches are present on high peaks south of the creek. The formation has a maximum thickness of about 4,200 ft (1,280 m) near Red and White Mountain, as determined from structure sections (pl. 1, secs. A-A', C-C'), but it thins rapidly eastward toward the Gore Range. In the valley of the North Fork of the Piney River 2–3 mi (3–5 km) north of the quadrangle, the Maroon is only 1,700 ft (518 m) thick in the area just west of the Gore fault. East of the fault, where it lies on Precambrian rocks, only 100–300 ft (30–90 m) of it is present beneath the Chinle Formation (Tweto and others, 1970).

CHARACTER

The Maroon Formation resembles the Minturn Formation in lithology—except that it is almost uniformly red, contains only very minor carbonate beds, and grades irregularly upward into a predominating fine-grained facies. A measured section of the part of the formation preserved on Jacque Peak in the Kokomo district (Tweto 1949; 1958) shows that the lower 2,000 ft (610 m) of the formation consists of: sandstone, 35 percent; siltstone and shale, 25 percent; grit, 22 percent; and conglomerate, 18 percent. All these rocks are feldspathic and micaceous, just as are those of the underlying Minturn Formation. Some of the conglomerate beds contain abundant cobbles greater than 4 in. (10 cm) in diameter, and some contain 18-in. (45-cm) boulders. Many of the siltstone beds are calcareous, and some contain thin beds or lenses of fine-grained gray limestone.

In the area north of Gore Creek, the lower 3,000–3,500 ft (900–1,050 m) of the Maroon is moderately well exposed along Red Sandstone Creek and along the jeep road on the ridge to the west of this creek. The exposed rocks are principally brick-red sandstone, siltstone, grit, and conglomerate, just as on Jacque Peak, though collectively a little less coarse in grain. A few nonpersistent beds of gray dense unfossiliferous limestone 2–5 ft (0.6–1.5 m) thick are present among the clastic rocks. The upper 1,000–1,500 ft (300–450 m) of the Maroon is poorly exposed but seems to consist mainly of brick-red sandstone, siltstone, and grit. Much of the siltstone is limy, and some on the slopes above the Eagle River is gypsiferous. One thin bed of mottled gray and red algal limestone about 3,700 ft (1,130 m) above the Jacque Mountain can be traced with difficulty for several miles across the area (pl. 1). We consider it unlikely that this bed correlates with the South Canyon Member or the Yarmony Member of Sheridan (1950) because the red beds above it include much sandstone and grit.

Detrital material in siltstone and silty limestone in the upper part of the Maroon is of the same arkosic composition as that in the grits. In the siltstones, quartz, microcline, plagioclase, muscovite, and chlorite are principal constituents; magnetite is a rather abundant accessory mineral, and tourmaline and zircon are less abundant. The coloring matter is chiefly earthy red hematite or brown limonite concentrated at the grain boundaries. Some of the plagioclase grains are slightly altered, but many are fresh. In the silty limestones, the calcite matrix encloses abundant angular fragments of quartz and subordinate chert, microcline, plagioclase, muscovite, chlorite, and magnetite. The microcline and plagioclase are fresh. The magnetite is in rounded grains. Earthy red hematite coats the clastic grains

and, in some of the limestones, this coating is accompanied by small but well defined crystals of red hematite.

FOSSILS AND AGE

No diagnostic fossils have been found in the Maroon in the Minturn quadrangle, and very few have been found in it or in closely associated units elsewhere in the region. A piece of fossil wood from a level about 200 ft (60 m) below the Chinle Formation on Red and White Mountain was tentatively referred to the genus *Dadoxylon* by R. A. Scott of the U.S. Geological Survey (written commun., 1961), who noted that this species occurs in all the post-Silurian periods of the Paleozoic. Limestone samples from two localities were examined by P. E. Cloud, Jr., of the U.S. Geological Survey (written commun., Feb. 7, 1961). Cloud found no microfossils in the insoluble residues. From thin-section study, he reported abundant fecal pellets 0.4–1.2 mm in diameter in a mottled pink and gray limestone from the saddle between Buffer and Indian Creeks. In a light-gray subaphanitic limestone from sec. 8, T. 5 S., R. 81 W., he found—in different specimens—tiny ostracods and "subspherical to bladder shaped objects about 0.3 mm in diameter and up to 1.2 mm long that suggest a siphonaceous alga similar to *Gymnocodium*." Cloud noted that if the objects are gymnocodium algae, they imply warm shallow water and a Permian age. The ostracods, which were examined by specialist G. I. Sohn of the U.S. Geological Survey, were unidentifiable.

Fossils found in the South Canyon Dolomite Member near Glenwood Springs indicate an age similar to that of the Permian Phosphoria and Kaibab Formations (Baas and Northrop, 1950; 1963). Poorly preserved fossils from the Yarmony Limestone Member of Sheridan (1950) were classed as Middle or Late Pennsylvanian or Permian in age by N. D. Newell (Brill, 1942). Far to the south, in the Salida area, reptilian remains occur in the Sangre de Cristo Formation at a level 1,800 ft (550 m) above a limestone unit that Brill (1952) correlated with the Jacque Mountain. The reptilian fossils were classed as Early Permian (Wolfcampian) in age by Brill (1952), but later collections from the same locality were classed as Late Pennsylvanian (Missourian) by Vaughn (1969).

Thus, the Maroon Formation of the Minturn quadrangle and neighboring areas probably is of Pennsylvanian and Permian age. It is underlain without evident stratigraphic break by rocks of Middle Pennsylvanian (Des Moinesian) age and overlain by rocks of Early Permian (Leonardian) age, and reptilian fossils in the lower middle part of the generally equivalent Sangre de Cristo Formation have been assigned either to the Late Pennsylvanian or the Early Permian.

ORIGIN

The Maroon Formation records a continuation of the sedimentation that produced the Minturn Formation, but under somewhat changed environmental conditions. The average finer grain of the Maroon as contrasted to that of the Minturn and the general decrease in grain size upward within the Maroon suggest that the source land area to the east became progressively less mountainous. Presumably, the abrupt mountain front that existed along the Gore fault in Minturn time gradually was transformed by erosion to a gentler front which migrated eastward through Maroon time, thus continually increasing the distance between the main source of sediments and the site of deposition. The absence of fossiliferous marine limestones, such as those of the Minturn, and the absence of any strata indicating a marine origin—except near the evaporite basin—suggest that the pattern of alternating marine and terrestrial conditions that characterized the Minturn gave way to dominantly terrestrial conditions of sedimentation. The sediments of the Maroon in the Minturn quadrangle are interpreted as stream channel and floodplain deposits at the east and as grading westward into coastal plain or tidal flat and local lagoonal deposits. In the lower part of the formation, these deposits intertongue westward with marine evaporites. The thin and nonpersistent limestones in the Maroon probably formed in desiccation ponds or lagoons rather than in marine waters. Farther west, carbonate rocks, such as those of the South Canyon, represent marine conditions.

The consistent red color of the Maroon also indicates a change in environment from that of the bulk of the Minturn, though the uppermost part of the Minturn was also affected by the change. Raup (1966) concluded from the clay mineral assemblage and particularly from the absence of detrital kaolinite in the fine-grained red beds of the Minturn, Maroon, and State Bridge Formations that the source material could not have been laterite, as has been often assumed, but that the source material was a product of weathering in a semiarid to arid environment. Walker (1967) concluded from an extensive study of red beds in the Maroon and Minturn and from close mineralogic parallels with red beds that are forming at present in Baja California that the red color formed after the deposition of the sediments, by alteration of iron-bearing minerals, in an arid environment. We agree in general with these conclusions but would qualify them somewhat.

The widespread occurrence of evaporites and eolian deposits in the Upper Pennsylvanian and Permian rocks of the Rocky Mountain region (McKee, Oriel, and others, 1967) suggests a regionally arid climate, as does the absence of plant and animal remains in the Maroon

Formation. The abundance of fresh feldspars, even in the siltstones of the Maroon, and the presence of unaltered detrital magnetite and biotite suggest mechanical weathering in an arid environment rather than chemical weathering in a humid, laterite-producing environment. However, hematite does occur as discrete, apparently detrital flakes in company with unaltered detrital biotite and magnetite in some of the siltstones and impure limestones. Such hematite must have been transported to the site of deposition rather than forming there by alteration or by subsequent redistribution of ferric iron by ground water. Assuming, as the clay mineralogy seems to dictate, that lateritic soils did not exist as a source of the detrital hematite, a source might nevertheless be produced by normal weathering in an upland somewhat less arid than the environment of deposition.

One of the factors contributing to the redness of the red beds is the presence of films of hematite in minute fractures within quartz clasts, giving them a pink or red cast. Such quartz occurs as pebbles even in the gray, buff, and green conglomerates of the Minturn Formation. Reconnaissance of the entire Gore Range (Tweto and others, 1970) has revealed that quartz of this character occurs in many hematite-stained fracture zones in the Precambrian rocks of the range. Rocks of the Gore fault zone, for example, are stained red by hematite and contain the hematite-impregnated quartz through widths of hundreds of feet in places. Presumably, this hematite is a product of geologically recent weathering. However, the Gore fault and many of the numerous other faults in the range originated in Precambrian time (Tweto and others, 1970); thus, they were in existence and were exposed to weathering in Pennsylvanian and Permian time. Such faults or fracture zones might have been a source of some hematitic material in the red beds. Most of the hematite, however, probably resulted from alteration of iron-bearing minerals in the depositional environment, as demonstrated by Walker (1967), and from redistribution by ground water of iron liberated by alteration. Alteration of iron-bearing minerals and redistribution of iron need not have been, in their entirety, penecontemporaneous with sedimentation. Indeed, some evidently occurred much later. The lower red zone in the Minturn, for example, transects bedding in a wavy manner that suggests ground-water control; in part at least, this red color may be related to the present topography. On the other hand, the occurrences of typical red-bed rocks, such as pebbles or fragments in nonred conglomerates of the upper Minturn, and of red siltstone chips in dense gray limestone in the Maroon, though rare, indicate that red beds were in existence at the time these conglomerates and limestones were deposited.

TRIASSIC SYSTEM

CHINLE FORMATION

The Upper Triassic Chinle Formation is the only Triassic unit recognized in the Minturn quadrangle. The Chinle is preserved in the quadrangle only in an area of less than a square mile on the northeastern slope of Red and White Mountain. In this area, and also in the Mount Powell quadrangle to the north, it consists of a basal white sandstone or conglomerate 10–25 ft (3–7.5 m) thick overlain by red siltstone. The basal sandstone or conglomerate, earlier referred to the Shinarump Member (Lovering and Tweto, 1944), was later classed as the Gartra Member of the Chinle (Poole and Stewart, 1964). On Red and White Mountain the Gartra seems to be conformable with the underlying Maroon Formation, but a few miles to the northeast, in the Mount Powell quadrangle, it fills shallow channels in the top of the Maroon and in places shows an angular discordance of 1°–2° with the Maroon.

The Chinle is overlain unconformably by the Jurassic Entrada Sandstone. On the northeast shoulder of Red and White Mountain, the red siltstone of the Chinle is about 70 ft (21 m) thick. About a mile to the west, on the west and northwestern ridge of Red and White Mountain, Poole and Stewart (1964) measured 225 ft (68 m) of the siltstone between the Gartra and the Entrada. Thus, a significant unconformity between the Chinle and Entrada is indicated; this pre-Entrada unconformity has been widely recognized in Colorado.

As exposed within the small area on the side of Red and White Mountain, the Gartra Member is about 10 ft (3 m) thick and consists of coarse-grained gray sandstone. On the northwestern side of Red and White Mountain, Poole and Stewart (1964; also F. G. Poole, written commun., 1956) found the Gartra to consist of 25 ft (7.6 m) of crossbedded conglomeratic sandstone. The pebbles consist of quartz, chert, and quartzite and are as much as 3 in. (7.6 cm) in maximum dimension. The sandstone also contains silicified wood in fragments or in segments of logs. A few miles north of the boundary between the Minturn and Mount Powell quadrangles, the Gartra is in some places a massive crossbedded coarse-grained sandstone and in others a conglomerate characterized by abundant silicified wood (Tweto and others, 1970).

The red siltstone of the Red and White Mountain area is divided by Poole and Stewart (1964) into a lower mottled member and an upper red siltstone member. The mottled member, about 25 ft (7.6 m) thick, consists of red and purple mudstone, siltstone, and sandstone. The red siltstone member consists of brick red siltstone, much of which is calcareous, and subordinate fine-grained red sandstone. As seen in thin section, the

siltstone from Red and White Mountain consists of silt-sized angular fragments of quartz and equant grains of calcite, fairly abundant accessory leucoxene in rounded grains, and interstitial red hematite. Very sparse, small flakes of muscovite are also present but no detrital feldspar fragments were observed. The calcite appears to be detrital rather than a matrix cement as it is in the Maroon siltstones. The scarcity of mica and absence of feldspar suggest that the rock is more mature than the siltstones of the underlying Maroon and Minturn Formations; possibly the Chinle rocks were derived in part from the reworking of red beds in these older formations.

JURASSIC SYSTEM

Two Upper Jurassic formations, the Entrada Sandstone and the Morrison Formation, were mapped in the Red and White Mountain area, the only locality where rocks of Jurassic age are preserved in the Minturn quadrangle. The Morrison of this locality and also of the area immediately north of the quadrangle (Tweto and others, 1970) contains much sandstone in its lower part. Some of this sandstone may be equivalent to units of the Sundance Formation as recognized in the State Bridge area by Pippingos, Hail, and Izett (1969) or to the Curtis Formation of Baker, Dane and Reeside (1936).

In the area just north of the Minturn quadrangle, the Entrada is absent and the Morrison rests, successively eastward, on Chinle, Maroon, and—a few miles east of the Gore fault—on Precambrian rocks (Tweto and others, 1970). Some part of the erosion that destroyed the Chinle or reduced it to thin remnants may be attributed to the pre-Entrada period of erosion discussed in the preceding section. A part, however, was caused by pre-Morrison erosion that removed the Entrada in a belt near the Gore fault and beveled an even surface across rocks of the Maroon Formation and remnants of the Chinle. East of the Gore fault, this surface beveled Precambrian rocks also.

ENTRADA SANDSTONE

As exposed on Red and White Mountain, the Entrada consists of about 60 ft (18 m) of cliff-forming, massive, bluff-to orange-weathering crossbedded sandstone. A generally similar character and thicknesses ranging from 62 to 109 ft (19 to 33 m) are reported in localities from 8 to 20 mi (13 to 32 km) west of the quadrangle (Sheridan, 1950). In outcrop, the Entrada appears to be conformable with the underlying Chinle Formation and the overlying Morrison, but regional relations indicate that both contacts are unconformities.

The sandstone of the Entrada on Red and White

Mountain is compact, homogeneous, and fine grained. It consists of well-sorted subangular to subrounded equant sand grains about 0.1 mm in diameter and of small amounts of interstitial clay and orange goethite. The scattered coarse sand grains that characterize the Entrada in many places were not noted at this locality. The grains of the sandstone are mostly quartz, but chert is fairly abundant and a few grains of fresh microcline and slightly argillized plagioclase are also present. The interstitial clay is a mixture of hydromica and kaolinite, which locally contains small specks and irregular masses of goethite. No detrital heavy minerals were observed in thin section.

MORRISON FORMATION

In the small area of exposure on Red and White Mountain, the Morrison Formation consists of about 250 ft (76 m) of sandstone and shale unconformably overlying the Entrada Sandstone and unconformably underlying the Cretaceous Dakota Sandstone. This thickness is small as compared with about 500 ft (150 m) of Morrison in the southern part of the Mount Powell quadrangle (Tweto and others, 1970) and the 350–400 ft (105–120 m) shown on a regional isopach map (Craig and others, 1955). The abundance of sandstone in the Morrison at Red and White Mountain suggests that only the lower part of the formation is present and that the upper part was eroded prior to deposition of the Dakota.

The Morrison of Red and White Mountain, and the lower half of the formation as exposed just north of the Minturn quadrangle, consists of predominant sandstone, subordinate interbedded green and gray clay shale, and a few beds of fine-grained gray limestone. The upper part of the formation—north of the quadrangle—is mainly variegated shales.

The sandstone is characterized by uneven, lenticular bedding and by abundant particles of white clay that give the rock a chalky appearance. The clay occurs interstitially and also as discrete grains or granules. Some beds of the sandstone contain scattered granules and pebbles of chert and quartz. Thin sections show that the grains in the sandstone are poorly sorted, subangular to subrounded, and from 0.2 to 2 mm in diameter. In most parts of the rock these grains have the interlocking sutured grain boundaries of a quartzite, but in small irregular areas a few millimeters in diameter, the individual sand grains are separated by a matrix of fine-grained calcite. In the basal sandstone, the detrital sand grains consist largely of quartz, with subordinate chert, calcite, and fresh microcline, in order of decreasing relative abundance. A few rounded detrital grains of zircon and green tourmaline are present also. Sandstone above the basal bed

is similar in character except that it contains chalky white grains of argillized feldspar and a few rounded masses as much as 2 mm in diameter of white clay. Specks of light-brown limonite averaging about 1 mm in diameter are abundantly and evenly disseminated through some of the rock.

Limestone of the Morrison is typically dense, thin bedded, lithographic, and medium gray to light bluish gray. Some of it contains irregular olive-gray chert nodules as much as one-half inch (1 cm) long. Some beds, and particularly a 5- to 10-ft (1.5- to 3-m) thick bed that is 10-15 ft (3-4.5 m) above the base of the formation, contain abundant spherical algal structures 1-3 mm in diameter that were identified as charophyte remains by Richard Rezak, formerly of the U.S. Geological Survey (oral commun., 1951). The presence of charophytes is conclusive evidence of the nonmarine origin of this limestone (Peck, 1957, p. 1).

CRETACEOUS SYSTEM DAKOTA SANDSTONE

The Dakota Sandstone is the youngest formation in the sequence of consolidated sedimentary rocks preserved in the Minturn quadrangle. Only two small remnants of the Dakota—on the northeastern slope of Red and White Mountain—remain in the quadrangle, but the sandstone is widespread to the northwest and north. Just north of the quadrangle (Tweto and others, 1970), the Dakota is 150-160 ft (45-48 m) thick. Except for 25-35 ft (7.5-10.5 m) of dark-gray thin-bedded shaly sandstone at the top, it consists entirely of light-gray sandstone. In some places the sandstone is medium to thick bedded and contains thin argillaceous seams and nodules; in others it is very massive, crossbedded, and is composed of a clean quartz sand. Lenses of conglomerate a few inches thick occur locally at the base of the sandstone or scattered through the lower 5-10 ft (1.5-3 m) of it. At localities farther north, as much as 40 ft (12 m) of conglomerate is present at the base of the Dakota. Pebbles in the conglomerate are typically about one-half inch (1 cm) in diameter, are well rounded, and consist of chert, quartz, and white silicified volcanic rock.

The sandstone of the Dakota is brittle but is hard and resistant, and it has a tendency to fracture into blocks that slide on the shales of the underlying Morrison Formation and slopes below. An area of several square miles east of Red and White Mountain is littered with blocks of Dakota, and it is evident that the two small patches of Dakota bedrock near the top of the mountain are the last remnants of an extensive sheet that has been destroyed by sliding of detached blocks.

UPPER CRETACEOUS AND TERTIARY IGNEOUS ROCKS

Igneous rocks younger than Precambrian occur only in scattered areas in the Minturn quadrangle. They include (1) a persistent sill of quartz latite porphyry in basal strata of the Belden Formation along the canyon of the Eagle River; (2) scattered small dark dikes in the Gore Range; and (3) patches of basalt and tuff on the sides of the Piney Rivery valley in the northwestern corner of the quadrangle. The sill is a northern extension of the group of porphyry bodies that characterize the Colorado mineral belt at this general longitude. The northwestern edge of the main belt of abundant and varied porphyry bodies is in the Pando area, about 5 mi (8 km) south of the Minturn quadrangle.

PANDO PORPHYRY SILL

The quartz latite porphyry of the sill exposed along the canyon of the Eagle River was named the Pando Porphyry by Tweto (1951), who traced it to the Leadville area, where distinctive altered facies of it had been known as "White porphyry" and "Mount Zion porphyry" (Tweto, 1956). Throughout the area between Gilman and Leadville, the Pando Porphyry occurs principally in one or more sills near the base of the Belden Formation, but it also forms sills in the Sawatch Quartzite and the Minturn Formation. The sills become thinner and less numerous northward; from near Pando northward into the Minturn quadrangle, only one sill is present. This sill—in the Belden—is more than 100 ft (30 m) thick near the quadrangle boundary and about 80 ft (24 m) thick at Gilman. North of Gilman it tapers more rapidly and apparently comes to a wedge end in a covered area south of the mouth of Two Elk Creek.

Geologic relations show that the Pando is the earliest and most widespread of all the porphyries in the mineral belt in the southern Gore and Mosquito Ranges. Isotopic dating by the K-Ar method established a Late Cretaceous age of about 70 m.y. (million years) for it (Pearson and others, 1962).

The Pando Porphyry is altered wherever exposed in the Minturn quadrangle and through most of the region to the south. The only known unaltered occurrences of it are in the center of a source plug or stock north of Leadville. The widespread pervasive alteration is deuteric. In mineralized areas, a later hydrothermal alteration is superposed on the deuteric alteration, but as the chemistry of the two stages was generally similar, the second alteration merely accentuated the first one, and the two are difficult to distinguish.

The deuterically altered porphyry consists mainly of

an aphanitic groundmass; phenocrysts constitute only 1–10 percent of the rock. The phenocrysts are principally altered plagioclase, typically in prisms 2–4 mm long, and smaller shreds of altered biotite. Quartz phenocrysts are generally present in smaller amounts, and potassium feldspar and smoky muscovite phenocrysts locally are scattered sparsely through the rock. The altered porphyry is light gray to orange gray or pinkish gray and weathers buff to yellowish gray.

As seen in thin section the deuterically altered rock consists of a slightly trachytoid groundmass and sparse phenocrysts. The phenocrysts are mainly plagioclase (oligoclase) and biotite, invariably strongly altered, but also they include quartz in rounded to subhedral grains and occasional grains of moderately fresh potassium feldspar. The groundmass consists of these same minerals together with anorthoclase. Spene and apatite are minor accessory minerals.

In outcrop, sills of Pando Porphyry generally are characterized by a thin platy structure near and parallel to the contacts and by a crude columnar structure in the interior (fig. 18). Primary flow structures,

described in detail by Tweto (1951), include textural layering, mineral orientations in the outer parts of a sill at right angles to the orientation in the body of the sill, intrusive-stage folds and faults, and the platy parting, which was produced by differential laminar flow. These features were interpreted by Tweto to indicate a relatively viscous magma as compared with other porphyries that do not show these features. The structural features indicate intrusion from the south-southeast, the general direction of the presumed source pluton near Leadville.

Chill zones in the Pando Porphyry sills generally are only a few inches thick, but locally they were thickened to as much as 3 ft (0.9 m) by the intrusive-stage drag folds and thrust faults. The contacts between the chilled and unchilled porphyry are sharp discontinuities that reflect differential flow while the sill magma cooled and solidified. The chilled porphyry is glassy in appearance, though microscopic study shows that most of it is finely crystalline.

Sedimentary rocks in contact with Pando Porphyry generally show only slight metamorphism. Black shale,



FIGURE 18.—Columnar structure in sill of Pando Porphyry exposed in cut on U.S. Highway 24, one-half mile (0.8 km) north of Gilman. Thin-bedded strata of the Belden Formation are above the sill, and a karst pinnacle of Leadville Dolomite casts shadow on embankment below highway.

the common wallrock of the porphyry, is only slightly hardened and slightly bleached for a few inches adjoining the contact. Black limestone is slightly bleached but otherwise unaltered. Where the Pando intrudes Leadville Dolomite 2-3 mi (3-5 km) south of Red Cliff, the gray dolomite is slightly reddened for about 2 in. (5 cm) from the contact. As seen in thin section, the dolomite is finely brecciated and is cut by minute veinlets of quartz and hematite. The dolomite also contains a few specks of hematite and a few blades of sericite that may have been introduced from the sill.

In contrast to the negligible effect of the sill on its wallrocks, the wallrocks seem to have affected the deuteric alteration within the sill, for the type of alteration seems to correlate with the type of wallrock. Where the Pando Porphyry sill intrudes shale of the Belden Formation, the sill is characterized by a sericite-anorthoclase type of alteration. In contrast, small sills of Pando in Sawatch Quartzite just south of the quadrangle in the Pando area (Tweto, 1953) are characterized by chlorite-allophane alteration. The difference in alteration with difference in wallrocks suggests that the wallrocks either influenced or caused deuteric alteration, probably by supplying water to the cooling sills which, as judged by metamorphic effects and structural features, were intruded as "dry" and viscous magmas.

Where the enclosing rock is shale, the dominant mineral in the Pando Porphyry is moderately coarse-grained sericite which makes up a large part of the groundmass of the porphyry. Biotite is altered to coarse sericite or muscovite accompanied by calcite, leucoxene, and small crystals of included apatite (fig. 19). Chlorite is absent. The feldspar phenocrysts are irregularly

replaced by an isotropic clay identified microscopically as allophane. Both the feldspar and the allophane are veined by anorthoclase or by a more sodic plagioclase, which remains fresh. In the remaining allophanized portions of the feldspar grains, fine-grained sericite later formed abundantly. Except in the altered biotite grains, calcite or other carbonates are lacking in the deuterically altered porphyry, though they are generally present where the rock was further altered by late hydrothermal solutions. Pyrite is locally present in small amounts in the deuterically altered porphyry. Quartz and apatite are unaltered.

Where the Pando Porphyry has quartzite walls, biotite in the porphyry is changed to chlorite, and feldspars are extensively allophanized. The chlorite is accompanied by minor amounts of sericite, muscovite, montmorillonite, and leucoxene (fig. 20). Some chlorite is partly replaced by montmorillonite which, in turn, is replaced by sericite. Both the plagioclase and the potassium feldspar are strongly allophanized, and the allophanized plagioclase is partly altered to hydromica (about 10 percent) with some sericite. Potassium feldspar phenocrysts are strongly allophanized and contain many small irregular masses of chlorite which probably represent former inclusions of biotite. Moderately coarse sericite is abundant in the groundmass where it apparently represents groundmass biotite. Pyrite and carbonate are absent in the chloritized porphyry in quartzite and no evidence of silicification was observed.

The early allophane in both rocks and the accompanying chlorite in the one suggest only the addition of water and some leaching of iron. The abundant sericite and accompanying anorthoclase and late sodic

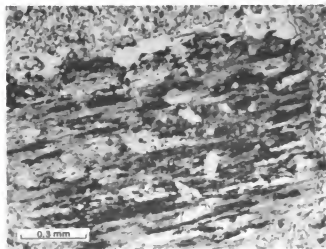


FIGURE 19.—Pando Porphyry showing phenocryst of biotite altered to sericite, leucoxene, and calcite, and sericitic groundmass. Crossed polars.

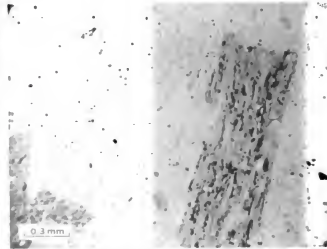


FIGURE 20.—Pando Porphyry showing biotite phenocryst altered to chlorite and opaque oxides. Potassium feldspar phenocryst at left is allophanized. Plain transmitted light.

plagioclase of the other rock suggest addition of alkalis at a later stage. At the time of intrusion, the wallrocks were almost certainly water saturated, as indicated by mudstone dikes near some porphyry contacts in the Pando-Leadville area; these dikes must have been emplaced as mud slurries. A sill of relatively dry magma intruded into saturated rocks might first absorb water nearly free of solutes, perhaps in the vapor phase, and then, with passing time and the transfer of heat farther into the wallrocks, water containing alkalis leached from shales might be supplied. Where the wallrocks consisted almost entirely of clean quartz sandstone or quartzite, alkalis were not available in quantity, and alteration stopped at the allophechlorite stage, except that alkalis liberated by allophechlorization of the feldspars and chloritization of biotite became available to form the relatively minor hydromica and sericite of these rocks. In the shale environment, the alkali-bearing solutions from the wallrocks probably contained a relatively high proportion of potassium, inasmuch as the potassium feldspar crystals are little sericitized, whereas biotite is completely altered to sericite and leucosene.

The formation of potassium and sodium feldspars would decrease the ratio of alkalis to hydrogen ion, and, as shown in the diagrams of Hemley and Jones (1964, figs. 1 and 2), this would shift the field of equilibrium from feldspar towards mica and ultimately to kaolinite-pyrophyllite. The shift from feldspar to mica is evident in the mineralogic relations in the altered porphyry; but the kaolinite-pyrophyllite stage was not reached, probably because equilibrium in saturation between wallrocks and sill was reached in a relatively short time, ending the transfer of solution to the sill. During the process of deuteric alteration, iron and magnesium were largely expelled, though some iron was fixed locally as pyrite or siderite.

DIKE ROCKS

Scattered small dikes of dark fine-grained igneous rocks occur along faults in the Precambrian rocks of the Gore Range, especially near the northern boundary of the quadrangle. The dikes are somewhat more abundant northward in the Mount Powell quadrangle but are absent southward through the remainder of the Gore Range (Tweto and others, 1970). Only one small dike has been found in the sedimentary rocks; this dike cuts grit of the Minturn Formation on Pitkin Creek about one-half mile (0.8 km) from Gore Creek.

The dikes are latite, dacite, and quartz basalt porphyries, some of which have lamprophyric characteristics. In the Slate Creek area and northward into the Mount Powell quadrangle, most of the dikes more than 4 or 5 ft (1.2 or 1.5 m) wide contain sanidine phenocrysts in

their inner zones, but the small dikes are aphanitic. These dikes are inferred to be related to the trachytic intrusive and volcanic center at Green Mountain in the Mount Powell quadrangle (Tweto and others, 1970). The dikes are considerably altered deuterically and therefore cannot be closely characterized petrographically. They seem to have consisted originally of a groundmass of small andesine laths and magnetite grains in a matrix of low-index feldspar, possibly anorthoclase, and phenocrysts of labradorite, potassium feldspar, hornblende, augite, and minor biotite and quartz. Some contain as much as 3 percent apatite. Calcite and chlorite are abundant alteration products, and one dike, 1.2 mi (1.9 km) southwest of Upper Slate Lake, contains the zeolite scolecite in abundance. The rock is classed as a lamprophyric latite.

Dacite porphyry dikes on the western side of the Gore Range, on the slopes above the upper Piney River, are characterized by abundant phenocrysts of andesine, some of which are as much as an inch (2.5 cm) in length and by small anhedral grains of hornblende. The groundmass is a very fine grained aggregate of oligoclase, quartz, potassium feldspar, biotite, and magnetite. Spinel is a relatively abundant accessory mineral, and apatite, epidote, and allanite are present in small amounts.

A short dike on the ridge between Bighorn and Pitkin Creeks and the dike in the Minturn Formation near the mouth of Pitkin Creek are quartz basalt. In the dike on the ridge, some of the quartz is in rounded grains that may be xenocrystic, although quartz occurs also in the groundmass. In the dike on Pitkin Creek, quartz occurs both in the groundmass and as 2-3 mm phenocrysts with square cross-section, suggesting original cristobalite. The plagioclase phenocrysts of the basalt porphyries are labradorite, An_{58-60} , and the plagioclase of the groundmass is andesine, An_{40} . The dike on the ridge contains about 25 percent of pyroxene in the form of aegirine-augite and pigeonite. The pigeonite rims and replaces the aegirine-augite. The dike on Pitkin Creek contains 11 percent augite and 5 percent biotite. The magnetite content of the two rocks is 5 and 8 percent, respectively.

The dike rocks are considered to be of middle to late Tertiary age. The basalts presumably are related to the basalts of the Piney River which, as shown in the following discussion, are Miocene in age. The latites and dacites seem to be related spatially and compositionally to the Green Mountain intrusive-volcanic center in the Mount Powell quadrangle. Geologic evidence suggests that this center is of late Tertiary age (Tweto, 1957), although a single fission-track age of about 30 m.y. (Naeser and others, 1973) suggests a late Oligocene age.

VOLCANIC ROCKS

Basalt and tuff or volcanic ash occur in patches high on the sides of the Piney River valley in the northwestern corner of the quadrangle. Basalt caps a ridge and knob northeast of the junction of Meadow Creek and the Piney River between the 9,500- and 9,800-ft contours, and it occurs also in a small patch high on the east slope of Red and White Mountain at the 10,300-ft contour. Tuff or ash crops out in a narrow belt at the top of the cliffs on the west side of the canyon of the Piney north of Dickson Creek, between the 9,400- and 9,750-ft contours. The tuff probably underlies much of the area covered by surficial deposits on the east and north slopes of Red and White Mountain (pl. 1).

These occurrences are erosional outliers of a moderately extensive basaltic volcanic field in the Piney River area and along the Colorado River north of the quadrangle. As mapped by Brennan (1969) and Donner (1949), this volcanic field extends from about 3 mi (5 km) north of the Minturn quadrangle northwestward about 14 mi (22 km) to Yarmony Mountain, north of the Colorado River. The volcanic sequence consists of superposed basalt flows which locally are separated by beds of volcanic ash or by lenticular fluvialite deposits. Donner (1949) distinguished at least nine flows, each 25–150 ft (7.6–45.7 m) thick, in the State Bridge area; he also mapped a persistent bed of tuff and breccia between the fifth and sixth flows. Taggart (1962) recognized more than 25 flows, each 5–40 ft (1.5–12.2 m) thick, on Piney Ridge, east of the Piney River, and he noted thin beds of calcareous tuff between some of them. In the lower valley of the Piney River, tuffaceous sedimentary rocks several hundred feet thick overlie the basaltic rocks (Brennan, 1969). On the basis of lithology, vertebrate fossils, and intercalated ash beds, the sedimentary rocks might be assigned to the Troublesome Formation of Middle Park, the North Park Formation, or the Browns Park Formation, all of Miocene age (Izett, 1968; also oral commun., 1970).

The tuff in the Minturn quadrangle crops out for about a mile (1.6 km) northwestward from the Dickson Ranch, at a level about 800–900 ft (240–270 m) above the Piney River. It lies on a gullied surface with relief of as much as 75 ft (22.8 m) cut over strata of the Maroon Formation. It is overlain by 50–75 ft (15–22.8 m) of surficial materials, which are discussed in the following section. Maximum exposed thickness of the tuff is about 200 ft (61 m). The tuff is light brown to yellowish white, coherent and tough but porous and friable, and distinctly "light" in weight, or specific gravity. Much of the tuff contains charcoal specks, and the upper 50 ft (15 m) contains abundant chunks of white opal as well as fragments of opalized twigs or rootlets. Bedding is

faint or absent. As seen microscopically, the tuff consists principally of pyroclastic materials but contains a minor fraction of foreign materials, such as microcline, rounded quartz grains, epidote, muscovite, and probably some biotite. The pyroclastic fraction consists in part of faintly anisotropic, turbid, partly devitrified glass and in part of isotropic glass shards, crystal fragments of plagioclase, potassium feldspar, biotite, and hornblende. Refractive index of the glass is 1.49 as determined by G. A. Izzett of the U.S. Geological Survey.

The basalt in the Minturn quadrangle is near andesite in composition and is notable for the presence of rather abundant potassium feldspar in the groundmass. The rock is dark gray, vesicular, and aphanitic, except for a few plagioclase phenocrysts as much as 4 mm long. These phenocrysts are conspicuously zoned and have cores of labradorite with rims of oligoclase. Grains of augite about 1 mm in diameter constitute about 25 percent of the rock. Olivine is present in scattered grains about the same size as the augite. Both the augite and the olivine are extensively altered to iddingsite and to a fine-grained low-index chlorite. The groundmass is a very fine grained mixture of twinned acicular andesine, tabular orthoclase, and sparse accessory magnetite. Flows near State Bridge were described by Donner (1949) as olivine-bearing hypersthene andesites and olivine basalts.

The stratigraphic relationship between the tuff and the basalt in the Minturn quadrangle is not evident, owing to the isolated exposures. Absence of basalt beneath the tuff suggests that the tuff may be the older, but the two rocks could intertongue, or if the basalt were discontinuous, the tuff could be the younger. Further, the precise relation of the tuff to the sequence of tuffs and siltstones farther north is unknown, but on the basis of general similarity in character, they are assumed to be of about the same age.

Fossil dog remains from the tuffaceous sedimentary rocks on the lower Piney River (E 1/4, sec. 1, T. 3 S., R. 83 W.) were described as *Cynodesmus casei* and assigned to the early Miocene by Wilson (1939). Reappraisal of this fossil and study of other vertebrate fossils found later in these strata led G. Edward Lewis of the U.S. Geological Survey (written commun., May 1, 1970) to assign a late Miocene age. Lewis referred Wilson's specimen to *Tomarctus thomsoni* (Matthew) rather than to *Cynodesmus casei* and, from other fossil collections in the area, identified:

1. The dogs *Amphicon sp.* and *Tomarctus sp.*
2. The oreodont *Brachycrus sp.* close to *B. tvaughani* Schultz and Falkenbach and *B. wilsoni* Schultz and Falkenbach
3. The horse *Merychippus sp.* close to *M. innensis* (Cope)

Basalt from Yarmony Mountain in the Piney River



FIGURE 21.—Rugged topography formed by glaciation in Gore Range. View southwestward from Upper Slate Lake.

basalt field has been dated isotopically as 21–24 m.y. (early Miocene) in age (Mutschler and Larson, 1969). As the basalts underlie the fossiliferous tuffs and siltstones, this age is consistent with the late Miocene age of the vertebrate fossils.

PHYSIOGRAPHY AND UPPER TERTIARY AND QUATERNARY UNCONSOLIDATED DEPOSITS

Physiographically, the Minturn quadrangle consists of three main units, corresponding to the threefold division in its bedrock geology. The Gore Range, on the northeast, is characterized by deep canyons and knife-edge ridges created by intense glaciation (fig. 21). The flank of the Sawatch Range, on the southwest, is an area of shallower glacial canyons, separated by broad, evenly inclined dip slopes (fig. 22) that rise southwestward toward high and rugged peaks that lie outside the quadrangle. The broad area between the two ranges, corresponding in general to the area underlain by the Minturn and Maroon Formations, is an area of smooth ridges and slopes and deep stream valleys (fig. 23).

The fluvial and glacial erosional processes that produced these landscapes also produced deposits, such as stream gravels, moraines, and colluvial blankets. Although the preserved deposits are small in comparison to the volume eroded, they provide a record of

the character and timing of the erosional processes. This record begins with local and generally scanty deposits of late Tertiary age and extends with increasing clarity through the Pleistocene Epoch to the present.

The earliest deposits related to the existing topography and physiography are the tuff and basalt of the Piney River area at the north edge of the quadrangle. These volcanic materials were deposited in a broad valley that was centered approximately over the pres-



FIGURE 22.—Dip slopes on flank of Sawatch Range. View northwestward across mouth of Bishop Gulch; canyon of Cross Creek in middle distance.



FIGURE 23.—Typical topography in area of Minturn Formation. View northwestward across valley of Gore Creek toward Bald Mountain (on skyline). Gore fault (arrow) is in front of crest of Bald Mountain; Precambrian rocks in back of the fault.

ent valley. Within the quadrangle, where the valley of the Piney River was greatly deepened by glacial erosion and related stream cutting, remnants of the old valley bottom as defined by the volcanic rocks are several hundred feet above the present stream (pl. 1, sec. D-D'). Farther north, however, the volcanic rocks extend to the bottom of the present valley, indicating that the valley was both wide and deep in Miocene time. Other streams in the sedimentary terrane, such as Gore, Red Sandstone, and Turkey Creeks and the Eagle River probably occupied similar valleys in a rolling upland of low relief in the Miocene, but no direct evidence of this has been found.

Aside from the volcanic rocks in the old valley of the Piney River, the oldest deposit related to the present physiography is a thick and old colluvium that mantles the high slopes in the northwestern part of the quadrangle. The colluvium covers some of the tuff along the Piney River; hence, it is younger than late Miocene. Shallow cirques of the earliest recognized glaciation are incised below some of the colluvium-mantled slopes, and in places the colluvium seems to extend beneath ancient glacial drift. The colluvium is, therefore, preglacial. It is judged to be Pliocene and possibly early Pleistocene in age.

The glacial history of the Pleistocene Epoch is represented by an exceptionally rich record, as almost every drainage of consequence in the quadrangle was glaciated at least once. This record takes the form both of erosional features, such as canyons and cirques, and of depositional features, such as moraines and valley trains of outwash gravels. Studies made subsequent to our main field work in the Minturn quadrangle indicate that as many as nine distinct episodes of glacial advance and retreat occurred in the mountains of central

Colorado (Tweto, 1961). Of these, two are tentatively correlated with the pre-Bull Lake glaciations defined by Richmond (1960, 1964); two are correlated with the Bull Lake Glaciation; three are correlated with the Pinedale Glaciation (Blackwelder, 1915; Richmond 1960); and two are Neoglacial or Holocene. All nine are represented by deposits in the Minturn quadrangle, but they are depicted only in two main groups on the map: (1) pre-Bull Lake and (2) Bull Lake and Pinedale undivided, although deposits of these two glaciations are separately distinguished in a few critical areas. Deposits of the two Neoglacial episodes exist in many of the cirques of the Gore Range but were not mapped. Relicts of the later of these, if not of both, are represented by many ice-cored rock glaciers in the high cirques. The glacier shown on the map (pl. 1) at the head of Black Creek was active in 1942 when discovered by Lovering, but it had degenerated to a boulder- and snow-covered body of stagnant ice by 1969 when it was revisited by Bruce Bryant in connection with the study of the Gore Range Primitive Area (Tweto and others, 1970).

The glacial epoch was a time of pronounced erosion of valleys and canyons, both by glacial ice and by streams. At the time of the pre-Bull Lake glaciations, deep canyons, such as those of the Eagle River and upper Gore Creek, did not yet exist. The early Eagle Glacier, for example, occupied a broad valley whose bottom was at the level of Gilman and the present canyon rims, as shown by the relation of ancient glacial drift to the topography. By the time of the succeeding Bull Lake Glaciation, the canyon had been cut to a depth of about 400 ft (120 m) in hard rocks, as shown by the location of a till of early Bull Lake age on the canyon sides. By the time of the Pinedale Glaciation, the canyon had reached its present depth of 500–600 ft (150–180 m), or was even a trifle deeper. No deepening of the valleys has occurred since the Pinedale Glaciation and, in fact, many of the valleys have been aggraded by a combination of stream action, colluvial processes, growth of alluvial fans, and landsliding.

Some part of the canyon cutting was certainly accomplished by the glaciers, but the bulk of it seems to have been produced by stream erosion, as the cutting occurred after the valley or canyon was occupied by one glacier and before it was occupied by the next. Melting of ice many cubic miles in volume upstream from a canyon may have been a factor in the canyon cutting, but it probably was not the only factor. Canyon cutting occurred after early glaciation in many places in the Cordilleran region (Richmond, 1965), suggesting that climatic or orogenic factors might also have been involved.

TERTIARY AND PLEISTOCENE(?) COLLUVIUM

The upper slopes and tops of smooth ridges northeast and southeast of Red and White Mountain are mantled in places by thick colluvium that contains abundant blocks of light-colored sandstone from the Dakota, Morrison, and Entrada Formations. In other places, bedrock surfaces on the Maroon Formation are littered with the sandstone blocks, or with irregular masses or nodules of varicolored chert, or both. Gradation of sandstone-bearing colluvium into areas of isolated sandstone blocks resting on bedrock suggests that the isolated blocks are residual from the erosion of the colluvium. Some of the sandstone blocks are partly replaced by varicolored chert. The same chert has also locally replaced grit and thin limestone beds of the Maroon Formation at the erosion surface on which the blocks rest. This suggests that the chert-forming process was related to weathering at and following the time in which the sandstone-bearing colluvium accumulated.

The colluvium consists of angular and subangular sandstone fragments of various sizes up to several feet across, scattered limestone fragments, and pieces of chert in a brown sandy or clayey matrix. Gullies through the colluvium indicate that it is as much as 50–75 ft (15–22.8 m) thick. Because the colluvium is on slopes below the small area of Mesozoic rocks capping Red and White Mountain and contains no materials other than Mesozoic rocks and minor debris from the Maroon Formation, it is believed to represent an apron of debris that formed as cliffs of the Mesozoic sandstones retreated toward the crest of Red and White Mountain. The debris accumulated on the side of the broad old valley of the Piney River, and it extended over the volcanic rocks that also coat the sides of that old valley. Because these volcanic rocks are Miocene and possibly late Miocene in age, and because the colluvium predates the earliest recognized glaciation, the colluvium is regarded as Pliocene and possibly early Pleistocene in age.

The chert associated with the colluvium is distinctive in its varied color and in the extreme irregularity of the pieces or lumps in which it occurs. It differs markedly from the olive-gray chert that is present in minor amount in the Morrison Formation on Red and White Mountain and could not have been derived from that source. The chert is scattered over the broad, mature erosion surface that forms the divide between the Piney and the Eagle Rivers southeast of Red and White Mountain. It is especially abundant in the channel of an intermittent stream that joins Buck Creek from the north at about the 10,000-ft contour.

Most of the loose chert is free of matrix materials, but some pieces show remnants of sandstone, limestone, or grit. Chert in sandstone blocks is in globular or veinlike forms. Chert in limestone and grit of the Maroon Formation at the stripped erosion surface is in small, sharply angular, blocky bodies.

The chert is white to dark gray and various shades of yellow, red, and brown; much of it is variegated. Most of it is dense, but the larger lumps commonly contain veins lined by quartz or—rarely—by calcite. In all types of occurrence, the chert generally shows several generations of deposition. As seen in thin section, chert that has replaced limestone at the outcrop of the Maroon Formation consists in large part of fine-grained quartz, the earliest silica mineral. Thin layers of fine-grained hematite coat this quartz. The quartz is cut by veinlets of coarser chaledony in fibers that have an ordered arrangement and that maintain optical continuity across the hematite bands. The chaledony is in turn coated by quartz in microvoids, and some of these openings contain still later growths of chaledony, quartz, or calcite.

A good example of chert that has replaced arkosic red sandstone of the Maroon Formation was seen in a boulder near the head of Buck Creek. The chert, in an irregular body about 3 ft (1 m) long, has a dark-red hematite-rich core. This core is veined and is rimmed by salmon-pink chert that contains far less hematite. The sandstone adjoining the chert is pitted by solution cavities and is decolorized in a band about an inch wide.

The occurrence, character, and paragenesis of the chert together indicate that the chert formed under supergene conditions, at and near the base of the colluvium covering an old erosion surface. The successive generations of deposition recorded in the chert indicate fluctuating conditions that could well reflect fluctuations in amount and in composition of descending ground waters. The leaching of hematite in red beds by the chert-depositing solutions, and the wide ranges in iron content suggested by color contrasts in the chert, indicate that solutions that were able to dissolve hematite existed at times. Because hematite is stable in most natural solutions of inorganic composition, these features strongly suggest that the solutions contained organic compounds. Vegetation at the surface of the colluvium would have been a ready source for such compounds.

PRE-BULL LAKE GLACIATIONS

During the two pre-Bull Lake glaciations more of the quadrangle was covered by ice than in any subsequent time. Glaciers existed during one or both of the early glaciations in several areas that were never glaciated again: in tributary gulches on both sides of Wearyman, Two Elk, and Mill Creeks, and at the heads of Turkey,

Timber, Lime, Willow, Game, Spraddle, Freeman, and Dickson Creeks. The largest of the early glaciers occupied the valley of the Eagle River from the southern edge of the quadrangle northwestward to Minturn. This glacier originated more than 15 mi (24 km) to the south of the quadrangle, and glaciers in the valleys of Fall and Cross Creeks were tributary to it within the quadrangle. Deeply weathered till that is the chief evidence of this glacier occurs in scattered patches, either as blanketlike deposits without morainal form or as damlike bodies in the valleys of sidestreams and gulches. One of the larger till bodies lies on the dip slope west of Gilman, where it extends from a little above the canyon rim upslope to about the 9,500-ft contour. Location of this and other remnants of the till indicate that the valley occupied by the glacier descended rapidly from the level of Gilman, 550 ft (170 m) above the present Eagle River, to the level of a rock bench on the north side of Martin Creek, 250 ft (75 m) above the valley floor at Minturn. Morainal remnants at this locality are the most distal that have been found; if the glacier extended farther, the evidence has been destroyed.

Trunk glaciers also existed in the Gore Creek and the Piney River drainages during the pre-Bull Lake glaciations. Along Gore Creek, evidence of these glaciations is in the form of scattered blanketlike deposits of till high on the valley walls, above the lateral moraines of Bull Lake age. The old glaciers in the Piney River drainage spread southward over the drainage divide into the drainages of Red Sandstone and Indian Creeks. The ridge between Indian and Freeman Creeks, for example, is capped by old till that contains boulders of Dakota Sandstone. The sandstone is thought to have been derived from an underlying colluvial blanket and to have originated on Red and White Mountain, though, conceivably, it could have come from remnants of a sedimentary cover on the Gore Range.

The older of the two pre-Bull Lake tills is typically red brown to brown and contains soft, weathered boulders in a tough, clayey matrix. Where extensively eroded, however, it is buff to light brown and sandy. The younger till has the same general characteristics but is a lighter shade of brown and not quite so clayey and tough. In many of the smaller old cirques and glacial valleys, these tills are heavily mantled with colluvium derived from the cirque walls, and hence they are shown on the map as "landslide and colluvium." Weathering and colluvial creep have destroyed or have buried any cliffs that existed in the old cirque walls, forming basins with characteristic steep smooth slopes at the heads of minor stream valleys. The Vail ski area owes the excellence of its ski runs to this modified glacial topography.

BULL LAKE GLACIATION

The Bull Lake Glaciation was characterized by the longest and thickest glaciers ever to occupy the Minturn quadrangle. The glaciation was in two episodes or stades, separated by a period of time long enough to allow appreciable modification of the moraines of the first stade and some weathering of the till before the second glacial advance occurred. Large lateral moraines along the valley sides hundreds of feet above the valley bottoms are the hallmark of these two glacial advances. Terminal moraines are inconspicuous because they were extensively eroded by the meltwater streams from younger glaciers with fronts farther up the valleys.

In general, the glaciers of the earlier stade extended farther down the valleys than did those of the later stade, but in many places ice of the later stade reached higher levels on the valley walls than in the early stade. Because of this and also because ice of the late stade extensively eroded the lateral moraines of the early stade in places, morainal evidence of the early stade of the Bull Lake is much less abundant than for the late stade.

Although the two sets of Bull Lake moraines differ preceptibly in degree of modification and weathering, together they are intermediate between the generally formless and deeply weathered pre-Bull Lake morainal deposits and the hummocky and bouldery moraines of fresh till characteristic of the Pinedale Glaciation. The Bull Lake moraines typically form benches on the valley walls, but where unimpeded by such walls, they form ridges. These ridges generally have smooth slopes with few or no boulders lying on them, in contrast to rough and bouldery morainal ridges characteristic of the Pinedale. Stream adjustment to the Bull Lake moraines is complete, and extensive segments of the moraines have been eroded in the process.

EAGLE RIVER AND TRIBUTARIES FROM SAWATCH RANGE

In the early stade of the Bull Lake, a glacier deep enough to have covered Iron Mountain at Red Cliff entered the quadrangle from the south and extended at least to Minturn. Morainal evidence of this glacier is scanty. Patches of lateral moraine lie just above the canyon rim west of the river and, near the lower end of the canyon, till of this age lies on bedrock 150 ft (45 m) above the river. Although the glacier was very large south of the quadrangle, it seems to have tapered rapidly between Red Cliff and Minturn. It may have reached Minturn only because of nourishment from the Fall Creek and Cross Creek tributary glaciers.

During the late stade of the Bull Lake, the Eagle

Glacier terminated about at Red Cliff. No terminal moraine remains, and probably none was formed, for all the drainage from a very extensive glacial system was here funneled into the narrow canyon of the Eagle River, presumably as a torrent that might have carried away almost all of the debris of the terminal area.

Bull Lake glaciers in the valley of Fall Creek formed prominent high compound lateral moraines that extend for 3–4 mi (5–6.5 km) along the valley. Ice of the early stade joined the Eagle Glacier at the level of a bedrock sill 250 ft (76 m) above the present canyon, and that of the second stade formed a small terminal moraine one-half mile (0.8 km) short of the mouth of this hanging valley. Ice of both stades also spilled prongs southward into the valley of Peterson Creek. The big lateral moraines lie on pre-Bull Lake tills, as along Notch Mountain Creek, and extensive blankets of the early tills extend upslope from them.

The Cross Creek drainage contained large Bull Lake glaciers that originated in cirques several miles southwest of the quadrangle. Unlike Fall Creek and many other valleys, Cross Creek valley contains only short segments of lateral moraines of any age, presumably because glacial movement and erosion were too vigorous to allow them to form or survive. In the terminal moraine area at the mouth of Cross Creek, only the northern portions of the Bull Lake terminal moraines are preserved. These are in the form of high morainel ridges. The older ridge curves northward, as if joining a glacier in the valley of the Eagle River, but the younger one extends straight eastward to a truncated front above the Eagle River where it rests on bedrock 60–75 ft (18–23 m) above the valley floor. Clearly, the late Bull Lake Cross Creek Glacier, and also the next succeeding Pinedale Glacier, forced the Eagle River eastward against the valley wall, causing erosion that accounts for the spectacular cliffs of the Minturn Formation between Minturn and the mouth of Eagle Canyon (fig. 12).

The valleys of Grouse and West Grouse Creeks were occupied by Bull Lake glaciers that were very narrow but had lengths of 5–6 mi (8–10 km). Moraine of the late stade of the West Grouse Glacier is at the level of the Eagle River below Minturn. An even narrower glacier of probable Bull Lake age descended the canyon of Stone Creek, at the western edge of the quadrangle, to a small terminal moraine between the 9,000- and 9,500-ft contours.

GORE CREEK DRAINAGE

The Gore Creek glaciers of Bull Lake time were the largest in the quadrangle. In both stades, ice reached levels 1,100–1,300 ft (335–400 m) above the present valley bottom in the vicinity of Black Gore, Bighorn,

and Pitkin Creeks. The glacier of the early stade descended Gore Creek to a terminal moraine area just southwest of the Gore Creek School, or to a point about 1.5 mi (2.5 km) from the Eagle River. The terminal moraine is much dissected, and as shown in road cuts, it rests on a bedrock surface that is 40–50 ft (12–15 m) above the present stream. The glacier of the second stade was about 2 mi (3 km) shorter; it extended to a terminal moraine area in the vicinity of Red Sandstone Creek. This moraine is also extensively dissected. The largest remnant is a terraced deposit outlined by the 8,250-ft contour just east of Red Sandstone Creek. Other remnants to the south of this are knobs and ridges of till separated by channels cut into the till by Gore Creek, probably in Pinedale time.

In both stades, the glacier coming from the head of Gore Creek, 3–4 mi (5–6.5 km) east of the quadrangle boundary, was heavily augmented by tributary glaciers within the quadrangle. Massive glaciers also descended Black Gore Creek from sources in the West Tenmile drainage east of the quadrangle. The ice from this source spilled through Vail Pass, bearing a load of telltale porphyries that are foreign to the Gore Creek drainage. A prominent lateral moraine of this origin caps the ridge east of Timber Creek at the 10,500-ft contour.

Other major tributaries of the Gore Creek glaciers came from the Bighorn, Pitkin, and Booth Creek drainages. Smaller tributaries from Spraddle Creek, Middle Creek, and possibly from Mill Creek existed during the early stade of the Bull Lake. Middle Creek also contained a glacier in the late stade, but this failed by about a mile to join with the Gore Glacier. The two forks of Red Sandstone Creek contained glaciers in both stades that formed large moraines southeast of Lost Lake. These glaciers extended only to the forks of the stream; thus, they failed by 4–5 mi (6.5–8 km) to reach the Gore glaciers.

PINEY RIVER

The Piney River drainage contained very large glaciers in both stades of the Bull Lake. The bulk of the ice came from what is essentially a single elongated cirque extending 3.5 mi (5.5 km) from the Booth Creek drainage divide to the sharp bend in the Piney River. Smaller amounts came from a hanging valley or cirque on the south side of Mount Powell, just north of the quadrangle, drained by the stream that joins the Piney River at the big bend and from a cirque drained by East Meadow Creek. Massive lateral moraines that were formed in the two stades of the Bull Lake and in the earliest stade of the Pinedale border the Piney River valley from near the big bend southwestward and westward for 6 mi (10 km). At their upper ends, these

moraines are 1,200–1,500 ft (360–450 m) above the present stream. Ice of the early stage of the Bull Lake spilled into the East Meadow Creek drainage on a wide front, forming extensive moraines in that valley. Ice of the second stage spilled into the East Meadow Creek drainage on a much smaller scale, through a saddle northwest of Piney Lake. The lower ends of the lateral moraines of the early stage, as well as any former terminal moraine, have been removed by erosion. The end of the eroded north lateral moraine is on the spur southeast of the mouth of Meadow Creek, 450 ft (135 m) above the Piney River. The end of the eroded south lateral moraine plugs the valley of Dickson Creek at Dickson Ranch, 550 ft (165 m) above the river. In contrast to the early moraines, the north lateral moraine of the late stage descends to a remnant of a terminal moraine in the canyon bottom. This indicates that the bedrock floor of this part of the canyon has remained at about the same level since Bull Lake time.

PINEDALE GLACIATION

With a few exceptions glaciers of the Pinedale Glaciation were far less extensive than the Bull Lake glaciers. The glaciation occurred in three episodes, or stades, of ice advance and retreat. Of these, the first was by far the most extensive, and in a few drainages in the region it equaled and even exceeded the late Bull Lake glaciers. Glaciers of the second and third stades of the Pinedale were everywhere much smaller than those of the first stage, and in many of the smaller drainages, they were absent.

Moraines of the Pinedale glaciers are hummocky, bouldery, and little modified. The till in them is sandy rather than clayey and, except as it might be colored by rocks, such as red beds, it is generally light gray in contrast to the yellow, buff, or brown colors characteristic of the older tills in surface or near-surface exposures. Soils are only weakly developed on the Pinedale Till and, practically speaking, are absent in many places.

The largest glaciers in the Minturn quadrangle during the Pinedale were in the valleys of Cross Creek and the Piney River. No glacier existed in the part of the Eagle Valley that is within the quadrangle, and Gore Creek Valley did not have a trunk glacier. An early Pinedale glacier did occupy the canyon of upper Gore Creek east of the quadrangle, but it terminated in the area between the mouths of Black Gore and Bighorn Creeks. Early Pinedale glaciers of Bighorn, Pitkin, and Booth Creeks reached the Gore Valley and deposited small moraines on its floor. Middle Pinedale moraines are a short distance up the canyons, and late Pinedale moraines are in the midportions of the canyons.

On Cross Creek, unlike all other drainages in the

quadrangle, glaciers of all three stades of the Pinedale descended to the terminal moraine area near the mouth of the creek. On the north side of this morainal area, the early Pinedale glacier formed a morainal ridge almost as high as the Bull Lake ridges. The ridge descends more rapidly than the Bull Lake ridges, however, and turns into a broad, low, complexly ridged terminal moraine near U.S. Highway 24 and the Eagle River. The middle Pinedale glacier was split near its terminus by the hill of rock in the center of the morainal area (pl. 1) and formed two morainal lobes within the terminal moraine horseshoe of the early Pinedale. The southern lobe rests on a low valley flat excavated out of part of the early Pinedale moraine. The late Pinedale glacier formed small morainal loops immediately south and west of the bedrock hill.

In the Piney River valley, the early Pinedale glacier was as high on the valley wall as the Bull Lake glaciers near Piney and Lost Lakes. From about this place, however, it descended to a prominent southwestward-sloping morainal bench 1.5 mi (2.5 km) west of Piney Lake and formed a small terminal moraine on the floor of the Piney River valley just above the mouth of Dickson Creek. The small terminal moraines of the middle and late stades of the Pinedale are in the vicinity of Piney Lake.

LANDSLIDE

The Minturn and Maroon Formations contain many incompetent shaly beds that make ideal surfaces for landsliding where the beds dip toward valleys. Additionally, the weak and platy-weathering rocks of these formations readily form a heavy "slopewash" or colluvium that creeps down the slopes and accumulates in slidelike piles in the basins or valleys. All the major valleys that cut the Minturn and Maroon Formations and many of the smaller ones have their slides splattered with landslides and colluvial accumulations. The larger slides are mainly of the dip-slope slide type, but some follow ground broken by faults, and many are on slopes oversteepened by glacial erosion. Most of the conspicuous slides are postglacial in age, and some are very recent or modern.

Incipient slides are evident in many places where open tension fissures as much as several feet wide and 20 ft (6 m) deep occur on hillsides that slope in the general direction of the dip. Such fissures (pl. 1) are especially common in a belt that extends from the head of Game Creek to the slopes south of Mill Creek and were probably caused by glacial oversteepening of Gore Valley. Clear evidence of recent movement was seen at the east end of a fissure that starts at the 10,600-ft contour on the nose extending north from a knob on the

Game Creek—Gore Creek Divide 2.1 mi (3.38 km) N 78° E of the mouth of Game Creek. Turf extends across the eastern end of the slowly widening fissure, but a few feet to the west a bare root 2 in. (5 cm) thick from a pine tree growing on the north wall extends through the air horizontally into a crack in the south wall about 20 in. (50 cm) away. The pine was cut down in 1963 and the tree rings indicated an age of 68 years. The two walls of the fissure must have been next to each other when the root first crossed into the south wall, as otherwise the root would have grown vertically downward, if it grew at all. Either the walls have moved apart so gradually that the growth of the root has kept it from breaking as the separation proceeded or else the roots were strong enough to withstand the pull of faster movement that took place after the tree was partly grown. The data show that the walls have separated at a minimum rate of about one-third inch (8 mm) per year, and it is probable that the separation of the walls began many years after the pine seed first sprouted.

Elsewhere, as on the slopes south of Vail, many open fissures show evidence of very recent movement. The relation of the fissured area shown on the geologic map (pl. 1) to Vail indicates that the possibility of sudden mass movement of the ground on the northward-dipping bedding planes in this area should be carefully appraised.

The large landslide at Whiskey Creek and another opposite Dowds constrict the valley of the Eagle River for about a mile downstream from Dowds. These slides forced the Eagle River against the northeast wall of its earlier valley, causing steep and cliffy slopes to be formed there. The construction of I-70 across these slides in 1969-70 induced much heaving and slumping of the slide material, indicating that the slides are still unstable. The Whiskey Creek slide overrides glacial outwash gravels that probably are as young as Pinedale; hence, it is probably postglacial in age. Farther west, near Stone Creek, gypsum has slid or flowed over these same gravels, reducing the width of the valley bottom from its former extent.

ALLUVIUM

Morainal areas in the valleys have many pockets and channels filled with alluvium or reworked glacial drift, and most of the stream courses are bordered by alluvial deposits. The landslide just above the mouth of Gore Creek and the terminal moraine at the mouth of Black Gore Creek both have formed natural dams in the past that impounded lakes above them. Delta deposits of crossbedded sand have formed in these lakes, and remnants of such deposits remain along the sides of the valleys. These deposits are included with "alluvium" on

the map (pl. 1) and so also are terrace gravels and fanglomerates.

STRUCTURE

The Minturn quadrangle contains elements of three major structural units—the Gore Range uplift on the northeast, the Sawatch Range uplift on the southwest, and a broad, northwest-trending, generally synclinal area of sedimentary rocks between the two major uplifts. The Gore Range is a fault-block range bordered on its southwestern side by the Gore fault—or fault zone—the largest and most complex fault in the quadrangle. The Sawatch Range, in contrast, is an anticlinal uplift of great size—90 mi (145 km) long and 40 mi (65 km) wide (fig. 24). The Minturn quadrangle includes only the eastern flank of the northward-plunging north end of the anticline. In this area, the flank of the anticline is disrupted only by minor faults, but several miles south of the quadrangle the eastern flank is disrupted by major graben faults of the upper Arkansas River valley (Tweto and Case, 1972).

Structural development of both the Gore Range and the sedimentary basin to the west was closely influenced by a long history of movement on the Gore fault. This fault was active in Precambrian, Paleozoic, Laramide (Late Cretaceous and early Tertiary), and late Tertiary times, and there is suggestive evidence of movement in Quaternary time. During the latter part of Paleozoic time, and perhaps intermittently earlier, the fault formed the western edge of a highland that extended eastward beyond the crest of the present Front Range—the Front Range highland of the Ancestral Rockies. (See Lovering, 1929.) As a structural and topographic unit created out of a part of the old highland, the Gore Range came into existence in Laramide time, but it was much modified and elevated as a fault block in late Tertiary time, accounting for its present relief (Tweto and others, 1970).

The Gore fault was also the border of the basin in which the Belden, Minturn, and Maroon Formations accumulated. Thus, it is not only a fault but also a zone of abrupt unconformity and wedgeout of sedimentary rock units. Folding or upturning of the sedimentary rocks along the fault may have begun in Pennsylvanian time. Folding that produced the present broadly synclinal structure of the sedimentary basin resulted from uplift of the Gore and Sawatch Ranges in Laramide time, but a minor part of it may have occurred in the late Tertiary, inasmuch as the volcanic rocks north of the quadrangle are synclinically folded.

In the Sawatch Range area, no evidence has been found anywhere of uplift prior to formation of the Sawatch anticline in Laramide time. This anticline was

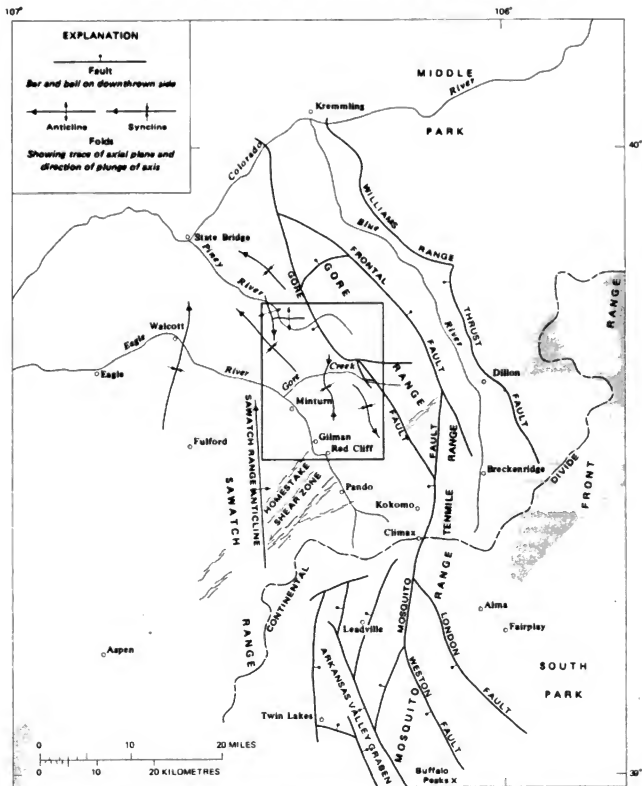


FIGURE 24.—Relation of Minturn quadrangle (outlined) to major structural features and Colorado mineral belt (patterned).

wedgeout of thousands of feet of sedimentary rocks elevated early in the Laramide orogeny, before the Gore Range (Tweto, 1975). Rise of the anticline tilted the sedimentary rocks northeastward through much of the Minturn quadrangle, forming the flank of the central syncline. This uniform tilt, or homoclinal dip, still characterizes a large area east of the Eagle River and south of Gore Creek. North of Gore Creek and, especially, from near the mouth of Gore Creek westward, a more complicated structural pattern now exists. Near the western border of the quadrangle, at least, this pattern is related to diapiric movement of gypsum as a result of excavation of the valley of the Eagle River. Folds and faults in this area probably have been developing almost continuously from the Laramide to the present.

GORE FAULT

The Gore fault delimits the western edge of the Precambrian terrane of the Gore Range for a distance of at least 45 mi (72 km), from the Mosquito fault in the Tenmile Range, several miles southeast of the Minturn quadrangle, to the Colorado River, 15 mi (24 km) north of the quadrangle (fig. 24). Through most of its course in the Minturn quadrangle the fault brings rocks of the Minturn Formation against Precambrian rocks, but in the north part of the quadrangle the Maroon Formation lies against the fault, and farther north various Mesozoic formations are against the fault.

In most places the Gore fault is not a single fracture but a wide and complex fault zone. Most of the fractures in this zone are in the Precambrian rocks, on the northeast or upthrown side of the fault surface that separates the Precambrian and the sedimentary rocks, though strands of the fault are present also in the sedimentary rocks in places. Many of the fractures in the fault zone are of Precambrian age, as will be discussed further; others are younger, but it is difficult to establish the time of origin of most fractures. Main periods of later movement along the fault zone, whether on reactivated or newly formed faults, occurred in the late Paleozoic, the Laramide, and the late Tertiary.

Precambrian origin of many of the fractures in the Gore fault zone is indicated by several lines of evidence (Tweto and Sims, 1963; Tweto and others, 1970): (1) the occurrence of Precambrian intrusive rocks such as pegmatite, aplite, and mafic diorite as dikes along the faults in places, or intruded into mylonitic rocks; (2) the presence of mylonitic rocks of Precambrian aspect beneath undeformed Pennsylvanian rocks and the occurrence of cobbles of the mylonite in the Pennsylvanian conglomerates; (3) the presence of intensely

sheared rocks beneath much less deformed Devonian(?) quartzite; and (4) the occurrence of little deformed dike rock dated isotopically at 1 b.y. on a fault of the Gore system at the Colorado River (Barclay, 1968).

Evidence of pre-Pennsylvanian Paleozoic movement along the Gore fault is shown by stratigraphic and fault relations. Of the pre-Pennsylvanian formations (table 1), the Harding Sandstone, the Dyer Dolomite, the Gilman Sandstone, and the Leadville Limestone are absent from upthrown fault blocks along the Gore fault. Along with the Manitou Dolomite of the area southeast of the quadrangle, they are concluded to have been erosionally truncated both in pre-Late Devonian and in pre-Pennsylvanian times and to wedge out beneath the Minturn Formation in a zone near and parallel to the Gore fault (Lovering and Johnson, 1933; Tweto and others, 1970). The Sawatch Quartzite, Peerless Formation, and Parting Formation reach the Gore fault (fig. 25), but the Sawatch is thinned to only 100 ft (30.5 m) beneath the Peerless, suggesting a possible "high" in the area of the Gore Range even in Cambrian time. The Peerless is only 20 ft (6 m) thick and tapers to a vanishing edge beneath the Parting Formation, indicating, along with absence of Ordovician rocks, extensive erosion before Late Devonian time. The Parting is exceptionally coarse grained and conglomeratic wherever exposed along the Gore fault, suggesting a land area in the vicinity of the Gore Range in Late Devonian time.

Fault relations suggest not only a land area but also active movement along the Gore fault zone in Paleozoic time. In the western of two fault blocks on the south slope of Bald Mountain (pl. 1; fig. 25), the Parting Formation lies on Precambrian rocks and is overlain by coarse Pennsylvanian conglomerate with an angular discordance of 17°. In the eastern fault block, one-half mile (0.8 km) away and 500 ft (150 m) lower, the Parting is underlain by the Peerless and Sawatch and overlain without angular discordance by strata of the Minturn Formation. The relations suggest that a north-trending fault—part of the Gore fault system—between the two blocks was active prior to deposition of the Parting and, again, prior to deposition of the Minturn. Similarly, in the valley of Black Gore Creek one-half mile (0.8 km) from Gore Creek, white quartzite and quartz granule conglomerate thought to be Parting but possibly Sawatch is turned up almost vertically, whereas rocks of the Minturn Formation 100 ft (30 m) away dip gently, suggesting a marked angular unconformity.

Major movement occurred on the Gore fault in Pennsylvanian and Permian time, as indicated by the

against Precambrian rocks in and along the Gore fault zone (pl 1, secs. *A-A'*, *B-B'*, *E-E'*). The occurrence of the Robinson Limestone Member of the Minturn Formation only 50–100 ft (15–30 m) above Precambrian rocks—or above thin patches of the Parting Formation lying on Precambrian rocks—on the mountain southeast of the junction of Gore and Black Gore Creeks has been noted in the discussion of the Minturn Formation. The best example of the abrupt wedgeout of the sedimentary rocks against the fault-scarp front of the old highland is in the Mount Powell quadrangle 3–4 mi (5–6.5 km) north of the Minturn quadrangle, where sedimentary rocks are preserved east of the fault. There, the entire Minturn and all but the uppermost 100–300 ft (30–90 m) of the Maroon wedge out in a zone no more than 3–4 mi (5–6.5 km) wide along the Gore fault (Tweto and others, 1970). In this area, the fault may even have been active in Jurassic time, as suggested by a marked difference in thickness of the Morrison Formation on the two sides, but no evidence of a scarp in Late Triassic time is seen in the Chinle Formation.

Most of the movement that placed sedimentary rocks in fault contact with Precambrian rocks and that

caused folding and overturning of the type shown in figures 25 and 26 is inferred to be of Laramide origin. However, it is difficult to separate with certainty the effects of Laramide fault movement from those of later Tertiary movements. Laramide deformation is proved more by regional geologic relations than by local ones, inasmuch as no sedimentary rocks younger than the Dakota are preserved within the quadrangle. On the northeastern side of the Gore Range, conglomerates of late Miocene(?) age show by their abundant content of Precambrian rocks that the range had been uplifted and had been stripped of its cover of Morrison and younger sedimentary rocks by that time, which was prior to the marked uplift in late Tertiary time (Tweto and others, 1970). The uplift that led to stripping of the sedimentary cover was almost certainly the Laramide in this range just as in most other major ranges in Colorado.

Extensive late Tertiary uplift and fault movement in the Gore Range has been documented by Tweto, Bryant, and Williams (1970). Some of this movement may have occurred along the strand of the Gore fault that separates the sedimentary and the Precambrian rocks, but most of it occurred along faults of the Gore



FIGURE 26.—Deformed strata of Minturn Formation in Gore fault zone at head of Spraddle Creek. View northwestward. One strand of fault lies in covered area between vertical strata of White Quail Limestone Member in center and inclined strata of Robinson Member and underlying Minturn rocks at right; main fault, which brings Precambrian rocks against the Minturn is just out of view to right.

fault zone within the Precambrian rocks. In the upper Piney River area, the late movement occurred on the series of long parallel faults of north-northwest trend (pl. 1). These are reactivated Precambrian faults. In the Gore Creek area, the late movement occurred on the fault strand that lies a short distance east of the sedimentary rocks. This strand is thought to be of Laramide origin.

From the north boundary of the quadrangle to Bald Mountain, the main strand of the Gore fault—separating the sedimentary and crystalline rocks—trends south-southeastward in a fairly straight line. At Bald Mountain, this fault intersects a west-northwest-trending fault zone in a complexly faulted area. The west-northwest-trending zone is a reactivated Precambrian fault zone that extends all the way across the range (pl. 1; Tweto and others, 1970) and is one of a family of persistent faults of this trend in the Gore Range. The line of displacement and upturning of sedimentary rocks turns eastward along the west-northwest-trending zone for about 2 mi (3 km) to beyond Booth Creek, and then it turns south-southeastward again. In the area of this bend, the fault is intersected by the faults with late displacement extending from the upper Piney River area. Southeast of the bend, an older unit of the Gore fault extends to a broad east-trending fault zone along Gore Creek, and the line of displacement jogs eastward along this zone. A younger strand of the fault—probably Laramide and Tertiary—cuts diagonally across the salient outlined by the two older faults in almost a straight line from Pitkin Creek to Gore Creek and beyond (pl. 1). In the area of the salient, near the mouths of Black Gore and Big Horn Creeks, other strands of the fault cut the sedimentary rocks. These are poorly delineated because of widespread cover of glacial deposits and uncertainties in distinguishing the effects of faulting as opposed to unconformity in an area with only scattered small outcrops.

A branch of the Gore fault extends south-southeastward up Black Gore Creek and then southward along Timber Creek, ultimately connecting with faults of the Pando area (Tweto, 1953). Also, old strands of the fault in Precambrian rocks near the mouth of Black Gore Creek project beneath strata of the Minturn Formation on the slopes east of the creek. From Gore Creek, the main young strand of the Gore fault extends into the adjoining Dillon quadrangle, where it intersects sedimentary rocks once again and forms a boundary between these and the Precambrian rocks (Tweto and others, 1970).

Most of the faults in the Gore fault zone are vertical or are steep normal faults (pl. 1, secs. A-A', E-E'), and the zone as a whole is interpreted to be essentially vertical. However, reverse and even low-angle thrust faults

are present locally. They probably formed in response to local stress conditions or in response to expansion of the Precambrian massif as it rose. Near Booth Creek, the fault strand between the Precambrian and the sedimentary rocks is a steep reverse fault that dips 80°–85° N. As shown in figure 25, section A-A', this fault is inferred to steepen to vertical at depth; the northward dip near the surface is interpreted to reflect expansion of the upthrown block of Precambrian rocks. Near Middle Creek, low-angle reverse and thrust faults are present in a small area at the edge of the Gore fault zone (pl. 1, map and sec. A-A'). The reverse and thrust faults are in the tip of a wedge between southeast- and south-trending faults in the area where the main Gore fault begins to turn eastward. The south-trending fault has a displacement of several hundred feet in the Gore fault zone (pl. 1, sec. A-A') but only a minor displacement farther south. Exposures are too poor in the small area of thrust faulting to reveal details of the complex structure there, but it is likely that the thrust fault is in a thin fault block underlain by an upward-steepening reverse fault as shown on plate 1 (map and sec. A-A').

GORE RANGE

The Gore Range has two major categories of structural features—the internal structure of early origin in the Precambrian rocks and later faults. The Precambrian gneisses were highly deformed plastically and then were sundured by granite intrusion, forming a gigantic breccia of gneiss blocks in a matrix of granite (pl. 1). Thus, the gneisses are structurally disorganized, and no attempt was made to study them in detail. In general, a broken irregular tongue of gneisses extends south-southeast along the crest of the Gore Range to the head of Bighorn Creek. The Cross Creek Granite which surrounds and intrudes this mass of gneisses has a structure that is nearly concordant with the broad outline of the area of gneissic rocks. To the west and east the foliation or planar structure of the granite strikes north-northwest; south of the area of metamorphic rocks, the structure of the granite strikes northeast or easterly. The north-northwest foliation trend along the western side of the range is paralleled by fractures of the Gore fault zone and probably influenced the trend of parts of the Gore fault.

The many faults in the Precambrian rocks of the range are of two main orientations, north-northwest and nearly east-west. Faults of the set trending north-northwest are long and straight, and most of them dip almost vertically. The set that trends nearly east-west includes a few widely spaced persistent faults that extend across the entire range (Tweto and others, 1970) and many shorter faults that subdivide the long blocks

outlined by the north-northwest-trending faults. Faults of both sets are typically fracture zones several feet to a few hundred feet wide, though a few narrow locally to a single fault plane. Many of the fracture zones are altered, and in general, the zones are marked by gullies and saddles on the slopes and ridges of otherwise hard rock. The density of the fault pattern in the Precambrian rocks contrasts markedly with the pattern of sparse faults in the bordering sedimentary terrane (pl. 1). This suggests that most of the faults in the range are Precambrian in age, as do other features noted in the discussion of the Gore fault. Many of the faults, however, were reactivated in late Paleozoic, Laramide, and late Tertiary time. One of the north-northwest-trending faults of the upper Piney River area, nearly 2 mi (3.2 km) east of the main Gore fault (pl. 1), contains in one area narrow slices of down-dragged red beds of the Minturn or Maroon Formation, indicating probable Laramide displacement of hundreds of feet.

SAWATCH RANGE

The part of the Sawatch Range included in the Minturn quadrangle consists of a core of Precambrian rocks covered by a thin mantle of sedimentary rocks that dip northeastward off the range, nearly in dip slopes (pl. 1, sec. B-B'). As in the Gore Range, the Precambrian rocks have an early fold structure and a later fracture structure, and the main elements of the fracture structure predate the Paleozoic rocks.

A major Precambrian structural feature, the Home-stake shear zone, lies just south of the quadrangle (fig. 24). This master zone, which trends northeast and consists of several individual shear zones in a belt 7-8 mi (11-13 km) wide, separates a metamorphic terrane to the southeast from the granitic terrane of Cross Creek Granite to the northwest (Tweto and Sims, 1963; Tweto, 1974). Fringe shear zones or faults of the Home-stake zone project into the Minturn quadrangle in the vicinity of Notch Mountain, Fall, and Peterson Creeks. They are exposed only locally, however, because of a widespread cover of Paleozoic rocks and glacial and col-luvial deposits. The strongest of these fracture zones extends northeastward for about a mile along the slope northwest of Notch Mountain Creek and then disappears beneath the Sawatch Quartzite (pl. 1). It is probably represented in the canyon of the Eagle River by some of the northeast-trending faults and veins in the Precambrian rocks near Gilman. The Ben Butler mine (fig. 8), for example, is on small veins in or near a wide shear zone that resembles the Precambrian shear zones, and both the veins and the shear zone end abruptly upward against the smooth and unbroken basal bed of the Sawatch Quartzite. Similarly, the San-

ta Cruz vein (fig. 8) is a wide and strong fracture zone in the Precambrian rocks but barely affects the overlying Sawatch Quartzite. These fracture zones and mines are described in the report on the Gilman district (Lovering and others, 1977).

Among faults of Laramide or younger age in this part of the Sawatch Range, the largest are in the area north of the latitude of Minturn, at the north end of the Precambrian core of the range. A prominent fault of east-northeast trend, downthrown to the north, extends from the Eagle River at the mouth of West Grouse Creek, to a fault along Stone Creek; west of Stone Creek, an en echelon fault of the same trend and displacement extends west-southwestward out of the quadrangle at least 2 mi (3 km). The two echelon faults are north-dipping normal faults and have displacements of 200-300 ft (60-90 m). No sign of the eastern fault could be found east of the Eagle River at Game Creek; the fault is inferred to end against a fault along the river. Evidence of a northwest-trending fault, upthrown to the northeast, along the river is seen in the repetition of the Gilman Sandstone on the two sides of the river at Minturn, and in the position of the dolomite bed of Dowds near Dowds (pl. 1, sec. B-B').

The fault along Stone Creek, very near the western border of the quadrangle, trends north-northeast and is upthrown about 250 ft (76 m) on its southeastern side. Its course along lower Stone Creek is uncertain because of slumping of shale and gypsiferous strata in the Belden and Minturn Formations.

In the area of the lower Stone Creek and Whiskey Creek, strikes and dips of the strata change erratically in short distances. A thrust fault that brings grits of the lower part of the Minturn Formation over gypsiferous strata cuts through this area (pl. 1). This fault probably is not a fundamental tectonic element of the Sawatch Range but is primarily a product of deformation and mass slumping at the edge of the gypsum basin. A fault along Whiskey Creek may be of the same origin. This fault is exposed only in a zone of vertical strata on the bank of the Eagle River. It projects southward beneath the landslide along Whiskey Creek but is not evident in the bedrock at the head of the slide. Neither is it seen to the north, across the Eagle River. There, it is inferred to end against east-west faults in a small area of landslide.

CENTRAL SEDIMENTARY BELT

The broad belt of sedimentary rocks between the Gore and Sawatch Ranges is predominantly synclinal in structure. Three northwest- to north-trending synclines, which are arranged echelon in a northwest-trending line, dominate the area structurally, though

other folds are present. The southeastern syncline, called the Black Gore syncline (pl. 1), closely parallels the Gore fault in the area from upper Mill Creek to Turkey Creek. The middle syncline, called the Vail syncline, extends from the Spraddle Creek area southward to the Two Elk Creek drainage. The northwestern and largest syncline, called the Red and White syncline, extends from lower Buffer Creek northwest to and beyond Red and White Mountain. As shown in the cross sections (pl. 1), these synclines are more pronounced at depth than at the surface because of the thinning of all the Paleozoic formations—and particularly the Minturn Formation—toward the Gore Range.

The Black Gore syncline (pl. 1, sec. E-E') is markedly asymmetric, with a wide, gently dipping southwestern limb and a narrow and steeper northeastern limb. Though interrupted by minor flexures, the southwestern limb is essentially homoclinal and is a part of the flank of the Sawatch anticline. The northeastern limb is a Gore Range structure and in part is due to drag along the Gore fault. As expressed in the rocks exposed at the surface—high in the Minturn Formation—the axis of the syncline is sinuous parallel to the Gore fault and lies less than a mile from the fault. As seen in cross section, however, the main synclinal axis is a mile farther southwest, owing to the thickening of the Minturn Formation in that direction. The Black Gore syncline dies out on the ridge between Mill and Gore Creeks, and it is overlapped on the west by the Vail syncline.

The Vail syncline (pl. 1) is a bowed, north-trending doubly plunging syncline that is prominently exposed on the sides of the valley of Gore Creek at Vail. The syncline is longitudinally faulted, and north of Gore Creek the east limb is turned up steeply against the fault (pl. 1). The northern part of the syncline, north of Gore Creek, is bounded on the west by a small anticline centered over Middle Creek. South of Gore Creek, the west limb is the homoclinal flank of the Sawatch anticline.

The fault zone that extends the length of the Vail syncline and beyond is called the Spraddle Creek fault zone. This fault zone extends south-southwestward from the Gore fault zone in the Bald Mountain-Spraddle Creek area nearly to Gilman. In the Bald Mountain area it is part of a complex of fault blocks where the Gore fault trends eastward. In this area it shows wide differences in amount of displacement, from as little as 100 ft (30 m) to more than 900 ft (275 m), reflecting both the differential movement of fault blocks and probable pre-Pennsylvanian and Pennsylvanian movements. From the head of Spraddle Creek, the fault extends southwestward into the eastern flank of the Vail syncline, separating steeply dipping beds of the syn-

clinal flank from gently dipping beds to the east. At Gore Creek the fault bends southward, slicing across the eastern flank of the Vail syncline to Two Elk Creek. Farther south, a series of short en echelon faults in the Minturn Formation suggests that the zone of deformation in the basement rocks persists to the vicinity of Gilman and might even project to fractures of the Homestake shear zone. Through most of its length, the Spraddle Creek fault is downthrown to the east, and from Gore Creek southward the displacements are less than 100 ft (30 m).

The Red and White syncline is a large and nearly symmetric syncline that occupies most of the area between the mouth of Gore Creek and the Piney River (pl. 1, sec. B-B'). In much of this area, rocks of the Maroon Formation—and also of the Chinle and younger formations in a small area on Red and White Mountain—are disturbed by many gentle flexures; thus, the syncline is scarcely evident from the attitudes of the strata as observed on the surface. The southeastern nose of the syncline is blunt and is an abrupt northwest-dipping monocline (pl. 1, sec. C-C') that extends along the north side of Gore Creek from the Eagle River to Red Sandstone Creek where it flattens somewhat and turns northward and then northwestward. On the spur north of Dowds, east-west faults with as much as 1,000 ft (305 m) of displacement increase the structural displacement along the monocline, inasmuch as they are downthrown to the north. In effect, the curving monocline or synclinal nose separates a southern area that is structurally a part of the flank of the Sawatch Range from a northern area that is part of a large structural basin in the area bordered by the Sawatch Range, White River Plateau, and northern Gore Range (figs. 1, 24).

In the vicinity of Dickson Creek, a small but sharp north-trending anticline—the Dickson anticline—is superposed on the lower northeastern flank of the Red and White syncline (pl. 1, sec. A-A'). The Dickson anticline enlarges northward and is a major structural feature along the Piney River near the quadrangle boundary (pl. 1, sec. D-D'). The anticline is cut acutely by two northwest-trending faults that have opposite displacements. The faults define a long narrow horst that is upthrown about 200 ft (60 m) on the northeastern side and nearly 1,000 ft (305 m) on the southwestern side (pl. 1, sec. D-D').

The area between the Dickson anticline and the Gore fault is occupied by the East Meadow anticline, which trends east, almost at right angles to the Dickson anticline (pl. 1, map and sec. B-B'). At the intersection of the two anticlines, on the slope southwest of the mouth of Meadow Creek, the tight nose of the East

Meadow anticline forms a crossfold on the flank of the Dickinson anticline (pl. 1). Much of the East Meadow anticline is concealed by glacial deposits, and its structure near the Gore fault could not be observed.

BEDDING FAULTS IN GILMAN AREA

The mine workings at Gilman and the cliffs in the canyon nearby expose many low-angle, or bedding-plane faults, and closely related small steep faults in the pre-Pennsylvanian rocks. Such faults probably are widespread in the quadrangle, but in the absence of near-perfect exposures they generally are not seen. The bedding faults record many different directions of movement and are interpreted as a complex system of adjustments to the regional flexural folding expressed by the Sawatch anticline and the synclinal region to the east.

The bedding faults occur persistently at certain stratigraphic horizons and also are scattered widely through the dolomites of the Dyer and Leadville. Stratigraphically, the lowest of the persistent fault zones is the Rocky Point zone near the top of the Sawatch Quartzite. The Rocky Point is a brecciated zone 2–10 ft (0.6–3 m) thick; it is subparallel to the bedding and is an important ore horizon in the quartzite. Slip surfaces within the zone indicate that the upper beds first moved northerly with respect to the lower ones and then, after or during fracturing that produced northeast-trending joints, they moved northeast down the dip.

One of the most persistent of the bedding faults follows the shaly layers in the upper part of the Harding Sandstone. It is exposed in a few places in mine workings and can be seen in a roadcut about 1.5 mi (2.4 km) southeast of Gilman. In the Eagle mine (fig. 8), the fault is marked by wet, gougy, "heavy" ground. Drag folds indicate that the upper block moved west; the amount of displacement was not ascertained but may amount to several hundred feet.

Persistent bedding fault zones also occur at the contact of the Parting Formation and Dyer Dolomite and in the Dyer at a horizon about 25 ft (7.6 m) above the contact. Both zones are altered and are mineralized in places, especially in the vicinity of some ore bodies. The faulted zone at the top of the Parting is a zone of thrust-fault movement; strata above the zone moved southwest almost straight updip, suggesting response to regional folding. Two periods of movement are shown in the fault zone in the Dyer, an early strike-slip movement that carried the upper beds northwest and a later normal-fault movement that displaced these beds due east. The uppermost persistent zone of bedding-plane

movement observed near Gilman is at the base of the Belden Formation. The fault zone is about 8 ft (2.4 m) thick where it is exposed beneath the porphyry sill in roadcuts just north of Rock Creek; drag folds and minor faults within the zone indicate a low-angle normal fault.

The bedding faults scattered through the Leadville Dolomite and Dyer Dolomite show movements of both the normal and reverse types. The amount and direction of movement on such faults is difficult to ascertain, but drag folds, grooves, striations, and gouge seams that displace conjugate systems of cross veinlets and that truncate folds and other structural features show the nature and the general magnitude of the movements. Bedding-plane thrust faults are apparently confined to relatively few surfaces; on these, the upper beds moved west and southwest updip relative to the underlying rocks. In contrast, normal-fault or down-dip movement of upper beds on bedding-plane slips was widespread. In some places steep calcite veinlets are displaced along planes an inch or so apart through many feet of section, and although the displacement along individual slips is rarely more than a few inches, the aggregate movement amounts to several feet in a bed 10 ft (3 m) thick. Not all the normal-fault movement was of this pervasive type, however, and much of it was concentrated in shaly beds.

In some places bedding-plane or low-angle faults turn abruptly into vertical faults whose walls moved past each other along a line parallel to the low-angle slip. A fault block lying between two vertical walls, and roofed and floored by bedding-plane slips or low-angle faults, acts as a separate tectonic tongue whose movement may not be reflected in the enclosing rocks. We refer to the steep faults bordering such blocks as tongue faults in the report on the Gilman district (Lovering and others, 1977). In the district, the permeable zones created by bedding-plane slips and tongue faults were important factors in the circulation of ground waters and ore solutions.

ECONOMIC GEOLOGY

The principal mineral deposits known in the Minturn quadrangle are in the Gilman district; they are described in a companion report (Lovering and others, 1977). The Gilman district, which ranks fifth in total output among the metal mining districts in Colorado, is a major source of zinc and has also produced large amounts of silver, copper, lead, and gold. The total value of the production through 1972 was about \$328 million. The main ore bodies of the district are replacement deposits in the pre-Pennsylvanian formations, prin-

cipally the Leadville Dolomite. Rocks of the Belden and Minturn Formations above the mineralized formations show little evidence of mineralization or of the rich ore bodies that lie beneath them. Had the Eagle River not cut a canyon through the mineralized area, it is doubtful that the ore deposits of the Gilman district would yet be known.

If ore deposits are concealed beneath the wide expanses of Pennsylvanian rocks elsewhere in the quadrangle, evidence of them—to judge by the Gilman district—may be scant and subtle. Accordingly, even minor indications of mineralization or hydrothermal alteration in the Pennsylvanian rocks may be significant as evidence of “leaks” from potentially larger mineralized bodies in the underlying Leadville and older carbonate rocks. We discuss below the few localities showing evidence of mineralization or alteration noted in our mapping in the sedimentary terrane, particularly in the Minturn Formation. More detailed mapping and geochemical studies would almost certainly reveal others.

Most of the visible evidence of mineralization in the Minturn Formation is found in the carbonate beds, generally near faults. In such occurrences, the carbonate rocks are irregularly recrystallized to a coarse-grained vuggy light-brown to pearly-gray dolomite. Brown siderite occurs in some of the vugs and in scattered veinlets cutting some of the hydrothermal dolomite. White barite is present locally, either as vug crystals or as small veinlets. Sulfide minerals occur sporadically, either as crystals in vugs or as small lumps and veinlets. Chalcopyrite is the most common sulfide mineral in these occurrences, though pyrite, sphalerite, or galena may predominate locally. Quartz crystals are abundant in the vugs in some localities. Fluorite is present in vugs in a few places, occurring as small colorless to pale-green cubic crystals. Silver is present in an unidentified form in some of the altered carbonate rocks, as indicated by assays of 1–3 ounces of silver per ton from a few samples that contained no visible sulfide minerals.

Small bodies of carbonate rocks showing these characteristics occur on the top of Battle Mountain, along faults near the head of Rock Creek, in dolomite reefs on Willow Creek, in two thin dolomite beds at the mouth of Wearyman Creek, along faults at the head of Wearyman Creek, along the Spraddle Creek fault north of Gore Creek and south of Mill Creek, and along the long east–west fault (pl. 1) east of Gilman. Where this fault crosses Turkey Creek, veins of chalcopyrite an inch (2.5 cm) or more in width cut limestone just north of the fault in the valley bottom on the northwest side of the creek; on the southeast side of the creek, boulders of limestone in landslide debris are partly dolomitized,

show zebra-rock structure, and contain disseminated siderite and chalcopyrite.

A small fluorite vein was noted on one of the en echelon faults at the southern end of the Spraddle Creek fault, on a shoulder south of Two Elk Creek, 3 mi (4.8 km) north-northeast of Gilman (pl. 1). The vein contains as much as 6 in. (15 cm) of pale-green fluorite through an exposed length of about 30 ft (9 m).

Uranium occurs in small amounts in red clastic rocks of the upper part of the Minturn Formation along the Black Gore Creek at the quadrangle boundary (Grossman, 1955). Exploratory drilling was done in the area in the 1950's, but little or no uranium production resulted. The drilling confirmed the unconformity beneath the upper part of the Minturn Formation in this area, as some of the drill holes passed into Precambrian rocks at shallow depth. Larger but low-grade deposits of uranium occur in the Gartra Sandstone Member of the Chinle Formation west of the quadrangle, near Red and White Mountain (Butler and others, 1962).

The Gore fault and many other faults in the Precambrian rocks of the Gore Range are accompanied in many places by hydrothermally altered zones, and, in a few places, by quartz or carbonate veins that locally contain traces of sulfide minerals. Many of the faults or veins are geochemically anomalous in one or more of several metals: copper, lead, zinc, gold, silver, molybdenum, bismuth, arsenic, antimony, cadmium, mercury, and tin (Tweto and others, 1970). Despite these anomalies, evidence of mineralization on a scale large enough to induce prospecting is scant. Quartz veins near the head of Deluge Creek, a northern tributary of Gore Creek a mile (1.6 km) east of the quadrangle boundary, locally contain the copper mineral bornite and are reported to have yielded a small amount of selected copper ore that was hauled out by pack burro. Similar but smaller copper-bearing quartz veins are exposed in cliffs beside Bighorn Creek between the 10,600- and 10,700-ft contours, but a prospect tunnel driven beneath the exposures encountered only tight unmineralized fractures. Narrow quartz-carbonate veins exposed in short prospect tunnels and trenches east of Pitkin Lake (lake at head of west fork of Pitkin Creek) contain silver-bearing copper and lead minerals in vuggy masses a few inches in diameter. At various places, but especially to the north of the Piney River, a few of the fracture surfaces in the Gore fault zone are coated with films of malachite or azurite a few square inches in area. About a mile (1.6 km) north of the quadrangle, malachite occurs as films on bedding planes and disseminated in sandstone of the lower part of the Morrison Formation upturned against the Gore fault. Though some of the sandstone contains as much as 1.2 percent copper and a little silver (Tweto and others,

1970, p. 91) the mineralized part is less than 100 ft² (9 m²) in area and is not of itself of commercial significance.

The geochemical anomalies and most of the vein material found along the faults in the Gore Range were concluded by Tweto, Bryant, and Williams (1970) to be products of metal-bearing solutions that passed through the fracture system in the Precambrian rocks enroute either to hot springs at the surface or to mineral deposits in sedimentary rocks now eroded away. In part, at least, these solutions were introduced into the fracture system after the late Tertiary uplift of the Gore Range; thus, they reflect a mineralization epoch younger than those of major mining districts nearby. However, some part of the mineralization and most of the alteration probably are products of earlier Tertiary or Laramide hydrothermal activity.

In the part of the Sawatch Range included within the quadrangle, little evidence of mineralization is seen. Jasperoid that has replaced carbonate rocks of the Dyer and Leadville Dolomites is present near Minturn, as indicated on plate 1, but it is nearly barren of metals other than iron (T. G. Lovering, 1972, p. 79-81). In the area southwest of Gilman, where the carbonate rocks are no longer preserved, short veins of jaspery quartzite breccia or of hematitic breccia occur in the Sawatch Quartzite in several places. As judged from the small size of prospect diggings on many of these veins, the jaspery and hematitic materials are barren of metal values in the commercial range, but, to our knowledge, they have not been tested geochemically for trace metals. Except in the Gilman district, no evidence of mineralization was observed in the Precambrian rocks of the Sawatch Range.

The rapid urbanization of the valley of Gore Creek has created a large demand for sand and gravel. The quadrangle is not well endowed with these materials. Because of the urbanization, deposits in the valley of Gore Creek are eliminated from availability. Other stream valleys in the sedimentary terrane contain little gravel, and what exists is of poor quality because it is derived from weak and inhomogeneous sedimentary rocks. The only large and readily accessible potential source of sand and gravel of good quality is in the moraines near the mouth of Cross Creek. These moraines consist almost entirely of materials derived from Precambrian rocks; though containing boulders, they could become a source of sand and aggregate of good quality. Moraines in the valley of the Piney River area are also potential sources of sand and gravel. However, these moraines contain a fraction of red sedimentary rocks from the Minturn and Maroon Formations; hence, they might not be as suitable for aggregate as the moraines of Cross Creek. They are also far less accessible than those of Cross Creek.

TYPE SECTION

Type section of the Minturn Formation

(Section begins at small knob at elevation 11,300 ft on ridge between Mill Creek and Two Elk Creek, midway between the mountains with elevations 11,400 and 11,223 ft, approximately sec. 22, unsurveyed T. 5 S., R. 80 W., Minturn 15-minute quadrangle, 1934 edition (pl. 1). Section measured southward down spur toward Two Elk Creek. Section is inaccurately offset, as indicated, and ends at intersection of U.S. Highway 24 and Rock Creek, 0.35 mi (400 m) north of Gilman, approximately SE $\frac{1}{4}$ sec. 13, unsurveyed T. 6 S., R. 81 W. Measured by T. S. Lovering, 1963.)

	Thickness (feet)	Distance above base (feet)
Maroon Formation:		
Sandstone and siltstone, highly micaceous, thin bedded; weather medium reddish gray.		
Conformable contact	6,308	
Minturn Formation:		
Jacque Mountain Limestone Member:		
135. Limestone. Upper part contains oolitic beds that grade laterally into mottled light- and dark- gray pseudoconglomerate consisting of algal nodules in lighter limestone matrix, cephalopods and fragmentary or poorly preserved brachiopods present but uncommon. Middle part is light gray, medium grained, and medium bedded. Lower 10 ft is thin bedded and irregular bedded, fine grained, and mottled pale pinkish gray and pale green. Pink color cuts across bedding	31	6,277
Clastic unit H:		
134. Sandstone, siltstone, and shale. Sandstone and siltstone are red, weather pale grayish red; many sandstone beds are crossbedded; siltstone is micaceous and platy. Shale is light green, weathers green and medium grayish red; breaks in flasse chips	330	5,947
133. Shale, red and green; and minor interbedded red sandstone and siltstone	35	5,912
132. Conglomeratic grit in massive resistant bed	12	5,900
131. Grit and interbedded sandstone and minor shale, medium- to dark- grayish red; some green mottling on fresh fracture; is thin to medium bedded. Grit is calcareous	108	5,792
130. Sandstone, dark red; has some interbedded calcareous siltstone and $\frac{1}{2}$ -in. beds of silty limestone	25	5,767
129. Conglomeratic grit and interbedded sandstone and siltstone. Grit is light- greenish gray; weathers light pinkish gray; is thin bedded; contains abundant 1- to 2-in. pebbles of quartz and felsitic Precambrian rocks and some pebbles of fresh mafic rock; grit is highly arkosic and some is calcareous. Siltstone is micaceous and greenish gray	100	5,667
128. Conglomerate, consists of pebbles, 4- to 6-in. cobbles and of a few 12-in.		

Type section of the Minturn Formation — Continued		Thickness	
Minturn Formation — Continued		(feet)	Distance
Clastic unit H — Continued			(feet)
128. Conglomerate — Continued			
boulders of Precambrian rocks in green-gray grit matrix	35	5,632	
127. Grit and conglomeratic grit, and minor interbedded sandstone and siltstone, as in unit 128	115	5,517	
126. Limestone, moderate to pale red, has light green spots; weathers light pinkish gray; is thin bedded, flaggy, and medium grained; contains abundant muscovite throughout, and upper layers also contain abundant medium to fine-grained biotite and pink feldspar	3	5,514	
125. Siltstone, sandstone, and shale, interbedded. Siltstone and shale are light green and weather reddish gray; sandstone is medium grayish red; sandstone and siltstone are very thin bedded to thin bedded; weather in flaggy to platy ledges; most beds are limy; some sandstones are crossbedded. Thin bedded conglomerate with pebbles 1–2 in. in diameter at 40 ft above base	73	5,441	
124. Grit and sandstone, interbedded, light-pinkish gray; weather medium to dark grayish red. Grits are about half feldspar and half quartz; contain scattered quartz and pegmatite pebbles 1 1/2 in. in maximum size; are calcareous. Conglomeratic grit bed near top of unit contains limestone fragments and grades laterally into limestone and calcareous grit. In lower middle part, unit is interbedded grayish-red and grayish-green siltstone and moderate-red sandstone. Near base, unit is moderate-red to grayish-red, fine to medium-grained thin-bedded sandstone, is calcareous; contains fresh mafic minerals grains	180	5,261	
123. Shaly siltstone, sandstone, and grit, interbedded. Siltstone weathers medium grayish green. The sandstone weathers light brownish gray. Sandstones are medium to coarse grained, some grades into grit; consists of quartz and mica with some feldspar and mafic minerals. Both grit and siltstone contain abundant feldspar in a green, probably chloritic, matrix. Grit predominates in the interval from 10 to 50 ft above the base of unit	70	5,191	
White Quail Limestone Member.			
122. Dolomite, light pinkish-gray, dense, thin-bedded; top 6 in. layer is reefoid, porous; weathers yellow brown	4	5,187	

Type section of the Minturn Formation — Continued		Thickness	
Minturn Formation — Continued		(feet)	Distance
White Quail Limestone — Continued			(feet)
121. Limestone, medium bluish gray, weathers medium light gray, except light bluish gray at top; is fine grained, medium crystalline, and medium to thin bedded; Locally oolitic; where oolitic, is light brownish gray. Weathers in slightly rounded slabby blocks; forms low ledge	8	5,179	
120. Gritty limestone and interbedded calcareous grit in about equal proportions. Limestone is medium blue gray; weathers medium light blue gray; contains feldspar, quartz, and mica; grades into grit by increase in clastic material. Both grit and limestone are crossbedded	10	5,169	
119. Limestone, mottled dark gray and brownish gray; weathers medium light bluish gray; is medium to fine crystalline and thin bedded; forms massive low cliff	14	5,155	
118. Covered. Probably interbedded shale, shaly limestone, and thin-bedded grit	10	5,145	
117. Limestone, dark gray, weathers medium bluish gray; is thin bedded	5	5,140	

(Section is offset 1 mile west on White Quail Limestone Member to spur extending south-southwest from 11,225 ft mountain on divide between Two Elk and Mill Creeks. Section continues south from this point down nose to base of basal limestone bed of Robinson Member, about 120 ft (37 m) above Two Elk Creek.)

Clastic unit G:

116. Sandstone, arkosic grit, and shale, interbedded. Sandstone is light greenish gray; weathers grayish green; is very thin bedded to thin bedded, fine to medium grained, micaceous, and arkosic; is dolomitic in lower part. Grit is pale greenish gray; weathers pinkish gray; has abundant fresh pink feldspar in fragments as much as 1/2 in. in diameter	131	5,009	
---	-----	-------	--

Elk Ridge Limestone Member

115. Limestone, light gray to dark blue-gray; weathers light to medium blue gray; is fine grained to dense, thin to medium bedded, except thick bedded at base; some bedding in lower part distorted by domed algal structures. Uppermost bed is black, dark gray weathering. At 20 ft above base, is 8-in. dolomite bed, weathers brownish gray; has bunched parallel grooves on bedding planes	30	4,979	
--	----	-------	--

Clastic unit F:

114. Quartz grit, light-gray, well-sorted, consists almost entirely of gritty quartz grains in calcareous cement	8	4,971	
--	---	-------	--

Type section of the Minturn Formation — Continued

Minturn Formation — Continued

Clastic unit F — Continued

	Thickness (feet)	Distance above base (feet)
113. Sandstone, grit, and shale, interbedded. Grit predominates in upper third of unit; is light pinkish gray; contains abundant pink feldspar. Sandstone is light yellowish gray to light greenish gray, thin bedded to very thin bedded, fine to medium grained, except that it contains coarse mica; lowest bed contains abundant plant material	115	4,856
112. Shaly siltstone and shale. Dark gray shale in upper part grades downward into shaly siltstone that weathers dark gray to brownish red and to platy to fissile chips. Grades upward into dark shale	145	4,711
111. Conglomeratic grit and gritty sandstone, pale greenish gray; weathers pinkish gray to light red, is very thin bedded and micaceous	90	4,621
110. Dolomite, pale bluish gray; weathers pale brownish gray; is medium bedded, medium grained, and fossiliferous	5	4,616
109. Shaly siltstone and arkosic sandstone, light yellowish gray to light pinkish gray, thin bedded, at 30 ft above base is 15 ft ledge of coarse grained cross-bedded sandstone containing abundant muscovite flakes and angular quartz fragments as much as 1/2 in. in diameter. Unit forms sandy slope covered with thin platy fragments of the sandstone, coarse pebbles and cobbles about 120 ft above the base indicate a concealed conglomerate	190	4,426
Robinson Limestone Member:		
108. Limestone, medium- and irregular-bedded, weathers light blue gray blotched with irregular yellow brown areas of argillaceous material. Unit is poorly exposed; forms low terracelike change of slope	5	4,421
107. Mostly covered but sparse outcrops show interbedded grits, conglomeratic grits, and yellowish-gray shaly siltstone	125	4,296
106. Limestone, light blue gray, fine-grained, thin bedded. Bedding is very irregular; contains abundant fossils and fossil fragments; fossils recrystallized to pinkish-white coarse calcite. Unit crops out in sporadic low ledges	15	4,281
105. Covered, probably sandstone and siltstone	65	4,216
104. Limestone, medium- to light gray; weathers light bluish gray and is medium to thick bedded; contains		

Type section of the Minturn Formation — Continued

Minturn Formation — Continued

Robinson Limestone Member — Continued

	Thickness (feet)	Distance above base (feet)
104. Limestone — Continued abundant fossils. In middle upper part, fossils dolomitized and yellowish and pinkish gray, giving rock a mottled appearance. Productids are abundant in lower layers. Upper part of unit forms smoothly rounded cliff 10–15 ft high	40	4,176
103. Shale and micaceous siltstone, interbedded, yellowish- to pinkish-gray. Upper part of unit is concealed in covered slope. Fault repeats 50 ft of section, and thickness of unit is corrected accordingly	150	4,026
102. Limestone and subordinate dolomite. Upper 8–10 ft is dolomite with reef structure, medium yellowish gray; weathers brownish gray; is medium coarse grained, thin bedded, and shaly; forms ledge 8 ft high. Remainder is light bluish gray, medium- to thick bedded limestone; has nodular structure	43	3,983
101. Sandstone and siltstone, shaly, yellowish- to pinkish gray	80	3,903
100. Dolomite, light gray; weathers medium brownish gray; is thick bedded, medium crystalline; weathers in low rounded ledge	8	3,895
99. Micaceous sandstone and siltstone, interbedded, light greenish gray; weathers light yellowish gray to light pinkish gray. Sandstone is medium grained, moderately even grained, and thin to medium bedded, contains abundant mica and argillized plagioclase grains. Unit is poorly exposed	150	3,745
98. Limestone and dolomite, reefoid. Limestone is light brownish gray; weathers medium blue gray, is thin to thick bedded. Dolomite is granular, mostly medium grained but locally coarse grained; vuggy at base. Top of reef forms cliff 10–30 ft high	65	3,680

(Section is offset 4 miles northwest on lineations of Robinson Member to point at elevation 9,650 ft on ridge between Game and Gate Creeks. At this locality, limestone of unit 98 is 120 ft thick. Section continues southwest into valley of Game Creek and along steep road in valley.)

Clastic unit E

97. Sandstone, siltstone, and minor dolomite. Sandstone and intergrading siltstone are greenish gray; weather medium yellowish brown, are thin bedded, arkosic, and micaceous, many beds are dolomitic; some contain abundant mafic grains. Dolomite is brownish gray; weathers medium yellow, is fine grained;

Type section of the Minturn Formation — Continued

Minturn Formation — Continued

Clastic unit E — Continued

	Thickness (feet)	Distance above base (feet)
97. Sandstone, siltstone, and minor dolomite — Continued contains fine quartz grains; occurs in scattered thin beds. Unit forms smooth slope; exposed only in jeep trail	234	3,446
96. Dolomite, medium blue-gray; weathers light brownish gray; is very finely crystalline and thin to medium bedded	6	3,440
95. Sandstone, conglomeratic grit, shaly siltstone, and shale. Unit is mostly greenish-gray, thin- to medium-bedded arkosic sandstone, with minor interbedded siltstone, shale, and conglomeratic grit. Most of unit weathers gray to light greenish gray. Many of sandstone beds grade into arkosic grit; some appear to be gypsiferous, none are calcareous; all weather readily. Conglomeratic grit contains pebbles 1/2 in. or less in diameter and local lenses of conglomerate. Shale is dark gray to greenish gray and finely micaceous. Siltstone is greenish gray to medium green, shaly, highly micaceous, and chloritic. Beds range in thickness from a few inches to a few feet and alternate in a random way. Unit weathers to a smooth slope and is not well exposed	530	2,910
94. Probable equivalent of Hornsiver Dolomite Member of Pando area. Dolomite, grit, sandstone, and shale. Upper part is sandy dolomite grading into dolomitic sandstone; is very micaceous; weathers orange brown; breaks into angular blocks and slabs. Middle part is interbedded conglomeratic grit and dolomitic sandstone; weathers brown speckled with orange-brown spots; is strongly crossbedded. Gritty dolomite at base is overlain by black shale with interbedded black dolomite in thin beds, up to 10 ft above base	54	2,856
93. Sandstone and grit (80 percent), shaly siltstone (10 percent), shale and dolomite (10 percent). Unit weathers pale yellowish brown to light orange brown and is thin to medium bedded. Unit has a few lenses of quartz-pebble conglomerate, pebbles are mostly less than 1 in. in diameter, but a few are as much as 2 in. Unit forms slope with a few ledges of sandstone cropping out	70	2,786
92. Shale, shaly siltstone, sandstone, and grit. Shale is dark gray; weathers medium gray. Siltstone is gray; weathers medium gray to brown and		

Type section of the Minturn Formation — Continued

Minturn Formation — Continued

Clastic unit E — Continued

	Thickness (feet)	Distance above base (feet)
92. Shale, shaly siltstone, sandstone, and grit — Continued light brown. Both shales and siltstones contain abundant plant remains. Sandstone and gritty sandstone weather light bluish gray to light yellowish gray; are thin to medium bedded, and contain scattered plant remains. Thin sandstone beds have current ripple marks	60	2,726
91. Grit, conglomeratic, gray to brownish-gray, medium- to thick bedded, unevenly calcareous. Pebbles are chiefly quartz	15	2,711
90. Siltstone, shale, and gritty sandstone, interbedded. Siltstone is micaceous, very fine grained, and grades into shale. Sandstone is arkosic and light green; weathers medium grayish green; is thin to medium bedded and medium grained to gritty. Unit has 1-ft bed of sandy calcareous dolomite about 30 ft above base. Unit forms smooth slope broken by ledgy layers of sandstone	55	2,656
89. Sandstone, dolomitic and gritty, yellowish-gray mottled with light yellowish-brown, medium-bedded ...	5	2,651
88. Grit, conglomeratic, weathers pale brownish gray to pale gray; is poorly cemented and poorly sorted; is medium to thick bedded, contains scattered pebbles 1/2–3 in. in diameter that include wide variety of Precambrian rocks. Unit forms covered slope with sporadic outcrops in rounded forms	94	2,557
87. Siltstone and gritty sandstone, arkosic; weathers brownish gray to light yellowish gray; are thin bedded to very thin bedded; contain abundant plant remains	6	2,551
86. Probable equivalent of Wearyman Dolomite Member of Pando area. Shale (80 percent), silty dolomite (10 percent), and micaceous sandstone (10 percent). Shale is dark gray; weathers light gray; is micaceous. Dolomite is gray; weathers brown; occurs as beds 1–3 in. thick. Sandstone is greenish gray; weathers brown, micaceous	27	2,524

Section is offset about 1.4 miles south on contact between probable Wearyman equivalent and top of underlying grit marker bed (pl. 1) to point N. 6° E. of Minturn Ranger Station, at top of highest bold cliffs at approximate elevation of 9,975 ft. Section continues southward down cliffs)

Clastic unit D:

85. Grit marker bed. Conglomerate and grit are light gray to pale green;

Type section of the Minturn Formation — Continued

Minturn Formation — Continued

Clastic unit D — Continued

85. Grit marker bed — Continued

weather pale pinkish gray to pale greenish gray; are medium bedded and crossbedded; alternate layers of fine- and coarse-grained conglomerate and interbedded grit give banded appearance. Most pebbles are less than 3 in. across, but some are as much as 1 ft.; are mostly granitic and metamorphic rocks, subangular to subrounded, tending toward flat ellipsoidal shapes. Unit forms highest sheer cliff on upper slope of Eagle Valley east of Minturn

Thickness
(feet)

Distance
above base
(feet)

193 2,331

84. Sandstone, grit, and minor interbedded siltstone and shale. Sandstone and grit are arkosic, micaceous, reddish green; weather light brownish gray to light greenish gray; are mostly thin bedded and slabby or flaggy. Shale is dark olive gray and fissile. There are ripple marks about 3 in. from crest to crest at 27 ft. above base of unit

33 2,298

83. Sandstone, grit, siltstone, and conglomerate, interbedded; are light green; weather pale greenish gray; are thin to thick bedded. Many beds contain coarse and poorly sorted fresh feldspar grains in a slightly dolomitic matrix of pyritic and micaceous sandstone. Some sandstone and grit beds show penecontemporaneous slumping and minor faulting. Conglomerates contain cobbles as much as 8 in. across; most conglomerate layers are nonpersistent and fill channels. Persistent conglomerate bed 2 ft. above base of unit is overlain by very thin bedded micaceous sandstone or laminated siltstone

56 2,242

82. Siltstone, grit, and dolomite, interbedded, thin- to medium-bedded. Siltstone is pale green; weathers pale greenish gray; is shaly, coarsely micaceous; contains abundant grit. Grit is laminated; consists of coarse quartz grains in chloritic and micaceous matrix. Dolomite is medium gray; weathers light orange brown; ranges from dolomitic sandstone through sandy dolomite to conglomeratic dolomite with lenticular reefy masses of dolomite

17 2,225

(Section is offset 1,000 ft. north on unit 82 and continues down cliff)

81. Grit and sandstone, pale-pinkish-gray to pale-yellowish-gray. Unit is mostly

Type section of the Minturn Formation — Continued

Minturn Formation — Continued

Clastic unit D — Continued

81. Grit and sandstone — Continued

thick bedded with a few nonpersistent layers of very thin bedded micaceous sandstone in upper half. Grit is conglomeratic, poorly cemented, and slightly dolomitic. Pebbles and cobbles in the grit are as much as 8 in. across, erratically distributed, subangular, and consist of Precambrian rocks and minor green micaceous arkosic sandstone and brown weathering dolomite. In profile unit forms high cliff with rounded forms

Thickness
(feet)

Distance
above base
(feet)

101 2,124

80. Grit, sandstone, and shale. Grit is pale greenish gray; weathers light greenish gray; consists of feldspar, quartz, and abundant mica; is thin bedded and flaggy. Sandstone is coarse to medium grained. Shale is medium greenish gray; weathers light grayish green; is micaceous and laminated; weathers to fissile chips

55 2,069

79. Dolomite, micaceous, conglomeratic, medium-pinkish-gray; weathers light yellowish brown to medium orange brown; is medium bedded and slabby; contains subrounded to subangular pebbles of Precambrian rocks $\frac{1}{2}$ –6 in. across

2 2,067

78. Grit, pale-bluish gray; weathers pale yellowish gray to pale orangish gray; is arkosic, poorly cemented, and very thick bedded; has grains 2–8 mm in diameter; contains shales in small lenses both parallel to bedding and crosscutting at steep angle; steep lenses are 1 in. thick and 6–10 in. long

23 2,044

77. Grit (80 percent), shale (15 percent), and dolomite (5 percent), interbedded. Grit is light gray; weathers pale greenish gray to light yellowish gray; is conglomeratic and dolomitic, medium bedded; contains quartz pebbles as much as 3 in. in diameter. Shale is dark gray; weathers light gray; is laminated and fissile. Dolomite is dark gray; weathers medium brown; is fine to medium grained; is thin to medium bedded and flaggy; occurs as lenticular beds

90 1,954

76. Grit, shale, and sandstone, interbedded, pale-yellowish-gray, thin- to thick-bedded. Grit is conglomeratic and calcareous; contains pebbles as much as 8 in. across; is in well defined beds with irregular but nearly parallel tops and bottoms; grades into very thin

Type section of the Minturn Formation — Continued		Thickness	
Minturn Formation — Continued		above base	
Clastic unit D — Continued		(feet)	(feet)
76. Grit, shale and sandstone — Continued			
bedded micaceous sandstone at top of unit. Shale layers are thickest in middle of unit	27	1,927	
75. Shale, very dark gray; weathers gray; contains minor interbedded brownish gray thin-bedded micaceous grit and siltstone. Unit is mostly covered	23	1,904	
74. Grit and conglomerate, with siltstone and shale partings. Some layers are dolomitic, changing on strike to gritty dolomite that pinches and swells in thickness from a few inches to 2 ft. Unit weathers light greenish gray to light grayish brown; is platy to slabby; forms cliff. Upper part contains quartz pebbles $\frac{1}{2}$ –3 in. across in matrix of poorly sorted sand and grit	33	1,871	
73. Conglomerate, light-brownish gray to light greenish gray, very thick bedded, poorly cemented, poorly sorted. Pebbles are subrounded to subangular, mostly of Precambrian rocks but a few of dolomite; matrix is coarse calcareous grit. Unit forms cliff pocked by caverns several feet high along vertical joints	46	1,825	
72. Grit (60 percent), shale (25 percent), and dolomite (15 percent), interbedded. Unit is thin to medium bedded. Grit is greenish gray to brownish gray; weathers pale brown; contains brown-weathering carbonate grains. Shale is light gray. Dolomite is dark gray to brownish gray; weathers medium brown; is fine grained and gritty	36	1,789	
71. Grit and conglomerate with a few shale partings. Unit is pale greenish gray to light brownish gray and thin to thick bedded. Conglomerate is poorly sorted; has pebbles 2–6 in. across in grit matrix. Unit forms prominent cliff 50 ft high	54	1,735	
70. Shale, siltstone, grit, conglomerate, and dolomite, interbedded. Shale is dark gray; weathers medium gray; is laminated and fissile. Siltstone and grit are greenish gray to brownish gray; are thin to medium bedded and very micaceous; siltstone is laminated. Conglomerate is pale pinkish gray; weathers pale greenish gray; is poorly cemented, most of pebbles are quartz. Some fine-grained grit and siltstone contain abundant plant fragments, especially rushlike leaves	74	1,661	

Type section of the Minturn Formation — Continued		Thickness	
Minturn Formation — Continued		above base	
Clastic unit D — Continued		(feet)	(feet)
69. Grit and sandstone, light gray to nearly white, weather pale brownish gray to medium light gray; is thin to very thick bedded, coarsely crossbedded, poorly sorted, and poorly cemented. Some beds are dolomitic; are light brown and cavernous where weathered. Grit contains pebbles of quartz, Precambrian rock, and dolomite	28	1,633	
68. Shale (70 percent) and dolomite (30 percent), interbedded. Shale is dark gray; weathers light to dark gray; is laminated to very thin bedded, and dolomitic near base. Dolomite in upper part is dark gray; weathers light yellow brown to light orange brown; is thin to medium bedded, dense, and almost lithographic; middle part is medium brownish gray, and gritty to conglomeratic; is pinkish gray, micaceous, and medium fine grained near base. Unit forms ledgy slope, mostly covered ...	95	1,538	
Clastic unit C:			
67. Reef dolomite of Lionshead, dark gray; weathers medium brown; is fine to medium grained, medium to thick bedded, and slabby or flaggy; contains poorly preserved fossils; is irregularly vuggy, with calcite crystals in the vugs. At 20–35 ft above base conglomeratic grit butts against side of reef in steep but sedimentary contact; dolomite above the grit contains abundant quartz pebbles. Upper surface of reef is irregular	48	1,490	
66. Sandstone, siltstone, and grit, interbedded. Sandstone and grit are light greenish gray to pale red; weather grayish brown to orange brown and, locally, to bright red; are calcareous, dolomitic, thin to medium bedded, and flaggy; is crossbedded in middle of unit. Siltstone is dark greenish gray and dusky red to light brown; weathers dark greenish gray, medium reddish gray, and medium orange brown; is very micaceous and very thin bedded to fissile	38	1,452	
65. Sandstone and minor shale, medium-light gray; weather light yellowish gray; are micaceous, medium grained, medium well sorted, and medium to thick bedded	13	1,439	
64. Shale (60 percent), siltstone (20 percent), and sandstone (20 percent), interbedded. Shale is dark			

Type section of the Minturn Formation — Continued		Thickness (feet)	Distance above base (feet)
Minturn Formation — Continued			
Clastic unit C — Continued			
54. Shale, siltstone, and sandstone —			
Continued			
greenish gray; weathers medium greenish gray; is interlayered with laminated micaceous siltstone that weathers to fissile chips. Sandstone is medium light gray, weathers dark gray to orange-brown; is thin to medium bedded			
63	Shale and dolomite. Shale is dark greenish gray; weathers dark grayish green; is silty, laminated, and fissile. Dolomite is medium grayish green; weathers medium grayish brown; is medium grained, medium bedded, and flaggy; contains abundant white- and black mica and fine grained sand	57	1,382
62	Grit, light grayish green; weathers light greenish gray; is arkosic, locally conglomeratic, medium bedded, and flaggy; contains a few siltstone partings	20	1,362
61	Shale, dark gray to dark greenish gray; weathers dark greenish gray; is very thin bedded to fissile; contains plant remains in lower part. In middle of unit is 18-in. bed of medium bluish-gray, medium-orange brown weathering dolomite	45	1,317
60	Grit, conglomeratic, pale greenish gray to pale pinkish gray, calcareous; weathers light pinkish gray; is very thin bedded and platy at top, massive in middle, and very thin bedded at base	14	1,303
59	Shale and minor shaly siltstone, black; weathers dark greenish gray to dark gray, in part is finely micaceous	18	1,285
58	Sandstone and grit, greenish- and pinkish gray; coarse grit at top of unit and medium fine-grained sandstone at base. Unit forms prominent continuous ledge with irregular profile	10	1,275
57	Grit (50 percent), shale (30 percent), and sandstone (20 percent), interbedded, light grayish-green. Sandstone and grit are thin to medium bedded. Sandstone is medium fine grained and micaceous. Shale is micaceous and fissile	17	1,258
56	Shale, shaly siltstone, and grit, grayish-green; weathers greenish gray. Grit is sandy to conglomeratic, forms ledges 2-4 ft thick on shaly slope	33	1,225
55	Shale and dolomite, interbedded. Shale is light greenish gray, micaceous, and fissile. Dolomite is in beds 2-4 in. thick, except 4 ft bed near top of unit	70	1,155
		19	1,136

Type section of the Minturn Formation — Continued		Thickness (feet)	Distance above base (feet)
Minturn Formation — Continued			
Clastic unit C — Continued			
54. Sandstone and conglomeratic grit,			
interbedded, pinkish gray to light gray except maroon to pink at base, medium thin bedded to massive, strongly crossbedded. Grit contains scattered pebbles, and a few lenses of conglomerate			
53	Sandstone, shaly siltstone, and shale, top is approximately top of lower red zone in section in this area. Sandstone is hematitic and chloritic; weathers dark red; is very thin to medium bedded; forms ledges 1-2 ft thick. Shaly siltstone and shale are red and laminated or fissile	20	1,116
52	Sandstone and grit, mottled light-greenish gray and light green; weather light pinkish gray. Grit is arkosic, locally conglomeratic, very micaceous, slightly calcareous, and crossbedded	21	1,095
51	Sandstone (40 percent), siltstone (30 percent), and shale (30 percent), interbedded; weather medium red, except some ledges weather light grayish green. Shale is red to dark green and hematitic to chloritic. Sandstone is red to medium greenish gray. Coarse conglomerate layer 10 ft below top of unit contains pebbles of Precambrian rocks and of greenish micaceous shale and siltstone	14	1,081
		51	1,030
Clastic unit B			
50	Dolomite bed of Dawds. Cherty dolomite, medium gray; weathers light grayish brown; is thin to very thin bedded and flaggy, with greenish-gray shale films on bedding planes. Chert is light to medium gray; some chert lenticles cut bedding in dolomite at low angle	6	1,024
49	Grit, sandstone, and siltstone, pinkish-gray to light greenish gray, weather medium red with light gray streaks. Unit is medium to thick bedded, has local lenses of micaceous conglomerate. Upper part of unit is very thin bedded hematitic shaly siltstone	26	998
48	Sandstone (70 percent), shale (20 percent), and siltstone (10 percent) interbedded. Sandstone is partly hematitic and dark red, and partly arkosic, chloritic, and gray; is thin to medium bedded, poorly sorted, and fine grained to gritty; includes some graywacke. Shale is medium green to dark greenish gray; weathers light green; is laminated and fissile. Siltstone is shaly, finely micaceous, hematitic, and laminated; some		

Type section of the Minturn Formation — Continued		Thickness	
Minturn Formation — Continued		(feet)	Distance
Clastic unit B — Continued			(feet) above base
46. Sandstone, shale, and siltstone — Continued			
hematitic layers show ripple marks, rill marks, and possible raindrop impressions	52	946	
47. Grit, sandstone, and siltstone. Poorly sorted conglomeratic grit alternates with well-sorted medium-grained arkosic sandstone containing abundant fresh pink feldspar grains. Grit is light greenish gray; weathers light gray to brownish gray; is thin bedded, but weathers in massive rounded forms. A little shaly siltstone occurs in middle of unit	37	909	
46. Shale, mudstone, and siltstone, interbedded; are thin to medium bedded. Shale is green; weathers light green. Mudstone is light brownish green; weathers yellowish brown to medium red; contains abundant medium- to coarse-grained muscovite, black mica, and other mafic minerals in a very fine grained slightly chloritized matrix	8	901	
45. Grit, conglomeratic, pale gray; weathers light gray to yellowish gray; is thin to medium bedded and flaggy; contains fresh feldspar, chloritized mafic minerals, and scattered 1-3 in. quartz pebbles	12	889	
44. Sandstone (80 percent) and shale (20 percent), interbedded. Sandstone is medium gray; weathers light brownish gray to medium red; is poorly sorted and gritty; contains fresh pink feldspar, chloritized coarse hornblende and biotite, and abundant white mica. Shale is light greenish gray	23	866	
43. Sandstone and grit, light greenish gray; weathers light yellowish brown; are thin to medium bedded, crossbedded, and flaggy. Layers of well-sorted, medium grained arkosic sandstone alternate with grit containing abundant quartz and Precambrian pebbles in highly micaceous matrix. Some layers contain abundant limonite spots and carbonized plant remains; also contain minor thin interbeds of fissile greenish gray shale	25	841	
42. Shale (70 percent), and sandstone (30 percent), interbedded. Shale is micaceous, silty, and light green, except lower 6 ft is red. Sandstone is pinkish gray; weathers light brownish gray; is arkosic, medium bedded, and locally crossbedded	10	831	

Type section of the Minturn Formation — Continued		Thickness	
Minturn Formation — Continued		(feet)	Distance
Clastic unit B — Continued			(feet) above base
41. Sandstone and minor interbedded siltstone. Uppermost bed is a medium-red fine-grained hematitic sandstone. Sandstone below is light greenish gray to light brownish gray; weathers pale greenish gray to pale pink; is medium to thick bedded, medium grained, well sorted, and arkosic; contains abundant brown limonite spots; has chlorite matrix. Siltstone is shaly, light greenish gray, very thin bedded to laminated, and contains abundant mica and chlorite	10	821	
40. Covered	28	793	
39. Sandstone, arkosic, conglomeratic, medium gray; weathers dirty brownish yellow; is medium to thick bedded, faintly crossbedded; is interbedded with light grayish-yellow fine grained micaceous thin-bedded sandstone	14	779	
38. Sandstone and grit, light gray to light-yellowish gray; weathers light yellowish brown to medium grayish brown. Sandstone is medium grained, well cemented, and thin bedded; weathers to platy slabs. Grit is thin to medium bedded, flaggy, and locally crossbedded; contains small quartz pebbles. A 5-ft bed of conglomeratic grit 35 ft above base of unit shows both trough and planar crossbedding	44	735	
37. Covered slope	35	700	
36. Sandstone, grit, and shale, interbedded. Sandstone is light greenish yellow, and thin to very thin bedded; consists of fine grained quartz and abundant medium-grained mica. Grit is light grayish white, very arkosic, locally conglomeratic, thin to medium bedded, flaggy, and crossbedded. Shale is pale grayish yellow; weathers light olive yellow; is micaceous and very thinly laminated	55	645	
35. Grit and interbedded shale. Grit is conglomeratic; contains green chloritic particles; is medium grayish red to medium grayish brown; weathers pale brownish yellow to dark grayish red; is thick bedded; contains 1/4-in. quartz pebbles. Shale is dark grayish red; weathers medium grayish red; is very thin bedded to fissile	94	551	
34. Sandstone, gray, medium-grained, crossbedded	10	541	

Type section of the Minturn Formation — Continued

Minturn Formation — Continued

Clastic unit B — Continued

	Thickness (feet)	Distance above base (feet)
33. Grit and conglomerate; has shale partings. Unit is light pinkish gray; weathers light grayish white to pale pinkish red with black seams; is very thick bedded; has planar crossbedding; contains many pebbles of green chloritic phyllite as well as pegmatite, granite, and metamorphic rocks; pebbles are as much as 3 in. across. Local channeling occurs between units ...	20	521
32. Grit and conglomerate, light-yellowish-brown to light-pinkish-gray; weathers medium orange brown to medium grayish red; are medium to very thin bedded, flaggy, and crossbedded. Pebbles are similar to those in unit 33	92	429
31. Grit and sandstone, arkosic, light-reddish-gray to light-yellowish-gray; weathers dark orange brown; are thin to medium bedded, and flaggy	35	394
30. Grit, grayish-red; weathers dark grayish red; is thin to medium bedded, flaggy, and arkosic; contains minor muscovite and chloritic phyllite	18	376

(Interval between unit 30 and top of Leadville Limestone is largely covered. Section is offset 3.7 mi southward to slope on north side of Rock Creek, north of Gilman, to corresponding stratigraphic position above Leadville. Section ends at top of amended type section of Balden Formation. (See fig. 9).)

Clastic unit A:

29. Grit; is in part conglomeratic; grades into quartz-pebble conglomerate, locally crossbedded	18	358
28. Shale, hematitic, dark-red; marks approximate base of lower red zone	5	353
27. Shale and sandstone, interbedded. Shale is green and fissile. Base of unit is 3-ft bed of brown-speckled gray sandstone	31	322
26. Sandstone and shale, interbedded. Shale is light green; forms 15-ft bed at top of unit. Sandstone is pinkish gray	71	251
25. Dolomite; contains abundant fossil fragments	2	249
24. Sandstone, greenish gray; weathers dark orange brown; is medium to thick bedded, and, in part, crossbedded; is arkosic and sideritic. Greenish micaceous shale in beds 1 ft or less thick occur in lower 15 ft of unit	35	214
23. Conglomerate and sandstone. Upper part is a light-pinkish-gray medium-bedded crossbedded medium- to fine-grained sandstone containing thin beds of conglomerate and lenses of		

Type section of the Minturn Formation — Continued

Minturn Formation — Continued

Clastic unit A — Continued

	Thickness (feet)	Distance above base (feet)
23. Conglomerate and sandstone — Continued green and red shale. This grades downward into pinkish-gray medium- to thick-bedded conglomeratic sandstone, and this grades into dark-red conglomerate at base. Conglomerate contains 1-in. pebbles of white and pink quartz, dark chert, and finely micaceous green shale fragments; matrix is micaceous	22	192
22. Shale, micaceous, green with dark-maroon-red streaks	1	191
21. Sandstone (70 percent), and shale (30 percent), interbedded. Sandstone is light greenish gray and thin to medium bedded, contains pebbles as much as 1/2 in. in diameter in a matrix of fine to coarse quartz grains. Shale is medium green; weathers light green; is very thin bedded	9	182
20. Grit, conglomeratic, light-green, weathers medium brown; is micaceous and poorly sorted; contains quartz pebbles 1/2 in. in diameter and minor feldspar	1	181
19. Shale, micaceous, green; mostly covered	17	164
18. Quartz-pebble conglomerate, light-gray; weathers light orange brown; is thick bedded; matrix is medium to coarse grained; pebbles are 1/2-1 1/2 in. in diameter	5	159
17. Dolomite, thin- to medium-bedded; is in persistent layers, has thin shale parting at top	2	157
16. Shale and sandstone, interbedded. Shale is fissile and thin bedded. Sandstone is medium bedded, fine grained to gritty, and micaceous; has clay cement	8	149
15. Conglomerate and sandstone, light-gray; weathers light brownish gray; are medium to thick bedded; have pebbles up to 3/4 in. that are mostly quartz but some that are chert, sandstone, and quartzite. Sandstone at base has irregular upper surface	8	141
14. Shale, dolomite, and grit, interbedded. Unit is mostly dolomite and dolomitic grit in upper half and mostly shale in bottom half. Shale is platy and dolomitic in middle and fissile at bottom. Grit is very dolomitic; contains dolomite nodules	7	134
13. Dolomite and shale. 1.5-ft dolomite bed at top is medium bedded, medium fine grained, and nonmicaceous; has		

Type section of the *Minturn Formation* — Continued
Minturn Formation — Continued
 Clastic unit A — Continued

	Thickness (feet)	Distance above base (feet)
13. Dolomite and shale — Continued few shale partings. Dolomite is underlain by 3 ft bed of fissile black noncalcareous shale with lenticular gritty dolomites 1–3 in. thick. 1 ft of gritty dolomite is at base	6	128
12. Shale and grit, interbedded. Shale is micaceous and pink; weathers light gray to yellow brown. Grit is chloritic, with some shale partings . .	8	120
11. Sandstone, light greenish gray; weathers medium orange brown to brownish gray; is poorly sorted, fine to coarse grained, very micaceous and crossbedded; has layers 1–6 ft thick; shale partings 1 in. to several inches thick occur between beds . . .	22	98
10. Shale (80 percent) and dolomite (20 percent), interbedded; beds are 1–3 in. thick. Shale is fissile in upper part and thin platy in lower part	8	90
9. Conglomerate. Pebbles are subangular to subrounded, 1/4–1.5 in. across but mostly about 1/4 in., are mostly quartz, but some are shale and black or gray chert (from Leadville(?) Limestone); some are coarse white quartzite (from Parling(?) Formation); Precambrian pebbles are minor. Rock contains spots of coarse-grained recrystallized carbonate and sparse grains of chalcocopyrite; weathers with many vugs, which probably represent leached carbonate	8	82
8. Shale and grit, micaceous; is very thin bedded in upper part and medium bedded at base. Grit is mostly quartz and mica	12	70
7. Shale and dolomite, interbedded; is in equal proportions. Shale is medium gray and thin bedded. Dolomite is gritty, greenish gray to brownish gray	12	58
6. Shale, dolomite, and grit, interbedded. Shale is medium gray, weathers light blue gray; is irregular and very thin bedded; contains lenses of grit as much as 1 ft thick and 10 ft long. Dolomite is greenish gray; weathers orange brown; is argillaceous, gritty, and micaceous; contains some chlorite; has angular quartz fragments as much as 1/2 in. in diameter	9	49
5. Sandstone and minor interbedded micaceous shale. Sandstone is medium grained, poorly sorted, micaceous, chloritic, and thin to thick bedded; occurs in lenticular beds; is crossbedded at top of unit.		

Type section of the *Minturn Formation* — Continued
Minturn Formation — Continued
 Clastic unit A — Continued

	Thickness (feet)	Distance above base (feet)
5. Sandstone and minor interbedded micaceous shale — Continued with foreset beds as much as 10 ft long	16	33
4. Shale and micaceous dolomite, interbedded. Shale is medium gray to dark gray; weathers medium light gray. Dolomite is micaceous and medium greenish gray; weathers brownish gray; occurs in lenticular nodular beds 1–8 in. thick	8	25
3. Grit, arkosic, medium gray to light-greenish-gray, medium grained; contains many thin partings of micaceous shale, grit bed locally cuts down into underlying shale as much as 30 in. and thickens correspondingly	2	23
2. Shale (80 percent), grit (15 percent), and dolomite (5 percent), interbedded. Shale is dark gray; weathers medium gray; contains arkosic grit in lenses 3–12 in. thick and 10–50 ft long. Dolomite is medium light gray; weathers light brownish gray	9	14
1. Sandstone, gritty, medium-light gray; weathers light gray, except orange-brown stain on joints from weathering of iron-bearing carbonate; is massive to thick bedded; lowest bed shows planar and trough crossbedding, contains sparse 1/2-in. quartz pebbles mixed with poorly sorted medium-fine to coarse quartz and altered feldspar grains; also contains abundant small grains and blebs of brown-weathering carbonate, presumably siderite	14	0

Channelled contact.

Belden Formation:

Black shale and limestone.

NOTE — Summary of measured thicknesses of major units.

	Feet	Meters
Jacque Mountain Limestone Member	31	9.45
Clastic Unit H	1,086	331.1
White Quail Limestone Member	51	15.55
Clastic Unit G	131	39.95
Elk Ridge Limestone Member	30	9.15
Clastic Unit F	553	168.6
Robinson Limestone Member	746	227.45
Clastic Unit E	1,156	352.45
Clastic Unit D	986	300.6
Clastic Unit C	508	154.9
Clastic Unit B	654	199.4
Clastic Unit A	376	114.6

Total measured thickness of the *Minturn*

Formation 6,308 1,923.2

REFERENCES CITED

- Baars, D. L., 1966, Pre-Pennsylvanian paleotectonics—Key to basin evolution and petroleum occurrences in Paradox basin, Utah and Colorado; *Am. Assoc. Petroleum Geologists Bull.*, v. 50, no. 10, p. 2082-2111.
- Baker, A. A., Dane, C. H., and Reeside, J. B., Jr., 1936, Correlation of Jurassic formations of parts of Utah, Arizona, New Mexico, and Colorado; *U.S. Geol. Survey Prof. Paper* 183, 66 p.
- Bail, S. H., 1906, Precambrian rocks of the Georgetown quadrangle, Colorado; *Am. Jour. Sci.*, 4th ser., v. 21, p. 371-389.
- Banks, N. G., 1967, Geology and geochemistry of the Leadville Limestone (Mississippian, Colorado) and its diagenetic, supergene, hydrothermal and metamorphic derivatives; *California Univ. (San Diego) Ph. D. thesis*, 298 p.
- , 1970, Nature and origin of early and late cherts in the Leadville Limestone, Colorado; *Geol. Soc. America Bull.*, v. 81, no. 10, p. 3033-3048.
- Barclay, C. S. V., 1968, Geology of the Gore Canyon Krumming area, Grand County, Colorado, U.S. Geol. Survey open-file rept., 187 p.
- Bass, N. W., 1944, Correlation of basal Permian and older rocks in southwestern Colorado, northwestern New Mexico, northeastern Arizona, and southeastern Utah; *U.S. Geol. Survey Oil and Gas Inv., Prelim. Chart* 7.
- , 1958, Pennsylvanian and Permian rocks in the southern half of the White River uplift, Colorado, in *Symposium on Pennsylvanian rocks of Colorado and adjacent areas*, Rocky Mtn. Assoc. Geologists, p. 91-94.
- Bass, N. W., and Northrop, S. A., 1950, South Canyon Creek Dolomite Member, a unit of Phosphoria age in Maroon Formation near Glenwood Springs, Colorado; *Am. Assoc. Petroleum Geologists Bull.*, v. 34, no. 7, p. 1540-1551.
- , 1953, Dotsero and Manitou Formations, White River Plateau, Colorado, with special reference to Clinetop algal limestone member of Dotsero Formation; *Am. Assoc. Petroleum Geologists Bull.*, v. 37, no. 5, p. 889-912.
- , 1963, Geology of Glenwood Springs quadrangle and vicinity, northwestern Colorado; *U.S. Geol. Survey Bull.* 1142-J, 74 p.
- Bassett, C. F., 1939, Paleozoic section in the vicinity of Dotsero, Colorado; *Geol. Soc. America Bull.*, v. 50, no. 12, p. 1851-1866.
- Behre, C. H., Jr., 1929, Revision of structure and stratigraphy in the Mosquito Range and the Leadville district, Colorado; *Colorado Sci. Soc. Proc.*, v. 12, no. 3, p. 37-57.
- , 1932, The Weston Pass mining district, Lake and Park Counties, Colorado; *Colorado Sci. Soc. Proc.*, v. 13, no. 3, p. 53-75.
- Behre, C. H., Jr., and Johnson, J. H., 1933, Ordovician and Devonian fish horizons in Colorado; *Am. Jour. Sci.*, 5th ser., v. 25, no. 150, p. 477-486.
- Berg, R. R., 1960, Cambrian and Ordovician history of Colorado, in *Weimer, R. J., and Haun, J. D., eds., Guide to the geology of Colorado*; *Geol. Soc. America, Rocky Mtn. Assoc. Geologists, and Colorado Sci. Soc.*, p. 10-17.
- Berg, R. R., and Ross, R. J., 1959, Trilobites from the Peerless and Manitou Formations, Colorado; *Jour. Paleontology*, v. 33, no. 1, p. 106-119.
- Bergendahl, M. H., 1969, Geologic map and sections of the southwest quarter of the Dillon quadrangle, Eagle and Summit Counties, Colorado; *U.S. Geol. Survey Misc. Geol. Inv. Map* 1-563.
- Bergendahl, M. H., and Koehmann, A. H., 1971, Ore deposits of the Kokomo-Tenmile district, Colorado; *U.S. Geol. Survey Prof. Paper* 652, 53 p.
- Blackwelder, Eliot, 1915, Post-Cretaceous history of the mountains of central western Wyoming; *Jour. Geology*, v. 23, p. 97-117, 193-217, 307-340.
- Boggs, Sam, Jr., 1966, Petrology of Minturn Formation, east-central Eagle County, Colorado; *Am. Assoc. Petroleum Geologists Bull.*, v. 50, no. 7, p. 1399-1422.
- Borcherdt, W. O., 1931, The Empire Zinc Company's operations at Gilman, Colorado; *Eng. and Mining Jour.*, v. 132, p. 99-105, 251-261.
- Brennan, W. J., 1969, Structural and surficial geology of the west flank of the Gore Range, Colorado; *Colorado Univ. Ph. D. thesis*, 109 p.
- Brill, K. G., Jr., 1942, Late Paleozoic stratigraphy of Gore area, Colorado; *Am. Assoc. Petroleum Geologists Bull.*, v. 26, no. 8, p. 1375-1397.
- , 1944, Late Paleozoic stratigraphy, west-central and north-western Colorado; *Geol. Soc. America Bull.*, v. 55, no. 5, p. 621-656.
- , 1952, Stratigraphy in the Permo-Pennsylvanian zuegog-syncline of Colorado and northern New Mexico; *Geol. Soc. America Bull.*, v. 63, no. 8, p. 809-880.
- Bryant, W. L., and Johnson, J. H., 1936, Upper Devonian fish from Colorado; *Jour. Paleontology*, v. 10, no. 7, p. 656-659.
- Burchard, E. F., 1911, Gypsum deposits in Eagle County, Colorado; *U.S. Geol. Survey Bull.* 470, p. 354-365.
- Butler, A. P., Jr., Finch, W. I., and Tweenhofel, W. S., compilers, 1962, Epigenetic uranium in the United States, exclusive of Alaska and Hawaii; *U.S. Geol. Survey Mineral Inv. Resource Map MR-21*, separate text.
- Campbell, J. A., 1967, Dispersal patterns in Upper Devonian quartzite sandstones in west-central Colorado, in *Oswald, D. H., ed., International Symposium on the Devonian System, Calgary, 1967*, v. 2; *Calgary, Alberta Soc. Petroleum Geologists*, p. 1131-1138, [1968].
- , 1970, Stratigraphy of Chaffee Group (Upper Devonian) west-central Colorado; *Am. Assoc. Petroleum Geologists Bull.*, v. 54, no. 2, p. 313-325.
- Cheney, M. G., 1940, Geology of North-Central Texas; *Am. Assoc. Petroleum Geologists Bull.*, v. 24, no. 1, p. 65-118.
- Chronic, John, McCallum, M. E., Ferris, C. S., and Eggler, D. H., 1969, Lower Paleozoic rocks in diatremes, southern Wyoming and northern Colorado; *Geol. Soc. America Bull.*, v. 80, no. 1, p. 149-156.
- Conley, C. D., 1965, Petrology of the Leadville Limestone (Mississippian), White River Plateau, Colorado [abs.]; *Mtn. Geologist*, v. 2, no. 3, p. 181-182.
- Craig, L. C., and others, 1955, Stratigraphy of the Morrison and related formations, Colorado Plateau region—A preliminary report; *U.S. Geol. Survey Bull.* 1009-E, p. 125-168.
- Crawford, R. D., and Gibson, Russell, 1925, Geology and ore deposits of the Red Cliff district, Colorado; *Colorado Geol. Survey Bull.* 30, 89 p.
- Cross, Whitman, Howe, Ernest, and Ranaome, F. L., 1905, Description of the Silverton quadrangle [Colorado]; *U.S. Geol. Survey Geol. Atlas*, Folio 120.
- Curtis, B. F., 1958, Pennsylvanian paleotectonics of Colorado and adjacent areas, in *Symposium on Pennsylvanian rocks of Colorado and adjacent areas*, Rocky Mtn. Assoc. Geologists, p. 9-12.
- Denison, R. H., 1951, Late Devonian fresh-water fishes from the western United States: Fieldiana—Geology, v. 11, no. 5, p. 221-261.
- Dings, M. G., and Robinson, C. S., 1957, Geology and ore deposits of the Garfield quadrangle, Colorado; *U.S. Geol. Survey Prof. Paper* 289, 109 p.
- Donnell, J. R., 1954, Tongue of Weber Sandstone in Maroon Formation near Carbonade and Redstone, northwestern Colorado; *Am.*

- Assoc. Petroleum Geologists Bull., v. 38, no. 8, p. 1817-1821.
- , 1958, The Weber Sandstone in the White River uplift, in *Symposium on Pennsylvanian rocks of Colorado and adjacent areas*. Rocky Mtn. Assoc. Geologists, p. 95-98.
- Donner, H. F., 1936, *Geology of the McCoy area, Eagle and Routt Counties, Colorado*. Michigan Univ. Ph. D. thesis.
- , 1949, *Geology of the McCoy area, Eagle and Routt Counties, Colorado*. Geol. Soc. America Bull., v. 60, no. 8, p. 1215-1248.
- Eldridge, G. H., 1894, Description of the sedimentary formations, in *Anthracite-Crested Butte folio* [Colorado]: U.S. Geol. Survey Geol. Atlas, Folio 9.
- Emmons, S. F., 1882, Abstract of report on geology and mining industry of Leadville, Lake County, Colorado: U.S. Geol. Survey 2d Ann. Rept., p. 201-290.
- , 1886, *Geology and mining industry of Leadville, Colorado*. U.S. Geol. Survey Mon. 12, 770 p.
- , 1898, Description of the Tenmile district quadrangle [Colorado]: U.S. Geol. Survey Geol. Atlas, Folio 48.
- Emmons, S. F., Irving, J. D., and Loughlin, G. F., 1927, *Geology and ore deposits of the Leadville mining district, Colorado*: U.S. Geol. Survey Prof. Paper 148, 368 p.
- Engel, A. E. J., Clayton, R. N., and Epstein, Samuel, 1958, Variations in isotopic composition of oxygen and carbon in Leadville Limestone (Mississippian, Colorado) and in its hydrothermal and metamorphic phases. *Jour. Geology*, v. 66, no. 4, p. 374-393.
- Folk, R. L., 1959, Practical petrographic classification of limestones. *Am. Assoc. Petroleum Geologists Bull.*, v. 43, no. 1, p. 1-38.
- Freeman, V. L., 1971, Stratigraphy of the State Bridge Formation in the Woody Creek quadrangle, Pitkin and Eagle Counties, Colorado: U.S. Geol. Survey Bull. 1324-F, 17 p.
- Gabelman, J. W., 1950, *Geology of the Fulford and Brush Creek mining districts, Eagle County, Colorado*: Mining Year Book 1950, Colorado Mining Assoc., p. 50-52.
- Grossman, E. L., 1955, Do Rado claims, Vail Pass district, Eagle County, Colorado (PRR-DEB-P-3-1756). In *Preliminary reconnaissance reports on reported occurrences of uranium deposits, Eagle County, Colorado*. Available from U.S. Dept. Commerce Natl. Tech. Inf. Service, Springfield, Va. 22161, as Rept. 172 537, 23 p.
- Guterman, F., 1890, Gold deposits in the quartzite formations of Battle Mountain, Colorado: Colorado Sci. Soc. Proc., v. 3, p. 264-268.
- Hallgarth, W. E., 1959, Stratigraphy of Paleozoic rocks in northwestern Colorado: U.S. Geol. Survey Oil and Gas Inv. Chart OC-59.
- , 1967, Western Colorado, southern Utah, and northwestern New Mexico, in McKee, E. D., Ortel, S. S., and others, *Paleotectonic investigations of the Permian System in the United States*. U.S. Geol. Survey Prof. Paper 515, p. 175-197.
- Hallgarth, W. E., and Skipp, B. A. L., 1962, Age of the Leadville Limestone in the Glenwood Canyon, western Colorado, in *Short papers in geology, hydrology, and topography*: U.S. Geol. Survey Prof. Paper 450-D, p. D37-D38.
- Hansen, W. R., and Peterman, Z. E., 1968, Basement-rock geochronology of the Black Canyon of the Gunnison, Colorado, in *Geological Survey research 1968*: U.S. Geol. Survey Prof. Paper 600-C, p. C80-C90.
- Harrison, J. E., and Wells, J. D., 1959, *Geology and ore deposits of the Chicago Creek area, Clear Creek County, Colorado*: U.S. Geol. Survey Prof. Paper 319, 92 p.
- Hayden, F. V., 1877, *Geological and geographical atlas of Colorado and portions of adjacent territory*. U.S. Geol. and Geog. Survey Terr., 20 pls.
- Hedge, C. E., Peterman, Z. E., and Braddock, W. A., 1967, Age of the major Precambrian regional metamorphism in the northern Front Range, Colorado: Geol. Soc. America Bull., v. 78, no. 4, p. 551-558.
- Hemley, J. S., and Jones, W. R., 1964, Chemical aspects of hydrothermal alteration with emphasis on hydrogen metasomatism: *Econ. Geology*, v. 59, no. 4, p. 538-569.
- Henbest, L. C., 1946, Correlation of the marine Pennsylvanian rocks of northern New Mexico and western Colorado [abs.]: *Washington Acad. Sci. Jour.*, v. 36, p. 134.
- , 1958, Significance of karst terrane and residuum in Upper Mississippian and Lower Pennsylvanian rocks, Rocky Mountain region, in *Wyoming Geol. Assoc. Guidebook 13th Ann. Field Conf., Powder River Basin*, 1958, p. 36-38.
- Hubert, J. F., 1960, Petrology of the Fountain and Lyons Formations, Front Range, Colorado: Colorado School Mines Quart., v. 55, no. 1, 242 p.
- Hunter, J. F., 1925, Precambrian rocks of the Gunnison River, Colorado: U.S. Geol. Survey Bull. 777, 94 p.
- Hutchinson, R. M., and Hedge, C. E., (editors), 1967, Precambrian basement rocks of the central Colorado Front Range and its 700-million-year history: *Geol. Soc. America, Rocky Mtn. Sec., Field Trip No. 1, 20th Ann. Mtg., Golden, Colo.*, 1967, 51 p.
- Izett, G. A., 1968, The Miocene Troublesome Formation in Middle Park, northwestern Colorado: U.S. Geol. Survey open-file rept., 42 p.
- James, H. L., 1966, Chemistry of the iron-rich sedimentary rocks. Chap. V, in Fleischer, Michael, ed., *Data of geochemistry*, 8th ed.: U.S. Geol. Survey Prof. Paper 440-W, 61 p.
- Johnson, J. H., 1934, Paleozoic formations of the Mosquito Range, Colorado: U.S. Geol. Survey Prof. Paper 185-B, p. 15-43 [1935].
- , 1944, Paleozoic stratigraphy of the Sawatch Range, Colorado: *Geol. Soc. America Bull.*, v. 55, no. 3, p. 303-378.
- Kirk, Edwin, 1931, The Devonian of Colorado: *Am. Jour. Sci.*, 5th ser., v. 22, p. 222-240.
- Koehnman, A. H., and Wells, F. G., 1946, Preliminary report on the Kokomo mining district, Colorado: Colorado Sci. Soc. Proc., v. 15, no. 2, p. 49-112.
- Langenheim, R. L., 1952, Pennsylvanian and Permian stratigraphy in Crested Butte quadrangle, Gunnison County, Colorado: *Am. Assoc. Petroleum Geologists Bull.*, v. 36, no. 4, p. 543-574.
- Lochman-Balk, Christina, 1956, The Cambrian of the Rocky Mountains and southwest deserts of the United States and adjoining Sonora Province, Mexico, in Rodgers, J., ed., *El sistema Cambrico, su paleogeografía y el problema de su base*: *Internat. Geol. Cong.*, 20th, Mexico v. 2, pt. 2, p. 529-657.
- Lovering, T. G., 1972, Jasperoid in the United States—its characteristics, origin, and economic significance: U.S. Geol. Survey Prof. Paper 710, 164 p.
- Lovering, T. S., 1929, Geologic history of the Front Range Colorado: Colorado Sci. Soc. Proc., v. 12, no. 4, p. 59-111.
- Lovering, T. S., and Johnson, J. H., 1933, Meaning of unconformities in stratigraphy of central Colorado: *Am. Assoc. Petroleum Geologists Bull.*, v. 17, no. 4, p. 353-374.
- Lovering, T. S., and Mallory, W. W., 1962, The Eagle Valley Evaporite and its relation to the Minturn and Maroon Formations, northwest Colorado, in *Short papers in geology, hydrology, and topography*: U.S. Geol. Survey Prof. Paper 450-D, p. D45-D48.
- Lovering, T. S., and Tweto, O. L., 1944, Preliminary report on geology and ore deposits of the Minturn quadrangle, Colorado: U.S. Geol. Survey open-file rept., 115 p. and map.
- Lovering, T. S., and Tweto, Ogden, 1953, *Geology and ore deposits of the Boulder County tungsten district, Colorado*: U.S. Geol. Survey Prof. Paper 245, 199 p. [1954].
- Lovering, T. S., Tweto, Ogden, and Lovering, T. G., 1977, Ore deposits of the Gilman district, Eagle County, Colorado: U.S. Geol. Survey Prof. Paper 1017 (In press).

- MacLachlan, M. E., 1959, Western Colorado and Utah, in McKee, E. D., and others, Paleotectonic maps of the Triassic system. U.S. Geol. Survey Misc. Geol. Inv. Map 1-300, p. 3, 8, 1960.
- Mallory, W. W., 1958, Pennsylvanian coarse arkosic redbeds and associated mountains in Colorado, in Symposium on Pennsylvanian rocks of Colorado and adjacent areas: Rocky Mtn. Assoc. Geologists, p. 17-20.
- , 1971, The Eagle Valley Evaporite, northwest Colorado—a regional synthesis: U.S. Geol. Survey Bull. 1311—E, 37 p.
- McKee, E. D., 1945, Stratigraphy and ecology of the Grand Canyon Cambrian, Pt. 1, in Cambrian history of the Grand Canyon region: Carnegie Inst. Washington Pub. 563, p. 4-168.
- McKee, E. D., Oriol, S. S., and others, 1967, Paleotectonic investigations of the Permian System in the United States: U.S. Geol. Survey Prof. Paper 515, 271 p.; and Paleotectonic maps of the Permian System: U.S. Geol. Survey Misc. Geol. Inv. Map 1-450.
- McKee, E. D., and Weir, G. W., 1953, Terminology for stratification and cross stratification in sedimentary rocks: Geol. Soc. America Bull., v. 64, no. 4, p. 381-390.
- Means, A. H., 1915, Geology and ore deposits of Red Cliff, Colorado: Econ. Geology, v. 10, no. 1, p. 1-27.
- Miller, A. K., and Youngquist, W. L., 1949, American Permian nautiloids: Geol. Soc. America Mem. 41, 218 p.
- Moench, R. H., 1964, Geology of Precambrian rocks, Idaho Springs district, Colorado: U.S. Geol. Survey Bull. 1182-A, 70 p.
- Morris, H. T., and Lovering, T. S., 1961, Stratigraphy of the East Tintic Mountains, Utah: U.S. Geol. Survey Prof. Paper 361, 145 p.
- Murray, F. N., and Chronic, John, 1965, Pennsylvanian conodonts and other fossils from insoluble residues of the Minturn Formation (Desmoinesian), Colorado: Jour. Paleontology, v. 39, no. 4, p. 594-610.
- Murray, H. F., 1958, Pennsylvanian stratigraphy of the Maroon Trough, in Symposium on Pennsylvanian rocks of Colorado and adjacent areas: Rocky Mtn. Assoc. Geologists, p. 47-58.
- Mutschler, F. E., and Larson, E. E., 1969, Paleomagnetism as an aid in age classification of mafic intrusives in Colorado: Geol. Soc. America Bull., v. 80, no. 11, p. 2359-2368.
- Myers, D. A., 1968, Stratigraphic distribution, Pennsylvanian fusulines, Manzano Mountains, New Mexico (abs.): Am. Assoc. Petroleum Geologists Bull., v. 52, no. 3, p. 542.
- Naeser, C. W., Izett, G. A., and White, W. H., 1973, Zircon fission-track ages from some middle Tertiary igneous rocks in northwestern Colorado: Geol. Soc. America Abs. with Programs, v. 5, no. 6, p. 498.
- Olcott, E. E., 1887, Battle Mountain mining district, Eagle County, Colorado: Eng. and Mining Jour., v. 43, p. 418-419, 436-437.
- Oriol, S. S., and Craig, L. C., 1960, Lower Mesozoic rocks in Colorado, in Weimer, R. J., and Haun, J. D., eds., Guide to the geology of Colorado: Geol. Soc. America, Rocky Mtn. Assoc. Geologists, and Colorado Sci. Soc., p. 43-58.
- Peale, A. C., 1874, Arkansas Valley-Eagle River-Sawatch Range, Chap. 3, in Report on the South Park region, Colorado: U.S. Geol. and Geog. Survey Terr. (7th Ann. Rept. Hayden), p. 239-246.
- , 1876, Report on valleys of Eagle, Grand, and Gunnison Rivers, Colorado: U.S. Geol. and Geog. Survey Terr. (8th Ann. Rept. Hayden), p. 73-180.
- Pearson, R. C., Hedge, C. E., Thomas, H. H., and Stern, T. W., 1966, Geochronology of the St. Kevin Granite and neighboring Precambrian rocks, northern Sawatch Range, Colorado: Geol. Soc. America Bull., v. 77, no. 10, p. 1109-1120.
- Pearson, R. C., Tweto, Ogden, Stern, T. W., and Thomas, H. H., 1962, Age of Laramide porphyries near Leadville, Colorado, in Short papers in geology and hydrology: U.S. Geol. Survey Prof. Paper 450-C, p. C78-C80.
- Peck, R. E., 1957, North American Mesozoic Charophyta: U.S. Geol. Survey Prof. Paper 294-A, 44 p.
- Peterman, Z. E., Hedge, C. E., and Braddock, W. A., 1968, Age of Precambrian events in the northeastern Front Range, Colorado: Jour. Geophys. Research, v. 73, no. 6, p. 2277-2296.
- Pettijohn, F. J., 1957, Sedimentary rocks (2d ed.): New York, Harper and Brothers, 718 p.
- Pipiringos, G. N., Hail, W. J., Jr., and Izett, G. A., 1969, The Chinle (Upper Triassic) and Sundance (Upper Jurassic) Formations in north-central Colorado: U.S. Geol. Survey Bull. 1274-N, 35 p.
- Poole, F. G., Baars, D. L., Drewes, H., Hayes, P. T., Ketner, K. B., McKee, E. D., Teschert, C., and Williams, J. S., 1967, Devonian of the Southwestern United States, in Oswald, D. H., ed., International symposium on the Devonian System, Calgary, 1967, V. 1: Calgary, Alberta Soc. Petroleum Geologists, p. 879-912 [1968].
- Poole, F. G., and Stewart, J. H., 1964, Chinle Formation and Glen Canyon Sandstone in northeastern Utah and northwestern Colorado: in Geological Survey research 1964: U.S. Geol. Survey Prof. Paper 501-D, p. D30-D39.
- Radabaugh, R. E., Merchant, J. S., and Brown, J. M., 1968, Geology and ore deposits of the Gilman (Red Cliff, Battle Mountain) district, Eagle County, Colorado, in Ore deposits of the United States, 1933-1967 (Graton Sales Volume) V. 1: Am. Inst. Mining Metall., and Petroleum Engineers, p. 641-664.
- Raup, O. B., 1966, Clay mineralogy of Pennsylvanian redbeds and associated rocks flanking ancestral Front Range of central Colorado: Am. Assoc. Petroleum Geologists Bull., v. 50, no. 2, p. 251-268.
- Resser, C. E., 1942, New Upper Cambrian trilobites: Smithsonian Misc. Coll., v. 103, no. 5, (Pub. 3693), 136 p.
- Richmond, G. M., 1960, Glaciation of the east slope of Rocky Mountain National Park, Colorado: Geol. Soc. America Bull., v. 71, no. 9, p. 1371-1382.
- , 1964, Three pre-Bull Lake tills in the Wind River Mountains, Wyoming—a reinterpretation, in Geology Survey research 1964: U.S. Geol. Survey Prof. Paper 501-D, p. D104-D109.
- , 1965, Glaciation of the Rocky Mountains, in The Quaternary of the United States: Princeton, N.J., Princeton Univ. Press, p. 217-230.
- Roth, Robert, and Skinner, John, 1930, The fauna of the McCoy Formation, Pennsylvanian, of Colorado: Jour. Paleontology, v. 4, no. 2, p. 332-352.
- Rothrock, D. P., 1960, Devonian and Mississippian systems in Colorado, in Weimer, R. J., and Haun, J. D., eds., Guide to the geology of Colorado: Geol. Soc. America, Rocky Mtn. Assoc. Geologists, and Colorado Sci. Soc., p. 17-22.
- Sandberg, C. A., and Mapel, W. J., 1967, Devonian of the Northern Rocky Mountains and Plains, in Oswald, D. H., ed., International Symposium on the Devonian System, Calgary, 1967, V. 1: Calgary, Alberta Soc. Petroleum Geologists, p. 843-877 [1968].
- Sando, V. J., 1967, Madison Limestone (Mississippian), Wind River, Washakie, and Owl Creek Mountains, Wyoming: Am. Assoc. Petroleum Geologists Bull., v. 51, no. 4, p. 529-557.
- Seeland, D. A., 1968, Paleocurrents of the late Precambrian to early Ordovician (basal Sauk) transgressive clastics of the western and northern United States, with a review of the stratigraphy: Utah Univ. Ph. D. thesis, 170 p.
- Sheridan, D. S., 1950, Permian(?), Triassic, and Jurassic stratigraphy of the McCoy area of west-central Colorado: Compass, v. 27, no. 3, p. 126-147.
- Sims, P. K., and Gable, D. J., 1964, Geology of Precambrian rocks, Central City district, Colorado: U.S. Geol. Survey Prof. Paper 474-C, 52 p.
- , 1967, Petrology and structure of Precambrian rocks, Central City quadrangle, Colorado: U.S. Geol. Survey Prof. Paper 554-E, 56 p.

- Singewald, Q. D., 1931, Depositional features of the "Parting" quartzite near Alma, Colorado. *Am. Jour. Sci.*, 5th ser., v. 22, p. 404-413.
- 1947, Preliminary geologic map and sections of the upper Blue River area, Summit County, Colorado: U.S. Geol. Survey Prelim. Map [Republished in Singewald, 1951].
- 1951, Geologic and ore deposits of the upper Blue River area, Summit County, Colorado: U.S. Geol. Survey Bull. 970, 74 p. [1952].
- Stevens, C. H., 1962, Stratigraphic significance of Pennsylvanian brachiopods in the McCoy area, Colorado: *Jour. Paleontology*, v. 36, no. 4, p. 617-629.
- Stevens, D. N., 1961, Cambrian and Lower Ordovician stratigraphy of central Colorado, in Berg, R. R., and Rold, J. W., eds., *Symposium on Lower and Middle Paleozoic rocks of Colorado: Rocky Mtn. Assoc. Geologists 12th Field Conf.*, p. 7-15.
- Stewart, J. H., Poole, F. G., and Wilson, R. F., 1972, Stratigraphy and origin of the Triassic Moenkopi Formation and related strata in the Colorado Plateau region: U.S. Geol. Survey Prof. Paper 691, 195 p.
- Sweet, W. C., 1954, Harding and Fremont Formations, Colorado: *Am. Assoc. Petroleum Geologists Bull.*, v. 38, no. 2, p. 284-305.
- Taggart, J. N., 1962, *Geology of the Mount Powell quadrangle, Colorado*: Harvard Univ. Ph. D. thesis, 239 p.
- Thomas, C. R., McCann, F. T., and Raman, N. D., 1945, Mesozoic and Paleozoic stratigraphy in northwestern Colorado and northeastern Utah: U.S. Geol. Survey Oil and Gas Inv. Prelim. Chart 16.
- Thompson, M. L., 1945, Pennsylvanian rocks and fusulinids of east Utah and northwest Colorado correlated with Kansas section: *Kansas Univ. Geol. Survey Bull.*, 60, pt. 2, 84 p.
- Thompson, W. O., 1949, Lyons Sandstone of Colorado Front Range: *Am. Assoc. Petroleum Geologists Bull.*, v. 33, no. 1, p. 52-72.
- Tillman, R. W., 1971, Petrology and paleoenvironments, Robinson Member, Minturn Formation (Desmoinesian), Eagle Basin, Colorado: *Am. Assoc. Petroleum Geologists Bull.*, v. 55, no. 4, p. 593-620.
- Tweto, Ogden, 1949, Stratigraphy of the Pando area, Eagle County, Colorado: *Colorado Sci. Soc. Proc.*, v. 15, no. 4, p. 147-235.
- 1951, Form and structure of sills near Pando, Colorado: *Geol. Soc. America Bull.*, v. 62, no. 5, p. 507-532.
- 1953, Geologic map of the Pando area, Eagle and Summit Counties, Colorado: U.S. Geol. Survey Mineral Inv. Field Studies Map MF-12 [1954].
- 1956, Geologic map of the Tennessee Pass area, Eagle and Lake Counties, Colorado: U.S. Geol. Survey Mineral Inv. Field Studies Map MF-34.
- 1957, Geologic sketch of southern Middle Park, Colorado, in Finch, W. C., ed., *Guidebook to the geology of North and Middle Park basins*, Colorado: Rocky Mtn. Assoc. Geologists, p. 18-31.
- 1958, Pennsylvanian stratigraphic section in the Minturn-Pando area, Colorado, in *Symposium on Pennsylvanian rocks of Colorado and adjacent areas*: Rocky Mtn. Assoc. Geologists, p. 80-85.
- 1961, Late Cenozoic events of the Leadville district and upper Arkansas valley, Colorado, in *Short papers in the geologic and hydrologic sciences*: U.S. Geol. Survey Prof. Paper 424-B, p. B133-B135.
- 1964, Geology [of Colorado], in *Mineral and water resources of Colorado*: U.S. 88th Cong., 2d sess., Senate Comm. Interior and Insular Affairs, Comm. Print, p. 11-27.
- 1968a, Geologic setting and interrelationships of mineral deposits in the mountain province of Colorado and south-central Wyoming, in *Ore deposits of the United States, 1933-1967* (Graton-Sales Volume), V. 1: Am. Inst. Mining Metall. and Petroleum Engineers, p. 551-588.
- 1968b, Leadville district, Colorado, in *Ore deposits of the United States, 1933-1967* (Graton-Sales Volume), V. 1: Am. Inst. Mining Metall. and Petroleum Engineers, p. 681-705.
- 1974, Geologic map of the Holy Cross 15-minute quadrangle, Eagle, Lake, Pitkin, and Summit Counties, Colorado: U.S. Geol. Survey Misc. Geol. Inv. Map I-830, [1975].
- 1975, Laramide (Late Cretaceous-early Tertiary) orogeny in the Southern Rocky Mountains, in Curtis, B. F., ed., *Cenozoic history of the Southern Rocky Mountains*: *Geol. Soc. America Mem.* 144, p. 1-44.
- Tweto, Ogden, Bryant, Bruce, and Williams, F. E., 1970, Mineral resources of the Gore Range-Eagles Nest Primitive Area and vicinity, Summit and Eagle Counties, Colorado: U.S. Geol. Survey Bull. 1319-C, 127 p.
- Tweto, Ogden, and Case, J. E., 1972, Gravity and magnetic features as related to geology in the Leadville 30-minute quadrangle, Colorado: U.S. Geol. Survey Prof. Paper 726-C, 31 p. [1973].
- Tweto, Ogden, and Lovering, T. S., 1947, The Gilman District, Eagle County, in *Vanderbilt, J. W., Mineral resources of Colorado: Denver, Colorado Mineral Resources Board*, p. 378-387.
- Tweto, Ogden, and Sims, P. K., 1963, Precambrian ancestry of the Colorado mineral belt: *Geol. Soc. America Bull.*, v. 74, no. 8, p. 991-1014.
- Vaughn, P. P., 1969, Upper Pennsylvanian vertebrates from the Sangre de Cristo Formation of central Colorado: *Los Angeles County Mus. Contr. Sci.* no. 164, 28 p.
- Walker, T. R., 1967, Formation of red beds in modern and ancient deserts: *Geol. Soc. America Bull.*, v. 78, no. 3, p. 353-368.
- Weller, J. M., chm., and others, 1948, Correlation of the Mississippian formations of North America: *Geol. Soc. America Bull.*, v. 59, no. 2, p. 91-196.
- Wilson, J. A., 1939, A new species of dog from the Miocene of Colorado: *Michigan Univ. Mus. Paleontology Contr.*, v. 5, no. 12, p. 315-318.

INDEX

(Italic page numbers indicate major references)

A	Page
Abstract	1
Age, Belden Formation	37
Cambrian	18
Cretaceous	58
Cross Creek Granite	14
Devonian	23
Dyer Dolomite	28
Gilman Sandstone	50
Jurassic System	37
Loudville Limestone	32
Maroon Formation	45
Minurn Formation	44
Mississippian	23
Molas Formation	33
Ordovician	21
Purkin Formation	26
Purkin Formation	26
Pennsylvanian	33
Permian	33
Swatch Quartzite	17
Tertiary	36
Triassic System	36
Algal structures	58
Aliphone	60
Alivern	69
Amphipyon sp.	64
Ammonite Buckles	33
Anthracopirifer optimus	44
rockymontana	48
Anthracopirifer rudimentalis	48
hermanni	50
Araspho National Forest	37
Arenisiphetis rugulosa	26, 44
ap	48
Avon, gypsum	78
Azurite	78

B	Page
Bald Mountain, fault blocks	71
Minurn Formation, boulders	47
Swatch Quartzite	15
thinning, Swatch Quartzite	19
Banks, quoted	31
Barnes	31
Battle Mountain, concealed area	74
Battle Mountain formation	38
Bedding faults	77
Belden, pre-, unconformity	32
Belden Formation	34
age	37
bedding faults	77
bedding faults, rugged area	35
channel	35
fossils	38
Gordon, Mackenzie, Jr., and	37
Yochelson, E. L., quoted	37
Herbst, L. G., quoted	35
section, amended type	38
still	58
Belden mine	34
Belden Shale Member	34
Ben Butler mine	75
Bighorn Creek, copper-bearing quartz veins	43
dk	47
Minurn Formation	47

B	Page
Biotite gneiss	8
Black Canyon Schist	7
Black Gore Creek, glaciers	67
Minurn Formation	47
upturned conglomerate	71
uranium	78
Black Gore syncline	76
Blue Limestone	23
Bulls Lake, outcrop knob	45
Bulls Creek, Robinson Limestone Member	45
Bornite	26
Butholite	26
Boulder Creek Granite	9, 10
Bruckneria sagittata	64
actini	64
Bradyon	50
Breccian gneiss	13
granite	13
Bright Angel Shale	21
Branson	20
Brevicrus boudier	48
Browns Park Formation	64
Buck Creek, chart	65
Bull Lake Glacier	68

C

C	Page
Caliche veinlets	77
Calcuttella	50
Calcuttella sp.	50
Cambrian System	15
Cassiope coral, undet.	48
Carlsbad tunneling	10
Central sedimentary belt	75
Chertley sp.	48
Chaffee Formation	23
Chaffee Group	24
Chalcophyllite	78
Chertstone, Belden Formation	35
Dyer Dolomite	28
Channel cuts, Dyer Dolomite	27
Chertophyllite	58
Cherokee Shale, fossils	51
Chan	63
Banks, quoted	31
Gilman district	27
Gilman Sandstone	29
Chert breccia marker	31
Chill zones	59
Chinle Formation	53, 56
China Member	56
Red and White syncline	76
uranium	78
Chonetella jeffordii	50
Cnidarian spines	48
Cirques, old, Vaid	66
Clastic dikes, Minurn Formation	43
Clastic unit A, Minurn Formation	47
described	87
Clastic unit B, Minurn Formation	43
described	85
ripple marks	43
Clastic unit C, Minurn Formation	43
described	84

C	Page
Clastic unit D, Minurn Formation	44
described	82
ripple marks	83
rubble lenses	84
Clastic unit E, Minurn Formation	44
described	81
ripple marks	82
Clastic unit F, Minurn Formation	45
described	80
Clastic unit G, Minurn Formation	45
described	80
Clastic unit H, Minurn Formation	46
described	79
Cinctostylus arcticus	48
Cinctostylus sp.	50
Cinctostylus ornatus	26
Coal, Belden Formation	34
Minurn Formation	52
Coffee Pot Member	30
Collierium	65
chart	65
Colorado Atlas	48
Composita ovalis	48
subtilis	48
Condriakyrus perplexa	48
Condriakyrus perplexa	48
Copper Mountain, Minurn Formation	47
Cardioid	12
Cretaceous System	58
Cryobryozoa sp.	50
Cross Creek, glaciers	67, 68
moraines	32
sand	79
Cross Creek batholith	9
diorite	12
history	14
Cross Creek Glacier	67
Cross Creek Granite	7, 8, 74, 75
age, C. E. Hedge, analyst	14
catclasia	11
diorite	13
feldspar	11
M. Seerwald, analyst	11
Cryptokyrus planicostatus	48
Curtis Formation	57
Cynodermus curvi	64

D

D	Page
Dacite porphyry dikes	61
Daderion	55
Dakota Sandstone	56
Dalage Creek, quartz vein, hornite	78
Darbya crassa	48
Demomeneus muricata	37, 50
nana	48
Devonian System	23
Devilmas	17
monia	21
maru	17
pectinoides	17
Dickson enticline	76
Dickson Creek, anticline	76
tuff	64
Dickson Ranch, tuff	64

	Page
Gore fault - Continued	
Maroon Formation	54
red beds	56
shales	24
veins	76
Gore Range	3, 8, 63, 74
durite	12
metamite	12
uplift	69
west dike	61
Gore River, glacier	66
Gore Valley, landslides	68
Gothic Formation	52
Gravel	79
Green Mountain volcanic center	61
Grit marker bed	82
Gymnocladium	55
H	
Harding Sandstone	22
bedding faults	77
section	23
Hedge, C. H., analyst, Cross Creek Granite	14
Hematite	60
Henshaw, L. G., quoted	37
Hemlock Formation, fossils	50
Hemlock Formation	42, 52
Honestake Creek, metamite	12
Honestake shear zone	18, 16, 75, 76
Swatch Quartzite	15
Hornblende Dolomite Member	82
fossils	48
Minturn Formation	44
I, J	
Iaho Springs Formation	7
Iakona	20
Igneous rocks	58
Jacque Mountain Limestone Member	34
age	48
described	79
fossils	51
Minturn Formation	46
stylolites	47
Jacque Peak, Maroon Formation	54
Jaspered	79
Jasperoid replacement	24
Jurassic System	57
Jurassic subvolcanic	48
K, L	
Kaibab Formation	55
Kanawha Formation	37
Kokomo district, Minturn Formation	44
Kolowah sp. A	48
Landslides	68
Stone Creek	76
Leadville Dolomite	30
bedding faults	77
jaspered	79
origin	31
section	31
Leadville Limestone	23, 30
age	32
correlation	32
facies boundary	30
fossils	32
Lepidodendron	52
Lima sp.	48
Lime Cliffs	44
Litoropholites pratensis	48
sp. index	48
Limestone reef dolomite described	84
Limestone reef dolomite, Minturn Formation	43

	Page
Madera Formation	42, 52
Malachite	78
Mantua Dolomite, exposures	22
Maroon formation	33, 34, 53
age	55
chert	53
correlation	53
fossils	55
fossil wood	65
landslides	68
paleogeography	55
Red and White syncline	78
thickness	54
Martin Creek, rock bench	66
Maximatus cherokanas	51
McCoy, Jacque Mountain Limestone Member	46
McCoy formation	52
Meadow Creek, anticlines	76
basalt	64
Merlella stratocutane	48
Mercykipus venosus	64
Metachasma rumpigius	81
metabolism	37, 50
age	61
Middle Creek	31
Middle Creek, anticline	76
Minturn Formation	47
Minturn Formation	45
thrust faults	74
Mogavilla sp.	37
Mill Creek, head, Jacque Mountain Limestone Member	47
landslides	68
Minturn Formation	45
White Quail Limestone Member	46
Minerals, ellipnone	40
enhydrite	34
azurite	78
barite	78
berite	77
calcite veinlets	10
feldspar, Cerlebed twins	10
chalcopyrite	78
coal	34
condurite	8, 12
epidote	13
fluorite	78
galena	74
garnet	8
Gilman ores	77
gypsum	34, 38
hematite	60
malachite	78
opal	64
phosphite	42
pyrite	78
scapolite	61
sericite	60
siderite	78
silimanite	8
aphanite	78
uranium	78
Minturn	3
Gilman Sandstone	34, 38
Minturn Formation	34, 38
age	48
Black Gore syncline	78
boulders, Bald Mountain	47
chert	42
clastic unit A	43, 85
clastic unit B	43, 85
clastic unit C	43, 84
clastic unit D	44, 82
clastic unit E	44, 81
clastic unit F	45, 80
clastic unit G	45, 80
clastic unit H	46, 79
coal	52

	Page
Minturn Formation - Continued	
correlation	48, 52
dolomite beds of Dwyka	43
dolomite reefs	43
Elk Ridge Limestone Member	45
facies changes	47
fossils	47
fossil plants	52
Gore fault	38
Hornblende Dolomite Member	44
Jacque Mountain Limestone Member	46
Kokomo district	44
landslides	68
biology	41
origin	52
paleogeography	52
phosphate	42
reef dolomite of Leadville	43
Resolution Dolomite Member	44
Robinson Limestone Member	44
sedimentary features	43
subdivisions	39
thickness changes	47
thinning, Gore fault	47
type section	43, 79
Waysman Dolomite Member	44
White Quail Limestone Member	45
Mississippi System	23
Monkopi Formation	54
Molas Formation	32
age	33
ores	46
regolith	32
section	35
Mosier Creek, Robinson Limestone Member	45
Monkopi sp.	50
Moraine, Bull Lake time	32
Criss Creek	32
Moraine material, West Tenmile area	67
Morgan Formation	52, 53
Morrison Formation	57
chert	58
fossils	57
malachite	78
Monkopi fault	71
Mosquito fault	78
Mosquito - Tenmile Range, Jacque Mountain Limestone Member	46
Mount Powell quadrangle, Cross Creek Granite	8
Mount Zion porphyry	58
Mulky coal	51
Multiseparia sp.	48
Mud chip conglomerates, Minturn Formation	43
Mudcracks, Minturn Formation	43
Mudstone dikes	61
N, O	
Nagaville coloradensis	50
New Jersey Zinc Co.	22
Newhouse tunnel, Harding Sandstone	3
Nodule, chert	65
North Fork Piney River	54
Maroon Formation	64
North Park Formation	64
North Mountain Creek, Honestake shear zone	78
Obolus monohar	21
Opalized wood	21
Ordovician System	21
Ore deposits	77
concreted	78
emplacement	78
host rocks	78
Leadville Dolomite	30
Rocky Point zone	27

Lead in the Environment

GEOLOGICAL SURVEY PROFESSIONAL PAPER 957





Lead in the Environment

T. G. Lovering, *Editor*

GEOLOGICAL SURVEY PROFESSIONAL PAPER 957

A compilation of papers on the abundance and distribution of lead in rocks, soils, plants, and the atmosphere, and on methods of analysis for lead used by the U.S. Geological Survey



UNITED STATES GOVERNMENT PRINTING OFFICE, WASHINGTON : 1976

UNITED STATES DEPARTMENT OF THE INTERIOR

THOMAS S. KLEPPE, *Secretary*

GEOLOGICAL SURVEY

V. E. McKelvey, *Director*

Library of Congress Cataloging in Publication Data

Main entry under title:

Lead in the environment.

(Geological Survey Professional Paper 957)

Bibliography: p.

1. Lead 2. Geochemistry. 3. Lead--Analysis.

I. Lovering, Tom Gray, 1921- II. Series: United States Geological Survey Professional Paper 957.

QE516.P3L4 553'.44 76-7962

For sale by the Superintendent of Documents, U.S. Government Printing Office

Washington, D.C. 20402

Stock Number 024-001-02911-1

CONTENTS

	Page
Summary, by T. G. Lovering.....	1
Inorganic chemistry of lead in water, by J. D. Hem.....	5
Organic chemistry of lead in natural water systems, by R. L. Wershaw.....	13
Distribution of principal lead deposits in the continental United States, by A. V. Heyl.....	17
Migration of lead during oxidation and weathering of lead deposits, by Lyman C. Huff.....	21
Lead in igneous and metamorphic rocks and in their rock-forming minerals, by Michael Fleischer.....	25
Abundance of lead in sedimentary rocks, sediments, and fossil fuels, by T. G. Lovering.....	31
Lead content of water, by M. J. Fishman and J. D. Hem.....	35
Lead in soils, by R. R. Tidball.....	43
Lead in vegetation, by H. L. Cannon.....	53
Lead in the atmosphere, natural and artificially occurring lead, and the effects of lead on health, by H. L. Cannon.....	73
Analytical methods for the determination of lead, by F. N. Ward and M. J. Fishman.....	81

ILLUSTRATIONS

FIGURE	Page
1. Diagram showing fields of stability for solid species and dominant solute species in system $Pb-H_2O$ as functions of pH and redox potential.....	6
2. Diagram showing fields of stability for solids and solubility of lead in system $Pb-CO_2-S-H_2O$ at 25°C and 1 atm pressure....	7
3. Map showing principal lead deposits of the United States.....	18
4. Graph and sketch showing relationship between unnamed vein and geochemical anomaly in residual soil, Porters Grove Range, Wis.	22
5. Histograms of lead distribution in granite, granodiorite, basalt, and gneiss.....	26
6. Histograms showing frequency of occurrence of lead in K-feldspar from granitic pegmatite and granitic rocks and in plagioclase from pegmatite.....	28
7. Graph showing lead content of common sedimentary rocks.....	32
8. Map and histogram showing distribution of lead in soils and other surficial materials of the United States.....	48
9. Map and histogram showing concentration and distribution of lead in soils of Missouri.....	50
10. Graph showing comparative lead content of soils and plants near Ameka lode, Nigeria.....	60
11. Graph showing lead in grass collected for 1,000 feet from highway in 1961 and in 1969.....	67

TABLES

TABLE	Page
1. Standard Gibbs free energies of formation of lead species and related solutes.....	6
2. Chemical equilibria and solubility equations for lead species in hydroxide and carbonate domains.....	7
3. Observed and calculated saturation concentrations of lead in U.S. surface waters collected during October and November 1970.....	9
4. Range of copper, lead, and zinc content of soils collected near ore veins.....	22
5. Ore-metal content of stream-sediment samples (minus 80-mesh) collected in and downstream from the Tombstone district, Arizona.....	23

	Page
TABLE 6. Mean lead contents of plants compared with mean lead contents of associated soils in both nonmineralized and mineralized areas	24
7. Published estimates of lead contents of igneous and metamorphic rocks	25
8. Summary of published analyses of lead content of igneous and metamorphic rocks	27
9. Range of variation of Ba/Pb ratio in igneous and metamorphic rocks	27
10. Lead content of feldspars	27
11. Lead content of other rock-forming minerals	29
12. Maximum and minimum concentrations of lead found in surface waters of the United States and Puerto Rico from 1960 to 1971	36
13. Lead concentrations in selected surface waters of the United States	37
14. Maximum and minimum concentrations of lead found in ground waters of several States and Puerto Rico from 1960 to 1971	39
15. Lead concentrations in residual soils from Wisconsin, grouped according to pH	44
16. Lead concentrations in selected soils developed under a variety of soil-forming factors	45
17. Lead concentrations in selected Scottish soils developed from different parent materials	46
18. Mean concentrations of lead in selected parent material types and derivative soils	46
19. Lead concentrations in tropical soils developed on different parent materials	46
20. Distribution of lead concentration and organic matter in soil profiles from the tropical climatic zone	47
21. Distribution of lead concentration in soil profiles from the temperate climatic zone	47
22. Cycling of lead in different environments	54
23. Normal lead concentrations in various classes of vegetation	55
24. Lead in garden produce	56
25. Seasonal variations of lead in trees and soils	56
26. Concentrations of lead in unpeeled and peeled garden produce from Maryland	57
27. Effects of lead and other metals on growth from four plant families	59
28. Lead in conifer twigs, needles, and subjacent mull, Coeur d'Alene district, Idaho	60
29. Lead content of vegetation and soils from several mining districts	62
30. Maximum lead and zinc contents of plants and drained peat, Orleans County, N.Y.	63
31. Lead indicator and accumulator plants rooted in mineralized ground	64
32. Lead contents of plants and soils as related to smelter contamination in Oklahoma and Colorado	66
33. Comparison of lead content between on-road and off-road samples of some soils and plants in Missouri	68
34. Lead concentrations in surface air in 1967 from selected sites along the 80th Meridian	74
35. Lead emissions in the United States, 1968	86
36. Normal lead content of some uncontaminated natural substances	86
37. List of minerals and alloys in which lead is a major constituent	86

LEAD IN THE ENVIRONMENT—SUMMARY

By T. G. LOVERING

Lead is a soft, heavy, malleable, relatively inert metal with a low melting point (327.4°C), which has been known and used by man since ancient times. It has the chemical symbol Pb (from its Latin name plumbum), atomic number 82, and atomic weight of 207.2, making it the heaviest of the common metals. It is the stable end product formed by the radioactive decay of uranium.

Metallic lead was used in antiquity for jewelry, plumbing, and cooking utensils. In modern times metallic lead and lead alloys are extensively used for storage battery plates, sheathing for electrical cables, small-caliber ammunition, shielding for X-ray apparatus and atomic reactors, type metal, bearing metal, and solder. Lead compounds are also important as components in the manufacture of paint, ceramics, and glass and as an anti-knock additive in gasoline. In 1970 the United States produced about 570,000 tons of lead and consumed about 1,380,000 tons. Much of the excess consumption was derived from recycled scrap metal, and the rest was imported chiefly from Canada and Mexico.

Ores of lead and zinc are often closely associated in deposits formed by replacement of limestone or dolomite. Lead ore is commonly present together with ores of copper, zinc, silver, arsenic, and antimony in complex vein deposits that are genetically related to silicious igneous intrusive rocks, but lead ore may occur in a variety of igneous, metamorphic, and sedimentary host rocks.

Although both metallic lead and the common lead minerals are nearly insoluble in pure water, they are appreciably soluble in certain organic acids; likewise, some of the lead compounds produced industrially are also considerably more water soluble than the element. If lead enters the human body in soluble form it accumulates there and can cause lead poisoning.

Airborne lead in smoke from smelters, or from the coking of coal with a high lead content, may produce toxic effects in plants, grazing animals, and humans exposed to the smoke for a long time. Lead poisoning may also result from the ingestion of lead-bearing paint by small children or of lead leached from pottery glazes by the citric acid in fruit juices.

Lead compounds released into the atmosphere in the exhaust fumes of automobiles have produced abnormally

high concentrations of lead in the blood of individuals continuously exposed to these fumes for long periods of time, but as yet there is no established instance of lead poisoning resulting directly from this source.

MIGRATION OF LEAD IN THE NATURAL ENVIRONMENT

Natural concentrations of lead in lead ore deposits do not normally move appreciably in normal ground or surface water, because any lead dissolved from primary sulfide ore tends to combine with carbonate or sulfate ions to form insoluble lead carbonate or lead sulfate or else to be adsorbed by ferric hydroxide. Mechanical disintegration and transportation of these insoluble lead compounds can remove lead from the surface of lead ore bodies and disperse it to some extent. Lead can also be leached by acid waters, particularly those that are rich in organic material, and travel in solution as soluble lead organic complexes. In this form it can be taken up by plants and enter the food chain, but examples are rare. In regions characterized by alkaline, neutral, or saline waters and soils, naturally occurring forms of lead do not enter either water or plants except in very minute traces. Lead minerals in a non-reactive host rock such as sandstone or quartzite have been known to dissolve in acid waters in amounts toxic to vegetation in a small area, but there are no known instances of lead poisoning in humans related to the natural occurrence of lead.

ABUNDANCE OF LEAD IN ROCKS, SEDIMENTS, FOSSIL FUELS, AND MINERALS

The average abundance of lead in the Earth's crust is approximately 15 ppm (parts per million), which is equivalent to half an ounce of lead per ton of rock. The lead contents of the common rock types that make up the crust of the earth range from about 30 ppm for granitic rocks, rhyolite, and black shale to about 1 ppm for evaporite sediments, basalt, and the ultramafic igneous rocks such as dunite, which are rich in iron and magnesium and poor in silica (table 36).

Unconsolidated continental sediments have a mean lead content very close to the mean crustal abundance of 15 ppm, but unconsolidated deep sea muds are appreciably

richer in lead, containing an average of about 60 ppm lead, and concentrations as high as 0.2 percent lead have been reported in sediments precipitated from hot brines in the Red Sea (table 36).

Coal contains an average lead concentration of about 10 ppm, and petroleum an average of less than 1 ppm of lead (table 36). Most of the lead in these fossil fuels concentrates in their ash when they are burned, although it has been estimated that during industrial burning coal may release as much as 6 percent of its original lead content into the atmosphere. Petroleum produces far less ash than coal, and inorganic constituents are much more highly concentrated in its ash.

Although lead is a major constituent of more than 200 known minerals (table 37), most of these are very rare, and only three are commonly found in sufficient abundance to form minable lead deposits. These three are galena, the simple sulfide of lead (PbS); anglesite, the lead sulfate (PbSO_4); and cerussite, the lead carbonate (PbCO_3). Galena is a common primary constituent of sulfide ore deposits; anglesite and cerussite normally form by the oxidation of galena close to the surface.

Lead is also present in trace amounts in many of the common rock-forming minerals (table 36). The amount of lead in any one of these minerals varies widely, and the greater the normal lead content of such a mineral, the greater the observed variation is likely to be. For instance, potash feldspar (orthoclase or microcline) generally contains the most lead of any of the common silicate minerals; yet, whereas samples from one group of pegmatite dikes in Norway yielded 280 ppm lead, similar samples from another group of pegmatite dikes in the same region contained less than 10 ppm. The maximum amount of lead this mineral can contain is unknown, but 2,800 ppm lead has been reported in a sample of a green variety of microcline called amazonite.

The common silicate minerals found in igneous rocks, in order of decreasing lead content, are (1) potash feldspar; (2) plagioclase feldspar and muscovite mica; (3) pyroxenes, amphiboles, and biotite mica; and (4) quartz. The common minerals of chemically precipitated sedimentary rocks (calcite, dolomite, gypsum, and halite) all normally contain less than 10 ppm lead. The lead content of the sedimentary clay minerals is extremely variable but is commonly on the order of 10–20 ppm.

NATURAL ABUNDANCE OF LEAD IN WATER

The concentration of lead in river water is low under natural conditions (table 36). Although small amounts of lead are widely distributed as a minor constituent in rock and soil minerals, lead is only slowly released by weathering processes. Even where the element is concentrated in ore deposits, the low solubility of lead in water that contains dissolved carbon dioxide species and

has a pH near neutrality generally will maintain concentrations of lead in solution below a few tenths of a milligram per litre. The waterborne element tends to be complexed by relatively insoluble organic matter and may also be extracted from water by organisms.

The median concentration of lead in river and lake water of the United States is about 2 $\mu\text{g/l}$ (micrograms per litre). Concentrations of lead in seawater range from a few hundredths of a microgram per litre (a value of 0.03 $\mu\text{g/l}$ is widely quoted) in the deeper parts of the ocean basins to 0.4 $\mu\text{g/l}$ observed at several places both nearshore and far offshore in surface waters of the Pacific Ocean. The higher nearshore and near-surface concentrations, however, are ascribable to atmospheric fallout of lead particles or washing out of such particles by rainfall. Concentrations of lead in rainfall over the United States have been reported to average 34 $\mu\text{g/l}$ over a 7-month period in 1966 and 1967, with a median value of about 10 $\mu\text{g/l}$. When the distribution of sampling points is correlated with reported concentrations, results show strongly the effects of industrial air pollution near cities.

ABUNDANCE OF LEAD IN SOILS

Soil samples collected from nearly a thousand localities throughout the conterminous United States ranged in lead content from <10 to 700 ppm and had a mean lead concentration of 16 ppm (Shacklette, 1971); only 6 percent of these samples contained more than 30 ppm of lead (table 36). Many of the soil samples with lead content in excess of 100 ppm were obtained from localities in western Colorado, but others came from widely scattered isolated sites.

Lead content of young residual soils is strongly influenced by that of the parent rock from which they are derived; however, this relationship is modified, and may be obscured, by other factors in mature soils developed on deeply weathered parent material. These factors include oxidation and reduction reactions, linking of organic compounds by lead ions (chelation), base exchange reactions by clay, adsorption of lead by hydroxides of iron and manganese, local solution and transportation by organic acids, and cycling by vegetation. In general, lead is more mobile in acid soils than in alkaline soils, tending to be leached out of the former and to form residual concentrations in the latter. Relatively high total-lead concentrations in alkaline soil may reflect residual concentration of lead in an insoluble form, which is not available to plants.

LEAD IN VEGETATION

Lead occurs naturally in small amounts in all plants (table 36). The concentration of lead in vegetation varies not only with the individual species, but also as a complex function of climatic variations, parts of the plant, composition of the soil in which the plant grows and of the rock from which this soil is derived, and finally the

effects of artificial contamination of both the water that nourishes the plant and the air that surrounds it.

Anomalously high concentrations of lead in plants may reflect natural contamination from lead deposits or artificial contamination of the plant's environment by man. Extensive analyses of plants from primitive areas, unaffected by either of these sources of contamination, are required to establish normal background values for lead in natural vegetation.

Median concentrations of lead in the ash of uncontaminated natural vegetation are highest for lichens (1,000 ppm), an order of magnitude lower in mosses (100 ppm), about 30-50 ppm in evergreen trees, and about 15-30 ppm in deciduous trees, shrubs and grasses; however, all of these types of vegetation exhibit a wide range in lead content (commonly an order of magnitude) on both sides of the median. The ash of uncontaminated domestic fruit and vegetable samples from the United States has a median lead content close to 10 ppm, which is the lower limit of the analytical method. The observed range for lead in the ash of these foods is from <10 to 100 ppm. The lead content of these plants expressed in dry weight varies from about one-fourth to less than one-tenth the lead content of the ash. Thus the highest observed lead-in-ash content of 100 ppm, for a tomato sample, corresponds to a dry-weight lead content of about 7 ppm and to a lead content for a fresh tomato of less than 1 ppm.

Studies of seasonal variation in the lead content of trees suggest that lead concentration is highest in early spring at the beginning of the growing season, declines during the summer, and rises again in the fall. Lead also tends to concentrate in certain parts of a growing plant. In trees, the highest lead concentrations are usually found in the older twigs; somewhat less lead occurs in the young twigs, seeds, and trunk wood, still less in the leaves or needles, and least of all in the roots. On the other hand, lead content of the leaves of certain vegetables appears to be higher than that of their stems, and the lead in fruits and root vegetables is largely concentrated in the skin or peel.

There appears to be a general tendency for lead to be more abundant in plant ash than in the soil, and more abundant in the soil than in the bedrock, but there are many exceptions.

The knowledge that certain plant species have the ability to absorb anomalous amounts of lead from lead-rich soils and their underlying parent materials has been used as a biogeochemical tool in prospecting for lead deposits for a quarter of a century. These accumulator plants include certain species of both evergreen and deciduous trees, as well as many shrubs and smaller plants.

Contamination of food and forage crops by artificial lead compounds contained in insecticide sprays, automobile exhaust fumes, and industrial smoke is a matter of concern to public health workers. Anomalously high lead concentrations have been found in leafy

vegetables and grasses grown in proximity to major highways, in crops grown on soil with a long history of treatment with lead-bearing insecticides, and in crops exposed to fallout from smelter smoke.

LEAD IN THE ATMOSPHERE

Lead enters the atmosphere largely in the exhaust fumes from internal combustion engines and, to a lesser extent, from the smoke produced by large-scale industrial burning of coal. Consequently the lead content of the air is highest in urban industrial areas and lowest in rural areas (table 36). The average lead concentration in the air of large metropolitan areas is about $2.5 \mu\text{g}/\text{m}^3$. In rural areas it is less than $0.5 \mu\text{g}/\text{m}^3$. The amount of lead present in the air at any particular place varies with traffic density, air temperature, and atmospheric conditions. The lead-bearing particles in the air are heavy and tend to collect in low areas with poor air circulation; lead concentrations greater than $40 \mu\text{g}/\text{m}^3$ have been measured in the air of vehicular tunnels. In spite of this tendency of lead to accumulate close to the ground, traces of it enter the upper atmosphere and are carried widely around the earth to return to the surface in rain or snow. The lead content of a snow sample collected in 1965 from the Greenland ice cap was approximately $0.4 \mu\text{g}/\text{l}$ of melted snow as compared to about $0.05 \mu\text{g}/\text{l}$ in melted ice that had formed in 1864.

METHODS FOR DETECTION OF LEAD

Lead may be determined in water, soil, and rock, and in the ash of plants and organic fuels by a wide variety of methods. The analytical methods employed for both water and solids in the laboratories of the U.S. Geological Survey include optical emission spectrography and atomic absorption spectrophotometry. In addition, X-ray, spectrographic, and colorimetric methods are employed for the analysis of rock, mineral, and soil samples; electron microprobe analysis of polished ore samples is used for the nondestructive determination of lead in high concentrations in small mineral grains.

Water samples are filtered to remove solid particles and are then acidified. In the atomic absorption method a lead-scavenging organic compound is first added to the water and then extracted with an insoluble organic fluid (methyl isobutyl ketone); this fluid is then introduced into the flame of the atomic absorption spectrophotometer. In the emission spectrographic method, lead and other metals are first precipitated by adding a suitable reagent to the water sample. The precipitate is filtered, dried, and introduced into the arc of the emission spectrograph for the simultaneous determination of the metals present.

The optical emission spectrograph is the most widely used laboratory tool for chemical analysis of solid samples that do not contain large amounts of organic carbon, because this method provides a simultaneous analysis for a large number of elements on a very small quantity of

sample material. In routine operation it will normally determine lead in concentrations as low as 5 ppm. Specific analyses for small traces of lead in such materials are made by the atomic absorption method, which, in routine operation, will give good results for lead in amounts as small as 1 ppm, and, with special sample preparation, this method can be used to detect even smaller amounts. Colorimetric methods with a sensitivity to about 20 ppm of lead are used for rapid field tests in reconnaissance geochemical exploration.

UNITS AND NOTATION

The amount of lead in natural materials is expressed in different ways for different substances by the authors of this report. Lead concentrations are generally reported in the following units:

For water—

$\mu\text{g/l}$ =micrograms per litre
 mg/l =milligrams per litre

For solids—

ppb=parts per billion
 ppm=parts per million
 $\mu\text{g/g}$ =micrograms per gram
 oz./ton=ounces per ton

For air—

ng/m^3 =nanograms per cubic metre
 $\mu\text{g/m}^3$ =micrograms per cubic metre
 g/ha =grams per hectare

Conversion factors—

1 ng=1 nanogram=0.00000001 gram
 1 μg =1 microgram=0.000001 gram
 1 mg=1 milligram=0.001 gram
 1 ppb=1 part per billion=0.000001 percent
 1 ppm=1 part per million=0.0001 percent
 1 part per thousand=0.1 percent
 1 oz./ton=31 parts per million=0.0031 percent
 1 g/metric ton (t)=1 part per million=0.0001 percent
 1 ha=1 hectare=1,000 square metres

Symbols

>=greater than
 <=less than
 ≈=approximately

INORGANIC CHEMISTRY OF LEAD IN WATER

By J. D. HEM

The concentration of dissolved lead in most natural water systems, which usually contain dissolved carbon dioxide and have a pH near 7, is very low—commonly less than $10\text{ }\mu\text{g/l}$ —partly because lead combines readily with carbonates, sulfates, and hydroxides normally present in such waters to form compounds of low solubility. Highly saline waters or strongly acid waters may contain appreciably higher concentrations of lead in solution, but such waters tend to be very restricted in distribution.

STABILITY FIELDS OF INORGANIC LEAD COMPOUNDS IN NATURAL WATER SYSTEMS

An outstanding characteristic of lead is its tendency to form compounds of low solubility with the major anions of natural water. The hydroxide, carbonate, sulfide, and more rarely, the sulfate of lead may act as solubility controls. Over most of the Eh-pH region, in which water is stable at 25°C and 1 atm (atmosphere) pressure, the divalent form, Pb^{+2} , is the stable species of lead. The more oxidized solid PbO_2 , in which lead has a $+4$ charge, is stable only in a highly oxidizing environment; thus Pb^{+4} probably has very little significance in controlling the behavior of lead in aqueous geochemical systems. If sulfur activity is very low, metallic lead can be a stable phase in alkaline or near-neutral reducing conditions in the presence of water.

Fields of stability for solid species of lead in the system $\text{Pb-H}_2\text{O}$ at 25°C are shown in figure 1. A dissolved activity of solute lead species of $10^{-8.32}\text{ mol/l}$ (equivalent to 1 g/l) was used to locate solid-solute boundaries. The stability fields of solids in the Eh-pH diagram would be enlarged at the expense of the areas of Pb^{+2} and Pb(OH)_2 if a higher dissolved lead activity were assumed.

The boundaries in figure 1 were calculated from thermodynamic data for lead assembled in table 1. The data were selected from published literature, mostly from the compilation of Wagman and others (1968). The range of published free energy values is rather large for some of the species of lead important in this study, and the choice of values can influence stability and solubility calculations substantially. Standard Gibbs free energy values compiled in the National Bureau of Standards Technical Notes (Wagman and others, 1968) should be

mutually compatible, but for a few of the lead species either no values are given or values in other publications appeared to be in better agreement with the consensus of published solubility information. Free energy values for PbS and PbCO_3 in table 1 were taken from Robie and Waldbaum (1968) because they seemed to give solubilities nearer those reported by most investigators, as quoted by Sillén and Martell (1964).

No value for the hydroxy-carbonate solid or PbSO_4aq is given in either the compilation by Robie and Waldbaum or that of Wagman and others. The value given by Wagman and others for PbOH^+ is not compatible with stability data for this complex given by Sillén and Martell (1964). The value chosen here is calculated from a stability constant published by Faucherre (1954), which agrees better with the considerable number of values for this ion determined by other investigators, even though it was calculated at 20°C rather than 25°C . The discrepancy introduced by this deviation from standard temperature is negligible. Faucherre's data were obtained for a solution of 0.06 ionic strength, and have been adjusted to zero ionic strength using the Debye-Hückel equation. Faucherre's work also provided data for the polynuclear ion $\text{Pb}_4(\text{OH})_6^{+4}$. Latimer's (1952) compilation of free energy data gave a value for $\text{Pb(OH)}_2\text{c}$ nearly 8 kcal less negative than the one given in table 1. The rather wide range in thermodynamic data adds a considerable factor of uncertainty to the solubility calculations.

The mixed oxide $\text{Pb}_2\text{O}_3\text{c}$ apparently is less stable than $\text{Pb(OH)}_2\text{c}$ in the system specified for figure 1 and does not appear in the Eh-pH diagram. The $\text{Pb(OH)}_2\text{c}$ value given in table 1 results in a large domain for this species in the Eh-pH diagram and almost eliminates the mixed hydroxy carbonate from consideration. The natural occurrence of this mineral, however, does suggest that the difference between the stabilities of mixtures of PbCO_3 and Pb(OH)_2 and of the basic carbonate likely favors the basic carbonate. If the free energy value of Latimer is used for the basic carbonate, the species has a narrow stability field near pH 8, and this field would be considerably enlarged if the carbon dioxide species concentration were assumed to be higher than the 10^{-3} mol/l used in drawing the boundaries in figure 2.

The system specified for figure 1 is highly simplified. To be more applicable to systems involving ordinary surface or underground water, the effects of dissolved carbon dioxide and sulfur species must be included. If a fixed total activity of dissolved carbon dioxide species and a fixed total activity of dissolved sulfur species are specified, stability fields of lead carbonate, sulfate, and sulfide can be shown. Figure 2 is an Eh-pH diagram for the system $\text{Pb}-\text{CO}_2-\text{H}_2\text{O}-\text{S}$ at 25°C and 1 atm pressure. Total activities of dissolved CO_2 and sulfur species are both 10^{-3} molar. Areas of stability of solids and the solubility of lead are shown in figure 2. Table 2 gives equations used for the solubility calculations in that part of the diagram where $\text{Pb}(\text{OH})_2$ c and carbonate or hydroxy carbonate are dominant.

As specified here, the activities of these dissolved carbon dioxide species do not necessarily involve a gas phase. Specifying a fixed partial pressure of carbon dioxide, as is sometimes done in solubility calculations of this type, tends to lead to a very high, probably unrealistic, concentration of carbonate in solution at the higher pH's.

From figure 2 it is evident that the solubility of lead is very low (less than $1 \mu\text{g/l}$) between pH 8.5 and 11, and is

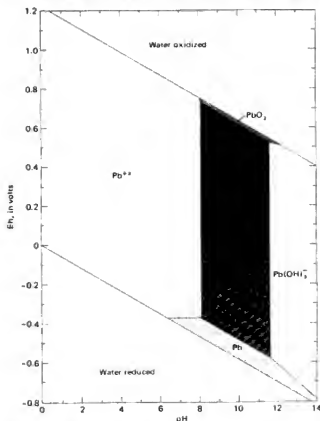


FIGURE 1.—Fields of stability for solids species (c; patterned) and dominant solute species in system $\text{Pb}-\text{H}_2\text{O}$ as functions of pH and redox potential. Dissolved lead activity $10^{-4.75}$ mol/l at 25°C and 1 atm pressure.

TABLE 1.—Standard Gibbs free energies of formation of lead species and related solutes.
[c, solid state; aq, dissolved]

Formula	Free energies ΔG_f° (kcal/mol)	Source of data
Pb^{2+} aq	-5.83	Wagman and others (1968).
PbOH^+ aq	-51.4 ¹	Calculated from Faucherre (1954).
$\text{Pb}(\text{OH})_2^0$ aq	-95.8	Wagman and others (1968).
$\text{Pb}(\text{OH})_3^-$ aq	-137.6	Do.
$\text{Pb}_4(\text{OH})_{14}^{2+}$ aq	-225.6 ¹	Calculated from Faucherre (1954).
PbCl^+ aq	-39.39	Wagman and others (1968).
PbCl_2^0 aq	-71.03	Do.
PbSO_4 aq	-187.38	Calculated from Kolthoff, Perlch, and Weiblen (1942).
PbO c ²	-44.91	Wagman and others (1968).
PbO c ¹	-45.16	Do.
$\text{Pb}(\text{OH})_2$ c	-108.1	Do.
PbS c	-22.96	Robie and Waldbaum (1968).
PbCO_3 c	-150.3	Do.
$\text{Pb}_3(\text{OH})_4(\text{CO}_3)_2$ c	-409.1	Laumer (1952).
PbSO_4 c	-194.36	Wagman and others (1968).
PbO_2 c	-51.95	Do.
Pb_3O_4 c	-143.7	Do.
H_2O l	-56.69	Do.
OH^- aq	-37.59	Do.
H_2S aq	-6.66	Do.
HS^- aq	2.88	Do.
SO_4^{2-} aq	-177.97	Do.
HSO_4^- aq	-180.69	Do.
H_2CO_3 aq	-148.94	Do.
HCO_3^- aq	-140.26	Do.
CO_3^{2-} aq	-126.17	Do.

¹A₂ 29°C.

²Yellow.

³Red.

⁴Liquid.

also low in all strongly reducing systems down to pH 2. However, between pH 6 and 8 the solubility of lead is a rather complex function of pH and total dissolved CO_2 and sulfur species. Lead can be relatively soluble in a dilute natural water below pH 6.5. In such a solution if the activity of dissolved CO_2 species were lower than 10^{-3} molar, the lead solubility would be greater than shown in the diagram. Some dilute river waters thus could be a favorable chemical environment for the solution of lead.

Within the field of stability for PbSO_4 , the solubility of lead is a function of the total sulfate concentration. This control is most effective at rather low pH and when sulfate concentrations are high. The dissolved ion-pair PbSO_4^0 aq is not a dominant form of dissolved lead unless sulfate activity exceed $10^{-2.42}$ mol/l. In a solution of this type ionic strength would be rather high, requiring a stoichiometric sulfate concentration of at least 500 mg/l to produce the specified activity of SO_4^{2-} ions. The PbSO_4^0 aq complex does influence the solubility of lead shown in figure 2, however, and was taken into account in locating the solubility lines. The solubility of lead is near 5 mg/l in most of the PbSO_4 c field; within this area solubility is constant above pH 2 because of the specified constant sulfur activity. Below pH 2 the lead solubility increases because some of the sulfate is converted to HSO_4^- at very

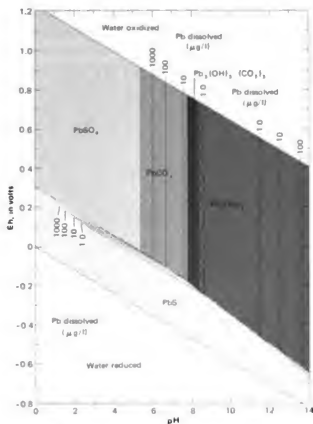


FIGURE 2.—Fields of stability for solids (i.e., patterned) and solubility of lead in system $\text{Pb-CO}_2\text{-S-H}_2\text{O}$ at 25°C and 1 atm pressure. Ionic strength 0.005.

low pH. Under reduced conditions the stable solid is galena, PbS , which has a very low solubility above pH 2.

The lead solubilities and regions of stability of solids shown in figures 1 and 2 are derived from theoretical chemistry, and certain variables are artificially fixed so that the results can be expressed on a two-dimensional graph. In effect, the defined systems retains only two degrees of freedom. Although some natural systems—for example, ground water in a mineralogically homogeneous aquifer—may have constraints enough to conform to a simple equilibrium model, the usual river or lake water is subject to changing conditions that increase the number of degrees of freedom, and a close conformance to equilibrium is unusual. However, the strong influence on lead solubility of the pH and alkalinity of the water may be reflected in analyses of river water, because the effect may be strong enough to be discerned even if equilibrium is not attained. Although available data are neither entirely reliable nor adequate in quantity, the best current information suggests that many surface waters in the United States carry concentrations of lead in solution whose values are close to those predicted from solubility calculations such as those represented in figure 2.

TABLE 2.—Chemical equilibria and solubility equations for lead species in hydroxide and carbonate domains

Chemical equilibria	
Equation	Source of constant
$[\text{Pb}^{2+}][\text{H}^{+}]^{-1}$	$= 10^{-8.15}$ Calculated from data in table 1.
$[\text{PbOH}^{+}][\text{H}^{+}][\text{Pb}^{2+}]^{-1}$	$= 10^{-8.12}$ Do.
$[\text{Pb(OH)}_2][\text{H}^{+}][\text{Pb}^{2+}]^{-1}$	$= 10^{-17.16}$ Do.
$[\text{Pb(OH)}_2][\text{H}^{+}][\text{Pb}^{2+}]^{-1}$	$= 10^{-19.04}$ Do.
$[\text{Pb}_2(\text{OH})_2][\text{H}^{+}][\text{Pb}^{2+}]^{-1}$	$= 10^{-17.35}$ Do.
$[\text{Pb}^{2+}][\text{HCO}_3^{-}][\text{H}^{+}]^{-1}$	$= 10^{-1.06}$ Do.
$[\text{PbSO}_4][\text{SO}_4^{2-}][\text{Pb}^{2+}]^{-1}$	$= 10^{-8.42}$ Do.
$[\text{HCO}_3^{-}][\text{H}^{+}][\text{H}_2\text{CO}_3]^{-1}$	$= 10^{-6.35}$ Garrels and Christ (1965).
$[\text{CO}_3^{2-}][\text{H}^{+}][\text{HCO}_3^{-}]^{-1}$	$= 10^{-10.33}$ Do.
$[\text{H}_2\text{CO}_3]_p[\text{CO}_2]^{-1}$	$= 10^{-1.47}$ Do.
Solubility equations	
$\Sigma \text{CO}_{2, \text{ diss.}} = \frac{[\text{H}_2\text{CO}_3]}{\gamma_{\text{H}_2\text{CO}_3}} + \frac{[\text{HCO}_3^{-}]}{\gamma_{\text{HCO}_3^{-}}} + \frac{[\text{CO}_3^{2-}]}{\gamma_{\text{CO}_3^{2-}}}$	
$\Sigma \text{Pb}_{\text{diss.}} = \frac{[\text{Pb}^{2+}]}{\gamma_{\text{Pb}^{2+}}} + \frac{[\text{PbOH}^{+}]}{\gamma_{\text{PbOH}^{+}}} + \frac{4[\text{Pb}_2(\text{OH})_2]}{\gamma_{\text{Pb}_2(\text{OH})_2}} + \frac{[\text{Pb(OH)}_2]}{\gamma_{\text{Pb(OH)}_2}} + \frac{[\text{Pb(OH)}_2]}{\gamma_{\text{Pb(OH)}_2}} + \frac{[\text{PbSO}_4]}{\gamma_{\text{PbSO}_4}}$	

Obtaining the solubility of Pb(OH)_2 by the use of data in table 1 leads to elimination of stability regions for several lead oxides shown in similar diagrams published by others. The field for PbO_2 is so small that it has very little significance, and it is not shown in figure 2. There are no areas of stability for the mixed valence oxide Pb_3O_4 or for the anhydrous PbO species. The low solubility of lead shown on the diagram, however, is a function of both hydroxide and carbonate effects and is likely to be real.

The basic lead carbonate $\text{Pb}_2(\text{OH})_2(\text{CO}_3)_2$, because of the rather low CO_2 concentration specified, has a small field of stability in the system defined in figure 2. However, there is only a small difference in free energy of formation between the actual double compound and a mixture of lead hydroxide and lead carbonate. The determination of which species might be formed in the vicinity of pH 8 by precipitation from a supersaturated solution could be mainly a matter of relative rates of reaction. Whether the stable solid is basic carbonate or a mixture of hydroxide and carbonate, the calculated equilibrium solubility of lead is essentially the same.

Other solids mentioned in the literature include hydroxy sulfates, nitrates, and chlorides of lead, none of which are stable in the system as defined. The solubility of lead phosphate is low enough to be a factor in some natural waters; generally, phosphate ionic species are not present in sufficient amounts in river and lake water to control the solubility of lead.

Other possibly significant solute species of lead have been described in the literature. The chloride complex PbCl^{+} will not be significant in solutions having less than about 1,000 mg/l of chloride. It could be a significant

factor in saline water. A considerable amount of data has been obtained on polynuclear hydroxide complexes of lead such as $Pb_4(OH)_4^{+4}$ and $Pb_5(OH)_4^{+2}$. For the most part, such species have been studied in more concentrated solutions of lead than the upper limit represented in figure 2. From the thermodynamic data it can be shown that polynuclear hydroxide species are not dominant factors in the aqueous chemistry of lead unless the concentration of lead is over 10^{-2} molar (Faucherre, 1954) and other complexing anions, such as sulfate and chloride are absent or in low concentrations. It seems reasonably certain that such conditions are rarely, if ever, attained in natural geochemical systems. Carbonate complexes such as $PbCO_3(aq)$ may be important in some waters but are not considered here.

EFFECTS OF TEMPERATURE AND IONIC STRENGTH

Except as noted, all the thermodynamic data in tables 1 and 2 are for a temperature of 25°C. This standard temperature is somewhat higher than that of most stream waters in the United States. At lower temperatures the solubilities of most minerals are somewhat decreased. However, the solubility of some carbonates increases as temperature declines. In a system having a CO_2 gas phase, the solubility of CO_2 also increases as temperature goes down and the dissociation reactions are affected.

Strictly speaking, solubility calculations made for 25°C are applicable only to systems at that temperature. If one is interested in testing a solution for adherence to equilibrium solubility at some other temperature, for example, at 5°, all the measurements on the system that would be affected by temperature should be made at 5°, and the results compared with solubility calculations adjusted to apply at 5°. Approximate temperature corrections for equilibrium constants can be made using standard chemical thermodynamic relationships. The alkalinity and pH measurements are seldom all made at the field temperature, however. Converting such values to ones that would represent some other temperature is not a simple matter.

Alkaline-earth metal carbonates decrease in solubility as temperature increases. The effect of temperature on solubility of lead carbonate does not appear to have been closely studied. A few stability constants quoted by Sillén and Martell (1964, p. 140, 141) suggest the solubility of lead carbonate may decrease with decreasing temperature, but temperature effects do not appear to be large. It does not seem worthwhile to calculate the solubility of lead at temperatures below 25° until more study has been given. However, the effect is probably not very large between 25° and 0°C, when compared to other factors that influence field application of solubility calculations.

Solutions of high ionic strength may retain substantially more lead in solution than do more dilute

waters. Ion pairing effects also become increasingly important at high ionic strength. The calculations given here do not apply to solutions whose total dissolved-solids concentration is much above 5,000 mg/l.

INORGANIC CONTROLS OF LEAD SOLUBILITY

As noted earlier in this discussion, lead forms carbonate, sulfate, sulfide, hydroxide compounds of low solubility. It is possible to show by equilibrium solubility calculations (fig. 2) that the concentration of lead species in solution should be less than 10 $\mu g/l$ at ordinary Earth-surface temperatures when HCO_3^- concentration is 61 mg/l or more and pH is between 7.6 and 12.6. A great many natural surface and ground waters are in this concentration range. If the pH is constant and bicarbonate alkalinity is increased, the solubility is proportionately decreased throughout the pH range characteristic of most freshwater. Calculations described by Hem and Durum (1973) showed that many river waters in the United States have lead concentrations near the solubility limits imposed by their pH levels and contents of dissolved CO_2 species.

The comparison of observed lead concentrations with theoretically calculated ones can never be expected to give more than a very approximate indication of what is happening in river water. The influences of changing temperature and pH on solubility may be substantial. It is not unlikely that apparent supersaturation could occur, perhaps as the result of kinetic barriers to crystallization of small particles. Close adherence to a solubility model can be expected to be rare or nonexistent; however, some waters have a so much greater capacity for lead solution than others that even a crude model can be useful. Although many waters do not have sufficient contact with lead compounds to be able to attain saturation, the opportunity for such contact is particularly favorable in urbanized areas or wherever there is heavy automobile traffic and extensive utilization of leaded gasoline. In such areas, the rainfall itself, along with dry fallout of particulate material from the atmosphere, can supply enough lead so that surface runoff reaching streams could contain substantial amounts—enough to reach saturation at times.

Lazrus, Lorange, and Lodge (1970) calculated that as much as 138 g of lead is deposited by rainfall per month on each hectare ($10^4 m^2$) in some parts of the northeastern United States. If the runoff in such an area is at a rate of about 50 cm of water annually (a commonly observed rate), the runoff would have to have an average lead concentration of 330 $\mu g/l$ to remove lead at a rate of 138 g/ha/mo. Higher or lower concentrations could be calculated for other areas and conditions. This figure for average concentration does indicate, however, that a large potential supply of lead is available for transport in runoff. Concentrations as high as 330 $\mu g/l$ could be stable in water having a pH near 6.5 and an alkalinity of about 25

mg/l HCO_3^- . Water having these properties is common in runoff from areas in New York and New England. Thus, the potential for high lead concentrations in river and lake waters does exist in some places, and careful monitoring of river and ground water quality is desirable.

In some other areas the composition of runoff water will be less favorable for lead solution. In many places the average pH and alkalinity are so high that less than $1 \mu\text{g}$ of lead could be retained in solution at equilibrium.

The most comprehensive data on lead concentrations in river water of the United States are included in a report by Durum, Hem, and Heidel (1971). However, their compilation does not include either the bicarbonate or pH determinations needed to apply solubility calculations in testing for adherence to equilibrium conditions. Some of

the sampling sites were points at which pH and alkalinity measurements are regularly made, and some applicable measurements were found in the computer-stored data for water quality stations.

Of the 720 samples obtained for the Durum, Hem, and Heidel study, 70 could be correlated with applicable pH and alkalinity determinations that had been made either on a sample obtained the same day as the sample for lead, or on one obtained within a few days, if the composition of the source was relatively constant (as in large lakes, for example). Lead was detectable in 39 of these samples, as shown in table 3.

This table gives a calculated range of lead concentration for each sample, based on pH and alkalinity. The lower number is the solubility in a very dilute solution; the

TABLE 3.—Observed and calculated saturation concentrations of lead in U.S. surface waters collected during October and November 1970

(Modified from Durum, Hem, and Heidel, 1971, and unpublished USGS records)

Sample source	Date sample collected (Oct. 1970, except as noted)	ΣHCO_3^- (Mg. l.)	ΣHCO_3^- (log mol/l)	pH	Pb ($\mu\text{g/l}$)	
					Calculated range	Observed
Raritan River near Manville, N.J.	12	75	-2.85	7.5	5.0- 15.0	3
Millstone River near Manville, N.J.	12	48	-3.09	7.4	12.0- 35.0	5
Manasquan River at Squamunk, N.J.	12	60	-2.96	7.1	18.0- 60.0	4
Delaware River at Trenton, N.J.	13	45	-3.12	7.7	4.0- 9.0	5
St. Johns River near Melbourne, Fla.	14	113	-2.66	7.6	3.0- 9.0	1
St. Johns River at Jacksonville, Fla.	2	103	-2.75	7.9	2.0- 5.0	2
Plantation Road Canal near Fort Lauderdale, Fla.	29	127	-2.49	7.6	2.0- 6.0	4
Caloosahatchee River near Opa, Fla.	29	199	-2.03	8.2	6- 15	1
Peace River at Arcadia, Fla.	Nov. 6, 1970	51	-3.05	7.9	3.0- 10.0	3
Phillipi Creek at Sarasota, Fla.	6	158	-2.56	8.0	1.2- 3.0	1
Alafia River at Lithia, Fla.	7	42	-3.09	7.2	15.0- 50.0	1
Swift Creek at Fcail, Fla.	6	15	-3.42	6.7	150.0- 400.0	1
Ochlocknee River near Havana, Fla.	15	32	-3.21	7.1	25.0- 80.0	4
Coosa River at Childersburg, Ala.	14	77	-2.83	7.4	5.0- 20.0	4
Alabama River at Claiborne, Ala.	9	50	-3.06	7.5	9.0- 25.0	9
Sispey Fork near Grayson, Ala.	22	38	-3.05	6.8	40.0- 150.0	6
Mahoning River, Ohio-Pennsylvania boundary	8	88	-2.85	7.3	8.0- 25.0	1
Catalochee Creek near Catalochee, N.C.	13	9	-3.53	7.2	40.0- 100.0	20
Tennessee River at Kentucky Dam, Ky. (near Paducah)	16	66	-2.90	7.5	6.0- 18.0	4
Washington Creek at Windigo, Mich.	15	68	-2.87	7.4	6.5- 20.0	2
St. Marys River, Sault Ste. Marie, Mich.	12	50	-3.04	7.7	5.0- 12.0	6
St. Clair River at Port Huron, Mich.	19	95	-2.79	8.3	1.0- 4.0	5
Detroit River at Detroit, Mich.	16	98	-2.78	8.2	1.5- 4.5	4
Missouri River at St. Joseph, Mo.	14	186	-2.45	8.0	9- 25	5
Mississippi River at East St. Louis, Ill.	13	229	-2.39	8.0	8- 25	7
North Sylamore Creek near Fifty Six, Ark.	30	146	-2.54	7.3	4.0- 12.0	10
Arkansas River below Little Rock, Ark.	7	100	-2.72	7.6	3.5- 10.0	11
Kiamichi River near Big Cedar, Okla.	6	10	-3.74	7.9	20.0- 60.0	84
Las Vegas Wash near Boulder City, Nev.	Nov. 19, 1970	258	-2.33	8.0	8- 2.0	2
Santa Ana River below Prado Dam, Calif.	8	518	-2.40	8.2	5- 1.2	34
Merced River, Happy Isles Branch, Yosemite, Calif.	20	9	-3.76	7.1	100.0- 300.0	2
Elder Creek near Branscomb, Calif.	7	75	-2.80	7.5	4.5- 12.0	2
North Fork Quinault River, near Amanda Park, Wash.	15	44	-3.08	7.4	10.0- 30.0	2
South Fork Coeur d'Alene River near Smeterville, Idaho	8	7	-3.24	5.8	1000.0- 5000.0	3
Hayden Creek near Hayden Lake, Idaho	21	47	-3.07	7.7	5.0- 15.0	3
Snake River near Shelley, Idaho	6	150	-2.57	8.2	8- 2.0	3
Rock Creek near Twin Falls, Idaho	19	335	-2.24	7.8	1.0- 3.0	2
Campbell Creek near Spenard, Alaska	16	48	-3.06	7.9	5.0- 10.0	2
Ship Creek near Anchorage, Alaska	16	59	-2.90	7.9	5.0- 15.0	1

higher represents the effect of increased ionic strength. Temperature effects are not directly recorded, but will generally have the effect of slightly decreasing the solubility of carbonates as temperature decreases. Most samples probably were 10°–15° cooler than the standard 25°C used in the calculations. The influence of temperature on lead solubility in these systems needs more investigation.

Of the 39 concentrations of lead determined, 12 are within the predicted solubility range and an additional 10 are reasonably close (within a factor of 2) to upper or lower limits.

The possible experimental and sampling errors are probably enough to explain these discrepancies. The remaining 17 samples include 15 that are well below saturation, a condition to be expected in a high percentage of the samples, owing to lack of sufficient opportunity to dissolve lead. There were only two samples in which a substantial degree of supersaturation occurred—one from the Mississippi River at East St. Louis, which was sampled during a high stage and may have been carrying colloidal particulate lead that could pass through the filter used in clarifying the sample, and the other from the Santa Ana River below Prado Dam, in the Los Angeles area of California, where lead fallout rates are probably very high, causing a situation also conducive to accumulation of colloidal particulate lead.

The principal value of these solubility calculations is in the aid they give to understanding the freshwater part of the geochemical cycle of lead and in the suggestion that hazards of increased lead in water supplies may be most severe in areas where runoff has both a relatively low dissolved-solids concentration and a low pH. It is not intended to imply that the equilibrium aspects of lead chemistry are the only important ones. Factors not considered here may be operating to prevent high lead concentrations from being reached in solutions that are below saturation. However, until more evidence is obtained that such factors are preventing lead from appearing in runoff, it seems obvious that lead concentrations in river and lake water require close attention.

NONSOLUTE LEAD IN WATER

A significant fraction of the total content of lead carried by river water may be in an undissolved state. This nonsolute lead can consist of colloidal particles in a hydrosolic suspension, a characteristic form of many metals having sparingly soluble hydroxides. It may also be present as larger undissolved particles of lead carbonate, oxide, hydroxide, or other lead compound, and can be incorporated in other components of the particulate lead of the runoff, either as sorbed ions or as surface coatings on sediment mineral particles. It can also be carried as a part of organic suspended matter in both living and nonliving forms.

The concentrations of lead usually reported represent an arbitrarily defined solute fraction, separated from the nonsolute fraction by filtration. Most filtration techniques cannot be relied upon to remove all colloidal-size particles, and on acidification of the filtered sample, as usually is done for preservation before analysis, the colloidal material that passed through is dissolved and is reported in that form. Usually the solids removed from a surface water sample by filtration are not analyzed for lead. Exceptions are the analyses reported for rivers in the USSR by Kononov, Ivanova, and Kolesnikov (1968), for which the only determinations of lead were on material removed by filtration. Their assumption appears to have been that solute lead was insignificant. Samples of ground water are not generally filtered before analysis. Content of colloidal material in such waters is probably negligible, however, owing to natural filtration effects during recharge and movement through the aquifer.

Even the lead in rainfall can be mainly particulate. Samples of rain were collected at the U.S. Geological Survey in Menlo Park, Calif., during the period January–April 1971. Filtration through membranes with 0.10- μ m-diameter pores removed as much as 90 percent of the lead. Several samples of runoff from a small stream draining part of the city of Palo Alto, Calif., were collected during this period. One of these contained 90 μ g/l of lead, about 90 percent of which could be removed by filtration. The sediment contained 0.11 percent lead.

Kopp and Kroner (1970, p. 14) reported lead in only 5 of 228 samples of suspended material obtained from composited river and lake samples. In one of these, however, the concentration was equivalent to 120 μ g/l in the original composite.

Dry atmospheric fallout of lead was measured during May and June of 1971 at Menlo Park, Calif. These measurements were made by exposing, for 1–2 weeks on the building roof, a large shallow polyethylene container in which distilled water was maintained at a depth of a few centimeters. The water and sediment accumulated were then analyzed for dissolved and particulate lead. This particulate fallout consistently contained 0.09 to about 0.10 percent of lead, and the fallout rate of lead ranged from 30 to 66 g/ha/mo. No measurable amount of rain fell during this period. Rates and composition of fallout obtained in this set of observations are similar to those reported earlier by Chow and Earl (1970) for the San Diego, Calif., area.

Before a meaningful estimate can be made of the effectiveness of runoff in transporting lead away from areas where it has been deposited by atmospheric fallout and rain, it will be necessary to obtain more information on the amounts of lead transported in nonsolute form, especially during periods when runoff rates are high, as well as corresponding information on the amount carried in solution. At present such data are almost totally

nonexistent. A laboratory study of sorption of lead by cation exchange (Hem, 1976) indicated that a major part of the lead in stream water may be adsorbed on suspended sediment.

REFERENCES CITED

- Chow, T. J., and Earl, J. L., 1970, Lead aerosols in the atmosphere—Increasing concentrations. *Science*, v. 169, p. 577-580.
- Durum, W. H., Hem, J. D., and Heidel, S. G., 1971, Reconnaissance of selected minor elements in surface waters of the United States, October 1970. U.S. Geol. Survey Circ. 645, 49 p.
- Faucherre, Jacques, 1954, Sur la constitution des ions basiques métalliques—2. Le plomb. *Soc. Chim. France Bull.*, v. 21, p. 128-132.
- Garrels, R. M., and Christ, C. L., 1965, *Solutions, minerals and equilibria*. New York, Harper & Row, 450 p.
- Hem, J. D., 1976, Geochemical controls on lead concentration in stream water and sediments. *Geochim. et Cosmochim. Acta*, v. 40 (in press).
- Hem, J. D., and Durum, W. H., 1975, Solubility and occurrence of lead in surface water. *Am. Water Works Assoc. Jour.*, v. 65, no. 8, p. 562-568.
- Kolthoff, I. M., Perlch, R. W., and Weiblen, D., 1942, Solubility of lead sulfate and lead oxalate in various media. *Jour. Phys. Chemistry*, v. 46, p. 561.
- Konovalov, G. S., Ivanova, A. A., and Kolesnikov, T. Kh., 1968, Dispersed and rare elements dissolved in the water and contained in the suspended matter of the main rivers of the U.S.S.R., in *Geochemistry of sedimentary rocks and ores* [in Russian]. Moscow Izdatel'stvo Nauka, 435 p.
- Kopp, J. F., and Kroner, R. C., 1970, Trace metals in waters of the United States—A five year summary of trace metals in rivers and lakes of the United States (Oct. 1, 1962-Sept. 30, 1967). U.S. Dept. Interior, Federal Water Pollution Control Admin., 29 p. and app.
- Latimer, W. M., 1952, The oxidation states of the elements and their potentials in aqueous solutions [2d ed.]. New York, Prentice-Hall, 392 p.
- Laurus, A. L., Lorange, Elizabeth, and Lodge, J. P., Jr., 1970, Lead and other metal ions in United States precipitation. *Environmental Sci. and Technology*, v. 4, p. 55-58.
- Robie, R. A., and Waldbaum, D. R., 1968, Thermodynamic properties of minerals and related substances at 298.15°K (25.0°C) and one atmosphere (1.013 bars) pressure and at high temperatures. U.S. Geol. Survey Bull. 1259, 256 p.
- Sillén, L. G., and Martell, A. E., 1964, Stability constants of metal-ion complexes [2d ed.]. London Chem. Soc. Spec. Pub. 17, 754 p.
- Wagman, D. D., Evans, W. H., Parker, V. B., Halow, I., Bailey, S. M., and Schumm, R. H., 1968, Selected values of chemical thermodynamic properties. U.S. Natl. Bur. Standards Tech. Note 270-3, p. 187-195.

ORGANIC CHEMISTRY OF LEAD IN NATURAL WATER SYSTEMS

By R. L. WERSHAW

Natural soil-water and sediment-water systems are extremely complex, consisting of a myriad of interacting organic and inorganic components. In this section we shall be concerned with the interaction of one of the inorganic components, lead, with the organic components of these systems.

The organic components of a soil-water system are an extremely diverse group of compounds (Saxby, 1969), including carbohydrates, amino acids, phenolic and quinonic compounds, organic acids, nucleic acids, enzymes, porphyrins and other heterocyclic compounds, lipids, terpenoids, and humic materials. (See Saxby, 1969; Spakhov and Spakhova, 1970; Greaves and Wilson, 1969; Kowalenko and McKercher, 1971; Ivanson and Sowden, 1969; and Kononova, 1966, for more complete discussions of the organic compounds in soils.)

In addition to the natural organic compounds present in soil, streams and lakes contain organic sediments and suspended solids that have been derived from municipal, agricultural, and industrial wastes. These wastes are made up of carbohydrates, proteins, nucleic acids, enzymes, lipids, and many of the other organic compounds of living systems. Oils, plasticizers, polymers, and an enormous number of other organic compounds are discharged to natural waterways by manufacturing and chemical industries.

The interaction of lead with the organic components of soil-water and sediment-water systems is still not well understood, but we shall review the work that has been done and attempt to draw what conclusions we can from the data available.

A number of studies have shown that the organic matter of soils and stream sediments apparently binds metals and reduces their mobility. However, as Mortensen (1963) has pointed out, although many workers have suggested that soil organic matter forms complexes with metals, and that these complexes are important in soil formation and plant nutrition, the evidence for existence of metal-soil organic matter complexes in nature is largely circumstantial.

Although a relatively large number of publications are available on the interaction of metals with organic materials of soils and waters (see Mortensen, 1963; Saxby, 1969), very few of the papers have dealt with interactions of

lead and organic material, and of these, most have been concerned with lead in soil-water systems; there are very few on the interaction of lead with organic materials in streams and lakes.

SURFACE WATER-SEDIMENT SYSTEMS

Herrig (1969) and Hellman (1970a, b, 1971) have studied the heavy metals in the waters and sediments of the Rhine River and its tributaries. Herrig found that both inorganic and organic lead compounds were being introduced into rivers as industrial and municipal wastes; the most common of these were lead oxide, metallic lead, lead stearate, lead palmitate and tetraethyl lead. Much of this lead was concentrated in the suspended and bottom sediments of high organic content. The sediments were more effective in removing lead than in removing copper or zinc (Hellman, 1970a).

The sediments of the lower Rhine contained about 10 times the amount of heavy metals found in those of the upper Rhine and its tributaries. Lead concentrations as high as 0.2 percent were found in some of the sediments; high heavy-metal concentrations in the sediments were associated with high concentrations in the river water. The high concentrations are orders of magnitude higher than the natural background levels and can only be due to municipal and industrial pollution. The high concentration of lead in sewage sludge indicates that municipal waste can be a major contributor of lead pollution in some streams (Gross, 1970). Even though the sediments remove large quantities of heavy metals from the water of rivers, they are still not efficient enough to totally decontaminate the water, and therefore the river water often contains high heavy-metal concentrations. Hellman (1970a) measured lead concentrations in the water as high as 85 $\mu\text{g/l}$, and the average for the length of the Rhine river was 51 $\mu\text{g/l}$.

The lead in the organic components of a sediment enters the sediment from two sources: (1) The plant and animal remains that provide the organic compounds to the sediment, and (2) the water that comes into contact with the sediment. The chelation of lead by the chemical components of living organisms tends to cause lead to accumulate in living tissue (MacLean and others, 1969;

Danielson, 1970; Bryce-Smith, 1971). This accumulation of lead is no doubt a major source of lead in organic sediments. However, both the organic and inorganic components of sediments will also remove lead from water. Therefore, as has been pointed out by Hellman (1970a), organic sediments will tend to decontaminate surface waters contaminated with lead and other heavy metals. However, one must also remember that sediments will tend to supply lead to waters with low lead concentrations in order to maintain chemical equilibrium. Therefore, even if the lead pollution of a surface water were to cease immediately, the sediments would continue to supply lead to the water and to its fauna and flora.

CHEMISTRY OF THE INTERACTIONS

Saxby (1969) has reviewed the literature of metal-organic chemistry in the geochemical cycle. He found that lead has been detected in the carbonaceous fractions of soils, coals, petroleum, bituminous rocks and asphalts, shales, sedimentary sulfides, and phosphate rocks. In general, however, very little is known about the molecular associations of metals in geological materials. Therefore, in our discussion we shall have to draw heavily upon studies that have been made on synthetic organic systems and medically important biological systems; however, the general chemical principles elucidated in these studies should also hold true for natural soil-water systems.

Two different types of organic lead compounds may be found in nature: (1) the so-called organo-lead compounds, in which the lead is covalently bonded to carbon atoms and the metal complexes, and (2) chelates, in which the lead is ionically bonded to organic ligands.

Lead normally exhibits both divalent and tetravalent states in organic compounds. When lead is covalently bonded to carbon it is generally more stable in the tetravalent state; relatively stable divalent lead derivatives are known, however. (See Shapiro and Frey, 1968, for a more complete discussion of lead bonding in organic compounds.)

Covalently bonded organo-lead compounds in natural systems undergo slow oxidation by air and photolysis when exposed to light. Most of these compounds except those in which the lead-carbon bonds are highly polar, such as the perfluoroalkyl lead compounds and R_4PbX and R_2PbX compounds in which X is an anion, are not hydrolyzed by water. In coordination compounds, such as metal complexes and chelates, ionic lead is normally divalent; however, organo-lead cations in which the lead is tetravalent may also be complexed by organic ligands.

Most of the detailed studies on the complexing of lead and other metals by organic ligands have been conducted by biochemists on the components of living systems; the same ligands however are present in the organic material of soils, natural waters, and sewage effluents.

Lead is generally most strongly bound to sulfur containing ligands and to phosphoryl groups (Passow, 1970), but it also forms coordination bonds with other ligands.

Vallee and Wacker (1970) have reviewed the chemistry of metalloproteins and have pointed out that lead interacts with proteins and enzymes by binding to carboxyl groups or sulfhydryl groups. The binding of lead and other heavy metals to a wide variety of enzymes inhibits the activity of the enzymes (Morrow and others, 1969; Hemberg and Nikkanen, 1970; Vallee and Wacker, 1970). Li and Manning (1955) have demonstrated that, in general, lead forms more stable complexes with proteins than do cadmium, zinc, or copper.

The binding of lead to enzymes and the consequent inhibition of enzymatic activity will undoubtedly affect the biological reactions that take place in streams, soils, and sewage treatment facilities, but unfortunately there are very few data on the interactions of lead with soil and water biochemical systems. However, the poisoning of enzyme systems in natural waters by heavy metals can be expected to drastically alter the rates of decomposition of organic wastes in these systems.

Heavy-metal cations may not always act as enzyme poisons in soil systems. Ladd and Builer (1970) have shown that divalent cations are effective in reducing the inhibition of the enzyme protease by humic acid. It appears that the humic acid binds to the enzyme, thereby preventing it from combining with substrate. If metal cations are present in the system, active sites on the humic acid will apparently preferentially bind to the cations and be unavailable for binding the enzyme. Lead also interacts with polynucleotides and viruses. Lead ions will cause the depolymerization of some polynucleotides such as ribonucleic acid (RNA) (Farkas, 1968) and deoxyribonucleic acid (Eichhorn, 1962; Izatt and others, 1971). In the depolymerization of RNA it appears that the lead binds the phosphate groups. This neutralizes the charge on the phosphate groups and renders the phosphodiester bonds more susceptible to hydrolysis by hydroxyl groups (Farkas, 1968). In the binding of lead to tobacco mosaic virus molecules the lead may displace protons of the hydroxyl groups (Fraenkel-Conrat, 1965).

In α amino acids, in more complex molecules containing α amino acids, and in molecules similar to 8-hydroxyquinoline and quinoline acid, lead and many other metals form five-membered chelate rings with reactive ligands. Charles and Freiser (1952), in their work on five-membered chelate rings, have measured the stability constants of lead chelates of *o*-aminophenol and *o*-aminobenzenethiol. Their data indicate that the order of decreasing stability for metal *o*-aminophenol is as follows: Cu, Ni, Zn, Co, Pb; for *o*-aminobenzenethiol, however, the order is Cu, Ni, Pb, Zn, Co. Lead forms more stable complexes with *o*-aminobenzenethiol than with *o*-

aminophenol, apparently because the lead-sulfur bond is stronger than the lead-oxygen bond.

Other groups of compounds such as carbohydrates, carboxylic acids, lipids, phenols, and oxygenated isoprenoids that have electron donor ligands similar to those of the proteins mentioned above would also be expected to complex lead. In this regard Hoogveen (1970) has demonstrated that lead is bound by phospholipids. Martin, Ervin, and Shepherd (1966) and Martin and Richards (1969) have shown that copper, zinc, iron, and aluminum form complexes with soil polysaccharides. These metal-polysaccharide complexes are generally more resistant to decomposition in soils than are uncomplexed polysaccharides. Although there are no experimental data on lead-polysaccharide complexes in soil, one would expect them to have properties similar to those of other heavy-metal polysaccharide complexes.

It is well established that soil humic materials such as humic acid and fulvic acid form complexes with metals (Kononova, 1966). Aleksandrova (1967) has classified the interactions of metals with humic materials into three categories: (1) Formation of heteropolar salts (an ion exchange phenomenon between strong bases and humic materials), (2) formation of coordination complexes, (3) formation of adsorption complexes with nonsilicate sesquioxides (adsorption of humus on sesquioxide gels). Most of the interactions of lead with humic materials that have been studied fall under the second category.

Humic acids and fulvic acids form stable complexes with lead (II) ions and other metal ions; these complexes may be separated from a mixture of humic acid or fulvic acid metal complexes by gel permeation chromatography (Mücke and Kleist, 1965; Klöcking and Mücke, 1969). Therefore, it should be possible to isolate intact, humic-metal complexes from soils and sediments.

Bondarenko (1968) found that the presence of fulvic acid in water increased the rate of solution of lead sulfide 10–60 times over a water solution at the same pH that did not contain fulvic acid. At pH values near 7, soluble lead-fulvic acid complexes were present in solution; at initial pH values between 7.4 and about 9, the lead-fulvic complexes partially decomposed, and lead hydroxide and carbonate were precipitated. At initial pH values of about 10, the amount of lead-fulvic acid complexes again increased. Bondarenko (1968) attributed this increase to dissociation of phenolic groups at high pH values, a phenomenon which increases the complexing capacity of the fulvic acid.

In addition to interactions in which a lead ion is bound by a single organic molecule, a single metal ion can be bound by two different organic molecules. It has been demonstrated, for example, that polyvalent cations act as bridges between clay minerals and humic and fulvic acids (Greenland, 1971).

SUMMARY AND CONCLUSIONS

The complexing of lead by most of the common sulfur-, phosphorus-, oxygen- and nitrogen-containing ligands means that lead will accumulate in both the living and nonliving organic components of soil-water and sediment-water systems. The living and non-living organic components are not independent of each other, but are constantly interacting, as the living components metabolize the nonliving components of the system and then die, contributing their remains to the pool of non-living compounds in the system. Some of the lower forms of life are consumed in the process by the higher forms of life and in this way chemical elements from the sediments are introduced into the food chain of the system; this food chain often ends with man. The fate of heavy metals in this process has not been elucidated; however, the sediment in a contaminated surface-water body will serve as a large reservoir which can provide lead and other metals to the biota of the system even after heavy metal pollutants have ceased to be introduced into the system. Unfortunately, in the case of heavy metals, much more attention has been paid to heavy metals dissolved in the water phase of surface water than to the complexed metals in the sediment phase which, in general, probably contain a considerably higher amount of metals than the water. The sediments will also act as a reservoir for providing dissolved heavy metals to the water when contamination levels are low.

High concentrations of lead in soils and sediments will have a marked effect upon enzyme systems, acting in some instances to reduce inhibition by other components of the systems. The alteration of the activity of some of the most basic components of living systems is certain to have a profound effect upon the biological and chemical processes taking place in natural systems.

ACKNOWLEDGMENT

This work could not have been completed without the diligent efforts of Miss Sarah Booker who did most of the literature search.

REFERENCES CITED

- Aleksandrova, L. N., 1967, Organomineral humic acid derivatives and methods of studying them: *Soviet Soil Sci.* 1967, no. 7, p. 903–913.
- Bondarenko, G. P., 1968, An experimental study of the solubility of galena in the presence of fulvic acids: *Geokhimiya* 1968, p. 631–636; translated in *Geochemistry International*, v. 5, p. 525–531.
- Bryce-Smith, D., 1971, Lead pollution—A growing hazard to public health: *Chemistry in Britain*, v. 7, p. 54–56.
- Charles, R. G., and Freiser, Henry, 1952, Structure and behavior of organic analytical reagents—2. Stability of chelates of α -amino-phenol and of α -aminobenzenethiol: *Jour. Am. Chem. Soc.*, v. 74, no. 6, p. 1385–1387.
- Danielson, Lennart, 1970, Gasoline contains lead: *Swedish Nat. Sci. Research Council, Ecological Research Comm. Bull.* 6, 45 p.
- Eichhorn, G. L., 1962, Metal ions as stabilizers or destabilizers of the deoxyribonucleic acid structure: *Nature*, v. 194, p. 474–475.

- Farkas, W. R., 1968, Depolymerization of ribonucleic acid by plumbous ion: *Biochimica et Biophysica Acta*, v. 155, p. 401-409.
- Fraenkel-Conrat, Heinz, 1965, Structure and function of virus proteins and of viral nucleic acid, in v. 5, of Neurath, Hans, ed., *The proteins—Composition, structure, and function*: New York, Academic Press, p. 99-151.
- Greaves, M. P., and Wilson, M. J., 1969, Adsorption of nucleic acids by montmorillonite: *Soil Biology and Biochemistry* [Oxford], v. 1, p. 317-323.
- Greenland, D. J., 1971, Interactions between humic and fulvic acids and clays: *Soil Sci.*, v. 111, no. 1, p. 34-41.
- Gross, M. G., 1970, Preliminary analyses of urban wastes, New York metropolitan region: Stony Brook, N.Y., Marine Sciences Research Center, New York State Univ., 35 p.
- Hellmann, Hubert, 1970a, Die Absorption von Schwermetallen an den Schwebstoffen des Rheinseins Untersuchung zur Entgiftung des Rheinwassers (ein Nachtrag) [Absorption of heavy metals by suspended solids in the Rhine River] Deutsche Gewässerkundliche Mitteilungen, v. 14, no. 2, p. 42-47; English abs. available in *Chem. Abs.*, v. 73, no. 48560b, 1970.
- 1970b, Die Charakterisierung von Sedimenten auf Grund ihres Gehaltes an Spurenmitteln [Characterization of sediments on the basis of their trace metal content]: Deutsche Gewässerkundliche Mitteilungen, v. 14, no. 6, p. 160-164; English abs. available in *Chem. Abs.*, v. 73, no. 115626d, 1971.
- 1971, Bestimmung von Metallen in Flussschlämmen mit Hilfe der Röntgenfluoreszenz—Bedeutung für die Praxis [Determination of metals in river sludge by X-ray fluorescence—Application in actual practice]: *Zeitschr. Anal. Chemie*, v. 254, no. 3, p. 192-195; English abs. available in *Chem. Abs.*, v. 74, no. 146178p, 1971.
- Hernberg, Sven, and Nikkanen, J., 1970, Enzyme inhibition by lead under normal urban conditions: *The Lancet*, v. 1, no. 7637, p. 63-64.
- Herrig, Hans, 1969, Untersuchen an flusswasser inhaltsstoffen [River water substances]: *Gas- und Wasserfach, Wasser-Abwasser*, v. 110, no. 50, p. 1385-1391; English abs. available in *Chem. Abs.*, v. 72, no. 35556a, 1970.
- Hoozevoort, J. Th., 1970, Thermoconductometric investigation of phosphatidylcholine in aqueous tertiary butanol in the absence and presence of metal ions, in Maniloff, Jack, Coleman, J. R., and Miller, M. W., eds., *Effects of metals on cells, subcellular elements, and macromolecules* [Rochester Conf. on Toxicity, 2d, 1969, Proc.]: Springfield Ill., Charles C. Thomas Pub., p. 207-229.
- Ivanson, K. C., and Sowden, F. J., 1969, Free amino acid composition of the plant root environment under field conditions: *Canadian Jour. Soil Sci.*, v. 49, p. 121-127.
- Izatt, R. M., Christensen, J. J., and Rytting, J. H., 1971, Sites and thermodynamic quantities associated with proton and metal ion interaction with ribonucleic acids, and their conjugate bases, nucleosides, and nucleotides: *Chem. Rev.*, v. 71, no. 5, p. 439-481.
- Klücking, Renate, and Mücke, Dietrich, 1969, Isolierung wasserlöslicher Huminsäuren (Fulvosäuren) aus ihrem Blei, (II)—Chelatverbindungen [Isolation of water soluble humic acids (fulvic acids) from their lead, (2)—Chelates]: *Zeitschr. Chemie*, v. 12, p. 455-454; English abs. available in *Chem. Abs.*, v. 72, no. 66020, 1970.
- Kononova, M. M., 1966, Soil organic matter—Its nature, its role in soil formation and in soil fertility [2d English ed.: translated from Russian by T. Z. Nowakowski and A. C. D. Newman]: London, Pergamon Press, 544 p.
- Kowalenko, C. G., and McKercher, R. B., 1971, Phospholipid components extracted from Saskatchewan soils: *Canadian Jour. Soil Sci.*, v. 51, p. 19-22.
- Ladd, J. N., and Butler, J. H. A., 1970, The effect of inorganic cations on the inhibition and stimulation of protease activity by soil humic acids: *Soil Biology and Biochemistry* [Oxford], v. 2, p. 35-40.
- Li, N. C., and Manning, R. A., 1955, Some metal complexes of sulfur-containing amino acids: *Jour. Am. Chem. Soc.*, v. 77, no. 20, p. 5225-5228.
- MacLean, A. J., Halstead, R. L., and Finn, B. J., 1969, Extractability of added lead in soils and its concentration in plants: *Canadian Jour. Soil Sci.*, v. 49, p. 327-334.
- Martin, J. P., Ervin, J. O., and Shepherd, R. A., 1966, Decomposition of the iron, aluminum, zinc, and copper salts or complexes of some microbial and plant polysaccharides in soil: *Soil Sci. Soc. America Proc.*, v. 30, p. 196-200.
- Martin, J. P., and Richards, S. J., 1969, Influence of the copper, zinc, iron, and aluminum salts of some microbial and plant polysaccharides on aggregation and hydraulic conductivity of Ramona sandy loam: *Soil Sci. Soc. America Proc.*, v. 33, p. 421-423.
- Morrow, J. J., Urata, G., and Goldberg, A., 1969, The effect of lead and ferrous and ferric iron on o-aminolevulinic acid synthetase: *Clin. Sci. [London]*, v. 37, p. 533-538.
- Mortensen, J. L., 1963, Complexing of metals by soil organic matter: *Soil Sci. Soc. America Proc.*, v. 27, p. 179-186.
- Mücke, Dietrich, and Kleist, Horst, 1965, Papierelektrophoretische untersuchungen an Huminsäure-metallverbindungen [Paper electrophoresis of metal-humic acid compounds]: *Albrecht-Thaer-Archiv*, v. 9, no. 4, p. 327-336; English abs. available in *Chem. Abs.*, v. 63, no. 9097a, 1965.
- Passow, Hermann, 1970, The red blood cell—Penetration, distribution, and toxic actions of heavy metals, in Maniloff, Jack, Coleman, J. R., and Miller, M. W., eds., *Effects of metals on cells, subcellular elements, and macromolecules* [Rochester Conf. on Toxicity, 2d, 1969, Proc.]: Springfield, Ill., Charles C. Thomas, p. 291-340.
- Saxby, J. D., 1969, Metal-organic chemistry of the geochemical cycle: *Rev. Pure and Appl. Chemistry*, v. 19, June, p. 131-149.
- Shapiro, Hyman, and Frey, F. W., 1968, The organic compounds of lead: *New York, Interscience*, 486 p.
- Spakhov, Yu. M., and Spakhova, A. S., 1970, Composition of free water-soluble organic compounds in the rhizosphere of some tree species: *Soviet Soil Sci.*, v. 2, no. 6, p. 703-710.
- Vallee, B. L., and Wacker, W. E. C., 1970, Metalloproteins, v. 5 of Neurath, Hans, ed., *The proteins—Composition, structure and function*: New York, Academic Press, 192 p.

DISTRIBUTION OF PRINCIPAL LEAD DEPOSITS IN THE CONTINENTAL UNITED STATES

By A. V. HEYL

The principal lead deposits in the continental United States are shown in figure 3. Most of the deposits and depositional districts are located within a few major tectonic and geographic regions of the United States. They are, from east to west, (1) the Appalachian foldbelt (Blue Ridge, Ridge and Valley, and Piedmont provinces) extending from Maine to Alabama; (2) several low domed uplifts within the little-disturbed craton of the greater Mississippi Valley (Central Lowland); (3) the Ouachita Mountains foldbelt (Ozark Plateaus) of Arkansas and Oklahoma; (4) the Rocky Mountains belt from Mexico and western Texas northward to western Wyoming and eastern Idaho (Middle and Southern Rocky Mountains); (5) the cordillera, which includes the Basin and Range province of New Mexico, Arizona, Nevada, western Utah, southeastern California, and southern Idaho, as well as the Sierra Nevada, Oregon Plateaus (Columbia Plateaus), Northern Rocky Mountains, and Cascade Mountains, and the main mountain ranges of Alaska (Pacific Mountain System); and (6) the Pacific foldbelt (Pacific Border province), which forms a narrow band in western California.

The deposits in the Mississippi Valley region (Central Lowland and Ozark Plateaus), Rocky Mountain belt (Northern and Southern Rocky Mountains provinces), and the cordillera (Basin and Range province) are the largest in the United States and have produced most of the commercial lead during the history of the United States. It is worthy of note, however, that the actual areas of lead deposits in these three regions are so small that even if all are taken into account they probably would not markedly increase the total crustal abundance of lead within these three regions. The deposits outside of these three regions are locally numerous, but they have not been major commercial sources of lead.

Lead is commonly associated with zinc and silver, and less commonly with gold, copper, fluorine, barium, cadmium, antimony, bismuth, and arsenic. In most districts lead is subordinate to zinc in total tonnage. The most notable exception is the southeastern Missouri district where lead is far more abundant than zinc (fig. 3,

loc. 1). This district has been our major source of lead since the 1870's.

Most of the major districts in Utah also have more abundant lead than zinc and silver has been a major byproduct. Likewise, in the Coeur d'Alene district of northern Idaho (fig. 3, loc. 3), which dominates lead production in the West, total lead production also exceeds that of zinc; this district is also the major source of silver in the United States.

Silver is associated with lead in most deposits in the western States, the quantity ranging from a minor byproduct to a major value of the ore. Many of the lead deposits mined in the foldbelts of the southern Rocky Mountains and in the Basin and Range region of the cordillera during the 19th and early 20th centuries were oxidized silver-enriched deposits worked mainly for their silver content.

The deposits in the Appalachian foldbelt (Blue Ridge, Piedmont, and Ridge and Valley provinces) are mainly zinc or copper-zinc deposits with relatively minor lead. A few of the largest deposits, such as the most productive zinc deposits in New Jersey, Pennsylvania, Maine, and east Tennessee, are almost free of lead. A few deposits, such as those at Edwards and Balmat, N.Y. (fig. 3, loc. 5), Blue Hill, Maine, and Austinville, Va. (fig. 3, loc. 6), contain enough lead to provide a commercial byproduct. Hundreds of other small deposits that contain lead are known throughout the Appalachian foldbelt.

The deposits in the Ouachita Mountain belt (Ozark Plateaus province) have also produced mainly zinc in the past, and lead is locally only abundant enough to provide a minor byproduct.

The cordillera and Rocky Mountain belt (Basin and Range and Southern Rocky Mountains provinces) contain many silver-bearing lead and lead-zinc deposits, and local concentrations of deposits are widely scattered throughout these regions. In the southern Rocky Mountains they are most abundant in the Colorado mineral belt (fig. 3, loc. 9), the San Juan Mountains, Colo. (fig. 3, loc. 10), and the Wasatch Range, northern Utah. In the cordillera, deposits are scattered throughout the Basin and Range and the

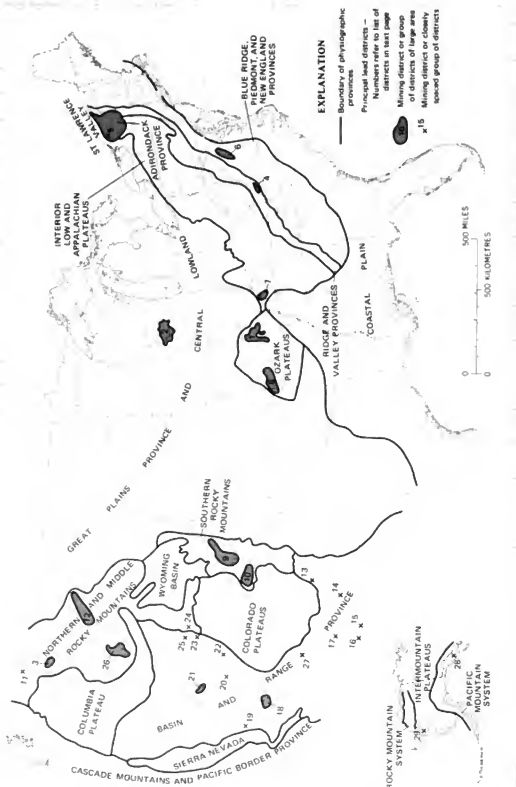


FIGURE 3.—Lead deposits in the United States that have produced or are known to contain more than 100,000 tons of lead. Districts or areas are listed in order of decreasing lead content. Compiled by A. V. Hryl, 1973.

- | | | |
|-------------------------------|---|---|
| 1. Northern Missouri | 9. Leadville, Red Cliff, Aspen, and other districts, Colorado | 23. San Francisco and San districts, Utah |
| 2. Illinois-Kentucky district | 10. New Juan Mountains region, Colorado | 24. Park City and Cornudas, Utah |
| 3. Central Alabama | 11. New Mexico districts | 25. West Mountains, Bingham, Rich Valley, and |
| 4. Southern Virginia | 12. northern Washington | 26. Warm Springs, Berkeley, Ashy Creek, and |
| 5. Bismarck, Idaho, N.V. | 13. southwestern Montana | 27. Big Lost River district, Idaho |
| 6. Illinois-Kentucky district | 14. Leadville, Aspen, and other districts, Colorado | 28. Ground Hog, Chalet Bay, and Tracy districts, Nevada |
| 7. Illinois-Kentucky district | 15. Leadville, Aspen, and other districts, Colorado | 29. Kuparuk River, Alaska |
| 8. Illinois-Kentucky district | 16. Leadville, Aspen, and other districts, Colorado | |
| | 17. Leadville, Aspen, and other districts, Colorado | |
| | 18. Leadville, Aspen, and other districts, Colorado | |
| | 19. Leadville, Aspen, and other districts, Colorado | |
| | 20. Leadville, Aspen, and other districts, Colorado | |
| | 21. Leadville, Aspen, and other districts, Colorado | |
| | 22. Leadville, Aspen, and other districts, Colorado | |
| | 23. San Francisco and San districts, Utah | |
| | 24. Park City and Cornudas, Utah | |
| | 25. West Mountains, Bingham, Rich Valley, and | |
| | 26. Warm Springs, Berkeley, Ashy Creek, and | |
| | 27. Big Lost River district, Idaho | |
| | 28. Ground Hog, Chalet Bay, and Tracy districts, Nevada | |
| | 29. Kuparuk River, Alaska | |

Northern Rocky Mountains provinces, but the greatest concentrations are in northern Idaho and adjacent eastern Washington. Similarly the wide cordillera belt that extends northward and westward through Alaska (Pacific Mountain System) contains most of the lead deposits known in that State.

Very few important lead-bearing deposits occur in the part of the Pacific foldbelt within the conterminous

United States (Cascade and Pacific Border province), although potentially important deposits are common in the Alaskan part of the Pacific foldbelt (Pacific Mountain System). Zinc deposits containing some lead occur on Santa Catalina Island and in other parts of southern California, in the Shasta copper district in northern California, and in Lane County, Oreg.

MIGRATION OF LEAD DURING OXIDATION AND WEATHERING OF LEAD DEPOSITS

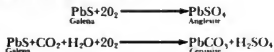
By LYMAN C. HUFF

Lead deposits, like deposits of other ore metals, commonly are surrounded by a zone in which the earth materials are enriched with the ore metal. During the oxidation and weathering of lead ore, some lead becomes incorporated in the soil, stream sediment, drainage waters, and plants. This dispersion of lead has been studied in detail around many lead deposits because it serves as a useful means of prospecting (Hawkes and Webb, 1962). Such studies show that some earth materials and plants near ore deposits may contain highly anomalous concentrations of lead and that such anomalous concentrations may extend outward from the ore deposits. These geochemical halos are an important factor in evaluating the lead content of our environment.

The lead content of most lead ores averages about 8 percent whereas the lead content of unmineralized rock is only about 15 ppm. This high contrast (about 5,000:1) indicates that, during weathering and erosion, the lead from the ore can be disseminated in earth materials in anomalous amounts throughout an area that is quite large by comparison with the original ore deposits. We will consider here the effects of supergene processes upon primary lead deposits and identify, insofar as they can be determined, the most important means of lead dispersal.

WEATHERING OF LEAD ORE

Geologic study has provided much information on the behavior of lead during oxidation and weathering of lead deposits. The predominant lead mineral in the primary ore is the sulfide, galena. During weathering, galena is slowly oxidized by atmospheric oxygen to either the sulfate (anglesite) or the carbonate (cerussite), as indicated by the following equations:



Cerussite usually is formed at a pH above 6 and anglesite at a pH below 6 (Garrels, 1960, p. 170-171). Where pyrite is present, Fe^{+3} in solution may facilitate oxidation of the galena. The CO_2 required in the formation of cerussite is provided by the carbon dioxide content of soil gas or, in

many instances, by the carbonate content of nearby limestones. Part of the lead may also be incorporated in clay minerals or in iron oxide coatings of complex composition. If the primary ore is rich in pyrite, a large part of the lead may become incorporated in the iron-oxide-rich gossans which characterize the weathered outcrops of such deposits.

The common supergene lead minerals are quite insoluble in natural waters. In weathered ore, dark-colored fragments of galena commonly are coated with a light-colored layer of anglesite or cerussite, showing the process of oxidation in progress. These oxidation products of lead do not leach away in soil moisture, but remain in the weathered rock. Many lead deposits have a high content of zinc, which oxidizes to soluble products that do leach away from the weathered ore. The behavior of lead during weathering thus contrasts sharply with that of zinc, sulfur, and other soluble oxidation components of the original ore. The lead content of weathered lead ore commonly is just as high as that of the original unweathered ore.

In the lead mining district of southwestern Wisconsin, residual concentrations of weathered galena fragments were found over some of the lead veins (Huff, 1952). These residual concentrations were left by the decomposition and mechanical washing away of the lighter minerals. As these residual concentrations had a high lead content and were easy to mine, they formed an important source of ore during the early development of this district. Such residual concentrations of lead are not common, but they do show the characteristic insolubility and limited leaching of lead minerals during weathering.

LEAD IN SOILS NEAR ORE DEPOSITS

As the weathered outcrops of lead deposits contain a large amount of lead, it might be suspected that soils on or near such deposits also would have a high lead content. Study in many places has shown this to be true. Some representative data (table 4) show that lead contents of 1,000 to 10,000 ppm are common in soils near outcrops of lead deposits.

TABLE 4.—Range of copper, lead, and zinc content of soils collected near ore veins
[Veins are classified in order of decreasing grade as C, commercial; SC, subcommercial; and M, mineralized (Huff, 1952, p. 586)]

Vein	Classification	Copper			Lead			Zinc		
		High (ppm)	Low (ppm)	High-low ratio	High (ppm)	Low (ppm)	High-low ratio	High (ppm)	Low (ppm)	High-low ratio
Unnamed vein, Porters Grove Ranger, Iowa County, Wis.....	SC	4,400	110	44	2,600	400	6
Iron King vein, Yavapai County, Ariz.....	SC	720	180	4	7,000	200	35	5,500	520	11
Collins East vein, Mammoth St. Anthony mine, Pinal County, Ariz.....	C	4,500	450	10
Unnamed copper vein, Pima County, Ariz.....	M	980	170	5
Apache vein, Gila County, Ariz.....	M	220	15	11
Pittsburgh vein, Coeur d'Alene district, Shoshone County, Idaho:										
Upper traverse.....		12,000	70	170	580	200	3
Lower traverse.....		13,000	190	100	1,800	230	8
Chicago vein, Blackbird district, Lemhi County, Idaho.....	C	1,600	220	7
Malachite vein, Jefferson County, Colo:										
West traverse.....	SC	5,300	50	106	500	80	5
East traverse.....	M	400	50	8
Union Copper veins, Gold Hill district, Cabarrus County, N.C.....	SC	720	150	5	2,500	150	17	680	220	3

Most supergene lead minerals are soft and disintegrate mechanically during weathering, so that much of the lead probably is concentrated in the fine-size fraction of the soil. Most geochemical exploration studies of soil are based upon analysis of a fine-size fraction, such as the minus-80-mesh fraction. These studies yield high lead values, indicating concentrations in the fines. Few analyses of all size fractions of soil have been made, however, and so little data are available on the relative concentration of lead in the various size fractions.

The dispersion of lead in residual soil is demonstrated effectively by study of soil samples collected near lead-rich veins (Huff, 1952). Soil samples collected across a lead-zinc vein in Wisconsin (fig. 4) show maximum lead content immediately over the vein. Soil on the hillside above the vein contains background amounts of lead. On the hillside below the vein, the lead content of the soil gradually decreases away from the vein through dilution as the soil creeps downhill. The distribution of zinc in the soil is somewhat different than that of lead. Probably this difference is caused by partial dispersion of zinc by solution in soil moisture, whereas the dispersion of lead is almost completely mechanical.

Some of the ore metals show a marked tendency to leach from the surface or A horizon of residual soils and to concentrate in the lower or B horizon, so that the B horizon attains a higher metal content than the A. Such leaching and redeposition has been recognized for zinc and copper but not for lead. Wherever such comparisons have been made the A horizon contains as much or more lead than does the B (see Keith, 1969, table 1).

In the southwestern Wisconsin lead-zinc district residual soil derived from lead deposits is overlain by a silty layer of colluvial loess. This loess is believed to be largely of Pleistocene age. Although the loess has been in contact with lead-rich residual soil for thousands of years, study shows that there has been little, if any, diffusion of lead in solution from the lead-rich soil into the loess

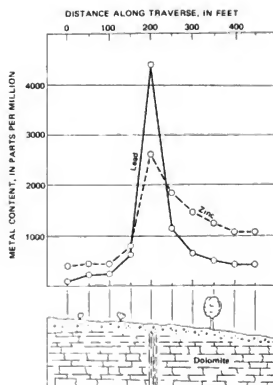


FIGURE 4.—Relationship between unnamed vein and geochemical anomaly in residual soil, Porters Grove Ranger, Iowa County, Wis. From Huff (1952, p. 524).

(Kennedy, 1956, p. 187-223). Similar studies made where glacial till overlies lead ore show little or no diffusion of lead in solution upward into the glacial till.

Surface soils may contain highly anomalous amounts of lead for 5 miles (8 km) or more from a major source of contamination such as a lead smelter. (Canney, 1959). In Yugoslavia, near a lead smelter which has operated for centuries, as much as 24,000 ppm lead has been measured in contaminated soil (Djurić and others, 1972). These high

concentrations result from airborne dust particles rich in lead which have been incorporated in the soil. The minimal leaching rate of lead from soils indicates that most of the lead added to surface soils from contaminating sources will remain in these soils indefinitely.

LEAD IN STREAM SEDIMENTS

In most mining districts the lead which creeps downhill in soils eventually is transported to creeks, or washes, where it is incorporated by running water into stream sediments.

Geochemical exploration studies show that stream sediments containing anomalous amounts of lead from mineralized areas can be traced downstream several miles from the source of the lead. It is assumed that the lead in such sediments, like that in soils, is mostly concentrated in the fine particles. Here again few analyses have been made of different size fractions to determine the extent of concentration in the fine particles.

Several studies of panning concentrates indicate that lead may also be concentrated in part in heavy minerals. In one area in New Mexico the heavy minerals containing lead have been identified (Griffiths and Alminas, 1968, p. 8) as fragments of linonite and wulfenite. Anglesite and cerussite are too soft to survive stream transportation as sand grains and are rarely found in heavy-mineral concentrates.

Reconnaissance mineral exploration of many large areas has been accomplished by sampling stream sediments and by analyzing these samples for lead as well as for other metals. A good example is a study in New Brunswick (Boyle and others, 1966). Stream-sediment samples commonly contain less than 100 ppm of lead (in the minus-80-mesh-size fraction); near known lead deposits they may contain more than 5,000 ppm of lead. Representative data for stream sediments collected by the author near Tombstone, Ariz., are given in table 5.

TABLE 5.—*Ore-metal content of stream-sediment samples (minus 80-mesh) collected in and downstream from the Tombstone district, Arizona*

[N.A., not analyzed]

Sample No.	Sample locality	Metal content (ppm)				
		Lead	Zinc	Silver	Methylmercury	Copper
Tombstone Gulch						
1	Near town and rich mines	4,500	4,300	26.0	120	175
35	0.5 mi (0.8 km) downstream from Sample 1	5,000	7,000	55.0	30	500
3	0.7 mi (1.1 km) downstream from Sample 1	5,500	6,000	66.0	16	500
2	1.9 mi (3.0 km) downstream from Sample 1	850	720	9.1	6	80
32	2.4 mi (3.9 km) downstream from Sample 1 and 0.4 mi (0.6 km) above Walnut Creek	550	660	6.1	< 1	50
Walnut Creek						
18	0.9 mi (1.5 km) below mouth of Tombstone Gulch	118	150	N.A.	N.A.	50
7	1.4 mi (2.2 km) below mouth of Tombstone Gulch	90	85	1.5	< 1	N.A.

LEAD IN MINE DRAINAGE

Measurable amounts of lead are rarely detected in either mine waters or drainage from mines. Representative data obtained near lead and zinc deposits in New Brunswick indicate a lead content of as much as 3,300 ppm in stream sediments but less than 0.001 ppm in stream waters. The water sample with the highest lead content, 2 ppm, was collected within a mine (Boyle and others, 1966, p. 24). In the same waters, the zinc content is as much as 1,000 ppm. The contrast shows the relative insolubility of lead. These results and other available data indicate that during weathering and erosion, little if any lead is removed in solution from lead deposits.

PLANTS

Plants growing in lead-rich soil absorb some lead from the soil. Later, when the plants die and decay, this lead is returned to the soil. The renowned geochemist V. M. Goldschmidt, after his chemical studies of coal ashes (1937), theorized that lead, as well as many other trace elements present in soil, tends to be absorbed by plants and plant humus. Thus, wherever soils are rich in lead, the plants also are likely to be rich in lead.

The extent to which plants accumulate lead from the soil (Webb and Millman, 1951; Worthington, 1955; and Malyuga, 1964) can be judged by the lead content of plants growing near areas of lead mineralization. Some studies have indicated an anomalous lead content in some plants but not in others (Cannon, 1960, table 3). Relative amounts of lead accumulated by various species can be evaluated by comparing the lead content of plant ash (which contains nearly all the inorganic constituents) with the lead content of the soil in which the plants are growing. Table 6 gives data of this type for three areas.

In most of these areas the lead content of plants is higher than that of the soil in the nonmineralized areas and lower than that of the soil in the mineralized area. In other words, the plants show less accumulation of lead from lead-rich soils. The reasons for this relationship between soils and plants with respect to lead is not completely understood. However, it does indicate that the ability of plants to accumulate lead from soils is limited.

Data given in another section of this report indicate considerable differences among plant species in ability to accumulate lead. Considering the large number of plant species, it is quite possible that some common plants which have never been investigated accumulate large amounts of lead. The mineralized areas, with high lead content in their soils, provide excellent environments to study the lead content of common, non-agricultural plant species. Because of the current interest in lead dispersion, additional studies of common plants in mineralized areas seem desirable to identify all species which accumulate lead.

TABLE 6.—Mean lead contents of plants compared with mean lead contents of associated soils in both nonmineralized and mineralized areas

[Data from the Mississippi Valley district from Keith (1969, p. 355-356); data from Alaska from Shackleton (1960, p. B102-B103); data from the Tombstone district collected by the author]

	Lead (ppm)	
	Nonmineralized area	Mineralized area
Upper Mississippi Valley		
Soils:		
Residual, A horizon	18	124
Plant ash:		
Elm, stems	162	78
Maple, stems	119	135
Oak, stems	150	99
Mahoney Creek lead-zinc deposit, Alaska		
Soils	20	1,300
Ash of all plant species sampled	90	160
Tombstone district, Arizona		
Soils:		
Alluvial	35	3,905
Plant ash:		
Mesquite, stems	53	239

CONCLUSIONS

The supergene dispersal of lead, unlike that of some other ore metals, takes place mostly by mechanical processes. Chemical changes are involved in weathering but the weathered products are relatively insoluble and are not leached from the rock by soil moisture. These soft insoluble lead minerals are incorporated in the fine-size fractions of the soil and stream sediments. They are dispersed by gravity and can be traced in ever-diminishing concentrations a long distance from their source.

The low solubility of the supergene lead minerals limits the amount of lead which dissolves in mine waters or is accumulated by plants. Available data on the lead content of mine waters indicate that it is normally very low. Some plants accumulate lead from lead-rich soil near ore deposits; this accumulation varies according to species and may amount to several hundred parts per million in the ash of some species. However, as shown elsewhere in

this report, high concentrations in plants have also been observed near lead smelters and near highways where plants absorb lead from industrial and automobile exhaust fumes.

REFERENCES CITED

- Boyle, R. W., Tupper, W. M., Lynch, J., Friedrich, G., Ziauddin, M., Shaliquallah, M., Carter, M., Bygrave, K., 1966, Geochemistry of Pb, Zn, Cu, As, Sb, Mo, Sn, W, Ag, Ni, Co, Cr, Ba, and Mn in the waters and stream sediments of the Bathurst-Jacquet River district, New Brunswick: Canada Geol. Survey Paper 65-42, 50 p.
- Ganney, F. C., 1959, Geochemical study of soil contamination in the Coeur d'Alene district, Shoshone County, Idaho: Mining Eng., v. 11, no. 2, p. 205-210.
- Cannon, H. L., 1960, Botanical prospecting for ore deposits: Science, v. 132, no. 3427, p. 591-598.
- Djurić, Đuljan, Kerin, Zarka, Graovac-Lepotavic, Ljubica, Novak, Ljiljajac, and Kop, Marija, 1972, Environmental contamination by lead from a mine and smelter: Archives Environmental Health, v. 23, no. 4, p. 275-279.
- Garrels, R. M., 1960, Mineral equilibria—At low temperature and pressure: New York, Harper and Bros., 254 p.
- Goldschmidt, V. M., 1957, The principles of distribution of chemical elements in minerals and rocks [7th Hugo Miller Lecture]: Chem. Soc. Proc. [London], Jan.-June [1957], p. 655-673.
- Griffitts, W. R., and Alminas, H. V., 1968, Geochemical evidence for possible concealed mineral deposits near the Monticello Box, northern Sierra Cuchillo, Socorro County, New Mexico: U.S. Geol. Survey Circ. 600, 13 p.
- Hawkes, H. E., and Webb, J. S., 1962, Geochemistry in mineral exploration: New York, Harper and Row, 415 p.
- Huff, L. C., 1952, Abnormal copper, lead, and zinc content of soil near metalliferous veins: Econ. Geology, v. 47, no. 5, p. 517-542.
- Keith, J. R., 1969, Relationships of lead and zinc contents of trees and soils, Upper Mississippi Valley district: Soc. Mining Eng. Trans., v. 244, no. 3, p. 353-356.
- Kennedy, V. C., 1956, Geochemical studies in the southwestern Wisconsin zinc-lead area: U.S. Geol. Survey Bull. 1000-E, p. 187-223.
- Malyuga, D. P., 1964, Biogeochemical methods of prospecting: New York, Consultants Bur., 205 p.
- Shackleton, H. T., 1960, Soil and plant relationships at the Mahoney Creek lead-zinc deposit, Revillagigedo Island, Southeastern Alaska, in Short papers in the geological sciences: U.S. Geol. Survey Prof. Paper 400-B, p. B102-B104.
- Webb, J. S., and Millman, A. P., 1951, Heavy metals in vegetation as a guide to ore—A biogeochemical reconnaissance in west Africa: Inst. Mining and Metallurgy Trans., v. 60, pt. 2, [no.] 537, p. 473-504.
- Worthington, J. E., 1955, Biogeochemical prospecting at the Shawangunk Mine (N.Y.)—A case study: Econ. Geology, v. 50, no. 4, p. 420-429.

LEAD IN IGNEOUS AND METAMORPHIC ROCKS AND IN THEIR ROCK-FORMING MINERALS

By MICHAEL FLEISCHER

LEAD IN IGNEOUS AND METAMORPHIC ROCKS

Most of the recent estimates of the lead content of igneous and metamorphic rocks (table 7) are based principally on the spectrographic analyses by Wedepohl (1956). Since the publication of his work, several hundred determinations by a variety of methods have been published. These are summarized in table 8 and are shown graphically for selected rock types in figure 5, in which the rocks analyzed have been classified under the names given by the respective authors. The data are in good general agreement with the averages previously proposed by Wedepohl and other researchers. It will be noted that the median values are generally slightly lower than the arithmetic averages, a consequence of the inclusion of a few very high determinations; thus, it is believed that the median value is generally more meaningful than the arithmetic average.

The data indicate that, within the probable error of the averages, the lead contents of plutonic rocks are generally about the same as those of their volcanic equivalents (table

8), granites correspond to rhyolites, diorites to andesites, and alkalic rocks to trachytes and phonolites.

The lead contents increase with increasing silica content and, in general, with content of potassium, but even within a single pluton or igneous complex correlations such as Pb/K, Pb/Rb, and Pb/Ba show wide variations. It is very doubtful that these ratios are useful as a tool for correlation. They are even less useful as a basis for prediction of lead contents. A few typical examples from recent papers for the variation of the Ba/Pb ratio are listed in table 9.

The average lead content for gneiss in table 8 is slightly lower than that for granitic rocks, but there are not sufficient data to permit drawing any conclusions as to whether lead is gained or lost during metamorphism, except to say that metasomatic reactions leading to the development of K-feldspar result in increased lead content. Milovskiy and Matveyeva (1970) studied three instances of granitization and found increases of average lead content in two, where lead increased from 13 to 30 ppm and from 8 to 18 ppm; in a third example the lead content remained constant at 40 ppm Pb.

The distribution of analyses for granite, granodiorite, basalt, and gneiss is shown in figure 5.

TABLE 7.—Published estimates of lead contents of igneous and metamorphic rocks

Rock Type	Lead (ppm)
Silicic rocks (granite, rhyolite)	220.0
Granite, high Ca	220.0
Granite, low Ca	115.0
Granodiorite	115.0
Intermediate rocks (diorite, andesite)	115.0
Quartz diorite	8.0
Diorite	110.0
Alkalic rocks	112.0
Ultramafic rocks	3.0
	1.1
	1.0
Rhyolite and obsidian	21.0
Dacite	11.0
Basalt and gabbro	6.0
	8.0
	6.0

¹Vinciguerra (1956, 1962).

²Wedepohl (1956).

³Turekian and Wedepohl (1961).

LEAD IN ROCK-FORMING MINERALS OF IGNEOUS AND METAMORPHIC ROCKS

From consideration of the ionic radii of the rock-forming elements of igneous rocks (values are from those of Whitaker and Muntus, 1970, for coordination number 6), one would expect lead (Pb^{+2} , 0.126 nanometres) to be concentrated in minerals of potassium (K, 0.146 nm), such as K-feldspars, biotite, and muscovite, and to occur to a lesser degree in minerals of calcium (Ca^{+2} , 0.108 nm) and sodium (Na^{+} , 0.108 nm). In igneous rocks one would also expect very close geochemical coherence between lead and barium (Ba^{+2} , 0.144 nm) and between lead and strontium (Sr^{+2} , 0.121 nm), and fair coherence of lead with rubidium (Rb^{+} , 0.157 nm).

In reality, however, although there is a general parallelism between the contents of lead and potassium,

LEAD IN THE ENVIRONMENT

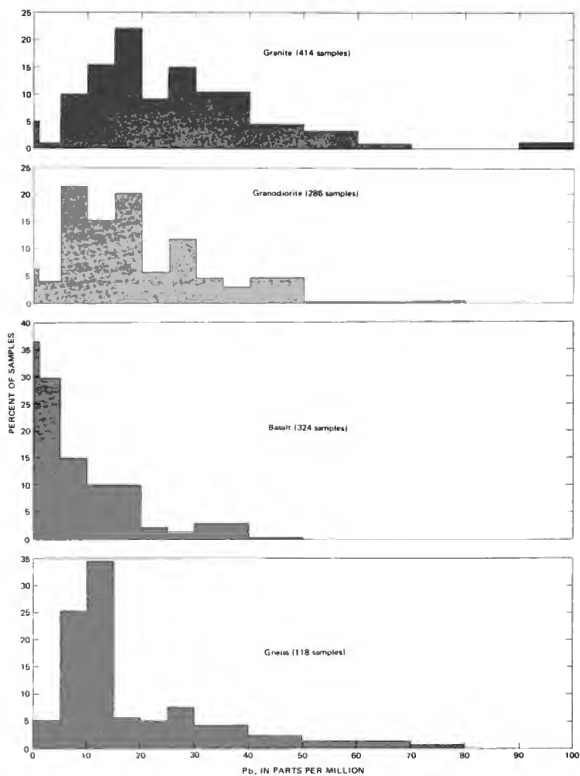


FIGURE 5.—Histograms of lead distribution in granite, granodiorite, basalt, and gneiss.

TABLE 8.—Summary of published analyses of lead content of igneous and metamorphic rocks.

(Lead content (ppm) indicated not determined)

Rock type	Number of analyses	Lead content (ppm)		
		Range	Arithmetic average	Median
Granitic rocks	536	0-200	25.0	18
Granodiorite, adamellite	317	0-80	22.0	16
Diorite, quartz diorite	122	0-76	14.0	11
Alkaline rocks	153	0-500	22.0	16
Ultramafic rocks	34	0-37	2.0	...
Rhyolite, obsidian	273	0-200	21.0	18
Latite, quartz latite	49	0-50	25.0	21
Dacite, rhyolite	121	0-300	12.0	11
Andesite	208	0-150	12.0	8
Basalt, gabbro, diabase	372	0-100	7.5	4
Trachyte, phonolite	33	0-60	18.0	16
Gneiss	274	0-80	20.0	12
Schist	81	0-100	15.0	15
Amphibolite	51	0-50	11.0	9

both in igneous rocks and in the individual minerals of those rocks, examination in detail shows extremely wide and unsystematic variations in the K/Pb ratio. The same may be said of the relation between lead and rubidium contents; likewise, the ratios of lead to barium and lead to strontium vary over an extremely wide range and show no systematic relation to crystallization trends.

In discussing this problem, Heier (1962 p. 426) stated. Lead does not show any special relation to any of the elements substituting for potassium in K-feldspars. Because Pb²⁺ is both divalent and smaller than K⁺, it should be strongly captured according to classical distribution rules. However, the data *** show that lead tends to be enriched in the most fractionated (pegmatite) K-feldspars. This contradiction to Goldschmidt's rule is related to the large electro-negativity value of Pb²⁺, and the consequent increased covalent nature of the Pb-O bonds as compared to the K-O bonds.

DISTRIBUTION OF LEAD AMONG ROCK-FORMING MINERALS

Less than a dozen analyses have been published in which lead content has been determined for all the constituents of a given rock, and the material balances for these are not very good, presumably because of the low spectrographic sensitivity for lead. The few available analyses (Nockolds and Mitchell, 1948; Tauson and Kravchenko, 1956; Zlobin and Gorshkova, 1961) all show that 70-95 percent of the total lead in the rocks is present in K-feldspar plus plagioclase.

It should be noted that some of the accessory minerals of granitic rocks, especially those containing radioactive elements (for example, monazite, xenotime, uraninite, thorite, zircon, allanite, titanite), commonly contain far greater concentrations of lead than major rock-forming minerals; the contribution of accessory minerals to the total lead content of the rock, however, is generally small.

Because galena occurs in small amounts in many rocks, attempts have been made (Arnaudov and others, 1967;

TABLE 9.—Range of variation of Ba/Pb ratio in igneous and metamorphic rocks

Rock type	Range of Ba/Pb ratio	Reference
Rhyolite:		
Pitchstone	60-300	Carmichael and McDonald (1961).
Pantellerite	4-56	Gibson (1972).
Andesite	20-44	Peltz and others (1971).
Do	30-153	Taylor and others (1969).
Olivine basalt	36-129	Cummings (1972).
Ankaramite	75-360	Gunn and others (1970).
Dolerite	8-35	Walker (1969).
Granodiorite	17-210	Savu and others (1971).
Granite	23-76	Do.
Do	2-90	Saba and others (1968).
Gneiss	7-132	Khaffagy (1971).

Arnaudov and Pavlova, 1971) to measure "sulfide lead" (by leaching with a solution containing 25 percent NaCl+0.5N HCl) and "sulfate lead" (by leaching with a solution containing 25 percent NaCl); these experiments show that in nearly all samples of feldspars and muscovites, 70-95 percent of the lead present is in the silicate molecule.

LEAD CONTENT OF ROCK-FORMING MINERALS

The feldspars, as stated previously, are the principal carriers of lead in igneous and metamorphic rocks. Their contents of lead vary widely from locality to locality, and even in different samples from a single locality, but general trends are evident from table 10 and figure 6, where data for orthoclase and microcline are grouped together.

For rocks of granodiorite composition the content of lead is only slightly greater in K-feldspar than in coexisting plagioclase (indeed, a few analyses show more lead in the plagioclase), but the lead content of the plagioclase decreases with decreasing content of calcium. Consequently, the ratio of lead in K-feldspar to lead in plagioclase increases towards the granites proper and

TABLE 10.—Lead content of feldspars

(Lead content (ppm) indicated not determined)

Rock type	Number of analyses	Pb (ppm)		
		Range	Average	Median
K-feldspar (microcline and orthoclase)				
Rhyolite, latite, quartz latite ¹	162	2- 115	47	...
Granitic rocks ²	344	0- 150	36	20
Granitic pegmatite ³	428	0- 560	72	30
Amazontite, granitic pegmatite	174	<5-13,500	477	200
Plagioclase				
Rhyolite, latite, quartz latite	3	13-14	14	14
Granitic rocks ²	128	1-52	13	10
Granitic pegmatite	90	<5-148	46	35

¹These are mostly sandstone.²Granite, granodiorite, adamellite, gneiss.³Excluding amazonite.

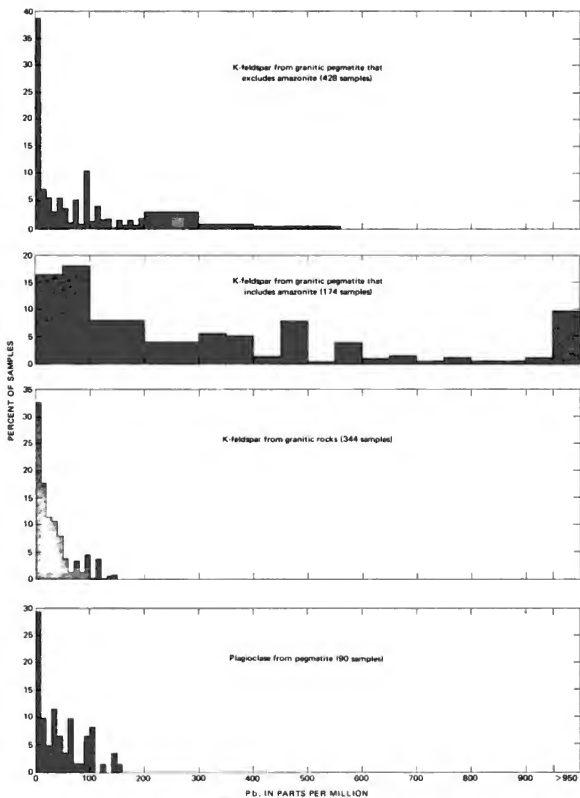


FIGURE 6.—Frequency of occurrence (percent of total samples) of lead in K-feldspar from granitic pegmatite that excludes amazonite, from granitic pegmatite that includes amazonite, and from granitic rocks, and in plagioclase from pegmatite.

further increases in the feldspars of granitic pegmatite. The K-feldspars of very late stages of granitic pegmatite (including the amazonite) show very high contents of lead, reaching maximum levels of 1.35 percent for amazonite (Alker, 1959) and 1.10 for green orthoclase (Cech and others, 1971).

Plots correlating lead content with Rb/Pb and Ba/Pb ratios show that these ratios tend to decrease as lead content increases, but the data scatter is so great that these ratios probably are not useful for correlation or prediction.

Data on other rock-forming minerals are assembled in table 11. Most of the data on muscovite are from Bradshaw (1967), who found significantly higher contents of lead in samples from granites associated with mineralization. The data of Parry and Nackowski (1963) and of Lovering (1969, 1972) indicate that the lead content of biotites from mineralized granitic rocks is slightly higher than in those from unmineralized granitic rocks; it is possible, however, that some of the variation is due to regional differences not connected with processes of mineralization. The average for chlorites seems to be higher than would have been anticipated; it may reflect introduction of lead during hydrothermal alteration, but more work is clearly needed. The low contents in quartz, pyroxene, amphibole, garnet, and olivine are as expected.

Very little work has been done on the fate of lead in the weathering of igneous rocks. The data of Butler (1953, 1954), however, indicate that most of the lead is taken up by minerals of the clay-size fraction.

SUMMARY

Averages for lead in the major types of igneous and metamorphic rocks as shown by recent analyses are in good agreement with the averages suggested by Wedepohl (1956). In the normal igneous or metamorphic rock series, the lead content increases with silica content and there is a rough correlation between contents of lead and potassium, but the variations are so great that ratios of lead to potassium, rubidium, or barium are not of much value for correlation or prediction. No distinct differences were noted between extrusive rocks and their intrusive equivalents.

The data do not clearly show whether lead is gained or lost during metamorphism, but indicate gain of lead during feldspathization or other types of potassium-metasomatism.

Most of the lead in igneous and metamorphic rocks is contained in feldspar; although some minor accessory minerals commonly contain more lead, their contribution to the total lead content of the rock is small. Late-stage K-feldspars of granitic pegmatite usually have the highest lead content of the common rock-forming minerals. The lead content of the late micaceous minerals (muscovite, biotite, and chlorite) is generally lower than

TABLE 11.—Lead content of other rock-forming minerals

Mineral and rock type	Number of analyses	Pb (ppm)	
		Range	Average
Muscovite:			
Granitic rocks:			
Mineralized ¹	55	4-100	21
Unmineralized ¹	99	1-450	7
Granite pegmatite.....	21	9-34	18
Schist.....	8	<10-77	42
Eclogite.....	2	(*)	10
Biotite:			
Granitic rocks.....	585	<1-450	29
Silicic volcanic rocks.....	17	<10-50	10
Schist.....	73	5-120	20
Pyroxenite.....	1	None	9
Biotite and phlogopite:			
Granite pegmatite.....	11	no data	13
Chlorite ¹	39	7-220	64
Quartz.....	51	0-50	5
Pyroxene.....	196	0-59	3
Amphibole.....	747	0-34	10
Garnet.....	21	1-46	8
Olivine.....	9	0-6	2

¹Granite, granodiorite, gneiss.

²Both analyses yielded 10 ppm.

³Nearly all from granitic rocks.

⁴Including two analyses of 216 and 545 ppm Pb.

⁵Excluding one analysis of 150 ppm Pb.

that of the feldspars, but higher than that of the other common rock-forming minerals. Micas from mineralized granitic rocks appear to contain slightly more lead than those from unmineralized rocks of similar composition.

REFERENCES CITED

- Alker, Adolf, 1959, Ein Amazonit pegmatit bei Park, Steiermark: Abh. Mineralog. Landesmuseums Joanneum, Graz, 1959, p. 1-6.
- Arnaudov, V., and Pavlova, M., 1971, The presence of lead in some mica-bearing pegmatites from southern Bulgaria [in Bulgarian, with Russian and English summary]: Bulg. Akad. Nauk Geol. Inst. Tr. Ser. Geokhimi., Mineral., Petrog., v. 20, p. 21-29.
- Arnaudov, V., Pavlova, M., and Petrusenko, Sv., 1967, Lead content in certain amazonites [in Bulgarian, with Russian and English summary]: Bulg. Akad. Nauk., Geol. Inst. Tr. Ser. Geokhimi., Mineral., Petrog., v. 16, p. 41-44.
- Bradshaw, P. M. D., 1967, Distribution of selected elements in feldspar, biotite, and muscovite from British granites in relation to mineralization: Inst. Mining Metallurgy Trans., sec. B, v. 76, [no.] 727, p. B137-B148.
- Butler, J. R., 1953, The geochemistry and mineralogy of rock weathering—I, The Lizard area, Cornwall: Geochim. et Cosmochim. Acta, v. 4, no. 4, p. 157-178.
- , 1954, The geochemistry and mineralogy of rock weathering—2, The Nordmarka area, Oslo: Geochim. et Cosmochim. Acta, v. 6, no. 5, p. 268-281.
- Carmichael, Ian, and McDonald, Alison, 1961, The geochemistry of some natural acid glasses from the north Atlantic Tertiary volcanic province: Geochim. et Cosmochim. Acta, v. 25, no. 3, p. 189-222.
- Cech, F., Misar, Z., and Povondra, P., 1971, A green lead-containing orthoclase [with German summary]: Tschernak Mineralog. U. Petrog. Mitt., v. 15, p. 213-231.
- Cummings, David, 1972, Mafic and ultramafic inclusions, Crater 160, San Francisco volcanic field, Arizona, in Geological Survey research 1972: U.S. Geol. Survey Prof. Paper 800-B, p. B95-B104.
- Gibson, I. L., 1972, The chemistry and petrogenesis of a suite of pantellerites from the Ethiopian rift: J. Petrology, v. 13, no. 1, p. 31-41.

- Gunn, B. M., Coy-Yll, Ramon, Watkins, N. D., Abranson, C. E., and Nougier, Jacques, 1970, Geochemistry of an oceanite-ankaramite-basalt suite from East Island, Crozet archipelago: *Contr. Mineralogy and Petrology*, v. 28, no. 4, p. 319-339.
- Heier, K. S., 1962, Trace elements in feldspars—A review: *Norsk Geol. Tidsskr.*, v. 42, no. 2, p. 415-454.
- Khafagy, Mahmoud, 1971, Zur Geochemie der Spitzer Gneise und der Paragneisse des Kampales, Niederösterreich: *Verh. Geol. Bundesanstalt*, 1971, no. 2, p. 171-192.
- Lovering, T. G., 1969, Distribution of minor elements in samples of biotite from igneous rocks, in *Geological Survey research 1969*: U.S. Geol. Survey Prof. Paper 650-B, p. B101-B106.
- , 1972, Distribution of minor elements in biotite samples from felsic intrusive rocks as a tool for correlation: U.S. Geol. Survey Bull. 1314-D, 29 p. [1971].
- Milovskiy, A. V., and Matveeva, S. S., 1970, Behavior of elements during the granitization of rocks [in Russian]: *Geologiya Rudnykh Metastozhd*, 1970, no. 3, p. 3-22; translated in *Internat. Geology Rev.*, v. 14, p. 623-638, 1972.
- Nockolds, S. R., and Mitchell, R. L., 1948, The geochemistry of some Caledonian plutonic rocks—A study in the relationship between the major and trace elements of igneous rocks and their minerals: *Royal Soc. Edinburgh Trans.* [1946], v. 61, pt. 2, p. 533-575.
- Parry, W. T., and Nackowski, M. P., 1963, Copper, lead, and zinc in biotites from Basin and Range quartz monzonites: *Econ. Geology*, v. 58, p. 1126-1144.
- Priz, Sergiu, Vasiliu, Cecilia, and Udrescu, Constanta, 1971, Petrology of magmatites from the Neogene subvolcanic zone, East Carpathians [in Rumanian with French and English summaries]: *Romania Com. Stat. Geologiei Anuarul*, v. 39, p. 177-256.
- Saha, A. K., Saukati, A. V., and Bhattacharya, T. K., 1968, Trace-element distribution in the magmatic and metasomatic granites of Singhbhum region, eastern India: *Neues Jahrb. Mineralogie Abh.*, v. 108, no. 3, p. 247-270.
- Savu, Haralambie, Vasiliu, Cecilia, and Udrescu, Constanta, 1971, Petrologic and geochemical study of the synorogenic and late orogenic granitoids from the Susita pluton, south Carpathians [in Rumanian, with French and English summaries]: *Romania Com. Stat. Geologiei Anuarul*, v. 39, p. 257-296.
- Tauson, L. V., and Kravchenko, L. A., 1956, Characteristics of lead and zinc distribution in minerals of the Caledonian granitoid of the Susamyr batholith in central Tian-Shan [in Russian]: *Geokhimiya*, 1956, no. 1, p. 81-89; translated in *Geochemistry*, 1956, no. 1, p. 78-88.
- Taylor, S. R., Capp, A. C., Graham, A. L., and Blake, D. H., 1969, Trace element abundances in andesites—2, Saipan, Bougainville, and Fiji: *Contr. Mineralogy and Petrology*, v. 23, no. 1, p. 1-26.
- Turekian, K. K., and Wedepohl, K. H., 1961, Distribution of the elements in some major units of the Earth's crust: *Geol. Soc. America Bull.*, v. 72, p. 175-192.
- Vinogradov, A. P., 1956, Regularity of distribution of chemical elements in the Earth's crust [in Russian]: *Geokhimiya*, 1956, no. 1, p. 6-52; translated in *Geochemistry*, 1956, no. 1, p. 1-43.
- , 1962, Average contents of the chemical elements in the principal types of igneous rocks of the Earth's crust [in Russian with English summaries]: *Geokhimiya*, 1962, no. 7, p. 555-571; translated in *Geochemistry*, 1962, no. 7, p. 641-664.
- Walker, K. R., 1969, The Palisades sill, New Jersey—A reinvestigation: *Geol. Soc. America Spec. Paper* 111, 178 p.
- Wedepohl, K. H., 1956, Untersuchungen zur Geochemie des Bleis [with English summ.]: *Geochim. et Cosmochim. Acta*, v. 10, no. 1-2, p. 69-148.
- Whittaker, E. J. W., and Munst, R., 1970, Ionic radii for use in geochemistry: *Geochim. et Cosmochim. Acta*, v. 34, no. 9, p. 945-956.
- Zlobin, B. I., and Gorshkova, M. S., 1961, Lead and zinc in alkaline rocks and their bearing on some petrologic problems [in Russian with English summary]: *Geokhimiya*, 1961, no. 4, p. 283-292; translated in *Geochemistry*, 1961, no. 4, p. 317-328.

ABUNDANCE OF LEAD IN SEDIMENTARY ROCKS, SEDIMENTS, AND FOSSIL FUELS

By T. G. LOVERING

SEDIMENTARY ROCKS AND SEDIMENTS

Lead is present in very small amounts in the common sedimentary rocks. Analytical data from the U.S. Geological Survey's rock analysis storage system for more than 2,500 sedimentary rock samples from various parts of the United States show average lead concentrations of about 32 ppm for carbonaceous shale, 23 ppm for siltstone, mudstone, claystone, and noncarbonaceous shale, 17 ppm for sandstone, and 11 ppm for limestone and dolomite. For all these rock types, median values are lower than the averages (fig. 7), and even the carbonaceous shale, which has the highest average lead content, contains only about 1 ounce of lead per ton (31 g/t) of average rock.

Comparable data on the lead content of these and other sedimentary rocks are found in the literature. Selected samples of carbonaceous shale from various formations in the Western United States contained from <10 to 70 ppm lead, with a median of 15 ppm (Davidson and Lakin, 1961, 1962). Vine (1966) collected four sets of black shale samples from various parts of the country and found median values in them ranging from 10 to 30 ppm of lead, and Wedepohl (1971) obtained an average lead value of 23.8 ppm from 200 bituminous shale samples taken from both the United States and Europe. Likewise, in an additional 73 samples of shale of Mesozoic to Holocene age, from Europe, Korea, Japan, the United States, and Trinidad, Wedepohl found an average of 23.8 ppm lead with a standard deviation of 15 ppm. Tourtelot (1962, pl. 4) found that the lead content of samples of Pierre Shale taken from widely separated localities in Montana, Wyoming, and South Dakota showed a narrow range of from 7 to 30 ppm with a median at 15 ppm. Krauskopf (1955, p. 416) gave an average value for lead in shale of 20 ppm; Newman (1962, p. 425) estimated the average lead content of Triassic mudstones on the Colorado Plateau as 13 ppm, and Cadigan (1971, p. 41-42) calculated a geometric mean of about 12 ppm lead for these rocks.

Published data on the lead content of normal sandstone are somewhat less abundant than those for shale and siltstone. Krauskopf (1955, p. 416) gave an average range of

10-40 ppm lead for sandstone. Wedepohl (1971, p. 241) found a mean value of 19.2 ppm lead in 45 Paleozoic and Mesozoic quartz sandstones from Germany. Lapchinskii and Lapchinskaya (1966, p. 123-127) reported an observed range of 16-52 ppm for lead in Carboniferous sandstone from Shebelinsk, Russia, and Razdorozhnyi (1966, p. 203-206) obtained a modal value of 10 ppm lead from sandstone samples of similar age from the Donets Basin of Russia.

Our data on normal lead in carbonate rocks (limestone and dolomite) are comparable with the average abundance of 8±4 ppm estimated by Graf (1960, p. 71) and with the average of 9 ppm given by Wedepohl (1971, p. 241) for 124 samples of European carbonate rocks.

Semiquantitative analyses of several hundred samples of phosphate rock from the Phosphoria Formation in Idaho (Sheldon and others, 1953; McKelvey and others, 1953) suggest that the normal lead content of this rock ranges from 10 to 100 ppm and that many of the samples contain >100 ppm of lead, indicating a slightly greater concentration of lead in phosphate rock than in carbonaceous shale. Bauxite, on the other hand, appears to be more comparable to the carbonate rocks in its lead content; samples of Arkansas bauxite had an average content of 7 ppm and a maximum content of 70 ppm lead (Gordon and Murata, 1952). However, some published analyses of European phosphorites and bauxites suggest the reverse relationship in the relative concentrations of lead in these two rocks. Orekhov (1968) reported a maximum value of 30 ppm lead in samples of lower Tertiary phosphorites of the Rostov region in Russia. Maksimovic (1968) found a range of 16-155 ppm, with an average of 69 ppm lead, in 120 samples of bauxite from Herzegovina, Yugoslavia. György (1957), however, gave lead concentrations in bauxite samples from western Hungary that are comparable to those reported for Arkansas bauxite.

The normal lead content of marine evaporite rocks appears to be even lower than that of the sedimentary carbonate rocks. Stewart (1963, p. Y33-Y39) presented

several analyses of these marine rocks and of the chloride and sulfate minerals of which they are composed. The highest lead value he gave is 5.4 ppm for a core sample of halite (NaCl); most of the halite samples, and also those of potash evaporites, contained less than 1 ppm of lead. The low lead content of potash evaporite sediments is somewhat surprising in view of the tendency for lead to concentrate in the potash feldspars of igneous rocks.

The presence of available lead in the marine environment is indicated by relatively high lead concentrations in samples of unconsolidated marine sediments. Turekian and Wedepohl (1961, p. 186) reported an average of 45 ppm lead in deep sea clay from the Atlantic and 110 ppm in corresponding samples from the Pacific. Ericson, Ewing, Wollin, and Heezen (1961, p. 229-231) analyzed more than 100 argillaceous bottom sediments from the Atlantic Ocean and the Caribbean Sea. These samples gave a median lead value of 60 ppm and a maximum of 240 ppm. Riley and Skirrow (1965, p. 49) reported an average

of 162 ppm of lead in deep sea clay samples; they believed more than half of this lead to have been derived from seawater (p. 57). Similarly, in deep sea nodules of iron and manganese oxides, they obtained nearly 1,000 ppm lead, which they thought was adsorbed from seawater by the hydrous colloidal oxides of iron and manganese.

Marine sediments deposited in shallow water appear to contain appreciably less lead than those deposited in deep water. Nearshore samples from the Pacific Ocean average only 20 ppm lead (Riley and Skirrow, 1965, p. 49), and similar lead contents are reported from Mediterranean Sea sediments (Bilyavskii, 1969), and Baltic Sea sediments (Lubchenko, 1970). However, in tectonically active areas, such as the Red Sea, where volcanic emanations and hydrothermal solutions mingle with marine water, lead content of the sediments can be greatly increased. Sediment samples from the bottom of hot brine pools in the Red Sea contain as much as 0.2 percent lead (Hendricks and others, 1969, p. 434).

This contrast between lead contents of deep and shallow marine sediments suggests that lead entering the marine environment has a tendency to move outward and downward toward the deeps. Such a theory would help to explain the low lead in evaporite sediments that formed in shallow basins; most of the lead may be presumed to have migrated seaward from these basins before the brines became sufficiently concentrated for the evaporite minerals to precipitate. Higher lead content of deep marine sediments may also be caused, in some places, by lead-bearing juvenile emanations entering the deep sea basins.

The normal lead content of unconsolidated terrestrial stream sediment appears to be comparable to that of shale. Holman (1963) found an average of 18 ppm lead in stream sediment samples from Nova Scotia. Analyses of more than 5,500 stream sediment samples from a large area in Maine yielded a mean of 25 ppm lead (F. C. Canney and Maurice Chaffee, written commun., 1971).

FOSSIL FUELS

The normal lead content of coal appears to be intermediate between that of shale and of the carbonate rocks, averaging about 10 ppm. Rao (1968) estimated that the lead content of Alaskan coal samples ranged from 1 to 50 ppm and averaged 10 ppm. Published lead analyses of organic fuels samples are normally given as percent lead in ash, inasmuch as lead cannot be determined by ordinary analytical methods in the presence of large amounts of organic carbon. The values given by Rao for the lead content of the ash of Alaskan coal samples are approximately one order of magnitude higher than his estimated values for the raw coal, ranging from 20 to 400 ppm and averaging 100 ppm. Abernathy, Peterson, and Gibson (1969) presented data on the lead content of the ash of large numbers of coal samples from the western, interior, and

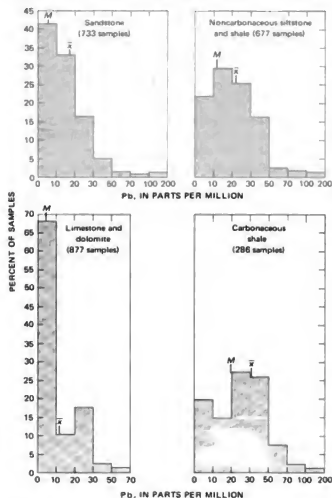


FIGURE 7.—Lead content of common sedimentary rocks (from U.S. Geological Survey's rock analysis storage system). M, median; \bar{x} , average.

eastern coal provinces of the United States. The average lead in ash was given as 29 ppm for the western province, 131 ppm for the interior province, and 55 ppm for the eastern province.

The published data suggest that the lead content of coal tends to decrease as its rank increases. Duell and Annell (1956) found lead contents in ash of low-rank-coal samples ranging from 100 to 1,000 ppm. Nunn, Lovell, and Wright (1953, p. 56) estimated a range of 10–100 ppm in the lead content of anthracite ash; and Chow and Earl (1970, p. 46) found a range of 10.0–33.8 ppm of lead in the ash of anthracite samples from Pennsylvania and Rhode Island.

Headlee and Hunter (1955, p. 151–155) ran some experiments on the partitioning of lead in coal among the products of combustion. They concluded that the ashing techniques used in the laboratory retain essentially all of the lead in the ash, but that ordinary burning of coal in industrial processes volatilizes about 6 percent of the lead originally present in the coal. If we use this figure, and assume a lead content of 10 ppm (0.001 percent) in the coal, it would require the combustion of approximately 10,000 tons of coal to introduce 1 pound (0.45 kg) of volatilized lead into the atmosphere. Industrial burning of coal samples with a lead content of 0.037 percent in the ash produced soot with a lead-in-ash content of 0.4 percent, and the ash of coal tar derived from this coal contained 2.84 percent lead (Headlee and Hunter, 1955, p. 155).

The lead content of petroleum, although generally lower than that of coal, is extremely variable. Hyden (1961, p. 44–59) published extensive tables showing the lead content of crude oil samples from different parts of the country. Lead ranges from <0.001 to 11.4 ppm and averages 0.025 ppm in the oil, and it ranges from <0.0015 to 300 ppm and averages 20 ppm in the ash. Donnell, Tailleux, and Tourtelot (1967) reported a maximum lead content of 200 ppm in the ash of samples of Alaskan oil shale.

REFERENCES CITED

- Abernathy, R. F., Peterson, M. J., and Gibson, F. H., 1969, Spectrochemical analyses of coal ash for trace elements: U.S. Bur. Mines Rept. Inv. 7281, 30 p.
- Bilyavskii, G. A., Mitropolskii, A. Yu., and Romanov, V. I., 1969, New data on the distribution of trace elements in the columns of bottom sediments in the Mediterranean Sea [in Ukrainian]: Akad. Nauk Ukrainy RSR, Dopevid, ser. B, v. 31, no. 12, p. 1059–1061; abs. in Chem. Abs., v. 72, no. 69311f, 1972.
- Cadigan, R. A., 1971, Geochemical distribution of some metals in the Moenkopi Formation and related strata, Colorado Plateau region: U.S. Geol. Survey Bull. 1344, 56 p.
- Chow, T. J., and Earl, J. L., 1970, Lead and uranium in Pennsylvanian anthracite: Chem. Geology, v. 6, no. 1, p. 43–49.
- Davidson, D. F., and Lakin, H. W., 1961, Metal content of some black shales of the western United States, in Short papers in the geologic and hydrologic sciences: U.S. Geol. Survey Prof. Paper 424-C, p. C329–C331.
- , 1962, Metal content of some black shales of the western continental United States, pt. 2, in Short papers in geology and hydrology: U.S. Geol. Survey Prof. Paper 450-C, p. C74.
- Deul, Maurice, and Annell, C. S., 1956, The occurrence of minor elements in the ash of low-rank coal from Texas, Colorado, North Dakota, and South Dakota: U.S. Geol. Survey Bull. 1036-H, p. 155–172.
- Donnell, J. R., Tailleux, I. L., and Tourtelot, H. A., 1967, Alaskan oil shale: Colorado School Mines Quart., v. 62, no. 3, p. 39–43.
- Ericson, D. B., Ewing, Maurice, Wollin, Goesta, and Heeren, B. C., 1961, Atlantic deep-sea sediment cores: Geol. Soc. America Bull., v. 72, p. 193–285.
- Gordon, Mackenzie, Jr., and Murata, K. J., 1952, Minor elements in Arkansas bauxite: Econ. Geology, v. 47, no. 2, p. 169–179.
- Graf, D. L., 1960, Geochemistry of carbonate sediments and sedimentary carbonate rocks—Pt. 3, Minor element distribution: Illinois State Geol. Survey Div. Circ. 501, 71 p.
- György, Bardossy, 1957, Bauxite in the region of Sacs and Nyirad [in Hungarian]: Magyar Állami Földt. Inté. Evkötöny, p. 433–454.
- Headlee, A. J. W., and Hunter, R. G., 1955, Changes in the concentration of the inorganic elements during coal utilization, in Characteristics of minable coals of West Virginia: West Virginia Geol. Survey [Rept.], v. 13a, p. 150–159.
- Holman, R. H. C., 1963, A regional geochemical reconnaissance of stream sediments in the northern mainland of Nova Scotia, Canada: Canada Geol. Survey Paper 63-25, p. 1–19.
- Hendricks, R. L., Reisbeck, F. B., Mahaffey, E. J., Roberts, D. B., and Peterson, M. M. A., 1969, Chemical composition of sediments and interstitial brines from the Atlantis II, discovery and chain deeps, in Degens, E. T., and Ross, D. A., eds., Hot brines and recent heavy metal deposits in the Red Sea: New York, Springer-Verlag, p. 407–440.
- Hyden, H. J., 1961, Distribution of uranium and other metals in crude oils: U.S. Geol. Survey Bull. 1100-B, p. 17–99.
- Krauskopf, K. B., 1955, Sedimentary deposits of rare metals: Econ. Geology, 50th Anniversary Vol [1905–1955], pt. 1, p. 411–463.
- Lapchinskii, Yu. G., and Lapchinskaya, L. V., 1966, Trace elements in carboniferous formations of the Shebelinsk natural gas deposits [in Russian]: Ukrain. Nauchno-Issled. Inst. Prirodnykh Gazov Trudy 1966, no. 2, p. 123–127; abs. in Chem. Abs., v. 67, no. 8398a, 1967.
- Lubchenko, I. Yu., 1970, Lead in recent Black Sea sediments [in Russian]: Akad. Nauk SSSR Doklady, v. 193, no. 2, p. 445–448.
- McKelvey, V. E., Armstrong, F. C., Gulbrandson, R. A., and Cambell, R. M., 1953, Stratigraphic sections of the Phosphoria formation in Idaho, 1947–48, pt. 2: U.S. Geol. Survey Circ. 301, 58 p.
- Maksimovic, Z., 1968, Distribution of trace elements in bauxite deposits of Herzegovina, Yugoslavia [in English]: Acad. Yugoslav Sci. Arts, Trav. Com. Int. Etude Bauxites, Oxydes, Hydroxydes Alum. 1968, no. 5, p. 63–70; abs. in Chem. Abs., v. 69, no. 88747g, 1968.
- Newman, W. L., 1962, Distribution of elements in sedimentary rocks of the Colorado Plateau—A preliminary report: U.S. Geol. Survey Bull. 1107-F, p. 337–445.
- Nunn, R. C., Lovell, H. L., and Wright, C. C., 1953, Spectrographic analysis of trace elements in anthracite: Anthracite Conf., 11th, Lehigh Univ. 1953, Trans., p. 51–65.
- Orekhov, S. Ya., 1968, Mineralogy and structural types of phosphorites of the Rostov region [in Russian]: Rostov na Donu Gosudarstvennogo Universiteta, Uchenye Zapiski, v. 53, no. 9, p. 273–287.
- Rao, P. D., 1968, Distribution of certain minor elements in Alaskan coals: Alaska Univ. Mineral Industry Research Lab. Rept. 15, 47 p.
- Rardoroshnyi, V. F., 1966, Copper, zinc and lead in rocks of small folding zone of Donets Basin (Lugansk geological district) [in Russian]: Polz. Iskop. Ukr. 1966, p. 203–206; abs. in Chem. Abs., v. 67, no. 83966b, 1967.
- Riley, J. P., and Skirrow, G., eds., 1965, Chemical oceanography, V. 2 London, New York, Academic Press, 508 p.

- Sheldon, R. P., Werner, M. A., Thompson, M. E., and Pierce, H. W., 1953, Stratigraphic sections of the Phosphoria formation in Idaho, 1949, pt. 1: U.S. Geol. Survey Circ. 304, 30 p.
- Stewart, F. H., 1963, Marine evaporites. U.S. Geol. Survey Prof. Paper 440-Y, p. Y1-Y32.
- Tournelot, H. A., 1962, Preliminary investigation of the geologic setting and chemical composition of the Pierre Shale, Great Plains region: U.S. Geol. Survey Prof. Paper 390, 74 p.
- Turekian, K. K., and Wedepohl, K. H., 1961, Distribution of the elements in some major units of the Earth's crust: Geol. Soc. America Bull., v. 72, no. 2, p. 175-192.
- Vine, J. D., 1966, Element distribution in some shelf and eugeosynclinal black shales: U.S. Geol. Survey Bull. 1214-E, p. E1-E31.
- Wedepohl, K. H., 1971, Zinc and lead in common sedimentary rocks, *app. to* Lavery, N. G., and Barnes, H. L., Zinc dispersion in the Wisconsin zinc-lead district: Econ. Geology, v. 66, p. 240-242.

LEAD CONTENT OF WATER

By M. J. FISHMAN and J. D. HEM

The lead content of water is usually described in terms of concentrations of the dissolved element. For research purposes, the U.S. Geological Survey, in testing water samples for trace elements, considers dissolved material to be particles small enough to pass through a 0.45- μ m-pore-diameter membrane. Although this is an arbitrary operational definition and some colloidal material may pass through the filter, the 0.45- μ m size limit is widely used. Where data are given here on dissolved lead, they may be assumed to represent material that passed through a 0.45- μ m-porosity filter. Until recently very little attention has been given to the minor-element content of material caught on the filter, and it is not possible to obtain from published literature any clear indication of the importance of the suspended fraction in the total quantity of lead transported by streams. There is some evidence, however, that, at times, considerable amounts may be present in suspension in streams carrying direct runoff from urbanized areas.

LEAD IN SURFACE WATERS

A considerable amount of information on lead concentrations in surface waters has been obtained since the late 1950's. However, the observations tend to be sporadic and scattered, and the details of the chemical behavior of the element and its occurrence in any single stream have not been fully explored. Kleinkopf (1960) reported a mean lead concentration of 2.3 μ g/l in waters from 440 lakes in the State of Maine, with a range of 0.03-115 μ g/l. Durum, Heidel, and Tison (1960) reported concentrations of a suite of minor elements, including lead, for samples from major streams throughout the world. Data from their report and supplementary unpublished analyses in U.S. Geological Survey files show a range of lead concentrations from 0 to 200 μ g/l, with an average of 8.4 μ g/l. There were 93 samples in this group, representing 27 streams, mostly in North America. Lead occurred in concentrations above the detection limit in more than 90 percent of the samples. The samples in the study by Durum, Heidel, and Tison were filtered before analysis, but the filter only removed particles over 1 μ m in diameter. Consequently these lead values may include some from material usually found in suspension as well as that in solution.

Since 1960, the U.S. Geological Survey has performed more than 1,600 lead determinations on surface-water samples collected throughout the United States. These samples were analyzed for lead by spectrographic and atomic-absorption techniques, which are discussed by M. J. Fishman (this report). Most of the samples were from one of three sources: (1) public water supplies, (2) water courses downstream from major municipal or industrial complexes, and (3) U.S. Geological Survey hydrologic bench-mark stations.

The dissolved-lead concentrations in these samples, representing surface waters in all 50 states as well as Washington, D.C., and Puerto Rico, range from "not detected" to 890 μ g/l. However, lead only rarely occurs in amounts exceeding the U.S. Public Health Service (1963) drinking water standard of 50 μ g/l lead. Only 13 of the more than 1,600 samples analyzed, or less than 1 percent, contained concentrations in excess of 50 μ g/l. Of the 13 samples, only 3 contained more than 100 μ g/l lead, or more than twice the U.S. Public Health Service limit. Eighty-six percent of the samples contained less than 10 μ g/l. Most surface waters, except for water courses downstream from major municipal and industrial complexes, evidently contain less than 10 μ g/l of dissolved lead.

Table 12 summarizes, by States, the maximum and minimum concentrations of lead found in surface waters of the United States. Also included in the summary are the percentage of samples containing less than 10 μ g/l and the number of samples that exceeded the U.S. Public Health Service drinking water limit. The data in this table, which cover the period from 1960 through 1971, were obtained from Durfor and Becker (1964), and Durum, Hem, and Heidel (1971), and from miscellaneous spectrographic data from analyses performed in the U.S. Geological Survey laboratory in Denver, Colo., under the direction of P. R. Barnett.

Table 13 shows lead concentrations in selected surface waters of the United States, as determined from miscellaneous spectrographic analyses.

Several in-depth studies of surface water in individual States and regions have also been carried out. Silvey (1967) reported an average concentration of 5.7 μ g/l of lead in streams of California in which the element could be

TABLE 12.—Maximum and minimum concentrations of lead found in surface waters of the United States and Puerto Rico from 1960 to 1971

	Number of samples	Number of samples equaling or exceeding mandatory maximum less than for drinking water ¹	Percent of samples having less than (10 µg/l)	Lead concentration (µg/l)	
				Maximum	Minimum
Alabama.....	76	1	96	50.0	ND
Alaska.....	9	0	100	5.0	< 1.0
Arizona.....	19	0	89	12.0	ND
Arkansas.....	32	0	81	20.0	< .8
California.....	40	0	68	34.0	< 1.0
Colorado.....	70	0	89	30.0	ND
Connecticut.....	50	1	72	50.0	< 1.0
Delaware.....	4	0	25	23.0	2.0
District of Columbia.....	4	0	100	5.8	< 1.0
Florida.....	37	0	100	6.0	< .7
Georgia.....	22	0	41	32.0	< 1.0
Hawaii.....	8	0	100	< 1.0	< 1.0
Idaho.....	26	0	100	6.0	< 1.0
Illinois.....	23	0	48	25.0	2.5
Indiana.....	46	0	89	20.0	ND
Iowa.....	14	0	100	5.7	< 1.0
Kansas.....	14	0	100	7.5	ND
Kentucky.....	10	0	60	20.0	< 1.0
Louisiana.....	19	0	95	11.0	< 1.0
Maine.....	7	1	57	890.0	5.0
Maryland.....	29	0	93	43.0	< 1.0
Massachusetts.....	24	1	75	87.0	1.3
Michigan.....	25	0	92	15.0	2.0
Minnesota.....	30	0	97	17.0	< 1.0
Mississippi.....	11	0	82	10.0	< 1.0
Missouri.....	103	0	84	38.0	< .5
Montana.....	25	0	96	23.0	< 1.0
Nebraska.....	21	0	81	10.0	< 1.0
Nevada.....	8	0	100	5.0	< 1.0
New Hampshire.....	5	1	80	70.0	4.0
New Jersey.....	130	2	88	240.0	< 1.0
New Mexico.....	34	0	91	10.0	ND
New York.....	211	0	92	22.0	< 1.0
North Carolina.....	27	0	70	32.0	< 1.0
North Dakota.....	22	0	86	37.0	< 1.0
Ohio.....	31	0	100	7.9	ND
Oklahoma.....	16	2	75	94.0	< 1.0
Oregon.....	14	0	100	< 1.0	< 1.0
Pennsylvania.....	65	1	71	55.0	2.0
Rhode Island.....	5	0	100	8.0	3.4
South Carolina.....	17	0	94	11.0	< 1.0
South Dakota.....	22	0	68	35.0	< 1.0
Tennessee.....	21	2	67	390.0	< 1.0
Texas.....	46	0	98	11.0	ND
Utah.....	28	0	89	12.0	< 1.0
Vermont.....	3	1	0	50.0	13.0
Virginia.....	16	0	81	42.0	< 1.0
Washington.....	17	0	100	7.0	< .5
West Virginia.....	22	0	86	44.0	< 1.0
Wisconsin.....	18	0	83	26.0	2.0
Wyoming.....	37	0	789	3.0	< 1.0
Puerto Rico.....	40	0	85	19.0	< 1.0
Total.....	1,673	13	86
Percent of total samples.....	86

¹10 µg/l as established by the U.S. Public Health Service (1965).

ND includes those values above 10 µg/l.

detected. However, lead concentrations were below the detection limit (0.6 µg/l) in 78 percent of the stream samples analyzed.

A comprehensive investigation of the distribution of dissolved lead in Florida surface waters was carried out by the U.S. Geological Survey in cooperation with the Bureau of Geology, Florida Department of Natural Resources, and other State and local agencies (C. S. Conover, written commun., 1971). More than 180 samples were analyzed; concentrations of lead ranged from 0 to 40 µg/l. The samples were collected during low (May 1970) and high (September 1970) streamflow conditions. The data for May 1970 indicate the following: (1) lead was found in about 60 percent of the samples in concentrations ranging from 1 to 30 µg/l; (2) 78 percent of all samples had lead concentrations equal to or less than 10 µg/l; and (3) 4 percent of all samples had concentrations of 30 µg/l. For September 1970, the following was observed: (1) lead was found in about 73 percent of the samples in concentrations ranging from 1 to 40 µg/l; (2) 75 percent of all samples had concentrations equal to or less than 10 µg/l; and (3) 7 percent of all samples had lead concentrations equal to or greater than 30 µg/l.

Several other investigators have reported the lead content of various lake and river waters. Boswell, Brooks, and Wilson (1967) reported that the lead concentration in the bottom waters of Lakes Joyce and Hoare in Antarctica were 340 µg/l and 83–91 µg/l, respectively. The lead content of the water of the Orange River at Vioolsdrif, Cape Province, Union of South Africa, was reported by DeVilliers (1962) to range from less than 0.001 to 136 ppm (1,360 µg/l), based on 24 samples collected over a period of 1 year. Zhukhovitskaya, Zamyatkina, and Lukashev (1966) reported that lead concentrations in streams of the upper Dnieper basin ranged from 0.01 to 0.55 ppb. Lukashev, Zhukhovitskaya, and Zamyatkina (1965) found that lead concentrations in the surface waters of the Poles'e territory near Pripyat in the Belorussian S. S. R. ranged from 2 to 13.3 ppb. Krainov and Korol'kova (1964) analyzed mineral waters of the Lesser Caucasus and found a maximum lead concentration of 40 µg/l. Turekian and Kleinkopf (1956) determined lead in 439 stream and lake waters of Maine by a semiquantitative spectrographic procedure. The average concentration of lead was 0.26 ppb. Heidel and Frenier (1965) reported on the lead concentration of 156 surface waters, including some samples from the estuary of the Patuxent River basin, Maryland. The lead content ranged from 0.9 to 11 µg/l, with an average of 5 µg/l. A survey of the concentration of lead and other trace elements in the Colorado, Columbia, Ohio, Mississippi, and Missouri Rivers and in the Great Lakes was presented by Kroner and Kopp (1965). In only a few samples did the lead concentration exceed the U.S. Public Health Service drinking water standard. For most samples the concentration of lead was below the detection

TABLE 13.—Lead concentrations in selected surface waters of the United States

Sample locality	Date of collection	Lead Concentration ($\mu\text{R/l}$)	Reference
Alabama:			
Sigbee Fork, near Grayson	Sept. 10, 1970	1	J. R. Ayrett (oral commun., 1971).
Cocosa River, at Gadsden	Sept. 30, 1970	2	Do.
Cahala River, near Centerville	Feb. 4, 1971	1	Do.
Arizona:			
West Bottom Creek, near Childs	Sept. 16, 1968	< 1	N. B. Garmony (written commun., 1971).
Canal (Gila River), near Arlington	Sept. 18, 1968	< 1	Do.
Arkansas:			
Bayou Melo, near Lonoke	Nov. 6, 1967	5	U.S. Geological Survey (1968a).
Bayou Bartholomew, near McGehee	Nov. 7, 1967	< 5	Do.
White River, at Clarendon	Nov. 6, 1967	4	Do.
Saline River, near Rye	Nov. 7, 1967	< 2	Do.
Ouachita River, at Arkadelphia	Nov. 8, 1967	3	Do.
Little River, near Ashdown	Nov. 9, 1967	1	Do.
Black River, at Black Rock	Nov. 16, 1967	< 4	Do.
Colorado:			
Arkansas River, at Granite	Jan. 19, 1967	30	U.S. Geological Survey (1967a).
South Platte River, near Henderson	Jan. 15, 1971	4	R. Brennan (written commun., 1971).
Connecticut:			
Naugatuck River, at Beacon Falls	Oct. 5, 1967	30	U.S. Geological Survey (1968b).
Hockanum River, near Rockville	Aug. 14, 1968	26	Do.
Florida:			
Sopchoppy River, near Sopchoppy	Mar. 10, 1970	6	R. L. Malcolm (written commun., 1971).
Iowa:			
Big Sioux River, at Akron	Apr. 4, 1967	3	U.S. Geological Survey (1967c).
Massachusetts:			
Connecticut River, at Northfield	July-Nov. 1970 (composite)	30	C. E. Knox (written commun., 1971) ¹
Hoosic River, below Williamstown	July-Dec. 1970 (composite)	3	Do.
Missouri:			
West Fork Black River, at Westfork	Oct. 24, 1967	5	U.S. Geological Survey (1968c).
Turkey Creek, near Joplin	Mar. 19, 1968	25	Do.
Spring River, near Waco	June 26, 1968	< 4	Do.
Sedalia Lake, near Sedalia	Oct. 29, 1970	1	A. Homyk (written commun., 1971).
James River, near Springfield	Feb. 16, 1971	< 4	Do.
Missouri River, near St. Louis	Mar. 12, 1971	4	Do.
Montana:			
Blackfoot River, near Lincoln	Aug. 22, 1969	< 3	U.S. Geological Survey (1969).
Nebraska:			
Disraeli River, near Thedford	June 13, 1967	13	L. R. Petri (written commun., 1971).
Missouri River, at Omaha	Mar. 19, 1971	2	A. Homyk (written commun., 1971).
New Hampshire:			
Pemigewasset River, at Woodstock	July-Oct. 1970 (composite)	70	C. E. Knox (written commun., 1971) ¹ .
New Jersey:			
Passaic River, at Chatham	Aug. 28, 1970	9	P. W. Anderson (written commun., 1971) ¹ .
Whippany River, at Morristown	do	5	Do.
Rockaway River, at Roseton	Sept. 1, 1970	5	Do.
Hackensack River, at River Vale	Sept. 2, 1970	12	Do.
Milstone River, near Manville	Sept. 3, 1970	< 2	Do.
Raritan River, near Manville	do	< 2	Do.
Assumpink Creek, at Trenton	do	< 3	Do.
Delaware River, at Trenton	Sept. 29, 1970	2	Do.
New Mexico:			
Pecos River, at Artesia	Apr. 7, 1970	< 2	K. Ong (written commun., 1971) ¹ .
Rio Mora, at Terroto	Oct. 5, 1970	.7	Do.
Mogollon Creek, near Cliff	Oct. 14, 1970	8	Do.
New York:			
Allegheny River, at Salamanca	Sept. 21, 1967	< 5	U.S. Geological Survey (1967b).
Oneida Lake, at Brewster	Oct. 1, 1969	< 2	R. J. Archer (written commun., 1971) ¹ .
Sisquesbanna River, at Johnson City	Apr. 6, 1970	1	Do.
Lake Champlain, at Crown Point	June 2, 1970	7	Do.
Niagara River, at City of Niagara Falls	Nov. 16, 1970	< 5	Do.
Lake Ontario, at Oswego	Dec. 9, 1970	4	Do.
Hudson River, at Poughkeepsie	Dec. 16, 1970	2	Do.
St. Lawrence River, at Alexandria Bay	Dec. 14, 1970	< 5	Do.
Black River, at Watertown	Feb. 22, 1971	1	Do.
North Carolina:			
Neuse River, at Raleigh	July 9, 1970	.7	R. Heath (written commun., 1971).
South Dakota:			
Belle Fourche River, at Wyoming-South Dakota boundary	Oct. 13, 1970	< 30	F. C. Boner (written commun., 1971).
Wyoming:			
Laramie River, at Laramie	Apr. 25, 1970	< 7	Do.
Cache Creek, near Jackson	Sept. 1, 1970	< 2	Do.
North Platte River, below Casper	Jan. 15, 1971	< 8	Do.
Bighorn River, at Kane	Jan. 26, 1971	< 5	Do.

¹See Pl. 2, Water Quality Records, of the U.S. Geological Survey's Water Resources Data series, for the respective State and water year.

limit of the spectrographic method used to analyze the samples.

The data of Durunt, Hem, and Heidel (1971) show a distinct regional pattern of dissolved-lead distribution in river water in the United States. Concentrations above the detection limit occurred in nearly all sources sampled in the States along the Atlantic Coast and in most sources in thickly populated regions around the Great Lakes. In the more thinly populated regions west of the Mississippi, a high proportion of the sources had less than $1 \mu\text{g/l}$ of lead, but relatively high concentrations appeared again along the Pacific Coast in streams of the Los Angeles, San Francisco, and Seattle areas. There were areas of higher concentrations in lead mining regions in Wisconsin, near the Ozark Mountains, and in northern Idaho and adjacent areas. The distribution pattern may be explained by considering the sources of environmental lead and by the solubility of lead carbonate and hydroxide from industrial wastes in river water.

Livingstone (1963) stated that from data then available it seemed likely that the global mean lead content for lakes and rivers ranged from 1 to 10 ppb. Data cited here suggest that this is a reasonable estimate for the dissolved fraction. In general, the presence of a few tens of micrograms per litre of lead in solution in river water appears to be most common in areas of heavy automobile traffic and extensive industrial development. In the vicinity of lead ore deposits, the content of lead in river water may also be in this range or higher.

Lead can be carried as a colloidal suspension of hydroxide in river water, and it may also be present as a coating on other mineral particles, or as ions sorbed on mineral surfaces. The available data do not clearly show the importance of suspended lead. Konovalov, Ivanova, and Kolesnikov (1968) determined lead concentrations in particulate material carried by 33 rivers in the U.S.S.R.; no data are given in their report for dissolved forms of lead. Concentrations of lead associated with sediment were as high as $152 \mu\text{g/l}$ of the original water sample, but most were below $40 \mu\text{g/l}$. The analyses for lead in solution apparently all showed concentrations below detection, but it is not certain that the methods used give results that are comparable with those of other investigations cited here.

LEAD IN PRECIPITATION AND RUNOFF WATERS

A large amount of lead is used each year in the United States as a gasoline additive. This lead is mostly dispersed in the atmosphere, and has a readily measurable influence on the composition of rainfall—and, hence, of runoff waters—especially in the more thickly populated parts of the country. Lazrus, Lotrange, and Lodge (1970) reported the average concentration of lead in rainfall to be $34 \mu\text{g/l}$ for 32 precipitation measuring stations throughout the United States during a 7-month period ending in March 1967. The concentrations of lead in rainfall in the north-

eastern part of the country, however, are known to exceed this average substantially. In addition, many of the dilute, relatively low pH solutions that constitute the usual river and lake waters in this region have a high capacity for retaining lead in solution at equilibrium. Many such waters could attain lead concentrations amounting to several hundred micrograms per litre before reaching chemical saturation. The potential for higher concentrations in the surface waters of industrialized and thickly settled regions does exist, although concentrations in this range have not yet become common enough to be brought to light by the rather thin distribution of sampling and analysis thus far accomplished. The amounts of lead used as gasoline additives each year in the United States are enough to give an average lead concentration near $150 \mu\text{g/l}$ for all the runoff leaving the conterminous 48 States in the average year. This figure, of course, indicates only that lead is available in amounts that are of considerable potential hydrochemical significance. Just how much lead might be expected to accumulate in a particular stream at a given time depends on many other factors. The greatest contributions to runoff in most large streams come from areas where population is relatively sparse and lead is less abundant. A considerable fraction of the lead brought down in rain or snow can be expected to be intercepted and retained by soil and vegetation; however, the direct runoff from urbanized areas may contain substantial lead concentrations at times, and further study will probably show that such occurrences are not rare.

It is important that studies of lead in river water be continued, with special efforts to measure solubility parameters (pH and alkalinity) and to determine the particulate fraction of lead in runoff, especially in early stages of runoff events.

LEAD IN GROUND WATERS

The lead concentrations found in ground waters of many States and Puerto Rico are summarized in table 14. Again, spectrographic techniques were used for determining the lead in most of these samples. Atomic-absorption techniques were used for a few samples. Of the 353 samples analyzed, only two contained lead concentrations exceeding the U.S. Public Health Service drinking water standards. Eighty percent of the samples contained less than $10 \mu\text{g/l}$ of lead.

The amounts of lead in ground waters used for public supplies in some of the larger cities of the United States were reported by Durlor and Becker (1964). Most of the samples represented treated water, and treatment may have influenced some of the concentrations. Results of 57 analyses, many representing mixed water from several wells, were given. Detectable concentrations of lead were present in 30 of these; the remainder had concentrations below detection. The lower limit of detection in these solutions was variable and rather high, generally above 2

TABLE 14.—Maximum and minimum concentrations of lead found in ground waters of some States and Puerto Rico 1960 to 1971.
(ND sought but not found)

Number of samples	Number of samples equalling or exceeding mandatory maximum for drinking water*	Percent of samples containing less than 10 µg/l	Lead concentration (µg/l)	
			Maximum	Minimum
Alabama	2	0	100	ND
Arizona	9	0	56	40
California	7	0	14	46
Colorado	103	0	96	5
Connecticut	1	0	100	< 8
Florida	14	0	78	40
Georgia	1	0	100	< 2.6
Hawaii	3	0	100	5.8
Illinois	2	0	100	7.5
Indiana	3	0	67	21
Kansas	3	0	67	4
Kentucky	5	0	100	< 2
Louisiana	4	0	100	4.5
Missouri	43	0	95	< 2
Montana	8	0	50	< 35
Nebraska	1	0	100	ND
New Jersey	8	0	75	< 22
New Mexico	13	0	31	30
New York	19	0	89	10
North Carolina	1	0	100	< 3
Ohio	26	0	54	30
Pennsylvania	27	0	74	29
Tennessee	5	0	100	3.2
Texas	14	0	86	38
Utah	1	1	0	62
Virginia	1	0	100	< 9
Washington	2	0	50	< 2.6
Wisconsin	1	0	100	7.4
Wyoming	20	1	90	240
Puerto Rico	6	0	33	(^b)
Total	353	2
Percent of total samples	80

*50 µg/l. as determined by U.S. Public Health Service (1963).

^bNo data one value above 10 µg/l.

^cAll values are reported as "less than," because of high dissolved solids.

µg/l. The highest value observed was 62 µg/l, but this was a definite anomaly; most concentrations observed were between 2 and 10 µg/l. Lead has a very low solubility in water that contains moderate concentrations of bicarbonate ions and has a pH near 8. Many ground waters display these properties, and thus are expected to be low in dissolved lead concentration.

Silvey (1967) found detectable amounts of lead in 17 percent of the samples from springs and in 15 percent of the samples from wells and oil-field brines collected at various sites in California. The average concentration of lead for the water in these samples was 17 µg/l for the springs and 2.8 µg/l for the wells and oil-field brines. However, one of the spring samples contained 143 µg/l, which strongly influenced the reported average.

The compilation of analyses of ground waters by White, Hem, and Waring (1963) contains a few values for lead

concentrations, although the element was not generally determined. The highest reported concentration was about 1,400 µg/l in water from Wilbur Spring, Colusa County, Calif. Several other saline or thermal waters contained a few tens or hundreds of micrograms per litre, but most analyses for lead indicated concentrations below detection limits. In general, the ground waters that contained significant concentrations of lead were either high in chloride or low in pH, and had relatively high temperatures.

More than 100 spring-water samples were collected east of the Continental Divide in Colorado (E. C. Mallory, Jr., written commun., 1971). The dissolved-solids content of these samples ranged from less than 50 mg/l to more than 28,000 mg/l. Lead concentrations were generally low; 68 percent of the samples contained 1 µg/l or less. Only four samples contained more than 10 µg/l, and the maximum concentration was 30 µg/l. Lead concentrations in Missouri ground waters were also found to be generally low (E. C. Mallory, Jr., written commun., 1971). Of the 43 samples analyzed, 42 contained less than 10 µg/l of lead; the remaining sample contained 10 µg/l. Kosolapova (1963) reported that the lead content of subsurface waters in the Olonek River basin of Russia ranged from 5 to 90 µg/l.

Goleva, Polyakov, and Nechayeva (1970) reported 15 analyses of ground waters associated with ore deposits and 21 analyses of mineral and saline ground waters from various localities in the USSR. In the waters from ore deposits, the highest lead concentration found was 1,680 µg/l, but all the rest were below 100 µg/l; the water containing the highest concentration was strongly acid, with a pH below 1.0. The mineral and saline waters generally contained from 1.9 to 11.4 µg/l of lead.

Acid mine drainage samples in some areas contribute large quantities of iron, manganese, aluminum, and other elements to surface waters. A number of acid mine waters from Pennsylvania and Maryland and one from West Virginia have been analyzed by a U.S. Geological Survey laboratory in Denver, Colo. The concentrations of iron, aluminum, and manganese in these samples are high, showing maximum values of 190,000, 130,000, and 13,000 µg/l, respectively. On the other hand, the lead concentrations were low; 86 percent of the samples contained less than 10 µg/l lead, and 80 percent contained less than 5 µg/l.

LEAD IN THERMAL WATERS

Several investigators have made chemical studies of the lead content of hot-springs waters. The lead content of the waters at Stubic, Yugoslavia, was reported by Miholić (1945) to be 0.003 mg/kg (approximately 3 µg/l). In seven hot springs of Shikabe, Hokkaido, Japan, Uzumasa and Akaiwa (1960) determined lead concentrations ranging from 0.09 to 0.36 mg/l. Noguchi and Nishiido (1969) deter-

mined lead in Tateyama-jigokudani hot springs in Toyama Prefecture, Japan. Eighteen samples were analyzed colorimetrically with dithizone, and the concentrations of lead found ranged from 0.00 to 1.25 mg/l. Minami, Sato, and Watanuki (1957, 1958) analyzed hot-spring waters of Tamagawa, Akita Prefecture, Japan. In 10 springs along the main Tamagawa stream, the lead concentrations ranged from 0.98 to 1.8 mg/l. In 10 springs in the Yukawa River, the average lead content was 1.29 mg/l.

Goleva, Polyakov, and Nechayeva (1970) gave analyses of four thermal waters from the U.S.S.R. One, from a fumarole at Ebeko volcano, had 34.7 $\mu\text{g/l}$ lead. The other three (carbonate and nitrogen-carbonate brines), obtained from the thermal area of Cheleken, had from 1,210 to 4,000 $\mu\text{g/l}$. These waters were very saline, containing more than 200 g/l of dissolved solids, and some of the other waters of this area were reported to contain up to 6 mg/l of lead.

LEAD IN SEAWATERS

Tatumoto and Patterson (1963) determined lead concentrations in seawaters off southern California using isotope dilution techniques. The lead content ranged from 0.08 to 0.4 $\mu\text{g/l}$ and averaged 0.2 $\mu\text{g/l}$. In deep waters, the concentration did not vary much and averaged 0.03 $\mu\text{g/l}$. Skurnik-Sarig, Zidon, Zak, and Cohen (1970) were unable to detect lead in Atlantic Ocean waters. However, in the Mediterranean Sea, the lead content at Ashdod and Palmachim, Israel, was 340 and 170 $\mu\text{g/l}$, respectively. In Black Sea samples, Belyaev (1966) reported that the lead content was 3.6 ppb. This value represents an average of determinations made in the course of 5 years at a number of sites. Loveridge and others (1960) stated that lead in seawater is associated with the suspended solids that are removed by filters that retain particles 1 μm in diameter or larger. The values found for dissolved lead in their study ranged from 0.6 to 1.5 $\mu\text{g/l}$.

REFERENCES CITED

- Belyaev, I. I., 1966, Distribution and content of trace amounts of heavy metal elements in Black Sea waters [in Russian]: Akad. Nauk Ukrain. SSR, Inst. Morskogo Gidrofiz. Trudy, v. 37, p. 199-213; abs. in Chem. Abs., v. 66, no. 118688w, 1967.
- Boswell, C. R., Brooks, R. R., and Wilson, A. F., 1967, Trace element content of the Antarctic Lakes: Nature, v. 213, p. 167-168; abs. in Chem. Abs., v. 66, no. 58736y, 1967.
- DeVilliers, P. R., 1962, The chemical composition of the water of the Orange River at Viooldrift, Cape Province: Rep. Suid-Afrika, Dept. Mynewe, Ann. Geol. Opname, v. 1, p. 197-208 [1963]; abs. in Chem. Abs., v. 62, no. 10220h, 1965.
- Durlor, C. N., and Bekker, Edith, 1964, Public water supplies of the 100 largest cities in the United States, 1962: U.S. Geol. Survey Water-Supply Paper 1812, 364 p.
- Durum, W. H., Heidel, S. C., and Tison, L. G., 1960, World-wide runoff of dissolved solids: Comm. Surface Waters, Internat. Assoc. Sci. Hydrology General Assembly, Helsinki 1960, Internat. Assoc. Sci. Hydrology Pub. 51, p. 618-628.
- Durum, W. H., Hem, J. D., and Heidel, S. G., 1971, Reconnaissance of selected minor elements in surface waters of the United States, October 1970: U.S. Geol. Survey Circ. 643, 49 p.
- Goleva, G. A., Polyakov, V. A., and Nechayeva, T. P., 1970, Distribution and migration of lead in ground waters [in Russian]: Geokhimiya 1970, p. 344-357; translated in Geochemistry Internat., 1970, p. 256-268.
- Heidel, S. G., and Frenier, W. W., 1965, Chemical quality of water and trace elements in the Patuxent River basin: Maryland Geol. Survey Rep. Inv. 1, 40 p.
- Kleinop, M. D., 1960, Spectrographic determination of trace elements in lake waters of northern Maine: Geol. Soc. America Bull., v. 71, p. 1231-1242.
- Konovalov, G. S., Ivanova, A. A., Kolesnikov, T. Kh., 1968, Trace and rare elements dissolved in water and carried by suspended sediments of principal rivers of the U.S.S.R., in Geochemistry of sedimentary rocks and ores: Moscow, Izdat. I'vso "Nauk", 435 p.
- Kosolapova, M. N., 1963, Microcomponents in natural waters of the Olenek River basin: Akad. Nauk SSSR Yakutskogo Filiala Sibirsk. Otd. Trudy, Ser. Geol. 1963, no. 16, p. 56-74; abs. in Chem. Abs., v. 59, no. 9673f, 1963.
- Krainov, S. R., and Korotkova, M. Kh., 1964, Distribution of some trace elements in the mineral waters of the Lesser Caucasus: Vsesoyuz. Nauchno-Issled. Inst. Gidrogeol. i Inzh. Geol. Trudy [N.S.], no. 9, p. 72-93; abs. in Chem. Abs., v. 61, no. 10439e, 1964.
- Kroner, R. C., and Kopp, J. F., 1965, Trace elements in six water systems of the United States: Am. Water Works Assoc. Jour., v. 57, no. 2, p. 150-156.
- Laurus, A. L., Lorange, Elizabeth, and Lodge, J. P., Jr., 1970, Lead and other metal ions in United States precipitation: Environmental Sci. and Technology, v. 4, p. 35-38.
- Livingstone, D. A., 1963, Chemical composition of rivers and lakes: U.S. Geol. Survey Prof. Paper 440-C, 64 p.
- Loveridge, B. A., Milner, G. W. C., Barnett, G. A., Thomas, A. M., and Henry, W. M., 1960, Determination of Cu, Cr, Pb, and Mn in sea water: Atomic Energy Research Estab. [Gt. Britain] [Rept.] R-3323, 36 p.; abs. in Chem. Abs., v. 54, no. 24118h, 1960.
- Lukashchik, K. I., Zhukhovskaya, A. L., and Zamyatkina, A. A., 1965, Heavy metals in surface waters of the Poles' territory near Pripyat in the Belorussian S.S.R. [in Russian]: Akad. Nauk Beloruss. SSR Doklady, v. 9, no. 3, p. 183-186; abs. in Chem. Abs., v. 63, no. 1584e, 1965.
- Miholj, Stanko, 1945, The chemical analysis of the hot-spring water at Stubik: Rad. Hrvatske Akad. Znanosti i Umjetnosti, Razreda Mat.-Prirodoslov., v. 278, no. 86, p. 195-211; abs. in Chem. Abs., v. 40, no. 4158-b, 1946.
- Minami, Eiichi, Sato, Gen, and Watanuki, Kunihiro, 1957, Arsenic and lead contents of the hot springs of Tamagawa, Akita Prefecture—[Pt. 1]: Nippon Kagaku Zasshi, v. 78, p. 1096-1100; abs. in Chem. Abs., v. 52, no. 11523e, 1958.
- 1958, Arsenic and lead contents of the hot springs of Tamagawa, Akita Prefecture—[Pt. 2]: Nippon Kagaku Zasshi, v. 79, p. 860-865; abs. in Chem. Abs., v. 52, no. 18968i, 1958.
- Noguchi, Kimio, and Nishido, Toshio, 1969, Behavior of copper, zinc, and lead in Tateyama-jigokudani hot springs in Toyama Prefecture [in Japanese]: Nippon Kagaku Zasshi, v. 90, no. 8, p. 781-786; abs. in Chem. Abs., v. 71, no. 105046p, 1969.
- Silvey, W. D., 1967, Occurrence of selected minor elements in the waters of California: U.S. Geol. Survey Water-Supply Paper 1535-L, 25 p.
- Skurnik-Sarig, Sarah, Zidon, Moshe, Zak, I., and Cohen, Yves, 1970, Lead determination in natural saline waters by UV spectrophotometry: Israel Jour. Chemistry, v. 8, no. 3, p. 545-549; abs. in Chem. Abs., v. 73, no. 101881a, 1970.
- Tatumoto, M., and Patterson, C. C., 1963, The concentration of common lead in sea water, in Geiss, J., and Goldberg, E. D.,

- compilers, Earth science and meteoritics. New York, Interscience, p. 74-89.
- Turekian, K. K., and Kleinkopf, M. D., 1956, Estimates of the average abundance of Cu, Mn, Pb, Ti, Ni, and Cr in surface waters of Maine: Geol. Soc. America Bull. 67, p. 1129-1131.
- U.S. Geological Survey, 1967a, Water resources data for Colorado, 1967—Pt. 2, Water quality records: Denver, Colo., U.S. Geol. Survey, Water Resources Div., 101 p.
- 1967b, Water resources data for New York, 1967—Pt. 2, Water quality records: Albany, N.Y., U.S. Geol. Survey, Water Resources Div., 160 p.
- 1967c, Water resources data for South Dakota, 1967—Pt. 2, Water quality records: Huron, S. Dak., U.S. Geol. Survey, Water Resources Div., 165 p.
- 1968a, Water resources data for Arkansas, 1968—Pt. 2, Water quality records: Little Rock, Ark., U.S. Geol. Survey, Water Resources Div., 155 p.
- 1968b, Water resources data for Connecticut, 1968—Pt. 2, Water quality records: Hartford, Conn., U.S. Geol. Survey, Water Resources Div., p. 129-247.
- 1968c, Water resources data for Missouri, 1968—Pt. 2, Water quality records: Rolla, Mo., U.S. Geol. Survey, Water Resources Div., p. 189-299.
- 1969, Water resources data for Montana, 1969—Pt. 2, Water quality records: Helena, Mont., U.S. Geol. Survey, Water Resources Div., 234 p.
- U.S. Public Health Service, 1963, Public Health Service drinking water standards [rev. 1962]: U.S. Public Health Service Pub. 956, 61 p.
- Urumasa, Yasumitsu, and Akaiwa, Hideo, 1960, Minor constituents of the springs of Shikabe, [Pt.] 58, of Chemical investigations of hot springs in Japan: Nippon Kagaku Zasshi, v. 81, p. 912-915; abs. in Chem. Abs., v. 55, no. 3885b, 1961.
- White, D. E., Hem, J. D., and Waring, G. A., 1963, Chemical composition of subsurface waters: U.S. Geol. Survey Prof. Paper 440-F, 67 p.
- Zhukhovitskaya, A. L., Zamyatkina, A. A., and Lukashev, K. I., 1966, Trace elements in the Upper Dnieper waters [in Russian]: Akad. Nauk Beloruss. SSR Doklady, v. 10, no. 11, p. 891-893; abs. in Chem. Abs., v. 66, no. 49131v, 1967.

LEAD IN SOILS

By R. R. TIDBALL

INTRODUCTION

Investigation of the lead content of agricultural soils was first stimulated by the known toxic effects of lead on plants, animals, and man; more recently, the development of geochemical prospecting techniques has resulted in analysis of nonagricultural soils for anomalous lead concentrations related to mineralization. Lead is among the trace elements listed as harmful to various plants and animals (McMurtrey and Robinson, 1938, p. 808; Swaine, 1955, p. vi), and the toxicity of lead is of continuing concern in human health (U.S. Public Health Service, 1966; Kehoe, 1971). Early interest in the concentration of lead in soil came as a result of pollution by effluent from smelters (Holmes and others, 1915) and pesticide sprays in orchards (Jones and Hatch, 1937, 1945). Geochemical prospecting activities, which greatly expanded in the 1930's (Hawkes, 1957, p. 314), stimulated interest in background concentrations of metals in soils as an aid to identifying mineralized zones. More recent interest stems from the contamination of soils along highways by automotive exhaust (Cannon and Bowles, 1962; Singer and Hanson, 1969; Ault and others, 1970; Dedolph and others, 1970; Motto and others, 1970; Schuck and Locke, 1970; Connor and others, 1971).

The natural concentration of any trace element in soil can be viewed in at least two ways. First, the concentrations of such elements may be expressed as *total* amounts, which include all modes of occurrence ranging from water-soluble salts to relatively immobile forms locked within the crystal lattice of primary minerals. Second, the concentrations may be expressed as *extractable* amounts that are soluble in a specified solvent. Such extractable quantities will vary depending on the solvent used and the strength of that solvent. Extractable quantities are of principal interest to the agricultural worker (Brewer, 1966, p. 216) because of efforts to equate extractable with "available" quantities for given plant species.

The objective in this report is to examine the soil as a natural reservoir of lead. Therefore, total concentrations are given here because they indicate the potential ability of the soil to supply lead (Mitchell, 1964, p. 331). In contrast,

the actual availability, as estimated by extractable amounts, depends on the interaction of many locally variable factors.

Average values are commonly expressed by either the arithmetic mean or the geometric mean. The familiar arithmetic mean is the sum of the values divided by the number of values. However, frequency distributions of trace-element concentrations in soils tend to be more nearly symmetrical on a logarithmic scale; therefore, a logarithmic transformation is appropriate. The best estimate of the most typical value in a log-normal distribution is given by the geometric mean, which is the anti-logarithm of the arithmetic mean of the log values (Miesch, 1967, p. B1-B2). The arithmetic mean will always be greater than the geometric mean. Many authors fail to identify which kind of mean they have used; therefore, the arithmetic mean is assumed to have been used in the literature cited in this report.

CHEMISTRY OF LEAD IN SOILS

The migration and ultimate distribution of lead within the soil result from combinations of factors that include chemical processes such as oxidation and reduction reactions, adsorption of cations on the exchange complex, chelation by organic matter and by other metal oxides, and cycling by vegetation. Most of these processes are in turn influenced by the regional factors involved in soil formation—climate, biota, topography, and, especially, parent material, all operating through time (Jenny, 1941).

Entrapment is one form in which lead occurs in the soil. A study of the soils in Bulgaria, for instance, showed that most of the lead occurred as inclusions in iron and aluminum hydroxides and in calcium carbonate (Iordanov and Pavlova, 1963). A small amount of lead was also present as pyromorphite ($Pb_3Cl(PO_4)_3$).

Lead tends to associate with the soil minerals in other ways as well. Lead is presumed to be adsorbed readily onto the exchange complex of clay minerals and is replaced only with difficulty (Mitchell, 1964, p. 337). Divalent lead should be adsorbed more strongly than monovalent potassium which has a similar ionic size (Goldschmidt, 1954, p. 402). The enrichment of lead in the B horizons of

some soils has been attributed in part to the presence of excess clay (Presant, 1971, p. 57). Lead also associates with amorphous iron sesquioxide and to a lesser extent with aluminum sesquioxide (Mitchell, 1964, p. 337). Although he did not specifically study lead, Jenne (1968) found that hydrous manganese and iron oxides play a predominant role in controlling the fixation of several heavy metals in the transition series. The sesquioxides and hydrous oxides may occur as surface coatings on particles of all sizes and, therefore, can exert an influence that is out of proportion to their concentration. Lead was found concentrated in that portion of the soil that was soluble in acidified hydrogen peroxide (Taylor and McKenzie, 1966). The soluble portion includes manganese minerals, organic matter, and other soluble minerals and salts. Presant (1971) found lead associated with free iron oxides in the B horizons of New Brunswick soils, but the correlation coefficient was not significant.

In general, most metals tend to be more available under acid conditions than under alkaline conditions (Hodgson, 1963, p. 141-144). In one study, plants grown in soils to which lead had been added took up more lead from acid soils than alkaline soils, but the effect was confounded somewhat by differing amounts of organic matter (MacLean and others, 1969). A summary of the composition of soils from Wisconsin, shown in table 15, suggests that greater total amounts of lead are found in the more alkaline soils; the pH-dependent stability of metal organic chelates may aid in explaining this distribution. Presant (1971) found negative correlations between total lead and pH in all soil horizons except the A₂ horizon. The effect of pH may be the indirect consequence of microbiological activity which in turn controls the oxidation and reduction of iron and manganese (Hodgson, 1963, p. 146). Studies of the distribution of the heavy metals within the soil profile based on pH alone may fail to give consistent results. Instead, the sorption-desorption exchange process should be viewed in terms of both the Eh and pH of the soil-water system, (Jenne, 1968, p. 342).

The movement of metals during the weathering process by means of organic chelating agents is another important

process in the chemistry of lead in soil. The following discussion is based on a review of these processes by Pauli (1966). The creation of organic chelating agents by biologic activity serves as one of the most effective processes of metal mobilization. These agents are either plant products, microbial metabolites, or humic compounds. The humic compounds, also known as humic acids (Drozdova, 1968), are three-dimensional, interlinked, aromatic polymers that result from the reaction of heteropolycondensation. This reaction splits simpler compounds and reconstitutes them into a more complex heteropolycondensate (polymer), some units of which are possibly linked together (chelated) by heavy metal cations. As the molecular weight of the polymer is built up through additional polycondensation, a complex lattice structure with diverse interconnections is developed. Thus cations, molecules, and even mineral particles may be enmeshed within a protective "cage." Clay minerals, especially those encrusted with iron oxides and hydroxides, adsorb the polymers, and even accommodate the smaller molecules in interlayer positions.

Metals initially become chelated according to their susceptibility, competition from other metals present, and the nature of the complexing agent. The continued fixation of the metal ion depends on the stability of the polymer and its ability to resist the forces of degradation. The metal binding force generally diminishes with increasing acidity, as we have seen. Experiments with calcium-humate and kaolin showed that lead was held by both substances at pH 5 but was released completely at pH 1.5 (Iordanov and Pavlova, 1963). Further, the complex polymers are more resistant to microbial attack than the simpler organic compounds. Cate (1959) suggests that the metal ions might be released from the polymer by an autocatalytic decomposition process. He speculates that in the podzolization process, lead is cycled to the ground surface by vegetation, is complexed by the humic polymers, is translocated down in the profile, and finally, is released for subsequent precipitation at the lower depth. Cate's model may approximate reality but it apparently fails to account for the lack of abundant movement of lead in weathering profiles.

Finally, the amounts and types of organic matter present appear to provide an important control on the movement of heavy-metal ions in soil systems. Evidence that suggests the importance of organic matter is summarized (Jenne, 1968, p. 340) into four categories: (1) known chelating ability of both synthetic and natural organics, (2) ability of plant material extracts to leach metals from soil material, (3) positive correlation found between concentrations of metal and organic matter of the soil, and (4) release of metals during oxidation treatment of organic matter by hydrogen peroxide. The association of lead and organic matter is not always empirically

TABLE 15.—Lead concentrations in residual soils from Wisconsin, grouped according to pH

[Data from computer storage of the U.S. Geological Survey; samples collected by H. T. Shalkie; spectrographic analysis by J. C. Hamilton; lower limit of detection 10 ppm. Means and deviations calculated according to methods of Meech (1967). Deviation ratio, the number of samples containing detectable concentrations versus the number of samples examined.]

Soil pH	Detection ratio	Lead concentration	
		Geometric mean (ppm)	Geometric deviation
Less than 6.5	105:133	17	1.84
6.5-7.5	155:168	21	2.21
Greater than 7.5	52:57	31	2.73

consistent however. For example, the results in table 20 for tropical soils show no apparent lead-organic matter relationship.

INFLUENCE OF PARENT MATERIAL

Parent material has been recognized in some cases as a fundamental control on the concentration of lead in the soil (Swaine and Mitchell, 1960; Hodgson, 1963; Mitchell, 1964, p. 321; Fleming and others, 1968) and, among the various regional factors in soil formation, it thus deserves special attention. The lead concentration of immature soils tends to be correlated directly with its concentration in the parent material. Thus most of the averages reported for lead in soils are similar to the average concentration of 16 ppm (Goldschmidt, 1954, p. 398) of lead in the Earth's upper lithosphere. As weathering progresses to a more advanced stage, other pedogenic factors may modify the distribution of lead within the soil profile (Wells, 1960; Tiller, 1963).

DISTRIBUTION OF LEAD IN SOILS

An extensive review of the literature on the lead concentration in soils was given by Swaine (1955, p. 83-87). In most soils from nonmineralized areas, concentrations range from 2 to 200 ppm. Average concentrations in these soils are generally between 5 and 25 ppm. Vinogradov (1959, p. 155-157) reported an average of 10 ppm lead in Russian zonal soils (see table 16); these results compared well with data from the literature, which were generally in the range of 10-50 ppm. Other selected summary statistics

from the literature and unpublished data of the U.S. Geological Survey are shown in table 16. Typical concentrations of lead in topsoils range from 10 to 30 ppm.

The concentration of lead in selected Scottish soils developed in a cool humid climate is shown in table 17 (Swaine and Mitchell, 1960). The higher concentrations of lead appear to be associated with granitic parent material.

Unpublished data from files of the U.S. Geological Survey, which are summarized in table 18, indicate no important differences between the concentration of lead in the parent material and that in the soil. Other data given in tables 19, 20, and 21 illustrate a range of lead concentrations in soils developed from different parent materials. The majority of values are less than 50 ppm and often less than 30 ppm. In general, the results are inconclusive in establishing soil/parent material relationships, because the natural variations in parent-material composition probably include the range of lead values observed among the soils. Further investigation in particular localities of interest to determine the magnitude of variation in both the soils and the parent material is necessary before meaningful relationships can be recognized.

The trace-element relationship between soil and parent material, if it exists, should permit prediction of the composition of the one from knowledge of the other. Oertel (1961) concluded on the basis of soils from Australia and Tasmania that such a prediction could not be satisfactorily reached; that is, a linear equation failed to describe the relationships accurately. However, a similar study of selected Belgian soils by Prabhakaran Nair and

TABLE 16.—Lead concentrations in selected soils developed under a variety of soil-forming factors
(Leaders (...) indicate no data)

Soil description	Number of samples	Range (ppm)		Mean (ppm) ^a	Deviation	Source of data
		Minimum	Maximum			
Finland, soils from moraine, sand, silt, clay, and peat	16	Vuorinen (1958).
Tartu and Mariik regions, U.S.S.R., soils	4	30	Borisova (1959).
Eastern European plain, soils. A horizon	13	<10	43	110	±18	Vinogradov (1959).
Kazakhstan region, U.S.S.R., desert soils, humus horizon	20	11	Dobrovolskiy (1960).
Kazakhstan region, U.S.S.R., salinized soils, humus horizon	6	10	Do.
Westfalen-Lippe, Federal Republic of Germany, agricultural soils	15	68	30	Balks (1961).
Westfalen-Lippe, Federal Republic of Germany, grassland soils	12	79	34	Do.
Dahomey, (Africa), tropical topsoils	5	3	23	Pinta and Ollat (1961).
People's Republic of China, soils	111	26	Fang, Sung, and Bing (1963).
Novosibirsk region, U.S.S.R., soils	43	10	30	Vitler and Khrapov (1963).
U.S.S.R., gray forest soils	25	10	45	Akhymov (1965).
New Brunswick, Canada, podzol soils. A horizon	53	13	Presant and Tupper (1965).
Kos'vinski (Kamen region, U.S.S.R., alpine soils, humus horizon)	100	Mikhailova and Mikhailov (1967).
Silesia, Poland, topsoils	94	728	Roszyk (1968).
Missouri, U.S.A., subsoils under cedar trees, off road	16	115	Connor and others (1971).
Wisconsin, U.S.A., soils	422	<10	>1000	724	±2.60	H. T. Shacklette (unpub. data, 1972).
Kentucky, U.S.A., red-yellow podzolic soils, A horizon	96	<7	96	114	±1.51	Connor and others (1976).

^aArithmetic mean assumed unless otherwise noted.

^bArithmetic mean and standard deviation estimated by methods described by Miesch (1962).

^cGeometric mean and geometric deviation estimated by methods described by Miesch (1962).

Cottenie (1971) reached just the opposite conclusion. The accuracy of prediction improved by grouping the soils within taxonomic classes.

TABLE 17.—Lead concentrations (in ppm) in selected Scottish soils developed from different parent materials

[Data from Swane and Mitchell (1966). Soil profile averages calculated by weighting each horizon according to thickness]

Parent material	Soil Pb
Igneous:	
Serpentine till	12
Olivine gabbro	13
Andesitic moraine	18
Granitic till	25
Metamorphic:	
Granitic gneiss	42
Quartz-mica schist till	54
Slate	18
Sedimentary:	
Sandstone till	12

TABLE 18.—Mean concentrations of lead in selected parent material types and derivative soils

[Unpublished data of the U.S. Geological Survey. Statistics calculated according to Marsch (1967). Leaders (—) indicate insufficient data for calculation. Direction ratio, the number of samples containing detectable concentrations versus the number of samples examined]

Sample material	Detection ratio	Range (ppm)		Geometric	Geometric
		Minimum	Maximum	mean (ppm)	deviation
Cambrian and Lower Ordovician rock, western craton, western United States ¹					
Sandstone:					
Soil	33:80	<20	130	16	±2.23
Parent material	3:80	<20	36	<20
Shale:					
Soil	28:72	<20	870	12	±3.45
Parent material	28:72	<20	1,500	12	±3.33
Carbonate:					
Soil	25:76	<20	350	11	±4.07
Parent material	12:76	<20	120	<20
Nonmineralized areas of Kentucky, Missouri, and Wisconsin ²					
Sandstone, siltstone, and quartzite:					
Soil	38:52	<10	30	11	±1.62
Parent material	6:11	<10	50	9	±2.45
Dolomite:					
Soil	37:38	<10	70	15	±1.90
Parent material	11:16	<10	70	13	±2.33
Limestone:					
Soil	27:27	15	50	23	±1.43
Parent material	5:8	<10	20	9	±1.56
Granite, rhyolite:					
Soil	12:12	10	70	18	±2.25
Parent material	6:6	15	50	25	±1.75

¹Collected by A. T. Marsch and J. J. Connor; analyzed on direct reader spectrophotometer. R. G. Harris, lower limit of detection, 20 ppm. Soil samples from surface horizon.

²Collected by H. T. Shacklette; semiquantitative spectrophotographic analysis by J. C. Hamilton. Lower limit of detection, 10 ppm. Soil values based on averages of samples from all horizons.

TABLE 19.—Lead concentrations in tropical soils developed on different parent materials

[Data from Nalovic and Pinta (1969). Leaders (—) indicate no data]

Parent material	Soil type	Pb (ppm)
Igneous:		
Basic rocks	Ferruginous	88.0
Basalt	Ferrallitic	17.5
Granite	do.....	40.0
Acid rocks	do.....	14.0
Volcanic ash	do.....	9.0
Metamorphic:		
Marble	do.....	19.0
Gneiss	do.....	40.0
Schist	Ferruginous	22.0
Sedimentary:		
Limestone	Ferrallitic	41.0
do.....	Ferruginous	21.0
Sandstone	do.....	20.0

TABLE 20.—Distribution of lead concentration and organic matter in soil profiles from the tropical climatic zone

Parent material and soil type	Soil depth (cm)	Organic matter (percent)	Soil Pb (ppm)
Dahomey, Africa (Pinta and Ollat, 1961)			
Clay (ferrallitic soil)	0-10	3.0	23
	40-60	8	20
	180-190	3	27
Unknown (ferruginous soil)	0-20	1.0	9
	40-60	.6	11
	80-100	6	14
Tertiary sediments (ferrallitic soil)	0-15	2.3	15
	20-30	.6	20
	80-90	.4	22
	375-385	.2	20
Madagascar (Nalovic and Pinta, 1969)			
Marble (red-brown ferrallitic soil)	0-18	8.2	21
	18-40	4.3	17
	40-85	.2	23
	85-130	.2	18
	150-280	.1	14
Calcareous material (ferruginous soil)	0-15	1.1	24
	15-200	.3	20
	200-240	.3	24
	>240	.1	18
Alluvium	0-40	1.2	19
	40-110	.2	19
	110-320	.2	22
	320-350	.2	19
	>350	.2	23

GEOGRAPHIC DISTRIBUTION OF LEAD IN SOILS OF THE UNITED STATES

The distribution of lead concentration in soils and other surficial materials at 964 sites throughout the United States is shown in figure 8. The symbols on the map represent concentrations within selected frequency classes as shown in the accompanying histogram. The distribution map is modified from Shacklette, Hamilton,

TABLE 21.—Distribution of lead concentration in soil profiles from the temperate climatic zone

Parent material	Soil depth or horizon	Soil Pb (ppm)
Wales (Ancher, 1968)		
	Depth (cm)	
Dolerite	0-5	150
	5-18	100
	18-16	100
Pumice tuff	0-5	80
	5-15	20
	15-25	4
	25-30	25
Rhyolite	0-10	180
	10-25	60
Mixed glacial drift	0-5	200
	5-11	100
Ireland (Fleming and others, 1968)		
	Horizon	
Granite (Brown podzolic soil)	A _p	25
	B ₁	20
	B ₂	20
	C	25
Shale (Brown podzolic soil)	A ₁	25
	B ₂	10
	C	15
Limestone (Gray-brown podzolic soil)	A ₁	15
	A ₂	60
	B _{2t}	50
	C	50
	Depth (cm)	
Peat over granite	0-8	120
	8-20	30
	20-11	3
	11-16	11
	Bedrock	20
New Brunswick, Canada (Preston and Tupper, 1968)		
	Horizon	
Mixed parent materials (nonmineralized terrain)	I-A	75
	II	15
	B ₁	36
	B ₂	28
	C	65
Wisconsin (unpub. data, U.S. Geological Survey)		
	Horizon	
Mixed parent materials (nonmineralized terrain)	A	24
	B	11
	C	22

^aAverage (arithmetic) lead in each horizon computed from 55 podzol profiles.

^bSamples collected by H. T. Shacklette, analyzed by J. C. Hamilton. Geometric means are estimated from a number of soil samples, as follows: A, 146 samples (no lead detected in 11 samples); B, 70 samples (no lead detected in 17 samples); C, 97 samples (no lead detected in 20 samples).

modified by lead fallout along the highways. However, collectors were asked to select quiet rural roads if possible, to avoid roadcuts or fills, to move away from the roadside, and to sample at a depth of about 8 inches (20 cm). Studies in the vicinity of highways show that the amount of lead decreases very sharply within the first 6 inches (15 cm) depth of soil (Lagerwerff and Specht, 1970; Motto and others, 1970). Thus, the risk of modification by fallout is believed to be minimal. The reader should avoid inferences about any single value, but rather examine only patterns of larger regions.

The largest regional patterns examined by Shacklette and others (1971) were "eastern" soils versus "western" soils. This division between east and west was established along the 97th meridian because that was the approximate boundary between Marbut's (1935) pedocals of the west and pedalfers of the east.¹ It also corresponds approximately to the division between moist soils of the east and dry soils of the west (U.S. Geological Survey, 1970, p. 86). The mean lead concentration in eastern soil samples is 14 ppm as compared with 18 ppm for western soil samples. Although the difference is small, it appears to reflect a real difference in the background lead content of soils of the two regions (statistically significant at the 95 percent confidence level).

The histogram in figure 8 shows that about 94 percent of the samples have lead concentrations that are equal to or less than 30 ppm. About 58 percent of the samples have concentrations equal to or less than the mean of 16 ppm. Thus, most of the sample sites across the country are typified by concentrations of 15-30 ppm, with few distinctive local geographic variations. Regions having many sites with lead concentrations below average include the Atlantic Coastal Plain and Gulf Coastal Plain from North Carolina to Texas, the High Plains of west Texas and southeastern New Mexico, the Lake States of Michigan, Wisconsin, and Minnesota, and parts of the northern Great Plains, particularly the Sand Hills of Nebraska. There were even fewer regional instances of above-average concentrations, although most of the sites in Colorado exhibit above-average lead concentrations: four samples with concentrations of 100 ppm were collected in the western half of Colorado. Otherwise, high concentrations in the range of 100-700 ppm are found only at widely scattered and isolated sites in the United States.

The distribution of lead in soil has been studied in detail in Missouri, which has large lead deposits and a well-established lead mining industry. Samples of agricultural soils were collected extensively throughout the State from the surface horizon (0-6 in. (0-15 cm) depth), through the

¹Pedocal and pedaffer are Marbut's terms for mature soils with and without a lime horizon, respectively.

Boengen, and Bowles (1971) with 101 additional sample values added. The sampling sites were located at approximately 50-mile intervals, and samples were collected either along highways or within various geologic study areas. There is some risk that the distribution shown has been

LEAD IN THE ENVIRONMENT

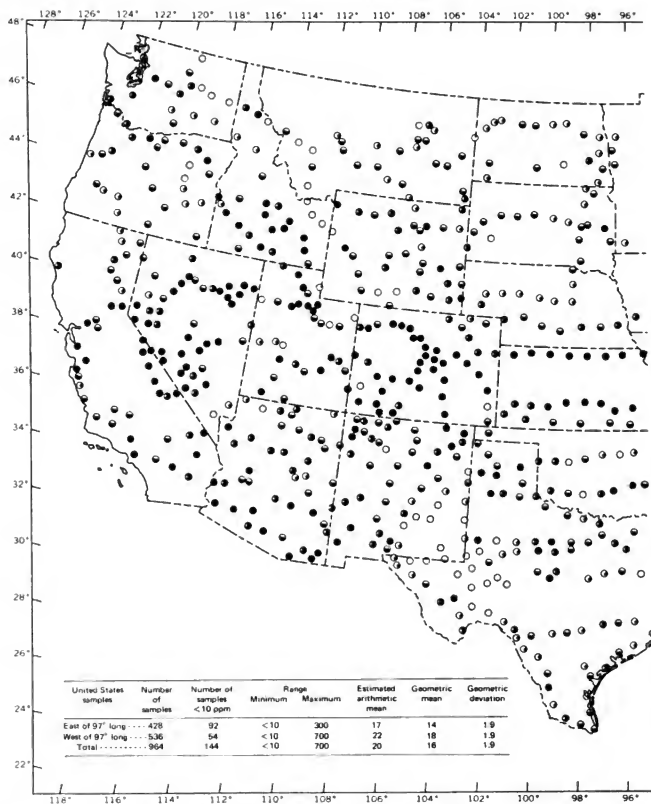
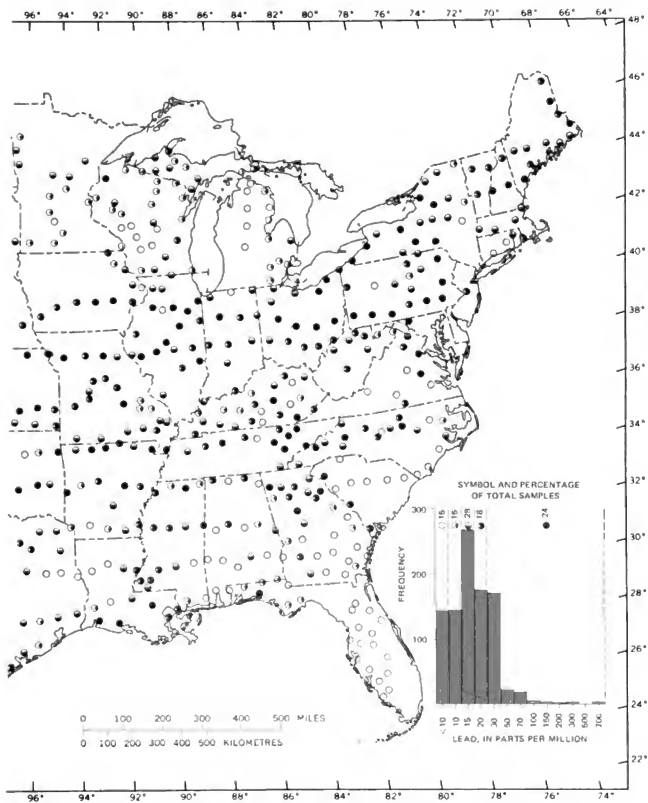


FIGURE 8.—Distribution of lead in soils and other surficial materials at 964 sites throughout the United States. Symbols correspond Map adapted from Shacklette, Hamilton, Boerngen, and Bowles (1971), supplemented with an additional 101 sites, data courtesy Neiman.



of this area exhibits considerable local variation within this midrange of lead concentration.

REFERENCES CITED

- Akhytseva, B. P., 1965, Content of trace elements in gray forest soils of the central chernozem belt [in Russian]: *Agrokhiymiya*, 1965, no. 9, p. 72-80; abs. in *Chem. Abs.*, v. 64, no. 3242r, 1966.
- Archer, F. C., 1965, Trace elements in some Welsh upland soils. *Jour. Soil Sci.*, v. 14, no. 1, p. 144-148.
- Ault, W. U., Senechal, R. G., and Erlebach, W. E., 1970, Isotopic composition as a natural tracer of lead in the environment: *Environmental Sci. and Technology*, v. 4, no. 4, p. 505-515.
- Balks, R., 1961, Lead content of soil [in German]: *Kali-Briefe, Fachgeb. I*, 1961, no. 11, p. 1-7; abs. in *Chem. Abs.*, v. 57, no. 1295e, 1962.
- Borisova, E. N., 1959, Natural lead concentration in the soil and in food products [in Russian]: *Kazanskiy meditsinskiy Zhurnal*, 1959, no. 4, p. 88-90; abs. in *Chem. Abs.*, v. 55, no. 9752a, 1961.
- Brewer, R. F., 1966, Lead, in Chapman, H. D., ed., *Diagnostic criteria for plants and soils*: Riverside, California Univ., Div. Agr. Sci., p. 213-216.
- Cannon, H. L., and Bowles, J. M., 1962, Contamination of vegetation by tetrathyl lead. *Science*, v. 137, p. 765-766.
- Cate, R. B., Jr., 1959, Organic translocation of metals: *Southeastern Geology*, v. 1, no. 3, p. 85-93.
- Connor, J. J., and Ebers, R. J., 1972, Geochemical survey of geologic units in U.S. Geological Survey, Geochemical Survey of Missouri—Plans and progress for third six-month period (July-December, 1970): U.S. Geol. Survey open-file report, p. 5-15.
- Connor, J. J., Shacklette, H. T., Ebers, R. J., Erdman, J. A., Miesch, A. T., Tidball, R. R., and Tourtelot, H. A., 1976, Background geochemistry of some rocks, soils, plants, and vegetables in the conterminous United States: U.S. Geol. Survey Prof. Paper 574-G.
- Connor, J. J., Shacklette, H. T., and Erdman, J. A., 1971, Extraordinary trace-element accumulations in roadside cedars near Centerville, Missouri, in *Geological Survey research 1971*: U.S. Geol. Survey Prof. Paper 750-B, p. B151-B156.
- Dedolph, Richard, Ter Haar, Gary, Holtzman, Richard, and Lucas, Henry, Jr., 1970, Sources of lead in perennial ryegrass and radishes: *Environmental Sci. and Technology*, v. 4, no. 3, p. 217-223.
- Dobrovolskiy, V. V., 1960, Microelements in several soils and soil-forming parent materials of Kazakhstan: *Soviet Soil Sci.*, 1960, no. 2, p. 120-127.
- Drozdova, T. V., 1968, Role of humic acids in concentrating rare elements in soils: *Soviet Soil Sci.*, 1968, no. 10, p. 1395-1396.
- Fang, C. L., Sung, T. C., and Bing, Yeh, 1963, Trace elements in the soils of northeastern China and eastern Inner Mongolia [in Chinese]: *Acta Pedologica Sinica*, 1963, v. 11, p. 130-142; abs. in *Chem. Abs.*, v. 60, no. 9048b, 1964.
- Fenneman, N. M., 1946, Physical divisions of the United States [map], with Characteristics [of the sections], by Fenneman, N. M., and Johnson, D. W.: U.S. Geol. Survey, scale 1:7,000,000.
- Fleming, G. A., Walsh, T., and Ryan, P., 1968, Some factors influencing the content and profile distribution of trace elements in Irish soils: *Internat. Cong. Soil Sci.*, 9th, Adelaide, Australia, Trans., v. 2, p. 341-350.
- Goldschmidt, V. M., 1954, *Geochemistry*: Oxford, Clarendon Press, 730 p.
- Hawkes, H. E., 1957, Principles of geochemical prospecting: U.S. Geol. Survey Bull. 1000-F, p. 225-355.
- Hodgson, J. F., 1963, Chemistry of the micronutrient elements in soils, in Norman, A. G., ed., *Advances in agronomy*, v. 15: New York, Academic Press, p. 119-159.
- Holmes, J. A., Franklin, E. C., and Gould, R. A., 1915, Report of the Selby Smelter Commission: U.S. Bur. Mines Bull. 98, 528 p.
- Iordanov, N., and Pavlova, M., 1965, Geochemistry of lead in soils [in Bulgarian]: *Izvestiya na Institutu Obshch. Neorganichna Khimiya Bulgarska Akademiya na Naukite*, 1965, no. 1, p. 5-14; abs. in *Chem. Abs.*, v. 60, no. 6657g, 1964.
- Jenne, E. A., 1968, Controls on Mn, Fe, Co, Ni, Cu, and Zn concentrations in soils and water—The significant role of hydrous Mn and Fe oxides, in Baker, R. A., ed., *Trace inorganic in water*: Washington, D. C., Am. Chem. Soc. (Advances in Chemistry Ser. 73), p. 337-387.
- Jenny, Hans, 1941, *Factors of soil formation—A system of quantitative pedology* [1st ed.]: New York, McGraw-Hill, 281 p.
- Jones, J. S., and Hatch, M. B., 1937, The significance of inorganic spray residue accumulations in orchard soils: *Soil Sci.*, v. 44, p. 37-63.
- , 1945, Spray residues and crop assimilation of arsenic and lead: *Soil Sci.*, v. 60, p. 277-288.
- Kehoe, R. A., ed., 1971, Papers read before the conference on inorganic lead, Amsterdam 1968: *Archives Environmental Health*, v. 23, no. 4, p. 245-311.
- Kiilgaard, T. H., Hayes, W. C., and Heyl, A. V., 1967, Metallic mineral resources in U.S. Geological Survey and the Missouri Division Geological Survey and Water Resources, Mineral and water resources of Missouri: U.S. 90th Cong., 1st sess., Senate Doc. 19, p. 41-63.
- Lagerweil, J. V., and Specht, A. W., 1970, Contamination of roadside soil and vegetation with cadmium, nickel, lead, and zinc: *Environmental Sci. and Technology*, v. 4, no. 7, p. 583-586.
- MacLean, A. J., Halstead, R. L., and Finn, B. J., 1969, Extractability of added lead in soils and its concentration in plants: *Canadian Jour. Soil Sci.*, v. 49, p. 327-334.
- McMurrey, J. E., Jr., and Robinson, W. O., 1938, Neglected soil constituents that affect plant and animal development, in *Soils and men—Yearbook of agriculture 1938*: Washington, U.S. Govt. Printing Office, p. 807-829.
- Marbut, C. F., 1935, *Soils of the United States, Pt. 3 of Atlas of American agriculture*: Washington, U.S. Govt. Printing Office, 98 p.
- Miesch, A. T., 1967, Methods of computation for estimating geochemical abundance: U.S. Geol. Survey Prof. Paper 574-B, 15 p.
- Mikhailova, R. P., and Mikhailov, I. S., 1967, Geochemical characteristics of soils above the timberline in the Kos'vinskii Kamen area [in Russian]: *Rastitel'nost' krainego Severa SSSR* 1967, no. 7, p. 146-150; abs. in *Chem. Abs.*, v. 69, no. 4589f, 1968.
- Mitchell, R. L., 1964, Trace elements in soils, in Brar, F. E., ed., *Chemistry of the soil* [2d ed.]: New York, Reinhold Publishing Corp., p. 320-366.
- Motto, H. L., Daines, R. H., Chalko, D. M., and Motto, C. K., 1970, Lead in soils and plants—Its relationship to traffic volume and proximity to highways: *Environmental Sci. and Technology*, v. 4, no. 3, p. 231-237.
- Myers, A. T., Havens, R. G., and Dunton, P. J., 1961, A spectrochemical method for the semiquantitative analysis of rocks, minerals, and ores: U.S. Geol. Survey Bull. 1084-I, p. 207-229.
- Nalovic, L., and Pinta, M., 1969, Recherches sur les éléments-traces dans les sols tropicaux—Etude de quelques sols de Madagascar [with English summary]: *Geoderma*, v. 3, no. 2, p. 117-132.
- National Research Council, Committee for the Study of Foliar Deposits, 1952, Pleistocene colluvial deposits of the United States, Alaska, and parts of Canada [map]: *Geol. Soc. America*, scale 1:2,500,000, 2 sheets.
- Oertel, A. C., 1961, Relation between trace-element concentrations in soil and parent material: *Jour. Soil Sci.*, v. 12, no. 1, p. 119-128.
- Pauli, V. W., 1966, Some recent developments in biogeochemical research: Alsace-Lorraine Service de la Carte Géologique, Bulletin [Strasbourg], v. 19, no. 3-4, p. 221-240.

- Pinta, M., and Ollat, C., 1961, *Récherches physico-chimiques des éléments-traces dans les sols tropicaux—1. Etude de quelques sols du Dahomey* [with English summary]: *Geochim. et Cosmochim. Acta*, v. 25, no. 1, p. 14-23.
- Prabhakaran Nair, K. P., and Goulet, A., 1971, Parent material-soil relationship in trace elements—A quantitative estimation: *Geoderma*, v. 5, no. 2, p. 81-97.
- Presant, E. W., 1971, Geochemistry of iron, manganese, lead, copper, zinc, arsenic, antimony, silver, tin, and cadmium in the soils of the Bathurst area, New Brunswick: Canada Geol. Survey Bull. 174, 93 p.
- Presant, E. W., and Tupper, W. M., 1965, Trace elements in some New Brunswick soils: *Canadian Jour. Soil Sci.*, v. 45, p. 305-310.
- Rozzyk, E., 1968, Lead in some very fine sandy soils of the lower Silesia: *Roczniki glebowe* [Warsaw] 19, p. 123-132; abs. in *Chem. Abs.*, v. 70, no. 5882u, 1969.
- Schuck, E. A., and Locke, J. K., 1970, Relationship of automotive lead particulates to certain consumer crops: *Environmental Sci. and Technology*, v. 4, no. 4, p. 324-330.
- Shacklette, H. T., Hamilton, J. C., Boering, J. G., and Bowles, J. M., 1971, Elemental composition of surficial materials in the conterminous United States: U.S. Geol. Survey Prof. Paper 574-D, 71 p.
- Singer, M. J., and Hanson, L., 1969, Lead accumulation in soils near highways in the Twin Cities metropolitan area: *Soil Sci. Soc. America Proc.*, v. 33, p. 152-153.
- Swaine, D. J., 1955, The trace-element content of soils: *Commonwealth Bur. Soil Sci. Tech. Commun.* 48, 157 p.
- Swaine, D. J., and Mitchell, R. L., 1960, Trace-element distribution in soil profiles: *Jour. Soil Sci.*, v. 11, no. 2, p. 347-368.
- Taylor, R. M., and McKenzie, R. M., 1966, The association of trace elements with manganese minerals in Australian soils: *Australian Jour. Soil Research*, v. 4, no. 1, p. 29-39.
- Tidball, R. R., 1972, Geochemical survey of soils, in U.S. Geological Survey, *Geochemical Survey of Missouri—Plans and progress for sixth six-month period (January-June, 1972)*: U.S. Geol. Survey open-file report, p. 19-57.
- Tiller, K. G., 1963, Weathering and soil formation on dolerite in Tasmania with particular reference to several trace elements: *Australian Jour. Soil Research*, v. 1, no. 1, p. 74-90.
- U.S. Geological Survey, 1970, *National atlas of the United States of America*: Washington, D. C., 417 p.
- U.S. Public Health Service, 1966, *Symposium on environmental lead contamination*: U.S. Public Health Service Pub. 1440, 176 p.
- Viler, G. E., and Khrapov, V. S., 1963, Content of trace elements in soils of the Baraba area in Novosibirsk Region [in Russian]: *Mikroelementy v Sibiri, Inform. Byul.* no. 2, p. 3-5; abs. in *Chem. Abs.*, v. 62, no. 10249g, 1965.
- Vinogradov, A. P., 1959, *The geochemistry of rare and dispersed chemical elements in soils* [2d ed.]: New York, Consultants Bur., 209 p.
- Vuorinen, J., 1958, On the amounts of minor elements in Finnish soils: *Maataloustieteellinen Aikakauskirja* [Helsinki], v. 30, p. 30-35; abs. in *Chem. Abs.*, v. 52, no. 14049e, 1958.
- Wells, N., 1960, Total elements in topsoils from igneous rocks—An extension of geochemistry: *Jour. Soil Sci.*, v. 11, no. 2, p. 409-424.

LEAD IN VEGETATION

By H. L. CANNON

Lead occurs naturally in small amounts in all plants, but the average concentration of lead in vegetation in highly populated countries has risen in the last several decades owing to man's activities. Because of this contamination from artificial lead, it is important that information on lead concentrations in plants be documented as to both date of collection and location with respect to sources of manmade lead. Information from primitive areas on lead in vegetation is therefore of prime value and should be collated and preserved. Only by comparison with such information can the effects of present-day contamination be properly assessed. Finally, averages for lead contents in vegetation are affected by natural variation in and among plants owing to differences in seasonal uptake, species, parts of the plant, and lead concentrations in the substrate.

THE BIOGEOCHEMICAL CYCLING OF LEAD

Bormann and Likens (1967) have pointed out that in the biological community the vertical extensions of the terrestrial ecosystem will be delimited by the top of the vegetation and by the depth to which roots penetrate into the regolith, and that the terrestrial ecosystem participates in the various larger biogeochemical cycles of the earth through a system of inputs and outputs. Thus, if we consider the geologic input, the weathering of the rocks will provide to the soil both elements incorporated in primary and secondary minerals and soluble ions that may be dissolved in the soil solution or adsorbed on the clay-humus complex. The degree of accumulation or loss in the ecosystem will vary with the response of a particular element to erosion and weathering. MacLean, Halstead, and Finn (1969) studied the uptake of lead by oats and alfalfa in soils with different levels of lead chloride, organic matter, and pH. They found that low humus content and high acidity of the soil increase lead uptake.

Lead, although not readily soluble, is absorbed by plants and stored in woody tissue to a considerable degree. An unpublished study of the uptake of lead by native plants and vegetables growing on various rock types in Hagerstown valley, Maryland, made by the author in

1958-59, suggests that there is a buildup of lead in the terrestrial ecosystem, inasmuch as median values increase from 11 ppm in rocks to 33 ppm in residual soils to 93 ppm in the ash of native vegetation in this particular area. Unfortunately at that time no consideration was given to the possibility of atmospheric lead, and the higher values in soils and vegetation probably reflect contamination from car exhaust. A similar progressive increase from rocks to vegetation was found by Lounamaa (1956), who studied native vegetation on various rock types in Finland and found lead to be concentrated in twigs and roots. Elsewhere, native vegetation and soils, largely on sandstone from the Navajo Reservation in New Mexico, were collected by the author in 1961 and 1962 using the same collection methods as those used in Maryland, but at sites considerably more remote from roads. Analyses showed a mean concentration of 20 ppm lead and a range of 5-700 ppm in the ash of 101 native plants that were rooted in soils having a mean of 18 ppm lead and a range of only 10-20 ppm. In both Maryland and New Mexico, the leaves of deciduous trees and the two most recent years of twig growth and needles of conifers were collected. The vastly different means of lead in plant ash from New Mexico (20 ppm) and from Maryland (93 ppm) are further interpreted to suggest the possibility of atmospheric contamination in the relatively more populated area of Maryland. A comparison of the cycling of lead from soil to tree leaves to humus for uncontaminated and contaminated areas is given in table 22.

The data suggest that lead is not concentrated in the humus under ordinary conditions, but that in areas of mining and smelting lead contamination of the humus and soil is largely unavailable to the vegetation or is held in the root and is not translocated to the upper portions of the plant to any appreciable degree.

Bolter and others (1972) made a more recent study of the cycling of lead in the so-called Viburnum Trend, or New Lead Belt, in southeastern Missouri. Several hundred soil and vegetation samples were collected and analyzed to delineate areas of anomalous high concentrations caused by the mining and smelting activity. Elevated heavy metal

TABLE 22.—Cycling of lead in different environments

[Leaves (—) indicate no data]

Source	Pb (ppm)				
	Leaves	Roots	Humus	Soil horizons	
	(in ash)	(in ash)		A	B
Uncontaminated ground					
Jefferson County, Colo.					
(on soil, 5 cm (1 in) from road)					
<i>Populus tremuloides</i> (aspen)	65	35	50	70	20
<i>Acer glabrum</i> (maple)	50	100	50	50	30
<i>Pinus ponderosa</i> (pine)	200	150	50	30	20
<i>Parosela taxifolia</i> (Douglas-fir)	200	60	50	30	20
Washington County, Md.					
(on limestone, 200 ft (66 ft) from road)					
<i>Carya cordiformis</i> (sho-korn)	100	—	20	30	—
<i>Carya ovata</i> (hickory)	200	—	30	20	—
<i>Fraxinus americana</i> (ash)	150	—	15	15	—
Cedar County, Mo.					
(on limestone)					
<i>Juniperus virginiana</i> (cedar)	100	—	80	50	—
<i>Quercus stellata</i> (oak)	30	—	85	—	—
Contaminated ground					
Joplin, Mo.					
(contaminated by drainage from mines)					
<i>Betula nigra</i> (elm)	500	1,500	1,700	2,000	—
<i>Quercus muhlenbergii</i> (oak)	150	—	5,200	1,200	—
Bartlesville, Okla.					
(contaminated from smelter)					
<i>Populus deltoides</i> (poplar)	120	—	2,500	2,500	—
<i>Allium porrum</i> (onion)	—	200	1,000	125	—
<i>Asparagus officinalis</i> (asparagus)	25	—	1,000	125	—

concentrations in soils were found to be mainly restricted to the humus and to the A horizons. A large part of the lead found in samples of leaves of vegetation was thought to be lead present on the surface of the leaves.

BACKGROUND LEAD CONCENTRATIONS IN VEGETATION

Before manmade contamination can be evaluated or the effect of mineralized ground appraised, the normal concentrations of lead that might be expected in various types of vegetation must be determined in samples from primitive areas with no manmade contamination and from results of sampling many years ago before manmade contamination had occurred. Warren and Delavault (1962) proposed, on the basis of analyses of uncontaminated Canadian plants, that the normal lead content of the twigs of trees be considered as 2.5 ppm in the dry weight and 50 ppm in the ash. They also suggested that the normal lead content of vegetables and cereal grains, which absorb less lead than trees, be taken as ranging from 0.1 to 1.0 ppm in the dry weight and from 2 to 20 ppm in the ash. Mitchell (1963) reported that in spring and summer pasture herbage normally contains less than 1 ppm lead in the dry weight, but that in autumn and winter it may contain several times this level.

However, unless the samples are collected from ground known to be unmineralized and are carefully screened to exclude any possibility of manmade contamination, a few

very high values will unduly raise the arithmetic mean. For this reason, a better measure of the expected "normal" value is the median concentration, as has been calculated for various classes of natural vegetation and given in table 23.

The lead medians for 193 deciduous tree tips (all from paloverde trees) and 131 leaves and stems (mostly from creosotebush) are considerably higher than values for other plants and may represent greater absorption of lead by these species. Large concentrations of lead are found in lichens and mosses, which are very slow growing. The normal levels of lead in garden vegetables are more difficult to establish, inasmuch as they are generally grown only in populated areas that are subject to airborne pollution and contamination from sprays. The results of analyses for lead in vegetables have been studied most intensively by H. V. Warren of British Columbia (Warren, 1972; Warren and Delavault, 1971). Median values from his data and those from Kehoe (1961) are given in table 24. A concentrated effort has recently been made by Warren (1972) to determine the "normal" (presumably median) concentrations of lead and other metals in vegetables. He concluded that variations in trace-element content of vegetables of both urban and rural areas are greater than have been generally realized and suggested a normal range for lead of 16-40 ppm in the ash or 1.6-2.0 ppm in the dry weight. These values are twice those he suggested earlier (Warren, 1961).

Median values for lead in vegetables that I collected in 1961-63 in New York, Maryland, and New Mexico are also shown in table 24. In many of the samples the amounts of lead were below the limit of detection by the spectrographic method used. All the samples of beet tops and onions and most of the cabbage samples had 10 ppm or more lead in the ash. The median lead in the dry weight of 111 vegetables was <1.3 ppm and that of 16 fruits about 0.25 ppm. One hundred vegetables collected by H. T. Shacklette in 1961 (written commun., 1961) from driftless and drift-covered areas in Wisconsin, Iowa, and Minnesota were analyzed colorimetrically by a method having a lower limit of detection of 25 ppm for lead in the ash. These vegetables were found to contain about 25 ppm lead in the ash or 1.3 ppm lead in the dry weight (table 24). A few of his samples were undoubtedly collected from mineralized ground. Both sets of values are lower than those reported by Warren (1972), but correspond rather well with those reported by Kehoe (1961) and suggested by Warren and Delavault (1962). The possibility must be kept in mind that many of Warren's (1972) samples from Great Britain were collected from Wales, where background lead in the soils and vegetation is considerably higher than normal, because of long-continued lead mining activities that have contaminated the valley alluvium and port-city soils with lead.

TABLE 25.—Normal lead concentrations in various classes of vegetation
[Leaders (—) indicate no data]

Locality	Number of samples	Part of plant	Median (ppm)		Range (ppm)		References
			Ash	Dry weight	Ash	Dry weight	
Conifer trees							
Western United States (wilderness areas)	20	Tips	50	1.8	30- 300	1 -10	H. L. Cannon (this paper).
Canada	17	2d-year twigs ..	25	8- 74	Warren and Delavault (1960).
Finland	83	Needles	30	<10-1,000	Lounamaa (1956).
Deciduous trees							
Western United States (wilderness areas)	193	Tips	36	2.5	5- 150	0.27- 13.0	M. A. Chaffee and H. L. Cannon (this paper).
	168	Stems	12	1.0	2- 50	16- 4.0	Do.
	178	Leaves	14.4	1.7	5- 70	<61- 9.1	Do.
British Columbia	15	2d-year twigs ..	31	11- 53	Warren and Delavault (1960).
Finland	97	Leaves	30	<10-1,000	Lounamaa (1956).
Sussex, England	4	30	1.0	7- 50	4- 2.0	Warren (1972).
Shrubs							
Western United States (wilderness areas)	131	Leaves	60	4.9	7- 100	0.57- 8.2	M. A. Chaffee and H. L. Cannon (this paper).
	56	Tips	21	1.8	7- 70	.57- 4.3	Do.
	110	Stems	41	2.1	7- 100	.57- 8.2	Do.
Canada	29	2d-year twigs ..	17	7- 46	Warren and Delavault (1960).
Finland	48	Tip	30	<10- 300	Lounamaa (1956).
Herbs							
Finland	50	10	1.8	<1.2- 3.0	Fletcher and Brink (1969).
	205	Leaves	10	<10- 100	Lounamaa (1956).
Grasses							
British Columbia	20	1.8	<1.2- 3.6	Fletcher and Brink (1969).
Western United States	226	Above ground ..	27	<20- 480	A. T. Miesch (written commun., 1970).
Western United States (wilderness areas)	15	do	20	1.6	<10- 70	< .8- 5.6	H. L. Cannon (this paper).
Finland	26	do	30	<10- 300	Lounamaa (1956).
Lichens							
Finland	59	Entire	1,000	30-6,000	Lounamaa (1956).
Colorado	10	do	1,000	81	300-1,500	12.3-150.0	LeRoy and Koksoy (1962).
Mosses							
Finland	16	Entire	100	<10-6,000	Lounamaa (1956).
Ferns							
Finland	93	Fronde	30	<10- 600	Lounamaa (1956).

SEASONAL VARIATIONS IN LEAD CONCENTRATIONS

The seasonal variation in the chemical composition of plants has been reported by many workers, but few studies have included the element lead. Guha and Mitchell (1966), however, studied seasonal variations of lead in three deciduous trees. They reported that concentrations in the dry weight of leaves decreased from May to June, owing to dilution from rapid growth, reached a maximum in mid-September, then decreased slightly in October, a pattern

which suggests a back translocation of lead into the twig. Concentrations in the petiole, blade, and inflorescence of sycamore are shown in table 25. Current studies in greater detail (R. L. Mitchell, oral commun., 1972) show a sharp peak in metal content in the early spring before the dilution drop.

The differences in concentrations of elements resulting from variation in uptake by species, parts of the plants, and season of collection were determined using four trees growing on unmineralized schist in a remote area of

Colorado more than half a mile (0.8 km) from the nearest road. The leaves, twigs, wood, roots, and, in some cases, fruit of two coniferous trees, *Pinus ponderosa* (Ponderosa pine) and *Pseudotsuga taxifolia* (Douglas-fir), and two deciduous trees, *Populus tremuloides* (aspen) and *Acer glabrum* (mountain maple), were sampled in spring,

TABLE 24.—Lead in garden produce

[Leads (—) indicate no data]

Type of produce	Number of samples	Lead in ash (ppm)		Lead in dry weight (ppm)	
		Median	Range	Median	Range
Great Britain and British Columbia					
Leafy vegetables ^a	30	14	2-260	2.5	0.2-96
Do ^b	8			17	0.5-94
Other vegetables ^b	20	25	4-100	1	2-11
Do ^c	115	31	4-620	21	10-20
Fruit ^d	5			0.8	0.4-18

New York, Maryland, and New Mexico

Fruit:					
Apples	8	10	<10-20	0.2	<0.2-0.59
Peaches	2	10	<10-10	3	<4-55
Pears	2	20	—	5	—
Total fruit	12	10	<10-20	0.5	<0.2-50
Nonleafy vegetables:					
Asparagus	5	<10	<10-50	<1	<0.9-5.75
Beans (green)	5	<10	<10-70	6.8	<50-84
Beans (shelled)	4	12	<10-20	98	<65-22
Beets	7	<10	<10-50	<1.8	<1-12.5
Carrots	8	<10	<10-50	<1.5	<0.9-9.9
Corn	15	<10	<10-70	<2.5	<2-1.05
Cucumbers	4	<10	<10-50	<1.5	<1-1.65
Green peppers	7	<10	<10-20	<1.5	<0.9-2.1
Onions	5	20	<10-20	1.5	7-1.84
Potatoes	9	<10	<10-30	<4.8	<4-1.65
Rhubarb	4	10	—	1	—
Salads	2	12	<10-20	1.4	<1.2-7
Squash	8	<10	<10-100	<1.4	—
Tomatoes	10	10	—	<1.6	—
Turnips	2	<20	—	<2.6	<30-6.8
Leafy vegetables:					
Cabbage	9	10	<10-30	2.5	<1.8-4.2
Beet tops	3	35	20-50	8	4.2-12.5
Kale	4	<20	<10-20	<2.5	<1.0-2.4
Lettuce	6	<10	<10-70	<3.5	<2-1.4
Total vegetables	116	<10	<10-100	<1.5	<0.2-14

Wisconsin, Iowa, and Minnesota^e

Fruit:					
Apple	5	25	<25-50	0.5	<0.5-1.0
Vegetables:					
Asparagus	5	150	25-300	12.0	2.5-30
Bean, pink (seed)	1	<25	—	<1.5	—
Bean, green (pod)	5	<25	<25-50	<1.6	<1.4-5.0
Bean (seed)	1	<25	<25-25	<2.5	<1.4-5.0
Cabbage	11	25	<25-25	<1.2	<1.8-3.5
Carrot	8	<25	<25-25	<2.4	<2.2-5.8
Cauliflower	2	<25	<25-25	<2.0	<2.0-2.1
Corn (field)	25	25	<25-150	4	<5-2.2
Corn (sweet)	4	<25	<25-50	5	<5-1.0
Cucumber	4	<25	<25-150	2.9	<2.4-18.7
Onion	7	<25	<25-25	<1.2	<1.1-1.1
Parasip	1	<25	—	<1.2	—
Pepper (sweet)	4	<25	—	<1.7	—
Potato (white)	10	25	<25-50	1.2	<0.5-2.1
Pumpkin	1	<25	—	<3.0	—
Radish (white)	1	<25	—	<4.1	—
Rhubarb	1	<25	—	<4.0	—
Rutabaga	2	<25	—	<2.5	—
Squash, Hubbard	1	<25	—	<1.2	—
Swiss chard	1	<25	—	<4.8	—
Turnip	1	<25	—	<5.9	—
Total	100	25	<25-300	1.5	<0.5-30

^aWarren and Delavault (1971).^bRutledge (1961).^cWarren (1972).^dH. T. Shackelair (written commun., 1970).

summer, and fall and analyzed for lead (table 25). Each value represents an average of several analyses. A drop in lead occurs as expected in the summer collections of pine, Douglas-fir, and aspen leaves, but not in maple. A drop is apparent in young twigs—again as expected—but also occurs in either the older twigs or older needles. As might be expected, the seasonal differences in older twigs are not so great nor so consistent as in young twigs in any species. However, the fact that seasonal differences of as much as four to nine times can occur in the young twigs and leaves of trees argues in favor of making all the collections for any project during the same month.

For prospecting purposes, Warren (1966) advised collecting older growth, preferably second year, which varies less seasonally in lead content and more consistently reflects anomalous lead contents in the soil than do other accessible parts of the tree.

TABLE 25.—Seasonal variations of lead in trees and soils

Material analyzed	Season or date									
	Sycamores from Craigieburn, Scotland (Guthrie and Mitchell, 1966)									
	(ppm, dry weight)									
	May 15	June 15	July 5	July 30	Aug 24	Sept 25	Oct 26			
Needle	0.9	0.6	1.1	0.8	1.0	1.3	1.4			
Leaf blade	3	9	1.8	1.8	1.5	3.1	2			
Inflorescence	2.5	1.1	.9	.5	.4	1	no data			
Colorado trees and soil (H. L. Carson, this report)										
	(ppm, average of three sample splits; soil collected under respective trees)									
	Spring		Summer		Fall		Other ^a			
	Ash	Dry wt	Ash	Dry wt	Ash	Dry wt	Ash	Dry wt		
Aspen										
Young leaves	65	4.6	20	1.1	45	5.9				
First-year twigs	40	2.9	20	1.1	50	5.4				
Older twigs	80	4.1	50	3.4	80	6.5				
Wood							80	1.2		
Roots							85	1.4		
Soil									50	
Humus									70	
A zone									20	
B zone									20	
Maple										
Young leaves	50	2.9	70	4.8	85	7.0				
First-year twigs	200	8	20	1.1	50	2				
Older twigs	500	15	200	8.8	100	7.3				
Seeds							30	90		
Wood							100	6.9		
Roots							100	8.5		
Soil									50	
Humus									50	
A zone									70	
B zone									20	
Pine										
Young needles	200	4	30	.96	50	1.25				
Older needles	200	1.89	300	6	300	8.1				
First-year twigs	300	9	100	2.5	570	8.8				
Older twigs	1,000	29	850	19	700	56				
Seeds on cones							600	16		
Wood							700	16		
Roots							150	5.6		
Soil									50	
Humus									50	
A zone									30	
B zone									20	
Douglas-fir										
Young needles	200	5.6	70	2.1	200	6.6				
Older needles	200	8.2	300	8.3	300	9.4				
First-year twigs	600	18	70	2.1	500	14				
Older twigs	1,750	44	1,750	35	1,500	82				
Seeds on cones							1,000	32		
Wood							700	14		
Roots							60	1.7		
Soil							45	1.7		
Humus									50	
A zone									30	
B zone									20	

^aSeasons not specified.^bIn root bark.

VARIATION IN LEAD CONTENTS WITH PARTS OF PLANT

Lead contents vary greatly in different parts of the plant. Jones (1959) reported higher concentrations of lead in leaves than in stems of kale and rape. John and Van Laerhoven (1972) found that the leaves of lettuce and spinach and the tuberous portions of radish and carrot plants accumulated markedly higher lead concentrations than did the heads—the edible portions—of cauliflower, broccoli, or oats. Guha and Mitchell (1966) found more lead in leaves than in stems of four deciduous trees. The data for aspen, maple, pine, and fir in Colorado (table 25) indicate considerable variation in different parts of a tree, as well as variation depending on season. Certainly in the conifers (pine and Douglas-fir), large concentrations of lead are stored in older twigs and cones. In the spring collection, Douglas-fir contained 5.6 ppm lead in the dry weight of leaves, 18 ppm in the first-year twigs, 44 ppm in older twigs, 32 ppm in cones, 14 ppm in wood, and only 1-7 ppm in roots. Lounamaa (1956) demonstrated a definite increase in concentration of lead in roots. This increase is not apparent in the data from Colorado, but large concentrations have been observed in roots of plants growing in highly mineralized ground.

Zimdahl and Arvick (1972) have measured lead uptake by sugar beets, corn, beans, and wheat grown in hydroponic solutions and in soil containing various levels of lead nitrate. Lead uptake by and distribution within the plants were directly related to the concentration of lead in the solution. Lead was concentrated in the root with limited translocation to the shoot. Similarly, the primary leaf of pinto beans contained less lead than did the stem but always more than the trifoliate leaf. The following table shows that massive amounts of lead can be absorbed by a plant when the metal is present in an available form. Translocation of lead is increased with increasing concentration from 100 to 1,000 ppm in the $Pb(NO_3)_2$ medium.

In vegetables fed lead in a nutrient solution, Motto, Daines, Chilko, and Motto (1970) reported as much as an eightfold increase in lead content of leaves, with a corresponding increase of as much as fortyfold (to a maximum

of 764 $\mu\text{g/g}$ in dry weight) in the roots. Shacklette (1963) found an average of 3.32 ppm lead in leaves and 3.84 ppm in branches of 22 samples of American elm collected in Wisconsin in nonmineralized soil.

Samples of cedar and oak that I collected for background material in Missouri had the following concentrations of lead, in parts per million:

	Cedar	Oak
First-year twigs with leaf scales.....	6
Leaves.....	1.6
First-year twigs.....	3.8
Wood.....	.54	1.5
Bark.....	5.5	12.5

The analyses show that, as compared to the bark, wood has a low lead content. Similar data are shown later in the discussion of lead contents in trees on contaminated ground.

Kennedy (1960) sampled needles, twigs, and cones of seven coniferous species in the Coeur d'Alene, Idaho, lead-zinc district and found marked accumulations in the twigs, with a maximum of 130 ppm in the dry weight for Douglas-fir twigs; concentrations in roots and humus were not measured.

The concentrations of lead in peeled and unpeeled vegetables and fruits were compared in a study of produce from Washington County, Md. (table 26).

Although these analyses include the entire vegetable and do not give a separate value for the skins, the difference between peeled and unpeeled produce is striking. Similarly, the contrast between the relatively high concentrations in the root crops and the relatively low ones in fruits reflects a true difference in distribution of lead. However, the values in the leafy vegetables, even though washed, may have been raised by vehicular exhaust lead, as many of the gardens were in contaminated areas.

TABLE 26.—Concentrations of lead in unpeeled and peeled garden produce from Maryland

(Analyses: Urena Oda, E. F. Conley, D. J. Fraser, and H. G. Neuman, U.S. Geological Survey. Numbers in parentheses indicate number of samples collected.)

	Unpeeled	Peeled
Root vegetables (26):		
Salsify.....	1.7	<2.2
Onions.....	1.84	1.3
Beets.....	16.5	<1.4
Potatoes.....	2.6	<.62
Carrots.....	2.1	<1
Fruits (8):		
Peaches.....	<.6	.53
Apples.....	.37	<.22
Leafy vegetables (22).....	5.24

PHYSIOLOGICAL EFFECTS OF LEAD ON PLANT GROWTH

Lead is not considered to be an element essential to plant growth, although Stoklasa (1913) reported that lead nitrate in small amounts increased the growth of plants; in large amounts, however, it proved toxic. Tsetsura (1948), also using solutions of lead nitrate, reported an increase in

Plant and part	100 ppm Pb		1,000 ppm Pb	
	Pb absorbed ($\mu\text{g/g}$) dry weight)	Root/shoot ratio	Pb absorbed ($\mu\text{g/g}$) dry weight)	Root/shoot ratio
Pinto bean:				
Root.....	32,400	231.4	54,100	4.1
Shoot.....	140		13,300	
Sugar beet:				
Root.....	54,300	84,800
Wheat:				
Root.....	9,300		16,000	
Shoot.....	260	35.8	5,800	2.8
Corn:				
Root.....	10,600		22,700	
Shoot.....	390	27.2	9,160	2.5

*Shoots not analyzed

the germination of seeds at low lead concentrations and a retardation at high levels. One question whether the stimulation in both experiments may not have been caused by the nitrate ion. Using lead acetate, Bonnet (1922) found that lead was readily taken into the root but that little was translocated to the leaves. Transpiration was greatly diminished, and the roots were short and thin. Seeds of many plants were found to be sensitive to lead, but corn was very tolerant and germinated after being soaked in lead acetate for 19 days. Hevesy (1923) used a radioisotope of lead to trace the localization of lead in different parts of the plant *Vicia faba* (horsebean). Only 0.3 percent of the lead was taken into the root from a 10^{-4} N solution in 24 hours but 60 percent of the lead from a 10^{-6} N solution was taken up in the same length of time. The percentage of lead that is translocated to the tops is greater in concentrated solutions because the roots are capable of binding nearly all of the lead in dilute solution. When the plants were moved to different solutions, Hevesy found that the tagged lead could be readily interchanged with other lead atoms or with copper atoms but not as readily with cadmium, zinc, chromium, barium, or sodium atoms. He also found that lead uptake by plants is not dependent on the absorption of water.

Hammet (1928) studied the effects of lead at the cellular level and found that lead retarded cell proliferation, while it allowed the cells to increase in size. Lead is most concentrated in areas of greatest mitotic activity (the area of rapid elongation), where a reaction takes place between the lead and an organic sulfhydryl.

Culture experiments by Scharer and Schropp (1936) showed that corn and rye were particularly resistant to lead toxicity but that barley, oats, and especially wheat were sensitive to lead poisoning. Recent sand culture studies with corn by Miller and Koeppel (1971) have clarified in several respects the effects of lead on plants in relation to other substances, particularly phosphorus. No effects on growth were noted when lead was absorbed under phosphorus-sufficient conditions, but under phosphorus-deficient conditions growth was retarded and corn died at a level of 6,000 μ mol lead. The age of the plant at the time of lead treatment was also found to be important, as the effects of lead were much more pronounced on the younger plants. Corn leaves accumulated large amounts of lead depending on the amount of lead applied and the phosphate condition of the plant; phosphate-deficient plants accumulated 5-10 times as much lead as the phosphate-sufficient plants.

Mitochondria studies (Miller and Koeppel, 1971) show that lead affects mitochondrial respiration, which is related to the phosphate status. Diaphorase experiments suggest that the sites of lead action are the specific flavoproteins for the oxidation of NADH and succinate. The lack of a lead effect on the oxidation of malate indicates that not all flavoproteins are sensitive to lead.

Malyuga (1964) reported that an unusual double-petaled form of the large poppy, *Papaver macrostomum*, grows in high-lead soil at Kadzharan. The double-petal form is created by a deeper incision of the petals, often to the base, which gives the impression of eight petals instead of four.

Other effects of lead on plants can be seen in the results of a study carried out by the author and L. W. Reichen in 1947. We grew sweetpeas, tomatoes, bluegrass, and violets in vermiculite at pH values of 7.6 and 5.8 and fed the plants increasing dosages of lead, copper, and zinc, both separately and in combination in Hoagland nutrient solution. The nutrient solution also contained small amounts of minor metals that had proved sufficient to maintain the control plants in healthy condition. The objectives of this experiment were to determine (1) the ultimate toxic limits for these three metals in representatives of several plant families, (2) the amounts of these metals that can be absorbed by these plants before toxic limits are reached, (3) the effects of each metal on uptake of other metals, and (4) the observable physiologic effects of these metals on plants. The experiment was originally conceived in connection with studies of a muck area in New York State that contained large quantities of zinc and lead (Cannon, 1955). That experiment was performed to determine whether the vegetation of the bogs could have extracted the metals from ground waters draining dolomites rich in zinc and whether observable physiological effects could be used as indicators of mineralized substrate.

In the 1947 study, the plants were fed the following solution, which was prepared in the laboratory and had a pH of 7.6:

10 cm³ MgSO₄ · 7H₂O
20 cm³ Ca(NO₃)₂ · 4H₂O
5 cm³ KH₂PO₄
12 cm³ minor elements in 0.5 l H₂O:
0.50 g MnSO₄
25 g ZnSO₄
25 g CuSO₄
75 g boric acid

Iron solution (0.5 percent FeSO₄ + 0.4 percent tartaric acid) was added three times a week as 0.6 cm³/l of solution. To lower the pH of the nutrient solution from 7.6 to 5.8, 10 cm³ of (NH₄)₂SO₄ was substituted for 10 cm³ of Ca(NO₃)₂ · 4H₂O. After the plants had become well established, increasing amounts of copper sulfate, lead acetate, and zinc acetate were added to the solution in milliequivalents for 1 month until the tolerance limits of the plants were reached. The plants were then harvested and analyzed by dithionite methods for copper, lead, and zinc contents. The results involving lead and its interactions with zinc and copper are summarized in table 27.

The uptake by plants under acid and alkaline conditions varied greatly among species. Sweetpeas and violets were unable to take up lead from the acid solutions, but at a pH of 7.6 the vines and leaves of sweetpeas contained as

TABLE 27.—*Effects of lead and other metals on growth of plants from four plant families*

[The original vermiculite contained 25 ppm lead. Control plants were germinated and grown in a nutrient solution at pH 7.6, their lead contents in the dry weight at harvest were as follows: sweetpea, 18 ppm; tomato, 18 ppm; bluegrass, 33 ppm; violet, 13 ppm. Leaders (...) indicate no data.]

Plant	Solution pH	Metal contents at harvest (ppm, dry weight)	Height at harvest (m)	Height at harvest (cm)	Effects of metals on growth
Plants grown in lead solution¹					
		Lead			
Sweetpea.....	7.6	8,200	60	152	Thin vines; no chlorosis; brittle roots.
	5.8	11	41	104	Healthy; slightly chlorotic.
Tomato.....	7.6	1,590	31	79	Healthy; buds still developing.
	5.8	130	14	36	Healthy; white tips on leaves.
Bluegrass.....	7.6	2,400	14-24	36-60	80 percent alive; still growing dark-blue-green smooth leaves.
	5.8	2,400	10-15	25-38	95 percent alive; still growing dark-blue-green rough leaves.
Violet.....	7.6	430	7.5	19	Dark green, glossy; healthier than control plant; seed pods developed.
	5.8	12	6	15	Dark-green dull leaves.
Plants grown in lead-copper-zinc solution¹					
		Lead	Copper	Zinc	
Sweetpea.....	7.6	190	1,700	4,300	60 152 Very thin vines.
	5.8	14	140	450	36 91 Tip dead; leaves crinkled.
Tomato.....	7.6	260	190	260	27 68 Slight chlorosis; a few buds.
	5.8	850	80	620	16 4 All leaves chlorotic.
Bluegrass.....	7.6	150	290	880	9-14 23-36 75 percent alive; smooth leaves.
	5.8	430	58	1,100	8-13 20-33 95 percent alive; rough leaves.
Violet.....	7.6	550	5,000	5 13 Advanced chlorosis; brittle roots.
	5.8	3.5 10 Dark glossy curled leaves.

¹Transpiration of water was much less from plants fed solutions containing lead.

much as 8,200 ppm lead dry weight. Bluegrass contained 2,400 ppm lead at pH's of both 7.6 and 5.8. Tomatoes concentrated more lead in an acid solution in the presence of excess copper and zinc. The symptoms of lead toxicity include thin weak stems, white leaf tips, brittle roots, and, in the more tolerant species, dark-blue-green foliage. Bluegrass and violets were extremely tolerant of lead and were, at the time of harvest, as healthy as the controls. Certainly, plants can extract lead from nutrient solution and do not appear in general to be as affected by lead as by zinc and copper.

ANOMALOUS LEAD CONCENTRATIONS IN PLANTS

Plants absorb lead in anomalous quantities from agricultural activity, from the air, from mineralized ground, and from contaminated alluvium along streams that drain areas of mining processing activity. Let us consider first the accumulation of lead by plants in mineralized ground and the species of plants that can grow there.

Plants rooted in soils naturally enriched in metals or in soils in which the metal occurs in an unusually available form have been subject to lead accumulation since plants first appeared on the Earth. Although plants growing in mineralized areas may contain lead at levels deleterious to the health of animals, including man, the areas of undisturbed mineralized ground are relatively small and are mostly in forested or uncultivated regions. Therefore, the greatest effect of lead from plants growing in a naturally

mineralized substrate may be on animals rather than on man. One exception may be vegetables raised commercially on peats enriched in lead.

The first analyses for lead in plants from a mineralized area were made in Sweden by Hedstrom and Nordstrom (1945), who developed a method of sampling trees along transects in favorable areas as a prospecting tool. At about the same time Hans Lundberg (written commun., 1947), in tracing the source of toxic lead in maple syrup from Pakenham, Ontario, found that the lead had originated in sap of trees growing in an area with a high soil-lead anomaly. Further studies showed high lead in maple at the Frontenac lead mine in Ontario and in *Ledum palustre* (crystal tea lendum) and *Betula* sp. (birch) at the Buchans mine in Newfoundland. In Missouri, Harbaugh (1950) also found lead levels in plants to be higher in mineralized ground than in barren ground, but not as consistently high as zinc levels were. Webb and Millman (1951) tested plants as a method of prospecting in Nigeria. They found that the concentrations of lead in twigs and leaves of savanna trees in the lead-zinc belt increase near mineralized ground and that the lead values gave pronounced geochemical anomalies many times wider than the lodes. The normal lead content in the ash of twigs of several species of trees averaged 1 ppm in unmineralized areas and ranged from 7 to 270 ppm in mineralized areas. Comparable anomalies were found in the leaves. Hawkes (1954) later compared lead content of soils along the same traverse (fig. 10).

Malyuga (1964) similarly compared lead contents of soil and ash of plant leaves and roots, that of roots being considerably higher than that of soil or leaves.

J. B. Cathrall and G. B. Gott (written commun., 1975) collected twigs and needles from eight species of conifers, from more than 600 trees in the highly mineralized *Coeur d'Alene* district, Idaho. Mull was collected from the same localities. The concentration of lead in the soils in which the trees grew ranged from 10 ppm to 1,500 ppm, with a median value of 28 ppm.

The plant ash was analyzed by an arc emission spectrographic method that permitted the determination of concentrations of as much as 5,000 ppm lead. The arithmetic means of lead in the ash of these samples was 3,088 ppm for twigs, 1,039 ppm for needles, and 1,611 ppm for mull (see table 28). The lead content of these samples, from all species, was consistently about three times higher in twigs than in needles and about two times higher in twigs than in mull. The mean value of lead in twigs, relative to lead in needles and mull, must be even greater, because 91 twig samples contain more than 5,000 ppm lead.

Worthington (1955) made a biogeochemical survey of the Showangunk lead-zinc-copper mine in New York State using white birch twigs and soil. The lead values and copper-zinc ratio were more useful than the copper or zinc values in outlining the orebody. In Finland, Salmi (1959) became interested in sampling peat as a method of prospecting glaciated country. At the copper-zinc-lead area in Vihanti Parish, he sampled leaves and twigs of *Ledum palustre* (crystallea ledum) and peat at the same traverse stations to test the method in an area where the ore had already been outlined. Anomalous metal in the plants

in an area not known to be mineralized was later explained by the discovery of a new ore body. Similar tests were made by Talipov (1964) in Uzbekistan where he reported concentrations of lead in soils to be 10–20 times above average and to accumulate in the humus layer; and Polikarpochkina, Polikarpochkina, and Abramov (1965) showed that dispersion halos of the metals in plants repeat the zonal structure of metal ores in the eastern Transbaikalian province.

High lead contents were found by Poskotin, Yushkov, Yurinskii, and Snegirev (1969) in birch, aspen, and pine in areas of mineral deposits. They concluded that the amount of lead depended on the depth to ore, plant species, age,

TABLE 28.—Lead in conifer twigs, needles, and adjacent mull, *Coeur d'Alene* district, Idaho

	Lead concentrations (ppm in ash)			Arithmetic mean	Geometric mean
	Total samples	Minimum	Maximum		
Douglas-fir					
Twigs	396	200	>5,000	3,288	2,775
Needles	425	100	>5,000	927	712
Mull	437	70	>5,000	1,564	1,105
Western white pine					
Twigs	37	200	>5,000	3,354	2,394
Needles	37	100	>5,000	2,777	1,558
Mull	37	100	>5,000	3,030	2,094
Grand fir					
Twigs	42	1,000	>5,000	2,958	2,739
Needles	42	200	>5,000	779	634
Mull	42	300	>5,000	1,940	1,591
Western hemlock					
Twigs	4	2,000	>5,000	4,250	3,942
Needles	4	500	>5,000	925	851
Mull	4	1,000	>5,000	2,250	2,060
Sub-alpine fir					
Twigs	40	200	>5,000	2,280	1,710
Needles	32	100	>5,000	734	642
Mull	32	100	>5,000	1,219	953
Lodgepole pine					
Twigs	39	200	>5,000	1,851	1,342
Needles	39	150	>5,000	1,419	876
Mull	37	150	>5,000	1,048	651
Ponderosa pine					
Twigs	5	150	1,500	710	412
Needles	5	150	500	270	246
Mull	5	100	1,000	400	306
All species					
Twigs	549	150	>5,000	3,080	2,478
Needles	605	100	>5,000	1,039	735
Mull	616	70	>5,000	1,611	1,117

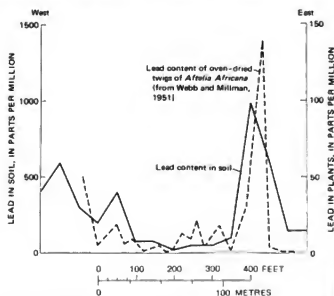


FIGURE 10.—Comparative lead content of soils and plants near Amekala lode, Nigeria (from Hawkes, 1954).

Lead frequency (number of occurrences in all species studied)			
Lead (ppm)	Twigs	Needles	Mull
0	0	0	0
70	0	0	1
100	0	4	9
150	1	1	1
200	11	11	27
300	9	69	55
500	7	89	83
700	24	151	15
1,000	82	118	120
1,500	36	46	67
2,000	104	36	119
3,000	109	13	68
5,000	115	14	29
>5,000	91	15	22

development of the root system, and mobility of lead in the particular geochemical environment. Brown and Meyer (1956) have also tested plants as a prospecting tool in the Edwards-Balmat district in New York and obtained positive results over known orebodies, although there was a wide variation in absorption by species.

A very thorough pilot study by Hornbrook (1969) of the Silvermine lead deposit, Cape Breton Island, Nova Scotia, indicates the scope and limits of geobotanical and biogeochemical prospecting methods. The data included 4,050 spectrographic determinations for lead in organic soil and plant material. The lead deposits are overlain by till that showed anomalous concentrations of lead, although the extent of the anomaly had been modified by glacial action. The pattern of lead anomalies in plant organs of different ages was compared, and anomalous concentrations in bark and twigs were sufficient to outline the extent of the ore. Although twigs contained more lead than bark, bark provided a more reliable basis for interpretation. The differences in lead concentration for different ages of twigs were not significant for prospecting purposes.

Several studies of lead uptake by plants in mineralized areas have been made by U.S. Geological Survey scientists. Shacklette (1960) made a study of vegetation and soils at the Mahoney Creek lead-zinc deposit in southeastern Alaska. The results given in table 29 show that mean lead concentrations increase from 90 ppm in the ash of plants from unmineralized ground to 160 ppm in the ash of plants rooted in soil over the vein. Shacklette suggested that the significance of differences between background, halo, and vein values of a species may be judged by the standard error. If a difference between two values is as great as or greater than twice the standard error, it can be considered a significant difference, not a sampling error.

Keith (1969) reported on similar studies of three deciduous tree species in the Upper Mississippi Valley lead-zinc district, where he collected 152 soils and 256 plants in mineralized areas and 306 soil and 368 plant samples in nonmineralized areas (table 29). It is apparent that, as expected, stems contain at least twice as much lead as leaves, but, contrary to expectations, lead is not noticeably concentrated in the trees growing on mineralized ground and is actually higher in nonmineralized areas. On the other hand, zinc (not shown here) was significantly concentrated in trees on mineralized ground. Keith believed the anomalously low concentrations of lead to be due to a higher pH in mineralized limestones in contrast to the surrounding areas of sandstone and glacial drift.

A study of lead in vegetation of the Ruby Hill lead-silver mining district in Arizona by Maurice Chaffee (written commun., 1970) shows the increase in lead uptake in an acid sulfide environment (table 29). The data show a remarkable concentration of lead in the older wood of sage and, in other vegetation, about a twofold increase in lead

over the levels in vegetation of the Upper Mississippi Valley limestone district.

Studies by Wallace (1971) show no effect of calcium on lead uptake by bushbeans, but a large increase in root absorption of lead when iron is added and a decrease with increments of NaHCO_3 .

Lead accompanied by zinc and cadmium may also accumulate in spring-fed peat bogs that drain dolomites of relatively high, but noneconomic, lead concentrations. When these peats are drained for "muck" farming of commercial vegetable crops, the metals become oxidized and are thus available to the vegetation to such an extent that vegetables cannot be grown in certain areas of highly mineralized peat. Such a situation developed on the "Manning muck" in Orleans County, N.Y., in 1938, but, during the last 30 years, the oxidized metals have been leached from the muck by ground and surface waters and neither wild plants nor vegetables now contain anomalous amounts of lead (Cannon, 1955, 1970). Some of the actual lead and zinc contents for the years 1946 and 1967-68 are given in table 30.

It is unfortunate that vegetables grown on the "Manning muck" were not analyzed for lead by Staker (1942) in 1938, as the median zinc content he recorded at that time was 140 ppm, and by 1946 the zinc content of native vegetation had dropped to one-third that level. Presumably, lead levels would have shown the same sharp decrease. In the 1946 collections, native vegetation (37 samples) had a median of 10 ppm and a range of 2-58 ppm lead in the dry weight; in the 1967-68 collections, native vegetation (7 samples) had a median of 4.7 ppm and a range of <0.5-10.2, and the vegetables (15 samples) had a median of <0.5 ppm and a range of <0.5-6.

LEAD INDICATOR AND ACCUMULATOR PLANTS

Certain species of plants that are tolerant of high-lead soils have been used as indicators in prospecting. These species may have adapted to living exclusively on rocks or soils that supply unusual amounts of a particular element, or they may have acquired an immunity to large amounts of an element by being able to reject the metal at the root site. Some indicator plants that have been found universally associated with a particular mineral assemblage absorb and concentrate large amounts of one or more metals in their storage tissues; others that do not concentrate large amounts of the metals in question may be species of wide distribution that favor mineralized ground under certain local conditions, because of a reduction in competition or a change in acidity, water conditions, or availability of major plant nutrients (Cannon, 1971).

Inasmuch as lead and zinc commonly occur together in ore deposits, it is difficult to establish positively that a particular plant is an indicator of lead. Plants that have

TABLE 29.—Lead content of vegetation and soils from several mining districts
[Number of samples, where specified, shown in parentheses]

Material analyzed	Plant part	Mean lead contents (ppm)		
Mahoney Creek Lead-zinc deposit, Alaska ¹				
		Background (± standard error)	Halo	Vein
<i>Menziesia ferruginosa</i> (rusty menziesia)	8-in. older stems.....	140±10 (20)	160±20 (10)	350±60 (5)
Do.....	Leaves and young stems.....	40±10 (20)	60±20 (10)	110±30 (5)
<i>Vaccinium ovalifolium</i> (whortleberry)	8-in. stems and leaves.....	40±10 (20)	60±20 (10)	100±30 (5)
<i>Tsuga heterophylla</i> (hemlock)	10-in. stems and needles.....	160±10 (18)	160±20 (9)	160±40 (5)
<i>Gaultheria shallon</i> (wintergreen)	10-in. stems and leaves.....	50±10 (15)	170±120 (8)	110±40 (4)
<i>Vaccinium parvifolium</i> (whortleberry)	8-in. stems and leaves.....	50±10 (4)	40±10 (4)	180±100 (2)
<i>Picea sitchensis</i> (spruce)	8-in. stems and needles.....	50 (1)	50 (1)	150 (2)
Mean of all plants.....		90±10	110±20	160±20
Soil samples.....		20±10	110±40	1,300±690
Upper Mississippi Valley district ²				
Nonmineralized areas				
		In ash of plants	In dry wt of plants	In dry wt of soils
<i>Ulmus</i> sp. (elm).....	Stems.....	102 (368)	4.9 (368)	78 (256)
	Leaves.....	29	3	3.7
<i>Acer</i> sp. (maple).....	Stems.....	119	4.7	26
	Leaves.....	44	4.5	6.5
<i>Quercus</i> sp. (oak).....	Stems.....	150	6.8	99
	Leaves.....	61	2.8	57
Soils:				
A Horizon.....			18	124
B Horizon.....			13	67
C Horizon.....			13	117
Ruby Hill mining district, Arizona ³				
		In ash	In dry wt	
<i>Pinus edulis</i> (pinyon).....	Needles.....	500	12.0	
	1- to 2-year twigs.....	500	13	
	Needles.....	500	11	
	1- to 2-year twigs.....	500	13	
	Needles.....	700	14	
	1- to 2-year twigs.....	700	16.8	
<i>Artemisia tridentata</i> (sage).....	1-year growth.....	700	42	
	Older wood and leaves.....	5,000	270	
	1-year growth.....	1,500	90	
	Older wood and leaves.....	> 5,000	> 220	
<i>Juniper</i> sp. (juniper).....	1-year growth.....	200	7.2	
	do.....	100	3.8	
	do.....	200	8.1	
<i>Cercocarpus ledifolius</i> (mountain mahogany)	do.....	700	36	
	do.....	700	36	
	do.....	2,000	88	
Median.....		700	15.4	
Range.....		100-5,000	3.8-220	

¹Collected by H. T. Shackleton, analyzed by D. R. Marx.²Analyzed by Maurice DeValliere and J. C. Hamilton.³Analyzed by E. L. Moser.

TABLE 30.—Maximum lead and zinc contents, in parts per million dry weight, of plants and drained peat, Orleans County, N.Y.

(N. unclassified Analysis H. W. Lakin, F. N. Ward, Laura Reichen, H. Almond, J. Grimaldi, H. Bloom, T. H. Harris, C. S. F. Pepp, From Lakin (1970))

	Year of collection	Lead		Zinc	
		Plant	Soil	Plant	Soil
<i>Portulaca oleraceus</i> (purslane)	1946	42	67	10,000	26,000
<i>Amorpha canescens</i> (sageweed)	1946	50	250	4,000	80,000
<i>Amorpha terreflora</i> (sageweed)	1946	5	250	2,000	80,000
<i>Cnicus discolor</i> (mistle)	1946	7	250	1,000	80,000
Soiler	1946	55	250	600	80,000
<i>Achillea millefolium</i> (yarrow)	1946	58	110	900	1,200
<i>Salix sp.</i> (willow)	1946	1	28	900	5,100
<i>Populus tremuloides</i> (poplar)	1946	4	110	860	5,200
<i>Solanum nigrum</i> (nightshade)	1946	10	67	10,000	26,000
<i>Solanum tuberosum</i> (potato)	1967-68	2.4	105	104	9,800
<i>Daucus carota</i> (carrot)	1967-68	2.0	58	156	5,200
<i>Elium repens</i> (cumin)	1967-68	N	10.5	11	400
<i>Brassica oleracea</i> (cabbage)	1967-68	N	16.5	150	2,800
<i>Cucurbita missouriensis</i> (squash)	1967-68	N	16.5	225	2,800
<i>Cnicus discolor</i> (mistle)	1967-68	0.7	21	487	6,200
<i>Pilea pumila</i> (cleome)	1967-68	3.0	58	150	51,000
<i>Rubus occidentalis</i> (wild raspberry)	1967-68	7.5	58	487	6,200
<i>Salix sp.</i> (willow)	1967-68	10.2	23	490	1,100

been reported as indicators or accumulators of lead are given in table 31. Plants that have been mentioned in the literature as being indicators of lead deposits in the Mississippi Valley lead-zinc district include white birch, cottonwood, and wild indigo. The association of *Amorpha canescens* (leadplant) with lead that has been mentioned in the early literature has not been verified. In northern Australia, zone of copper-lead-zinc minerals permits a more careful study of the tolerance of the various species that grow there (Cole, Provan, and Tooms, 1968). *Gomphrena canescens* R. B. (globe amaranth) and *Polycarpea synandra* F. Muell. var. *gracilis* (a pink), two of the indicator species, were found to tolerate 50,000 ppm zinc and 5,000 ppm lead in the soil. At another deposit, *Polycarpea glabra* (a pink), *Bulbostylis barbata* (bulletwood), and *Eriachne mucronata* indicated lead-zinc ores, the last concentrating as much as 50 ppm lead in the dry weight.

Although no trees were considered to be indicators of lead ores in studies that have been made by H. V. Warren in Canada and H. T. Shacklette in Alaska, very high contents of lead have been found in Douglas-fir, mountain hemlock, alder, birch, and heather. Shacklette (1965) described the distribution of a liverwort (*Cephalozia bicuspidata*) as entirely covering the surface of the ore, to the exclusion of all other species, at the Mahoney Creek lead-zinc mine in Alaska. The exposed ore contained 12.9 percent lead. The concentrations of lead in Canadian hemlock, arbutus, and several common adventive weeds from mineralized, drained peat in New York were also high, the lead content in the dry weight of coniferous species exceeding that of the peat. *Ledum palustre* in Finland was found by Salmi (1959) to accumulate high lead contents compared to other species. Thyssen (1942)

has reported a grass, *Molina altissima*, growing at Innerstetal, Germany, to contain 55,600 ppm lead in the ash. The grass species, *Agrostis tenuis*, appears to have adapted specifically to high-lead soils, and seed from selected heavy-metal-tolerant races of this species is being used as cover on mine dumps and tailings in Wales (Jowett, 1964; Wild and Wiltshire, 1971).

Some naturally lead poisoned areas have been studied and described in detail by Låg and Bølviken (1974). Occurrences of naturally lead poisoned soil and vegetation have been found in 5 different areas in Norway where deposits of galena occur in the bedrock. In the initial stages of poisoning, the forest trees and *Vaccinium* spp. (blueberry) are replaced by *Deschampsia flexuosa* (hairgrass), which grows profusely but without seed. Where lead poisoning is more advanced, the vegetation is abnormal or dying, and in highly mineralized soils, the ground is barren. *D. flexuosa* responds to increasing contents of lead in the soil with a corresponding decrease in the plant-Pb/soil-Pb ratio. After a low ratio of 0.6 percent is reached, at level of 1 percent lead in the soil, the ratio remains constant with increasing soil lead until the plant is killed. This defense mechanism of *D. flexuosa*, combined with a restricted availability of lead in the soil, effectively counteracts poisoning of the plant. Because plant growth is retarded, podzolization of the soil in these poisoned areas is lacking and erosion of moraine soils is increased, resulting in a stony soil surface. Låg and Bølviken believe the search for areas showing signs of natural heavy-metal poisoning to be a valuable method of geochemical prospecting.

ANOMALOUS LEAD CONCENTRATIONS IN PLANTS RESULTING FROM MAN'S ACTIVITY

LEAD ACCUMULATION RELATED TO MINING AND SMELTING ACTIVITY

The activities of man in the mining, milling, and smelting of ores have released considerable lead into the environment. These accumulations, because they occur as the result of activities in populated areas and because they may be released in a more available form than the original sulfide ores, may have a greater effect on health and disease than the lead in vegetation rooted in mineralized ground. Extensive studies are being conducted in Great Britain and Japan, where health problems have arisen in populations living in contaminated areas.

In Japan, lead analyses have been made of agricultural products grown near a large zinc refinery in Annaka City, where a chronic disease, itai itai, has been shown to be caused by contamination of water and rice crops by cadmium from the refinery (Kobayashi, 1972). Mulberry

TABLE 31.—Lead indicator and accumulator plants rooted in mineralized ground

Plant species	Indicator (I) or accumulator (A)	Locality	Maximum lead content (in ppm) reported			Reference
			In plants (ash)	In soil (dry weight)	In soil (dry weight)	
Conifers						
<i>Pseudotsuga menziesii</i> (Douglas-fir twigs).	A	British Columbia	2,200			Warren and Delavault (1960).
<i>Pseudotsuga taxifolia</i> (Douglas-fir tips).	A	Coeur d'Alene, Idaho	130	20,000		Kennedy (1960).
<i>Larix occidentalis</i> (larch tips).	A	do	100	1,000		Do.
<i>Pinus monticola</i> (white pine tips).	A	do	100	20,000		Do.
<i>Tsuga mertensiana</i> (mountain hemlock twigs).	A	Alaska	4,000			H. T. Shacklette (written commun., 1960).
<i>Tsuga canadensis</i> (Canada hemlock tips).	A	New York (peats)	40	10		Cannon (1955).
<i>Tsuga heterophylla</i> (Pacific hemlock stems).	A	British Columbia	1,100			Warren and Delavault (1960).
<i>Thuja occidentalis</i> (eastern arbutus tips).	A	do	19	13		Do.
<i>Thuja plicata</i> (giant arbutus stems).	A	British Columbia	3,100			Do.
<i>Picea</i> sp. (spruce wood).	A	Wisconsin	1,300			Thyssen (1942).
<i>Equisetum arvense</i> (horsetail stalks).	A	Warren, N.H. (ore).	420	140		Cannon, Shacklette, and Bastron (1968).
Do	A	Warren, N.H. (tailings)	344	86	21,000	Do.
Deciduous trees						
<i>Alnus crispa</i> (American green alder).	A	Alaska	5,000			H. T. Shacklette (written commun., 1960).
<i>Alnus sinuata</i> (Sitka alder)	A	do	4,000			Do.
<i>Populus</i> sp. (cottonwood twigs).	I	Wisconsin				A. V. Heyl (oral commun., 1948).
Do	A	Missouri	400	45	5,000	Cannon and Anderson (1971).
<i>Betula populifolia</i> (gray birch).	A	Alaska	5,000			H. T. Shacklette (written commun., 1960).
Do	I	Wisconsin				A. V. Heyl (oral commun., 1948).
<i>Betula glandulosa</i> (hitch stems).	A	British Columbia	25,000			Warren and Delavault (1960).
<i>Salix</i> sp. (willow roots).	A	Harz Mountains, Germany	17,300			Thyssen (1942).
<i>Betula lutea</i> (yellow birch twigs).	A	Joplin, Mo.	4,600	175	2,000	Cannon (1971).
Shrubs						
<i>Calluna</i> sp. (Alaskan heather).	A	Alaska	3,000			H. T. Shacklette (written commun., 1960).
<i>Vaccinium canadense</i> (huckleberry fruit).	A	Warren, N.H.	258	81	21,000	Cannon, Shacklette, and Bastron (1968).
<i>Holodiscus discolor</i> (rock spirea leaves).	A	Coeur d'Alene, Idaho	77	20,000		Kennedy (1960).
<i>Ledum palustre</i> (Labrador tea, twigs).	A	Finland	600		1600	Salmi (1959).
Herbs						
<i>Arenaria (Minuartia) verne</i> (leadwort).	A	North Wales	47,000			H. V. Warren (written commun., 1972).
<i>Portulaca oleracea</i> (common purslane).	A	New York (peat)	42	467		Cannon, Shacklette, and Bastron (1968).
<i>Ambrosia elatior</i> (common ragweed).	A	do	50	250		Do.
<i>Arcium minus</i> (small burdock).	A	do	58	110		Do.
<i>Polycarpha glabra</i> (pink).	IA	Australia				Nicolls, Provan, Cole and Toms (1964-65).
<i>Tussilago farfara</i> (coltsfoot).	I	Siegerland, Germany				Linstow (1929); Dorn (1937).
<i>Baptisia bracteata</i> (wild indigo).	I	Wisconsin				H. L. Cannon (unpub. data, 1948).

TABLE 31.—Lead indicator and accumulator plants rooted in mineralized ground—Continued

Plant species	Indicator (I) or accumulator (A)	Locality	Maximum lead content (in ppm) reported			Reference
			In plants		In soil	
			(ash)	(dry weight)	(dry weight)	
Herbs—Continued						
<i>Polycarpha synandra</i> v. <i>gracilis</i> (pink).....	IA	Australia.....			5,000	Cole (1965).
<i>Gomphrena canescens</i> (globe amaranth leaves).....	IA	do.....	49		5,000	H. E. King (written commun., undated).
(globe amaranth flowers).....	IA	do.....		114	5,000	Do.
(globe amaranth stems).....	IA	do.....		51	5,000	Do.
<i>Bulbostylis barbata</i> (bulletwood).....	IA	do.....				Nicolls, Provan, Cole, and Tooms (1964-65).
<i>Eriachne mucronata</i>	IA	do.....		50		Do.
<i>Campanula alpina</i> (alpine bellflower).....	IA	Caucasus.....	1,000			Starikov, Kononov, and Brushchin (1964).
Grasses						
<i>Molinia altissima</i> (Indian grass).....	IA	Innerstetal, Germany.....	35,600			Thyssen (1942).
<i>Deschampsia flexuosa</i>	I	Norway.....	2,000	99	17,200	Låg and Bølviken (1974).
<i>Agrostis tenuis</i> (subsp.).....	I	North Wales.....				Jowett (1964).
<i>Calamagrostis epigeios</i> (reed grass).....	A	Poland.....	> 100			Sarosiek (1959).
Ferns						
<i>Dryopteris crassula</i> (woodfern).....	A	Wisconsin.....		30	71	Cannon, Shacklette, and Bastron (1968).
<i>Dryopteris</i> spp.	A	Norway.....	4,100	410	23,300	Låg and Bølviken (1974).
<i>Ptyopteris spirulosa</i>	A	New Brunswick.....				Schmidt (1955).
Liverworts						
<i>Cephalosia bicuspidata</i>	I	Alaska.....			129,000	Shacklette (1965).
Algae						
<i>Spirogyra</i> type.....	A	Warren, N.H.	9,420	6,600	(¹)	Cannon, Shacklette, and Bastron (1968).

¹Pest.²Waters in which algae were growing contained 16 ppm total heavy metals.

growing on the hills above the refinery contained 41-160 ppm lead in the dry weight of the leaves, depending on the distance from the refinery. Leafy vegetables contained 4.4-260 ppm lead in the dry weight, root vegetables < 0.02-63 ppm, and fruits of vegetables < 0.4-11.0 ppm. A particular moss that covers the garden soils contained 370 ppm lead in the dry weight, 7,010 zinc, and 61 ppm cadmium. The lead uptake thus varies with species and plant part as well as distance. It was observed that the principal source of metals in the vegetation was by absorption through the roots from polluted soil rather than from direct deposition of metals from the air.

A comprehensive study by the U.S. Environmental Protection Agency was conducted in the Helena Valley area of Montana to determine the effects on vegetation of pollutants from the American Smelting and Refining Co. smelter (Hindawi and Neely, 1972). The lead content of vegetation was found to decrease with distance from the stack. Gordon (1972) reported samples from east Helena of plants and the soils in which they were grown to contain

lead in the dry weight, in parts per million, as follows:

	Vegetation lead	Soil lead
Washed lettuce.....	10-26	49-550
Unwashed lettuce.....	26-460	370-1,400
Conifer needles.....	40-125	370-1,100

Hindawi and Neely (1972) grew alfalfa, pinto beans, carrots, beets, petunias, and tobacco in greenhouses in vermiculture, exposing the growing plants to ambient air, and in garden soils outdoors, at the same distances from the stack, in order to test how much lead might be absorbed from the soil and how much from the air in the vicinity of a smelter. Their results, reported for unwashed produce, in parts per million, are as follows:

Distance from smelter (mi)	(km)	Vermiculture (A)	Local garden soil (B)	Absorbed from soil (B-A)
0.4	0.6	7.4	48.3	40.9
.8	1.3	3.0	5.4	2.0
2.5	4.0	1.5	3.0	1.5
4.5	7.2	.6	1.0	.4

¹Believed to reflect contamination by duststorm that arose during sampling.

If one assumes that the plants grown in vermiculite in the greenhouse but receiving ambient air are receiving the same atmospheric lead insult as the outdoor plants, then by subtraction it would appear that about half of the lead measured in unwashed produce may be absorbed from the soil and half from the air.

During the 19th century, several parts of Wales were intensively mined for lead. Fields adjacent to and down-stream from the mines became contaminated by airborne and waterborne heavy-metal compounds; these fields still contain high concentrations of these metals. Work by Alloway and Davies (1971) showed that herbage, consisting largely of the grasses *Festuca* and *Lolium*, and soils in this area have the following lead contents in parts per million dry weight:

	Range	Mean	Standard deviation
Herbage	30-100	63.2	24.5
Soil (total)	90-2,976	1,652.0	878.3
Soil (available ¹)	16-1,020	323.8	292.7

¹Acetic acid extractable.

Radishes were then grown in 15 gardens of north Cardiganshire, some close to and some remote from mines. The radishes had lead contents ranging from 4.6 to 33.1 ppm dry weight, with a mean content of 13.1 ppm and standard deviation of 7.4.

Lagerwerff, Brower, and Biersdorf (1972) collected soil and grass samples along 4 transects extending 6,684 feet (2,400 m) from a smelter in Galena, Kan., near the Missouri border, after the smelter had discontinued operations involving lead production. In the direction of prevailing winds, lead content of the unwashed grass ranged from 98.4 ppm (dry weight) at 1,082 feet (330 m) from the smelter to 16.2 ppm at 6,684 feet (2,400 m). They also observed that the pastures near the smelter had been invaded by switchgrass (*Panicum virgatum*) and broomsedge (*Andropogon virginicus*), which are both tolerant of the combination of low pH and high heavy-metal concentration in the soil.

In 1968 the U.S. Geological Survey sampled birch and oak trees, their humus, and the alluvium in which they were growing, along a stream in a forested mining area near Joplin, Mo.; old mine diggings and pits were visible under the undergrowth. Although this locality had no air contamination from lead at the time of sampling, concentration of lead in the bark was comparable to that in the first-year twigs. The lead content was higher in the birch, which is an accumulator, than in the oak. Results of the study are as follows (number of samples collected are given in parentheses):

	Lead (ppm)	
	In ash	In dry weight
<i>Betula lutea</i> (birch) (2):		
Leaves	315	25.0
Twigs (1st-year)	4,600	175.0
Wood	900	14.0
Bark	2,900	73.0
Roots	1,600	50.0

	Lead (ppm)	
	In ash	In dry weight
<i>Quercus muhlenbergii</i> (oak) (2):		
Leaves	140	6.4
Twigs (1st-year)	1,200	48.0
Wood	375	9.4
Bark	1,500	178.0
Humus		1,700.0
Alluvium		2,000.0

Smelters and refineries, commonly located in well-populated areas, may contribute considerable amounts of lead to the atmosphere; this airborne lead, in turn, contaminates the soil and vegetation. Warren, Delavault, and Cross (1966) found as much as 1,600 ppm lead in the ash of birch leaves growing 3 miles (5 km) from the Trail smelter in British Columbia.

Studies have been made by the U.S. Geological Survey near several zinc-lead smelters. Analyses of plants and soils collected near the Bartlesville, Okla., and Leadville, Colo., smelters are given in table 32. The tree sampled at Leadville was the nearest pine to the smelter able to grow in the contaminated soil and was considerably dwarfed. The smelter had not been operative for 15 years at the time of sampling.

TABLE 32.—Lead contents of plants and soils as related to smelter contamination in Colorado and Oklahoma

[Leadless (...) indicate no data. From Cannon and Anderson (1971); analysis: T. F. Harris and C. S. F. Papp]

Sample No D-13	Material analyzed	Lead (ppm)	
		In ash	Converted to dry wt
Bartlesville, Okla. 1,500 ft (466 m) from smelter			
387	<i>Populus deltoides</i> (cottonwood), leaves.....	120	11.2
410	<i>Populus deltoides</i> (cottonwood), wood.....	190	2.5
411	<i>Populus deltoides</i> (cottonwood), bark.....	500	34
406	Top 0.5 in. (1.25 cm) soil.....	2,500
407	1-5 in. (2.5-12.7 cm) soil.....	2,500
7,000 ft (2,100 m) from smelter			
390	<i>Ulmus americana</i> (elm), leaves.....	120	7.2
388	<i>Asparagus officinalis</i> (asparagus), tops.....	40	2.4
389	<i>Allium porrum</i> (onion), bulb.....	200	11
408	Humus.....	1,000
409	Soil.....	125
Leadville, Colo. ¹ 1,000 ft (300 m) from smelter			
452	<i>Carex</i> sp. (sedge), tops.....	500	49
3,300 ft (975 m) from smelter			
453	<i>Pinus edulis</i> (pine), needles.....	2,500	40
454	<i>Pinus edulis</i> (pine), branch wood (including bark).....	18,000	342

¹Smelter inoperative since 1956.

LEAD ACCUMULATION RELATED TO AGRICULTURAL ACTIVITIES

Contamination of the soil due to agricultural activities stems generally from efforts to reclaim or increase the fertility of the land, or from sprays used on crops to combat insect or fungal infestation. Tailings from lead-zinc mines are occasionally used for fertilizer, but a study by Hawkes and Lakin (1949) in east Tennessee where such practice is common showed that the amounts added were small and did not affect the level of lead in the soil. Residual lead can be detected in soils that have been sprayed in the past and this lead may be translocated to the edible parts of produce. Warren (1961) compared trees in orchards in Okanogan County, Wash., that had been sprayed 10 years earlier with trees that had never been sprayed. The unsprayed trees contained less than 1 ppm lead whereas sprayed trees contained 40, 50, and 100 ppm. A garden in Canadaigua, N.Y., which had been sprayed repeatedly, but which was well protected from street contamination, was sampled by the author and found to contain 300 ppm lead in the soil, 700 ppm in the ash (44 ppm in dry weight) of raspberry canes, and 300 ppm lead in the ash (12 ppm in dry weight) of the berries.

LEAD ACCUMULATION RELATED TO URBAN AIR POLLUTION

The effects of lead in the atmosphere on the lead content of vegetation were pointed out by Warren and Delavault (1960), who found higher values in Canadian plants collected near roadsides than in those remote from roads. Warren and Delavault (1962) further investigated this anomaly by sampling similar vegetation in two localities in England—in an area of Sussex remote from a road and in London. Their results for twigs of the previous year's growth showed these lead contents, in parts per million:

Species	Sussex locality		London locality	
	Dry weight	Ash	Dry weight	Ash
Lime.....	0.4	8	5	50
Yew (needles).....	.4	7	6	100
Willow.....	1.0	35	2	30
Birch.....	1.0	36	8	160
Oak.....	.8	30	20	280
Ash.....	2.0	30	14	160
Hazel.....	2.0	50	52	680

In Maryland the lead content of the ash of vegetables collected near roads was also shown to be higher than that of vegetables farther from roads (Cannon and Bowles, 1962), as shown in the following table (analyst, E. F. Cooley):

Distance from road (ft)	Distance from road (m)	Number of samples analyzed	Lead content (ppm) Mean	Lead content (ppm) Range
1-25	4-8	29	80	10-500
25-50	8-16	29	66	10-700
50-100	16-160	45	45	<10-150
>100	>160	28	20	<10-200

To test the significance of these findings, Cannon and Bowles (1962) sampled grass in four directions for 1,000 feet (304 m) from major highways in the Denver area in early June of 1961. The samples were washed in tapwater and analyzed using an emission spectrograph. The lead contents along all four traverses decreased logarithmically with distance from the highway, from 30 ppm to a background of 2 ppm at 900 feet (274 m). In 1969, the samples were re-collected in early June along the only traverse remaining in pasture. The lead content had risen about 1,000 percent and had spread considerably farther from the highway. The highest lead content, 222 ppm dry weight, was found at a distance of 5 feet (1.5 m) from the highway, and grass at 1,000 feet (304 m) contained 28 ppm (fig. 11) (Cannon and Anderson, 1971). Washed grass contained less than unwashed, although the samples were collected during a period of heavy rains.

Salmi (1969) reported a decrease in lead content of *Sphagnum tuscum* (moss) on the surface of a bog at distances of 0-984 feet (0-300 m) from a road in Finland. At about 33 feet (10 m) on one traverse, 27 ppm lead was measured, in contrast to a norm of 2 ppm. Purves and Mackenzie (1969, 1970) reported on significant differences in lead content of herbage in parklands of Scotland. The mean for rural herbage was 30.3 ± 2.3 ppm and that for urban (Edinburgh) herbage was 44.6 ± 4.2 ppm in dry weight. On the other hand, the inner leaves of cabbage collected from rural and urban areas showed significant

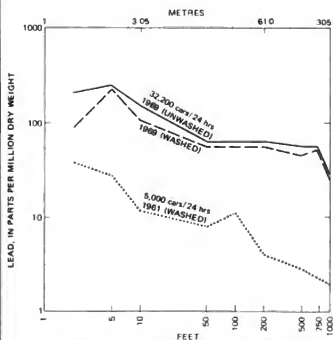


FIGURE 11.—Lead in grass collected for 1,000 feet (304 m) from highway in 1961 and 1969.

differences in boron, molybdenum, and zinc, but none in lead. Unwashed privet leaves were collected by Everett, Day, and Reynolds (1967) in areas close to and remote from highways in England. Leaves near highways had an average of 86 ppm dry weight, and leaves remote from highways had an average of 45 ppm dry weight.

A U.S. Geological Survey study in Missouri (Connor, Erdman, and others, 1971) found that roadside contamination has a much greater effect on the lead content of vegetation than it does on soils or rock outcrops. Thirty-two samples of cedar and 60 samples of grass were collected from locations both on (< 50 ft (15 m) away) and off (> 500 ft (152 m) away) secondary roads. The collections from these locations consisted of the terminal branches of cedar (*Juniperus virginiana*) and above-ground portions of grasses at a specified stage of development. The mixed grasses were mostly *Triodia flavens*, *Festuca elatior*, and *Setaria viridis*. The samples, which were not washed, were analyzed by emission spectrography. The results are shown in table 33. The differences in both cedar and grass are significant at the 0.05-ppm probability level; those in subsoils and rocks are not. These data show that lead reported in roadside soils is confined to surface soils, and that soils at a depth of several inches are unaffected. Cedar, which is an evergreen and thus exposed to contamination throughout the year, contained no more lead than did the grass. That cedar is an accumulator of lead was shown by one sample collected near Centerville, which contained 1,200 ppm lead dry weight (Connor, Shacklette, and Erdman, 1971). Further investigation has shown a geometric mean of 348 ppm dry weight in 15 cedar samples from the area. It is believed that the soil here has been contaminated by ore dust from trucks transporting ores from mine to smelter. These data can be compared with those of Lagerwerff and Specht (1970), who sampled grass at 8, 16, and 32 feet (about 2, 4, and 9 m) from major freeways near Washington, D. C., and soil at these sites at depths of 0-5, 5-10, and 10-15 cm. Lead contents in grass and soil decreased with distance; the levels of lead in grass ranged from a maximum of 68.2 ppm dry weight at 8 feet (2

m) to a minimum of 7.5 ppm at 32 feet (9 m) and in surface soil ranged from 540 ppm to 55 ppm. The data also show a reduction in lead content with depth. Dedolph, Ter Haar, Holzman, and Lucas (1970) were able to correlate the amounts of lead in grass with concentrations in air. At 40 feet (12 m) from the road, the air contained $2.3 \mu\text{g}/\text{m}^3$ and the grass averaged 15 ppm dry weight, and at 120 feet (36 m), the air contained $1.7 \mu\text{g}/\text{m}^3$ and the grass 8.4 ppm lead.

An increase in the lead content of plant foliage in the winter months has been reported by several workers and generally attributed to increased exposure time to air-pollution lead. Mitchell and Reith (1966) found an increase in pasture herbage from 1 ppm lead (dry weight) in early autumn to 30-40 ppm in the winter. However, they attributed the increase to either a translocation of lead from roots to tops during the winter months or a loss of organic matter through respiration rather than to surface contamination from the air.

The effects of washing on the lead values varies with season and rainfall conditions. In the study reported by Cannon and Anderson (1971), on grass collected in the spring shortly after a heavy rain, no great difference in lead content between washed and unwashed samples was noted. Ganje and Page (1972) compared the lead content of washed with unwashed samples of lima-bean leaves and pods, corn leaves, sugar-beet leaves, and tomato fruits collected in California near the Santa Ana and Riverside Freeways; they found a 30-70 percent decrease, depending on such factors as the extent of plant surface exposed, roughness of surface, and duration of exposure. Motto, Daines, Chilko, and Motto (1970) also found a ± 40 percent decrease in washed grass collected within 225 feet (68 m) of highways. Rains (1971), on the other hand, could not wash lead from *Avena fatua* (wild oats) that had grown in a lead-fallout region, nor could he extract it with water. He was, however, able to extract 50 percent with 0.01 M HCl and 95 percent with 0.01 M NH_4EDTA .

Whether the lead that cannot be washed from roadside plants is absorbed directly from the air through the leaves or is taken up from the contaminated soil has been debated. Certainly there can be no doubt concerning absorption from the air in regard to *Tillandsia usneoides* (Spanish moss), which has no root system and obtains all essential elements from the atmosphere. Analyses of 123 samples of Spanish moss collected by H. T. Shacklette (written commun., 1971) from the Atlantic and Gulf Coastal Plain areas ranged from 3.2 to 230 ppm lead in dry weight and had a geometric mean of 192 ppm; the contrast between samples from urban industrial areas and rural areas indicated the influence of atmospheric pollution in raising lead levels. Wherry and Buchanan (1926), who analyzed Spanish moss for some of the essential plant nutrients, found no difference between washed and unwashed samples. Martinez, Nathany, and Dharmarajan

TABLE 33.—Comparison of lead content between on-road and off-road samples of some soils and plants in Missouri
[Data from Connor, Erdman, and others, 1971; analyst, Harriet Norman]

Locality	Sample type	Number of samples	Lead content (ppm) ¹	
			On road ²	Off road ³
Various	Cedar branch tips	32	16	7
Do.	Soil	32	17	14
Kansas City, Mo.	Grass	30	29.0	9.7
Do.	Soil	30	10	14
Pacific, Mo.	Grass	30	17.0	4.5
Do.	Soil	30	10.0	3.5

¹Dry weight, geometric mean.

²Samples taken < 50 ft (15 m) from road.

³Samples taken > 500 ft (152 m) from road.

(1971) in most instances found no significant difference between unwashed samples of Spanish moss and those washed with ammonium acetate, but were able to extract more than one-third of the lead from a sample collected near a four-lane highway. These plants, however, have a highly developed system for extracting nutrients from the air and cannot be considered as representative of the entire plant kingdom.

Rühling and Tyler (1968) grew plants from roadside seed in contaminated soils obtained near highways. The plants contained only 5–10 ppm lead in the dry weight of the plant, whereas the same species of weeds that grew in the same soils along the roadside contained 68–950 ppm lead in the dry weight of washed samples. These data indicate absorption of lead from the atmosphere. Crops were grown by Ter Haar (1970) both in greenhouses supplied with filtered and ambient air and in plots planted in rows perpendicular to a busy highway. Of the 10 crop plants studied, only leaf lettuce, bean leaves, and the husk of sweet corn showed significant increases in lead content in unfiltered air compared to filtered air. In crops grown 30–520 feet (9–158 m) from a highway, soybeans and snap beans also showed higher lead contents nearer the highway. He concluded from these studies that natural lead in the soil is the main source of lead in edible crops and that airborne lead contributes only 0.5 to 1.5 percent of the lead content of the U.S. diet. More sophisticated experiments (Dedolph and others, 1970) at the Argonne Laboratory consisted of growing six harvests of ryegrass and three harvests of radishes in chambers ventilated with filtered and unfiltered air and in a field adjoining a highway traversed by about 29,000 vehicles per day. The data obtained from analyses of coded samples were subjected to statistical evaluation. Clearly defined differences in plant-lead content attributable to differences in the lead concentration of the atmospheric environment could be discerned in leaves of both species. Lead-enriched water applied to the plants had no effect on their lead content. Atmospheric lead had no effect on the lead content of the root or edible portion of the radish. They concluded that the radish and rye leaves contain on the order of 2.5 ppm lead dry weight, which is soil derived. Lead concentrations above this base level (maximum 15 ppm) reflect the average lead concentration in the atmosphere in which the plants were grown.

Schuck and Locke (1970) investigated crops routinely grown in fields near highways in the vicinity of Riverside, Calif., and concluded that lead particulate particles are not absorbed but exist as a topical dust coating, of which at least 50 percent can be removed by washing. In a cauliflower head, interior florets contained less lead than did the outer florets; maximum amounts were contained in the outer leaves of cabbage heads growing 25 feet (7 m) from the highway. No evidence of absorption through the

roots from water or from the high-lead soils that had been treated in the past with lead arsenate was observed.

Zimdahl and Arvik (1972) believed that the leaf cuticle is a primary barrier to entrance of atmospheric lead into the leaf and plays a more important role than stomatal penetration. Experiments with penetration of lead through cuticle membrane from leaves and fruits showed that less than 1 percent of the lead is able to penetrate the cuticular barrier. Whether atmospheric lead can be absorbed through the stomata of the leaf and translocated to other parts of the plant has not been determined, although lead isotopic studies should be able to resolve this question. Chow (1970) has shown that the isotopic composition characteristic of gasoline lead is of greater abundance in grass near highways and in surface soils than in soils at depth. Ault, Senechal, and Erleback (1970) studied tree rings and found no significant difference in isotopic ratio (Pb^{206}/Pb^{208}) with age. The ratios in all rings of wood were lower than that of roadside grass or of gasoline lead. The lead abundance in the outermost tree rings (0.34 ppm) was twice that of the 15- and 30-year-old rings (0.15 ppm). Either the uptake of lead was less in the past or lead is removed from the xylem layers after formation—perhaps along the radial ray cells of the woody part of the tree.

Algae, mosses, lichens, and others of the lower plant groups, because of their slow growth and unusually high concentrations of metals, have been proposed by several scientists as indicators of lead contamination. Rühling and Tyler (1968) suggested that mosses growing on trees in urban areas be used as an index for surveying deposition of airborne heavy metals. They found that the contents of lead in mosses in southern Sweden had risen from about 25 to 100 ppm from 1860 to 1968. Martinez, Nathany, and Dharmarajan (1971) suggested that Spanish moss, which is not a true moss but a highly specialized epiphytic angiosperm, be used as a sensor for lead in the Gulf States; they were able through this medium to establish gradients from line-and-point sources to pollutants. Rains (1971) found a particular species of *Avena fatua* (wild oats) to be highly tolerant of lead and suggested its use as an indicator.

Two sources of pollution-caused lead in the atmosphere that have not been mentioned in previous sections have been reported in British Columbia and England. Warren, Delavault, Fletcher, and Wilks (1971) described an episode in Richland, B.C., in 1970, when dust falling in a particular area of the town was found to contain 4.2 percent lead, soil within a radius of a few hundred feet contained as much as 4,000 ppm lead, and forage grown in this locality contained from 1.5 to 8.5 percent lead in the ash. Lead in unwashed vegetables contained as much as 6.5 ppm in wet weight but a maximum of 0.6 ppm after washing. Although, for the most part, the lead is not absorbed into the plant tissue, the lead on the plants was being consumed by cattle. The industrial plant credited

with being the source of the lead pollution has been closed voluntarily until control devices can be installed. Dunn and Bloxam (1932) reported on livestock deaths in England, which, although widely separated, were all on pastures near coke ovens. Soil downwind from the ovens contained as much as 7 ppm lead and grass contained as much as 46 ppm in the dry weight. Soils and grass upwind from the ovens had considerably lower lead contents. Further analysis showed the chimney soot to contain 342 ppm lead and the flue soot, 68 ppm.

SUMMARY

Plants absorb available lead from soils. Natural lead in plants growing in uncontaminated and unmineralized areas averages 2 ppm in the dry weight. As much as 350 ppm lead has been measured in the dry weight of vegetation rooted in soils developed from rocks containing lead ores; concentrations of as much as 664 ppm have been reported in vegetation subjected to the industrial and agricultural activities of man. A large percentage of lead in soil is not available to plants, and only in mining areas where high lead levels in soils occur is the growth of plants seriously affected. Of greater environmental significance is atmospheric lead from lead smelters, other types of industrial plants, and automobile emissions. Concentrations of lead in or on plants exposed to contaminated air decrease logarithmically with distance from the source. There is no clear evidence that lead from the atmosphere enters into the plant, except in the case of Spanish moss, which is highly specialized for absorbing atmospheric elements into the plant tissue. Washing and preparation of vegetables reduces the lead content to levels acceptable for human consumption, with the possible exception of lettuce and other leafy vegetables that are consumed raw; however, atmospheric lead in or on forages remains a hazard to livestock. Lead levels are increasing markedly and should be monitored on a continuous basis in urban and industrial areas.

REFERENCES CITED

- Alloway, B. J., and Davies, B. E., 1971, Heavy metal content of plants growing on soils contaminated by lead mining. *Jour. Agr. Sci. [Cambridge]*, v. 76, p. 321-325.
- Ault, W. U., Senchal, R. G., and Erelbach, W. E., 1970, Isotopic composition as a natural tracer of lead in the environment. *Environmental Sci. and Technology*, v. 4, no. 4, p. 305-311.
- Bolter, E., Hemphill, D., Wixson, B., Butcher, D., and Chen, R., 1972, Geochemical and vegetation studies of trace substances from lead smelting, in Hemphill, D. D., ed., Trace substances in environmental health-6 [6th Ann. Conf. Proc.]: Columbia, Missouri Univ., p. 79-86.
- Bonnet, E., 1922, Action des sels solubles de plomb sur les plantes [Action of soluble lead salts on plants]. *Acad. Sci. [Paris] Comptes rendus*, v. 174, no. 7, p. 488-491.
- Bormann, F. H., and Likens, G. E., 1967, Nutrient cycling: Science, v. 155, no. 3761, p. 424-429.
- Bradshaw, A. D., 1952, Populations of *Agrostis tenuis* resistant to lead and zinc poisoning. *Nature*, v. 169, p. 1098.
- Brown, J. S., and Meyer, P. A., Jr., 1959, Geochemical prospecting as applied by the St. Joseph Lead Company. *Internat. Geol. Cong.*, 20th, Mexico City 1956, Proc., v. 3 of Symposium on geochemical exploration, p. 623-639.
- Cannon, H. L., 1955, Geochemical relations of zinc-bearing peat to the Lockport dolomite, Orleans County, N.Y.: U.S. Geol. Survey Bull. 1000-D, p. 118-185.
- , 1970, Trace element excesses and deficiencies in some geochemical provinces of the United States, in Hemphill, D. D., ed., Trace Substances in Environmental Health-3 [3rd Ann. Conf. Proc.]: Columbia, Missouri Univ., p. 21-43.
- , 1971, The use of plant indicators in ground water surveys, geologic mapping, and mineral prospecting: *Taxon*, v. 20, no. 2-3, p. 227-256.
- Cannon, H. L., and Anderson, B. M., 1971, The geochemist's involvement in the pollution problem, in Cannon, H. L., and Hoppes, H. C., eds., *Environmental geochemistry in health and disease: Geol. Soc. America Mem. 123*, p. 155-177.
- Cannon, H. L., and Bowles, J. M., 1962, Contamination of vegetation by tetraethyl lead: *Science*, v. 137, no. 3552, p. 765-766.
- Cannon, H. L., Shacklette, H. T., and Bawron, Harry, 1968, Metal absorption by *Equisetum* (horsetail): *U.S. Geol. Survey Bull.* 1278-A, 21 p.
- Chow, T. J., 1970, Lead accumulation in roadside soil and grass: *Nature*, v. 225, p. 295-296.
- Cole, M. M., 1965, Biogeography in the service of man [inaugural lecture]: London, London Univ., Bedford College, 63 p.
- Cole, M. M., Provan, D. M. J., and Tooms, J. S., 1968, Geobotany, biogeochemistry, and geochemistry in mineral exploration in the Bulman-Waimuna Springs area, Northern Territory, Australia: *Inst. Mining and Metallurgy Trans.*, sec. B, v. 77, p. B81-B104.
- Comar, J. J., Erdman, J. A., Sims, J. D., and Ebens, R. J., 1971, Roadside effects on trace element content of some rocks, soils, and plants of Missouri, in Hemphill, D. D., ed., Trace Substances in Environmental Health-4 [4th Ann. Conf. Proc.]: Columbia, Missouri Univ., p. 26-31.
- Comar, J. J., Shacklette, H. T., and Erdman, J. A., 1971, Extraordinary trace-element accumulations in roadside cedars near Centerville, Missouri, in *Geological Survey research 1971*: U.S. Geol. Survey Prof. Paper 750-B, p. B151-B156.
- Dedolph, Richard, Ter Haar, Gary, Holtzman, Richard, and Lucas, Henry, Jr., 1970, Sources of lead in perennial ryegrass and radishes: *Environmental Sci. and Technology*, v. 4, p. 217-223.
- Don, Paul von, 1937, Pflanzen als Anzeiger für Erzlagerstätten [Plants as indicators of ore deposits]: *Der Biologe* [Munich], v. 6, p. 11-13.
- Dunn, J. T., and Bloxam, H. C., 1932, The presence of lead in the herbage and soil of land adjoining coke ovens, and the illness and poisoning of stock fed thereon: *Jour. Soc. Chem. Industry*, v. 51, p. 1007-1021.
- Everett, J. L., Day, C. L., and Reynolds, D., 1967, Comparative survey of lead at selected sites in the British Isles in relation to air pollution: *Food and Cosmetics Toxicology*, v. 5, p. 29-35; abs. in *Chem. Abs.*, v. 66, no. 98251t, 1967.
- Fletcher, Kenneth, and Brink, V. C., 1969, Content of certain trace elements in range forages from south central British Columbia: *Canadian Jour. Plant Sci.*, v. 49, no. 4, p. 517-520.
- Ganje, T. J., and Page, A. L., 1972, Lead concentrations of plants, soil, and air near highways: *California Agriculture*, April 1972, p. 7-9.
- Gordon, C. C., 1972, Effects of air pollution on indigenous animals and vegetation, in Helena Valley, Montana area, environmental pollution study: U.S. Environmental Protection Agency, Office of Air Programs Pub. AP-1, 179 p.

- Guha, M. M., and Mitchell, R. L., 1966, The trace and major element composition of the leaves of some deciduous trees—[Pt.] 2, Seasonal changes: *Plant and Soil* [Netherlands], v. 24, no. 1, p. 90-112, abs. in *Chem. Abs.*, v. 64, no. 180521, 1966.
- Hannet, P. S., 1928, Studies in the biology of metals: Protoplasm, v. 4, p. 183-191; v. 5, p. 135-141, p. 536-562.
- Harbaugh, J. W., 1950, Biogeochemical investigations in the Tri-State district: *Econ. Geology*, v. 45, no. 6, p. 548-567.
- Hawkes, H. E., 1954, Geochemical prospecting investigations in the Nyerba lead-zinc district, Nigeria: *U.S. Geol. Survey Bull.* 1000-B, p. 51-103 [1955].
- Hawkes, H. E., and Lakin, H. W., 1949, Vestigial zinc in surface residuum associated with primary zinc ore in East Tennessee: *Econ. Geology*, v. 44, no. 4, p. 286-295.
- Hedström, Helmar, and Nordström, Allen 1945, New aspects of ore prospecting [in Swedish]: *Medd. Jernkontors Gruvbyrå*, v. 59, p. 1-10.
- Hevesy, George, 1925, The absorption and translocation of lead by plants: *Biochem. Jour.*, v. 17, p. 459-445, 1925.
- Hindawi, I. J., and Neely, G. E., 1972, Soil and vegetation study, in Helena Valley, Montana area, environmental pollution study. U.S. Environmental Protection Agency, Office of Air Programs Pub. AP-1, p. 81-94.
- Hornbrook, E. H. W., 1969, A pilot project at the Silvermine lead deposit, Cape Breton Island, Nova Scotia, Sec. G. in *Progress report on biogeochemical research at the Geological Survey of Canada*: *Canada Geol. Survey Paper* 67-23, pt. 2, p. 65-94.
- John, M. K., and VanLaarhoven, C. J., 1972, Lead distribution in plants grown on a contaminated soil: *Environmental Letters*, v. 3, no. 2, p. 111-116.
- Jones, D. J. C., 1959, Chemical composition of kales and rapeseeds—[Pt.], 3. The minor elements: *Jour. Agr. Sci. [Cambridge]*, v. 53, p. 151-155.
- Jowett, D., 1964, Population studies on lead-tolerant *Agrostis tenuis*: *Evolution*, v. 18, p. 70-80.
- Kebow, R. A., 1961, The metabolism of lead in man in health and disease: *Harben Lecture*, no. 1, 1960, 18 p.; rept. in *Jour. Royal Inst. Public Health and Hygiene*, v. 24, p. 81-97.
- Keith, J. R., 1969, Relationships of lead and zinc contents of trees and soils, upper Mississippi Valley district. Soc. Mining Engineers Trans. [AIME], v. 244, p. 353-356.
- Kennedy, V. C., 1960, Geochemical studies in the Coeur d'Alene district, Shoshone County, Idaho, with a section on *Geology*, by S. W. Hobbs: *U.S. Geol. Survey Bull.* 1098-A, p. 1-55 [1961].
- Kobayashi, Jun, 1972, Air and water pollution by cadmium, lead, and zinc attributed to the largest zinc refinery in Japan, in Hemphill, D. D., ed., Trace substances in environmental health—5 [5th Ann. Conf. Proc.]: Columbia, Missouri Univ., p. 117-128.
- Låg, J., and Björken, B., 1971, Some naturally heavy-metal poisoned areas of interest in prospecting, soil chemistry, and geochemistry: *Norges Geol. Undersøkelser*, v. 304, Bull. 23, p. 73-96.
- Lagerwerff, J. V., Brower, D. L., and Bierdorf, G. T., 1972, Accumulation of cadmium, copper, lead, and zinc in soil and vegetation in the proximity of a smelter, in Hemphill, D. D., ed., Trace substances in environmental health—6 [6th Ann. Conf. Proc.]: Columbia, Missouri Univ., p. 71-78.
- Lagerwerff, J. V., and Specht, A. W., 1970, Contamination of roadside soil and vegetation with cadmium, nickel, lead, and zinc: *Environmental Sci. and Technology*, v. 4, p. 583-586.
- LeRoy, L. W., and Koksoy, Munim, 1962, The lichen—A possible plant medium for mineral exploration: *Econ. Geology*, v. 57, no. 1, p. 107-111.
- Linstow, O. von, 1929, *Bodenanzeigende Pflanzen* [Soil-indicating plants] [2d ed.]: Berlin, Preussischen Geol. Landesanstalt Abh., n. ser. 114, 246 p.
- Lounamaa, J., 1956, Trace elements in plants growing wild on different rocks in Finland: *Annales Botanici Societatis Zoologicae Botanicae Fennicae "Vanamo"*, v. 29, no. 4, 196 p.
- MacLean, A. J., Halstead, R. L., and Finn, B. J., 1969, Extractability of added lead in soils and its concentration in plants: *Canadian Jour. Soil Sci.*, v. 49, no. 3, p. 327-334.
- Mal'yuha, D. P., 1964, Biogeochemical methods of prospecting: *New York, Consultants's Bur.*, 205 p. [translated from the Russian].
- Martinez, J. D., Nathany, Madhusudan, and Dharmaratne, Venkatram, 1971, Spanish moss—A sensor for lead: *Nature*, v. 233, no. 5821, p. 564-565.
- Miller, R. J., and Koppke, D. E., 1971, Accumulation and physiological effects of lead in corn, in Hemphill, D. D., ed., Trace substances in environmental health—4 [4th Ann. Conf. Proc.]: Columbia, Missouri Univ., p. 186-193.
- Mitchell, R. L., 1965, Soil aspects of trace element problems in plants and animals: *Jour. Royal Agr. Soc. [Cambridge]*, v. 121, p. 75-86.
- Mitchell, R. L., and Reith, J. W. S., 1966, The lead content of pasture herbage: *Jour. Sci. Food and Agriculture [London]*, v. 17, p. 437-440.
- Motto, H. L., Dames, R. H., Chalko, D. M., and Motto, C. K., 1970, Lead in soils and plants—its relationship to traffic volume and proximity to highways: *Environmental Sci. and Technology*, v. 4, no. 3, p. 231-237.
- Nicolls, O. W., Provau, D. M. J., Cole, M. M., and Tooms, J. S., 1965, Geo-botany and geochemistry in mineral explorations in the Dugald River area, Clonduff district, Australia: *Inst. Mining and Metallurgy Trans. [London]*, v. 74, pt. 11, no. 705, p. 695-799.
- Polikarpchikina, V. V., Polikarpchikina, R. T., and Abramov, I. L., 1965, Dispersion halos in plants in areas of eastern Transbaikalia ore deposits [in Russian]: *Akad. Nauk SSSR, Sibirsk Otdeleniye Inst. Geokhim. Vopr. Geokhim. Izvreshchennykh Gorn. Porodi Rudn. Mestorozhd. Vost. Sibiri* 1965, p. 212-270; abs. in *Chem. Abs.*, v. 65, no. 1970h, 1966.
- Puskotin, D. I., Yushkov, Yu. N., Yurimkin, N. A., and Snegirev, A. D., 1969, Biogeochemical prospecting for chalcopryite and rare metal deposits in the Urals [in Russian]: *Vses. Soveshch. Po Primeneniiu Mikrotelementov Sel'skom Khozaystvu Meditsine, 5th, Irkutsk 1966* [1969]; abs. in *Chem. Abs.*, v. 75, no. 66117y, 1971.
- Purves, David, and Mackenzie, F. J., 1969, Trace-element contamination of parklands in urban areas: *Jour. Soil Sci. [Oxford]*, v. 20 no. 2, p. 289-290.
- 1970, Enhancement of trace-element content of cabbages grown in urban areas: *Plant and Soil* [Netherlands], v. 33, p. 483-485.
- Rains, D. W., 1971, Lead accumulation by wild oats in a contaminated area: *Nature*, v. 235, no. 5316, p. 210-211.
- Reese, M. L., 1957, A study of the microflora of two Cardiganshire rivers and the effect of local lead mines upon their algal population: *Water and Water Eng.*, v. 39, p. 26-28.
- Rühling, Åke, and Tyler, Germund, 1968, An ecological approach to the lead problem: *Botaniska Notiser*, v. 121, p. 321-342.
- Salmi, Matti, 1959, On peat-chemical prospecting in Finland: *Internat. Geol. Cong., 20th, Mexico City 1956, Proc.*, v. 2 of Symposium on geochemical exploration, p. 243-254.
- 1969, Contamination of roadsides in Finland [in Finnish]: *Terra*, v. 81, p. 229-233.
- Sarosiek, J., 1959, Lead content in *Calamagrostis epigeios* [in Polish with English summary]: *Soc. Botan. Polonica Acta*, v. 28, no. 23, p. 417-432; abs. in *Chem. Abs.*, v. 54, no. 15273d, 1960.
- Schlatter, K., and Schropp, W., 1936, The effect of lead upon plant growth [in German]: *Zeitschrift Pflanzenmehr Dúngung Bodenkr.*, v. 12, p. 31-33.
- Schmidt, R. C., 1955, Dispersion of copper, lead, and zinc from mineralized zones in an area of moderate relief as indicated by

- soils and plants: McGill Univ. M.S. thesis, 72 p., abs. in Canadian Mining Jour., v. 76, no. 6, p. 83.
- Schlack, E. A., and Lacke, J. K., 1970, Relationship of automotive lead particulates to certain consumer crops: Environmental Sci. and Technology, v. 4, p. 321-332.
- Shacklette, H. T., 1960, Soil and plant sampling at the Mahoney Creek lead-zinc deposit, Revillagigedo Island, southeastern Alaska, in Short papers in the geological sciences: U.S. Geol. Survey Prof. Paper 400-B, p. B102-B104.
- _____, 1963, Variation in element content of American elm tissue with a pronounced change in the chemical nature of the soil, in Short papers in geology and hydrology: U.S. Geol. Survey Prof. Paper 475-C, p. C105-C106.
- _____, 1965, Bryophytes associated with mineral deposits and solutions in Alaska: U.S. Geol. Survey Bull. 1198-C, 18 p.
- Staker, E. V., 1942, Progress report on the control of zinc toxicity in prat soils: Soil Sci. Soc. America Proc., v. 7, p. 387-392.
- Starikov, V. S., Kononov, B. T., and Brustein, I. M., 1964, Biochemical prospecting and the results of its use in the Gornaya Osetiya: Geokhimiya 1964, no. 10, p. 1070-1072; translated in Geochemistry International, v. 1, p. 1019-1021.
- Stoklasa, J., 1913, The influence of uranium and lead on plants: Acad. Sci. [Paris] Comptes rendus, v. 156, no. 2, p. 153-155.
- Talipov, P. M., 1964, Concentration of nonferrous metals in soils and plants of the Sary-Chechu and Uch-Kulach regions Uzbekistan: Geokhimiya 1964, no. 5, p. 457-467; translated in Geochemistry International, v. 1, p. 441-450.
- Ter Haar, Gary, 1970, Air as a source of lead in edible crops: Environmental Sci. and Technology, v. 4, no. 3, p. 226-229.
- Thyssen, S. W., 1942, Gechemische und pflanzenbiologische Zusammenhänge in Lichte der angewandten Geophysik [Geochemical relations and botanical relationships in the light of applied geophysics]: Beitr. zur angewandten Geophysik, v. 10, no. 1, p. 35-84.
- Tsutsura, M. N., 1948, The influence of boron and lead on the development and crops of sunflowers [in Russian]: [Scientific report of Dniepropetrovsk City Institute], v. 30.
- Wallace, Arthur, 1971, Regulation of the micronutrient status of plants by chelating agents and other factors: Los Angeles, California Univ. 34P51-53. Pub. by the author, Los Angeles, Calif.
- Warren, H. V., 1961, Some aspects of the relationships between health and geology: Canadian Jour Public Health, v. 52, p. 157-164.
- _____, 1966, Some aspects of lead pollution in perspective: Jour. College of General Practitioners, v. 11, p. 135-142.
- _____, 1972, Variations in the trace element contents of some vegetables: Jour. Royal College of General Practitioners, v. 22, p. 56-60.
- Warren, H. V., and Delavault, R. E., 1960, Observations on the biogeochemistry of lead in Canada: Royal Soc. Canada Trans., ser. 3, v. 54, p. 11-20.
- _____, 1962, Lead in some food crops and trees: Jour. Sci. and Food Agr. [London], v. 13, no. 2, p. 96-98.
- _____, 1971, Variations in the copper, zinc, lead, and molybdenum contents of some vegetables and their supporting soils, in Cannon, H. L., and Hopps, H. C., eds., Environmental geochemistry in health and disease: Geol. Soc. America Mem. 123, p. 97-108.
- Warren, H. V., Delavault, R. E., and Cross, C. H., 1966, Mineral contamination in soil and vegetation and its possible relation to public health, in Pollution and our environment: Canadian Council Resource Ministers Natl. Conf. [Montreal], Background Paper A3-5, 11p.
- Warren, H. V., Delavault, R. E., Fletcher, K. W., and Wilks, E., 1971, A study in lead pollution: Western Miner, Feb. 1971, p. 22-26.
- Webb, J. S., and Millman, A. P., 1951, Heavy metals in vegetation as a guide to ore—A biogeochemical reconnaissance in West Africa: Inst. Mining and Metallurgy Trans. [London], v. 60, p. 475-504.
- Wherry, E. T., and Buchanan, Ruth, 1926, Composition of the ash of Spanish-moss: Ecology, v. 7, no. 3, p. 503-506.
- Wild, H., and Wiltshire, G. H., 1971, The problem of vegetating Rhodesian mine dumps examined: Chamber of Mines [Rhodesia] Journal, v. 13, no. 11, p. 26-30; no. 12, p. 35-37.
- Worthington, J. E., 1955, Biogeochemical prospecting at the Shawangunk Mine—A case study: Econ. Geology, v. 50, no. 4, p. 420-429.
- Zundahl, R. L., and Arvik, J. H., 1972, Lead in soils and plants: Symposium on Environmental Chemicals—Human and Animal Health, Fort Collins [Colorado] 1972 (sponsored by U.S. Environmental Protection Agency and Insu. Rural Environmental Health, Colorado State Univ.), Proc., p. 33-40.

LEAD IN THE ATMOSPHERE, NATURAL AND ARTIFICIALLY OCCURRING LEAD, AND THE EFFECTS OF LEAD ON HEALTH

By H. L. CANNON

The amount of lead introduced into the environment from natural sources appears to be small compared to that made available in one way or another by man. This lead, in turn, is being absorbed by man at rates estimated by Patterson (1965) to be 30 times higher than inferred natural rates. Any discussion of lead in the environment must consider, therefore, the sources and effects of contamination lead in the world today. We are all exposed to lead in the air we breathe and in the food and water we ingest; furthermore, workers in particular industries and residents of particular areas are also exposed to occupational and industrial lead.

NATURAL ATMOSPHERIC LEAD

The amount of lead from natural sources that is released into the atmosphere is small, as shown by the following estimates by Patterson (1965):

Source	Lead ($\mu\text{g}/\text{m}^3$)
Silicate dust from soils	0.0005
Volcanic halogen aerosols	0.0003
Volcanic silicate smoke	0.00006
Forest fire smoke	0.00006
Aerosolic sea salts	0.00001
Meteorites and meteoritic smoke	0.0000002

The calculation of these values involved many assumptions, and the total of about $0.0005 + \mu\text{g}/\text{m}^3$ in the atmospheric reservoir is probably low. One source of lead in the atmosphere that may be important in mineralized areas is the exudate from vegetation. Curtin, King, and Mosier (1974) showed that heavy metals, including lead, are given off in vapor by vegetation; lead in condensed tree exudate measured from 1 to 12 ppb. Although the exudate in non-mineralized areas has a much lower lead content, the overall contribution is considerable. A small amount of lead is also released from the decay of radioisotopes. Inasmuch as emanations from the volcano, Mauna Loa, Hawaii, affect the general circulation of the trade winds, Kruger (1969) measured Pb^{210} levels as a means of studying atmosphere chemistry and transport processes. The comparatively large values of Pb^{210} in Hawaii indicate that little is removed from the atmosphere during the trade wind transport over the open ocean. The release of Pb^{210} from radon decay has been estimated at 2.260×10^{-12} curies per m^2 per year for annual rainfall in Great Britain, with a

mean air residency time of about 4 weeks (Hill, 1960). Because of man's widespread contamination of the air with lead throughout the world, data on natural levels of lead in the atmosphere are difficult to obtain. Certainly, in noncontaminated areas of the world, lead in the atmosphere averages less than $0.01 \mu\text{g}/\text{m}^3$ and perhaps less than $0.001 \mu\text{g}/\text{m}^3$. A median lead value of $0.019 \mu\text{g}/\text{m}^3$ was reported by the U.S. National Air Pollution Control Administration (1968) from 29 nonurban collections made in 1965; likewise, no significant lead ($< 0.001 \mu\text{g}/\text{m}^3$) was detected in the fourth quarter of that year at six stations in remote areas of the country, using especially sensitive methods of analysis.

LEAD CONTAMINATION OF THE AIR

Although the quantity of lead ingested from food and water is much higher than that taken in from urban air, inhaled lead is much more readily absorbed; probably some 20–40 percent of lead absorbed is derived from the air (Carroll, 1970). In general, the higher the atmospheric level the higher the blood level of lead and, presumably, the total body burden. The differences in the concentrations of lead in surface air collected by the Atomic Energy Commission along their 80th Meridian network in 1967 are shown in table 34 (Harley, 1970).

In data compiled by McCaldin (1966), mean atmospheric lead concentrations for particular sets of samples ranged from $0.3 \text{ ng}/\text{m}^3$ of lead in 149 samples from suburban stations of the National Air Sampling Network to $44.5 \text{ ng}/\text{m}^3$ in 7 samples collected from Boston's Summer Tunnel. Lazrus, Lorange, and Lodge (1970) reported on atmospheric precipitation samples collected from a nationwide network of 32 stations in the United States. The lead values averaged for each station ranged from 0 to 138 g of lead deposited on 1 hectare by 1 cm of precipitation.

An increase with time in lead in the atmosphere has been shown by Murozami, Chow, and Patterson (1969) who studied the annual ice layers in dated sections in northern Greenland. The lead content of the ice was less than $0.0005 \mu\text{g}/\text{kg}$ in 800 B.C.; $0.01 \mu\text{g}/\text{kg}$ in 1750, at the beginning of the Industrial Revolution; $0.07 \mu\text{g}/\text{kg}$ in

TABLE 31.—Lead concentrations in surface air in 1967 from selected sites along the 80th Meridian

[Data from U.S. Atomic Energy Commission (cited in Harter, 1970)]

Site sampled	Latitude	Lead (ng. m ⁻³)
Thule, Greenland	70° N	<0.01
Moosewater, Canada	56° N	0.06
New York, N.Y.	41° N	2.5
Sterling, Va.	39° N	.74
Miami, Fla.	26° N	1.7
Bimini, Bahama Islands	26° N	0.10
San Juan, P.R.	18° N	0.80
Bahia, Panama	9° N	0.23
Guayaquil, Ecuador	2° S	0.35
Lima, Peru	12° S	0.50
Chachabua, Peru	16° S	0.09
Antofagasta, Chile	24° S	0.06
Santiago, Chile	33° S	0.87
Punta Arenas, Chile	53° S	0.06

1940; and 2.5 $\mu\text{g/kg}$ in 1965. Lead contents of Antarctic ice are much lower, probably because much less lead is introduced by man into the air of the southern hemisphere than into that of the northern hemisphere.

Estimates of the residence time of lead in air range from 1 to 4 weeks depending on the size of the particulate matter with which the lead is associated (Lagerwerff, 1972). Measurements of aerial concentrations of Pb^{210} show an upward transport of the finer particulates into the troposphere and beyond. The aerosols then travel toward the poles, where they become concentrated and sink again into the atmosphere. The cycle is closed by surface air currents which move toward the equator.

The most significant contribution of lead to the atmosphere is from the combustion of leaded gasoline, as table 35 shows. According to TerHaar and Bayard (1971) the lead originates in the antiknock fluid, which contains PbBr_2 , PbBrCl , Pb(OH)Br , $(\text{PbO})_2\text{PbBr}_2$, and $(\text{PbO})_2\text{PbBrCl}$. After burning, the compounds recombine, so that after 18 hours 75 percent of the bromides and 30–40 percent of the chlorides disappear, and the proportion of lead carbonates and lead oxides are increased. A study of the aerosols in Fairbanks, Alaska, by Winchester, Zoller,

Duce, and Benson (1967) showed that although the weight ratio Cl:Pb averages close to that of ethyl fluid (0.34) the Br:Pb ratio is 4 times less than that of ethyl fluid (0.39). This information supports the theory that lead halide particles, formed initially by combustion of ethyl fluid, lose bromine by oxidation and volatilization. The extent of the lead contribution to the atmosphere from ethyl gasoline was proved by Chow and Johnstone (1965), who determined that the isotopic composition of the lead from ethyl gasoline and of aerosols from the Los Angeles basin were the same. The lead from car exhaust was identified also in mountain snows and in the surface waters of the ocean. This identification followed a joint study by the U.S. Public Health Service and the petroleum industry of the lead in the atmosphere of three cities—Cincinnati, Philadelphia, and Los Angeles—which was conducted from June 1961 to May 1962 (Ludwig and others, 1965), during which time 3,400 samples were collected from 20 stations. They found an average concentration of 1.4 ng/m^3 in Cincinnati, 1.6 ng/m^3 in Philadelphia, and 2.5 ng/m^3 in Los Angeles. Concentrations as high as 44 ng/m^3 were measured in a vehicular tunnel. The highest concentrations were found during the autumn and winter months and in the early morning hours. Other studies in the United States and elsewhere have substantiated these findings. Temperature inversion phenomena in San Diego, which prevent the vertical movement of air above the base of the inversion layer, were studied by Chow and Earl (1970). Although pollution in San Diego is relatively low compared to that of other cities, average weekly lead concentrations of as much as 8 ng/m^3 were measured.

A study by Daines, Motto, and Chilko (1970) has shown that a relationship exists between the amount of lead in the air and traffic volume, proximity to the highway, engine acceleration, and wind direction. They also found that traffic markedly affected lead content of air only in a relatively narrow zone along the highway, with the lead content decreasing more than 50 percent in the interval from 10 to 150 feet (3 to 46 m). Ault, Senchal, and Erlebach (1970) demonstrated that there are significant differences in lead isotopic ratios found in rock, soils, grasses, tree leaves, normal air particulate, and those found in coal, fly ash, gasoline, and fuel oil. The $\text{Pb}^{206}/\text{Pb}^{204}$ ratio of 18.2 in air within 500 feet (152 m) of a turnpike approached that of gasoline (18.3), whereas at greater distances the ratio averaged 18.7.

A less serious source of atmospheric lead is in fly ash which originates mainly from the burning of coal by power plants, steel mills, cement plants, and other industries. In a recent U.S. Geological Survey study of the coal and fly ash produced by power plants in the Southwest Energy Program, it was found that coal being produced for 10 power plants had a median content of 50 ppm lead in ash (73 samples), with a range of 30–200 ppm. Bottom ash had a median content of 30 ppm, with a range

TABLE 35.—Lead emissions in the United States, 1968

[Data from U.S. Environmental Protection Agency (cited in National Research Council, 1972)]

Emission source	Lead emitted (thousands lb)	
	(thousands lb)	(tons, yr)
Gasoline combustion	181,000	199,000
Coal combustion	920	1,000
Fuel oil combustion	24	26.5
Lead alkyl manufacturing	810	890
Primary lead smelting	174	192
Secondary lead smelting	811	892
Brass manufacturing	521	573
Lead oxide manufacturing	20	22
Gasoline transfer	36	39.5
Total	181,316	202,635

of 20–30 ppm; fly ash had a median content of 50 ppm lead with a range of 20–70 ppm. At the Four Corners plant, in San Juan County, N. Mex., fly ash collected in the stack was compared with the effluent falling on vegetation and soil of the surrounding area. The fly ash in the stack averaged 70 ppm lead and the effluent only 20 ppm. Analyses of the top one-half inch of soil along two 6.5-mile (10.4-km) traverses from the power plant indicated, for 1.5 miles (2.4 km), a lead content above the 20 ppm reported by Shacklette, Hamilton, Boerngen, and Bowles (1971) as average for U.S. soils, but the lead value at no point was greater than 30 ppm (Cannon and Anderson, 1972).

A major but relatively local source of atmospheric lead is the effluent from mining and smelting operations. Djurić, Kerin, Graovac-Leposavić, Novak, and Kop (1971) reported on a detailed study of lead levels in air, water, plants, and urine in the environs of a lead smelter in Yugoslavia. The smelter lies in a basin, has been operative since 1746, and currently produces 22,000 tons (19,800 t) of lead annually. The stack had no filtering devices until 1969. Samples of air collected in 1967 from three villages in the valley had a lead content ranging from 1.3 to 84.0 ng/m³, with considerable variation on different sampling dates. Lead contents in soils ranged from 91 to 24,880 mg/kg, compared with 0.8–37.4 mg/kg in uncontaminated soil. The river that received effluent from the smelter ranged in lead content from 685.12 mg/l at the smelter to 2.89 mg/l 22 km below the smelter. Above the smelter the river contained only 0.001–0.02 mg/l. Analyses of food and forage show relatively low lead levels in peeled produce but high levels of lead in lettuce and hay; the lead levels in hay are toxic to cattle if the hay is used exclusively and continuously as forage. Milk, meat, and honey were also contaminated, the lead content in milk being 40 times the national average in the United States. Lead in the environment is being absorbed by the inhabitants at levels sufficient to induce a physiologic response.

A study has been made of the distribution of lead around two smelters in Toronto, Canada, and of blood lead levels in the local families. The lead fallout was shown to originate from episodic large-particulate emissions from near-ground sources rather than from stack fumes. Between 13 and 30 percent of the children living in the contaminated areas had absorbed excessive amounts of lead, but probably the lead was ingested from contaminated dusts rather than from drinking water, home-grown vegetables, air, or paint pica. Of the children who had absorbed excessive lead, most of those selected for special study showed metabolic changes; 10–15 percent of this selected group showed subtle neurological dysfunctions and minor psychomotor abnormalities (Roberts and others, 1974).

Cases of lead poisoning have been reported among workers and residents near a lead smelter in India where the daily flue emissions contained almost 2,000 lb (900 kg)

of lead; in Colombia, families living in lead foundries exhibit chronic symptoms, and many children die from lead poisoning (Haley, 1969).

Lead poisoning in 75 children in Smeltertown, an area of 120 families near El Paso, Tex., where lead has been smelted since 1887 (Wall Street Journal, 1972a, b), has recently shown the urgency of the problem in this country. An intensive monitoring program has been initiated to study the effects on the environment of the so-called New Lead Belt (Wixson and others, 1972) in Missouri, which accounted for more than 80 percent of the total United States lead production in 1973. Lead levels in soils, air, plants, and water are being carefully checked and the effects of lead pollution on grazing animals are being studied. Long-term studies should contribute much to our knowledge of the long-range effects of low-level lead contamination on the health of animals, including man.

Cigarettes represent a minor but common source of lead. Although most of the lead remains in the ash, an intake of 20 ng per pack from the smoke has been estimated by Horton (1966). Studies by the Air Pollution Control Administration have demonstrated that in urban areas smokers have 1.24 times more blood lead than nonsmokers and in rural areas, 1.42 times more blood lead (Hofbauer, 1960).

LEAD CONTAMINATION OF WATER AND FOOD

Pollution lead may be ingested from several sources. A main source of lead poisoning in underprivileged children is pica, or an abnormal craving to ingest odd things including fragments of lead-based paint from cribs and walls (Haley, 1969). A decrease in plumbism from this source can be expected as current laws ordering the substitution of titanium-based paints on nursery furniture become effective. Cooking in earthenware pottery with a lead glaze or the use of such pottery as containers for acid foods can be a cause of lead poisoning (Klein and others, 1970). Vegetables and fruits are easily contaminated by lead-arsenate sprays and, although less lead arsenate is used than formerly, a buildup of the metals occurs in the soils of old orchards where a reservoir of lead is available to crops long after the use of lead arsenate has ceased. Experimental work by Jones and Hatch (1945) showed that crops grown in soil taken from an orchard with a spray record of 22 years assimilated from 1 to 3 times more lead in the above-ground portions and 2 to 8 times in the below-ground portions than the same crops grown in unsprayed soil; a maximum lead value of 35 ppm in dry weight of peeled eggplant was recorded.

Lead may also be introduced into cultivated land through the use of tailings from lead-zinc mines or of high-lead limestones for fertilizer. Warren, Delavault, and Cross (1966) have reported on the use of a limestone containing 45 ppm lead for fertilizer on land which then produced oats containing 3–4 ppm lead in the dry weight.

The soil and vegetation in the vicinity of mining operations (even though long defunct) may be contaminated by waste and spoil piles. The lower part of the Tamar Valley district of west Devon and Cornwall in Great Britain is a richly mineralized area which was mined for base metals in the 19th century. Soils from pastures and gardens contain unusually high contents of lead; garden soils had a maximum of 522 ppm total lead and 36 ppm available lead (extractable with acetic acid) (Davies, 1971). Radishes were used as a convenient test crop to measure actual uptake. They contained as much as 74 ppm lead in the ash. Davies (1972) concluded that the inhabitants of this valley are exposed to a greater lead insult than similar populations elsewhere in Great Britain.

Drinking water standards have been set by the U.S. Public Health Service at 0.5 mg/l maximum for lead. Although ground-water lead levels have remained relatively unaffected, man has increased lead in surface waters through agricultural practices, fallout of lead alkyl aerosols, contact with scrap and waste heaps, and mining activities. However, according to Patterson (1965), in rural areas the atmospheric washout of lead alkyl products should immediately be fixed in the clay fractions of the soil and thus make little contribution to the surface waters except through storm sewers. Sewer treatment plants contribute lead to surface waters, although about 65 percent of the lead in drinking water is removed in treatment processes, according to Horton (1966). He stated that lead is frequently present in unfiltered surface waters at levels well above the maximum permissible concentration but is generally much lower in filtered water. Analyses of 42 sewage sludges from rural and industrial towns in England and Wales show very large concentrations of certain trace elements. The sludges contained from 120 to 3,000 ppm lead and had a median content of 700 ppm in dry weight (Berrow and Webber, 1972).

Contributions of lead to ground and surface waters from rainfall can range as high as 0.49 mg/l in areas of industrial contamination or high traffic volume. However, Lazrus, Lorange, and Lodge (1970) have shown that there is, on the average, twice as much lead in atmospheric precipitation as in municipal water supplies, suggesting that the lead precipitates or is adsorbed on suspended matter and is thus filtered out in processing. Ettlinger (1966) showed maximum lead in surface water to be associated with metal-working and chemical industries, but concluded that only a fraction of the lead in surface water remains dissolved.

Lead piping and lead solder used with copper tubing may also be a significant source of lead in water distribution systems. According to Patterson (1965) many of our largest cities use lead pipe exclusively for water service connections. She has estimated a per capita contribution of 5 µg/l of lead from lead used in water distribution systems.

EFFECTS OF INGESTED LEAD ON LIVESTOCK

In animals, the toxic effects of lead ingested in contaminated vegetation have often been noted. Horses, especially young ones, are particularly susceptible to lead poisoning. Chronic lead poisoning in six foals on three different properties within 5 miles (8 km) of the Trail smelter in British Columbia and subsequent poisoning of introduced horses has been described by Schmitt and others (1971). The symptoms were loss of weight, muscular weakness, stiffness of joints, and harsh, dry coats. A thorough investigation showed that young horses were more susceptible than old horses, and that lead rather than zinc, arsenic, or cadmium was the cause of the illness. Soil, forage, and blood levels of the horses on the three properties were as follows:

Property	Distance from smelter (miles)	Lead in top 1 inch soil (ppm)	Lead in forage (ppm dry weight)	Mean lead in blood (µg/100 g)
A	2.0	750	38	22.6
B	1.5	620	90	31.6
C	.5	2,900	264	37.6

In all but a few fruits and vegetables grown within 5 miles (8 km) of the smelter, lead concentrations were considered to be acceptable for human consumption, and human urine lead levels were not elevated.

The death of four horses that had been corralled on the tailings pond of an old gold mine near Evergreen, Colo., was investigated by D. M. Sheridan and H. L. Cannon of the U.S. Geological Survey (unpub. data, 1970). The drinking water for the horses contained high concentrations of fluorine but the autopsy report showed lead poisoning. A noxious weed, *Grindelia squarrosa*, evident in the hay fed to the horses, which had been cut at a city country club, was subsequently found to contain 1,540 ppm lead in the dry weight. Inasmuch as the grass in the hay contained only 5.2 ppm, *Grindelia* appears to be an accumulator of toxic levels of lead.

Horses subsequently died in a pasture near Centerville, Mo., where 15 samples of cedar were reported by Connor, Shacklette, and Erdman (1971) to contain as much as 1,200 ppm lead in the dry weight, with a geometric mean of 348 ppm dry weight. The area was believed to have been contaminated by lead from ore trucks.

An outbreak of acute lead poisoning among cattle pastured near a lead smelter was studied by veterinarians from the University of Minnesota (Hammond and Aronson, 1964). The forage contained 148–285 ppm lead in the dry weight. Acute bovine lead poisoning resulted from long-term continuous intake of contaminated forage, whereas horses in the same environment responded by long-delayed onset of the classical syndrome of chronic equine plumbism. These and other case histories suggest that airborne lead absorbed by and adhering to plants may be more hazardous to grazing animals than to man.

OCCUPATIONAL LEAD

Plumbism from occupational lead used in automobile body manufacture and repair, foundries, electrolyte printing, storage battery manufacture, secondary smelters, and munition plants was a hazard in this country before 1945. Improved occupational practices since that time and the introduction in 1945 of safe working standards for lead levels in air and urine have been responsible for decreasing exposure to airborne lead in dust and fumes by several orders of magnitude (Stokinger, 1966). In a study of workers who are regularly exposed to gasoline additives, it was found that garage mechanics show elevated lead levels in urine, but the levels are below the present acceptable limits. Although inhalation intoxication and skin absorption have caused problems in other countries (Haley, 1969), controls instituted in the United States have resulted in safe handling of lead alkyls, tetraethyl lead, and tetramethyl lead during manufacture. Nevertheless, after the manufactured products leave the plant, they may still pose a hazard through careless handling by the consumer; for instance, acute plumbism among children has been caused by burning old battery cases for fuel in fireplaces and cookstoves (National Research Council, 1972).

The contributions of lead to the environment that result from man's activity are much greater, therefore, than the lead that is available in the environment from natural sources. Considerably improved controls and monitoring programs are indicated.

ABSORPTION AND EFFECTS OF LEAD ON HEALTH

The human body tends to discriminate against the heavier metals in favor of the lighter, using the lighter in metabolic processes and being poisoned by the heavier (Patterson, 1965). The chemistry of lead is similar to that of barium in its behavior in the body, particularly in regard to deposition in and mobilization from the skeleton.

Lead in animals (including man) is concentrated largely in bone, although small amounts of lead occur in other types of tissue. Amounts that have been reported are as follows (Haley, 1969):

Tissue	Lead (μg/100 g)
Long bone.....	670-5,590
Flat bone.....	210-1,110
Liver.....	40- 280
Kidney.....	15- 160
Muscle.....	10- 170
Brain.....	10- 90

Bone represents the greatest storage site of lead, which is bound to bone by absorption or exchange at the surfaces of bone salt crystals, or is combined with the sulfate in the organic matrix. However, according to work by Kehoe (1961), the average individual appears to be in lead balance; the body burden of lead is established early in life and does not change appreciably throughout the life span.

Haley (1969) reported lead concentrations in blood from 10 to 26 $\mu\text{g}/\text{ml}$; however, the lead levels of blood can be raised experimentally to as much as 450 $\mu\text{g}/100\text{ g}$ by heavy dosages in food and air, with accompanying increases in urinary and fecal lead (Kehoe, 1964). Lead interferes with normal maturation of erythroid elements in the bone marrow and inhibits hemoglobin synthesis in precursor cells (Kench and others, 1952). Lead also affects prophylin metabolism and interferes with the activity of several enzymes.

Although less than 10 percent of lead ingested by man is absorbed, 20-25 percent of respiratory intake may be retained and absorbed. Epidemiologic studies of blood lead levels show a logarithmic regression on estimated atmospheric exposure, according to Goldsmith and Hexter (1967), who postulated that further increases in atmospheric lead will result in predictable, progressively higher lead levels in the population. In a group of workers who were exposed to industrial lead and who had blood lead levels of 0.045-0.14 $\text{mg}/100\text{ g}$, the serum transaminase activity was increased, suggesting that subclinical liver impairment may occur at levels below the "safe" level of 0.07 $\text{mg}/100\text{ g}$ (Hofreuter, 1960). Experiments by Schroeder, Vinton, and Balassa (1963) with lead-fed rats showed increased mortality rates in both sexes and renal and hepatic accumulations of lead similar to those in adult humans. However, there is evidence that the average intake of lead from food has not changed from its level during the three-decade period prior to 1965, because the increase in environmental lead in food has been balanced by the decrease in use of lead in agricultural chemicals and in food processing and packaging (Lewis, 1965).

In children, overt manifestations of acute lead poisoning, plumbism, differ from those of adults, and the mortality rate is relatively high. Symptoms may include anemia, gastrointestinal distress, and encephalopathy. The last may result in early death, permanent symptoms of brain damage, or complete recovery (Haley, 1969). Adult or chronic lead poisoning requires years to develop to the critical level, which is recognizable by symptoms such as headache, muscle pains, constipation, abdominal tenderness, colic, weight loss, and fatigue (Johnstone, 1961). Kidney damage from lead has not been identified in the United States although it is commonly reported in European countries; this difference may be due to poorer industrial hygiene in European countries. Renal lesions, which may be caused by lead ingestion, have been shown to lead to hypertension and may also predispose to gout as a result of defective urate secretion (Emmerson, 1965). An important symptom of chronic plumbism is the neuromuscular involvement, usually of the extensor muscles, as in wrist drop. Chronic exposures to lead in the water supply have been shown to result in increased miscarriages and stillbirths; the pregnant woman and her

fetus are highly susceptible to lead poisoning (Wilson, 1966).

The poisoning of industrial workers with organic lead alkyls—tetraethyl or tetramethyl lead—causes a different set of symptoms called the acute brain syndrome. These symptoms include irritability, insomnia, emotional instability, tendon reflexes, and tremor. Delusions and hallucinations may occur (Sanders, 1965). However, lead alkyls decompose rapidly and are largely handled physiologically as inorganic water-soluble lead (Tepper, 1966). Although, according to Haley, there are no documented cases of lead poisoning in children or adults attributable to airborne lead from the combustion of leaded gasoline, continuous monitoring has been advised and realistic lead tolerance levels advocated after further study.

REFERENCES CITED

- Ault, W. U., Senechal, R. G., and Erlebach, W. E., 1970, Isotopic composition as a natural tracer of lead in the environment; *Environmental Sci. and Technology*, v. 4, no. 4, p. 305-314.
- Berrow, M. L., and Webber, J., 1972, Trace elements in sewage sludges. *Jour. Sci. Food and Agriculture* [London], v. 23, p. 95-100; abs. in *Chem. Abs.*, v. 76, no. 117245u, 1972.
- Cannon, H. L., and Anderson, B. M., 1972, Trace element content of the soils and vegetation in the vicinity of the Four Corners Power Plant, Pt. 3 of Coal resources work group report: U.S. Dept. Interior, Southwest Energy Study, open-file report, 44 p.
- Carroll, R. E., 1970, Trace element pollution in air, in Hemphill, D. D., ed., *Trace substances in environmental health—3*, [3d Ann. Conf. Proc.] Columbia, Missouri Univ., p. 227-231.
- Chow, T. J., and Earl, J. L., 1970, Lead aerosols in the atmosphere—Increasing concentrations: *Science*, v. 169, p. 577-580.
- Chow, T. J., and Johnstone, M. S., 1965, Lead isotopes in gasoline and aerosols of Los Angeles Basin, California: *Science*, v. 147, p. 502-505.
- Connor, J. J., Shacklett, H. T., and Erdman, J. A., 1971, Extraordinary trace-element accumulations in roadside cedars near Centerville, Missouri, in U.S. Geological Survey research 1971: U.S. Geol. Survey Prof. Paper 750-B, p. B151-B156.
- Curtin, G. C., King, H. D., and Mosier, E. L., 1974, Movement of elements into the atmosphere from coniferous trees in subalpine forest of Colorado and Idaho: *Jour. Geochem. Explor.*, v. 3, no. 3, p. 245-263.
- Daines, R. H., Motto, Harry, and Chiklo, D. M., 1970, Atmospheric lead—its relationship to traffic volume and proximity to highways: *Environmental Sci. and Technology*, v. 4, no. 4, p. 318-322.
- Davies, B. E., 1971, Trace metal content of soils affected by base metal mining in the West of England: *Oikos* [Copenhagen], v. 22, no. 3, p. 1-7.
- , 1972, Occurrence and distribution of lead and other metals in two areas of unusual disease incidence in Britain: *Internat. Symposium on Environmental Health Aspects of Lead*, Amsterdam 1972, Proc., p. 125-134.
- Djurić, Dušan, Kerin, Zarka, Gracovac-Leposavic, Ljubica, Novak, Ljiljana, and Kop, Marija, 1971, Environmental contamination by lead from a mine and smelter: *Archives Environmental Health*, v. 23, no. 4, p. 275-279.
- Emmerson, B. T., 1965, The renal excretion of urate in chronic nephropathy: *Australian Annals of Medicine*, v. 14, p. 295-303.
- Ettinger, M. B., 1966, Lead in drinking water: *Symposium on Environmental Lead Contamination*, 1965, U.S. Public Health Service Pub. 1440, p. 21-27.
- Goldsmith, J. R., and Hexter, A. C., 1967, Respiratory exposure to lead—Epidemiological and experimental dose-response relationships: *Science*, v. 158, no. 3797, p. 132-134.
- Haley, T. J., 1969, A review of the toxicology of lead: *Am. Petroleum Inst. Air Quality Mon.* 69-7, 53 p.
- Hammond, P. B., and Aronson, A. L., 1964, Lead poisoning in cattle and horses in the vicinity of a smelter: *Conf. Veterinary Medicine*, 1963, New York Acad. Sci. Annals, v. 111, no. 2, p. 595-611.
- Harley, J. H., 1970, Discussion of sources of lead in perennial ryegrass and radishes: *Environmental Sci. and Technology*, v. 4, p. 225.
- Hill, C. R., 1960, Lead-210 and polonium-210 in grass: *Nature*, v. 187, p. 211-212.
- Holfreuter, D. H., 1960, Evaluating the health hazards of exposure to lead and carbon monoxide: *Air Pollution Medical Research Conf.*, San Francisco 1960 [Proc.], available from U.S. Dept. Health, Education, and Welfare, Public Health Service, Air Pollution Div., Cincinnati, Ohio 45226.
- Horton, R. J. M., 1966, Major sources of lead pollution: *Symposium on Environmental Lead Contamination*, 1965, U.S. Public Health Service Pub. 1440, p. 137-142.
- Johnstone, R. T., 1964, Clinical inorganic lead intoxication: *Archives Environmental Health*, v. 8, no. 2, p. 250-255.
- Jones, J. S., and Hatch, M. B., 1945, Residues and crop assimilation of arsenic and lead: *Soil Sci.*, v. 60, p. 277-288.
- Kchor, R. A., 1961, The metabolism of lead in man in health and disease: *Harben Lecture*, no. 1, 1960, 18 p.; reprinted in *Jour. Royal Inst. Public Health and Hygiene*, v. 24, p. 81-97.
- , 1964, Metabolism of lead under abnormal conditions: *Archives Environmental Health*, v. 8, no. 2, p. 235-243.
- Kench, J. E., Lane, R. E., and Varley, H., 1952, Urinary coproporphyrins in lead poisoning: *British Jour. Medicine*, v. 9, p. 133-137; abs. in *Chem. Abs.*, v. 46, no. 11450h, 1952.
- Klein, Michael, Nemer, Rosalie, Harpur, Eleanor, and Corbin, Richard, 1970, Earthenware containers as a source of fatal lead poisoning: *New England Jour. Medicine*, v. 283, no. 13, p. 669-672.
- Kruger, Paul, 1969, Lead-210 in surface air along the slopes of Mauna Loa volcano, Hawaii: U.S. Atomic Energy Comm. Rept. ST-326-PA-16-3, 24 p.; available only from U.S. Dept. Commerce Natl. Tech. Inf. Service, Springfield, Va. 22161.
- Lagerwerff, J. V., 1972, Lead, mercury and cadmium as environmental contaminants, Chap. 23 in *Micro nutrients in agriculture*: Madison, Wis., Soil Sci. Soc. America, p. 593-696.
- Larus, A. L., Lorange, Elizabeth, and Lodge, J. P., Jr., 1970, Lead and other metal ions in United States precipitation: *Environmental Sci. and Technology*, v. 4, no. 1, p. 53-58.
- Lewis, K. H., 1965, The diet as a source of lead pollution: *Symposium on Environmental Lead Contamination*, 1965, U.S. Public Health Service Pub. 1440, p. 17-20.
- Ludwig, J. H., Diggs, D. R., Hesselberg, H. E., and Maga, J. A., 1965, Survey of lead in the atmosphere of three urban communities, a summary: *Am. Indus. Hygiene Assoc. Jour.*, v. 26, p. 270-284.
- McCaldin, R. O., 1966, Estimation of sources of atmospheric lead and measured atmospheric lead levels: *Symposium on Environmental Lead Contamination*, 1965, U.S. Public Health Service Pub. 1440, p. 7-15.
- Murozani, M., Chow, T. J., and Patterson, C. C., 1969, Chemical concentrations of pollutant lead aerosols, terrestrial dusts, and sea salts in Greenland and Antarctic snow strata: *Geochim. et Cosmochim. Acta*, v. 33, p. 1247-1294.
- National Research Council, Division of Medical Sciences, Committee on Biological Effects, 1972, *Lead—Airborne lead in perspective*: Natl. Acad. Sci., 330 p.
- Patterson, C. C., 1965, Contaminated and natural lead environments of man: *Archives Environmental Health*, v. 11, p. 344-360.
- Roberts, T. M., Hutchinson, T. C., Pasiga, J., Chatopadhyay, A., Jervis, R. E., and VanLoon, J., 1974, Lead contamination around

- secondary smelters—Estimation of dispersal and accumulation by humans. *Science*, v. 186, p. 1120-1122.
- Sanders, L. W., 1965, Lead excretion and health of antiknock blenders. *Archives Environmental Health*, v. 10, no. 6, p. 886-892.
- Schmitt, Nicholas, Brown, Gordon, Devlin, E. L., Larsen, A. A., McCausland, F. D., and Savile, J. M., 1971, Lead poisoning in horses, an environmental health hazard. *Archives Environmental Health*, v. 23, no. 3, p. 185-195.
- Schroeder, H. A., Vinton, W. H., Jr., and Balassa, J. J., 1963, Effects of chromium, cadmium, and lead on the growth and survival of rats. *Jour. Nutrition*, v. 80, no. 1, p. 48-54.
- Shacklette, H. T., Hamilton, J. C., Boerngen, J. C., and Bowles, J. M., 1971, Elemental composition of surficial materials in the conterminous United States. U.S. Geol. Survey Prof. Paper 574-D, 71 p.
- Stokinger, H. E., 1966, Recent history of lead exposure in U.S. industry, 1935-1965: Symposium on Environmental Lead Contamination, 1965, U.S. Public Health Service Pub. 1440, p. 29-35.
- Tepper, L. B., 1966, Under what circumstances is direct contact with lead dangerous? Symposium on environmental lead contamination, 1965, U.S. Public Health Service Pub. 1440, p. 59-62.
- TerHaar, G. L., and Bayard, M. A., 1971, Composition of airborne lead particles. *Nature*, v. 232, p. 553-554.
- U.S. National Air Pollution Control Administration, 1968, Air quality data from national air surveillance networks and contributing State and local networks [1966 ed.]. U.S. Natl. Air Pollution Control Admin. Pub. APTD 68-9, 157 p.
- Wall Street Journal, 1972a, El Paso mayor seeks Federal aid in area hit by lead poisoning. New York, Wall Street Jour., March 24, 1972.
- , 1972b, Lead-poisoning issue eclipses pollution suit fought against Asarco. New York, Wall Street Jour., March 31, 1972.
- Warren, H. V., Delavault, R. E., and Crow, C. H., 1966, Mineral contaminations in soil and vegetation and its possible relations to public health, in *Pollution and our environment*. Canadian Council of Resources Ministers Natl. Conf. (Montreal), Background Paper A3-3, 11 p.
- Wilson, A. T., 1966, Effects of abnormal lead content of water supplies on maternity patients. *Scottish Medical Jour.*, v. 11, p. 73-82.
- Winchester, J. W., Zoller, W. H., Duce, R. A., and Bemon, C. S., 1967, Lead and halogens in pollution aerosols and snow from Fairbanks, Alaska. *Atmospheric Environment*, v. 1, no. 2, p. 105-119.
- Wixson, B. G., Bolter, Ernst, Gale, N. L., Jennett, J. C., and Purushothaman, K., 1972, The lead industry as a source of trace metals in the environment: Environmental Resources Conf. on Cycling and Control of Metals, Columbus, Ohio, Battelle Memorial Inst., Proc., 11 p.

ANALYTICAL METHODS FOR THE DETERMINATION OF LEAD

By F. N. WARD and M. J. FISHMAN

DETERMINATION OF LEAD IN SOILS AND ROCKS

Methods of chemical analysis with enough sensitivity to measure the low concentrations of lead in soil and rock samples are numerous. Such methods are based on familiar operations of optical emission spectrography, X-ray spectrography, molecular absorption (colorimetry), and atomic absorption. In a review of available methods, a certain amount of judgment has to be exercised in choosing those to be discussed; accordingly, the following discussion will be devoted to the methods most commonly used by the U.S. Geological Survey.

OPTICAL EMISSION SPECTROGRAPHY

Optical emission spectrographic methods are used to determine the lead content of soils, rocks, and minerals at the 5- to 10-ppm level, with a relative standard deviation of 10-20 percent. Such precision is attained with a semi-quantitative procedure variously designated as the three-step or six-step semiquantitative spectrographic method. Better precision is attained with strictly quantitative procedures, but the semiquantitative methods are so widely used in the Geological Survey that some discussion of them is in order.

Quantitative data are achieved by comparing the spectra from unknown soil and rock samples with spectra of standard mixtures obtained under identical conditions of instrumental parameters, sample handling, and so on. The standard spectra are produced from mixtures of different amounts of pure compounds incorporated in matrices whose chemical compositions are similar to those of the host materials of the unknowns. The mixtures of pure compound plus matrix material are accordingly referred to as standard mixtures or simply as standards.

Within an order of magnitude, the concentration of lead in standards differs by a common factor, the cube root of 10 (Myers and others, 1961; Barnett, 1961). An explanation of the theoretical basis of this common factor is beyond the scope of this paper. It suffices to say that within an order of magnitude a series of lead standards would contain the following amounts of lead: the first standard, 1 percent; the second standard, 0.464 percent; the third, 0.215 percent, and so on.

Ward and others (1963) stated that these values could be rounded off respectively to 1, 0.5, 0.2, and 0.1 percent. Within an order of magnitude change in lead concentration, three standards were used and the method was called a three-step semiquantitative spectrographic method. The differences between the standards were called concentration ranges, and these ranges were rather broad. Many spectrographers felt that by inserting additional standards at the logarithmic midpoints of these ranges they could achieve better precision and accuracy. The method henceforth became known as a six-step semiquantitative spectrographic method.

After using both three-step and six-step procedures for a few years many Survey spectrographers concluded that the value of the additional midpoint standards for obtaining more accurate results was debatable and that the time required to prepare the midpoint standards as well as the extra space required on the photographic plate might offset any advantage.

Currently both methods are used in the Geological Survey, although most appraisal studies and exploration programs need only the three-step, or three-standards, procedure.

In applying the method, the spectrographer prepares a standards plate having spectral lines produced by lead concentrations of 1.0, 0.5, 0.2, and 0.1 ppm, and he designates the midpoints of the ranges delineated by these standards as 0.7, 0.3, and 0.15 ppm, respectively. He compares the spectral line of lead from an unknown with the line produced by one of these standards or, if the unknown lies at a midpoint between two standards, with the range delineated by two standards lines. This range is often called a bracket and the midpoint further specified as the geometric midpoint.

Shacklette and others (1971, p. 225) described this method for reporting semiquantitative results as follows.

The values obtained by spectrography were reported in geometric brackets having boundaries 1.2, 0.83, 0.56, 0.38, 0.26, 0.18, 0.12 and so forth, percent; the brackets are identified by their respective geometric midpoints, 1.0, 0.7, 0.5, 0.3, 0.2, 0.15, and so forth. Thus, a reported value of 0.3 percent for example, identifies the bracket from 0.26 to 0.38 percent as the analyst's best estimate of the concentration present. The precision of a reported value is approximately plus or minus one bracket at the 68-

percent level of confidence, and plus or minus two brackets at the 95-percent level.

The lead content of the unknown is thus reported with one of the following numbers: 1.0, 0.7, 0.5, 0.3, 0.2, 0.15, and 0.1, and the reported value for lead will always be one of these numbers expressed as a power of 10 that depends on the relative concentration.

Ideally, the composition of the matrix or material to which pure lead compounds are added to form this series of standards should approximate the composition of the samples as closely as possible, especially with regard to major components. These major components cause changes in the sample excitation, which, along with the spectral lines and physical nature of the samples, affect spectral lines and intensities of the lead analyte. These effects are magnified because of the predominance of the matrix in the standard mixture. For highest accuracy, therefore, standards would have to be incorporated in several different kinds of matrices—for instance, gossan, silicate, or carbonate—and ultimately the number of standards would become unwieldy.

In practice, a compromise is made, and most lead determinations are made on the basis of standards prepared in one or two matrices modified to approximate the vast number of geologic materials analyzed. Further modifications—such as the addition of graphite to the unknown sample in a 2:1 ratio—are made to promote uniform excitation and inhibit the effect of major components in the matrix.

In these semiquantitative methods, spectra of unknowns are compared visually with spectra of standards, and occasionally faulty comparisons along with possible computational errors give rise to shocking results which usually prove embarrassing. Aware of these possibilities, spectrographers of the U.S. Geological Survey worked for several years to develop systems in which human participation was minimized and as many operations as possible were performed instrumentally. The problem was twofold. First, they had to make an instrument to read the line intensities recorded on the plates; however, each plate is unique and has to contain built-in flagging so that the instrument will measure the intensity of the most appropriate line or lines of the elements of interest including lead. Second, the Survey spectrographers had to devise computer programs to perform as many computations as possible, including corrections for matrix and background, and present the final readout in a format useful to geologists. The computer program was devised first and is described by Helz, Walthall, and Bernan (1969); the instrument development came later and is given by Helz (1973). Subsequent applications and improvements are described by Dorrzapf (1973).

X-RAY SPECTROGRAPHY

In the U.S. Geological Survey, lead determinations are made routinely by X-ray spectrographic methods. These

methods are not generally considered as trace methods, but after chemical pretreatment sensitivities as low as 50 ppm with a relative standard deviation of about 20 percent are achieved.

MOLECULAR ABSORPTION (COLORIMETRY)

For more than 25 years, trace amounts of lead in soils and rocks have been determined by molecular absorption methods. The common name for this process—colorimetry—is descriptive, but the process is one of absorption. Under specific conditions lead reacts with certain organic reagents—for instance, dithizone—to form colored species which can be extracted into immiscible solvents such as carbon tetrachloride or xylene.

The absorption of the colored species by these solvents occurs maximally at discrete frequencies, and the amount of absorption can be related to the concentration of lead in the soil or rock sample.

Molecular absorption methods of lead analysis are so numerous that a thorough review is beyond the scope of this paper, but procedures included by Sandell (1959) illustrate some of the available methods. For real samples of igneous rocks the sensitivity of the method is as low as 1 ppm (Thompson and Nakagawa, 1960).

Rapid field methods based on the reaction of lead with dithizone have a sensitivity limit of 20 ppm, which is adequate for reconnaissance studies.

ATOMIC ABSORPTION SPECTROMETRY

Atomic absorption methods for lead in soils and rocks as used in our laboratory were described by Ward and others (1969). Sensitivities as low as 1 ppm are routinely achieved, and under special conditions, such as by using a Delves spoon, the sensitivity can be lowered by one or two orders of magnitude.

Some typical lead values determined routinely by an atomic absorption method are as follows: five repeat determinations on a sandstone yielded 12–16 $\mu\text{g/g}$ lead, with a relative standard deviation of 12 percent; corresponding values on a granite were 22–24 $\mu\text{g/g}$, with a relative standard deviation of 5 percent.

ELECTRON PROBE

The electron probe is useful for determining lead concentrations greater than about 0.1 percent. In ordinary soils and vegetation and in many rocks, the lead concentration is too low for measurement by the probe. In minerals, however, the local concentration of lead may easily exceed the threshold amount, and the probe is most useful for determining such enrichments.

DETERMINATION OF LEAD IN VEGETATION

One routine spectrographic method for determining lead in plant ash calls for mixing equal parts of ash with quartz to simulate the silicic matrix in which the standard powders are incorporated. The obvious advantage is that

the same standard plates can be used on plant ash and silicic rock samples. The obvious disadvantage is that the sensitivity given above for lead in soils and rocks by optical emission spectrography is only 10-20 ppm. This sensitivity is adequate for many species of vegetation, but is inadequate for some specific applications.

Recently Mosier (1971, 1972) incorporated standard powders in a plant-ash base and, with a split-slit technique using a Hartmann diaphragm and a step filter assemblage, achieved a simultaneous recording of 35 elements including such volatile elements as silver, arsenic, bismuth, antimony, and others. Using this procedure Mosier determined amounts as small as 1 ppm lead in plant ash, with a relative standard deviation of 20 percent.

Trace amounts of lead in organic matter can also be measured by analytical methods based on molecular absorption (colorimetry) and atomic absorption. Methods based on X-ray spectrography may also be used after special sample treatment, but many different species contain less than threshold amounts and such X-ray methods are less useful than other procedures discussed here.

Molecular absorption methods for determining lead in vegetation are similar to those for soils and rocks except in sample size and treatment before analysis. Usually a 2-g sample of air-dried and ground vegetation is used; the minimum lead content that can be determined is near 0.25 ppm.

Atomic absorption methods for lead in vegetation are again similar to those for lead in soils and rocks, except in sample size and treatment. Ashing is necessary and can be accomplished either with oxidizing acids or by ignition in a muffle furnace at temperatures of 450°-500°C under controlled conditions to avoid losses.

Detection limits for lead of 0.02 $\mu\text{g}/\text{ml}$ are quoted in the literature (Perkin-Elmer Corporation, 1971). Such limits are achieved with conventional atomic absorption techniques, but with a flameless procedure, Fernandez and Manning (1971) detected as little as 0.4 $\mu\text{g}/\text{g}$. Ward and others (1969) defined sensitivity in more practical terms, and, using a new procedure, they achieved a sensitivity of 1 $\mu\text{g}/\text{g}$ in plant ash. Five samples of fir ash contain 30-60 $\mu\text{g}/\text{g}$ lead. On the basis of 1 percent ash, these values are equivalent to 1.2-2.4 $\mu\text{g}/\text{g}$ lead in air-dry sample.

DETERMINATION OF LEAD IN WATER

The literature on analytical methods for the determination of lead in water is voluminous. U.S. Geological Survey personnel have periodically reviewed the literature of analytical chemistry applied to water analysis; the last such review was published in 1973 (Fishman and Erdmann, 1973). These reviews are a good source of references to published descriptions of analytical procedures for lead, and we will not attempt to duplicate

these references here. The principal methods used by the U.S. Geological Survey for determining lead in aqueous solutions are atomic absorption spectrophotometry and emission spectroscopy. For example, the analyses for this report, which were performed by U.S. Geological Survey personnel using these techniques, and which are described by M. J. Fishman (this volume), were determined on water samples filtered at the time of collection through 0.45- μm membrane filters and acidified with nitric acid to a pH less than 3.

Atomic absorption spectrophotometric methods are being used routinely for the direct determination of many trace elements; however, lead normally occurs in freshwater at concentrations less than can be directly detected by atomic absorption. Therefore, a preconcentration procedure is essential if lead is to be determined by atomic absorption. Brown, Skougstad, and Fishman (1970) described a rapid simple accurate and sensitive preconcentration procedure in which lead is chelated with ammonium pyroldine dithiocarbamate (APDC) at a pH of 2.8, and the chelate is then extracted with methyl isobutyl ketone (MIBK). The extract is aspirated into the flame of an atomic absorption spectrophotometer. Water containing from 1.0 to 20.0 $\mu\text{g}/\text{l}$ lead may be analyzed by this procedure; higher concentrations must be reduced by dilution. None of the substances commonly occurring in natural water interferes with this method. Fishman and Midgett (1968) reported that results obtained by this procedure are in good agreement with those obtained spectrographically.

With the emission spectrograph, lead in water is determined simultaneously with many other minor elements. Three methods are described by Barnett and Mallory (1971). The first method consists of evaporating the water and analyzing the residue, and is used for the analysis of samples whose dissolved-solids concentrations do not exceed about 1,000 mg/l . This method is sensitive, precise, and reasonably accurate. The lower limits of detection vary with the quantity of dissolved solids; however, in order to achieve lower limits of detection for water samples containing more than 1,000 mg/l dissolved solids, it is necessary to separate lead and other minor elements from the major constituents prior to analysis. In the second method, lead and 20 other metallic elements are precipitated with thioacetamide, and the resultant sulfides are converted to oxides and analyzed. With the third procedure, 18 elements, including lead, are precipitated by complexing with tannic acid, thionalide, and 8-hydroxyquinoline. The precipitates are ashed and the resulting oxides analyzed.

REFERENCES CITED

- Barnett, P. R., 1961, An evaluation of whole-order, $\frac{1}{2}$ -order, and $\frac{1}{4}$ -order reporting in semiquantitative spectrochemical analysis: U.S. Geol. Survey Bull. 1084-H, p. 183-206.

- Barnett, P. R., and Mallory, E. C., Jr., 1971, Determination of minor elements in water by emission spectroscopy: U.S. Geol. Survey Techniques Water-Resources Inv. TW15-A2, 31 p.
- Brown, Eugene, Skougstad, M. W., and Fishman, M. J., 1970, Methods for collection and analysis of water samples for dissolved minerals and gases: U.S. Geol. Survey Techniques Water-Resources Inv. TW15-A1, 160 p.
- Dorrapd, A. F., Jr., 1975, Spectrochemical computer analysis—argon-oxygen d-c arc method for silicate rocks: U.S. Geol. Survey Jour. Research, v. 1, no. 5, p. 559-562.
- Fernandez, F. J., and Manning, D. C., 1971, Atomic absorption analysis of metal pollutants in water using a heated graphite atomizer: Atomic Absorption Newsletter, v. 10, no. 3, p. 65-69.
- Fishman, M. J., and Erdmann, D. E., 1973, Water analysis: Anal. Chemistry, v. 45, no. 5, p. 361R-403R.
- Fishman, M. J., and Midgett, M. R., 1968, Extraction techniques for the determination of cobalt, nickel, and lead in fresh water by atomic absorption, in Baker, R. A., ed., Trace inorganics in water: Washington, Am. Chem. Soc. (Advances in Chemistry Ser. 73), p. 230-235.
- Helz, A. W., 1973, Spectrochemical computer analysis—Instrumentation: U.S. Geol. Survey Jour. Research, v. 1, no. 4, p. 475-482.
- Helz, A. W., Walihall, F. G., and Berman, Sol., 1969, Computer analysis of photographed optical emission spectra: Appl. Spectroscopy, v. 23, no. 5, p. 508-518.
- Mosier, E. L., 1971, A method for semiquantitative spectrographic analysis of plant ash for use in bio-geochemical exploration [abs.]: Soc. Appl. Spectroscopy Natl. Mtg., 10th, St. Louis 1971, Program, p. 65.
- , 1972, A method for semiquantitative spectrographic analysis of plant ash for use in biogeochemical and environmental studies: Appl. Spectroscopy, v. 26, no. 6, p. 636-641.
- Myers, A. T., Havens, R. G., and Duntun, P. J., 1961, A spectrochemical method for the semiquantitative analysis of rocks, minerals, and ores: U.S. Geol. Survey Bull. 1084-I, p. 207-229.
- Perkin-Elmer Corporation, 1971, Analytical methods for atomic absorption spectrophotometry [rev. ed.]: Norwalk, Conn., Perkin-Elmer Corp., 584 p.
- Sandell, E. B., 1959, Colorimetric determination of traces of metals [3d ed.]: New York, Interscience, 1032 p.
- Shacklette, H. T., Hamilton, J. C., Boeringen, J. G., and Bowles, J. M., 1971, Elemental composition of surficial materials in the conterminous United States: U.S. Geol. Survey Prof. Paper 574-D, 71 p.
- Thompson, C. E., and Nakagawa, H. M., 1960, Spectrophotometric determination of traces of lead in igneous rocks: U.S. Geol. Survey Bull. 1004-F, p. 151-164.
- Ward, F. N., Lakin, H. W., Canney, F. C., and others, 1965, Analytical methods used in geochemical exploration by the U.S. Geological Survey: U.S. Geol. Survey Bull. 1152, 100 p.
- Ward, F. N., Nakagawa, H. M., Harms, T. F., and VanSickle, G. H., 1969, Atomic-absorption methods of analysis useful in geochemical exploration: U.S. Geol. Survey Bull. 1289, 45 p.

TABLES 36 & 37

TABLE 36—Normal lead content of some uncontaminated natural substances
(Estimated from data given in this report)

Material	Median	Normal range
ppm		
Crust of the earth	15	Unknown
Common rocks		
Granite	18	10 - 100
Rhyolite	18	10 - 100
Gabbro	4	< 1 - 25
Basalt	4	< 1 - 25
Schist	15	< 1 - 50
Gneiss	12	< 1 - 50
Amphibolite	10	< 1 - 25
Sandstone	15	10 - 50
Siltstone and shale	15	3 - 50
Carbonaceous shale	20	5 - 100
Limestone	5	3 - 15
Sediments		
Terrestrial	15	5 - 40
Marine	60	50 - 150
Lakes	15	5 - 50
Fossil fuels		
Coal	10	5 - 50
Oil	02	005 - 1
Common minerals		
Potassium feldspar	10	10 - 150
Plagioclase feldspar	15	5 - 50
Muscovite mica	20	5 - 70
Biotite mica	30	5 - 100
Hornblende	10	5 - 30
Quartz	5	3 - 30
Calcite	5	1 - 15
μg/g		
Water		
Rivers	6	0.1 - 100
Lakes	1	1 - 50
Hot springs	100	10 - 1,000
Oceans	2	0.1 - 10
μg/m ³		
Air	0.02	< 0.001 - 0.1
ppm in ash		
Vegetation		
Evergreen trees	50	10 - 100
Deciduous trees	25	10 - 50
Shrubs	25	10 - 50
Grasses	20	10 - 100
Mosses	100	10 - 1,000
Fruits and vegetables	< 10	< 10 - 50

TABLE 37—List of minerals and alloys in which lead (Pb) is a major constituent

[Compiled by Michael Fleischer. This list includes minerals considered to be valid or doubtful species. Minerals containing two anions are listed under both, with the exception of compounds containing halides. For example, halogates, $PbAl_2(SO_4)(AsO_4)OH_2$, is listed both under sulfates and under phosphates, arsenates, vanadates, and antimonates, however, $Pb_3(AsO_4)_2Cl_2$ is listed under phosphates, arsenates, vanadates, and antimonates, but not under halides. References for unnamed minerals, given in parentheses, show volume and page number of American Mineralogist where the mineral is described.]

Name	Formula
Alloys	
Plumbopalladinite	Pb_2Pd
Polarite	$Pb(Pb_{10}Bi)$
Unnamed (v. 46, p. 464)	Pb_2Pb
Unnamed (v. 53, p. 1063)	$Pb_2Pb_{11}Bi$
Minerals	
Arsenates	
Finsterlinite	$Pb_3(AsO_4)_2Cl$
Trigonite	$Pb_3MnHf(AsO_4)_2$
Carbonates	
Beyerite	$(Ca,Pb)_3(Bi,Cu)_2CO_3 \cdot 2H_2O$
Californite	$Pb_3(Cu,Pb)(SO_4)(CO_3)(OH)_2$
Cerussite	$PbCO_3$
Dendrite	$Pb_3(CO_3)_2(OH)_2 \cdot 2H_2O$
Hydrocerussite	$Pb_3(CO_3)_2(OH)_2$

TABLE 37—List of minerals and alloys in which lead (Pb) is a major constituent—Continued

Name	Formula
Minerals—Continued	
Carbonates—Continued	
Leadhillite	$Pb_6(SO_4)_2(CO_3)_4(OH)_2$
Nadolomite	$Pb_6Mg_4(CO_3)_4(SO_4)_2 \cdot 5H_2O$
Phosphinite	$Pb_3(CO_3)_2Cl_2$
Plumbosulfite	$Pb_3(CO_3)_2(SO_3)(OH)_2$
Schillingite	$Pb_3Ca_2Cu_2(CO_3)_4(OH)_2 \cdot 6H_2O$
Suzanneite	$Pb_3(SO_4)_2(CO_3)_2(OH)_2$
Wherryite	$Pb_3(CuCl)_2(SO_4)_2(Cl,OH)_2O$
Halides	
Bideauxite	$Pb_6AgCl_3 \cdot (F,OH)_2$
Blancite	$Pb_3Cl_2(OH)_2$
Bulrite	$Pb_3Cu_2Ag_2Cl_3(OH)_2 \cdot H_2O$
Chlorosulphite	$Pb_3CuCl_3(OH)_2O_2$
Cotunnite	$PbCl_2$
Cumengite	$Pb_3Cu_2Cl_3(OH)_2 \cdot H_2O$
Duboisite	$Pb_3Cu_2Cl_3(OH)_2$
Friederite	$Pb_3Cl_2(OH)_2$
Laurionite	$Pb_3Cl_2(OH)_2$
Lorettoite	$Pb_3CuCl_3(OH)_2$
Nadolite	Pb_3Cl_2
Mendipite	Pb_3CuCl_3
Naderite	Pb_3CuCl_3
Paralaurionite	Pb_3CuCl_3
Pentastite	$Pb_3Cl_2(OH)_2$
Percyite	$Pb_3CuCl_3(OH)_2$
Perite	Pb_3CuCl_3
Phosphinite	$Pb_3Cu_2Cl_3$
Pseudobulrite	$Pb_3Cu_2Cl_3(OH)_2 \cdot 2H_2O$
Pseudocumengite	$K_2PbCl_3(OH)_2$
Schwartzembergite	$Pb_3(Cu,Ag)_2(OH)_2O_2$
Unnamed (v. 55, p. 1814)	
Iodates	
Schwartzembergite	$Pb_3(I,Br)_2Cu_2(OH)_2$
Unnamed (v. 55, p. 1814)	
Molybdates, tungstates	
Raspite	$PbWO_4$
Stolzite	$PbWO_4$
Wallerite	$PbMoO_4$
Oxides	
Bindheimite	$Pb_3Si_2O_7(O,OH)$
Cesarite	H_2PbMoO_6
Clarkite	$Pb_3(Ca,Pb)_2(SO_4)(OH)_2$
Coronadite	$Pb(Mn^{2+},Mn^{3+})_2O_8$
Curite	$Pb_3U_2O_7 \cdot 4H_2O$
Fourmarierite	$PbU_2O_7 \cdot 4H_2O$
Hemaphysite	$Pb_3Fe_2O_7(OH,Cl)_2$
Litharge	PbO (terragene)
Magnetoplumbite	$(Pb,Mn)_2Fe_2O_7$
Massicot	PbO , orthorhombic
Mauzyite	$Pb_3U_2O_7$ (oxide?)
Maria-vandendriesscheite	$PbU_2O_7 \cdot nH_2O$, n less than 12
Minam	PbO_2
Murdochite	$Pb_3Fe_2O_7$
Plattnerite	PbO_2
Plumbocerrite	$PbFe_2O_7$
Plumbophenochlore	$(Pb,U,Ca)_2(Nb,Ta)(OH)_2$
Quemelite	$Pb_3Mo_2(OH)_2$
Vandendriesscheite	$PbFe_2(O,OH)_2 \cdot 2H_2O$
Richtertite	$Pb_3U_2O_7$ (oxide?)
Sennite	$(Fe,Mn,Pb)_2TiO_7$
Uraninite	$(U,Th,Pb)_2O_7 \cdot xH_2O$
Vandendriesscheite	$PbFe_2(O,OH)_2 \cdot 2H_2O$
Wilhendorfite	$(Pb,Ca)_2U_2O_7 \cdot 2H_2O$
Unnamed (v. 55, p. 1816)	$PbO_{1.6}$
Phosphates, arsenates, vanadates, antimonates	
Bayldonite	$Pb_3Cu_2(AsO_4)_2(OH)_2$
Bertrandite	$PbFe_2(AsO_4)_2(SO_4)(OH)_4$
Bruckebuschite	$Pb_3MnFe(VO_4)_2 \cdot 2H_2O$
Carminite	$Pb_3Fe_2(VO_4)_2(OH)_2$
Carynite	$(Ca,Nb,Pb)_2(Mn,Mg)_2(AsO_4)_2$
Chervetite	$Pb_3V_2O_7$
Corkite	$PbFe_2(PO_4)_2(SO_4)(OH)_2$
Crocoite	$PbCrO_4$
Dreosulite	$Pb_3Zn_2(VO_4)_2 \cdot 3H_2O$
Dewindite	$Pb(UO_2)_2(PO_4)_2 \cdot 3H_2O$
Dufite	$PbCr(AsO_4)(OH)$
Dumontite	$Pb(UO_2)_2(PO_4)_2 \cdot 3H_2O$
Enderbite	$Pb_3Fe_2(PO_4)_2 \cdot 2H_2O$
Ferrite	$(Pb,Ba)_2(PO_4)_2 \cdot 2H_2O$
Formosine	$(Pb,Cu)_2[Cr,AsO_4](OH)$
Forsythite	$(Ba,Pb)(UO_2)_2(VO_4)_2 \cdot 5H_2O$
Grothmannite	$Pb_3Fe_2(PO_4)_2$
Geoprosadite	$Pb_3(AsO_4)_2$
Grayite	$(Th,Pb,Ca)PO_4 \cdot H_2O$
Halimondite	$Pb_3(UO_2)_2(AsO_4)_2$

TABLE 37.—List of minerals and alloys in which lead (Pb) is a major constituent—Continued

Name	Formula
Minerals—Continued	
Phosphates, arsenates, vanadates, antimonates—Continued	
Hedyphane	$(\text{Ca,Pb})_{12}(\text{AsO}_4)_{12}\text{Cl}_2$
Hidalgite	$\text{PbAl}_2(\text{SO}_4)_2(\text{AsO}_4)(\text{OH})_2$
Himadite	$(\text{Pb}_2\text{Al})_2(\text{PO}_4)_2(\text{SO}_4)(\text{OH})_2$
Higleyite	$\text{Pb}_2(\text{UO}_2)_2(\text{AsO}_4)_2(\text{OH})_2 \cdot \text{H}_2\text{O}$
Lusungite	$(\text{Sr,Pb})_2\text{Fe}_2(\text{PO}_4)_2(\text{OH})_2 \cdot \text{H}_2\text{O}$
Mimeteite	$\text{Pb}_2(\text{AsO}_4)_2\text{Cl}_2$
Monomellite	$(\text{Pb,Ca})_2(\text{SO}_4)_2$
Mottramite	$\text{Pb}_2(\text{Ca,Zn})_2(\text{VO}_4)_2(\text{OH})_2$
Moussanite	$\text{PbFe}_2(\text{VO}_4)_2(\text{OH})_2$
Parsonite	$\text{Pb}_2(\text{UO}_2)_2(\text{PO}_4)_2 \cdot 2\text{H}_2\text{O}$
Phosphogummite	$\text{PbAl}_2(\text{PO}_4)_2(\text{OH})_2 \cdot \text{H}_2\text{O}$
Pyrrhotite	$\text{Pb}_2(\text{UO}_2)_2(\text{PO}_4)_2 \cdot 4\text{H}_2\text{O}$
Pyrochlore	$\text{Pb}_2(\text{VO}_4)_2(\text{OH})_2$
Pyromorphite	$\text{Pb}_5(\text{PO}_4)_3\text{Cl}$
Rensselaerite	$\text{Pb}_2(\text{UO}_2)_2(\text{PO}_4)_2(\text{OH})_2 \cdot 7\text{H}_2\text{O}$
Sahlite	$\text{Pb}_2(\text{AsO}_4)_2(\text{OH})_2$
Schulzeite	$\text{Pb}_2(\text{AsO}_4)_2(\text{OH})_2$
Tsumebite	$\text{Pb}_2(\text{Ca,Pb})_2(\text{SO}_4)_2(\text{OH})_2$
Vandinite	$\text{Pb}_2(\text{VO}_4)_2\text{Cl}_2$
Vauquelinite	$\text{Pb}_2\text{Cu}_2(\text{CO}_3)_2(\text{PO}_4)(\text{OH})_2$
Unnamed (v. 51, p. 258)	$\text{Pb}_2\text{Cu}_2(\text{AsO}_4)_2(\text{SO}_4)(\text{OH})_2$
Unnamed (v. 52, p. 1585)	$\text{Pb}_2\text{Fe}_2(\text{AsO}_4)_2(\text{OH})_2 \cdot \text{H}_2\text{O}(\text{?})$
Unnamed (v. 47, p. 418)	$\text{Pb}_2\text{Fe}_2\text{ arsenate}$
Unnamed (v. 47, p. 418)	$\text{Pb}_2\text{Zn arsenate}$
Silicates	
Alamsonite	Pb_2SiO_4
Baryllite	$\text{Pb}_2(\text{SiO}_3)_2$
Ekanite	$(\text{Th,U})_2(\text{Ca,Pb,Pb})_2\text{Si}_2\text{O}_{10}$
Eggspringite	$(\text{Ca,Pb})_2\text{Si}_2\text{O}_7$
Gaonite	$\text{Pb}_2(\text{CaSiO}_3)_2$
Hancockite	$(\text{Pb,Ca,Sr})_2(\text{Al,Fe})_2(\text{SiO}_3)_2(\text{OH})_2$
Hemihedrite	$\text{Pb}_2(\text{Ca,Sr})_2(\text{SiO}_3)_2(\text{OH})_2$
Hypocrite	$(\text{Pb,Ca,Ba})_2(\text{SiO}_3)_2(\text{OH})_2$
Jaguite	$\text{Pb}_2(\text{Ca,Sr})_2(\text{OH})_2$
Joestite	$(\text{Pb,Ca,Mn})_2(\text{SiO}_3)_2(\text{OH})_2$
Kasolite	$\text{Pb}_2(\text{UO}_2)_2(\text{SiO}_3)_2 \cdot \text{H}_2\text{O}$
Kentrolite	$\text{Pb}_2\text{Mn}_2\text{Si}_2\text{O}_7$
Larsenite	Pb_2SiO_4
Margaronite	$\text{Pb}_2(\text{Ca,Mn})_2\text{Si}_2\text{O}_7$
Melanconite	$\text{Pb}_2\text{Fe}_2\text{Si}_2\text{O}_7$
Molybdoophyllite	$\text{Pb}_2\text{Mg}_2\text{Si}_2\text{O}_7(\text{OH})_2$
Naxosite	$\text{Pb}_2(\text{Ca,Sr})_2\text{Si}_2\text{O}_7$
Plattnerite	$\text{Pb}_2(\text{Al})_2(\text{SiO}_3)_2$
Rehobothite	$\text{Pb}_2\text{Ca}_2(\text{SiO}_3)_2(\text{OH})_2$
Wickenburgite	$\text{Pb}_2\text{Ca}_2(\text{SiO}_3)_2(\text{OH})_2$
Sulfates, chromates, selenates, selenites, tellurates	
Anglesite	PbSO_4
Beaverite	$\text{Pb}_2(\text{Ca,Fe,Al})_2(\text{SO}_4)_2(\text{OH})_2$
Bendatite	$\text{Pb}_2\text{Fe}_2(\text{AsO}_4)_2(\text{SO}_4)(\text{OH})_2$
Calcedonite	$\text{Pb}_2(\text{Ca,Sr})_2(\text{SO}_4)_2(\text{OH})_2$
Corkite	$\text{Pb}_2(\text{Fe,Al})_2(\text{SO}_4)_2(\text{OH})_2$
Crocoite	PbCrO_4
Demonsmarkite	$\text{Pb}_2(\text{Ca,U})_2(\text{UO}_2)_2(\text{SeO}_4)_2(\text{OH})_2 \cdot 2\text{H}_2\text{O}$
Fluorocrocoite	$\text{Pb}_2\text{Ge}_2(\text{SO}_4)_2(\text{OH})_2 \cdot \text{H}_2\text{O}$
Formate	$(\text{Pb,Cu})_2(\text{Al,Cr,As})_2(\text{OH})_2$
Hemihedrite	$\text{Pb}_2\text{Zn}_2(\text{CO}_3)_2(\text{SiO}_3)_2(\text{OH})_2$
Hidalgite	$\text{Pb}_2(\text{Al})_2(\text{SO}_4)_2(\text{OH})_2$
Himadite	$(\text{Pb,Sr})_2(\text{Al}_2\text{PO}_4)_2(\text{SO}_4)(\text{OH})_2$
Ironite	$\text{PbCrO}_4 \cdot \text{H}_2\text{O}$
Izote	$\text{Pb}_2(\text{UO}_2)_2(\text{SO}_4)_2(\text{OH})_2$
Lamarite	Pb_2SO_4
Leadhillite	$\text{Pb}_2(\text{SO}_4)_2(\text{CO}_3)_2(\text{OH})_2$
Lunarite	$\text{Pb}_2\text{Cu}_2(\text{SO}_4)_2(\text{OH})_2$
Moertrumite	$\text{Pb}_2(\text{UO}_2)_2\text{TeO}_4$
Molybdonite	PbSeO_4
Vauquelinite	$\text{PbMn}_2\text{Al}_4(\text{CO}_3)_2(\text{SO}_4)_2 \cdot \text{H}_2\text{O}$
Naslettite	$\text{Pb}_2(\text{SeO}_4)_2(\text{SO}_4)$
Oluchite	$\text{Pb}_2\text{Ca}_2(\text{SO}_4)_2(\text{OH})_2$
Oluchite	$\text{Pb}_2\text{Ca}_2(\text{SO}_4)_2(\text{OH})_2$
Palmerite	$\text{Pb}_2\text{Cu}_2(\text{SO}_4)_2$
Phenocrichrome	$\text{Pb}_2\text{Fe}_2\text{SO}_4$
Phosphogummite	$\text{Pb}_2\text{Fe}_2(\text{SO}_4)_2(\text{OH})_2$
Rehobothite	$\text{Pb}_2\text{Ca}_2(\text{SO}_4)_2(\text{OH})_2$
Schenckite	$\text{Pb}_2(\text{Ca,Sr})_2(\text{SO}_4)_2(\text{OH})_2$
Sunnite	$\text{Pb}_2(\text{SO}_4)_2(\text{CO}_3)_2(\text{OH})_2$
Tsumebite	$\text{Pb}_2\text{Cu}_2(\text{SO}_4)_2(\text{OH})_2$
Vauquelinite	$\text{Pb}_2\text{Cu}_2(\text{CO}_3)_2(\text{SO}_4)(\text{OH})_2$
Wherryite	$\text{Pb}_2\text{Cu}_2(\text{CO}_3)_2(\text{SO}_4)_2(\text{OH})_2$
Unnamed (v. 51, p. 258)	$\text{Pb}_2\text{Cu}_2(\text{AsO}_4)_2(\text{SO}_4)(\text{OH})_2$
Sulfides, selenides, tellurides	
Albite	PbTe
Berkite	$\text{Pb}_2\text{Fe,Pb}_2\text{S}_2$
Clausenite	PbSe
Galenite	PbS

TABLE 37.—List of minerals and alloys in which lead (Pb) is a major constituent—Continued

Name	Formula
Minerals—Continued	
Sulfides, selenides, tellurides—Continued	
Parkite	$\text{Ni}_2(\text{Bi,Pb})_2\text{S}_2$
Shandite	$\text{Ni}_2(\text{Pb,Sb})_2$
Unnamed (v. 53, p. 1421)	Pb,Bi,Te
Unnamed (v. 55, p. 1444)	$(\text{Pb,Bi})_2\text{Te}_2$
Unnamed (v. 55, p. 1067)	$(\text{Pb,Pb})_2\text{As}_2$
Sulfonates	
Albite	$\text{PbCu}_2\text{B}_2\text{O}_7$
Andorite	$\text{PbAg}_2\text{Sb}_2\text{O}_7$
Beumhauserite	$\text{Pb}_2(\text{Cu,Ag})_2\text{B}_2\text{O}_7$
Benjaminite	$\text{Pb}_2(\text{Cu,Ag})_2\text{B}_2\text{O}_7$
Berryite	$\text{Pb}_2(\text{Cu,Ag})_2\text{B}_2\text{O}_7$
Bonchevite	$\text{PbBi}_2\text{S}_2(\text{?})$
Boulangerite	$\text{Pb}_3\text{Sb}_2\text{S}_{11}$
Bournonite	$\text{Pb}_2\text{Sb}_2\text{S}_{11}$
Burnsite	$\text{Pb}_2\text{Bi}_2\text{S}_{11}$
Caennite	$\text{Pb}_2\text{Bi}_2\text{S}_{11}$
Concrite	$\text{Pb}_2\text{Bi}_2\text{S}_{11}$
Cylindrite	$\text{Pb}_2\text{Bi}_2\text{S}_{11}$
Dadosite	$\text{Pb}_2\text{Sb}_2\text{S}_{11}$
Daphnite	$\text{Pb}_2\text{Ag}_2\text{Sb}_2\text{S}_{11}$
Dufrenoyite	$\text{Pb}_2\text{Ag}_2\text{Sb}_2\text{S}_{11}$
Fiselyite	$\text{Pb}_2\text{Ag}_2\text{Sb}_2\text{S}_{11}$
Franchite	$\text{Pb}_2\text{Sb}_2\text{S}_{11}$
Franchetite	$\text{Pb}_2\text{Ag}_2\text{Sb}_2\text{S}_{11}$
Frederickite	$\text{Pb}_2\text{Sb}_2\text{S}_{11}$
Galenobismutite	PbBi_2S_2
Groenlandite	$\text{Pb}_2\text{Sb}_2\text{S}_{11}$
Groenlandite	$\text{Pb}_2\text{Cu}_2\text{Sb}_2\text{S}_{11}$
Gladite	$\text{Pb}_2\text{Ag}_2\text{Sb}_2\text{S}_{11}$
Graustone	$\text{Pb}_2\text{Ag}_2\text{Sb}_2\text{S}_{11}$
Groenlandite	$\text{Pb}_2(\text{Bi,Ag})_2\text{S}_{11}$
Gustavite	$\text{Pb}_2\text{Ag}_2\text{Sb}_2\text{S}_{11}$
Hammarite	$\text{Pb}_2\text{Ag}_2\text{Sb}_2\text{S}_{11}$
Hauchite	$(\text{Pb,Te})_2\text{Ag}_2\text{Sb}_2\text{S}_{11}$
Heteromorphite	$(\text{Pb,Tl})_2(\text{Cu,Ag})_2\text{As}_2\text{S}_{11}$
Hutchinsonite	$(\text{Pb,Tl})_2(\text{Cu,Ag})_2\text{As}_2\text{S}_{11}$
Jamiesonite	$\text{Pb}_2\text{FeSb}_2\text{S}_{11}$
Jordanite	$(\text{Pb,Tl})_2\text{Ag}_2\text{Sb}_2\text{S}_{11}$
Kobellite	$\text{Pb}_2(\text{Bi,Sb})_2\text{S}_{11}$
Launayite	$\text{Pb}_2(\text{Ag,Cu})_2\text{As}_2\text{S}_{11}$
Lengbachite	$\text{Pb}_2(\text{Ag,Cu})_2\text{As}_2\text{S}_{11}$
Lillianite	$\text{Pb}_2\text{Bi}_2\text{S}_{11}$
Lindströmite	$\text{Pb}_2\text{Cu}_2\text{Sb}_2\text{S}_{11}$
Lüsengite	$\text{Pb}_2\text{Ag}_2\text{Sb}_2\text{S}_{11}$
Madocite	$\text{Pb}_2(\text{Bi,Ag})_2\text{S}_{11}$
Marrite	$\text{Pb}_2\text{Ag}_2\text{As}_2\text{S}_{11}$
Menzingerite	$\text{Pb}_2\text{Cu}_2\text{Sb}_2\text{S}_{11}$
Monimite	$\text{Pb}_2\text{Bi}_2\text{S}_{11}$
Nagaitite	$\text{Pb}_2(\text{Ag,Cu})_2\text{Sb}_2\text{S}_{11}$
Neyite	$\text{Pb}_2(\text{Cu,Ag})_2\text{Bi}_2\text{S}_{11}$
Niessite	$\text{Pb}_2(\text{Cu,Ag})_2\text{Bi}_2\text{S}_{11}$
Orythrite	$\text{Ag}_2\text{Pb}_2\text{Sb}_2\text{S}_{11}$
Paragonite	$\text{Pb}_2\text{FeSb}_2\text{S}_{11}$
Plagioclase	$\text{Pb}_2\text{Sb}_2\text{S}_{11}$
Platynite	$\text{Pb}_2\text{Bi}_2\text{S}_{11}$
Platynite	$\text{Pb}_2\text{Bi}_2\text{S}_{11}$
Ramsdellite	$\text{Ag}_2\text{Pb}_2\text{Sb}_2\text{S}_{11}$
Rathite	$(\text{Pb,Tl})_2\text{As}_2\text{S}_{11}$
Rehobothite	$\text{Pb}_2\text{Ag}_2\text{Sb}_2\text{S}_{11}$
Robinsonite	$\text{Pb}_2\text{Sb}_2\text{S}_{11}$
Sakharovite	$(\text{Pb,Fe})_2(\text{Bi,Sb})_2\text{S}_{11}$
Sartorite	$\text{Pb}_2\text{As}_2\text{S}_{11}$
Schirmerite	$\text{Pb}_2\text{Ag}_2\text{Bi}_2\text{S}_{11}$
Seligmannite	$\text{Pb}_2\text{Sb}_2\text{S}_{11}$
Semseyite	$\text{Pb}_2\text{Sb}_2\text{S}_{11}$
Sorbyite	$\text{Pb}_2(\text{Bi,Ag})_2\text{S}_{11}$
Sterryite	$\text{Pb}_2(\text{Bi,Ag})_2\text{S}_{11}$
Tessite	$\text{Pb}_2\text{Sb}_2\text{S}_{11}$
Tininite	$\text{Pb}_2(\text{Bi,Sb})_2\text{S}_{11}$
Twinite	$\text{Pb}_2(\text{Bi,Ag})_2\text{S}_{11}$
Uvarovite	$\text{Pb}_2(\text{Bi,Sb})_2\text{S}_{11}$
Vermite	$\text{Pb}_2(\text{Bi,Ag})_2\text{S}_{11}$
Wallite	$\text{Pb}_2(\text{Cu,Ag})_2\text{As}_2\text{S}_{11}$
Whiteite	$\text{Pb}_2\text{Bi}_2\text{S}_{11}$
Whiteite	$\text{Pb}_2\text{Bi}_2\text{S}_{11}$
Zinkenite	$\text{Pb}_2\text{Bi}_2\text{S}_{11}$
Unnamed (v. 5, p. 136)	$\text{Pb}_2\text{As}_2\text{S}_{11}$
Unnamed (v. 55, p. 1067)	$\text{Pb}_2\text{As}_2\text{S}_{11}$
Unnamed (v. 55, p. 1445)	$\text{Pb}_2\text{Ag}_2\text{Cu}_2\text{Bi}_2\text{S}_{11}$
Unnamed (v. 54, p. 1067)	$\text{Pb}_2\text{Ag}_2\text{Cu}_2\text{Bi}_2\text{S}_{11}$
Unnamed (v. 38, p. 525)	$\text{Pb}_2\text{Ag}_2\text{Cu}_2\text{Bi}_2\text{S}_{11}$
Unnamed (v. 55, p. 533)	$\text{Pb}_2\text{Bi}_2\text{S}_{11}$

INDEX

[Page numbers of major references are in *italics*]

A	Page	D	Page		Page
Abundance	2	Delusions	73	Inorganic chemistry, water	5
Accumulator plants	61, 26	Deoxyribonucleic acid	13	Invertebrate	5
Agricultural waste	13	Deposits, distribution	12	Insomnia	28
Air pollution	1, 2, 3, 39, 54, 66, 67, 71	mineral associations	12	Ionic radii	23
Alaska, air pollution	74	Detection	1	Ionic strength, solubility	9
Alkalinity, solubility	5, 39, 44	Durite	23	Iowa, vegetation	54
Allanite	22	Distribution, ore deposits	12, 46	Iron sesquioxide	44
Aluminum sesquioxide	44	Dolomite	1, 2, 31		
Amphibole	2, 29	Dunite	1		
Analytical methods	1, 81			J. K. L.	
Andrew	23			Japan, health problems	63
Arenaria	22	E		thermal water	30
Angleite	2, 21, 23	Electron probe	3, 42	Kobayashi damage	77
Anomalous concentrations	39	Emotional instability	28	Lakes	2, 36
Antarctica	74	Encephalopathy	77	Lane County, Oreg.	19
surface water	36	Evaporites	1, 32	Leaching	1
Antimony	1			Lichen	3
Associations, ore deposits	1, 12	F		Limestone	1, 21, 31
Atlantic Coastal Plain, concentration	42	Feldspar	2, 25, 27, 42	Limonite	29
Atmosphere	1, 2, 3, 39, 54, 66, 67, 71	Flavoprotein	36	Liver	22
Atomic absorption spectrometry	1, 31, 42	Florida, surface water	36	Levenock, poisoning	26
Automobile exhaust	1, 3, 36, 67	Ford	23	Los Angeles, air pollution	14
		Fossil fuels	2, 42		
B		G		M	
Barley, toxicity sensitivity	38	Galena	2, 7, 21, 27	Manganese	2
Basalt	1, 25	Garnet	28	Maryland, surface water	36
Bauxite	31	Gasoline additive	1, 38, 71	vegetation	55, 54, 57
Biogeochemistry	11	Gas/natural system	22	Mediterranean Sea	30
Biocite	2, 23	Geochronological system	71	Metabolic effects	22
Black Sea	40	Geothermal halo	22	Metamorphic rocks	21
Blood damage	72	Gneiss	25, 27	Mica	2, 25, 27
Bluegrass, toxicity sensitivity	56	Gout	72	Michigan, concentration	1, 21, 32
Bone damage	72	Grain	23	Migration	1, 21, 32
Brain damage	72, 78	toxicity sensitivity	58	Minerals	2, 27
British Columbia, livestock poisoning	26	Granite	1, 25	Mining	23, 39, 42, 26
Bulgaria, soil	43	Granodiorite	25, 27	Minnesota, concentration	42
		Grass	3	vegetation	24
C		Great Britain, health problems	63	Miscarriage	72
Calcite	2	soil	36	Mississippi River	36
Carbonate	1, 2, 5, 7, 21	Great Lakes	26	Missouri, ground water	30
Cattle, poisoning	26	Greenland	1	livestock poisoning	26
Cerussite	2, 21, 27	Ground water	6, 48	soil	56, 53
Chelation	2, 14	Gulf Plain, concentration	31	vegetation	53, 46, 48
Chemistry	1, 12, 42	Gypsum	2	Missouri district	17
Cigarette smoke	73			Missouri River	26
Cinnamite, air pollution	24	H		Molecular absorption	42
Clay	2, 21	Hair	2, 32	Monazite	22
Claystone	31	Hallimination	2, 32	Montana, vegetation	65
Coal	2, 12	Halos	21, 60	Mosses	5
Coeur d'Alene district, Idaho	17, 57, 60	Health hazards	21, 72	Mudstone	31
Colloid particles	10, 39, 38	High Plains, concentration	42	Municipal waste	13
Colorado, concentration	42	Homes, poisoning	26	Muscovite	2, 25, 32
livestock poisoning	26	Hot springs water	25		
soil	66	Hydrologic suspension	40	N	
soil	2	Hydroxides	5, 2, 8	Nebraska, concentration	42
vegetation	2	Hypertension	27	Neuromuscular damage	72
Colorado mineral belt	12			New Lead Belt, Mo.	53
Colorado River	36	I		New Mexico, air pollution	25
Colorimetric analysis	3, 42	Idaho, surface water	38	vegetation	53, 54
Columbia River	26	vegetation	12, 60	New York, vegetation	54
Consumption, U.S.	1	Igneous rocks	23		
Coordination compounds	14	Indicator plants	42	O	
Copper, association	1	Industrial safety	22		
plant toxicity resistance	38	Industrial waste	2, 3, 13, 34	Oats	25
Corn, toxicity resistance	58			toxicity sensitivity	58

	Page
Occupational hazards	22
Ocean water	2, 12, 40
Ohio River	36
Oil-field brines	39
Oil shale	33
Oklahoma, smelter	46
Olivine	28
Optical emission spectrography	3, 31, 42
Ore deposits	1, 12
effect on soils	27
Organic chemistry, water	13
Organic compounds	1, 2, 13
Oxidation	1, 27
Ozark Mountains, surface water	38
P	
Pain	1, 23
Perfluoralkyl compounds	13
Pesticide	33
Petroleum	2, 33
pH, solubility	3, 23, 44
Philadelphia, air pollution	24
Phenol	25
Phosphate	1
Phosphorus formation, Idaho	31
Phosphorus, plant toxicity resistance	58
Pica	23
Plagioclase	2
Plants	2, 22, 24
analysis	62
Poisoning	1, 22, 22
Polychloride complexes	13
Pollution, air	1, 28, 24, 66, 67, 72
soil	66
water	13, 22, 13
Polymers, leachates	14
Poppe, toxicity resistance	58
Posah, feldspar	4
Pottery, glaze	1, 23
Precipitation	34
Production, U.S.	1
Prospecting	21, 41, 36, 39, 41
plants	3
Pycnomorphite	43
Pyroxene	2, 29
Q, R	
Quartz	2, 39
Quartzite	1
Radioactive decay	23
Randall	2, 44
Red Sea	2, 32
Rhyolite	1, 23

	Page
Rhombic acid	14
Rivers	2
Runoff water	32
Rural v. urban pollution	3
S	
San Diego, air pollution	24
San Juan Mountains	17
Sandstone	1, 31
Santa Catalina Island, Calif.	13
Saturated, surface water	8
Seasonal variation, concentration in plants	3, 35
Seawater	2, 32, 40
Sedimentary rocks	11
Sediments	22, 22
Shale	1, 31
Shasta copper district, Calif.	19
Shrub	3
Silicate	31
Silver	1
Smelting	3, 41, 25
Soil	2, 22, 47
Missouri	53
Solubility	1, 3, 2, 4, 23, 33, 38, 38
Spectrographic analysis	3
Springs	38
Stability fields, inorganic compounds	3
Stillbirth	22
Strain sediments	21
Subsurface water	5, 38
Sulfate	1, 2, 3, 8, 33
Sulfide	2, 4
Supergene processes	21
Supersaturation, surface water	8
Surface water	2, 6, 22, 36
Surface water-sediment systems	23
Suspended particles	10, 33, 38
Sweetwater, toxicity sensitivity	58
T	
Thermal water	32
Thermodynamics, water	4
Theoret	27
Tranite	22
Tomatoes, toxicity sensitivity	58
Tombstone, Ariz.	23
Toxemia, air pollution	24
Toxicity, animals	1
humans	1, 22, 22
plants	32
Toxite	23
Tree	1, 36, 32, 60
Troposphere	24

	Page
U	
Uranamics	1
Union of South Africa, surface water	36
Uranium	22
Urban v. rural pollution	3
U.S.S.R., ground water	39
surface water	30
thermal water	40
V	
Vegetation	2, 22, 12, 23, 23
analysis	62
Viburnum Trend, Mo.	33
Violence, toxicity sensitivity	58
Vitruvius	14
W	
Wales, mining	46
vegetation	34
Wasatch Range	12
Washington County, Md.	32
Water	13
Water	2, 23, 28
analysis	62
inorganic chemistry	1
ocean	2, 32, 40
organic chemistry	13
pollution	23
solubility	1, 3, 2, 4, 23, 33, 38
subsurface	5, 38
surface	2, 6, 22, 36, 40
thermodynamics	8
Weathering	27, 33
Wheat, toxicity sensitivity	58
Wiscum, concentration	42
ore deposits	21
surface water	38
vegetation	54
Wulfenite	23
X, Y, Z	
X-ray spectrography	1, 62
Xenotime	22
Yugoslavia, air pollution	23
thermal water	38
Zinc, migration	22
ore deposits	1
plant toxicity resistance	58
Zircon	22

Calderas of the San Juan Volcanic Field, Southwestern Colorado

GEOLOGICAL SURVEY PROFESSIONAL PAPER 958





Calderas of the San Juan Volcanic Field, Southwestern Colorado

By THOMAS A. STEVEN and PETER W. LIPMAN

GEOLOGICAL SURVEY PROFESSIONAL PAPER 958

*Eighteen major ash-flow tuff sheets
were deposited and perhaps as many
related calderas developed during
emplacement of an underlying shallow
batholith in late Oligocene time*



UNITED STATES DEPARTMENT OF THE INTERIOR

THOMAS S. KLEPPE, *Secretary*

GEOLOGICAL SURVEY

V. E. McKelvey, *Director*

Library of Congress Cataloging in Publication Data

Steven, Thomas August, 1917-

Calderas of the San Juan volcanic field, southwestern Colorado.

(Geological Survey Professional Paper 958)

Bibliography: p.

Supt. of Docs. no.: I 19.16:958

I. Calderas--Colorado--San Juan Mountains. 2. Volcanic ash, tuff, etc.--Colorado--San Juan Mountains. 3. Batholiths--Colorado--San Juan Mountains.

I. Lipman, Peter W., joint author. II. Title. III. Series: United States Geological Survey Professional Paper 958.

QE524.S85 551.2'1'0978838 75-619377

For sale by the Superintendent of Documents, U.S. Government Printing Office
Washington, D.C. 20402
Stock Number 024-001-02783-6

CONTENTS

	Page		Page
Abstract	1	Central San Juan caldera complex—Continued	
Introduction	1	Bachelor caldera	19
General geology	3	Manimah Mountain(?) caldera	20
Early eastern calderas	4	Source of the Wason Park Tuff	22
Platoro and Summitville calderas	4	San Luis and Cochetopa Park calderas	22
Bonanza caldera	6	Compound subsidence of the San Luis caldera	25
Western San Juan caldera complex	7	Subsidence of the Cochetopa Park caldera	26
Ute Creek caldera	7	Resurgence of the San Luis caldera	27
Lost Lake caldera (buried)	8	Postcaldera lavas	27
San Juan, Uncompahgre, and Silverton calderas	10	Creede caldera	27
Uncompahgre and San Juan collapses	10	Late general magmatic uplift	29
Postcollapse lavas and sediments	11	Block-faulted area	30
Intracaldera ash-flow tuffs	12	Discussion	30
Silverton collapse	12	Development of the batholith	30
Resurgens doming	12	Relation of ash-flow eruption and caldera subsidence	31
Lake City caldera	13	Differentiation in local cupolas	31
Central San Juan caldera complex	16	Resurgence	32
Mount Hope caldera	16	Mineralization	33
La Garita caldera	18	References cited	34

ILLUSTRATIONS

FIGURES 1-25. Maps:	Page
1. Calderas in the San Juan volcanic field in relation to Bouguer gravity field	2
2. Generalized geology of the Platoro and Summitville calderas	5
3. Distribution of La Jara Canyon Member of Treasure Mountain Tuff in relation to Platoro caldera	6
4. Distribution of Ojito Creek and Ra Jadero Members of Treasure Mountain Tuff in relation to Summitville caldera	6
5. Geologic map of Ute Creek and Lost Lake calderas	8
6. Distribution of Ute Ridge Tuff in relation to Ute Creek caldera	9
7. Distribution of Blue Mesa Tuff in relation to Lost Lake caldera	9
8. Distribution of Dillon Mesa Tuff in relation to Uncompahgre caldera	10
9. Western San Juan caldera complex after subsidence related to eruption of the Sapinero Mesa Tuff	11
10. Distribution of Sapinero Mesa Tuff in relation to San Juan and Uncompahgre calderas	12
11. Distribution of Crystal Lake Tuff in relation to Silverton caldera	13
12. Western San Juan caldera complex after subsidence of the Silverton caldera and general resurgence	14
13. Generalized geology of the western San Juan caldera complex showing distribution of rocks related to the Lake City caldera	15
14. Generalized geology of the Mount Hope caldera and adjacent areas	17
15. Distribution of the upper member of Maconic Park Tuff in relation to Mount Hope caldera	18
16. Restored Bachelor and La Garita calderas	20
17. Distribution of the Fish Canyon Tuff in relation to the La Garita caldera	21
18. Distribution of Carpenter Ridge Tuff in relation to Bachelor caldera	21
19. Distribution of Mammoth Mountain Tuff in relation to probable source area	22
20. Distribution of Wason Park Tuff in relation to possible source area	22
21. Generalized geology of the San Luis and Cochetopa Park calderas in relation to remnants of the Bachelor and La Garita calderas	23
22. Generalized geology of the Creede and San Luis calderas in relation to remnants of the Bachelor and La Garita calderas	24
23. Distribution of Nelson Mountain Tuff in relation to San Luis caldera	26
24. Distribution of the Cochetopa Park Tuff in relation to Cochetopa Park caldera	26
25. Areas where erosional remnants of Snowshoe Mountain Tuff are preserved in relation to the Creede caldera	28

TABLE

TABLE 1. Ash-flow stratigraphy in the San Juan volcanic field	Page
	4

CALDERAS OF THE SAN JUAN VOLCANIC FIELD, SOUTHWESTERN COLORADO

By THOMAS A. STEVEN and PETER W. LIPMAN

ABSTRACT

Calderas in the San Juan volcanic field in southwestern Colorado formed largely in late Oligocene time (30-26 m.y. ago) in response to recurrent large-volume ash-flow eruptions. The ash-flow deposits overlie a coalescing assemblage of early Oligocene (35-30 m.y.) andesitic stratovolcanoes that formed the southwest part of a widespread composite volcanic field in the southern Rocky Mountains. A nearly one-to-one relationship exists between large-scale pyroclastic eruptions and calderas: 18 major ash-flow sheets have been identified, 15 calderas are known, 2 are postulated on indirect evidence, and another one may possibly be identified in the northeast part of the volcanic field. In general, the different caldera cycles confirm the successive stages of development described by Smith and Bailey in 1968, except that few calderas demonstrate all stages of activity. On the other hand, almost every stage is exceptionally well developed in one or more of the calderas.

The development of the calderas is believed to chronicle the emplacement of successive segments of an underlying shallow batholith that is indicated by a major gravity low having sharp marginal gradients. Early calderas in the eastern part of the field formed in areas of clustered andesitic volcanoes and are not clearly associated with the main gravity low. These early calderas are believed to have formed above local high-level magma chambers that developed in the roots of the volcano clusters before the main body of the batholith rose to shallow depths. Post-collapse volcanics are largely of andesitic composition, indicating that only limited volumes of silicic differentiates formed at the tops of these chambers and that these differentiates were depleted by the ash-flow eruptions.

The western San Juan caldera complex also formed in an area of clustered earlier andesitic volcanoes, but are above the western part of the batholith indicated by gravity data. Large volumes of silicic differentiates formed within the batholith and were spread widely by ash-flow eruptions. Five calderas formed within a period of about 2 m.y. (in the interval from 29 to 27 m.y. ago), and contrasting lithologies of the ash-flow sheets related to the calderas require sequential development of cupolas and magmatic differentiation within them. Postsubsidence lavas that were erupted after emplacement of the most voluminous of these ash-flow sheets were largely of mafic quartz latite to andesite compositions, indicating temporary depletion of silicic differentiates in the source magma chamber. In the same area, a sixth caldera formed 4.5 m.y. later in response to eruption of a petrologically distinct ash-flow tuff believed to have had an origin different from the earlier ash-flow tuffs.

Development of the central San Juan caldera complex began about 28 m.y. ago, during the period of ash-flow eruptions and caldera collapses in the western San Juan Mountains, and was largely complete by the end of the Oligocene, 26 m.y. ago. During this 2-m.y. span, recurrent pyroclastic eruptions caused deposition of eight major ash-flow sheets and formation of at least seven calderas. The calderas are above the main eastern segment of the gravity low and are believed to mark the

culminating upward movement of magma in this part of the batholith. Contrasting lithologies of sequential ash-flow sheets, which were derived from clustered and, in some places, nested caldera sources, require rapid development of successive cupolas above the batholith and of local differentiation within them. Most of the postsubsidence lavas that were erupted late in the different caldera cycles are coarsely porphyritic quartz latites compositionally related to the associated ash-flow tuffs; apparently even the most voluminous ash-flow eruptions did not deplete the silicic differentiates at the top of this part of the batholith. Concurrent eruption of andesitic rocks from scattered volcanoes not closely associated with the calderas is evidence of the presence of more mafic undifferentiated magma at depth, however.

The life span of the batholithic magma chamber, as indicated by ash-flow eruptions and caldera subsidence, appears to have been brief. Voluminous andesitic material was erupted from widely scattered centers throughout early Oligocene time (35-30 m.y. ago). Toward the end of this period, the first local magma chambers 10-30 km across had risen to shallow depths beneath some of the major volcano clusters, and had differentiated sufficiently to supply large volumes of silicic ash. Within the next 4 m.y. (30-26 m.y.), the main batholith rose to shallow depths in segments indicated by the main caldera complexes; vast quantities of ash were erupted and numerous calderas collapsed into the partly evacuated magma chambers. However, within another 4 m.y. (by 22 m.y. ago), the batholith had coagulated sufficiently to allow a younger, petrologically distinctive magma to penetrate to comparably shallow depths and retain its compositional identity.

INTRODUCTION

The San Juan Mountains, southwestern Colorado (fig. 1), consist mainly of volcanic rocks that form the largest remnant of a major composite volcanic field that covered most of the southern Rocky Mountains in middle Tertiary time (Steven and Epis, 1968; Steven, 1975). This remnant is an eroded volcanic plateau (Steven, 1968), in which coalescing early andesitic volcanoes were widely overlain by the silicic tuffs of 18 major and several minor ash-flow sheets and by related lavas and breccias (Lipman and others, 1970). The sources of all the larger ash-flow sheets were near-surface magma chambers that were rapidly evacuated during voluminous pyroclastic eruptions, thereby causing collapse of overlying calderas. This paper reviews the history of the ash-flow field and its related calderas and summarizes the general relations that seem common to most individual cycles of pyroclastic eruption

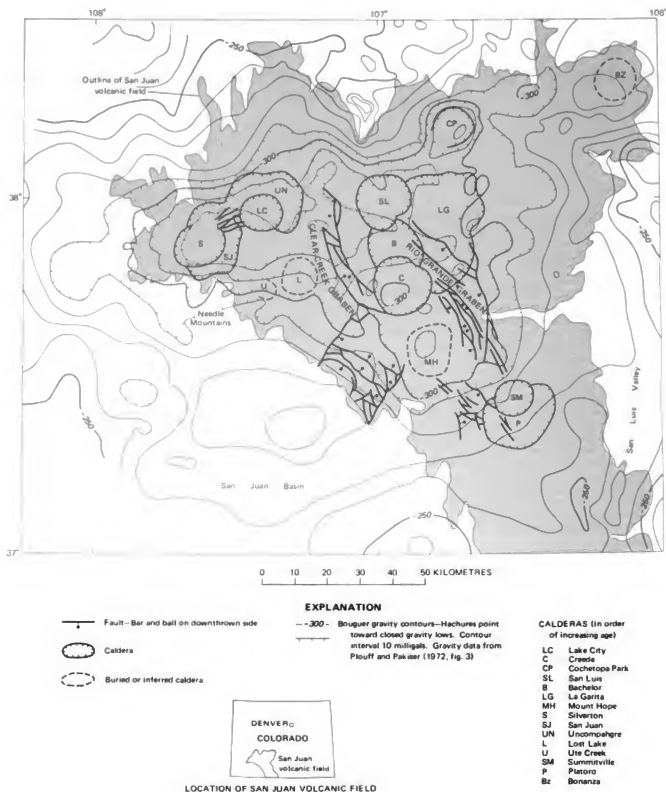


FIGURE 1.—Calderas in the San Juan volcanic field (patterned) in relation to Bouguer gravity field.

and caldera subsidence in the San Juan field.

The sequence of events we have determined for each of the calderas conforms well to the succession of stages in the development of a typical resurgent caldera described by Smith and Bailey (1968), although few of the San Juan calderas demonstrate all stages of activity. On the other hand, almost every stage is exceptionally well developed in one or more of the San Juan calderas.

GENERAL GEOLOGY

The general evolution of the San Juan volcanic field has been described by Lipman, Steven, and Mehnert (1970) and will be outlined only briefly here. Volcanic activity began in latest Eocene or earliest Oligocene time, probably between 40 and 35 m.y. ago.¹ The early rocks are largely intermediate in composition (andesite, rhyodacite, and mafic quartz latite) and were erupted from many scattered stratovolcanoes. These volcanoes were especially active in the interval from 35 to 30 m.y. ago, and the products derived from them coalesced into a composite volcanic field covering more than 25,000 km².

About 30 m.y. ago the character of volcanic activity changed markedly to predominantly pyroclastic eruptions, and large-volume quartz latitic and rhyolitic ash flows spread widely from many centers. Most of the larger sheets show evidence of compound cooling, and evidently were formed by many individual ash flows that followed one another in rapid succession. The earliest ash flows came largely from the northeastern and southern parts of the San Juan field, and were erupted from clusters of the early stratovolcanoes; caldera collapse resulting from the ash-flow eruptions largely destroyed the upper parts of these volcanoes. Postsubsidence eruptions around these early calderas were largely of intermediate-composition lavas and breccias that commonly are virtually indistinguishable from the early intermediate rocks of the composite volcanic field.

Beginning about 29 m.y. ago, ash-flow eruptions broke out in the western part of the San Juan volcanic field where five calderas formed in less than 2 m.y. The first two of these calderas are largely covered and are imperfectly understood, but the last three evolved in a manner generally similar to the early calderas farther east. They developed in an area of clustered andesitic central volcanoes whose vent areas were largely destroyed by caldera subsidence. Postsubsidence eruptions here were also mainly of intermediate-composition lavas and breccias that closely resemble those of the early volcanoes.

About 28 m.y. ago, while ash flows were still erupting and calderas forming in the western San Juan Mountains,

major pyroclastic eruptions began in the central part of the San Juan volcanic field. A sequence of eight major ash-flow sheets formed, and caldera subsidences have been identified or inferred at all the ash-flow source areas. Postsubsidence eruptions around most of the central San Juan calderas were of viscous quartz-latitic and rhyolitic lavas closely related in composition to the ash-flow tuffs. Although some more mafic volcanoes were active during this same interval, they were not closely associated in space with the developing calderas. Ash-flow activity terminated in the central San Juan Mountains about 26.5 m.y. ago.

In early Miocene time, about 25 m.y. ago, the character of the erupted material changed from the andesitic and derivative rocks that formed the early San Juan volcanoes and succeeding ash-flow tuffs to fundamentally basaltic materials with some associated high-silica alkali-rich rhyolites. This change approximately coincided with inception of basin-and-range faulting in the adjacent San Luis Valley segment of the Rio Grande trough (Lipman and Mehnert, 1975). Fundamentally basaltic eruptions in the San Juan field continued intermittently until about 5 m.y. ago. The only large-volume rhyolitic ash-flow tuff deposited during the period of fundamentally basaltic activity is the Sunshine Peak Tuff, about 22.5 m.y. old (Melnert and others, 1973a), which formed from ash flows that accumulated in and around the concurrently developing Lake City caldera in the western part of the San Juan volcanic field.

In all, 15 calderas are now known in the San Juan volcanic field, and indirect evidence suggests that at least two and perhaps three more exist.

A large negative Bouguer gravity anomaly underlies the area containing most of the calderas (fig. 1), and is believed to reflect a major underlying batholith (Plouff and Pakiser, 1972). Sharp gradients at the margins of the anomaly indicate that the top of the batholith is relatively shallow. The change from eruption of intermediate-composition rocks by widely scattered early stratovolcanoes to eruption of the more silicic ash flows probably took place as this batholith rose and differentiated beneath the central part of the field. When the roofs of the more differentiated and gas-charged cupolas of the batholith failed, great volumes of ash were erupted rapidly, and unsupported segments collapsed to form the calderas. The sequential development of the calderas is believed to reflect the progressive emplacement of the different high-level plutons of a composite batholith.

The calderas in the San Juan volcanic field became comprehensible to us only after the complex stratigraphy of the related ash-flow units and associated rocks was determined by regional mapping of the Durango 1°×2° quadrangle (Steven, Lipman, Hail, and others, 1974) and

¹ Except where otherwise noted, all ages and age designations are from Lipman, Steven, and Mehnert (1970) or Steven, Mehnert, and Chudakovich (1967).

adjacent parts of the Montrose 1°20' quadrangle. This regional work has led to major revisions in stratigraphic nomenclature established by earlier studies of local areas (Steven, Lipman, and Olson, 1974; Lipman and others, 1973). The volcanic stratigraphy of the ash-flow units as understood in 1975 is given in table 1. For a more complete summary of the total volcanic stratigraphy, the reader should consult the above references and particularly the explanation of the Durango quadrangle map.

EARLY EASTERN CALDERAS

The oldest calderas in the eastern part of the San Juan field—the Bonanza caldera and the nested Platoro and Summitville calderas—are widely separated and the related ash-flow sheets do not overlap. Thus, the relative ages of eruption and caldera development at the two centers are uncertain (table 1). All these cycles are younger than the dated rocks in the early intermediate-composition volcanoes (34.7-31.1 m.y.) and are older than the Fish Canyon Tuff (27.8 m.y.). The only age relations among these rocks that can be told directly by superposition are those between the several members of the Treasure Mountain Tuff that are derived from the Platoro and Summitville calderas. K-Ar ages of the Treasure Mountain Tuff related to the Platoro and Summitville calderas appear older than those obtained from tuffs related to any of the calderas in the western San Juan Mountains, but present data do not permit interpretation of age relations between the Bonanza caldera and any of the other older calderas.

Both the Bonanza caldera and the Platoro and Summitville calderas formed within clusters of earlier andesitic stratovolcanoes, and they are on or just outside of the margin of the shallow batholith that gravity data suggest underlies the San Juan volcanic field (fig. 1) (Plouff and

Pakiser, 1972). The Bonanza caldera is located near the northeast end of a narrow gravity low that extends east-northeast from the main anomaly; this caldera probably is localized above a satellite pluton. The Platoro and Summitville calderas are outside the sharp gradient along the southeast side of the main gravity low, and thus are probably not above the near-surface part of the main batholith. Quite possibly these early calderas developed above local high-level magma chambers that formed in the roots of earlier volcanoes before the main batholith had risen to its present near-surface position.

PLATORO AND SUMMITVILLE CALDERAS

The Platoro and Summitville calderas in the southeastern part of the volcanic field (fig. 1) constitute a composite collapse structure about 20 km in diameter that formed as a result of recurring eruptions of ash flows of the Treasure Mountain Tuff (Lipman and Steven, 1970; Lipman, 1975a, b). The Platoro caldera and the nested younger Summitville caldera (fig. 2) formed within a cluster of six or seven intermediate-composition stratovolcanoes of the Conejos Formation. These central volcanoes had been extensively eroded and the intervening basins filled with the resultant detritus, producing a widespread low-relief surface. Ash-flow activity began 30-29 m.y. ago when at least 500 km³ of phenocryst-rich quartz-latic ash that now constitutes the La Jara Canyon Member of the Treasure Mountain Tuff was erupted from sources in the Summitville-Platoro region and spread 30-40 km in all directions (fig. 3). Caldera collapse began before these eruptions were complete, and the late ash flows forming the La Jara Canyon Member ponded within the collapsing caldera to a thickness of more than 800 m. Similar concurrent eruption and collapse characterized other large calderas in the San Juan Mountains, when the

TABLE 1.—Ash-flow stratigraphy in the San Juan volcanic field

Ash-flow unit	Estimated volume (km ³)	Dominant composition	Age (m.y.)	Related caldera
Sunshine Peak Tuff	100-500	Silicic rhyolite	22.5	Lake City.
Snowshoe Mountain Tuff	> 500	Quartz latite	26.5(?)	Creede.
Cochetopa Park Tuff	< 100	Zoned rhyolite to quartz latite	> 26.4 < 26.7	Cochetopa Park.
Nelson Mountain Tuff	> 500	do	> 26.4 < 26.7	San Luis.
Rat Creek Tuff	< 100	Rhyolite	> 26.4 < 26.7	Early stage San Luis.
Wason Park Tuff	100-500	do	> 26.4 < 26.7	Unknown.
Mammoth Mountain Tuff	100-500	Zoned rhyolite to quartz latite	26.7	Do.
Carpenter Ridge Tuff	> 500	Rhyolite, locally zoned to quartz latite	> 26.7 < 27.8	Bachelor.
Crystal Lake Tuff	25-100	Rhyolite	> 26.7 < 27.8	Silverton.
Fish Canyon Tuff	> 5,000	Quartz latite	27.8	La Garita.
Masonic Park Tuff (upper member)	> 500	do	28.2	Mouth Hope.
Sapinero Mesa Tuff	> 1,000	Rhyolite	> 27.8 < 28.4	Uncompahgre and San Juan.
Dillon Mesa Tuff	25-100	do	> 27.8 < 28.4	Uncompahgre(?).
Blue Mesa Tuff	100-500	do	> 27.8 < 28.4	Low Lake(?).
Ute Ridge Tuff	> 500	Quartz latite	28.4	Ute Creek.
Treasure Mountain Tuff:				
Ra Jado Member	100-500	do	> 29.1 < 29.8	Summitville
Ojo Creek Member	40-70	do	> 29.1 < 29.8	Do.
La Jara Canyon Member	> 500	do	29.8	Platoro.
Bonanza Tuff		do	> 27.8	Bonanza.

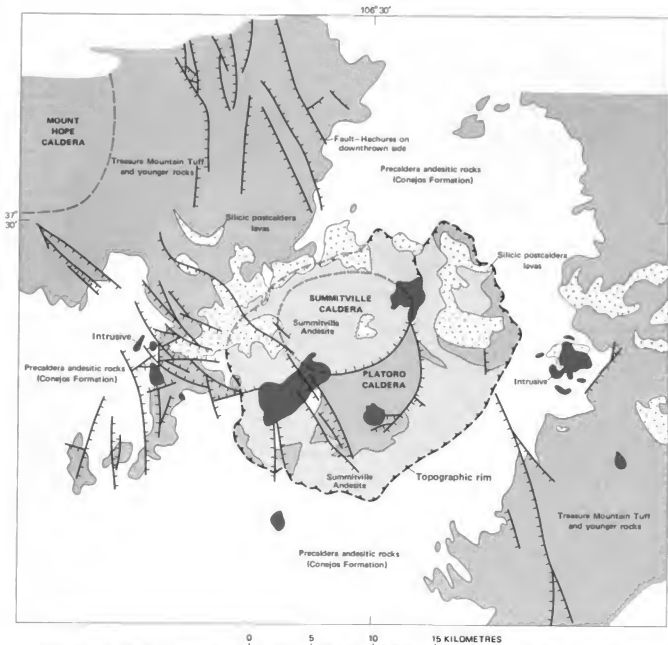


FIGURE 2.—Generalized geology of the Platoro and Summitville calderas. Control moderate to good where boundaries of calderas are shown by solid symbols; conjectural where shown by open symbols.

roofs of the magma chambers lost support before eruptions were completed.

The thick La Jara Canyon tuffs within the Platoro caldera are topographically and structurally high as a result of resurgent uplift shortly after collapse. Early resurgence is demonstrated by the presence in the core of the caldera of monolithologic talus breccias that were derived from the La Jara Canyon Member and that intertongue with lavas that filled the structural moat adjacent

to the resurgent block. The resurgent core forms a nearly unbroken block that dips homoclinally to the southwest, in contrast with the fractured domical uplifts that characterize many other known resurgent calderas.

After resurgence was virtually complete, the marginal moat of the Platoro caldera was filled by as much as 1 km of dark andesitic lavas and interbedded volcanoclastic sedimentary rocks of the lower member of the Summitville Andesite. These andesitic lavas, in essence, represent



FIGURE 3.—Distribution of La Jara Canyon Member (diagonal lines) of Treasure Mountain Tuff in relation to Platoro caldera (P) and San Juan volcanic field (shaded). Base for figures 3, 4, 6-8, 10, 11, 15, 17-20, and 23-25 from U.S. Geological Survey, Colorado State map, 1:500,000, 1968.

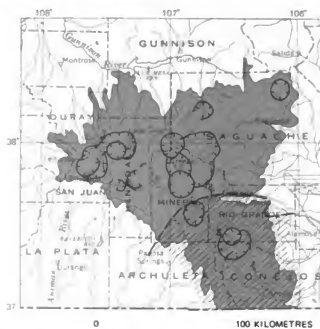


FIGURE 4.—Distribution of Ojito Creek and Ra Jadero Members (diagonal lines) of Treasure Mountain Tuff in relation to Summitville caldera (S) and San Juan volcanic field (shaded).

a continuation of the same type of volcanic activity that characterized the development of the Cotejos Formation, with which they are readily confused in the field.

A younger collapse structure, the Summitville caldera, occupies the northern part of the Platoro caldera (fig. 2). This caldera apparently formed when ash-flows constituting the upper sheets of the Treasure Mountain Tuff, including the Ojito Creek and Ra Jadero Members, were erupted after the Platoro caldera itself was nearly filled by lavas of the lower member of the Summitville Andesite. The Ojito Creek and Ra Jadero tuffs (fig. 4) are nearly coextensive with those in the La Jara Canyon Member and their constituent ash must have been erupted from the same general area. Although the volumes of these upper two members are much less than that of the La Jara Canyon Member (table 1), they are large enough to suggest associated caldera collapse (Smith, 1960, fig. 3). In addition, the Summitville caldera is indicated by (1) a large-displacement (800+ m) arcuate fault marking the main ring-fracture fault on the southeast side of the caldera (fig. 2), (2) fragmentary exposures of the topographic wall, especially on the northeast side, and (3) the concentration of the products of late igneous activity and mineralization around the margins of the caldera. The caldera probably was not resurgent, but was filled by thick lavas of the upper member of the Summitville Andesite, and many key geologic relations are largely buried. In

addition, extensive late intrusion and hydrothermal alteration further obscured relations.

Porphyritic rhyodacitic to rhyolitic lavas and genetically related dikes and granitic stocks were emplaced repeatedly around the margins of the Platoro and Summitville calderas during the interval between 29 and 20 m.y. ago, with dated events at 29.1, $>26.7 < 27.8$, 25.8, 22.8, and 20.2 m.y.; these shallow intrusions and associated rocks locally were hydrothermally altered and mineralized.

BONANZA CALDERA

A caldera in the vicinity of the old mining camp of Bonanza in the northeast part of the San Juan volcanic field has been postulated by Karig (1965), Mayhew (1969), Bruns (1971), Knepper and Marrs (1971, p. 261), and others.

The oldest rocks in the Bonanza area are andesitic to latitic flows and breccias of the Rawley Andesite and Hayden Peak Latite (Burbank, 1932; Mayhew, 1969) that form an interfingering assemblage. We interpret these rocks to be the near-source facies of one or more local volcanoes equivalent in age to the Conejos Formation near the Platoro area. These rocks are overlain by the Bonanza Tuff, a densely welded quartz-latitic ash-flow tuff that once formed a widespread sheet over much of the northeastern part of the San Juan volcanic field. Near Bonanza, remnants of this sheet must have been deeply faulted into the older andesitic pile, probably as a result of caldera subsidence. Younger andesitic flows and breccias

cover at least some of the Bonanza Tuff that occurs within the subsided block (Knepper and Marrs, 1971, pl. 1).

Few generalizations can be made about the Bonanza caldera from available published data. However, we consider it significant that, as in the Platoro caldera complex, subsidence took place within an area of older intermediate-composition volcanoes and that post-subsidence lavas are predominantly andesitic in composition.

WESTERN SAN JUAN CALDERA COMPLEX

Six calderas in the western San Juan Mountains are located above the main western lobe of the gravity low that has been interpreted to represent a shallow batholith. The first five of these calderas, the Ute Creek, Lost Lake, San Juan, Uncompahgre, and Silverton, formed within the brief span of about 2 m.y., and the five related ash-flow deposits superficially resemble each other enough to have once been included within a single formation (the now-abandoned Gilpin Peak Tuff of Luedke and Burbank, 1963).

Of these five calderas, only the Ute Creek caldera is not clearly within the gravity low, but instead is located at the sharp gradient along the south side of the gravity low (fig. 1). This structure may have formed above a local magma chamber that either was too deep or, after ash-flow eruptions, did not retain enough relatively light silicic differentiate at its top to be detected by gravity measurements. The other four early calderas are well within the area of the gravity low, and, of these, three are closely clustered and have overlapping cycles of development. These cycles are believed to represent high-level magmatism and volcanic eruption related to the main upward movement of magma in this western part of the batholith.

The last subsidence structure, the Lake City caldera, formed about 5 m.y. after the earlier calderas subsided, and the associated ash-flow tuff contrasts markedly in composition and appearance with the earlier ash-flow tuffs. During the 5-m.y. interval, the main batholith is believed to have congealed sufficiently for a petrologically distinct batch of magma to penetrate to shallow depths and still retain its compositional identity.

UTE CREEK CALDERA

The southern margin of the caldera that formed during eruption of the Ute Ridge Tuff is exposed for about 3 km along the canyon of Ute Creek (figs. 5 and 6). Elsewhere, the eastern and northern topographic wall of the caldera can be located closely at only two places, one near the mouth of Ute Creek and the other along the south side of Pole Creek Mountain, near the eastern end of the mountain. The downdropped block within these limits may have subsided as a trapdoor that has no ring-fracture zone along its west side.

Along Ute Creek, intracaldera Ute Ridge Tuff, more than 300 m thick, is juxtaposed against Precambrian melsyenite and quartzite and an older unnamed crystal-poor ash-flow tuff of Tertiary age, whereas an outflow layer of the Ute Ridge Tuff is only about 130 m thick and extends out over an irregular surface cut on the older rocks. The probable, caldera-boundary fault between the thick section of Ute Ridge Tuff and the adjacent rocks is occupied by a quartz monzonite intrusive (fig. 5); another similar intrusive cuts the thick section of Ute Ridge Tuff north of lower Ute Creek.

In the vicinity of Ute Creek, a younger ash-flow sheet, the Blue Mesa Tuff, unconformably overlies the Ute Ridge Tuff, quartz monzonite intrusives, and Precambrian rocks. A chilled vitrophyre at the base of the Blue Mesa is in contact with all these older rocks, and north of Ute Creek a thin lens of andesite occurs locally along the unconformity. Development of the structural discordance between the thick section of Ute Ridge Tuff and the juxtaposed older rocks thus closely accords in time with eruption of the Ute Ridge Tuff, and seems most easily accounted for by caldera subsidence related to that eruption. Subsidence concurrent with eruption is indicated by the thick section of Ute Ridge Tuff within the downdropped block, in contrast with the relatively thin outflow sheet. Although we saw no evidence for post-subsidence resurgence, two quartz monzonite intrusive bodies along and near the southern margin apparently were emplaced late in the Ute Creek caldera cycle.

The topographic caldera wall along the east side of the downdropped block is closely controlled near the mouth of Ute Creek, where the top of a buried hill of older andesitic volcanic breccias (San Juan Formation) is exposed a few hundred metres east of the thick section of Ute Ridge Tuff that lies within the caldera. Several kilometres northwest, across the Rio Grande, another buried hill of andesitic breccias of the San Juan Formation is exposed along the south side of Pole Creek Mountain. The Ute Ridge and Blue Mesa Tuffs wedge out against this hill, which may represent a remnant of the northeast caldera wall.

Thick Ute Ridge Tuff is excellently exposed along the Rio Grande inside the west-facing semicircular arc described by the intrusive-filled fault along Ute Creek and the two buried hills of andesite breccia. The rude layers representing the many successive ash flows in the Ute Ridge Tuff dip about 5° east as part of a much later regional tilting that affected the whole western San Juan area, but otherwise are undeformed westward from the arcuate wall for 12-15 km. The tops of at least two buried hills of Precambrian crystalline rocks extending well up into the Ute Ridge Tuff are exposed along the Rio Grande 3-9.5 km west of the arcuate wall.

These incompletely exposed relations suggest that the

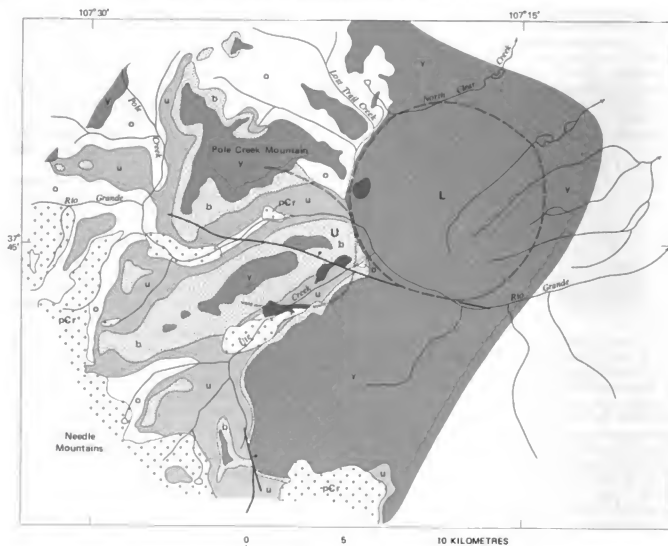


FIGURE 5.—Geologic map of Ute Creek (U) and Lost Lake (L) calderas. pCr, Precambrian rocks; a, precaldera volcanic rocks; u, Ute Ridge Tuff; b, Blue Mesa Tuff; y, postcaldera volcanic rocks; black, intrusive rocks. Open rectangles indicate approximate boundaries of postulated buried calderas.

source of the Ute Ridge Tuff was in a hilly area cut on older Precambrian rocks and Tertiary andesitic rocks, and that the pyroclastic eruptions caused concurrent subsidence of a trapdoor block that was faulted along the south, east, and north but probably only downwarped on the west. The fragmentary structural and topographic wall exposed in places along Ute Creek and Pole Creek Mountain reflects the abrupt boundaries of subsidence in these directions, whereas the downwarped(?) western margin is obscured by the relatively flat lying upper part of the Ute Ridge Tuff exposed along the Rio Grande.

LOST LAKE CALDERA (BURIED)

A distinctive arcuate drainage pattern along the upper Rio Grande (fig. 5) reflects a buried caldera related to

eruption of the ash composing the Blue Mesa Tuff. All rocks in this area dip regionally about 5° east and northeast; eastward across the arcuate drainage pattern, however, the dips increase to 10°-15° and then flatten again to form an arcuate monocline. Fracturing related to this monocline provided a zone of weakness later etched out by stream erosion. The monocline involves the Dillon Mesa and Sapinero Mesa Tuffs and younger units in this area, and reflects minor late subsidence around the western periphery of an older buried caldera.

The western margin of the largely buried Lost Lake caldera closely follows the arcuate monocline. The wall of the caldera is closely controlled near the mouth of Ute Creek, where a hill of older andesitic mudflow breccia protrudes up into the ash-flow section and represents a

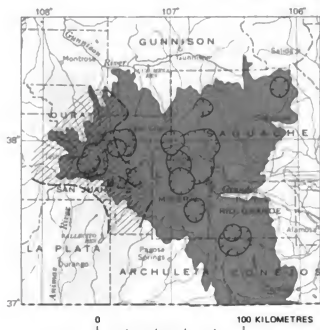


FIGURE 6.—Distribution of Ute Ridge Tuff (diagonal lines) in relation to Ute Creek caldera (U) and San Juan volcanic field (shaded).

wedge-shaped septum between the Ute Creek and Lost Lake calderas (fig. 5). Farther north, the northwestern wall of the Lost Lake caldera follows Lost Trail Creek for about 5 km; this segment of the caldera is marked, on the west side of the creek, by early, intermediate-composition andesitic rocks in the wall of the caldera and, on the east side, by caldera-filling rocks. No constraints are known on the east side of the caldera, however, and the projected margin (fig. 5) is drawn simply to close out the eastern side of a circular area that conforms to the arcuate monocline and drainage pattern to the west. The Lost Lake caldera, like several others in the San Juan volcanic field, possibly may have subsided as a trapdoor block with an incomplete ring-fracture zone and hinged eastern margin.

The oldest rocks exposed within the Lost Lakes caldera are the nearly identical Dillon Mesa and Sapinero Mesa Tuffs. These rocks form the lower parts of prominent cliffs along the Rio Grande, and are best exposed along the north side of the river opposite the mouth of Ute Creek. At this locality, the lower cliffs consist of Dillon Mesa Tuff; the upper 150 m of this unit is well exposed but, as the base is everywhere below the level of the river, its total thickness is not known—although it probably greatly exceeds the 0–100 m of Dillon Mesa Tuff exposed on Pole Creek Mountain west of the caldera. The overlying Sapinero Mesa Tuff, which forms the upper cliffs, is about 130 m thick, about the same as it is on Pole Creek Mountain. Evidently the Dillon Mesa ponded within and passively filled the caldera, and the succeeding Sapinero Mesa Tuff was deposited across it without appreciable thickening.

The Lost Lake caldera cuts off the Ute Ridge Tuff (fig. 5), and in turn was largely filled by the Dillon Mesa Tuff. These stratigraphic relations limit the time of caldera subsidence to the period during which the ash of the Blue Mesa Tuff was erupted. Of all the major ash-flow sheets in the upper Rio Grande area, only the Blue Mesa Tuff lacks an exposed source. The Blue Mesa is a widespread sheet (fig. 7) that pinches out against Precambrian rocks in the Needle Mountains on the south, extends westward to the eroded edge of the volcanic rocks near Telluride, and wedges out to the north against older volcanic rocks north of the Gunnison River, more than 80 km north of the upper Rio Grande area. To the east, the Blue Mesa Tuff is covered by younger rocks and its distribution is unknown (Steven, Lipman, Hail, and others, 1974). The Blue Mesa Tuff and older rocks are sufficiently well exposed north and west of the upper Rio Grande area that a caldera source can be eliminated in most of these areas. The source therefore most likely lies within the covered part of the sheet—and thus in the Lost Lake caldera.

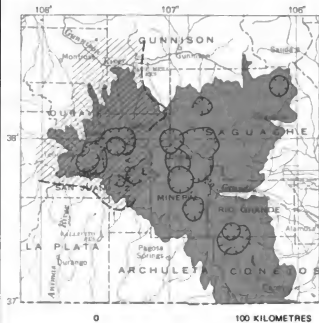


FIGURE 7.—Distribution of Blue Mesa Tuff (diagonal lines) in relation to Lost Lake caldera (L) and San Juan volcanic field (shaded).

The Blue Mesa Tuff is a uniform-textured, moderately phenocryst poor, densely welded ash-flow tuff over most of its exposed extent. In the upper Rio Grande area, however, the phenocrysts are larger and more abundant than elsewhere, and the unit is weakly compositionally zoned, becoming more mafic upward. A rhyodacitic lava flow also occurs locally between the Blue Mesa and the over-

lying Dillon Mesa Tuff on the north side of Pole Creek Mountain and just west of the arcuate monocline; this is the only known locality of lava-flow activity at this horizon. These areally restricted variations suggest a nearby source for the Blue Mesa Tuff.

No evidence was seen for resurgent doming of the Lost Lake caldera after subsidence. However, only the upper parts of the caldera fill can be seen, and the oldest rocks exposed are along the margins of the caldera, where the effects of resurgence would have been minimal. Thus, a low dome could exist a depth and not be reflected by the younger rocks that cover the caldera area.

SAN JUAN, UNCOMPAGHGRE, AND SILVERTON CALDERAS

The geologic history of the caldera complex in the western San Juan Mountains has recently been reinterpreted by Lipman, Steven, Luedke, and Burbank (1973), and the discussion here is taken largely from them. The western San Juan Mountains were the site of a cluster of intermediate-composition central-vent volcanoes in early Oligocene time, 35-30 m.y. ago. The near-source facies of these volcanoes consists of complex accumulations of lavas, breccias, and pyroclastic debris, which pass laterally into coalescing volcanoclastic aprons consisting predominantly of mudflow breccias and, at the margins, of conglomeratic and other stream-worked debris. The clustered volcanoes formed part of the great field of early intermediate-composition volcanic rocks that covered much of the southern Rocky Mountains in early Oligocene time (Lipman and others, 1970; Steven and Epis, 1968; Steven, 1975).

Ash-flow sheets from nearby sources at the Ute Creek and Lost Lake calderas covered the lower flanks and coalescing outflow aprons of these volcanoes, and wedged out against highlands built up around the central vents.

UNCOMPAGHGRE AND SAN JUAN COLLAPSES

The volcanic cycles that led to the development of the San Juan, Uncompahgre, and Silverton calderas probably began when the relatively small volume of material constituting the Dillon Mesa Tuff (table 1; fig. 8) was erupted shortly before 28 m.y. ago. No direct evidence can be marshalled to tie this eruption with any specific increment of subsidence, but the unit seems to be radially distributed around the area of the Uncompahgre caldera, and is thickest and most densely welded near the margins of this possible source area. Renewed eruptions of similar rhyolitic ash-flow tuff material about 28 m.y. ago led to widespread emplacement of the Sapinero Mesa Tuff, and to simultaneous collapse of the Uncompahgre and San Juan calderas (fig. 9).

The Sapinero Mesa Tuff spread widely (fig. 10) from its source area at these calderas, and had an estimated volume in excess of 1,000 km³. It has been traced northeastward for more than 90 km, northward 65-70 km; and south-



FIGURE 8.—Distribution of Dillon Mesa Tuff (diagonal lines) in relation to Uncompahgre caldera (U) and San Juan volcanic field (shaded).

eastward 40-45 km. Apparently it wedged out southward against the older highland of Precambrian rocks in the Needle Mountains. The western flank of the volcanic pile has been removed by erosion, and the original extent of the Sapinero Mesa Tuff in this direction is not known. Outflow Sapinero Mesa Tuff is generally less than 100 m thick, whereas the intracaldera Eureka Member is at least 700 m thick in places and the base is only locally exposed. This disparity in thickness between outflow and intracaldera facies is common among the San Juan calderas, and is interpreted to indicate subsidence concurrent with eruption; the intracaldera accumulation is generally somewhat younger than most of the outflow sheet.

Approximate contemporaneity of subsidence of the Uncompahgre caldera and eruption of the Sapinero Mesa Tuff can be demonstrated convincingly on the basis of geologic evidence (Lipman and others, 1973), and similar general relations of intracaldera and outflow accumulations of Sapinero Mesa Tuff for the San Juan caldera imply a similar timing. Subsidence of the two calderas was accompanied by widespread landsliding and avalanching of the steep caldera walls, and abundant debris from these sources is interleaved marginally with the intracaldera ash-flow accumulations (Eureka Member) in both calderas. By this process the topographic walls of the two calderas actually merged locally to form a single depression with a distorted dumbbell shape; the two main subsided blocks were joined across a low divide when the septum between them largely caved away (fig. 9).

The simultaneous development of adjacent but separate

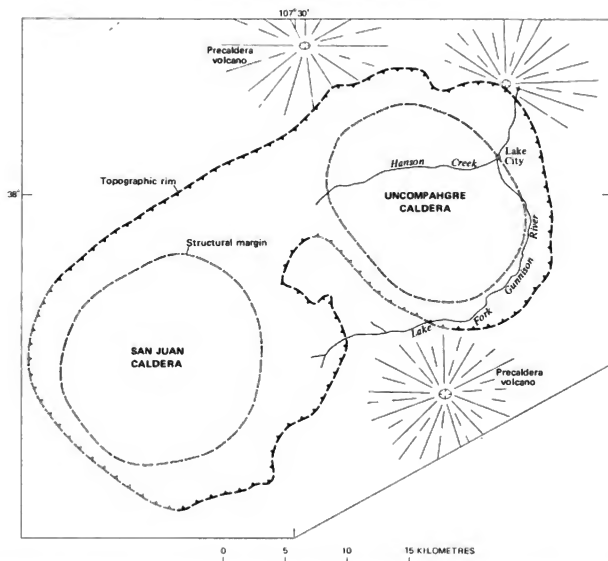


FIGURE 9.—Sketch map of the western San Juan caldera complex after subsidence related to eruption of the Sapinero Mesa Tuff. Control moderate to good where boundaries are shown by solid symbols; conjectural where shown by open symbols.

calderas was followed by merged later stages of the local caldera cycles. The calderas were resurgently domed together over an extended period of time, while the depressions were being filled with lavas and sediments from local sources and with ash-flow tuffs from concurrently developing calderas to the east. Renewed ash-flow eruptions forming the Crystal Lake Tuff during this period of resurgence and caldera filling led to subsidence of a local trapdoor block, the Silverton caldera, nested within the older San Juan caldera. These generally concurrent developments will be discussed separately in the following paragraphs, although the events are closely related and are manifestations of the same basic volcanic processes.

POSTCOLLAPSE LAVAS AND SEDIMENTS

The first postsubsidence eruptions within the San Juan and Uncompahgre calderas were mostly of viscous, coarsely porphyritic lavas of predominantly rhyodacitic and quartz-latic composition. These heaped up in the vicinity of their vents to form prominent local domes and thick flows, surrounded by lower areas where pyroclastic and reworked debris accumulated as bedded tuffs and volcanoclastic sediments. Some of these lower areas apparently were the sites of local ponds in which finely stratified deposits formed. This assemblage of thick porphyritic flows and associated bedded deposits is best displayed within the San Juan caldera, where it has been called the Burns Formation. It can be recognized as a

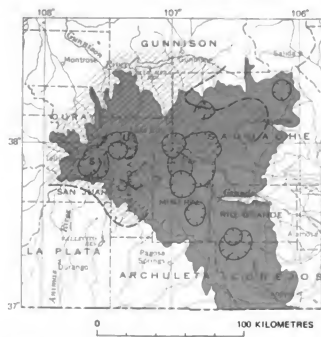


FIGURE 10.—Distribution of Sapinero Mesa Tuff (diagonal lines) in relation to San Juan (S) and Uncompahgre (U) calderas and San Juan volcanic field (shaded).

distinctive assemblage across the low divide into the northwest part of the Uncompahgre caldera; eastward, sedimentary rocks predominate and there are only minor porphyritic lavas.

The lavas filling the depression changed in composition upward to dark fine-grained andesite flows. These lavas were appreciably more fluid than the viscous porphyries of the Burns Formation, and the resulting flows are thinner and more widespread. Sedimentation in low areas continued, and the resulting bedded rocks are indistinguishable from many of those in the underlying Burns Formation. Local volcanic activity diminished later in the period of infilling, and volcanoclastic sedimentary rocks compose the upper layers of fill. The sequence of predominant andesitic flows grading upward into predominant sedimentary beds is best displayed in northeastern parts of the San Juan caldera, where the flows were originally called the pyroxene andesite unit and the overlying bedded rocks the Henson Tuff (Cross and others, 1905, 1907). Later, Luedke and Burbank (1963) combined both of these units into a redefined Henson Formation. Across the north side of the Uncompahgre caldera, the proportion of andesite flows to sedimentary rocks decreases eastward, and in the northeast part of the Uncompahgre caldera, the whole section generally equivalent to the Burns and Henson Formations consists largely of similar-appearing sedimentary rocks.

Rocks equivalent to the caldera-filling Burns and Henson Formations are found outside the calderas only on

the southeast side, where andesitic flows and breccias overlie the Sapinero Mesa Tuff and underlie younger ash-flow units derived from sources to the east.

INTRACALDERA ASH-FLOW TUFFS

The Burns and Henson rocks forming the bulk of the fill in the San Juan and Uncompahgre calderas are overlain by a sequence of ash-flow tuffs, mostly from caldera sources in the central San Juan Mountains, interlayered with locally derived sedimentary and volcanic rocks. The basal unit of this upper sequence is the Fish Canyon Tuff, derived from the La Garita caldera source area about 27.8 m.y. ago. Overlying ash-flow units consist in sequence of the Crystal Lake Tuff (derived from the Silverton caldera), the Carpenter Ridge Tuff (from the Bachelor caldera), Wason Park Tuff (caldera source not identified), and Nelson Mountain Tuff (from the San Luis caldera). Locally derived sediments closely similar to those in the Henson and Burns Formations separate all these ash-flow units at one place or another, and locally derived lavas of generally intermediate composition intervene between the Crystal Lake and Carpenter Ridge Tuffs, the Carpenter Ridge and Nelson Mountain Tuffs, and overlie the Nelson Mountain Tuff within and adjacent to the Uncompahgre caldera.

SILVERTON COLLAPSE

Eruption of the Crystal Lake Tuff (fig. 11) during the period of caldera filling resulted in trapdoor subsidence of the Silverton caldera within the older San Juan caldera (fig. 12). A block 15 km across, consisting in its upper parts of thick sections of Burns and Henson lavas and sediments, was displaced more than 600 m downward along its southern margin, whereas a sharp monocline cut by a deeply faulted graben marks its northeastern margin. Even in the present deeply dissected topography, the core of the trapdoor block stands nearly as high as the ash-flow deposits in the adjacent terrain, suggesting that no great thickness of Crystal Lake Tuff could ever have existed there. This suggestion accords with relations noted at other lesser calderas in the San Juan volcanic field related to small- to moderate-volume ash flow eruptions, where subsidence usually followed eruption and in places did not form complete ring-fracture zones.

RESURGENT DOMING

Resurgence of the San Juan, Uncompahgre, and Silverton calderas differed in several important aspects from resurgence at many of the other calderas in the San Juan volcanic field. Although it apparently began shortly after subsidence, uplift of the volcanic source areas probably continued for more than a million years through the period of infilling by locally derived lavas and sediments and by ash-flow tuffs from extraneous sources. As uplift continued rhyolitic magma regenerated beneath the San Juan caldera and erupted catastrophically as the ash-flows of the Crystal Lake Tuff, with related sub-

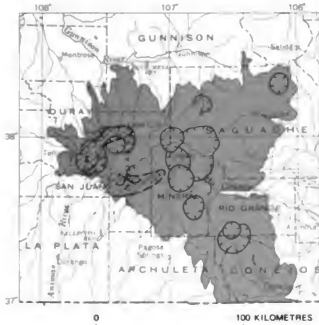


FIGURE 11.—Distribution of Crystal Lake Tuff (diagonal lines) in relation to Silverton caldera (S) and San Juan volcanic field (shaded).

sidence of the Silverton caldera. Structures that formed during this later subsidence appear to merge with some of the structures formed by uplift and seem to have developed concurrently.

Early resurgence is indicated by local angular unconformities between slightly tilted and eroded welded tuffs in the intracaldera Eureka Member of the Sapinero Mesa Tuff and overlying intermediate-composition lavas in the Burns Formation, as first noted by Luedke and Burbank (1968, p. 183). The extent of this early resurgence cannot be determined from the sparse evidence now available. Later magmatic uplift is indicated by the broad doming of the whole area of the San Juan and Uncompahgre calderas that affected the younger caldera fill as well. This broad uplift apparently was episodic, inasmuch as the ash-flow units overlying the Burns and Henson Formations appear to have been confined to a moat area around at least the eastern and northern margins of the uplifted core of older rocks, and yet in turn were tilted by further uplift of the core.

Longitudinal distention fractures along the crest of the broad domal uplift formed the deeply infaulted Eureka graben, which extends northeastward from the San Juan caldera into the uncollapsed septum between the San Juan and Uncompahgre calderas, where it is cut off abruptly by the much younger Lake City caldera. This graben offsets the caldera-filling Burns and Henson Formations as much as 0.5 km along the major faults, and, in places, graben faults cut small remnants of the younger Crystal Lake Tuff.

At its southwest end, the trend of the Eureka graben changes sharply, turning from northeast to northwest and giving the downfaulted area the distinctive bootlike shape shown in figure 12 (Burbank, 1951; Burbank and Luedke, 1969). The intersection of the northeast-trending Sunnyside fault and northwest-trending Ross Basin fault at the instep of the boot is intensely mineralized and is the site of the highly productive Sunnyside mine. This area has been studied in detail by many geologists and is well illustrated on a geologic map by Burbank and Luedke (1969, pl. 2). The fractures and veins pass smoothly around a sharp right-angle bend, and seem to have formed concurrently. To the northwest, as shown in the same illustration, several important veins and faults begin at the footwall of the Ross Basin fault as northeast-trending fractures generally parallel to the leg of the boot, but after several kilometres they swing sharply east and southeast to parallel the instep of the boot. This change in direction would again seem to require coexistent distentional stresses related to both major trends of the Eureka graben.

Whereas the northeast-trending fractures are along the crest of the broad dome of the simultaneously uplifted San Juan and Uncompahgre calderas, the northwest-trending fractures that define the foot of the boot are within the monoclinical hinge area along the north side of the younger Silverton caldera. The northwest-trending fractures thus appear to represent distentional fractures related to trapdoor subsidence of this block. Thus, in order for these different fault systems to have merged so completely, eruption of the Crystal Lake Tuff and subsidence of the Silverton caldera must have been concurrent with a major episode of uplift of the older calderas. Later or continued uplift of the broad dome is suggested by several minor northeast-trending faults that cut the foot of the Eureka graben boot (Burbank and Luedke, 1969, pl. 2).

Except for its having been formed during the period of general uplift, the Silverton caldera itself shows no evidence of being resurgently domed. Development of the spectacular radial and other intricate vein and dike patterns just outside the northwest and southeast margins of the Silverton caldera (Burbank, 1941; Varnes, 1963) may have resulted from this special stress environment. No other San Juan caldera has similar intricate patterns of fracture-related structures.

LAKE CITY CALDERA

After about a 4-m.y. period of greatly reduced volcanic activity in the western San Juan Mountains, ash-flow eruptions that produced the Sunshine Peak Tuff began about 22.5 m.y. ago in the Lake City area (Lipman and others, 1973; Mehnert and others, 1973a). Outflow Sunshine Peak Tuff must have been deposited widely in the region, although only small erosional remnants have survived. Concurrently with these eruptions, an elliptical block about 12 by 15 km across, nested within the southern

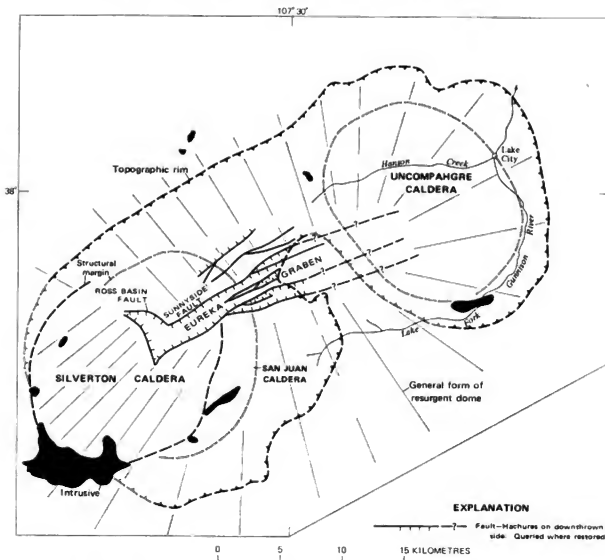


FIGURE 12.—Sketch map of the western San Juan caldera complex after subsidence of the Silverton caldera and general resurgence. Control moderate to good where boundaries are shown by solid symbols; conjectural where shown by open symbols.

part of the older Uncompahgre caldera, subsided to form the Lake City caldera (fig. 13). The last-erupted part of the Sunshine Peak accumulated to a thickness of as much as 1 km within the concurrently subsiding caldera, and great landslide avalanches caved off the caldera wall, spread across the caldera floor, and intertongued with the accumulating ash flows.

The ring fault along which this collapse occurred is continuously exposed for about 300° of arc around the caldera; it is nearly everywhere a single fault, typically marked by only a metre or so of gouge and minor hydrothermally altered rock. It is exposed over topographic relief of as much as 600 m, and is everywhere steep, dipping inward from 75° to nearly vertical.

Shortly after the ash-flow eruptions ceased, lava flows and domes of viscous silicic quartz latite, fed largely from vents along the ring fault, accumulated around the margins of the caldera floor. These lavas tend to overlie the Sunshine Peak Tuff conformably and dip quite steeply in places. They probably largely predate resurgent doming, although the effects of doming on them are difficult to distinguish reliably from primary dips of the flows. An east-northeast-trending line of rhyolite intrusives was emplaced in the moat area of the older Uncompahgre caldera, north of the Lake City caldera. These rocks are closely similar in composition to the Sunshine Peak Tuff, but apparently were emplaced somewhat more recently, with one intrusive yielding a K-Ar age of about 18 m.y. (H. H. Mehnert, written commun., 1974).

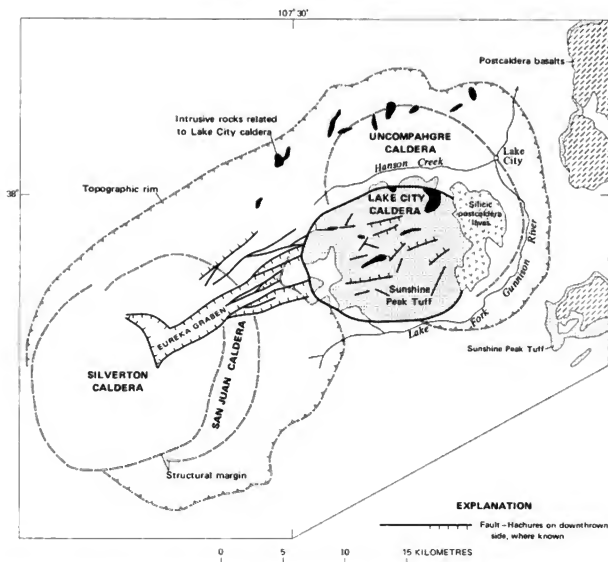


FIGURE 13.—Generalized geology of the western San Juan caldera complex showing distribution of rocks related to the Lake City caldera.

Resurgence of the Lake City caldera produced a simple dome characterized by outward dips of 20° - 25° on its flanks and a northeast-trending apical graben over its distended crest. The trend of this graben reflects reactivation of the trends of the earlier Eureka graben system, which was related to resurgence of the Uncompahgre and San Juan calderas. Most of the mapped faults of the Lake City resurgent structure have relatively small displacements—10-50 m—and some seem to be little more than cracks that localized weak hydrothermal alteration. Chaotic caldera-collapse breccias are widely exposed below the intracaldera tuffs on the southwest side of the Lake City caldera, and the resurgence appears to have been somewhat asymmetrical, with maximum uplift in this area. Resurgence resulted from upward movement of

magma which crystallized as a shallow stock of granite porphyry.

Gently dipping upper contacts of the granite porphyry are exposed at the bottoms of several deep erosional valleys within the core of the Lake City caldera, and the most intensely altered rock within the resurgent dome occurs around margins of the granite porphyry. Parts of the northern ring fault are occupied by a short, thick, discontinuous ring dike, which broadens and becomes coarser grained downward. The top of the granite porphyry is within 1 km of the top of the Sunshine Peak Tuff indicating crystallization at very shallow depths beneath the resurgent dome.

Most of the original topographic wall of the Lake City caldera has been eroded, and only a few small remnants are

preserved southwest of Lake City. The present valleys of Henson Creek and the upper Lake Fork of the Gunnison River, which define a striking elliptical drainage pattern just outside the structural boundary of the Lake City caldera, are not directly controlled by any major fault structures. They more likely developed in debris that accumulated in a low topographic moat along the margin of the resurgent dome of the Lake City caldera outside the limits of the subsided block, and were subsequently superimposed onto older rocks of the caldera wall.

CENTRAL SAN JUAN CALDERA COMPLEX

The central San Juan caldera complex developed above the eastern part of the gravity anomaly (fig. 1) between 28.2 and 26.5 m.y. ago. Within this brief span of less than 2 m.y., eight major ash-flow sheets were erupted, at least seven calderas formed, and numerous local volcanic rock units accumulated. These caldera cycles thus had an average duration of only about a quarter of a million years, and in at least one case, the cycles of two nearby calderas overlapped in time.

We believe that these intense pyroclastic eruptions and resulting caldera subsidences marked the culmination of upward movement of magma to form the eastern part of the underlying batholith. As the roof above this segment of the batholith became progressively thinner, it was breached by numerous ash-flow eruptions of great magnitude, and related calderas subsided at the ash-flow source areas. The development of the numerous clustered and partly overlapping calderas that followed one another in rapid succession, and the common marked contrasts between lithologies—ranging from phenocryst-rich quartz latites to phenocryst-poor rhyolites—of successive ash-flow deposits, required rapid congealing of the upper parts of the local cupolas and equally rapid reestablishment of new cupolas and magmatic differentiation within them. The pyroclastic eruptions and caldera subsidences apparently ceased when the upper part of the batholith congealed to a thickness sufficient to contain the magmatic pressures.

MOUNT HOPE CALDERA

The Mount Hope caldera (fig. 14) is almost completely buried by younger rocks, primarily the Fish Canyon Tuff, but fragmentary evidence suggests that it was the source of two phenocryst-rich quartz latite ash-flow sheets of the Masonic Park Tuff. The lower sheet has been recognized only within 10–15 km of the caldera, but the upper sheet (fig. 15) extends 30 km west of the caldera, to the margin of the San Luis Valley 30 km east, and into New Mexico 75 km southeast (Steven, Lipman, Hail, and others, 1974).

The topographic wall along the north margin of the Mount Hope caldera is exposed for about 6 km. This wall cuts sharply across the lower ash-flow sheet of the Masonic Park Tuff, andesitic flows and breccias of the Sheep

Mountain Andesite, thick quartz latite flows of the volcanics of Leopard Creek, and the upper ash-flow sheet of the Masonic Park Tuff. Total relief along the exposed section of this wall is about 500 m. The caldera is filled with Fish Canyon Tuff that is at least 1.4 km thick and extends over adjacent rocks on the south, east, and northeast sides of the caldera. Adjacent to the caldera, the Fish Canyon Tuff generally rests directly on the upper sheet of the Masonic Park Tuff.

The exposed segment of the topographic wall indicates that the caldera subsided after the ash flows forming the widespread upper sheet of Masonic Park Tuff were erupted (28.2 m.y. ago), and the basin formed by subsidence was in turn filled passively by the next succeeding major ash-flow sheet, the Fish Canyon Tuff (27.8 m.y. old). In addition to these stratigraphic constraints on the age of the caldera, other evidence, as follows, indicates that the Masonic Park Tuff was derived from a source within the Mount Hope caldera: (1) the position of the caldera well within the Masonic Park ash-flow sheet (fig. 15) and adjacent to the thickest sections of this formation; (2) intertonguing of the Masonic Park Tuff with andesite lavas of the Sheep Mountain Andesite and with other locally derived lavas near the rim of the Mount Hope caldera; and (3) the presence near the south and southwest edges of the caldera of bedded welded tuffs at the base of the upper ash-flow sheet of the Masonic Park that are believed to represent agglutinated ash fall, a depositional process only likely close to the eruptive source (Lipman, 1975a, fig. 26).

An earlier complex history of eruptions from the same general source is indicated by scattered exposures north-west and west of the Mount Hope caldera and in the highly faulted area southwest of the caldera (fig. 14). In these areas, the several individual ash flows within the composite older ash-flow sheet of Masonic Park Tuff intertongue with dark andesite flows and breccias of the Sheep Mountain Andesite that apparently formed a number of local volcanoes near the western margin of the later Mount Hope caldera. Just northwest of the Mount Hope caldera, the intertongued assemblage of Masonic Park Tuff and Sheep Mountain Andesite is overlain by thick coarsely porphyritic quartz latite lavas (volcanics of Leopard Creek), and these in turn are overlain by the thick upper sheet of Masonic Park Tuff (Steven and Lipman, 1973).

We interpret these relations to indicate early concurrent eruptions of quartz latitic ash flows of Masonic Park Tuff and andesitic lavas and breccias from local Sheep Mountain volcanoes. The ash-flow eruptions were apparently of small volume, and it is not known whether they were accompanied by caldera subsidence. Viscous quartz-latitic lavas forming a thick local assemblage (volcanics of Leopard Creek) were erupted along the

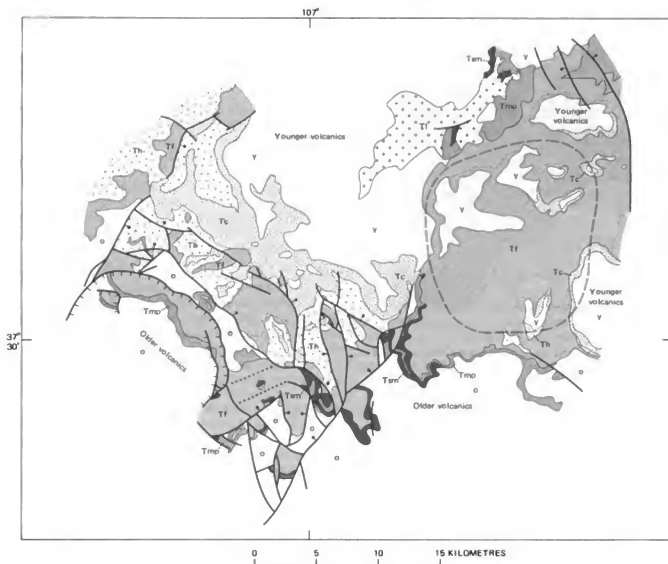


FIGURE 14.—Generalized geology of the Mount Hope caldera and adjacent areas. o, precaldera (older) volcanic rocks; Tmp, Masonic Park Tuff; Tsm, Sheep Mountain Andesite; Tf, Fish Canyon Tuff; Th, Huerto Formation; Tl, volcanics of Leopard Creek; Tc, Carpenter Ridge Tuff; y, volcanic rocks younger than Carpenter Ridge Tuff. Open rectangles outline the buried caldera. Heavy lines indicate faults; bar and ball or hachures on downthrown sides; dotted where buried.

northwest side of the postulated source area following accumulation of the older Masonic Park ash-flow tuffs and Sheep Mountain andesitic flows and breccias. Renewed eruptions of quartz-latic ash flows identical in composition and appearance to the older sheet of Masonic Park Tuff spread great volumes of tuff in all directions from the source area, thereby forming the widespread upper sheet of Masonic Park Tuff and resulting in subsidence of the Mount Hope caldera.

The Mount Hope caldera was not resurgently domed immediately after subsidence to any discernible extent; the Fish Canyon Tuff filled a hole more than 1.4 km deep and

the floor of the fill is not exposed. Later broad uplift of the caldera area is indicated by the progressive overlap of younger ash-flow units onto the eastern side of the caldera fill (fig. 14). This uplift apparently was more a trapdoor uplift than a dome, with the western side preferentially uplifted. This later uplift probably was roughly concurrent with major faulting west and southwest of the Mount Hope caldera that will be discussed later. The Mount Hope caldera forms a type generally transitional between the earlier and later calderas of the San Juan field. Mount Hope is like the earlier calderas in its associated andesitic volcanism and the quartz-latic composition of



FIGURE 15.—Distribution of the upper member of Masonic Park Tuff (diagonal lines) in relation to Mount Hope caldera (M) and San Juan volcanic field (shaded).

the erupted tuffs; yet this caldera is well within the main gravity anomaly (fig. 1) and is associated with more silicic lava flows, as represented by the volcanics of Leopard Creek.

LA GARITA CALDERA

The La Garita caldera (fig. 16), the largest in the San Juan volcanic field, ranks among the great calderas in the world. The original topographic basin was at least 40 km across from north to south, and the subsided block within this basin appears to have been nearly 30 km across. The original east-west diameter of the caldera was somewhat less, but the precise dimensions cannot be established because the western part of the La Garita caldera has since been destroyed by later caldera subsidences.

The La Garita caldera is located near the center of the San Juan volcanic field, above the east-central part of the triangular-shaped batholith indicated by gravity data (fig. 1). Subsidence took place 27.8 m.y. ago (Lipman and others, 1970, p. 2340), in response to eruption of more than 3,000 km³ of the phenocryst-rich quartz-latic ash of the Fish Canyon Tuff (fig. 17). This unit spread over an area of more than 15,000 km²; it is 30-200 m thick over wide areas and accumulated to a thickness of more than 1.4 km within the concurrently subsiding caldera.

Whereas many of the older San Juan calderas formed near clusters of earlier andesitic volcanoes (the Bonanza, Platoro-Summitville, San Juan, Uncompahgre, and Mount Hope calderas), any such relationship is more difficult to determine for the La Garita caldera because of

its size. The intrusive core of an older volcano is exposed along the eastern wall of the La Garita caldera, and other volcanic centers are near the east, west, and north sides of the caldera, but exposures are inadequate to indicate whether these volcanoes were concentrated near the caldera.

A more important localizing factor may have been the position of the La Garita caldera with respect to the underlying batholith. The caldera occupies much of the roof above the broadest part of the batholith indicated by the gravity anomaly (fig. 1); this part of the roof was repeatedly disrupted by ash-flow eruptions and caldera subsidences throughout the less than 2 m.y. that remained of the period of intermediate to silicic volcanic activity. The recurrent volcanic activity and related subsidences here must have reflected equally active high-level magmatism throughout the eastern part of the batholith.

Little can be reconstructed of the early development of the La Garita caldera. The floor of the caldera is nowhere exposed, and the eastern and northern margins that survived later caldera subsidences are marked by a structural moat deeply filled with younger volcanic deposits. Little air-fall ash occurs below the outflow sheet, so premonitory eruptions seem to have been minor. In addition, no compositional zoning was noted anywhere in the outflow sheet of Fish Canyon Tuff, and the basal rocks seem indistinguishable from those elsewhere in the unit. Apparently, large volumes of ash were erupted quite suddenly from a major chamber containing relatively homogeneous phenocryst-rich quartz-latic magma.

The disparity in thickness between the intracaldera (more than 1.4 km thick) and outflow parts (generally less than 200 m thick) of the Fish Canyon Tuff requires subsidence concurrent with eruption. Compaction foliation and rude layering, marked in places by less-welded partings, are virtually parallel throughout the caldera fill, and indicate that block subsidence was concurrent with filling.

Little igneous activity or sedimentation seems to have occurred immediately after subsidence, and the first demonstrable event was broad resurgent doming of the core. The crest of the dome was relatively flat over an area at least 5 km across, and the preserved eastern and northeastern flanks dip 5°-15° radially outward from the crest. Minor tensional faults separate flat from inclined segments of the core, and also separate inclined segments that dip in different directions. Maximum relief from the northeast moat to the crest of the dome was more than 1.4 km. The western and southwestern flanks of the resurgent dome have since caved into younger calderas, and have been covered by younger volcanic units.

Most of the moat is deeply filled by younger volcanic rocks, or has been destroyed by younger caldera subsidences. The lower fill, along the northeast side of the

caldera, consists of Carpenter Ridge Tuff, in places showing evidence of having accumulated in shallow water. Minor tuffaceous sedimentary rocks exposed locally in this area probably represent deposition by small streams or in local ponds.

No late ring-fracture igneous activity is evident along the eastern or northern sides of the La Garita caldera, but the major rhyolite dome along Miners Creek, partly exposed in a deep canyon 6 km west of Creede (Steven and Ratté, 1965), is older than the Carpenter Ridge Tuff, and may have erupted through the western ring-fracture zone of the La Garita caldera.

The eastern wall of the La Garita caldera apparently stood especially high, and most subsequent units from the central San Juan caldera complex were trapped against it. Elsewhere, the younger ash flows overtopped the La Garita caldera rim and spread widely. This high part of the caldera wall marks the truncated end of a line of major older andesitic volcanoes that extended west-northwest from the Summer Coon center 10 km north of Del Norte (Lipman, 1968), through the Baughman Creek and upper La Garita Creek centers, to the Sky City center exposed in the eastern topographic wall of the caldera (fig. 16). These volcanoes were deeply eroded prior to eruption of the Fish Canyon Tuff, but protruded through all but the youngest subsequent ash-flow units.

BACHELOR CALDERA

The Bachelor caldera, the source of rhyolite ash flows that formed the widespread Carpenter Ridge Tuff (fig. 18), collapsed along the west margin of the La Garita caldera (fig. 16). The age of the Carpenter Ridge Tuff and of the Bachelor caldera is bracketed by K-Ar ages of 27.8 m.y. for the older Fish Canyon Tuff and 26.7 m.y. for the younger Mammoth Mountain Tuff.

The outflow Fish Canyon and Carpenter Ridge Tuffs are separated by andesite flows and breccias of the Huerto Formation that formed a series of volcanoes near the present edge of volcanic rocks south and southwest of the Bachelor caldera. After eruption of the andesites, the area southwest of the Mount Hope caldera (fig. 14) was intricately downfaulted toward the caldera complex, as described later. During the Huerto eruptions and later faulting, magma accumulated in a newly developed high-level chamber beneath the west side of the La Garita caldera, and differentiated to a silicic phenocryst-poor rhyolite which erupted to form the Carpenter Ridge Tuff. Southeast of the caldera, the Carpenter Ridge is locally compositionally zoned from rhyolite upward into quartz latite.

Eruption of the Carpenter Ridge Tuff was accompanied by subsidence of an oval-shaped caldera about 15 by 25 km across. Tuff more than 1.5 km thick accumulated within the subsiding caldera, whereas the outflow sheet generally is less than 400 m thick. As in other calderas in the San

Juan Mountains, these relations are believed to indicate subsidence concurrent with eruption.

The floor and eastern wall of the Bachelor caldera are exposed locally northeast of Creede. In this area, a rough fault-block topography marked by tectonically shattered rocks, fault scarps, and talus breccia developed on the older rocks (Steven and Ratté, 1965, p. 17). These fault blocks underlie the Bachelor caldera fill and form the eastern caldera wall, where they mark the progressive breaking down of the resurgent core of the La Garita caldera toward the younger subsidence feature to the west. In part these fault blocks may represent inward sliding of the Bachelor caldera wall toward the main ring-fracture zone during Carpenter Ridge eruptions.

Similar relations on the west side of the caldera may be represented by the intertonguing of Shallow Creek Quartz Latite with the intracaldera Bachelor Mountain Member of the Carpenter Ridge Tuff, as described by Steven and Ratté (1965, p. 23). This intertonguing was mapped in the early 1950's before any of the calderas in the central San Juan Mountains had been recognized. In retrospect it seems plausible that the layers of Shallow Creek Quartz Latite within the Bachelor caldera fill may instead be avalanche and landslide breccia derived from a major quartz latite dome (fig. 8) that formed the nearby oversteepened caldera wall, a relationship which has been found in many other intracaldera fills in the San Juan Mountains. This suggestion needs to be checked in the field.

Three small ash flows resembling Fish Canyon Tuff appear to intertongue with the intracaldera Bachelor Mountain Member of the Carpenter Ridge Tuff on the east side of the Bachelor caldera (Steven and Ratté, 1965, p. 18). These relations, if valid, indicate that neighboring cupolas on the underlying batholith were sufficiently locally restricted to permit contrasting magmas to coexist locally and earlier magma types to persist while the Carpenter Ridge rhyolite was differentiating.

The core of the Bachelor caldera was resurgently domed shortly after subsidence, and a fragmented cross section of the dome can be seen in the north wall of the younger Creede caldera. The top of the Carpenter Ridge Tuff is more than 700 m higher at the crest of the dome than it is near the eastern and western ring-fracture zones. Tensional fractures that formed during doming dropped local blocks nearly 500 m near the crest of the uplift, and longitudinal normal faults, including the ancestral Amethyst fault in the Creede mining district (Steven and Ratté, 1965, p. 55-56), extended north-northwest down the axis of the uplift. These faults marked the initial fracturing of an area that was recurrently broken during later volcanic episodes, and was widely mineralized at the time when the ores of the Creede mining district were deposited.

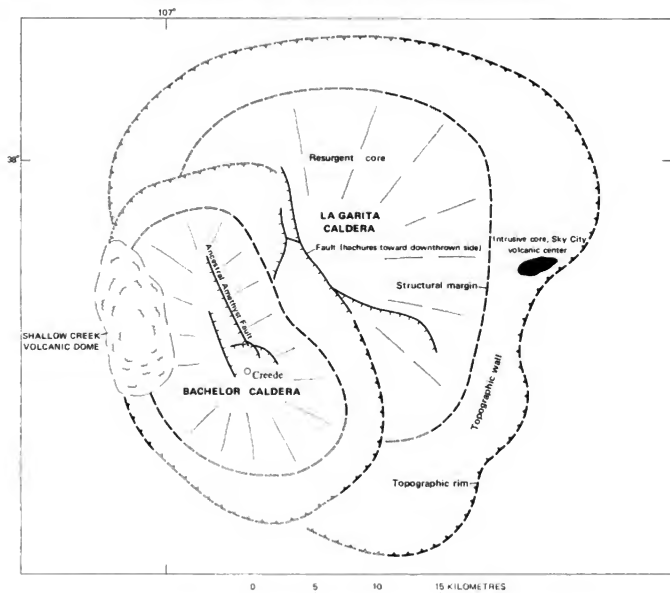


FIGURE 16.—Restored Bachelor and La Garita calderas. Control moderate to good where boundaries are shown by solid symbols; conjectural where shown by open symbols.

Small plugs of rhyolite cut the intracaldera tuffs near the center of the Bachelor caldera. These plugs are most abundant in the rocks that are cut by tensional faults and that were pervasively brecciated during resurgent doming. Evidence is ambiguous, but the rhyolite plugs may have been emplaced before brecciation and, thus, prior to resurgence. No postresurgence igneous activity related to the Bachelor caldera cycle has been recognized.

The shattered intracaldera Bachelor Mountain Member of the Carpenter Ridge Tuff on the resurgent dome was altered during the waning stages of the Bachelor caldera cycle. The shattered tuff was intensely silicified and largely healed to a massive rock. The K_2O content of the

silicified rock increased markedly from about 5 percent to as much as 11 percent (Raté and Steven, 1967, p. H13); this increase is reflected by abundant very fine grained orthoclase in the matrix. In the northern part of the Bachelor caldera, the intracaldera tuffs were variably bleached and altered, and disseminated pyrite was erratically introduced. No significant economic mineral deposits related to the Bachelor caldera cycle are known, however.

MAMMOTH MOUNTAIN(?) CALDERA

Indirect evidence suggests that subsidence took place during eruption of the Mammoth Mountain Tuff, but the

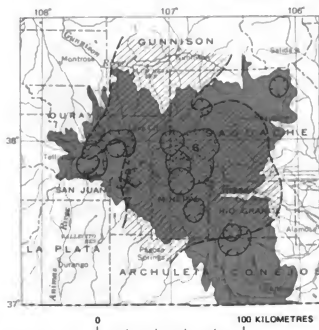


FIGURE 17.—Distribution of the Fish Canyon Tuff (diagonal lines) in relation to La Garita caldera (G) and San Juan volcanic field (shaded).

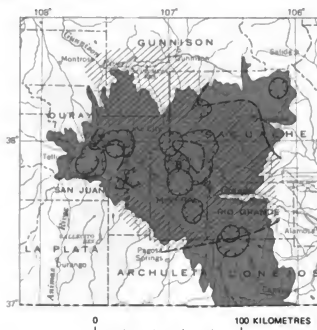


FIGURE 18.—Distribution of Carpenter Ridge Tuff (diagonal lines) in relation to Bachelor caldera (B) and San Juan volcanic field (shaded).

postulated caldera has been largely destroyed by the younger Creede caldera and covered by younger rocks.

The Mammoth Mountain eruptive cycle began with local episodic pyroclastic eruptions that formed a sequence originally called Farmers Creek Rhyolite by Steven and Ratté (1964, 1965) and Ratté and Steven (1967); subsequent regional work has indicated that these rocks were primarily local products of premonitory eruptions in the Mammoth Mountain cycle (Steven, Lipman, Hail, and others, 1974; Steven and Ratté, 1973) that were deposited just northeast of the postulated source beneath the younger Creede caldera. The early episodic pyroclastic eruptions progressed into a pulsating, nearly continuous, ash-flow eruption that flooded (fig. 19) the lower parts of the rough topography left by subsidence and resurgence of the La Garita and Bachelor calderas (fig. 1). Most of these Mammoth Mountain ash flows welded into coherent, dense tuff that shows obscure compound cooling (Ratté and Steven, 1967, p. H18-H33).

The Mammoth Mountain Tuff accumulated to a thickness of more than 500 m in the moat of the resurgent Bachelor caldera, where it is strongly zoned from phenocryst-poor rhyolite at the base to phenocryst-rich quartz latite at the top (Ratté and Steven, 1964, 1967). The Mammoth Mountain Tuff wedges out against and is absent over the top of the resurgent core of the Bachelor caldera, and was contained on the northeast and southwest by the outer topographic wall of the caldera. A 300- to 400-m-thick sheet of densely welded quartz latite tuff of the

Mammoth Mountain Tuff extends southeast from the postulated source within the subsequently formed Creede caldera to the southeast topographic wall of the La Garita caldera where it wedges out abruptly. Remnants of crystal-rich Mammoth Mountain Tuff 5-20 m thick are preserved near the Continental Divide 35-40 km south of Creede, indicating that the unit spread widely in this direction over the smooth top of Carpenter Ridge Tuff.

Near the postulated source, the products of the Mammoth Mountain eruptive cycle show structural relations that may indicate nearby caldera subsidence related to the ash-flow eruptions. The rudely layered rocks at the base of the section—the Farmers Creek Tuff (Farmers Creek Rhyolite of Steven and Ratté, 1965)—and most of the overlying phenocryst-poor tuff are inclined 10°-15° NE. The dip of this compaction foliation flattens in the younger quartz-latitic rocks; the change in dip is about coincident with the change in lithology and takes place within a vertical span of about 50 m. This change in dip is interpreted to reflect structural disturbance during Mammoth Mountain eruptions, a structural disturbance perhaps related to caldera collapse at the source vents.

Most of any Mammoth Mountain caldera that may have existed was destroyed by the younger Creede caldera. The size or shape of the postulated caldera is unknown, except that it must be within the topographic wall of the Creede caldera, which exposes pre-Mammoth Mountain rocks on its northern, eastern, and southwestern segments. Numerous viscous quartz-latitic lava flows that probably

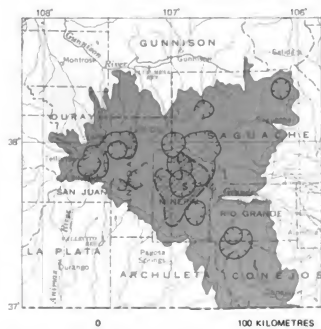


FIGURE 19.—Distribution of Mammoth Mountain Tuff (diagonal lines) in relation to probable source area (S) and San Juan volcanic field (shaded).

accumulated near their own vents overlie the Mammoth Mountain Tuff east and northeast of the Creede caldera and may represent the outer parts of flows and domes erupted marginally around the postulated Mammoth Mountain caldera.

SOURCE OF THE WASON PARK TUFF

The Wason Park Tuff is a simple cooling unit of rhyolitic ash-flow tuff that spread widely over the central San Juan volcanic field (fig. 20) and seems centered on the younger Creede caldera (fig. 1). North of the Creede caldera, the Wason Park fills the upper parts of the same rough topography that confined the Mammoth Mountain Tuff. It is largely confined to the moats around the resurgent La Garita and Bachelor calderas where it rests on thick tongues of Mammoth Mountain Tuff, and it thins or wedges out laterally against the resurgent cores or topographic walls of these calderas. To the west, south, and southeast, however, the Wason Park Tuff spread widely as a thin sheet on top of older ash-flow sheets.

The Wason Park Tuff has a volume greater than 100 km³ (Ratté and Steven, 1967, p. H34) and is sufficiently voluminous that subsidence should have resulted at the source (Smith, 1960, fig. 3), but no caldera structure is exposed within the area covered by the sheet. The only area large enough for subsidence related to Wason Park Tuff is under the younger Creede caldera, which is near the center of the area of distribution of the thickest and most densely welded Wason Park Tuff. White pumice blocks characteristic of the Wason Park Tuff are larger near the Creede

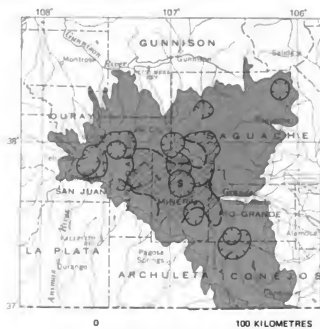


FIGURE 20.—Distribution of Wason Park Tuff (diagonal lines) in relation to probable source area (S) and San Juan volcanic field (shaded).

caldera than in the distal parts of the sheet (Ratté and Steven, 1967, fig. 16), and may indicate proximity to source. A local lava flow closely similar in lithology to the densely welded Wason Park Tuff underlies the Wason Park along the northeast rim of the Creede caldera (Ratté and Steven, 1967, fig. 15B), again suggesting a nearby source.

SAN LUIS AND COCHETOPA PARK CALDERAS

Although completely separate subsidence structures, the San Luis and Cochetopa Park calderas (figs. 21 and 22) are so intertwined in evolution that they are considered together. Furthermore, the San Luis caldera appears to be a compound structure consisting of two overlapping subsided blocks that formed in sequence during separate periods of ash-flow eruptions.

Stratigraphic uncertainties preclude confident interpretation of the evolution of these calderas. The history of past usages of the Rat Creek, Nelson Mountain, and Cochetopa Park as rock-stratigraphic units chronicles the confusion that has stemmed from attempts to correlate virtually identical rock types from area to area; nearly every report dealing with these units that has been published since 1964 treats them differently. This report continues this confusing practice because none of the previous usages permits reconstruction of a coherent history of evolution of the calderas.

In its type locality in the Creede mining district (Steven and Ratté, 1964, 1965), the Rat Creek Tuff consists largely of soft white nonwelded to slightly welded relictized tuff,

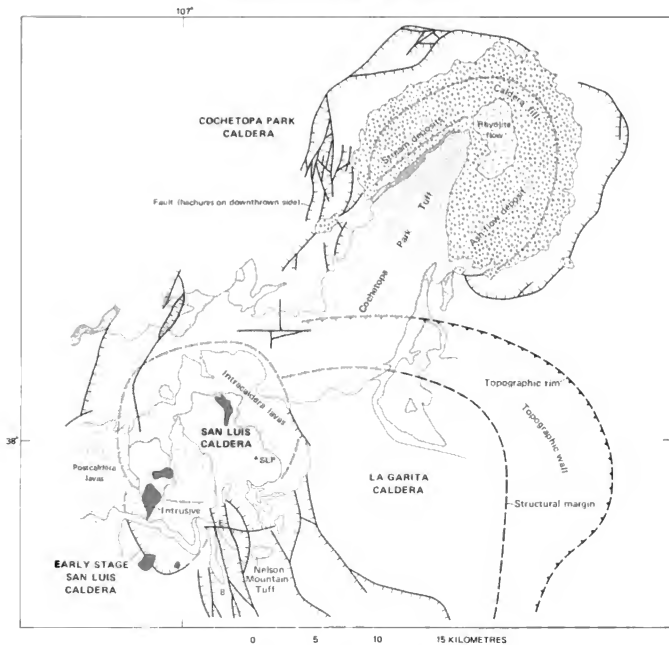


FIGURE 21.—Generalized geology of the San Luis and Cochetopa Park calderas in relation to remnants of the Bachelor (B) and La Garita calderas. Control moderate to good where boundaries are shown by solid symbols; conjectural where shown by open symbols. E, general area of the Equity mine; SLP, San Luis Peak.

with a ledge of densely welded tuff 10-30 m thick just above the middle. The Rat Creek is overlain by Nelson Mountain Tuff, a densely welded quartz latite containing 15-30 percent phenocrysts. Steven and Rattré (1965, p. 37) included in the Nelson Mountain the large mass of propylitized densely welded tuff (the Equity Quartz Latite as used by Emmons and Larsen, 1923) that fills the lower part of the San Luis caldera, although they could not prove physical continuity.

After extensive regional mapping in the central and northern San Juan Mountains, Steven, Lipman, and Olson (1974, p. A80) concluded that the densely welded rocks in the San Luis caldera were probably the intracaldera equivalent of the Rat Creek Tuff, and called them the Equity Member of that formation. Overlying densely welded tuffs on the north and northeast sides of the caldera were correlated with the lithologically identical Nelson Mountain Tuff at its type locality. These overlying welded

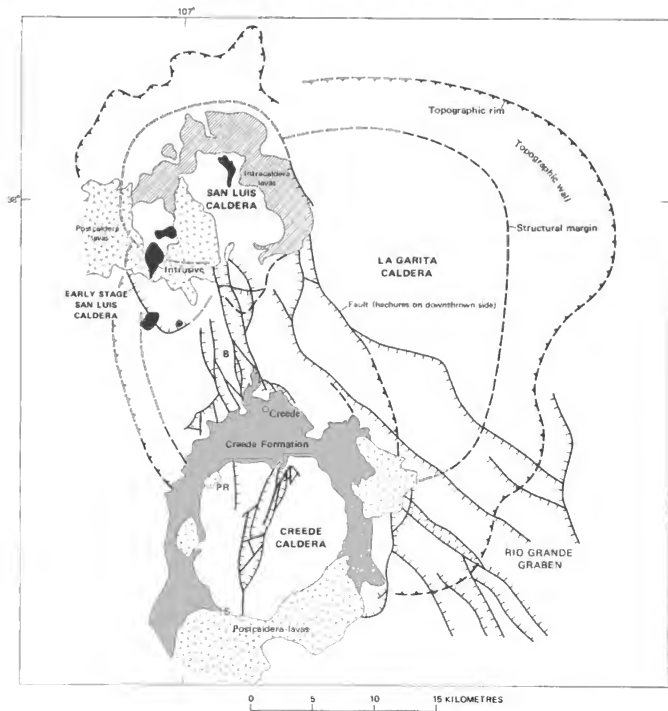


FIGURE 22.—Generalized geology of the Creede and San Luis calderas in relation to remnants of the Bachelor (B) and La Garita calderas. Control moderate to good where boundaries are shown by solid symbols; conjectural where shown by open symbols. PR, Point of Rocks volcano; S, Spar City.

tuffs extend into their apparent source area in the Cochetopa Park caldera to the northeast. Younger post-subsidence tuffs filling the Cochetopa Park caldera were called the Cochetopa Park Member of the Nelson Mountain Tuff.

Continued work in the northwestern San Juan Mountains has shown that something is wrong with this interpretation of the stratigraphic assemblage. Major densely welded ash-flow tuffs in the Lake City area (40 km northwest of Creede) almost certainly are equivalent to the

Nelson Mountain Tuff at its type locality in the Creede mining district, but details of distribution and volume make it highly unlikely that they were derived from the Cochetopa Park caldera. This forces the following tentative conclusions:

1. The correlation of Nelson Mountain Tuff in its type locality in the Creede district with lithologically identical tuffs northeast of the San Luis caldera probably is wrong.
2. The original correlation of Nelson Mountain Tuff with the densely welded (Equity) tuffs in the San Luis caldera by Steven and Ratté (1964, 1965) probably is correct. The Equity Member is therefore removed from the Rat Creek Tuff and assigned to the Nelson Mountain Tuff.
3. The densely welded tuffs north and northeast of the San Luis caldera, apparently derived from the Cochetopa Park caldera, constitute a separate unit younger than the Rat Creek and Nelson Mountain Tuffs. We therefore remove the Cochetopa Park Member from the Nelson Mountain Tuff and raise it to formational rank as the Cochetopa Park Tuff.

The interpretations that follow assume that these tentative conclusions are generally correct, but repeated examinations of critical field relations and petrographic studies have failed to develop the firm criteria for distinguishing these units that will be required for confident evaluation of our evolutionary model.

COMPOUND SUBSIDENCE OF THE SAN LUIS CALDERA

As currently (1975) understood, the Rat Creek Tuff appears to be a relatively low volume assemblage of poorly welded rhyolitic ash-flow tuffs confined largely to the vicinity of the Creede mining district (Steven and Ratté, 1965). Several factors imply a nearby source: (1) at least one local volcano of Rat Creek age is well exposed in the heart of the Creede district (Steven and Ratté, 1965, p. 35); (2) a local ledge of densely welded tuff occurs just above the middle of the Rat Creek Tuff within the Creede district; and (3) a small subsidence structure (caldera) of Rat Creek age is located along the northwest side of the Creede district. This last structure, described below, is here considered an early stage in the development of the compound San Luis caldera (fig. 21).

The regional sheet of Rat Creek Tuff ranges widely in thickness because of rough underlying topography. It is 150-200 m thick through the central part of the Creede district, but to the northeast it wedges out completely against an eroded fault scarp cutting the resurgent core of the La Garita caldera. North of the Creede district, the Rat Creek is cut off by the topographic wall of the main San Luis caldera.

In the early stage of the San Luis caldera along Miners Creek northwest of the Creede district (fig. 21), soft zeolitized tuffs that are physically continuous with type Rat Creek Tuff fill a partly exposed subsidence structure that has a steep arcuate fault along the south and southwest sides. To the north and northeast, this caldera is largely covered by younger rocks and relations are almost totally obscured; the map pattern (figs. 21 and 22) implies that the northern part of the caldera caved into the main San Luis caldera which developed shortly afterward.

Soft tuffs of the Rat Creek accumulated to a thickness of more than 350 m within the early caldera and are at least twice as thick as nearby correlative outflow tuffs. The intracaldera tuffs are flat lying and show no evidence of resurgence. The faulted margin is largely obscured by massive landslides, but it can be estimated to within a few metres along one gully where it appears to be very steep. Elsewhere the fault is indicated by juxtaposition of soft intracaldera Rat Creek Tuff and flat-lying older rocks in the wall. Two intrusives were emplaced along or near the faulted margin. One is a major neck, more than 1 km across, that clearly occupies the fault; the other forms a low knob, 500 m across, completely surrounded by landslide debris.

Several features indicate a Rat Creek age for the early caldera. The wall outside the faulted margin includes rocks as young as Wason Park Tuff, which is the next oldest ash-flow unit in the San Juan Mountains, and locally may include the overlying andesite of Bristol Head which is directly beneath the Rat Creek Tuff just east of the early caldera. The local ledge of densely welded tuff in the upper part of outflow Rat Creek Tuff extends westward to the vicinity of the early caldera, but is nowhere found within the caldera, although the area of its projected position is well exposed. However, the caldera margin, whose development probably accounts for this discordance, is covered by surficial debris and younger lavas. The caldera fill is overlain by typical Nelson Mountain Tuff that extends from its type locality westward across the area of the early San Luis caldera. The Nelson Mountain forms an unbroken rim across the trend of the older faulted caldera margin without any change in thickness or evidence of deformation.

The main San Luis caldera (figs. 21, 22, and 23) is now thought to have subsided concurrently with eruption of the Nelson Mountain Tuff, and at least 1.5 km of phenocryst-rich quartz latite accumulated within the subsiding basin, whereas the outflow sheet nearby is only about 300 m thick. This thick mass of intracaldera ash welded into a dense, nearly homogeneous rock with only a few local less-welded partings. Later propylitic alteration further homogenized the rock and obscured partings. The base of the intracaldera Nelson Mountain Tuff is exposed locally within the north-central part of the caldera core

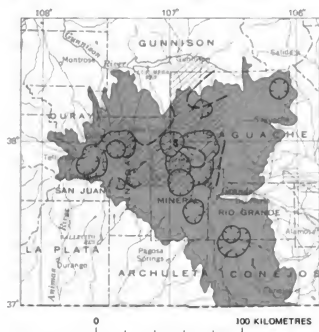


FIGURE 23.—Distribution of Nelson Mountain Tuff (diagonal lines) in relation to San Luis caldera (S) and San Juan volcanic field (shaded).

where densely welded quartz latite directly overlies a local hill, probably a volcanic dome, of older rhyolite. Some probable Carpenter Ridge Tuff is exposed on the north flank of this hill, but its relations with the adjacent rhyolite are obscure. No soft tuff representative of Rat Creek ash flows is exposed on this buried hill, but the lower parts of the caldera floor where such tuff deposits might more reasonably be expected are nowhere exposed.

Subsidence of the main San Luis caldera produced a broad basin nearly 15 km across. Intermediate to silicic lavas and breccias of the volcanics of Stewart Peak accumulated within the northern and eastern parts of this basin, and were locally accompanied by deposits of stream and lake sediments (figs. 21 and 22). Most intracaldera lavas around the eastern side of the caldera are rhyolacite and quartz latite, but perlitic rhyolite flows are abundant along the north margin. All known dike and neck feeders for the intracaldera lavas are within the caldera core. The eastern margin of the caldera block again subsided locally during eruption of the intracaldera lavas, as indicated by a fault with at least 500 m of throw that places the lower part of the volcanics of Stewart Peak within the caldera against older Fish Canyon Tuff in the wall. The fault passes under unbroken Cochetopa Park Tuff to the north, and ledges of this younger unit representing successive ash flows both to the north and south intertongue with younger lavas on the Stewart Peak sequence, providing an upper age limit for the renewed subsidence.

SUBSIDENCE OF THE COCHETOPA PARK CALDERA

Ash flows of the Cochetopa Park Tuff that were deposited in the San Luis caldera area (fig. 1) during accumulation of the intracaldera volcanics of Stewart Peak had their source in the Cochetopa Park area, some 30 km northeast. Minor phenocryst-poor rhyolite ash accumulated near the source, but the eruptions soon changed to crystal-rich quartz latite that is seemingly identical with the Nelson Mountain Tuff. The Cochetopa Park ash flows followed the nearly filled moat around the northern side of the La Garita caldera (fig. 1) and inter-tongued with the volcanics of Stewart Peak within the San Luis caldera (fig. 24).

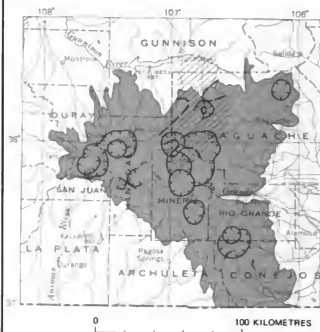


FIGURE 24.—Distribution of the Cochetopa Park Tuff (diagonal lines) in relation to Cochetopa Park caldera (C) and San Juan volcanic field (shaded).

In contrast with the larger San Juan calderas, where subsidence occurred concurrently with ash-flow eruptions, the Cochetopa Park caldera collapsed after major eruptions had ceased, as indicated by lack of thickening of the intracaldera tuff. In further contrast with the larger calderas, the Cochetopa Park caldera did not form a complete circular structure, but subsided as a trap-door bounded by a horseshoe-shaped fault. The southwestern margin did not fracture, but merely bent downward and tilted eastward. A trough, probably representing a graben, formed along the northwest side of the caldera core, and a tilted, northeast-trending ridge of Cochetopa Park Tuff dipping 5°-10° E. extended beyond the middle of the caldera (fig. 21). An inner ring-fracture zone can be postulated to account for major subsidence (fig. 21).

Maximum displacement on the northeastern side of the trapdoor is 700-800 m, as judged from the height of the topographic wall in this direction.

After the inner trapdoor block had subsided, or perhaps concurrently with subsidence, the walls of the caldera slumped inward along arcuate faults that nearly surround the downfaulted parts of the caldera. The breakaway zone near the hingeline of the trapdoor on the west side of the caldera is a splintered area of many faults and jumbled relations between blocks. Elsewhere, the slumped blocks are bounded by curved, linking faults that are concave toward the subsided trapdoor. Locally along the northeast side, no slumping took place.

Minor pyroclastic eruptions after subsidence of the Cochotopa Park caldera deposited local moderately to densely welded ash-flow tuffs near the hingeline and thick nonwelded pumiceous ash-flow tuff within the caldera east of the medial ridge (fig. 21). The trough (graben?) northwest of the medial ridge was filled with sandy tuffaceous stream deposits and a few layers of air-fall tuff. The two facies merge in the northeastern part of the caldera about on trend with the medial ridge. Layering in the tuffaceous caldera fill is flat and shows no resurgence of the caldera core. In places the caldera fill covers arcuate faults of the outer slumped zone and provides an upper limit on the age of that faulting.

A thick rhyolite flow with a prominent black vitrophyre at its base was erupted through the caldera fill about on trend with the medial ridge, and eroded remnants still persist as the feature called Cochotopa Dome.

RESURGENCE OF THE SAN LUIS CALDERA

Whereas minor resurgence of the San Luis caldera may have preceded or accompanied eruption of the intracaldera volcanics of Stewart Peak, most resurgence took place later. Densely welded layers of the Cochotopa Park Tuff, representing many successive ash flows from the Cochotopa Park caldera, intertongue with the upper volcanics of Stewart Peak and are involved in this resurgent uplift. North of the caldera, the Cochotopa Park Tuff is inclined less than 10° in various directions, but near the caldera margin the layers are bent up along a curving hingeline and dip 20° - 25° radially outward from the resurgent core. In part, this hingeline is marked by a fault with little displacement and the change in dip is sharp; elsewhere no fault is apparent and the change in dip is less abrupt. South of the caldera, resurgence is locally marked by an abrupt change in dip from flat layers of Nelson Mountain Tuff outside the caldera to layers dipping 15° or so southward off the dome within the caldera. Near the Equity mine in the northern part of the Creede district, however, local resurgence uplifted a triangular block, 1.5-3 km on a side, nearly a kilometre (Steven and Ratté, 1965).

This resurgence was somewhat asymmetrical to the San Luis caldera. The small remnant of the early subsided block along the southwest side of the caldera is not domed, and evidence of resurgence is apparently limited to the main caldera and to an area extending about a kilometre beyond the eastern and northeastern structural margin of the caldera. The edge of resurgent uplift on the north side of the San Luis caldera is just inside the outer topographic wall, and possibly is outside the buried structural margin.

The minimum structural relief caused by resurgence is a little less than a kilometre, as indicated by the elevation difference between the top of flat-lying Nelson Mountain Tuff outside the caldera and the top of San Luis Peak within the caldera. On the north side of the caldera, this difference is about 1.4 km, whereas on the south side it is about 0.7 km; as discussed later, this contrast reflects tilting caused by late general uplift of the roof of the batholith that underlies the central part of the San Juan volcanic field.

POSTCALDERA LAVAS

Resurgence of the San Luis caldera was followed by development of a line of volcanoes that extends westward from the caldera about 14 km. The eastern part of these postcaldera volcanic rocks, as shown in figures 21 and 22, consists of coarsely porphyritic lavas and breccias (the quartz latite of Baldy Cinco) that were erupted from many local vents, some within the western part of the San Luis caldera. Over most of their extent, these lavas and breccias rest on flat ledges of densely welded Nelson Mountain Tuff or Cochotopa Park Tuff, but on the east they abut and wedge out against tilted volcanics of Stewart Peak and Nelson Mountain Tuff in the resurgent core of the San Luis caldera. Apparently most of the western third of the caldera was once covered by these rocks. Lavas of similar age and composition (quartz latite of Rambouillet Park) (Steven, 1967) extend farther southwest, toward the south-east margin of the Uncompahgre caldera.

CREEDE CALDERA

The Creede caldera (fig. 22) formed in response to eruption of the Snowshoe Mountain Tuff about 26.5 m.y. ago and is the youngest subsidence structure in the central San Juan caldera complex. Its form is clearly reflected in the modern landscape. (See frontispiece, Ratté and Steven, 1967, for a color panorama of the Creede caldera.) The excellently preserved topographic form of this structure has resulted primarily from burial of all but the higher parts of the resurgent core by stream and lake sediments of the upper Oligocene Creede Formation that were not removed by erosion until late Cenozoic time (Steven, 1968, p. 114). Development of the Creede caldera was considered in detail by Steven and Ratté (1965, p. 58-62), and Smith and Bailey (1968, p. 625-626) used it as one of their seven examples of typical resurgent cauldrons.

The Creede caldera subsidence was localized along the southwest margin of the La Garita caldera (fig. 22); it obliterated the south part of the Bachelor caldera and the larger part of any calderas related to eruptions of the Mammoth Mountain and Wason Park Tuffs.

Initial eruptions of the phenocryst-rich quartz latite forming the Snowshoe Mountain Tuff spread a thin, poorly welded sheet over the flat surfaces of earlier ash-flow tuffs in adjacent areas (fig. 25). Subsidence began shortly thereafter and proceeded concurrently with eruption. More than 1.4 km, and perhaps more than 2 km, of nearly uniform crystal-rich ash accumulated within the subsiding basin; most of this is densely welded, but a few partings are less welded.

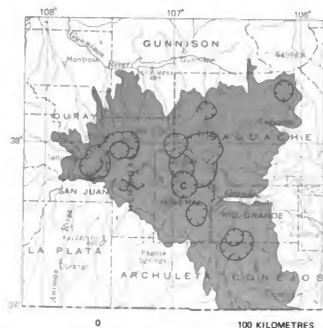


FIGURE 25.—Areas where erosional remnants of Snowshoe Mountain Tuff are preserved (diagonal lines) in relation to Creede caldera (C) and San Juan volcanic field (shaded).

Tongues of talus and rockfall breccia (Steven and Ratté, 1965, p. 42) extend into at least the upper 700 m of the intracaldera Snowshoe Mountain Tuff along the western side of the caldera, and probably are present but unexposed elsewhere within the intracaldera tuffs. These breccias clearly indicate subsidence concurrent with accumulation of the Snowshoe Mountain Tuff, and demonstrate that the developing caldera wall exposed rocks as old as Wason Park Tuff at least episodically during subsidence. The successive rude layering and compaction foliation in the Snowshoe Mountain Tuff are virtually parallel, and indicate that the core of the caldera sank as a coherent mass, rather than in piecemeal blocks.

Final subsidence left a basin 12–15 km across, with steep walls rising 1–1.4 km above the flat floor. These walls were

unstable, and great masses fell off to form tongues of rockfall breccia that extended over the caldera floor. The northeast wall of the caldera, where densely welded Mammoth Mountain and Wason Park Tuffs overlie soft tuffs, was particularly susceptible to avalanching, and a broad crescent-shaped scallop, 8 km wide and 3 km deep, developed in the outer wall. Breccias derived from the northeast wall of the caldera (Steven and Ratté, 1965, p. 42–43) have been identified more than halfway across the caldera, 8–10 km from their source.

The core of the Creede caldera was strongly domed after subsidence, and the center of the dome was uplifted more than 1.5 km above the structural moat left around the periphery. The eastern part of the uplift is a simple half dome with the layers of Snowshoe Mountain Tuff dipping radially outward 25°–45°. A deep north-trending graben extends across the center of the uplift; displacement is minor near the north and south ends of the graben, but exceeds 700 m near the center of the dome. Internal structure of the graben is complex (Steven and Ratté, 1965, pl. 1), but its general form is a fractured keystone block across the distended top of the resurgent dome. The west part of the resurgent core was less regularly uplifted; the northern flank was tilted northwest and broken by faulting and the western flank was tilted generally westward and was progressively more uplifted toward the south.

A small dome of autobrecciated rhyolite (Point of Rocks volcano) formed along the west side of the Creede caldera at some time just preceding, during, or immediately after resurgent doming. Pebbles of similar rhyolite have been found in some avalanche breccias caught in jumbled fault blocks along the keystone graben, suggesting that this volcano may have formed before resurgence. On the other hand, the eruption may have followed resurgent uplift, inasmuch as a local exposure shows the feeding neck to be nearly vertical where it cuts across strongly inclined layers of Snowshoe Mountain Tuff.

Resurgence of the Creede caldera was followed by eruption of flows and domes of Fisher Quartz Latite at places around the periphery and by deposition elsewhere of the stream and lake sediments and travertine of the Creede Formation. Closely accordant K–Ar age determinations of Fisher lavas indicate that this stage in the Creede caldera cycle took place about 26.4 m.y. ago. Most of the postcaldera lavas were erupted from centers northeast and south of the caldera. Ash-flow deposits in the concurrently deposited Creede Formation are most abundant toward the south, indicating that Fisher centers in this direction supplied much of the ash that elsewhere was reworked into the predominant stream-and-lake-sediment facies. Travertine in the Creede Formation was deposited widely around the periphery of the caldera; consideration of the timing of deposition and of carbon isotope ratios led

Steven and Friedman (1968, p. B32-B33) to conclude that the carbonate was derived from underlying sedimentary carbonate units by resurgent magma rising into the roots of the Creede caldera. The Creede Formation is presently exposed over a vertical range of more than 700 m; the bottom of the basin of deposition is not exposed and the top of the formation is eroded. The original thickness of the formation was more than a kilometre and was possibly as much as 1.4 km.

The final major stage in structural disruption that has been recognized in the vicinity of the Creede caldera was strong local faulting accompanied by mineralization in the Creede mining district adjacent to the north margin of the caldera (Steven and Ratié, 1965) and in the Spar City mining district along the south margin of the caldera (Steven, 1964). Steven (1972) and Steven and Eaton (1975) have interpreted the faulting and mineralization in the Creede district to have resulted from local intrusion of a stock into the roots of a preexisting broken zone. This intrusion may have been the terminal stage of the Creede caldera cycle or, more probably, may have been a later unrelated event, inasmuch as K-Ar age determinations on adularia from the OH vein in the Creede district indicate that mineralization took place there about 24.6 m.y. ago (M. A. Lanphere, P. M. Bethke, P. B. Barton, written commun., 1973), nearly 2 m.y. after caldera subsidence.

LATE GENERAL MAGMATIC UPLIFT

A broad zone extending from the Platoro caldera complex northwest through the central San Juan caldera complex was broken by normal faults late in the period of caldera development. Faults that developed at this time extend along the crest of the eastern part of the gravity low (fig. 1); these faults are thought to reflect uplift and distention related to a general buoyant rise of the whole eastern part of the batholith, where evidence for concurrent magmatism is strong.

Faulting took place in two general segments—the Rio Grande graben (figs. 1 and 22) extending southeast from the central caldera complex, and the Clear Creek graben (fig. 1) extending tangentially northwest from the caldera complex. Some faults in the Rio Grande graben were recurrently active, particularly near the northwest end, where we recognized several increments of displacement related to the progressive breakdown of the southwestern half of the La Garita caldera. Recurrent movement is also evident at the southeast end of the graben system, where Miocene basalts of the Hinsdale Formation are locally involved. The main graben faulting, which integrated some of the earlier faults into a regional pattern, took place during the Creede caldera cycle. Many of the faults cut Nelson Mountain Tuff and are in turn overlapped by unbroken Fisher Quartz Latite that was erupted late in the Creede caldera cycle. The northwest-trending faults are generally parallel to the trend of the underlying batholith.

This same part of the batholith was the source of repeated ash-flow eruptions and caldera subsidences during and just before graben development, indicating high-level activity in the underlying magma chamber. Some Rio Grande graben faults terminate to the southeast against a north-trending fault that closely parallels the eastern margin of the gravity low—again implying a close relationship between the faulting and distention of the roof above an active segment of the batholith.

As shown on figure 1, the Clear Creek graben (Steven, 1967) extends tangentially northwest from the southwest side of the central San Juan caldera complex. Its trend is parallel to the southwest side of the gravity low in the south-central part of the volcanic field. Where the graben extends across the gravity low toward the north, it separates an area of then-recent ash-flow eruptions and caldera subsidences to the east from an area of older ash-flow eruptions and caldera subsidences to the west. The graben reflects distention of the roof of the batholith, and it also marks relative uplift of the area to the east (Steven, 1967), toward the area of concurrently active magmatism. To the north, faulting changes from a graben to a west-facing normal fault and then to a northwest-facing monocline that bends around the northwest side of the San Luis caldera and dies out as it approaches the margin of the gravity low. As discussed earlier, the Nelson Mountain Tuff is about 0.7 km higher to the south of the San Luis caldera than it is to the north—a discordance believed to measure some of the late general uplift of the area above the batholith.

The Clear Creek graben began to develop during the closing stages of the San Luis caldera cycle, and may have been about concurrent with the Creede caldera cycle. The west-facing normal fault at the north end of the graben already existed when the quartz latite of Baldy Cinco was erupted, inasmuch as lavas of this unit poured over and covered a scarp related to the fault. Relations are ambiguous near the Creede caldera at the southeast end of the graben, where widespread glacial till obscures much of the bedrock. We saw no evidence that the graben existed when the Creede Formation was being deposited, yet none of the faults can be demonstrated to cut the Creede Formation. At least one fault on trend with the Clear Creek graben cuts Fisher Quartz Latite flows in the Spar City mining district on the south side of the Creede caldera, but this might reflect late reactivation of an earlier fault.

The Rio Grande and Clear Creek grabens are thus believed to reflect general distention and minor buoyant uplift of the eastern part of the batholith, where intense ash-flow activity and caldera subsidence demonstrated concurrent high-level magmatism in the underlying batholith. The faulting dies out southeastward and northwestward as it approaches the margins of the related gravity low, and no related graben faults of this age are

present in the western part of the gravity low where ash-flow eruptions and caldera subsidences are older. However, the intricate pattern of veins and small faults that radiate outward from the Silverton caldera may reflect analogous broad uplift during waning stages of volcanism in that area.

BLOCK-FAULTED AREA

An area west and southwest of the Mount Hope caldera is also broken by faults that were recurrently active during the period of caldera formation. This structurally somewhat anomalous area seems localized where the south margin of the gravity low, and presumably of the subvolcanic batholith (fig. 1), extends southwest across a thick wedge of Paleozoic-Mesozoic sedimentary rocks marking the northern extension of the San Juan Basin (fig. 1). The faults have the general pattern of a short ladder (fig. 14), with two northeast-trending faults bounding an area cut into narrow blocks by irregularly northwest trending steep faults. Several periods of movement can be discerned.

The oldest faulting followed deposition of the intertongued Masonic Park welded tuffs and Sheep Mountain andesitic lavas, and preceded deposition of the Fish Canyon Tuff. A later period of faulting is indicated in the eastern part of the highly faulted area, where andesitic breccias and minor flows in the Huerto Formation thin abruptly from more than 1,500 m to about 70 m thick eastward across a buried scarp on the Fish Canyon Tuff. This scarp probably marks a local fault that was active between deposition of the Fish Canyon Tuff and the Huerto Formation.

The main faulting followed eruption of the andesitic lavas and breccias of the Huerto Formation. The ladder-shaped pattern of faults formed at this time and the general result was to depress the area toward the caldera area to the north. These faults are superimposed on the steep gravity gradient along the south side of the underlying batholith (fig. 1), and the general effect of the faulting was to warp a local segment of the roof downward toward the batholith across its southwestern margin. This faulting did not coincide with any particular ash-flow eruption, but rather followed accumulation of episodically erupted andesitic lavas and breccias at a number of local volcanic centers. The movement thus probably resulted from magmatic movements within the batholith and distention along its south margin. This distention may have been in part localized by the relatively incompetent prevolcanic sedimentary sequence in this area.

Many of the faults that formed during the main post-Huerto faulting were reactivated later, after the Carpenter Ridge Tuff accumulated. In places, this reactivated movement was in the same direction as the earlier movement, and in other places, the direction of displacement was reversed. Most of the post-Carpenter Ridge faulting

appears to have reflected minor readjustments in the already broken roof of the batholith.

The youngest faults within this area reflect shallow gravity sliding of the south flank of the volcanic pile out over underlying Cretaceous shales. Fracturing took place along crescentic faults facing southward toward the edge of the volcanic plateau (fig. 14). The rocks enclosed within these faults were dropped downward toward the south, and tilted northward 30° or more by concurrent rotation. These faults are related to the present erosional scarp along the south side of the volcanic plateau, and are not directly related to the older faults that resulted from magmatic movement during late Oligocene volcanic activity.

DISCUSSION

DEVELOPMENT OF THE BATHOLITH

Calderas and related subsidence structures in the San Juan volcanic field are situated within a marked negative gravity anomaly that is believed to reflect an underlying shallow batholith. Successive ash-flow eruptions and caldera collapses in the volcanic pile above this batholith probably mark the local culminations of upward movement of magma: when the roof of an individual chamber became so thin that it failed, voluminous ash was erupted rapidly and a caldera collapsed into the partly evacuated magma chamber. Resurgent upward movement of magma domed many of the calderas and caused extrusion of lavas along the earlier formed structures. High-level magmatism, as manifested by volcanic eruptions and related structural adjustments, diminished at each center as the underlying cupola crystallized.

Using this model, we can trace the development of the high-level batholith beneath the San Juan volcanic field from the histories of the successive calderas. The early calderas are widely scattered and are either on the margins of the gravity low or on outward projections from it. Most of these early calderas developed within clusters of older andesitic stratovolcanoes, and the postsubsidence eruptions were commonly of intermediate lavas similar to the older andesites. We interpret these calderas to have developed above isolated high-level cupolas of magma that developed in the roots of older volcanoes before the main body of the batholith rose to its present position. The upper parts of these cupolas differentiated to quartz latite and low-silica rhyolite, which formed the ash-flow tuffs associated with the early calderas, but the quantity of silicic material was limited, and the postsubsidence lavas were from the underlying relatively undifferentiated andesitic magma.

The later calderas and associated structures are above the main body of the batholith as indicated by gravity data. At least 12 separate calderas formed within about 3 m.y. This intense activity is believed to reflect the rise of the

batolith in two main high-level segments corresponding to the two main caldera complexes. The segment beneath the western San Juan Mountains rose to shallow depths about a million years before the central San Juan segment, but high-level magmatic activity in each segment overlapped in time.

The top of the batholithic mass of magma was extensively differentiated—to phenocryst-poor rhyolite in the upper parts of local cupolas, and to large volumes of phenocryst-rich quartz latite beneath. Ash-flow eruptions in the western San Juan Mountains depleted the more silicic differentiates in the upper parts of the magma chambers, and the postsubsidence lavas were more mafic intermediate-composition rocks from progressively greater depths in the chambers. In the central San Juans, however, even the largest ash-flow eruptions did not exhaust the differentiated material in the underlying chambers, and the postsubsidence lavas that were erupted around the calderas are typically porphyritic quartz latites which are related in composition to the associated ash flow tuffs. Local andesitic volcanoes not closely associated with the calderas tapped deeper, little-differentiated parts of the batholith throughout the period of ash-flow eruptions and caldera subsidences.

The Lake City caldera in the western part of the San Juan volcanic field, which is related to eruptions of the petrologically distinct alkali rhyolite of the Sunshine Peak Tuff, collapsed about 4 m.y. later than the youngest major eruptions of andesitic and derivative rocks from the central and western parts of the San Juan volcanic field. This late caldera is believed to have formed above a later high-level magma chamber unrelated to the earlier segments of the batholith.

These interpretations suggest some time limitations on the magmatic life span of a shallow, composite batholith 100 km across. After about 5 m.y. (during the period from 35 to 30 m.y. ago) of intensive eruption of andesitic lavas from many scattered centers, local magma chambers 10-30 km across had risen to shallow depths beneath some of the larger volcano clusters, and had differentiated sufficiently to supply large-volume eruptions of silicic ash. Within the next 4 m.y. (30-26 m.y.) the batholith evolved from this collection of scattered chambers to a broad shallow mass of extensively differentiated magma, and then to virtual dormancy. Within another 4 m.y. (26-22 m.y.), the lower part of the batholith had coagulated sufficiently to permit a younger, petrologically distinctive body of magma to work its way up to similar shallow depths, while still retaining its compositional identity.

RELATION OF ASH-FLOW ERUPTIONS AND CALDERA SUBSIDENCE

An essentially one-to-one relationship exists between major eruptions of ash flows and subsidence of calderas in

the San Juan volcanic field. Unresolved is the volume of ash required to make this maxim operative. Most of the ash-flow sheets we have mapped have either very small (<10 km²) or moderate (100-500 km²) to large (>500 km²) volumes; caldera subsidence is known or suspected to have been associated with all the moderate-volume sheets and invariably accompanied the large-volume sheets. Several of the calderas associated with moderate-volume ash-flow sheets did not form complete circular collapse structures, but subsided as trapdoors hinged on one side. Such calderas generally were not resurgently domed after subsidence. Calderas associated with large-volume sheets, on the other hand, generally are complete subcircular structures, and commonly were resurgently domed after collapse.

All large-volume ash-flow units are much thicker within the calderas, typically by an order of magnitude, than in the surrounding outflow areas. This relationship is most easily explained by subsidence concurrent with eruption. Many of the large-volume units are compositionally zoned from early rhyolite to later quartz latite. In most, the rhyolite is confined to the base of the outflow sheet, commonly near the source, and the exposed intracaldera tuff is entirely quartz latite. This suggests that by the time ash-flow eruptions had removed sufficient magma to cause collapse, the rhyolitic material at the top of the chamber was usually exhausted. Alternatively, initiation of collapse may have disrupted the vent systems and caused tapping of deeper, less differentiated parts of the magma chamber. No generalization can be made concerning the beginning of subsidence relative to composition of the ash being erupted, however, as the relative volumes of rhyolitic versus quartz-latitic ash vary widely from one sheet to another. At the extremes, no rhyolite at all has been found at the base of the Fish Canyon Tuff, which forms the largest sheet in the San Juan field, whereas rhyolite dominates in both the outflow and intracaldera facies of the large-volume Sapinero Mesa and Carpenter Ridge Tuffs.

DIFFERENTIATION IN LOCAL CUPOLAS

Evidence for independent differentiation at separate volcanic source areas supports the idea that the successive calderas developed above local cupolas that projected above the general top of the batholith. This postulate is inherent in our interpretation of the development of the widely scattered early calderas, but appears valid for the clustered calderas in the western and central San Juan complexes as well.

In the western San Juan caldera complex, contrasting phenocryst-rich quartz-latitic Ute Ridge Tuff and phenocryst-poor rhyolitic Blue Mesa Tuff were erupted sequentially from calderas only a few kilometres apart, and individual magma chambers with separate

differentiation seem required. The later series of eruptions of rhyolitic Dillon Mesa and Sapinero Mesa Tuffs, progressively more mafic lavas and breccias of the Burns and Henson Formations, and rhyolitic Crystal Lake Tuff, all from within the confines of the San Juan-Uncompahgre-Silverton caldera cluster, chronicle the sequence of depletion of the differentiated magma at the top of one major cupola, establishment of another cupola, further differentiation, and, finally, renewed eruptions of regenerated rhyolite. Inasmuch as only about 2 m.y. intervened between eruptions of the Ute Ridge and Crystal Lake Tuffs, these sequential high-level magmatic processes must have progressed rapidly.

The major La Garita caldera in the central San Juan Mountains occupied much of the roof of the eastern segment of the batholith. The associated ash flows show virtually no evidence of compositional zoning; evidently, little highly silicic material had accumulated at the top of the broad magma chamber that supplied the enormous quantities of ash for the Fish Canyon Tuff. The magma chambers that developed successively along the west side of the La Garita caldera, however, were strongly differentiated. Rhyolite is a major constituent in the Carpenter Ridge, Mammoth Mountain, and Wason Park Tuffs, which followed in succession from closely associated source areas. Each of these units has distinctive phenocryst characteristics requiring separate development, and the first two are strongly compositionally zoned upward from phenocryst-poor rhyolite to phenocryst-rich quartz latite. All three of these units evidently developed under conditions that permitted local differentiation within sequentially formed restricted chambers.

The later Rat Creek, Nelson Mountain, Cochetopa Park, and Snowshoe Mountain Tuffs are from more widely scattered centers, for which local cupolas can readily be postulated. Except for the rhyolitic Rat Creek Tuff, these units are mostly composed of closely similar phenocryst-rich quartz latite, although the Cochetopa Park Tuff has some rhyolitic ash at its base. The overlap in time of the areally separate San Luis and Cochetopa Park caldera cycles also indicates concurrently developing, separated cupolas containing individually differentiated batches of magma.

Considering the number of calderas that developed sequentially within the approximately 4 m.y. of ash-flow activity above the San Juan batholith, differentiation must have been relatively rapid to generate silicic magma at the tops of the individual cupolas. This is particularly true for the succession of Fish Canyon, Carpenter Ridge, Mammoth Mountain, and Wason Park Tuffs, where the related calderas and source areas apparently overlap and the individual high-level magma chambers had to develop and differentiate in sequence.

RESURGENCE

Two broad types of magmatic uplift and general uplift related to calderas in the San Juan volcanic field have been recognized—in one, the uplift was closely confined to the caldera and the immediately adjacent area and occurred soon after collapse; in the other, however, broader uplift involved major segments of the roof of the batholith and occurred over an extended period. These two types of magmatic uplift merge and are, in places, difficult to distinguish.

Virtually none of the smaller calderas in the San Juan volcanic field show evidence of resurgent doming after subsidence. Fairly clear-cut relations indicating no resurgent doming are found at the Summitville, Ute Creek, Silverton, and Cochetopa Park calderas, as well as at the buried or postulated Lost Lake, Mammoth Mountain, and Wason Park calderas. Of these, the Silverton, Cochetopa Park, and probably the Ute Creek calderas subsided as trapdoor blocks with horseshoe-shaped incomplete ring-fracture zones interrupted by monoclinial hinges on one side; the buried Lost Lake caldera possibly may have subsided in a similar manner. The Summitville caldera is deeply buried by a fill of andesite flows, and the postulated Mammoth Mountain and Wason Park calderas were largely or completely destroyed by younger subsidences.

Most major San Juan calderas were resurgently domed shortly after subsidence. The Platoro, La Garita, Bachelor, San Luis, Creede, and Lake City calderas display such doming particularly well, and the Bonanza caldera may belong to this group. These are the typical resurgent cauldrons so well described by Smith and Bailey (1968), in which uplift was a definite stage in the caldera cycle (stage V) and was closely confined to the collapsed block and a narrow belt around the margin. Uplift clearly seems to have resulted from the rise of a central pluton beneath the subsided block, and often was accompanied by escape of magma along the marginal ring-fracture zones. The uplifted blocks within these calderas range from nearly symmetrical domes cut by tensional fractures (the Creede, Lake City, San Luis, and probably La Garita and Bachelor calderas) to tilted trapdoor blocks (the Platoro caldera).

Less well defined is the long-continued uplift of the area of the western San Juan caldera complex. Although some typical resurgence—in the sense described by Smith and Bailey (1968)—of both the San Juan and Uncompahgre calderas may have taken place, the main uplift was of long duration and involved an oval-shaped area that included both calderas. It began shortly after collapse of the San Juan and Uncompahgre calderas, continued through filling by locally derived lavas and sediments of the Burns and Henson Formations, eruption of the Crystal Lake tuff and resultant subsidence of the Silverton caldera, and further filling by ash flows from intracaldera sources in

the central San Juan Mountains. Quite possibly the total period of recurrent uplift spanned a million or more years. This long-continued activity may have resulted in part from general buoyant uplift by the major magma chamber that underlay the whole western caldera complex.

Another example of late general uplift is the Mount Hope caldera. We saw no evidence for postcollapse resurgence, and the succeeding Fish Canyon Tuff appears to have passively filled a deep depression. After filling, however, the whole area of the caldera was broadly upwarped, and so several of the overlying ash-flow sheets wedged out laterally against a low dome in the caldera area. Again, slight buoyant uplift above either a persisting cupola of magma, or a later renewed incursion of magma, would account for the relations seen. This type of uplift, and to a lesser extent that displayed in the Uncompahgre and San Juan calderas in the western part of the volcanic field, seems transitional to the broad buoyant uplift that affected the whole eastern part of the shallow batholith, as described in the section on "Late magmatic uplift."

MINERALIZATION

Only about a third of the calderas in the San Juan volcanic field are significantly mineralized (Steven, Luedke, and others, 1974). These calderas all had complex postsubsidence histories involving recurrent intrusion and extrusion of magma along the ring-fracture zones and related grabens. Some mineralization may have taken place during terminal stages of the associated caldera cycle, but the association of mineralization with a given caldera cycle generally seems tenuous, and the caldera seems principally to have provided fractures that guided later igneous intrusion and hydrothermal activity.

The Creede mining district occupies a radial graben on the north side of the Creede caldera. Faulting began during resurgence of the Bachelor caldera, and was reactivated several times later during the volcanic history of the area. The last faulting took place either late in the Creede caldera development cycle or shortly thereafter, when a generally equidimensional area 5-6 km across just outside the Creede caldera wall was broken, probably by intrusion of a stock at depth (Steven and Eaton, 1975). Important silver, lead, zinc, copper, and gold ores were deposited widely in fractures in the heart of the broken area (Steven and Ratté, 1965). The Creede caldera subsided about 26.5 m.y. ago, whereas the ores were deposited about 24.6 m.y. ago (M. A. Lanphere, P. M. Bethke, and P. B. Barton, written commun., 1973). These dates are perhaps too widely separated for the mineralization to be considered a terminal phase of the Creede caldera cycle of development and should, instead, be considered a later, unrelated event.

Mineralization around the nested Platoro and Summitville calderas is even less closely tied to the caldera cycles.

The calderas formed 29-30 m.y. ago in response to the repeated ash-flow eruptions of the Treasure Mountain Tuff (Lipman and Steven, 1970; Lipman, 1975a). The ring-fracture zones of these calderas were the sites of repeated igneous intrusion that began shortly after caldera subsidence and continued to about 20 m.y. ago. Significant mineral deposits seem to be concentrated where ring fractures of the Summitville and Platoro caldera complex intersect a regional northwest-trending fault zone (fig. 1) in the Summitville, Stunner, and Platoro mining districts. Other mineralized areas in or near this complex, at Crater Creek, Jasper, and Cat Creek, are also localized by caldera-margin faulting and igneous activity. The ores at Summitville have been dated by K-Ar methods as 22.4 m.y. old (Mehnert, Lipman, and Steven, 1973b), and thus are much too young to be tied to the main caldera cycles.

The western San Juan Mountains have a complex history of mineralization with several distinct periods of ore deposition extending over an interval of about 15 m.y. in late Tertiary time (Lipman and others, 1976). In the Lake City area, scattered mineral deposits, currently of limited economic significance, occur in the intrusive cores of intermediate-composition stratovolcanoes that were active between 35 and 30 m.y. ago, before any of the ash-flow eruptions that resulted in caldera collapses. Significant vein and disseminated mineralization occurred within northern parts of the Uncompahgre caldera after it collapsed about 28 m.y. ago, but before collapse of the Lake City caldera during eruption of the Sunshine Peak Tuff 22.5 m.y. ago. This timing is indicated by mineralized areas cut off by the younger subsidence and fragments of mineralized rock in landslide debris within adjacent parts of the Lake City caldera fill. Additional vein and disseminated mineralization occurs within and adjacent to the Lake City caldera, and is therefore younger than 22.5 m.y. old.

Major veins that follow faults of the Eureka graben (fig. 13) between the Lake City and Silverton calderas seem also to have formed after collapse of the Lake City caldera, although the graben faults existed as pre-Lake City structures. Later mineralization seems indicated by the following field relations: (1) We saw no altered rocks or vein fragments in landslide breccias within the Lake City caldera adjacent to the Eureka graben, although veins and mineralized rocks along graben faults extend to the structural margin of the caldera. (2) At Engineer Pass on the northwest side of the Eureka graben, silicic quartz porphyry intrusions that cut the Sunshine Peak Tuff, which was erupted from Lake City caldera, occur at the junction of a hydrothermally altered breccia pipe with associated mineralized veins and have yielded K-Ar and fission-track ages of 15-22 m.y. (H. H. Mehnert and C. N. Naeser, written commun., 1974). These silicic quartz porphyry intrusives, which form a well-defined northeast-trending belt extending about 40 km from northwest of

Silverton to north of Lake City, range from quartz latite to silicic rhyolite and granite. They are petrologically distinct from dated intrusions of the main cycle of ash flows and caldera collapse, which occurred at about 28 m.y., but they have close petrographic affinities to magmas of the 22.5-m.y. Lake City cycle.

In the productive Red Mountain district, on the west side of the Silverton caldera, intense alteration and breccia-pipe mineralization are similarly associated with silicic quartz-porphry intrusions that have been dated at 22-23 m.y. (H. H. Mehnert and C. N. Naeser, written commun., 1974), suggesting that mineralization in this area is young and genetically unrelated to the Silverton caldera cycle. The ages of the major vein systems south-east and northwest of the Silverton caldera are less certain, but at least some of the major veins southeast of Silverton cut quartz-porphry intrusions similar to those in the Engineer Pass and Red Mountain areas, and replacement ores associated with the rich veins on the northwest side of the Silverton caldera have yielded adularia K-Ar ages of 11-17 m.y. (F. S. Fisher and H. H. Mehnert, written commun., 1974). Thus, much—perhaps all—of the productive mineralization structurally associated with the Silverton caldera appears to have occurred at least 6-10 m.y. later than formation of the caldera 28 m.y. ago. The caldera appears to have acted mainly as a structural control, with some mineralization genetically associated with quartz-porphry intrusions that are petrologically distinct from volcanic rocks erupted during the caldera-forming process.

The primary function of calderas in mineralization thus appears to be the preparation of zones of weakness in the roofs of major magma-chambers. If conditions at depth are favorable, some of these zones are the sites of recurrent igneous intrusion and extrusion, locally accompanied by hydrothermal activity and mineralization. Whether this activity is the terminal stage of a specific caldera cycle, or is later and generally independent, seems accidental at our present incomplete state of knowledge.

REFERENCES CITED

- Bruns, D. L., 1971, *Geology of the Lake Mountain northeast quadrangle, Saguache County, Colorado*: Colorado School Mines M.S. thesis, 79 p.
- Bruns, D. L., Epis, R. C., Weimer, R. J., and Steven, T. A., 1971, Stratigraphic relations between Bonanza center and adjacent parts of the San Juan volcanic field, south-central Colorado, in *New Mexico Geol. Soc. Guidebook 22d Ann. Field Conf.*, San Luis Basin Colorado, 1971: p. 183-190.
- Burbank, W. S., 1932, *Geology and ore deposits of the Bonanza mining district, Colorado, with a section on History and production*, by C. W. Henderson: U.S. Geol. Survey Prof. Paper 169, 166 p.
- , 1941, Structural control of ore deposition in the Red Mountain, Sneffels, and Telluride districts of the San Juan Mountains, Colorado: Colorado Sci. Soc. Proc., v. 14, no. 5, p. 141-261.
- , 1951, The Sunnyside, Ross Basin, and Bonita fault systems and their associated ore deposits, San Juan County, Colorado: Colorado Sci. Soc. Proc., v. 15, no. 7, p. 285-304.
- Burbank, W. S., and Luedke, R. G., 1969, *Geology and ore deposits of the Eureka and adjoining districts, San Juan Mountains, Colorado*: U.S. Geol. Survey Prof. Paper 535, 75 p. [1970].
- Cross, Whitman, Howe, Ernest, and Irving, J. D., 1907, *Description of the Ouray quadrangle, Colorado*: U.S. Geol. Survey Geol. Atlas, Folio 153, 20 p. [text], 3 maps.
- Cross, Whitman, Howe, Ernest, and Ransome, F. L., 1905, *Description of the Silverton quadrangle, Colorado*: U.S. Geol. Survey Geol. Atlas, Folio 120, 34 p. [text], 4 maps.
- Emmons, W. H., and Larsen, F. S., 1923, *Geology and ore deposits of the Creede district, Colorado*: U.S. Geol. Survey Bull. 718, 198 p.
- Karig, D. E., 1965, Geophysical evidence of a caldera at Bonanza, Colorado, in *Geological Survey research 1965*: U.S. Geol. Survey Prof. Paper 525-B, p. B9-B12.
- Knepper, D. H., Jr., and Marrs, R. W., 1971, *Geological development of the Bonanza-San Luis Valley-Sangre de Cristo Range area, south-central Colorado*, in *New Mexico Geol. Soc. Guidebook 22d Ann. Field Conf.*, San Luis Basin, Colorado, 1971: p. 249-264.
- Lipman, P. W., 1968, *Geology of the Summer Coon volcanic center, eastern San Juan Mountains, Colorado*, in Epis, R. C., ed., *Cenozoic volcanism in the southern Rocky Mountains: Colorado School Mines Quart.*, v. 65, no. 3, p. 211-236.
- , 1975a, *Evolution of the Platoro caldera complex and related volcanic rocks, southeastern San Juan Mountains, Colorado*: U.S. Geol. Survey Prof. Paper 852, 128p.
- , 1975b, *Geologic map of the Platoro caldera area, southeastern San Juan Mountains, Colorado*: U.S. Geol. Survey Misc. Inv. Map 1-828. (In press.)
- Lipman, P. W., Fisher, F. S., Mehnert, H. H., Naeser, C. W., Luedke, R. G., and Steven, T. A., 1976, *Multiple ages of mid-Tertiary mineralization and alteration in western San Juan Mountains, Colorado*: *Econ. Geology* (in press).
- Lipman, P. W., and Mehnert, H. H., 1975, *Late Cenozoic basaltic volcanism and development of the Rio Grande depression in the southern Rocky Mountains*, in Curtis, B. F., ed., *Cenozoic history of the southern Rocky mountains*: Geol. Soc. America Mem. 144, p. 119-154.
- Lipman, P. W., and Steven, T. A., 1970, *Reconnaissance geology and economic significance of the Platoro caldera, southeastern San Juan Mountains, Colorado*, in *Geological Survey research 1970*: U.S. Geol. Survey Prof. Paper 700-C, p. C19-C29.
- Lipman, P. W., Steven, T. A., Luedke, R. G., and Burbank, W. S., 1973, *Revised volcanic history of the San Juan, Uncompahgre, Silverton, and Lake City calderas in the western San Juan Mountains, Colorado*: U.S. Geol. Survey Jour. Research, v. 1, no. 6, p. 627-642.
- Lipman, P. W., Steven, T. A., and Mehnert, H. H., 1970, *Volcanic history of the San Juan Mountains, Colorado, as indicated by potassium-argon dating*: Geol. Soc. America Bull., v. 81, no. 8, p. 2329-2352.
- Luedke, R. G., and Burbank, W. S., 1963, *Tertiary volcanic stratigraphy in the western San Juan Mountains, Colorado*, in *Short papers in geology and hydrology*: U.S. Geol. Survey Prof. Paper 475-C, p. C39-C44.
- , 1968, *Volcanism and cauldron development in the western San Juan Mountains, Colorado*, in Epis, R. E., ed., *Cenozoic volcanism in the southern Rocky Mountains: Colorado School Mines Quart.*, v. 65, no. 3, p. 175-208.
- Mayhew, J. D., 1969, *Geology of the eastern part of the Bonanza volcanic field, Saguache County, Colorado*: Colorado School Mines M.S. thesis, 94 p.
- Mehnert, H. H., Lipman, P. W., and Steven, T. A., 1973a, *Age of the Lake City caldera and related Sunshine Peak Tuff, western San Juan Mountains, Colorado*: *Ischron West*, no. 6, p. 31-33.

- , 1973b, Age of mineralization at Summitville, Colorado, as indicated by K-Ar dating of alunite: *Econ. Geology*, v. 68, no. 3, p. 399-401.
- Plouff, Donald, and Pakver, L. C., 1972, Gravity study of the San Juan Mountains, Colorado, in *Geological Survey research 1972*: U.S. Geol. Survey Prof. Paper 800-B, p. B183-B190.
- Ratte, J. C., and Steven, T. A., 1964, Magmatic differentiation in a volcanic sequence related to the Creede caldera, Colorado, in *Short papers in geology and hydrology*: U.S. Geol. Survey Prof. Paper 475-D, p. D49-D55.
- , 1967, Ash flows and related volcanic rocks associated with the Creede caldera, San Juan Mountains, Colorado: U.S. Geol. Survey Prof. Paper 524-H, 58 p.
- Smith, R. L., 1960, Ash flows: *Geol. Soc. America Bull.*, v. 71, no. 6, p. 795-842.
- Smith, R. L., and Bailey, R. A., 1968, Resurgent calderons, in Coats, R. R., Hay, R. L., and Anderson, C. A., eds., *Studies in volcanology*: *Geol. Soc. America Mem.* 116, p. 613-662.
- Steven, T. A., 1964, Geologic setting of the Spar City district, San Juan Mountains, Colorado, in *Short papers in geology and hydrology*: U.S. Geol. Survey Prof. Paper 475-D, p. D123-D127.
- , 1967, Geologic map of the Bristol Head quadrangle, Mineral and Hinsdale Counties, Colorado: U.S. Geol. Survey Geol. Quad Map GQ-631.
- , 1968, Critical review of the San Juan peneplain, southwestern Colorado: U.S. Geol. Survey Prof. Paper 594-I, 19 p.
- , 1972, Geologic environment of ore deposition in the Creede district, San Juan Mountains, Colorado [abs.]: *Econ. Geology*, v. 66, no. 8, p. 1270.
- , 1975, Middle Tertiary volcanic field in the southern Rocky Mountains, in Curtis, B. F., ed., *Cenozoic history of the southern Rocky Mountains*: *Geol. Soc. America Mem.* 144, p. 75-94.
- Steven, T. A., and Eaton, G. P., 1975, Geologic environment of ore deposition in the Creede district, San Juan Mountains, Colorado: *Econ. Geology*, v. 70, No. 6, p. 1023-1037.
- Steven, T. A., and Epis, R. C., 1968, Oligocene volcanism in south-central Colorado, in Epis, R. C., ed., *Cenozoic volcanism in the southern Rocky Mountains*: *Colorado School Mines Quart.*, v. 63, no. 3, p. 241-258.
- Steven, T. A., and Friedman, Irving, 1968, The source of travertine in the Creede Formation, San Juan Mountains, Colorado, in *Geological Survey research 1968*: U.S. Geol. Survey Prof. Paper 660-B, p. B29-B36.
- Steven, T. A., and Lipman, P. W., 1975, Geologic map of the Spar City quadrangle, Mineral County, Colorado: U.S. Geol. Survey Geol. Quad. Map GQ-1052.
- Steven, T. A., Lipman, P. W., Hail, W. J., Jr., Barker, Fred, and Luedke, R. G., 1974, Geologic map of the Durango quadrangle, southwestern Colorado: U.S. Geol. Survey Misc. Geol. Inv. Map 1-764.
- Steven, T. A., Mehnert, H. H., and Obradovich, J. D., 1967, Age of volcanic activity in the San Juan Mountains, Colorado, in *Geological Survey research 1967*: U.S. Geol. Survey Prof. Paper 575-D, p. D47-D55.
- Steven, T. A., Lipman, P. W., and Olson, J. C., 1974, Ash-flow stratigraphy and caldera structures in the San Juan volcanic field, southwestern Colorado, in Coher, G. V., and Wright, W. B., *Changes in stratigraphic nomenclature by the U.S. Geological Survey, 1972*: U.S. Geol. Survey Bull., 1394-A, p. A75-A82.
- Steven, T. A., Luedke, R. G., and Lipman, P. W., 1974, Relation of mineralization to calderas in the San Juan volcanic field, southwestern Colorado: U.S. Geol. Survey Jour. Research, v. 2, no. 4, p. 405-409.
- Steven, T. A., and Ratte, J. C., 1964, Revised Tertiary volcanic sequence in the central San Juan Mountains, Colorado, in *Short papers in geology and hydrology*: U.S. Geol. Survey Prof. Paper 475-D, p. D54-D63.
- , 1965, Geology and structural control of ore deposition in the Creede district, San Juan Mountains, Colorado: U.S. Geol. Survey Prof. Paper 487, 90 p.
- , 1973, Geology of the Creede quadrangle, Mineral and Saguache Counties, Colorado: U.S. Geol. Survey Geol. Quad. Map GQ-1053.
- Varnes, D. J., 1963, Geology and ore deposits of the South Silverton mining area, San Juan County, Colorado: U.S. Geol. Survey Prof. Paper 378-A, 56 p.



